JOURNAL OF BIOLOGICAL REGULATORS & HOMEOSTATIC AGENTS
Volume 30, No. 2, April - June, 2016

CONTENTS

EDITORIAL

AN OVERVIEW OF THE HISTORY, APPLICATIONS, ADVANTAGES, DISADVANTAGES AND PROSPECTS OF GENE THERAPY

M. JAFARLOU[1], B. BARADARAN[2], T.A. SAEDI[3], V. JAFARLOU[4], D. SHANEHBANDI[2], M. MARALANI[5] and F. OTHMAN[1]

[1]Department of Human Anatomy, Faculty of Medicine and Health Sciences, Universiti Putra Malaysia, Serdang, Selangor, Malaysia; [2]Immunology Research Center, Tabriz University of Medical Sciences, Tabriz, Iran; [3]Institute of Biosciences, Universiti Putra Malaysia, Serdang, Selangor, Malaysia; [4]Department of Surgery, Imam Reza Hospital, Tabriz University of Medical Sciences, Tabriz, Iran; [5]Health Sciences Institute, Dokuz Eylul University, Izmir, Turkey

Received April 20, 2015 – Accepted March 9, 2016

Gene therapy has become a significant issue in science-related news. The principal concept of gene therapy is an experimental technique that uses genes to treat or prevent disease. Although gene therapy was originally conceived as a way to treat life-threatening disorders (inborn defects, cancers) refractory to conventional treatment, it is now considered for many non–life-threatening conditions, such as those adversely impacting a patient's quality of life. An extensive range of efficacious vectors, delivery techniques, and approaches for developing gene-based interventions for diseases have evolved in the last decade. The lack of suitable treatment has become a rational basis for extending the scope of gene therapy. The aim of this review is to investigate the general methods by which genes are transferred and to give an overview to clinical applications. Maximizing the potential benefits of gene therapy requires efficient and sustained therapeutic gene expression in target cells, low toxicity, and a high safety profile. Gene therapy has made substantial progress albeit much slower than was initially predicted. This review also describes the basic science associated with many gene therapy vectors and the present progress of gene therapy carried out for various surface disorders and diseases. The conclusion is that, with increased pathobiological understanding and biotechnological improvements, gene therapy will become a standard part of clinical practice.

Gene therapy is delivering nucleic acid polymers as drugs into a patient's cells for treatment. Cells, tissue and all individuals modified by gene therapy are considered to be genetically modified or transgenic (1- 5). Indeed, gene therapy is capable of eradicating cancerous cells, halting cardiovascular diseases, correcting genetic weakness, and neurological disorders as well as completely removing infectious pathogens (6-12).

However, the significant point is that gene therapy is not a novel idea. According to Joshua Lederberg (1963), "We might anticipate the interchange of chromosomes and segments. The permanent application of molecular biology will be the direct control of nucleotide sequences in human chromosomes, coupled with recognition, selection and integration of the desired genes. It will only be a

Key words: gene therapy, somatic, germ line, viral vectors

Mailing address:
Prof. Dr. Fauziah Othman,
Department of Human Anatomy, Faculty of Medicine and Health Sciences, University Putra Malaysia,
43400, Serdang, Selangor, Malaysia
Tel.: +60(3)89472330
e-mail: fauziah@upm.edu.my

0393-974X (2016)

matter of time . . . before polynucleotide sequences can be grafted by chemical procedures onto a virus DNA." The first clinical study using gene transfer was reported in 1960 (13).

Gene therapy and the use of genomics are related in some aspects but they should be distinguished from each other in discovering new medicines and diagnostic techniques.

In 5 patients with metastatic melanoma, a retroviral vector to transfer the neomycin resistance marker gene into tumor-infiltrating lymphocytes was used by Rosenberg and his colleagues (13-16). These lymphocytes then were expanded *in vitro* and later reinfused into the respective patients. By showing in that first study that retroviral gene transfer was protected from or not exposed to danger or risk, it led to numerous other studies. In fact, more than 900 clinical trials have been approved worldwide since 1989 (17). After the initial idea of gene therapy explained by Joshua Lederberg in 1963, research on human genetics did not accelerate until the 1980s (18).

Somatic cell gene therapy

In general, the genetic makeup of the individual is not impacted by the change, and consequently the alteration is not transmitted to the individual's descendents. Gene therapy of somatic cells can enhance and contribute to the normal functioning of a disabled organ. Gene therapy of somatic cells is a technology with various applications in human health. One variant of somatic cell gene therapy is DNA vaccines which, in a procedure similar to that of conventional vaccines, prepares the ground for the cells of the immune system to fight certain diseases (19- 23).

Somatic gene therapy can be divided into two ex vivo and in vivo gene therapies.

Ex vivo is where cells are first cultured or synthesized outside the body and then transplanted back in. In certain gene therapy clinical trials, cells from the patient's bone marrow or blood are separated and grown in the laboratory. The cells are exposed to the suitable viral vectors which are carrying the desired gene. The vectors enter the cells and inserts the desired gene into the cells' DNA. The cells grow in the laboratory and are then returned to the patient by injection into a vein. It is obvious that introducing the desired containing cells into an organism may trigger immune responses. The cells also may not function as desired, malfunction, or not entirely work at all (24). *In vivo* is where genes are directly delivered to the organism, such as through a vector or other means. This form of gene therapy is called *in vivo* because the gene is transferred to cells inside the patient's body and may hold more risks than its *ex-vivo* counterpart, such as a possible immune reaction from the organism. Vectors used in *in-vivo* gene therapy include viruses, bacterial plasmids, nanoparticles (25).

Germ-line gene therapy

By introducing corrective genes into reproductive cells (sperm and eggs) or zygotes, the germ-line gene therapy is produced. The objective of this is to create a favorable or advantageous genetic change that is transmitted to the offspring. When genes are introduced in a reproductive cell, descendant cells can inherit the genes (18).

Via the use of pluripotent cells, or cells that can differentiate into any other cell type, stem cell therapy is produced. Stem cells exist in developing embryos and in some tissues of adults. The goal of this therapy is to regenerate or repair a damaged organ or tissue. Indeed, it is similar to a conventional transplant. Since it uses the individual's own cells, the procedure has a reduced probability of rejection. For instance, stem cells differentiated into nerve cells could help patients suffering from paralysis to recover movement, or they can be utilized in order to rejuvenate the cardiac muscles in patients suffering heart strokes (24). Furthermore, in the future there is a likelihood of utilizing an individual's stem cells to produce certain tissues or organs *in vitro*. Finally, stem cell research could take a quantum leap forward by merging gene therapy with genetic engineering to create stem cells that can be used to generate healthy tissues and organs (18, 19).

Some arguments for and some arguments against germ-line cell gene therapy are mentioned in the literature.

Arguments for germ-line cell gene therapy:

i. providing a bright prospect for the cure and treatment of several diseases;

ii. being the only treatment procedure for a number of genetic diseases;

iii. extending the benefits across generations (i.e., due to the elimination of genetic defects in the genome of the individual, the benefits are passed down to the descendents).

Arguments against germ-line cell gene therapy:

i. involving a multitude of poorly-understood steps and impossibility of estimating long-term results;

ii. opening the door to human genetic modifications which could be prone to inhumane misuse and unethical application;

iii. being very costly and consequently being beyond the easy reach of the common people;

iv. being possible to extend the cure to a person's offspring only if the defective gene was directly modified, but probably not if a new gene was added to another part of the genome (18, 19).

Applications

The design of gene therapy has two key purposes: i) introducing genetic material into the cells to recompense for the unusual genes, and ii) to make an advantageous and favorable protein. Gene therapy can be capable of introducing a common copy of the gene for restoring protein function, if an essential protein is caused by a mutated gene to be missing or faulty (27).

If a gene is directly inserted into a particular cell, it will not usually be able to function. A vector is a carrier, which is genetically engineered for gene delivery instead of a gene. There are some particular viruses that can deliver the gene. This gene delivery is performed by infecting the cell and, as a result, these viruses are usually used as vectors (27).

After the viruses are modified they are used in humans, and because of their modifications they cannot lead to disease. Some of the virus types perform the integration of their genetic material (containing the new gene) in a human cell's chromosome (retroviruses). Although the DNA of some virus types is introduced into the cell's nucleus (for example adenoviruses), the integration of the DNA is not carried into a chromosome (27).

The vector can be injected intravenously directly into a particular cell in the body, where the specific cells take it up. In addition, the patient's cell sample can be removed and put into contact with the vector in the setting of the laboratory. Then the cells that introduce the vector are put back into the patient. If the treatment is a success, a functioning protein will be made by the new gene, which has been delivered by the vector (27, 28).

A large number of technical challenges need to be overcome by researchers before gene therapy becomes a particular method for treating diseases. For example, more effective solutions need to be discovered by the scientists for delivering genes and targeting them into particular cells. In addition, they need to make sure that the new genes are controlled by the body.

Approaches to gene therapy

According to Baranyi et al. (14), two methods have been presented to introduce the genes into a cell: i) non-viral vectors (29-32), and ii) viral vectors (33-36). To date, 70% of the clinical trials have used the viral vectors. Although the efficiency of viral vectors is very extensive in transferring the genes, some safety risks can also be created by them. The transfer of the genes, which is mediated by the viral vectors, is called transduction. Retroviruses (e.g. HIV), adenoviruses, adeno-associated viruses, herpes simplex viruses, lentiviruses and hybrid viruses (which combine the positive features of more than one virus) are some of the different types of viruses used as vectors in gene therapy (33, 36). Although it is believed that the viral vectors are more dangerous than non-viral vectors, the efficiency of the non-viral vectors is lower than the viral vectors in transferring genes. The transfer of the genes, which is mediated by non-viral vectors is known as transfection.

There is an advantage for viral vectors to achieve more efficient transfer of the genes *in vivo*. Despite the use of duplication deficient vectors, significant safety problems are still posed by the viral vectors. The two most common viruses used in clinical trials are derived from Moloney Murine Leukemia Virus (MoMLV; ~28%) and a serotype

5 adenovirus (Ad5; ~26%), a retrovirus. The target of the MoMLV vectors is dividing cells, and their efficacy is reasonably high. In addition, since they randomly integrate into the target cell chromosome, they lead to stable transfer of the gene. MoMLV vectors have a basic disadvantage in the insertional mutagenesis risk, which is caused by the retroviral genome integration into the host genome (37, 38). Furthermore, dividing cells are required by the retroviral vectors for successful transduction, to some extent they are dangerous to target the transfer of the gene to quiescent well-differentiated types of cells (for example in epithelial tissues). Ad5 vectors are capable of the transduction of both non-dividing and dividing cells and making the transfer of the genes easy and highly efficient. Another important issue is that the Ad5 vectors integrate into a chromosome too rarely and they can be found in the nucleus of the cell that has been targeted in an epichromosomal location. Therefore, if the targeted cell is divided, just one of the daughter cells will be the recipient of the gene that has been transferred and with the following cycles of the division of the cell, the gene will be considerably weakened. One of the most important disadvantages of the Ad5 vector is that an effective host-immune reply is included in them. In addition, it is of significant importance to recognize that diverse viral vectors can vary in the capability of transducing different types of cells. Most of the time, this will reflect the existence or lack of cell covering receptor proteins that can intercede viral entry into the targeted cell (38).

Problems

Since the first clinical gene therapy was performed, extensive attention has been devoted to gene therapy (13), to which considerable private and public sector investments have been devoted. In addition, the research activities in this field have been significantly increased. There are a large number of studies on preclinical animal models and they have provided concept proofs for different potential clinical applications. Furthermore, there have been some fundamental developments in understanding the biology of the vector and improving the production and design of vectors.

Despite what has been mentioned above, the progress of clinical studies has been slow. In addition, a significant hindrance in the field took place in September 1999 when several deaths resulting from gene therapy were reported (26). In a clinical trial, an 18-year-old man died at the University of Pennsylvania. In this trial an adapted Ad5 vector was used for the gene delivery for ornithine decarboxylase, a lacking hepatic enzyme. Based on a study in the university, the death of this man was caused by a huge reaction of immunity to the applied Ad5 vector. This case was extensively publicized and it led to congressional as well as Food and Drug Administration (FDA) hearings about conducting trials of clinical gene therapy. A transient hold was subsequently lifted on all of the clinical trials on adenoviral vector. FDA conducted a study which discovered that this clinical trial had a large number of possible violations in monitoring and performance. The case was settled after 5 years of study in February, 2005. The case of Gelsinger caused gene therapy to undergo a great deal of skepticism and criticism. It was obvious that a number of errors occurred in that special case, and as a result, all the trials in gene therapy are now under much restricted regulations by FDA and the National Institute of Health (NIH).

Approximately one year after the case of Gelsinger, the first report on a significantly improved trial of gene therapy was presented. In 2000 in Paris, Cavazzana-Calvo and her group presented the outcome of a study in which two children going through a harsh combined immunodeficiency disorder (SCID-XI) were confined to live in an isolated environment (28). An MoMLV was used by these researchers to transfer a curative gene into the *ex vivo* lymphocytes of the patients, and after the cells were amplified, they were returned to the patients. Both of the patients were capable of continuing normal lives and leave hospital. After these cases, there were other patients who were cured and treated in these series of studies. However, as a drawback, three out of eleven patients who where cured by the MoMLV vector directly developed leukemia as a result of the process of transferring the gene (37). Apparently, the integration of the MoMLV was in a non-random

manner close to LM02 gene (LIM domain only 2) in all of the eleven patients. The activation of LM02 gene was performed by this integration and resulted in leukemia. All of the patients underwent leukemia treatment and were cured, and as a result, a significant collaborative scientific attempt was initiated to recognize the mechanisms that can affect the integration of MoMLV.

CONCLUSION

Gene therapy as a powerful new technology has been under discussion for about twenty years and a great deal of interest has been given to its procedure. The early trials led to great expectations in the scientific community. Despite some disappointments occurring, a large number of researchers believe that the scientific and technical details need the time factor to be perfected and the procedures to become routine (38).

From the gene therapy of stem cell research, other promising results have been reported in patients with type-B hemophilia in Philadelphia at Stanford University and the children's Hospital, where patients who were treated by gene therapy indicated a reduction of blood coagulation (39).

A defective gene in the ADA enzyme causes a disease called ADA deficiency which is presented on the human chromosome 20. This disease has been one of the focuses of the gene therapy in a large number of institutions. In one of the study cases, a number of patients who were treated with the corrective gene had the ability to regain their immune systems and now they are able to live normal lives outside the special bubbles for isolation, which are required for maintaining a microbe free environment. The patients began the production of a correct ADA enzyme after they received gene therapy.

The trial of SCIS-XI will most likely reflect the way that the gene therapy is heading in the next one or two decades: the path of success, but with several difficulties. This therapy also has the potential use for curing more complex diseases, such as coronary diseases and cancer, which seems promising. Gene therapy is still going through its infancy period and it is believed that as time goes by and it matures, it will be an effective treatment for countless genetic diseases that may have an effect on humanity.

More credibility is added by these experiences to the general viewpoint presented by Leiden in 1995 in an editorial that the field of gene therapy, which is still going through its infancy and, regardless of some drawbacks, is perfectly founded in primary scientific ideologies with promising clinical outcomes for the future (39).

REFERENCES

1. Wang D, Gao G. State-of-the-art human gene therapy: Part I. Gene delivery technologies. Discov Med 2014; 18:67-77.
2. Bigda JJ, Koszałka P. Wacław Szybalski's contribution to immunotherapy: HGPRT mutation and HAT selection as first steps to gene therapy and hybrid techniques in mammalian cells. Gene 2013; 525:158-61.
3. Chen ZY, Lin Y, Yang F, Jiang L, Ge SP. Gene therapy for cardiovascular disease mediated by ultrasound and microbubbles. Cardiovasc Ultrasound 2013; 11.
4. Wagner E. Advances in cancer gene therapy: tumor-targeted delivery of therapeutic pDNA, siRNA, and dsRNA nucleic acids. J Boun 2007; 12:77-82.
5. Waerzeggers Y, Monfared P, Viel T, Winkeler A, Voges J, Jacobs AH. Methods to monitor gene therapy with molecular imaging. Methods 2009; 48:146-60.
6. Bunnell BA, Morgan RA. Gene therapy for infectious disease. Clin Microbiol Rev 1998; 11:42-56.
7. Kawase Y, Ladage D, Hajjar RJ. Rescuing the failing heart by targeted gene transfer. J Am Coll Cardiol 2011; 57:1169-80.
8. Meissner TB, Mandal PK, Ferreira LMR, Rossi DJ, Cowan CA. Genome editing for human gene therapy. Meth Enzymol 2014; 546:273-95.
9. Navarro-Yepes J, Zavala-Flores L, Anandhan A, et al. Antioxidant gene therapy against neuronal cell death. Pharmacol Ther 2014; 142:206-30.
10. Gelfand Y, Kaplitt MG. Gene therapy for psychiatric disorders. World Neurosurg 2013; 80:11-18.
11. Kantor B, McCown T, Leone P, Gray SJ. Clinical applications involving CNS gene transfer. Adv Genet 2014; 87:71-24.

12. Cross D, Burmester JK. Gene therapy for cancer treatment: past, present and future.. Clin Med Res 2006; 4:218-27.
13. Rosenberg SA, Aebersold P, Cornetta K, et al. Gene transfer into humans-immunotherapy of patients with advanced melanoma, using tumor-infiltrating lymphocytes modified by retroviral gene transduction. N Engl J Med 1990; 323:570-78.
14. Baranyi L, Slepushkin V, Dropulic B. Ex Vivo Gene Therapy: Utilization of Genetic Vectors for the Generation of Genetically Modified Cell Products for Therapy, in: Gerson, E.C.L.L. (Ed.), Gene Therapy of Cancer (Third Edition). Academic Press, San Diego, 2014; pp. 3-18.
15. Gebremedhin S, Singh A, Koons S, Bernt W, Konopka K, Duzgunes N. Gene delivery to carcinoma cells via novel non-viral vectors: Nanoparticle tracking analysis and suicide gene therapy. Eur J Pharm Sci 2014; 60:72-79.
16. Wirth T, Ylä-Herttuala S. 12 - Gene transfer vectors (DNA vehicles) and their incorporation into biomaterials for bone repair. In Biomaterials for Bone Regeneration, P. Dubruel, and S.V. Vlierberghe, eds. Woodhead Publishing 2014; pp. 374-405.
17. Edelstein M.L, Abedi MR, Wixon J, Edelstei R.M. Gene therapy clinical trials worldwide 1989-2004-an overview. J Gene Med 2004; 6: 597-602.
18. Razi Soofiyani S, Baradaran B, Lotfipour F, Kazemi T, Mohammadnejad L. Gene therapy, early promises, subsequent problems, and recent breakthroughs. Adv Pharm Bull 2013; 3:249-55.
19. Genetics Home Reference [WWW Document], 2015. URL http://ghr.nlm.nih.gov/ (accessed 12.10.15).
20. Witherspoon DJ, Wooding S, Rogers AR, Marchani EE, Watkins WS, Batzer MA, Jorde LB. Genetic similarities between and within human populations. Genetics 2007; 176:351-59.
21. Gottschalk U, Chan S. Somatic gene therapy. Present situation and future perspective. Arzneimittelforschung 1998; 48:1111-20.
22. O'Malley BW, Ledley FD. Somatic gene therapy. Methods for the present and future. Arch. Otolaryngol. Head Neck Surg 1993; 119:1100-107.
23. Grossman M, Raper SE, Kozarsky K. Successful ex vivo gene therapy directed to a liver in a patient with familial hypercholesterolemia. Nat Ganet 1994; 6:335-341.
24. Wolff JA, Malone RW, Williams P. Direct gene transfer into mouse muscle in vivo. Science 1990; 247:1465-68.
25. Raper SE, Chirmule N, Lee FS, Wivel NA, Bagg A, Gao G, Wilson JM. Batshaw ML. Fatal systemic inflammatory response syndrome in a ornithine transcarbamylase deficient patient following adenoviral gene transfer. Mol Genet Metab 2003; 80:148-58.
26. Braddon VR, Chiorini JA, Wang S, Kotin RM, Baum BJ. Adenoassociated virus-mediated transfer of a functional water channel into salivary epithelial cells in vitro and in vivo. Hum Gene Ther 1998; 9:2777-85.
27. Cavazzana-Calvo M, Fischer A. Gene therapy for severe combined immunodeficiency: are we there yet? J Clin Invest 2007; 117:1456-65.
28. Brown MD, Schätzlein AG, Uchegbu IF. Gene delivery with synthetic (non viral) carriers. Int J Pharm 2001; 229:1-21.
29. Ramsey JD, Vu HN, Pack DW. A top-down approach for construction of hybrid polymer-virus gene delivery vectors. J Control Release 2010; 144:39-45.
30. Kunath K, von Harpe A, Fischer D, Petersen H, Bickel U, Voigt K, Kissel T. Low-molecular-weight polyethylenimine as a non-viral vector for DNA delivery: comparison of physicochemical properties, transfection efficiency and in vivo distribution with high-molecular-weight polyethylenimine. J Control Release 2003; 89:113-25.
31. Swami A, Kurupati RK, Pathak A, Singh Y, Kumar P, Gupta KC. A unique and highly efficient non-viral DNA/siRNA delivery system based on PEI-bisepoxide nanoparticles. Biochem Biophys Res Commun 2007;362:835-41.
32. Giacca M, Zacchigna S. Virus-mediated gene delivery for human gene therapy. J Control Release 2012; 161:377-88.
33. Lesch HP, Makkonen KE, Laitinen A, Määttä AM, Närvänen O, Airenne KJ, Ylä-Herttuala S. Requirements for baculoviruses for clinical gene therapy applications. Journal of Invertebr Pathol 2011; 107:106-12.
34. Aucoin MG, Perrier M, Kamen, AA. Critical assessment of current adeno-associated viral vector production and quantification methods. Biotechnol.

Adv 2008; 26:73-88.
35. Segura MM, Garnier A, Durocher Y, Ansorge S, Kamen A. New protocol for lentiviral vector mass production. Biochem Eng J 2010; 48:362-77.
36. Walther W, Stein U. Viral vectors for gene transfer: a review of their use in the treatment of human diseases. Drugs 2000, 60:249-71.
37. Dulak J, Uchto J, Jozkowicz A. 50 years of gene therapy--a contribution of Wacław Szybalski to science and humanity. Gene 2013; 525:149-50.
38. Ponder KP. Hemophilia gene therapy: a holy grail found. Mol Ther 2011; 19: 427-28.
39. Leiden JM. Gene therapy--promise, pitfalls, and prognosis. N Engl J Med 1995; 28:871-73.

EDITORIAL

EXTRACORPOREAL SHOCKWAVES AS REGENERATIVE THERAPY IN ORTHOPEDIC TRAUMATOLOGY: A NARRATIVE REVIEW FROM BASIC RESEARCH TO CLINICAL PRACTICE

M.C. D'AGOSTINO[1], R. FRAIRIA[2], P. ROMEO[3], E. AMELIO[4], L. BERTA[5], V. BOSCO[6], S. GIGLIOTTI[7], C. GUERRA[4], S. MESSINA[8], L. MESSURI[9], B. MORETTI[10], A. NOTARNICOLA[10], G. MACCAGNANO[10], S. RUSSO[11], R. SAGGINI[12], M.C. VULPIANI[13] and P. BUSELLI[14]

[1]Humanitas Research Hospital and Humanitas University, Rozzano, Milano, Italy; [2]Department of Medical Sciences, University of Torino, Turin, Italy; [3]Orthopedic Clinic of the University of Milan, Galeazzi Orthopedic Institute, Milan, Italy; [4]University Hospital, Verona, Italy; [5]Med & Sport 2000, Turin, Italy; [6]Private Clinic Madre Fortunata Toniolo, Bologna, Italy; [7]ASL Napoli1 Centro, Napoli, Italy; [8]Welfare Italia, Lodi, Italy; [9]Chiavari Hospital ,Genova, Italy; [10]Department of Medical Sciences of Basis, Neurosciences and Organs of Sense, Faculty of Medicine and Surgery, University of Bari, Bari, Italy; [11]Department of Surgery, Orthopedic, University "Federico II", Napoli, Italy; [12]Department of Medical, Oral and Biotechnological Sciences, University "G. D'Annunzio", Chieti, Italy; [13]Physical Medicine and Rehabilitation Unit, St. Andrea Hospital, University "La Sapienza", Roma, Italy; [14]Department of Neuro Ostheo Articular Sciences, Cremona Hospital, Cremona, Italy

Received November 27, 2015 – Accepted March 8, 2016

Extracorporeal Shock Wave Therapy (ESWT), after its first medical application in the urological field for lithotripsy, nowadays represents a valid therapeutical tool also for many musculoskeletal diseases, as well as for regenerative medicine applications. This is possible thanks to its mechanisms of action, which in the non-urological field are not related to mechanical disruption (as for renal stones), but rather to the capacity, by mechanotransduction, to induce neoangiogenesis, osteogenesis and to improve local tissue trophism, regeneration and remodeling, through stem cell stimulation. On the basis of these biological assumptions, it becomes clear that ESWT can represent a valid therapeutic tool also for all those pathological conditions that derive from musculoskeletal trauma, and are characterized by tissue loss and/or delayed healing and regeneration (mainly bone and skin, but not only). As a safe, repeatable and non–invasive therapy, in many cases it can represent a first–line therapeutic option, as an alternative to surgery (for example, in bone and skin healing disorders), or in combination with some other treatment options. It is hoped that with its use in daily practice also the muscle–skeletal field will grow, not only for standard indications, but also in post–traumatic sequelae, in order to improve recovery and shorten healing time, with undoubted advantages for the patients and lower health service expenses.

The first medical applications of Extracorporeal Shock Wave Therapy (ESWT) were performed in the early nineties as urological lithotripsy (disruption of kidney stones); soon after, its

Key words: extracorporeal shock waves, ESWT, tendinopathy, traumatology, bone healing, mechanobiology, mechanotransduction, tissue regeneration

Mailing address:
Dr Angela Notarnicola,
Department of Medical Sciences of Basis,
Neurosciences and Organs of Sense, Faculty of Medicine and Surgery,
University of Bari, Piazza Giulio Cesare 11, 70124 Bari, Italy
Tel.: +39 0805592938
e-mail: angelanotarnicola@yahoo.it

0393-974X (2016)

field of clinical application expanded to some musculoskeletal diseases (tendon pathologies, bone healing disturbances, vascular bone diseases) and, more recently, to the field of regenerative medicine, vulnology and dermatology (wound healing disorders, scars and ulcers) and neurology (spasticity and similar syndromes) (1-4).

A recent clinical application has been for andrologic disturbances (induratio penis plastic and erectile dysfunction), based on its positive effects on local microcirculation (5). Ischemic heart disease represent another recent field of ESWT application, again for its regenerative and trophic effects, although it must be still considered as an experimental indication (6).

From the general point of view, ESWT, as a non-invasive procedure, avoids side-effects, is repeatable, well accepted and tolerated by the patients (with correct diagnosis and application), and can be considered a strategic therapeutic tool not only in orthopedics, but also in traumatology and regenerative medicine, where delayed healing in many cases is due to tissue loss and de-vascularization, especially when all other non-invasive treatments were ineffective or surgery failed (1).

Brief history of shock waves

Shock Waves (SW) are acoustic (mechanical) waves and are one of the most efficacious ways of dissipating energy. They are ubiquitous in nature and in the universe (the roar of a plane flying at supersonic speed, the propellers of a ship spinning around very rapidly, the shooting of a bullet, the thunder of the storm, as well as the implosion of a supernova) (7).

Already known as a physical entity from the beginning of the 19th century, only during the Second World War, after fortuitous observations, did scientists begin to study their possible useful application on humans (besides technical usage), by exploiting their potential for disruption. Indeed, after early experimental attempts at destroying brain tumors, from 1960 their interest regarded the possibility of breaking up kidney stones (urolithiasis), and Extracorporeal Shock Waves Lithotripsy (ESWL) was applied for the first time in urolithiasis at the beginning of the 1990s in Munich (8). In 1991, again after some fortuitous observations, it was discovered that, besides a pure mechanical action, SW could produce some other important therapeutic effects, and related to a biological action (bone healing enhancement). Valchanou and Michailov in 1991 published the first international article, demonstrating the possibility to successfully treat bone healing disturbances by SW treatment, that is, in a non-urological application (9).

Since 1991, SW rapidly has gained further increasing interest (as Orthotripsy) for the treatment of many musculoskeletal diseases (especially bone healing disorders and tendon pathologies), However, until recently it was considered a "pioneering technique" for the following reasons:

i) The technique was inherited from urological applications, where the goal is breaking (pure mechanical action);

ii) since mechanical forces were implicated, the idea of breaking calcification was predominant for a long time;

iii) despite many scientific results published in the scientific literature, demonstrating the effectiveness of ESWT as a biological tool (not purely a mechanical one), a great deal still had to be learnt about the mechanisms of action of SW in tissue and cellular level.

The mechanisms of action: from mechanics to biology

SW are "acoustic" waves (mechanical energy), characterized by a definite shape with an initial positive, very rapid part of high amplitude, followed, after a few microseconds, by a sudden phase of mild negative pressure, afterwards returning to the ambient (basic) values. The physical characteristics for clinical applications were stated by an international "Consensus Conference" in 1997; according to the parameters recognized by national and international Scientific Societies, they must have the following characteristics: high peak pressure (>500 bar); short duration (<10 microseconds); rapid rise in pressure (<10 ns) (7, 8). There are three methods to generate focused shockwaves for focused SW (fSW): electrohydraulic (EH), electromagnetic (EM) and piezoelectric (PE). All three have in common that the

waves are generated in water (inside the applicator). Focused shockwaves are generated in water because the acoustic impedance of water and biologic tissue is comparable. As a result of this, reflection is limited and waves are better transferred into the body. A difference between these three methods is the moment at which the shockwave forms. EH generators produce focused shockwaves at origin, immediately after the spark gap, while EM and PE generators form shockwaves nanoseconds later by means of focusation of waves that are generated.

Radial Waves (rSW) are acoustic waves as well (mechanical force), which, unlike fSW, are produced by a ballistic or "pneumatic" source (10). In this case, the source (applicator) is composed of a barrel handpiece, containing a metallic bullet, that is accelerated at a very high speed by compressed air. High kinetic energy is produced and impacts against the tip of the applicator, which is directly in contact with the body surface: in this way, the kinetic energy accumulated during running is transmitted to the area of treatment. Unlike fSW, radial waves propagate in the body in a radial fashion, from which derives the term "radial waves". From the physical point of view, they are not focused in the deeper layers, but preferably they join the more superficial layers in the area of treatment and can be thus successfully applied in many therapeutic indications, especially in the field of soft tissues diseases (11).

As already anticipated, SW in non-urological fields have to be considered as "mechanical forces at the service of biology": in other words, by applying some mechanical stimulations (SW) it is possible to obtain some biological reactions, also known as Mechanobiology/Mechanotrandsuction. "Mechanotransduction" is a biological pathway according to which many cell types, after perceiving and processing the mechanical information from the extracellular environment (as biomechanical forces), turn them into biochemical responses, thus influencing some fundamental cell functions such as apoptosis, proliferation, migration and differentiation. At first, mechanotransduction was extensively studied in endothelial cells in relation to shear stress stimulation, but nowadays its role is also known in function and physiology of many other cell types (such as bone cells, fibroblasts, bone cells, and mesenchymal stem cells) (12).

Recently, thanks also to the studies in mechanobiology, there is a renewed interest in the scientific literature regarding the importance of mechanical stimuli on living beings, and the influence that biomechanical deformations can have on cellular biology and physiology, in health and diseases, especially with the purpose of possible therapeutic applications (13).

SW can be nowadays properly considered a form of "mechanotherapy", the research and studies of which regarding "physical" stimulations are not limited to describe and quantify the final general (positive or negative) results, but to analyze in detail the pathway of actions, at a biological level, that these "physical means" may produce on the tissues and cells treated.

As already mentioned, nowadays it is scientifically proven that SW, on biological structures, although acting as pure mechanical force, do not induce a disruptive effect, but actually induce some biological effects on cells and tissues, whose metabolism and functions can be positively stimulated.

From a general point of view, ESWT - as mechanotherapy - plays a vital role in positively influencing local tissue homeostasis and some cell functions, with the final result of stimulating the self-healing abilities. Evidence from the literature (basic science and clinical trials), in fact, seem to indicate that this effect implies the SW capability of inducing proliferation, migration and differentiation of stem cells, which significantly contributes to tissue healing and regeneration. Besides stem cells and bone marrow stromal cells, many other cells can be considered as targets for mechanotrasduction following SW stimulation; these include tenocytes, bone cells and their precursors, endothelial cells, and fibroblasts amongst others. In other words, the regenerative potential of SW seems to be attributable, ultimately, to the influence on tissue trophism and regeneration and neoangiogenesis as well (1, 14). As will be explained in more detail, this can make SW a strategical therapeutic tool in muscle–skeletal traumatology, where tissue loss and devascularization can be, in most cases, the detrimental cause of complications and delayed healing.

Undoubtedly, the most important clinical field where ESWT plays a key role as "mechanotherapy" is represented by bone healing disorders and bone vascular diseases, also considering that these pathologies represent the vast majority of the sequelae in traumatology, of which the healing time, discomfort and troubles for the patient as well as socio-economical detrimental effects are well known.

Post-traumatic bone pathology

Bone healing disorders (pseudoarthrosis or delayed osteogenesis) can be the results of a severe trauma with bone and soft tissue damage, and/or the consequence of an inadequate treatment (surgical or conservative); sometimes they can derive from a failed osteosynthesis with loss of stability; sometimes they are related to subjective medical conditions and lifestyles that negatively interfere with bone healing.

Many clinical studies and experimental works confirm SW as an important therapeutic tool for improving osteoregenerative processes in pseudoarthrosis and bone healing delay as a valid alternative to surgery in several cases, as well as the potential for positively interfering with an altered bone turnover (as takes place when bone marrow edema is present) or for enhancing local bone trophism (as in osteonecrosis and related syndromes) (1, 15).

Another interesting field of application for ESWT in post–traumatic bone conditions is stress fractures. Also in this case, due to an altered biomechanical environment and to repeated strains and overload, sometimes associated to abnormal anatomical conformations (especially in the foot), there is an imbalance in local bone turnover, with a prevailing reabsorption phase. If not properly treated early, besides persisting and sometimes worsening pain, this may involve - as a final result - a real fracture. Also in these cases, ESWT application, in association with some other prescriptions (mainly rest and not weight–bearing), results as a good strategy to accelerate bone healing and pain relief, thus allowing a more rapid return to sport and daily activities (15).

From a general point of view, bone can be considered the tissue where mechanobiological pathways are better expressed in their different forms: this in partly due to its mechanosensitivity and its complexity at the tissue and physiological level. Basic studies, in fact, demonstrate that mechanical stimulation can act on the bone at different levels: surely SW action is exerted on bone and periosteal cells and their precursors, but also in the cross–talk between osteoblasts and osteoclasts and the local microvessels (16). There is evidence, in fact, of the following effects:

- direct stimulation of osteoblasts/periosteal cells (17);
- osteogenic cell differentiation from mesenchymal precursors (18);
- accelerated migration of osteoblasts (19);
- early expression of angiogenesis-related growth factors, endothelial nitric oxide synthase (eNOS), vascular endothelial growth factor (VEGF) (angiogenetic effect, supporting tissue regeneration) (20);
- orthotopic bone regeneration through stimulation of the periosteum (21);
- reduction of osteoclasts activity, through inhibition of pro-osteoclastogenic factors (22).

It is important to underline that, as with surgery, also for ESWT the clinical cases and patients have to be strictly selected in advance, as not all of them are suitable for ESWT. For the success of the therapy, some conditions have to be met: first of all, anatomical stability and, secondly, to apply SW with a proper device, in order to ensure that adequate levels of energy are achieved. Also the possibility to target exactly the area to be treated, in terms of depth and surface localization (by fluoroscopy or ultrasound–guided) are important factors not to be overlooked. For biomechanical stability, it is important to verify the presence of eventual synthesis loosening; if not stabilized, it should be possible to surgically stabilize and apply SW soon after, or apply a cast, according to the anatomical site, the age of the patients, and radiographic appearance. It is very important to remember another great advantage of ESWT, that is the possibility to be applied even in the presence of metal implants, as well as in the presence of soft tissue critical conditions, such as skin loss and devascularization.

Tendon pathology

Nowadays, although initially described for bone healing disturbances, ESWT is perhaps more well known, amongst musculoskeletal applications, for

the treatment of tendinopathies and enthesiopathies, independently of the presence of calcifications (1, 10).

ESWT seems to be effective in treating tendon pathologies, and not simply a "palliative" therapy but as a "curative" treatment; other than resolving pain and inflammation at short–medium term follow-up, in fact, SW could positively play an important role in tendon metabolism and structure, by exerting a local trophic effect (at long term follow-up) (1, 2). Many encouraging results on the application of SW in chronic tendinopathies have been recently published, especially as an effective intervention to be considered when other non–surgical treatments have failed, although the specific mechanisms of action remain partly unknown (22).

Histological descriptions in animal models demonstrated that ESWT, in injured tendons, may reduce edema, swelling, and inflammatory cell infiltration. Lesion site undergoes intensive tenocyte proliferation and progressive tendon tissue regeneration, related to high level TGF-β1 and IGF-I expression, as in the early stage of tendon healing, therefore the authors hypothesized that physical SW stimulation may increase tendon mitogenic responses (21).

Tendon cells, differentiated and progenitors, as well the collagen structure are potential targets of shock waves. *In vivo* experimental studies showed typical changes in tendon structure characterized by a transient and dose-dependent inflammatory reaction, neovessel proliferation at the bone-tendon junction associated with the release of proangiogenic regulatory factors [NO synthase (NOS) and VEGF] and proliferating GF (PCNA) (23).

In vitro, different energy setting results in a proliferative action on cells related to gene expression of collagen types I and III and TGF-β1, followed by the production of NO and collagen synthesis (24). Moreover, the expression of tenocytic markers such as scleraxis, tenomodulin, tenascin-C, and type I and III collagens, as well interleukin (IL)-6 and MMPS 1 and 13 have been observed in tenocyte cultures (25).

Besides the expression of specific tendon cells markers, *in vitro* experiments suggested the capability of shock waves to modulate, in tendon cells, the release sequence of anti-inflammatory cytokines (Il-1, Il-6, Il-10) which did not induce MMPs synthesis, but was correlated to the expression of growth factors (TGFβ1- VEGF), almost simulating the physiologic process of tendon healing (26).

It has been described that SW may provide faster post-injury recovery when applied on human primary cultured tenocytes derived from ruptured tendons versus the healthy ones. The Authors underline that these data seem to suggest a possible shock wave-induced mechanisms of tissue repair. Not only do some studies seem to confirm the positive influence of SW on metabolism and function of tendon cells, but some also describe increased expression of lubrycin after SW exposure, thus suggesting a possible beneficial effect in counteracting the formation of adhesions, especially in post–surgical conditions (21, 26).

Tissue healing, regeneration and remodeling

These effects derived from SW application add further value to this mechanotherapy, which can be thus applied in all clinical conditions characterized by skin loss and/or tissue vascular impairment and hypoxia. This can be of particular interest especially for all those post–traumatic conditions (mainly crash and hand traumas), where the impact can simultaneously destroy both bone and soft tissues, sometimes with open fractures and tissue loss. In all these critical conditions, often surgical intervention must be rapid and only provisional at first, with the aim, at a later time, of carrying out a revision surgery, both for definitive stabilization and/or skin coverage (26). In both situations, SW application can be a useful therapeutic tool for enhancing and improving tissue revascularization and regeneration. Moreover, it can be applied even in local compromised conditions, without fear of side effects or adverse reactions. The indication to treat precociously or even pre–operatively all those unsafe conditions, in order to avoid major complications or guarantee a better and rapid improvement during follow–up (27) is still speculative nowadays, but it already has an experimental background.

More recently, SW stimulation in animal models, after intramuscular silicone injection, were associated with decreased formation of the dense fibrous envelope and, when applied in multiple sessions,

it was possible to observe active reduction of the fibrous capsule, related to a synergistic changes in pro- and anti-fibrotic proteins (respectively, TGF-β1 and matrix metalloproteinase 2), thus revealing that SW stimulation could decrease capsule formation, while inducing fibrotic tissue remodeling/resorption (28). Based on this and some other analogue experimental and clinical experiences, it seems possible to argue that SW would enhance not simply "healing" processes, but even induce a real "regenerative" effect, where fibrous tissue is reduced at first, or secondly remodeled, as in scar tissue. Although further studies in tissue regeneration and remodeling are necessary, recent knowledge seems to demonstrate that SW can influence the TLR3 pathway, thus implying that this mechanotherapy could act as immunomodulator in wound healing, mainly through an anti-inflammatory strategy (29).

Moreover, some experimental preliminary data demonstrated, for the first time, the possibility to positively interfere *in vitro* with macrophage activity, in particular, stimulation of pro-resolving macrophages (M2) and inhibition of pro-inflammatory macrophages (M1) (30). These data could be an innovative finding in SW mechanobiology, as only recently the critical role was demonstrated of the innate immunity system in a series of interconnected biochemical and cellular events, responsible for tissue healing, regeneration and remodeling (30).

Alhough the field of fibrous tissue remodeling needs further clinical and basic science confirmation, it is already proved that it is possible, by applying ESWT, to reduce pain, swelling and redness in post - surgical scars (as for example in "pillar pain") (32).

Another interesting application of ESWT is in the treatment of myositis ossificans (MO), which is a fairly common evolution in sports activity and can be due to direct trauma or to repeated micro-injuries. The traditional therapeutic approach relies on a variety of treatments, such as physical therapy but evidence of their proven clinical efficacy is lacking. The latest therapeutic option is surgical removal, however, this is a demolitive procedure and is frequently associated with a significant loss of functional integrity. The current literature indicates that shock waves offer an efficacious therapeutic opportunity for restoring the physiologic conditions of muscle-tendon extensibility (33). ESWT is non-invasive, inexpensive and without side effects and could be a viable alternative to surgery.

Tissue engineering

Most of the clinical procedures to restore bone loss include autograft or allograft transplantation, or the use of synthetic materials. Autograft transplantation is the clinically preferred treatment option today but suffers from limited supply and donor site. Allografts, although more readily available, could implicate disease transmission and are seldom used in clinical practice. In view of these problems, different therapeutic approaches have been attempted: tissue engineering emerged as a concept to assist the regeneration of body tissue defects which are too large to self-repair as well as to substitute the biological functions of damaged and injured organs by using cells with proliferative and differentiative potential (34).

In recent times, Berta et al. (35) treated normal fibroblasts with low- to medium- energy shock waves and evaluated fibroblast viability, the growth rate and pattern, and gene expression for TGF-β1 and collagen types I and III - the main factors involved in the repair process. Shock waves had a dose-dependent stimulatory effect on cell proliferation. The pattern of expression of TGF-β1 mRNA showed higher values in treated fibroblasts. Moreover, ESW treatment enhanced expression of the genes encoding collagen types I and III.

The effect of ESW treatment on fibroblasts as a model of therapeutic application of the mechanical source was recently the subject of an extensive literature review (36). In summary, the factors most involved in tissue repair induced by ESW treatment are the following: endothelial nitric oxide synthase (eNOS) and vascular endothelial growth factor (VEGF) which are related to TGF- β1 increase. The data have been related to the increase of angiogenesis observed in ESW-treated tissues, an additional factor in accelerating the repairing process. Most recently, ESW therapy was shown to enhance fibrocartilage regeneration at the healing interface in a delayed tendon-bone insertion healing model, providing

mechanical cues and upregulating expression of fibrocartilage-related makers and cytokines (37).

It has already been extensively described above that shock waves are widely used to treat musculoskeletal disorders, thanks to their efficacy in favoring callus formation in long-bone fractures: in addition to the factors described above, it has recently been shown that the increase of bone morphogenetic protein-2 (BMP-2) induced by the ESW treatment of MG-63 osteoblast-like cells is a further component involved in bone healing (38). *In vitro* studies have shown that treatment with SWs influences cell proliferation, enhancing transmembrane currents, as well as the voltage dependence of Ca-activated and K channels (39). Other studies suggested that exposure to extracorporeal SWs enhances mesoblast recruitment at the junction of ossified cartilage and the production of TGF-b1 and VEGF-A, which are chemotactic and mitogenic, for the recruitment and differentiation of mesenchymal stem cells to promote bone regeneration of segmental defects in rats (40). More recently, a direct dose-dependent stimulatory effect of SWs on the proliferation and differentiation of osteoblasts from normal human cancellous bone was reported.

Muzio et al. (41) showed that ESW initially trigger a rise in cell number and osteogenic activity in MG-63 human osteoblast-like cells colonizing bioactive glass scaffolds; at a later stage they induce a further increase in osteogenic activity, as evidenced by more numerous and larger calcium deposits observed in scaffolds colonized by ESW-treated cells. In the same study, a direct effect of ESW on BMP expression was described for the first time, as it was found that the osteo-inductive effect of SWs was mediated by increased expression of ALP, osteocalcin, type I collagen, BMP-4, BMP-7 and BMP-2. Moreover, ESW were shown to be capable of favoring the colonization of the scaffolds as well as stimulating osteoblast activity.

Besides trying to enhance the regenerative ability of damaged bone, a further challenge of tissue engineering is to identify novel cell-based therapies when repair processes are deficient. Bone contains a variety of different cell types: vascular cells, marrow cells, pre-osteoblasts, osteocytes, chondroblasts and osteoclasts, all carrying out distinct cellular functions to allow the bone to work as a highly dynamic organ. Whereas all these cells are necessary to build up a real bone, the sources of cells which are regarded to be sufficient for engineering a bone-like construct in vitro are limited. Human mesenchymal stem cells (MSC) are a promising candidate cell type for musculoskeletal regenerative tissue engineering because of their capacity for self-renewal and multipotent differentiation. Interactions among biochemical and mechanical signals result in bone formation and repair. Recently, Catalano et al. (42) reported that ESW treatment can promote and improve osteogenic medium-induced differentiation of ASC into osteoblast-like cells. The ability was confirmed of ESW to promote the process of ASC differentiation even when used alone, and to boost the process of differentiation induced by the osteogenic medium.

Although all the mechanisms accounting for the effects of ESW in ASC differentiation into osteoblast-like cells are still far from being elucidated, the results reported by Uddin and Quin (43), who described the enhancement of osteogenic differentiation and proliferation in human mesenchymal stem cells by LIPUS stimulation, are in accordance with data published by Sun et al. (44). More recently, important signaling pathways involved in the mechanotransduction of extracorporeal shock waves were defined. A time-dependent cascade of events was suggested that starts with ROS production elicited by ESW and finally comes to a modulation of ALP protein function in terms of phosphatase activity and calcium deposits (42).

The combination of autologous ASCs and ESW treatment represents an important step for tissue engineering procedures in the treatment of bone tissue damage. It is worth underlining the clinical importance of having tissue-engineered scaffolds with a high bone regenerative potential to be associated to osteogenic stimulation due to ESW exposure. Moreover, a not negligible aspect is provided by the fact that, by using stem cells from adipose tissue, the ethical problems related to the use of embryonic stem cells may be overcome.

Additional *in vivo* work is required to determine

the real therapeutic potential of ESW, and clinical trials will definitively assess the use of ESW as an additional tool for improving the outcome of regenerative treatment. As research at the cellular level continues to expand, the opportunity for growth is limitless, with cell-based applications and tissue engineering potentially setting the stage for how regenerative medicine is practiced today and in the future.

CONCLUSIONS

In 1997 Haupt wrote: " ... in patients in whom conservative treatment has failed, surgery used to be the only choice, but its success rate barely exceeds that of shock wave therapy and surgery can still be done if shock wave therapy fails. Extracorporeal shock waves will have an impact on orthopedics comparable to its effect in urology. Scientific evaluations, professional certifications, quality assurance and reimbursement issues present great challenges ..." (45).

Much progress has been made since SWs were first applied in urology and soon after in the musculoskeletal field: in some ways, it seems that the pioneering thought of Haupt was true and perhaps we have exceeded expectations.

Nowadays, on the basis of our narrative review, we can declare the "SW pioneering phase" as closed, while opening the very new and revolutionary phase of tissue regeneration, with important therapeutic implications in muscle–skeletal traumatology sequelae and with further promising perspectives in regenerative medicine, cell therapy and tissue engineering in the near future.

However, we must emphasize that the lack of studies and meta-analyses of systemic revisions do not allow us to demonstrate the effectiveness of the shock waves with high levels of evidence. Our optimistic conclusions on the effects of shock waves are currently downsized if we take into account those of other authors who recommend to conduct prospective, (randomized) controlled trials comparing ESWT versus placebo (46, 47).

REFERENCES

1. Notarnicola A, Moretti B. The biological effects of ESWT on tendon tissue. Muscles Ligaments Tendons J 2012; 2(1):33-7.
2. Schaden W, Fischer A, Sailler A. Extracorporeal shock wave therapy of nonunion or delayed osseous union. Clin Orthop Relat Res 2001; 387:90-4.
3. Saggini R, Figus A, Troccola A, Cocco V, Saggini A, Scuderi N. Extracorporeal shock wave therapy for management of chronic ulcers in the lower extremities. Ultrasound Med Biol 2008; 34(8):1261-71.
4. Santamato A, Notarnicola A, Panza F, et al. SBOTE study: extracorporeal shock wave therapy versus electrical stimulation after botulinum toxin type a injection for post-stroke spasticity-a prospective randomized trial. Ultrasound Med Biol 2013; 39(2):283-91.
5. Chung E, Cartmill R. Evaluation of clinical efficacy, safety and patient satisfaction rate after low-intensity extracorporeal shockwave therapy for the treatment of male erectile dysfunction: an Australian first open-label single-arm prospective clinical trial. BJU Int 2015; 115:46-49.
6. Ito K, Fukumoto Y, Shimokawa H. Extracorporeal shock wave therapy for ischemic cardiovascular disorders. Am J Cardiovasc Drugs 2011; 11(5):295-302.
7. Karzova MM, Yuldashev PV, Khokhlova VA, Ollivier S, Salze E, Blanc-Benon P. Characterization of spark-generated N-waves in air using an optical schlieren method. J Acoust Soc Am 2015; 137(6):3244-52.
8. Shrivastava SK, Kailash. Shock wave treatment in medicine. J Biosci 2005; 30(2):269-75.
9. Valchanou VD, Michailov P. High energy shock waves in the treatment of delayed and nonunion of fractures. Int Orthop 1991; 15(3):181-4.
10. Speed C. A systematic review of shockwave therapies in soft tissue conditions: focusing on the evidence. Br J Sports Med 2014; 48(21):1538-42.
11. Gerdesmeyer L, Maier M, Haake M, Schmitz C. Physical-technical principles of Extracorporeal Shockwave Therapy (ESWT). Orthopade 2002; 31:610-17.
12. Marshall KL, Lumpkin EA. The molecular basis of mechanosensory transduction. Adv Exp Med Biol

2012; 739:142-55.
13. Khan KM, Scott A. Mechanotherapy: how physical therapists' prescription of exercise promotes tissue repair. Br J Sports Med 2009;43(4):247-52.
14. Sansone V, D' Agostino MC, Bonora C, Sizzano F, De Girolamo L, Romeo P. Early angiogenic response to shock waves in a three-dimensional model of human microvascular endothelial cell culture (HMEC-1). J Biol Regul Homeost Agents 2012; 26(1):29-37.
15. Leal C, D´Agostino MC, Gomez-Garcia S, Fernandez A. current concepts of shockwave therapy in stress fractures. Int J Surgery 2015; 24(Pt B):195-200.
16. Lai JP, Wang FS, Hung CM, Wang CJ, Huang CJ, Kuo YR. Extracorporeal shock wave accelerates consolidation in distraction osteogenesis of the rat mandible. J Trauma 2010; 69(5):1252-58.
17. Tam KF, Cheung WH, Lee KM, Qin L, Leung KS. Osteogenic effects of low-intensity pulsed ultrasound, extracorporeal shockwaves and their combination - an in vitro comparative study on human periosteal cells. Ultrasound Med Biol 2008; 34(12):1957-65.
18. Cheng JH, Wang CJ. Biological mechanism of shockwave in bone - Review. Int J Surg Forthcoming 2015; 24(Pt B):143-6.
19. Xu JK, Chen HJ, Li XD, et al. Optimal intensity shock wave promotes the adhesion and migration of rat osteoblasts via integrin β1- mediated expression of phosphorylated focal adhesion kinase. J Biol Chem 2012; 287(31):26200-12.
20. Wang CJ, Huang HY, Pai CH. Shock wave-enhanced neovascularization at the tendon-bone junction: an experiment in dogs. J Foot Ankle Surg 2002; 41(1):16-22.
21. Chen YJ, Wang CJ, Yang KD, et al. Extracorporeal shock waves promote healing of collagenase-induced Achilles tendinitis and increase TGF-beta1 and IGF-I expression. J Orthop Res 2004; 22(4):854-61.
22. Kearney CJ, Hsu HP, Spector M. The use of extracorporeal shock wave-stimulated periosteal cells for orthotopic bone generation. Tissue Eng Part A 2012; 18:1500-8.
23. Mani-Babu S, Morrissey D, Waugh C, Screen H, Barton C. The effectiveness of extracorporeal shock wave therapy in lower limb tendinopathy: a systematic review. Am J Sports Med 2015; 43(3):752-61.
24. Wang CJ, Wang FS, Yang KD, et al. Shockwave therapy indices neovascularization at the tendon-bone junction. A study in rabbits. J Orthop Res 2003; 21(6):984-9.
25. Vetrano M, D'Alessandro F, Torrisi MR, Ferretti A, Vulpiani MC, Visco V. Extracorporeal shock wave therapy promotes cell proliferation and collagen synthesis of primary cultured human tenocytes. Knee Surg Sports Traumatol Arthrosc 2011; 19:2159-68.
26. Han SH, Lee JW, Guyton GP, Parks BG, Courneya JP, Schon LC. Effect of extracorporeal shock wave therapy on cultured tenocytes. Foot Ankle Int 2009; 30:93-8.
27. Antonic V, Mittermayr R, Schaden W, Stojadinovic A. Evidence supporting extracorporeal shock wave therapy for acute and chronic soft tissue wounds. Wounds 2011; 23(7):204-15.
28. Ottomann C, Hartmann B, Tyler J, et al. Prospective randomized trial of accelerated re-epithelization of skin graft donor sites using extracorporeal shock wave therapy. J Am Coll Surg 2010; 211(3):361-7.
29. Fischer S, Mueller W, Schulte M, et al. Multiple extracorporeal shock wave therapy degrades capsular fibrosis after insertion of silicone implants. Ultrasound Med Biol 2015; 41(3):781-9.
30. Kuo YR, Wang CT, Wang FS, Yang KD, Chiang YC, Wang CJ. Extracorporeal shock wave treatment modulates skin fibroblast recruitment and leukocyte infiltration for enhancing extended skin-flap survival. Wound Repair Regen 2009; 17(1):80-7.
31. Sukubo NG, Tibalt E, Respizzi S, Locati M, d'Agostino MC. Effect of Shockwaves on Macrophages: A possible role in tissue regeneration and remodeling. Int J Surg Epub 2015; 24(Pt B):124-30.
32. Mantovani A, Biswas SK, Galdiero MR, Sica A, Locati M. Macrophage plasticity and polarization in tissue repair and remodelling. J Pathol 2013; 229(2):176-85.
33. Romeo P, D'Agostino MC, Lazzerini A, Sansone VC. Extracorporeal shock wave therapy in pillar pain after carpal tunnel release: a preliminary study. Ultrasound Med Biol 2011; 37(10):1603-8.
34. Buselli P, Coco V, Notarnicola A, et al. Shock waves in the treatment of post-traumatic myositis ossificans. Ultrasound Med Biol 2010; 36 (3):397-409.
35. Stock UA, Vacanti JP. Tissue engineering: current state and prospects. Annu Rev Med 2001; 52:443-51.
36. Berta L, Fazzari A, Ficco AM, Enrica PM, Catalano MG, Frairia R. Extracorporeal shock waves enhance

normal fibroblast proliferation in vitro and activate mRNA expression for TGF-beta1 and for collagen types I and III. Acta Orthop 2009; 80(5):612-7.
37. Frairia R, Berta L. Biological effects of extracorporeal shock waves on fibroblasts. A review. Muscles Ligaments Tendons J 2012; 1(4):138-47.
38. Chow DH, Suen PK, L. Huang, et al. Extracorporeal shockwave enhanced regeneration of fibrocartilage in a delayed tendon-bone insertion repair model. J Orthop Res 2014; 32(4):507-14.
39. Muzio G, Martinasso G, Baino F, Frairia R, Vitale-Brovarone C, Canuto RA. Key role of the expression of bone morphogenetic proteins in increasing the osteogenic activity of osteoblast-like cells exposed to shock waves and seeded on bioactive glass-ceramic scaffolds for bone tissue engineering. J Biomater Appl 2014; 29(5):728-36.
40. Lee JY, Kim SN, Lee IS, Jung H, Lee KS, Koh SE. Effects of extracorporeal shock wave therapy on spasticity in patients after brain injury: a meta-analysis. J PhysTher Sci 2014; 26(10):1641-47.
41. Chen YJ, Wurtz T, Wang CJ, et al. Recruitment of mesenchymal stem cells and expression of TGF-beta 1 and VEGF in the early stage of shock wave-promoted bone regeneration of segmental defect in rats. J Orthop Res 2004; 22(3):526-34.
42. Muzio G, Vernè E, Canuto RA, et al. Shock waves induce activity of human osteoblast-like cells in bioactive scaffolds. J Trauma 2010; 68(6):1439-44.
43. Catalano MG, Marano F, Rinella L, et al. Extracorporeal shockwaves (ESWs) enhance the osteogenic medium-induced differentiation of adipose-derived stem cells into osteoblast-like cells. J Tissue Eng Regen Med 201; Epub.
44. Uddin SM, Qin YX. Enhancement of osteogenic differentiation and proliferation in human mesenchymal stem cells by a modified low intensity ultrasound stimulation under simulated microgravity. PLoS One 2013; 8(9):e73914.
45. Sun D, Junger WG, Yuan C, et al. Shockwaves induce osteogenic differentiation of human mesenchymal stem cells through ATP release and activation of P2X7 receptors. Stem Cells 2013; 31(6):1170-80.
46. Haupt G. Shock waves in orthopedics. Urologe A 1997;36(3):233-8.
47. Schmitz C, Császár NB, Milz S, Schieker M, Maffulli N, Rompe JD, Furia JP. Efficacy and safety of extracorporeal shock wave therapy for orthopedic conditions: a systematic review on studies listed in the PEDro database. Brit Med Bull 2015; 116:115-38
48. Warmuth M, Schumacher I. Extrakorporale Stosswellentherapie (ESWT) bei ausbleibender oder verzo¨gerter Frakturheilung. Systematischer Review. Decision Support Document Nr. 62; 2012.

EDITORIAL

HEADACHE, MIGRAINE AND OBESITY: AN OVERVIEW ON PLAUSIBLE LINKS

D. LAINO[1], G. VITALITI[2], P. PARISI[3], P. PAVONE[2], A. VERROTTI[1], R. LUBRANO[4], N. MATIN[5] and R. FALSAPERLA[2]

[1]Department of Pediatrics, Perugia University, Perugia, Italy; [2]General and Emergency Paediatrics Operative Unit, Policlinico-Vittorio Emanuele University Hospital, University of Catania, Catania, Italy; [3]Child Neurology, Chair of Pediatrics, NESMOS Department, Faculty of Medicine and Psychology, Sapienza University, c/o Sant'Andrea Hospital, Rome, Italy; [4]Pediatric Nephrology Operative Unit, Sapienza University of Rome, Rome, Italy; [5]Teheran University of Medical Sciences, Teheran, Iran

Received February 10, 2016 – Accepted April 6, 2016

Headache can represent different disorders with different etiologies; including cardiac, cerebral, vascular, psychiatric, metabolic, neurologic diseases. Recent studies have highlighted that obesity is significantly associated with headache and disability in adults. This rule also applies to children. This review focuses on literature data studying any eventual relationship between headache, migraine and obesity [shown in Body Mass Index (BMI)] in children. Research data have highlighted that there is a relationship between headache physiopathology and central and peripheral mechanisms responsible for food assumption. In this regard, neurotransmitters such as serotonin, and peptides such as orexin and adipocytokines (adiponectin and leptin) seem to play a key role both in food assumption and in headache pathogenesis. These data further emphasize the potential association between headache and BMI. Therefore, those therapeutic strategies aiming to decrease BMI may represent a model of useful treatment to understand whether weight loss reduces the incidence and the severity of headache in obese children. In conclusion, considering the effects of obesity and weight loss on the natural history of headache, important changes are expected in therapeutic management of paediatric headaches.

Headache and obesity are two common challenges of public health both in adults and children. In paediatric patients, headache is one of the most common chronic conditions with a prevalence of 10-29% of infants and adolescents (1). Similarly, the prevalence of obesity is following an increasing trend in children of every age (2). Between 1964 and 1970, infantile obesity prevalence was approximately 5%, while in 2003-2004 this data rose to 17% (3). In the United States, 12% of the population has some kind of headache and one-third of the population is obese (4). In the last thirty years, the increased prevalence of overweight people has been associated with a number of medical and psychological conditions. Chronic headache in paediatric age has been associated with functional disability, while other literature data have demonstrated an increased risk of psychopathology (4). On the other hand, obesity in children has been associated with type II diabetes, high blood pressure values and psychosocial discomfort (5).

Key words: headache and obesity, etiopathogenesis, paediatric age, new therapeutic targets

Mailing address:
Dr Giovanna Vitaliti,
AOU Policlinico-OVE
Via Plebiscito n. 628,
95100 Catania, Italy
Tel.: +39 0957435254
e-mail: giovitaliti@yahoo.it

0393-974X (2016)

DISCLOSURE: ALL AUTHORS REPORT NO CONFLICTS OF INTEREST RELEVANT TO THIS ARTICLE.

Both diseases are linked to a reduced quality of life compared to healthy subjects (6). Finally, both headache and obesity represent an economic burden for any National Health System (NHS). The costs associated with headache medical care exceed 11 billion dollars per year (7), while those of obesity are estimated around 147 billion dollars (8), with indirect costs of 65 billion dollars over the global economic overload (9).

Recent literature data suggest a possible relationship between chronic headache and obesity: obesity is associated with a higher incidence and severity of headache, as well as a higher prevalence of migraine (10).

The aim of our review was to analyse the results of literature data on the association between obesity and headache possibly evolving to migraine. Moreover, we have investigated the potential role of weight loss on migraine management and eventual etiopathogenic mechanisms relating weight loss to the decreased incidence of headache.

MATERIALS AND METHODS

The major studies, clinical trials, case reports and reviews on the eventual association between obesity and headache/migraine, published from 1960 until the present time were selected.

Given the lack of an electronic database that contains all publications of all medical journals and that a restriction of only one database could be associated with a systematic bias, it was necessary to combine multiple databases for a comprehensive literature search. For this reason, an electronic literature search was carried out in MEDLINE via PubMed interface, EMBASE, SCOPUS, Google Scholar, and the Cochrane Library for all articles published from inception to October 2015.

Database-specific search strings were developed and included search terms describing obesity (population/exposure/intervention) and paediatric headache/migraine (study design/description of cases). A combination of medical subject headings and keywords was used. Titles and abstracts of identified papers were screened by two independent reviewers to determine whether they met the eligibility criteria of interest to develop our review. Subsequently, full texts of the remaining articles were independently retrieved by the two reviewers for eligibility.

We finally confirmed our results by performing a second revision of the literature data and selected articles, to be sure not to have omitted important scientific results.

RESULTS

Definition and prevalence of obesity

At present two systems are used to define overweight and obesity in preschool children: the International Obesity Task Force (IOTF) system and the referring standard World Health Organization (WHO) system. The first one, usually indicated for infants and adolescents between 2 and 18 years of age, was developed on a database of 97.876 males and 94.851 females, included from birth to 25 years of age, belonging to six different countries (Brazil, United Kingdom, Hong Kong, Norway, Oman and the USA) (11). WHO classification was used for children between 0-59 months of age, based on a cohort of 888 children and 6697 breast-fed infants and children coming from tertiary countries (12). This cohort of patients included infants and children of six different countries (Brazil, Ghana, India, Norway, Oman and the USA).

The first years of life after birth represent an important period for the development of obesity and its long-term compliances. In fact, a study on a USA cohort of children showed that a rapid weight increase between 0 and 4 months of age was associated with a higher incidence of overweight at the age of 7 years and in adolescence (13). Other studies highlighted how the early and rapid weight increase in small for gestational age (SGA) infants was associated with higher BMI, particularly with central obesity at early infancy (14), and with higher blood pressure values in adulthood (15).

Two systems of Nutritional Survey, the National Health and Nutrition Examination Survey (NHANES) and the Paediatric Nutrition Surveillance System (PedNSS), have documented an increase in the prevalence of overweight in children who are under 5 years old (16). These increases are evident in all paediatric age groups, including infants less than 6 months of age. The increase in the rate of overweight

was higher in black and Hispanic children than white patients, similarly to what was reported by NHANES and PedNSS.

Definition and prevalence of migraine

Migraine is a common condition in paediatric age and presents a higher prevalence during adolescence. A systematic review of 64 cross-sectional studies with a total of 227,249 subjects showed an overall mean prevalence of 54.4% for headache 9.1% for migraine (17). In prepuberal ages, migraine was more prevalent in boys, although after puberty this prevalence reverted and females were more affected (17).

Migraine is defined by the International Headache Society (IHS) as recurrent headache manifesting with or without aura, lasting 4 to 72 hours (18). However, in children the duration is shorter than adults, the headache is often bifrontal or bitemporal rather than unilateral and it should be noted that paediatrics have difficulty in expressing severity of symptoms and associated symptoms (18).

Migraine involves 3-10% of paediatric patients and 50/1000 schoolchildren in the United Kingdom and approximately 7.8 million children in Europe (19).

Studies in developing countries indicate that migraine is the most common diagnosis in children with headache and is rarely diagnosed in infants under 2 years of age due to the lack of communication in this age group, with difficulties linked to the clear explanation of symptoms. Moreover, migraine severity seems to have an increase directly proportionate to age (18). In prepuberal age, it equally involves males and females, while after puberty there is a higher prevalence in female subjects (18, 19).

Etiopathogenic mechanisms

The association between headache and migraine is linked to an increased release of pro-inflammatory mediators: the neurogenic inflammation derived from activation of the trigeminal vascular system seems predominantly responsible for pain in migraine. The stimulation of gangliar trigeminal nociceptors induces the release of pro-inflammatory molecules, such as Calcitonine-Gene Related Peptides (CGRP) and P-molecule (20). Literature data have shown an increase in CGRP levels in plasma of adult obese subjects and in venous blood of obese animal models, as well as in patients with migraine (20). In obese murine models, the exogenous administration of CGRP increases fat accumulation and CGRP is found elevated before the onset of obesity. Moreover, it is known that CGRP and its receptors are actually important targets for the pharmacological treatment of migraine (21).

The P-molecule has been identified in adipose tissue and has been involved in the increase of fat deposits and in the onset of the pro-inflammatory cascade associated with obesity (20). Moreover pro-inflammatory adipocytokine levels, such as tumor necorsis factor-alpha (TNF-alpha) and Interleukin-6 (IL-6) have been found increased in obesity (20-22) and at the onset of acute headache (22).

Similarly, leptin stimulates the release of cytokines and seems to be involved in the increased sensibility to pain (20-22). Moreover, high leptin concentrations in obese subjects are usually associated with increased susceptibility to inflammatory and chronic autoimmune diseases (20-22). Although little is known on the role of leptin in migraine, one recent study has highlighted how leptin was not elevated in patients with episodic headache in respect to controls, even if this difference was no more evident after statistical adjustment for patients with migraine and reduced fat mass (20-22).

Finally, Protein C reactive (PCR) levels, which are usually increased during systemic inflammation, have also been found increased both in children with migraine and in obese subjects (23). Therefore, the inflammatory condition subtending obesity may be responsible for the inflammatory state characterizing migraine, also contributing to the onset of acute episodes of headache (23).

Several neurotransmitters and peptides responsible for food assumption, which are usually under hypothalamic control, seem to have a key role in migraine etiopathogenesis. Serotonin is a neurotransmitter commonly associated with obesity, migraine and hunger. Serotonin has a key role in the process of food assumption, including sense of fullness. Serotonin-agonist drugs reduce hunger, causing a secondary weight loss (24). On the other hand, migraine has been described as a condition characterized by cerebral deficit of serotonin. Therefore, a plausible hypothesis is that in migraine

patients there is a tendency towards hunger (24).

At present, there is an increasing interest in the role of orexins, especially orexin A, in hunger control: orexins are also involved in migraine pathogenesis. Orexin A levels are increased in cerebral spinal fluid of migraine patients (25). As a molecule with antinociceptive properties, orexin A is involved in a compensatory response to chronic pain (25). Orexins are involved in hunger regulation (25). Moreover, literature data have shown that orexin A administration increases hunger and delays the sense of fullness in rats (25), while antagonists of orexin receptor 1 (OR1) reduces hunger in rats (25). In addition to epidemiological evidence, clinical and basic data suggest that several neurotransmitters and cytokines modulating food assumption can play a key role in migraine pathogenesis; nevertheless, further studies are necessary to confirm this relationship.

Finally, some psychological events and conditions are considered fundamental on the association between migraine and obesity. In fact, evidence of a possible relationship between stress and headache/migraine have recently been established (26). Moreover, depression can contribute to reinforce this link. Recent studies have examined anxiety and depression in migraine pathogenesis: in patients under treatment for migraine, both were more frequent in obese than in non-obese subjects. Their link with a high frequency of migraine and disability was stronger in patients affected by anxiety and depression (26).

DISCUSSION

Obesity and migraine are common conditions in childhood and in adulthood. Literature data on adults has established a link between these two morbidities. The consequences of obesity and weight increase on migraine can have important implications in its clinical management and few studies have examined the implications of weight loss on migraine, and whether weight loss can improve headache severity in childhood.

In studies on adults, obesity seems to be associated with increased incidence of daily chronic headache, as far as frequency and severity of acute episodes of migraine are concerned; previous studies highlighted an increased incidence of migraine, above all the type associated with aura, in obese females (27). It has therefore been suggested that, in females, migraine with aura is associated with high levels of oestrogens secreted by the adipose tissue (27). In this regard, Kaplan showed that obese females with migraine have more severe and frequent acute episodes (27).

Recent studies have highlighted a direct relationship between migraine and obesity in paediatric patients. More recently, Hershley et al. examined the effect of weight and weight loss on different migraine parameters in 913 paediatric patients (71% of whom presented migraine). The authors observed that BMI percentile at baseline visit was directly associated with migraine frequency. Reduction in BMI was associated with reduction in migraine frequency at 3- and 6- month follow-up visits in overweight and obese children, but not in normal-weight subjects (28).

In a study of Klinik et al. on 124 children, the authors analysed the link between obesity influence on migraine severity, suggesting that obesity represents a risk factor for the frequency and severity of migraine attacks during infancy and adolescence (29). In that study, even if acute headache severity and symptoms did not differ between obese and non-obese children, the authors found an association between obesity and frequency of migraine attacks in affected children and adolescents. Obese patients had more frequent acute episodes than non-obese children. These results are similar to those previous studies on adult obese patients. Vomiting was more frequent in obese females than non-obese migraine patients (29). Moreover, no significant difference was found between obese and non-obese females with regard to the presence of aura, prodromal or concomitant symptoms of migraine. In another study of Klinik et al., obesity did not have any effects on symptoms associated with migraine, such as aura, phono/photophobia, nausea and vomiting (29). On the contrary, Bigal et al. observed important differences of refractory migraine between obese and non-obese adults, after prophylactic treatment (30). Nevertheless, the decrease in the number of days of serious attacks was higher among obese patients, suggesting that obese migraine subjects responded better to prophylactic treatment than normal weight patients. However, new therapeutic perspectives include dietetic adjustments,

increase of physical activity and psychological support, which can be effective both for obese children and adolescents. A multistep, comprehensive and varied approach will be the effective part of a multidisciplinary program of weight management in obese children with migraine, even if further studies are necessary to confirm the role of this approach. Resuming the results of these studies is difficult due to the differences of treatment, duration and type of intervention. Even if obesity has a complex development involving environmental and genetic factors, an imbalance between energetic intake and waste is one of the etiologies. Therefore, those strategies to modify the lifestyle should include increase of structured and non-structured physical activity and decrease in sedentary activities.

CONCLUSIONS

Literature data show a link between obesity and migraine, in that both are influenced by genetic and inflammatory mediators. Priority should be given to the identification of risk factors and pathogenic mechanisms involved in the onset of chronic migraine. Moreover, the link between migraine and BMI has been clearly demonstrated, therefore, those therapeutic interventions to modify BMI can represent a useful therapeutic model to analyse whether a moderate weight loss reduces the frequency and severity of headache, and its progression towards migraine. Further studies on the pathogenic mechanisms that link weight loss and headache/migraine will clarify future potential therapeutic strategies.

REFERENCES

1. Ornello R, Ripa P, Pistoia F, Degan D, Tiseo C, Carolei A, Sacco S. Migraine and body mass index categories: a systematic review and meta-analysis of observational studies. J Headache Pain 2015; 16:27.
2. Ravid S. Migraine & paediatric obesity: a plausible link? Indian J Med Res 2015; 139:343-8.
3. Ogden CL, Carroll MD, Curtin LR, McDowell MA, Tabak CJ, Flegal KM. Prevalence of overweight and obesity in the United States, 1999–2004. JAMA 2006; 295:1549-55.
4. Powers SW, Gilman DK, Hershey AD. Headache and psychological functioning in children and adolescents. Headache 2006; 46:1404-15.
5. Verrotti A, Di Fonzo A, Penta L, Agostinelli S, Parisi P. Obesity and headache/migraine: the importance of weight reduction through lifestyle modifications. Biomed Res Int 2014; 420858.
6. Schwimmer J, Burwinkle T, Varni J. Health-related quality of life of severely obese children and adolescents. JAMA 2003; 289:1813-19.
7. Hawkins K, Wang S, Rupnow M. Direct cost burden among insured US employees with migraine. Headache 2008; 48:553-63.
8. Finkelstein EA, Trogdon JG, Cohen JW, Dietz W. Annual medical spending attributable to obesity: payer-and service-specific estimates. Health Aff (Millwood) 2009; 28:822–31.
9. Trogdon JG, Finkelstein EA, Hylands T, Dellea PS, Kamal-Bahl SJ. Indirect costs of obesity: a review of the current literature. Obes Rev 2008; 9:489-500.
10. Verrotti A, Carotenuto M, Altieri L, et al. Migraine and obesity: metabolic parameters and response to a weight loss programme. Pediatr Obes 2015; 10:220-25.
11. Cole TJ, Bellizzi MC, Flegal KM, Dietz WH. Establishing a standard definition for child overweight and obesity worldwide: international survey. BMJ 2000; 320:1240-43.
12. WHO Multicentre Growth Reference Study Group. WHO Child Growth Standards based on length / height, weight and age. Acta Paediatr Suppl 2006; 450:76-85.
13. Stettler N, Kumanyika SK, Katz SH, Zemel BS, Stallings VA. Rapid weight gain during infancy and obesity in young adulthood in a cohort of African Americans. Am J Clin Nutr 2006; 77:1374-78.
14. Ong KK, Ahmed ML, Emmett PM, Preece MA, Dunger DB. Association between postnatal catch-up growth and obesity in childhood: prospective cohort study. BMJ 2000; 320:967-71.
15. Law CM, Shiell AW, Newsome CA, et al. Fetal, infant, and childhood growth and adult blood pressure: a longitudinal study from birth to 22 years of age. Circulation 2002; 105:1088-92.
16. Ogden CL, Flegal KM, Carroll MD, Johnson CL. Prevalence and trends in overweight among US children and adolescents, 1999–2000. JAMA 2002;

288:1728-32.
17. Wöber-Bingöl Ç. Epidemiology of migraine and headache in children and adolescents. Current pain and headache reports 2013; 17:1-1.
18. Oleson J. The international classification of headache disorders. Cephalalgia 2004; 24:9-160.
19. Evers S. Drug treatment of migraine in children. A comparative review. Paediatr Drugs 1999; 1:7-18.
20. Bond DS, Roth J, Nash JM, Wing RR. Migraine and obesity: epidemiology, possible mechanisms and the potential role of weight loss treatment. Obes Rev 2011; 12:362-71.
21. Mannix LK, Fan X, Assaid C, Assaid C, Furtek C, Jones CJ, Lines CR, Rapoport AM; MK-0974 Protocol 004 study group. Randomized controlled trial of an oral CGRP receptor antagonist, MK-0974, in acute treatment of migraine. Neurology 2008; 70:1304-12.
22. Stofkova A. Leptin and adiponectin: from energy and metabolic dysbalance to inflammation and autoimmunity. Endocr Regul 2009; 43:157-68.
23. Vanmolkot FH, de Hoon JN. Increased C-reactive protein in young adult patients with migraine. Cephalalgia 2007; 27:843–6.
24. Blundell JE, Halford JCG. Serotonin and appetite regulation: implications for the pharmacological treatment of obesity. CNS Drug 1998; 9:473-95.
25. Sarchielli P, Rainero I, Coppola F, Rossi C, Mancini M, Pinessi L, Calabresi P. Involvement of corticotrophin-releasing factor and orexin-A in chronic migraine and medication-overuse headache: findings from cerebrospinal fluid. Cephalalgia 2008; 28:714-22.
26. Tietjen GE, Peterlin BL, Brandes JL, et al. Depression and anxiety: effect on the migraine-obesity relationship. Headache 2007; 47:866-75.
27. Kaplan Y. Effects of obesity on migraine in women. J Neurol Sci (Turkish) 2006; 23:295-302.
28. Hershey AD, Powers SW, Nelson TD, et al; American Headache Society Pediatric Adolescent Section. Obesity in the pediatric headache population: a multicenter study. Headache 2009; 49:170-77.
29. Kinik ST, Alehan F, Erol I, Kanra AR. Obesity and paediatric migraine. Cephalalgia 2010; 30:105-9.
30. Bigal ME, Gironda M, Tepper SJ, Feleppa M, Rapoport AM, Sheftell FD, Lipton RB. Headache prevention outcome and body mass index. Cephalalgia 2006; 26:445-50.

EDITORIAL

ENDOCRINOLOGY OF THE SKIN: INTRADERMAL NEUROIMMUNE NETWORK, A NEW FRONTIER

Al. CARAFFA[1], E. SPINAS[2], S.K. KRITAS[3], G. LESSIANI[4], G. RONCONI[5], A. SAGGINI[6], P. ANTINOLFI[7], J. PIZZICANNELLA[8], E. TONIATO[9], T.C. THEOHARIDES[10] and P. CONTI[11]

[1]University of Perugia, Perugia, Italy; [2]Department of Surgery and Odontostomatological Sciences, University of Cagliari, Italy; [3]Department of Microbiology and Infectious Diseases, School of Veterinary Medicine, Aristotle University of Thessaloniki, Macedonia, Greece; [4]Vascular Medicine Unit, Villa Serena Hospital, Città Sant'Angelo, Italy; [5]Clinica dei Pazienti del Territorio, Policlinico Gemelli, Rome, Italy; [6]Department of Dermatology, University of Rome Tor Vergata, Rome, Italy; [7]Department of Orthopedics, Hospital, Perugia, Italy; [8]University of Chieti, Chieti, Italy; [9]Department of Medical, Oral and Biological Sciences, University of Chieti, Chieti, Italy; [10]Molecular Immunopharmacology and Drug Discovery Laboratory, Tufts University, Boston, MA USA; [11]Immunology Division, Medical School, University of Chieti-Pescara, Chieti, Italy

Received March 25, 2016 - Accepted June 6, 2016

Endocrinology systems exert an important effect on vascular function and have direct actions on blood vessels. Estrogens provoke an increase in skin elasticity, epidermal hydration, skin thickness, reduce skin wrinkles and augment the content of collagen and the level of vascularisation. Therefore, there is an intricate cross-talk between skin conditions and stress. In stress, β2-adrenoreceptor (β2AR) pathway, cortisol, epinephrine and norepinephrine increase DNA damage and interfere with the regulation of the cell cycle, contributing to aging and skin diseases. Substance P is a neuropeptide released in the skin from the peripheral nerve and is related to stress and inflammation. SP provokes infiltration of inflammatory cells in the skin and induces a variety of cytokines/chemokines. Corticotropin-releasing hormone (CRH), produced by mast cells, is a neuropeptide also expressed in skin and responds to stress. CRH initiates diverse intracellular signaling pathways, including cAMP, protein kinase C, and mitogen-activated protein kinases (MAPK). Under stress, CRH, glucocorticoids, epinephrine and cytokines are generated. Moreover, the release of ACTH binds the receptor MC2-R and stimulates the generation of glucocorticoids such as corticosterone and cortisol, which interact with the transcription factors AP-1 and NF-kB. In skin keratinocytes, ACTH promotes the generation of pro-inflammatory cytokines, which enhances T-cell activity. Cortisol is immunosuppressive by inhibiting Th1 and Th2 cell response, antigen presentation, antibody and cytokine/chemokine production. However, glucocorticoids are certainly helpful in Th1-mediated autoimmune disorders. On the other hand, cytokines, such as TNF, IL-1 and IL-6, stimulate the generation of CRH and activate HPA axis in inflammatory states. Here, we describe for the first time a cross-talk between endocrinology and skin, including pro-inflammatory cytokines and neurogenic inflammatory pathways.

Key words: skin, endocrinology, inflammation, neuroimmunology, CNS, cytokine.

Mailing address:
Dr Pio Conti, Affiliated Professor,
Molecular Immunopharmacology and Drug Discovery Laboratory,
Tufts University, Boston, MA 02111, USA;
Professor of Immunology, Post Graduate School of Medicine,
University of Chieti-Pescara, Viale Unità d'Italia, 73, 66100 Chieti, Italy
e-mail: pconti@unich.it

0393-974X (2016)

DISCLOSURE: ALL AUTHORS REPORT NO CONFLICTS OF INTEREST RELEVANT TO THIS ARTICLE.

There is an intricate cross-talk between skin conditions and stress which has been reported since Roman times. In fact, there is a direct relationship between skin diseases, endocrinology and psychological stress, although there may sometimes be an overlapping between, endocrinology, inflammation, and immunology of skin diseases (1).

The estrogen receptors, ERα, ERβ, and GPER, are expressed in all vertebrates and a few invertebrates and are located in diverse tissues, such as liver, colon, bone, brain, salivary gland and skin (2). Estrogens are known to affect vascular function and have direct actions on blood vessels (3). Estrogen treatment increases skin elasticity, epidermal hydration, skin thickness, reduces skin wrinkles and augments the content of collagen and the level of vascularisation. In addition, administration of topical estrogen increases keratinocyte proliferation and epidermal thickness. Estrogen augments TGF-β and TGF-β type II receptor expression, which is related to dermal fibroblast proliferation and extracellular matrix (ECM) secretion (4). On the other hand, it down-regulates the expression of matrix metalloprotease-I (MMP-1), with an increase of collagen content demonstrated in estrogen-treated skin (5).

Corticotropin releasing hormone (CRH), is a 41-amino-acid neuropeptide which is expressed in skin, responds to stress and is an important mediator of the hypothalamic–pituitary–adrenal (HPA) axis (6). Two different CRHs exist, CRH1 and CRH2; CRH1 is expressed in human skin where it regulates coetaneous immune cells and the endocrine system. CRH production increases in stress and mediates inflammatory skin diseases, such as psoriasis and atopic dermatitis (AD) (5). CRH exerts its biological effects by binding CRHR, initiating diverse intracellular signaling pathways, including cAMP, protein kinase C, and mitogen-activated protein kinases (MAPK). It is well known that under stress, the central nervous system (CNS) releases CRH, glucocorticoids, epinephrine and cytokines which are local inflammatory hormones (6). Cytokines are polypeptides which initiate their action by binding specific receptors on the membrane of target cells (7). It has been reported that stress can induce or exacerbate multiple diseases including skin disorders (8). The effect of stress, through CRH binding CRH-R1, on the skin is exercised primarily by the hypothalamic-pituitary-adrenal (HPA) axis. In this context, the release of ACTH binds the receptor MC2-R and stimulates the generation of glucocorticoids such as corticosterone and cortisol, which interact with the transcription factors AP-1 and NF-kB. In skin keratinocytes, ACTH promotes the generation of pro-inflammatory IL-18, which enhances T-cell activity and acts on Th2 cytokines generation (9).

In addition, it is well known that cortisol is immunosuppressive by inhibiting Th1 and Th2 cell response, antigen presentation, antibody and cytokine/chemokine generation. CRH, via cAMP acts on melanocytes and skin fibrblasts by producing corticosterone and ACTH which is also generated by keratinocytes and Langerhan cells.

CRH is produced by mast cells and inhibits the proliferation of epidermal keratinocytes by acting on the G0-G1 cycle and induces differentiation by transcription factors. In the skin, CRH stimulates the proliferation of fibroblasts and melanocytes, induces mast cell degranulation, increases vascular permeability, inhibits apoptosis, promotes angiogenesis through VEGF, up-regulates lipogenesis enzymes in human sebocyte and mediates inflammatory responses through IL-6 generation; while it down-regulates the inflammatory IL-18 in keratinocytes. In addition, stress induces the release of the corticotropin-releasing factor which leads to the generation of glucocorticoids (10). Stress hormones in the skin activate APC cells, an effect that can be inhibited by glucocorticoids (11).

Cytokines, such as TNF, IL-1 and IL-6, stimulate the generation of CRH and activate HPA axis in inflammatory states. Th1 cells primarily secrete IFN-γ, IL-2 and TNF involved in inflammation, while Th2 cells generate IL-4, IL-10 and IL-13 and promote humoral immunity. Furthermore, CRH antagonist may aid in preventing stress-induced Th1-suppression, exhibiting therapeutic qualities (12).

IL-12 is produced by activated macrophages and other APCs, and is the principal inducer of Th1 cells. Th1 cell-derived IFN-γ activates T cytotoxic cells, NK cells and macrophages. IL-12, TNF and IFN-γ

stimulate inflammatory products including nitric oxide. Moreover, IL-12 and IFN-γ are important for the control of bacterial infections. The inhibition of H2 antagonists may result in an increase of Th1 responses that could be useful in the management of certain skin infections, while glucocorticoids are certainly helpful in Th1-mediated autoimmune disorders.

T helper cells are divided into Th1, Th2, Th9, Th17 and Th22 cells and are characterized by specific cytokine generation patterns. All these cells and other immune cells possess vitamin D receptor, where vitamin D can be linked and decrease pro-inflammatory cytokine released from these cells and other immune cells such as mast cells and skin keratinocytes (13).

In the skin, vitamin D undergoes various hydroxylation steps to produce the biologically-active form of vitamin D3. Provitamin 7-dehydrocholesterol, mostly found in the Malpighi layers is synthesized in the sebaceous gland of the skin and is transformed into vitamin D3 (cholecalciferol) after skin irradiation (285/315 nm UV light) and after skin absorption is transported by the bloodstream. Vitamin D provokes an increase of the anti-inflammatory cytokine IL-10; while IL-12 decreases, an effect that contributes to inhibit inflammatory immune cells and skin inflammation. In psoriatic patients, the use of vitamin D3 and D2 inhibit keratinocyte differentiation and proliferation showing therapeutic effects. This disorder is worsened by acute stress which is mediated by VEGF. In addition, psoriasis is characterized by an increase of epidermal vascularization, keratinocyte hyperproliferation, and inflammation mediated by inflammatory markers such as IL-17A, IL-17F, and IL-8. Vitamin D and Treg exert a therapeutic effect on the skin by inhibiting beta-defensin (HBD)2, HBD3, IL-17A, IL-17F, and IL-8. In fact, Tregs are able to alleviate clinical signs of immediate-type hypersensitivity reactions in IgE-mediated skin allergy (13).

Chronic inflammatory skin disease, such as atopic dermatitis (AD) shows an impaired cutaneous barrier function due to abnormalities in the skin. Immunological studies and epidemiological investigations on atopic dermatitis (AD) have suggested a link between vitamin D deficiency and

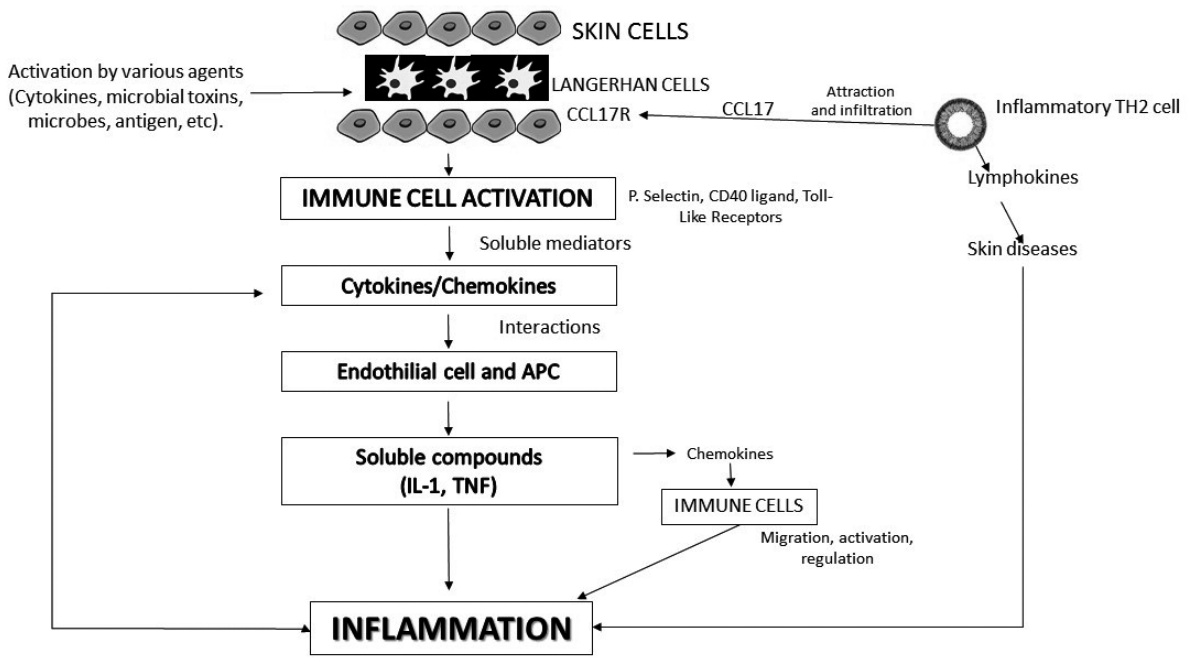

Fig. 1. *Skin cell activation (Langerhans cells) by various agents leading to cytokines/chemokines generation provoking inflammatory responses and skin disorders.*

allergic skin diseases (13). Vitamin D deficiency is associated with a higher risk of contracting AD with unknown mechanism. In addition, vitamin D-deficient mice have an increased contact hypersensitivity response compared to those with normal vitamin D levels. Therefore, it has been established that this vitamin enhances the barrier function in the skin and often ameliorates atopic skin disease.

JAK-STAT pathway is a signal transduction pathway for numerous cytokines which binds its receptor and leads to JAK activation and STAT phosphorylation (14). This pathway is involved in the dysregulation of T-cell response in chronic inflammatory skin diseases, such as atopic dermatitis and allergic diseases.

When injected in the skin, TNF and IL-1 often mimic host responses to infection, inflammation, injury or immunologic challenge, while IL-4 and IL-10 therapies are quite effective in several skin pathologies such as psoriasis and atopic dermatitis (15). Therefore, the use of anti-inflammatory cytokines/chemokines as therapeutics for inflammatory skin diseases remains a promising approach.

Substance P is a neuropeptide released in the skin from the peripheral nerve and is related to stress and inflammation. SP is a neuroinflammatory compound which provokes infiltration of inflammatory cells in the skin and induces a variety of cytokines such as TNF, IL-1, IL-6, IL-12 and certain chemokines. Stress can induce DNA damage through the β2-adrenoreceptor (β2AR) pathway and cortisol, epinephrine and norepinephrine increase DNA damage and interfere with the regulation of the cell cycle, contributing to aging and skin diseases.

It has been reported that an excess of fat mass, due to hormonal dysfunction results in the production of chemokines, such as monocyte chemoattractant protein-1 (MCP-1), which helps to recruit inflammatory cells, including mast cells and macrophages, in fat tissue (16).

Nerves in the skin may produce neuropeptides, such as substance P, neutrophins and NGF, which may contribute to the inflammatory response in skin disorders, including allergy and pruritus. In addition, NGF skin mast cells act by binding the high affinity tyrosine kinase receptors, such as TrkA, TrkB, and TrkC, stimulate cytokine production and promote neurogenic inflammation (17). Activated mast cells, keratinocytes and Langerhans cells represent an immune barrier, which produce chemokines, substance P, growth factors, TNF, IL-1β, and other inflammatory cytokines.

In the skin, vitamin D provokes recruitment of T cells through the increases of expression of the chemokine receptor 10 (CCR10) and inhibits dendritic cell migration, IL-12 and IL-23 cytokine production.

Acne vulgaris is a common skin disease which is increased in stress conditions (18). CRH, which is detected on sebocytes, promotes lipogenesis and induces cytokines IL-6 and IL-11 generation in keratinocytes mediating inflammatory responses. Acne is also worsened by ACTH and alpha MSH which contribute to sebum formation. SP is increased in acne condition where it promotes the proliferation and differentiation of sebaceous glands, and induces gene expression of PPAR-γ which plays a role in stimulating sebocyte lipogenasis. Adipose tissue which produces pro-angiogenic factors, such as vascular endothelial growth factor, is also involved in skin inflammation.

The adipokine leptin is a hormone predominantly synthesized and secreted by adipocytes with a 16-kDa, and a protein containing 167 amino acids, resulting the most important intracellular signal transduction pathway signal transducer and activator of transcription 3 (STAT3) (19). In human epidermis, leptin is present at the gene and protein level and is mainly generated by subcutaneous adipocytes. Leptin has pro-angiogenic activities, is involved in the induction of endothelial dysfunction and is related with obesity and its metabolic disorders. Leptin acts as a metabolic hormone, plays an important role in regulating skin metabolism and body mass. Moreover, high leptin levels may accelerate skin inflammation.

Here, we show for the first time that there are feedback mechanisms and cross-talk between brain and skin, and pro-inflammatory cytokines and neurogenic inflammatory pathways. However, further studies are necessary in order to clarify the complex mechanism(s) that regulate the neuroimmune network and pathophysiological skin functions.

REFERENCES

1. Theoharides TC, Spanos C, Pang X, et al. Stress-induced intracranial mast cell degranulation: a corticotropin-releasing hormone-mediated effect. Endocrinology 1995; 136(12):5745-50.
2. Janik ME, Bełkot K, Przybyło M. Is oestrogen an important player in melanoma progression? Contemp Oncol (Pozn) 2014; 18(5):302-6. doi: 10.5114/wo.2014.43938.
3. Gruber CJ, Tschugguel W, Schneeberger C, Huber JC. Production and actions of estrogens. N Engl J Med 2002; 346(5):340-52.
4. Findlay JK, Drummond AE, Britt KL, et al. The roles of activins, inhibins and estrogen in early committed follicles. Mol Cell Endocrinol 2000; 163(1-2):81-87.
5. Thornton MJ. Estrogens and aging skin. Dermatoendocrinol 2013; 5(2):264-70.
6. Theoharides TC, Donelan JM, Papadopoulou N, Cao J, Kempuraj D, Conti P. Mast cells as targets of corticotropin-releasing factor and related peptides. Trends Pharmacol Sci 2004; 25(11):563-8.
7. Kutukculer N, Azarsiz E, Aksu G, Karaca NE. CD4+CD25+Foxp3+ T regulatory cells, Th1 (CCR5, IL-2, IFN-γ) and Th2 (CCR4, IL-4, Il-13) type chemokine receptors and intracellular cytokines in children with common variable immunodeficiency. Int J Immunopathol Pharmacol 2016; 29(2):241-51.
8. Petra AI, Panagiotidou S, Stewart JM, Conti P, Theoharides TC. Spectrum of mast cell activation disorders. Expert Rev Clin Immunol 2014; 10(6):729-39.
9. Ying Chen and John Lyga. Brain-Skin Connection: Stress, Inflammation and Skin Aging. Inflamm Allergy Drug Targets 2014; 13(3):177-90.
10. Shaik-Dasthagirisaheb YB, Conti P. Chemokine network involved in inflammatory skin diseases. Ann Clin Lab Sci 2015; 45(4):452-57.
11. Elenkov IJ, Chrousos GP. Stress, cytokine patterns and susceptibility to disease. Baillieres Best Pract Res Clin Endocrinol Metab 1999; 13(4):583-95.
12. Calcagni E, Elenkov I. Stress system activity, innate and T helper cytokines, and susceptibility to immune-related diseases. Ann N Y Acad Sci 2006; 1069:62-76.
13. Toniato E, Spinas E, Saggini A, et al. Immunomodulatory effects of vitamin D on skin inflammation. J Biol Regul Homeost Agents 2015; 29(3):563-67.
14. Kotenko SV, Pestka S. Jak-Stat signal transduction pathway through the eyes of cytokine class II receptor complexes. Oncogene 2000; 19(21):2557-65.
15. Li Z, Zhou J, Zhu D, Zhang Q, Huang M, Han Y, Zhou S. Role of endogenous TNF-a in cardiomyocyte apoptosis induced by bacteria lipoprotein and the protective effect of IL-10. Eur J Inflamm 2015; 13(2):117-25.
16. Toussirot E, Aubin F, Dumoulin G. relationships between adipose tissue and psoriasis, with or without arthritis. Front Immunol 2014; 5:368.
17. Rivera J, Fierro NA, Olivera A, Suzuki R. New insights on mast cell activation via the high affinity receptor for IgE. Adv Immunol 2008; 98:85-120.
18. Zouboulis CC. Acne as a chronic systemic disease. Clin Dermatol 2014; 32(3):389-96.
19. Popovic V, Damjanovic S, Dieguez C, Casanueva FF. Leptin and the pituitary. Pituitary 2001; 4(1-2):7-14.

REGULATORY EFFECT OF miRNA ON MULTI-DIRECTIONAL DIFFERENTIATION ABILITY OF MESENCHYMAL STEM CELL IN TREATMENT OF OSTEOPOROSIS

ZW. TENG[1], Y. ZHU[2], Q. NA[1], XG. ZHANG[1], H. ZHAO[1], GJ. WEI[3], J. ZHAO[1], XW. ZHANG[1], GZ. WANG[1], J. LIANG[1], ZJ. ZHANG[4] and YG. LIU[5]

[1]Department of Orthopedic Surgery, The People's Hospital of Yuxi City, The 6th Affiliated Hospital of Kunming Medical University, Yuxi, Yunnan, China; [2]Department of Nephrology, The People's Hospital of Yuxi City, The 6th Affiliated Hospital of Kunming Medical University, Yuxi, Yunnan, China; [3]Department of Orthopedic, The First Affiliated Hospital of Harbin Medical University, Harbin, Heilongjiang, China; [4]Department of Orthopedic Surgery, General Hospital of Jizhong Energy Fengfeng Group, Handan, Hebei, China; [5]Department of Orthopedic Surgery, Affiliated Hospital of Hebei University of Engineering, Handan, Hebei, China

Received October 8, 2015 – Accepted March 1, 2016

This study was designed to evaluate the effect of miRNA acting in regulating multi-directional differentiation ability of mesenchymal stem cell in treatment of osteoporosis (OP), with the aim of finding a new idea and approach for clinical treatment of OP. Estrogen deficiency-induced OP mice model was established by means of ovariectomy (OVX). Additionally, a sham group was set up for control. Bone Marrow Mesenchymal Stem Cells (BMMSCs) of OVX group (O/BMMSCs) and BMMSCs of sham group (S/BMMSCs) were separately cultured. Then surface markers of BMMSCs were detected. Multi-directional differentiation ability was identified in the two groups by giving cells targeted induced stimulation. It was found that the bone trabecula, bone density and bone volume fraction of distal femoral metaphysis in the OVX group were much lower than those of the sham group. Moreover, trabecular bone space in the OVX group became larger; O/BMMSCs and S/BMMSCs both had normal expression of surface markers as well as potentials of osteogenic and adipogenic differentiation; O/BMMSCs had a weaker osteogenic capability but a stronger adipogenic capability than S/BMMSCs. All the findings suggest that the regulatory effect of miRNA on multi-directional differentiation ability plays a vital role in the treatment of OP, and there is a close correlation between them; deficiency or functional defect of BMMSCs can result in the occurrence of OP.

Osteoporosis (OP) refers to a systematic bone disease which is induced by the reduction of primary osteoporosis and degradation of bone microstructure (1-3). OP is mainly induced by imbalanced bone remodeling induced by weakened osteogenic capability (4, 5). Mesenchymal Stem Cells (MSCs) can differentiate into osteoblasts and play an important role in bone remodeling. A recent study (6) found that miRNA can regulate multi-directional differentiation ability of MSCs based on its target binding feature, thus playing a significant role in occurrence, development and treatment of OP (7, 8).

miRNA within cells changes under disease conditions, and the regulatory effects occurring

Key words: miRNA, multi-directional differentiation ability, bone marrow mesenchymal stem cells, osteoporosis

Mailing address:
Dr Yugang Liu,
Department of Orthopedic Surgery,
Affiliated Hospital of Hebei University of Engineering,
Handan, 056002, Hebei, China
e-mail: liuyuganglygg@163.com

0393-974X (2016)

DISCLOSURE: ALL AUTHORS REPORT NO CONFLICTS OF INTEREST RELEVANT TO THIS ARTICLE.

afterwards can induce changes in a series of biological functions (9). Another study (10) suggests that miR-375 can lower expression of phosphoinositide-dependent kinase 1 (PDK1) by targeted binding with it, therefore inducing glucose to stimulate expression of insulin gene and DNA synthetic ability decrease.

Stem cells with a wide application prospect have been the hot spot in medical and biological fields (11-12). Every miRNA has multiple target genes and several miRNA can also regulate the same gene. They play an important role in regulating growth, development, aging and death of the body (13). This study aims to explore the regulatory effect of miNRA on multi-directional differentiation ability of MSCs in the treatment of OP to offer a reliable clinical basis for treatment of OP.

MATERIALS AND METHODS

The main instruments and equipment used in this experiment included micro-computed tomography (CT) (General Electric Co., Ltd., Germany), 10 cm culture dish, 6-well plate, 96-well plate (Corning company, USA), centrifuge (Xiangyi Centrifuge Instrument Co., Ltd., China), carbon dioxide constant temperature incubator (Thermo Co., Ltd., USA), inverted phase contrast microscope (Olympus Corporation, Japan), YJ-875 benchtop (Suzhou Purification Equipment Factory, China).

Reagents used included 1% pentobarbital sodium (Shanghai Chemical Reagent Center, China), fetal calf serum (Sijiqing, China), α-Minimum Essential Medium (α-MEM), penicillin, streptomycin (Gibco, USA), glutamine (Invitrogen, USA), etc. All animal experiments involved in this study were reviewed and approved by the animal ethics committee.

Construction of estrogen deficiency induced OP mice model

Twenty female C57BL/6J mice, aged eight weeks, were selected and classified into an ovariectomy group (n=10) and a sham group (n=10). 1% pentobarbital sodium was injected into mice through the abdominal cavity. Then mice were disinfected. An incision was cut along the median line on the back to separate skin and muscle. Bilateral ovaries and the surrounding adipose tissue of mice in the OVX group were removed. Then the muscle layer and skin were sutured. In the sham group, only adipose tissue around the bilateral ovaries was removed.

Identification of estrogen deficiency mice model of OP

Four weeks later, mice were detected with micro-CT. Femoral metaphysis bone trabecula parameters, such as bone mineral density (BMD), bone volume fraction (BV/TV), trabecular space (Tb. Sp) and trabecular number (Tb. N), were analyzed to identify whether the model had been successively established.

Isolated culture of Bone Marrow Mesenchymal Stem Cells (BMMSCs) of OVX and sham group

Four weeks after surgery, all mice were sacrificed and then disinfected by soaking in 75% ethyl alcohol. Femur and tibia were separated and then soaked in α-MEM containing 20% fetal calf serum, 100 U/mL penicillin and streptomycin. After femur head and tibia head were removed, bone marrow was blown out and made into suspension, and then cultured in an incubator (37°C, 5% CO_2).

Identification of label on the surface of BMMSCs of OVX and sham group

Firstly, P3 generation of BMMSCs of mice in theOVX group and sham group were digested. Then the cells were washed by phosphoric acid solution (PBS) and centrifuged for 5 min. Supernate was removed afterwards. Cell density was adjusted and then the liquid was transferred to EP tube. Every EP tube was added with anti- major histocompatibility complex (MHC)-II, anti-CD73, CD34, CD45, CD29 (phycoerythrin label) and stem cell antigen-1 (SCA-1) (fluorescein isothiocyanate label), 2 μL for each. Then the tubes were placed ina refrigerator (4°C). Two hours later, cells were centrifuged, washed by PBS and resuspended. Finally, propidium iodide positive percentage (PI%) was analyzed using flow cytometry.

Identification of osteogenic differentiation ability of BMMSCs of OVX group and BMMSCs group

BMMSCs were inoculated in a 6-well plate and cultured by MEM-α. After cells adhered to the wall, osteogenic induction liquid was added. Alizarin red staining was performed three weeks later. After washing with PBS, overall and microscopic appearances of

mineralized nodule were observed by naked eye and inverted microscope, respectively. Quantitative analysis was made as per the following procedures. PBS in wells was absorbed and then cetyl pyridinium chloride was added, 1 ml each well. After the mineralized nodule dissolved, the solution was transferred to a 96-well plate, 100 µl for each well. Finally, a microplate reader was used at 540 nm.

Identification of adipogenic differentiation of BMMSCs of OVX group and sham group

BMMSCs were inoculated in a 6-well plate (2×10^5/well) and cultured with α-MEM containing 20% fetal calf serum. When cells adhered to the wall, culture solution was alternated by adipogenic induction liquid. Staining was performed after 14-day cultivation. Thirty minutes later, the cells were washed by PBS. Difference of lipid droplet between the two groups was observed under an inverted microscope. Then quantitative analysis was made by staining with Oil Red O. Detailed procedures are as follows. Firstly, PBS was removed from the wells. Then isopropanol was added to dissolve lipid droplet, 1 ml for each well. The other procedures were the same as the above section.

Statistical analysis

Quantitative analysis was repeated three times. SPSS17.0 software was used to analyze data. Difference of values between the two groups was compared using *t*-test. Difference was considered to be statistically significant if $P<0.05$.

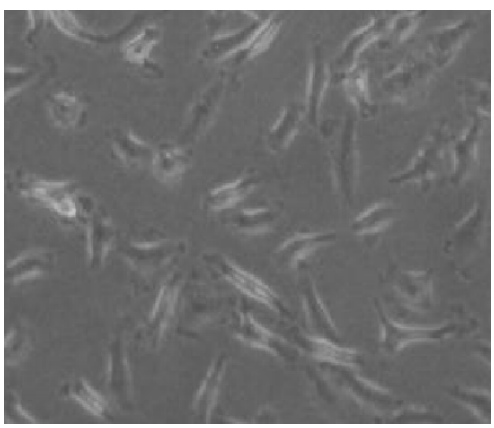

Fig. 1. *Cultivation of primary generation BMMSCs.*

RESULTS

Construction and identification of estrogen deficiency-induced OP mice model

It was found from micro-CT images that femoral metaphysis bone trabecula parameters such as BMD, BV/TV and Tb N in the OVX group were much lower than those of the sham group.

Isolated culture results of BMMSCs of OVX group and sham group

After one week cultivation of primary generation BMMSCs, most BMMSCs adhered to the wall and became fusiform, and some colonies also formed (Fig. 1).

Identification results of label on the surface of BMMSCs

BMMSCs is a cell group mixing with surface antigens of MMCs and epithelial cells such as SCA-1, CD29 and CD73 but not including surface antigens of hematopoietic stem cell and costimulatory molecules such as CD34, MHC-II and CD45. In the sham group, 96.9% BMMSCs showed positive SCA-1 expression, 77.1% BMMSCs expressed

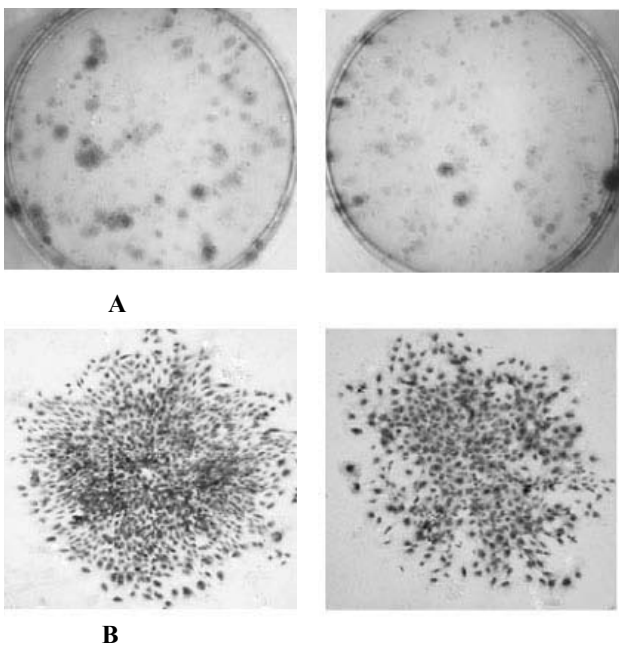

Fig. 2. *Comparison of proliferation ability of O/BMMSCs (**A**) and S/BMMSCs (**B**).*

positive SD29 and 63.4% BMMSCs expressed positive CD73; expression rates of MHC-II, CD45 and CD34 were 2.6%, 3% and 4%, respectively; in the OVX group, 95.5% BMMCCs showed positive SCA-1 expression, 75.7% BMMSCs expressed positive CD29 and 69.2% expressed positive CD73; expression rates of MHC-II, CD45 and CD34 were 3.1%, 2.7% and 2.5%, respectively.

Identification results of osteogenic differentiation ability of BMMSCs of OVX group and sham group

Twenty-one days after osteogenic induction, we observed mineralized nodules in both groups under inverted microscope, and the number of mineralized nodules in the OVX group was less than that of the sham group (Fig. 2). Quantitative detection showed that absorption value of BMMSCs in the OVX group was lower than that of the sham group.

Identification results of adipogenic differentiation ability of BMMSCs of OVX group and sham group

Fourteen days after adipogenic induction, oil red O staining was performed. Lipid droplets were observed under an inverted microscope, but the number of lipid droplets in the OVX group was much higher than that of the sham group. Moreover, quantitative detection suggested that absorption value of BMMSCs in the OVX group was higher than that of the sham group. Details are shown in Fig. 3.

Regulatory effect of miRNA on BMMSCs

MSC, an important member of stem cell family, is a multipotential stem cell. MSCs, which were first discovered in bone marrow, have attracted more and more attention for their characteristics of multiple differentiation potential, hematopoietic

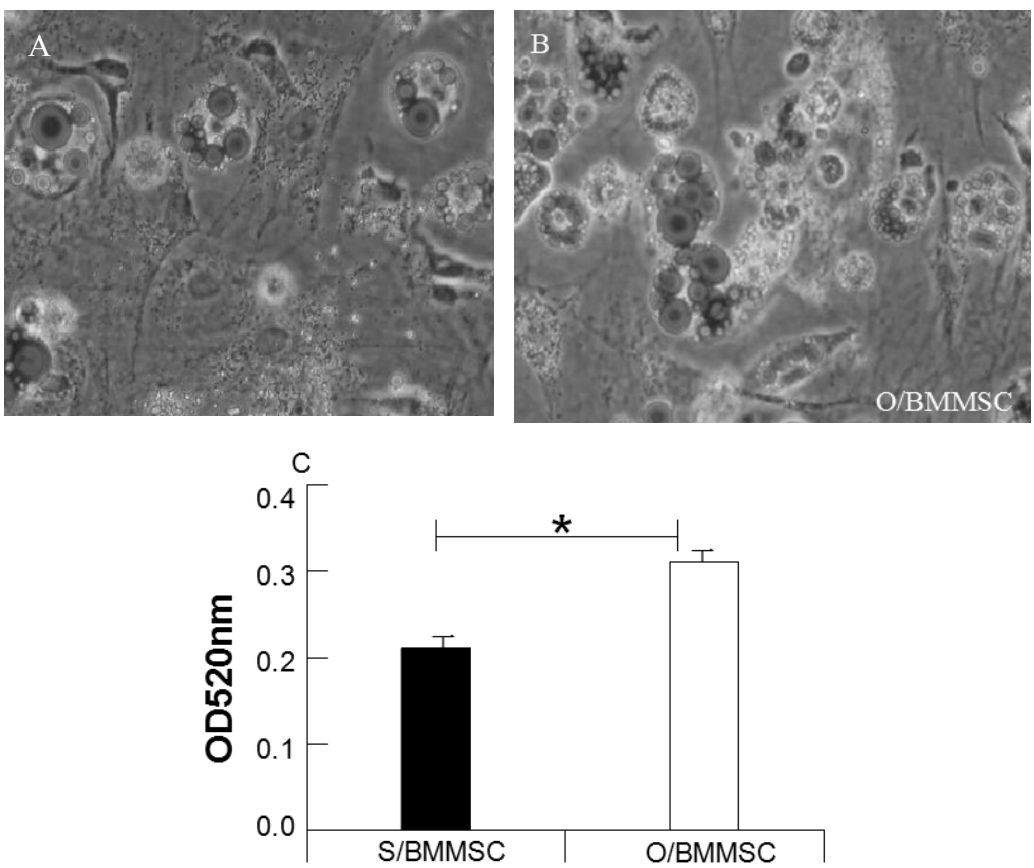

Fig. 3. *Oil red O staining results of BMMSCs of sham group and OVX group. **A**) BMMSCs in sham group observed under microscope 14 days after adipogenic induction. **B**) BMMSCs in OVX group observed under microscope 14 days after adipogenic induction. **C**) quantitative statistics of oil red O staining. *p<0.05)*

support, stem cell implantation promotion and self replication. MSCs have been applied in the treatment of hematological system diseases, cardiovascular disease, liver cirrhosis and nervous system disease, knee joint meniscus injury and autoimmune disease, and have saved many lives. Furthermore, MSCs have a long-term development potential in nerve system repai. Fig. 4 shows BMMSCs of mice observed under microscope.

DISCUSSION

Studies have suggested that functional defect of BMMSCs is one of the primary causes of reduced generation of osteoporotic bone (14, 15). It has been proved that MSCs play an important role in more than five kinds of major tissues in the human body and can also repair bone and support vascular hematopoiesis (16). With immunological properties, MSCs can treat immune and inflammatory disease by playing an immunoregulatory effect via multiple approaches.

MSCs, a small cell group derived from non-hematopoietic stem cells, exist in bone marrow and connective tissue. In 1970, Friedenstein et al. (17) successfully isolated multi-potential MSCs from bone marrow for the first time and pointed out fibroblast-like MSCs were capable of differentiating into fat cells, chondrocytes and osteoblasts and, moreover, could provide a micro-environment for the generation of hematopoietic stem cell.

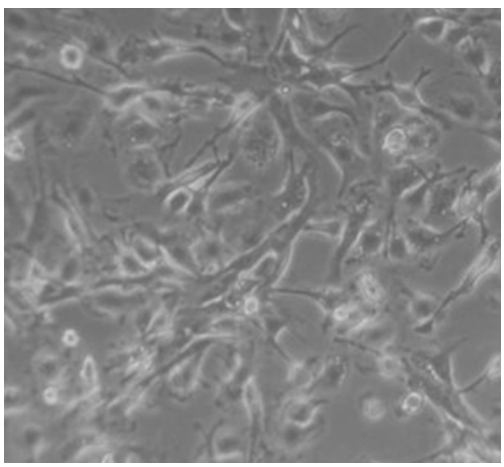

Fig. 4. *BMMSCs of mice.*

Studies on immunoregulation properties of MSCs can be divided into two types, one which blocks or treats rejection reaction of allotransplant with MSCs, and the other restrains abnormal immunoresponse of patients with immunological and inflammatory diseases with MSCs (18). Multiple animal models which were designed having graft-versus-host disease, kidney failure, disseminated sclerosis, rheumatoid arthritis, Crohn's disease and inflammatory bowel disease have been applied in research on immune properties of MSCs. In addition, there is also evidence suggesting miRNA plays a vital role in regulating, updating and multi-directional differentiating stem cells (19). miRNA can keep properties of stem cells, sustain unchanged stem cell proliferation, downregulate genes which sustain undifferentiated state of stem cells, activate stem cell lineage-specific gene and promote directional differentiation of stem cells (20-22).

The innate immune system plays an important role in the immunoreaction process of the human body (23). MSCs can have immunomodulatory effects by interacting with innate immunocytes such as dendritic cells, macrophages and neutrophile granulocytes.

MSCs are able to directly regulate immune response by acting on antigen-presenting cells (APC) (21). Dendritic cell, an APC with the strongest function, can activate the functions of T lymphocytes. MSCs can restrain the generation of T lymphocytes by secreting IL-6, regulating the expression of CD40 and CD86 on the surface of dendritic cells and inhibiting the antigen presentation of dendritic cells (24-26).

Hundreds of miRNAs found in animals and humans possess molecular cell regulating gene expression, indicating miRNA is likely to be involved in regulating gene expression, which is of great significance for future research in this field (27-29). BMMSCs are attracting more and more attention for their special immunoregulation function. Multiple immune and inflammatory diseases, such as systemic lupus erythematosus (SLE), graft-versus-host disease and multiple sclerosis, can all be treated with BMMSCs (30). Allogenic BMMSCs are usually

used for treating immune disease. Therefore, the health condition of BMMSC provider is in a close correlation to treatment effect of immune disease. Kastrinaki et al. (31) found that BMMSCs from patients with rheumatoid arthritis had insignificantly different immunoregulation effect with BMMSCs from healthy people. Moreover, Calkoen et al. (32) also found that MSCs from patients with systematic arthritis had normal immunoregulatory effects. But BMMSCs from patients with graft-versus-host disease have been found to result in more serious immune rejection reaction (33). Therefore, it is of great importance to confirm whether the immunoregulatory effect of BMMSCs can be affected in patients with some diseases.

OP induced by female hormone deficiency in females is a commonly seen senile chronic disease. As the female ages, female hormone secretion reduces and bone absorption increases. Clinical performance of OP induced by menopause is similar to mouse model of OP (34). Pendás found that older people tended to have lower bone density compared to the bone density in their youth. Moreover, bone cortical thickness has a significant decline with aging (35).

This experiment, using mice with estrogen deficiency-induced OP, was carried out to confirm changes of immunoregulation function of BMMSCs. Bilateral ovaries were removed from mice to construct estrogen deficiency-induced OP mice model. We found estrogen deficiency-induced OP mice had decreased BMD, Tb. N and BV/TV compared to fat-removed mice. BMMSCs have a potential of multi-directional differentiation and self-renewing. Hence, we cultured BMMSCs from mice in the OVX group and sham group with osteogenic induction liquid and adipogenic induction liquid, and found they could differentiate into osteoblasts and lipoblasts. But BMMSCs in the OVX group had weaker osteogenic capability and stronger adipogenic capability compared to the sham group. Santiago et al. (36) pointed out that BMMSCs had weak osteogenic capability but strong adipogenic capability in OP patients, which is consistent with results obtained in this experiment. BMMSCs surface antigen detection also proved that BMMSCs in the OVX and sham group both expressed MSCs and epidermic cell surface label SCA-1, CD73 and CD29, but showed up low expression of non-stem cell surface label, MHC-II, CD34 and CD45.

Based on the immunoregulatory effect of BMMSCs and target regulatory effect of miRNA, we set up an estrogen deficiency-induced OP mice model and explored whether BMMSCs had changes of miRNA expression which could lead to immunoregulatory abnormality of BMMSCs.

In conclusion, MSCs with potentials of self-renewing and multi-directional differentiation exist in tissues such as bone marrow, cord blood and fat. MCSs are considered as the ideal candidate cell for bone defect diseases such as OP and osteitis, and are expected to be one of the most potential cells in tissue engineering and clinical treatment. miRNA can regulate MSCs to differentiate into bone under certain conditions, therefore, it plays an important role in bone reconstruction and is the basis of bone formation and metabolism. Reduced bone formation induced by defect of osteogenic differentiation ability is an important pathogenic mechanism for OP.

ACKNOWLEDGEMENTS

This study was supported by joint special fund of Applied Fundamental Research of Kunming Medical University granted by Science and Technology Office of Yunnan, grant no. 2014FZ048.

REFERENCES

1. Eastell R. Identification and management of osteoporosis in older adults. Medicine 2013; 41:47-52.
2. Eastell R. Osteoporosis. Medicine 2013; 41(10):586-91.
3. Papanikou M, Kotsopoulou A. Osteoporosis and somatization of anxiety. Proc Soc Behav Sci 2014; 113:54-61.
4. Grob GN. Pathologizing old age: the case of osteoporosis. MD Advis 2011; 4(2):20-22, 24-27.
5. Abdallah BM, Kassem M. The use of mesenchymal (skeletal) stem cells for treatment of degenerative diseases: current status and future perspectives. J

Cell Physiol 2009; 208(1):9-12.
6. Bianco P, Robey PG, Simmons PJ. Mesenchymal stem cells: revisiting history, concepts, and assays. Cell Stem Cell 2008; 2(4):313-19.
7. Anastasilakis AD, Polyzos SA, Toulis KA. Role of wingless tail signaling pathway in osteoporosis: an update of current knowledge. Curr Opin Endocrinol Diabetes Obes 2011; 18:383-88.
8. Oheim R, Beil FT, Barvencik F, Egermann M, Amling M, Clarke IJ, Pogoda P. Targeting the lateral but not the third ventricle induces bone loss in ewe: an experimental approach to generate an improved large animal model of osteoporosis. J Trauma Acute Care Surg 2012; 72:720-26.
9. Soltis AR, Saucerman JJ. Robustness portraits of diverse biological networks conserved despite order-of-magnitude parameter uncertainty. Bioinformatics 2011; 27(20): 2888-94.
10. Zhang Q, Xiao XH, Li M, et al. miR-375 and miR-30d in the effect of chromium-containing Chinese medicine moderating glucose metabolism. J Diabet Res 2014; 2014(1):173-89.
11. Elham E, Wang Y H, Wang L, et al. Combined closed-circuit acute normovolemic Hemodilution and deliberate hypotension in a Jehovah's witness: a case report. Chin J Tissue Eng Res 2015; 18(14):2167-72.
12. Li CH, Wang XW, Wang QT. Immunomodulatory effect of mesenchymal stem cells. Prog Mod Biomed 2009; 43(2):425-30.
13. Zhang BH, Pan XP, Anderson TA. miRNA: a new player in stem cells. J Cell Physiol 2006; 209(2):266-69.
14. Hideaki K, Hideki A, Arinobu T. Bone marrow stromal cells (bone marrow-derived multipotent mesenchymal stromal cells) for bone tissue engineering: Basic science to clinical translation. Int J Biochem Cell Biol 2010; 43 (3):286-89.
15. Nemeth K, Mezey E. Bone marrow stromal cells as immunomodulators. A primer for dermatologists. J Dermatolog Sci 2015; 77:11-20.
16. Ren JQ, Stroncek DF, Zhao Yingdong, et al. Intra-subject variability in human bone marrow stromal cell (BMSC) replicative senescence: Molecular changes associated with BMSC senescence. Stem Cell Res 2013;11(3):1060-73.
17. Friedenstein AJ, Chailakhjan RK, Lalykina KS. The development of fibroblast colonies in monolayer cultures of guinea-pig bone marrow and spleen cells. Cell Tissue Kinet1970; 3(4):393-403.
18. Dennis GJ, Mond JJ. Corticosteroid-induced suppression of murine B cell immune response antigens. J Immunol 1986; 136(5):1600-604.
19. Redshaw Z, Sweetman D, Loughna PT. The effects of age upon the expression of three miRNAs in muscle stem cells isolated from two different porcine skeletal muscles. Differentiation 2014; 88(4-5):117-23.
20. Houbaviy HB, Murray MF, Sharp PA. Embryonic stem cell-specific miRNAs. Dev Cell 2003; 5(2):351-58.
21. Ishii H, Saito T. Radiation-induced response of micro RNA expression in murine embryonic stem cells. Med Chem 2006; 2:555-63.
22. Kleftogiannis D, Korfiati A, Theofilatos K, Likothanassis S, Tsakalidis A, Mavroudi S. Where we stand, where we are moving: Surveying computational techniques for identifying miRNA genes and uncovering their regulatory role. J Biomed Inform 2013; 46(3):563-73.
23. Mann DL, Topkara VK, Evans S, Barger PM. Innate immunity in the adult mammalian heart: for whom the cell tolls. Transact Am Clin Climatolog Assoc 2010; 121:34-50; discussion 50-1.
24. Jiang XX, Zhang Y, Liu B. Human mesenchymal stem cells inhibit differentiation and function of monocyte derived dendritic cells. Blood 2005; 105:4120-26.
25. Ramasamy R, Fazekasova H, Lam EW, Soeiro I, Lombardi G, Dazzi F. Mesenchymal stem cells inhibit dendritic cell differentiation and function by preventing entry into the cell cycle. Transplantation 2007; 83:71-76.
26. Aggarwal S, Pittenger MF. Human mesenchymal stem cells modulate allogeneic immune cell responses. Blood 2005; 105:1815-22.
27. Wu XJ, Zeng R, Wu SK, Zhong JX, Yang LW, Xu JF. Comprehensive expression analysis of miRNA in breast cancer at the miRNA and isomiR levels. Gene 2015; 557:195-200.
28. Chang JY, Chang MY, Wu YL, Syu FJ. Development of a miRNA biochip platform. Biomarkers and Genomic Medicine, 2014; 6(4):154-58.
29. Báez A, Martín-Antonio B, Piruat JI, Barbado MV, Prats C, Álvarez-Laderas I, Carmona

M, Pérez-Simón JA, Urbano-Ispizua Á. Gene and miRNA expression profiles of hematopoietic progenitor cells vary depending on their origin. Biol Blood Marrow Transplant 2014; 20(5):630-39.

30. Uccelli A, Moretta L, Pistoia V. Mesenchymal stem cells in health and disease. Nat Rev Immunol 2008; 8(9):726-36.
31. Kastrinaki G, Lorentzou S, Konstandopoulos A G. Soot oxidation kinetics of different ceria nanoparticle catalysts. Emiss Cont Sci Technol 2015; 1(3):247-53.
32. Calkoen E, Koning PJD, Geest RJVD, Roos AD, Westenberg JJ, Roest A. Vortex flow in the left atrium in healthy controls and patients with mitral valve regurgitation after atrioventricular septal defect correction: evaluation with 4D flow MRI and particle tracing. J Cardiov Magn Reson 2015; 17(1):1-2.
33. Nauta AJ, Westerhuis G, Kruisselbrink AB, Lurvink EGA, Willemze R, Fibbe WE. Donor-derived mesenchymal stem cells are immunogenic in an allogeneic hostand stimulate donor graft rejection in a nonmyeloablative setting. Blood 2006; 108:2114-20.
34. Egermann M, Goldhahn J, Schneider E. Animal models for fracture treatment in osteoporosis. Osteoporos Int 2005;16(2):S129-38.
35. Pendás A, Zhou Z, Cadinanos J, Freije JMP, Wang JM, Hultenby KR. Defective prelamin A processing and muscular and adipocyte alterations in Zmpste24 metalloproteinase–deficient mice. Nat Genet 2002; 31(1):94-99.
36. Santiago-Mora R, Casado-Diaz A, De Castro MD, Quesada-Gomez JM. Oleuropein enhances osteoblastogenesis and inhibits adipogenesis: the effect on differentiation in stem cells derived from bone marrow. Osteop Int 22(2):675-84.

TARGETING LEUKEMIC SIDE POPULATION CELLS BY ISATIN DERIVATIVES OF NICOTINIC ACID AMIDE

A.M. NAGLAH[1,2], Z. SHINWARI[3], M.A. BHAT[1], M. AL-TAHHAN[3], M.A. AL-OMAR[1] and A. AL-DHFYAN[3,4]

[1]Department of Pharmaceutical Chemistry, College of Pharmacy, King Saud University, Riyadh, Saudi Arabia; [2]Peptide Chemistry Department, Chemical Industries Research Division, National Research Centre, Dokki, Cairo, Egypt; [3]Stem Cell & Tissue Re-Engineering Program, Research Center, King Faisal Specialized Hospital and Research Center, Saudi Arabia; [4]Department of Pharmacology and Toxicology, College of Pharmacy, King Saud University, Riyadh, Saudi Arabia

Received September 9, 2015 – Accepted March 16, 2016

Side population (SP) cells mediate chemoresistance in leukemia. However, chemical inhibition approach to target SP cells has been poorly studied. Herein, we report the discovery of isatin derivatives of nicotinic acid amide as potent side population cell inhibitors. The selected derivatives showed superior potency over the reference drug verapamil. Furthermore, the treatment increased chemosensitivity and inhibited the cell proliferation on three different leukemic cell lines, K562, THP-1 and U937, suggesting that both SP and the bulk of leukemic cells are affected. Moreover, treatment with the most potent compound Nic9 reduced the expression of ABCG2, demonstrating that side population inhibition effect of the target derivatives is at least via ABCG2 inhibition. Importantly, the target derivatives induced erythrocyte/dendritic differentiation to leukemic cells mainly through Musashi/Numb pathway modulation.

Leukemia can be described as abnormal hematopoietic tissue initiated by a few leukemic stem cells (LSCs) that undergo an aberrant and poorly regulated process of organogenesis similar to that of normal hematopoietic stem cells (1). One of the main properties of cancer stem cells (CSCs) is resistance to a given therapy and ability to survive the primary treatment and relapse. A number of factors may govern this phenomenon, including stem cell quiescence, protected niche environment, upregulated expression of xenobiotic efflux pumps, and enhanced anti-apoptotic and DNA repair pathways (2). CSCs can be isolated and enriched by a variety of techniques and methods, including cell surface markers and dye excluded side population (SP). Dye excluded SP method was first described in murine bone marrow and SP cells represented a small subset of cells that were enriched at least 1000-fold in hematopoietic stem cell (HSC) activity (3). The SP cells are identified according to their ability to efflux the Hoechst dye at a higher pace than the remaining tumor cells termed the main population (non-SP). Furthermore, the degree of efflux activity seems to correlate with the maturation state, so that cells displaying the highest efflux activity are

Key words: isatin, nicotinic acid amide,, side population cells (SP), chemoresistance, cell proliferation, ABCG2, Musashi/Numb pathway

Mailing address:
Dr Abdullah Al-Dhfyan,
Stem Cell & Tissue Re-Engineering Program, Research Center,
King Faisal Specialized Hospital & Research Center,
MBC-03, PO Box 3354, Riyadh 11211, Saudi Arabia
Tel.: +966 506286770 - Fax: +966 1 4647272
e-mail: aaldhfyan@kfshrc.edu.sa

0393-974X (2016)

DISCLOSURE: ALL AUTHORS REPORT NO CONFLICTS OF INTEREST RELEVANT TO THIS ARTICLE.

the most primitive in terms of differentiation potential (4). More importantly, in the patients with B-cell chronic lymphocytic leukemia, SP cells appeared resistant to conventional B cell-chronic lymphocytic leukemia (B-CLL) treatments, such as fludarabine, bendamustin or rituximab (5). Accordingly, in order to block the chemoresistance of leukemic cells, there is an urgent need to develop small molecule inhibitors of side population (SP) cells. Nicotinic acid derivatives and its isomers have anti-bacterial, anti-oxidant, anti-inflammatory, anti-carcinogenic and anti-tubercular activities (6). Isatin constitutes an important class of bioactive compounds exhibiting caspase inhibition and anti-proliferative activity (7-9). One of the main ways to treat leukemia is by induced differentiation. The concept of differentiation therapy of cancer is ~40 years old. Despite many encouraging results obtained in laboratories, in both *in vitro* and *in vivo* studies, the only really successful clinical application of differentiation therapy was all-trans-retinoic acid (ATRA)-based therapy of acute promyelocytic leukemia (APL) (10). One of the main pathways that regulate stem/differentiation state of leukemic cells is Musashi/Numb pathway. The Musashi (Msi) family is a group of RNA-binding proteins characterized by two RNA recognition motifs (RRMs) and is evolutionarily conserved (11). In mammals, the function of Msi has been found to activate Notch signaling through the translational repression of NUMB, which represses an intracellular Notch signaling, by binding to the 3′ untranslated region (UTR) of the Numb mRNA thereby activating self-renewal state (12). In our laboratory, through small screening program, we reported the discovery of many active small molecules that are able to target different subpopulation of CSCs, including SP cells and CD133 positive cells and ALDH positive, cells (13-15). Herein, we report the discovery of isatin derivatives of nicotinic acid amide as potent SP cell inhibitors and differentiation cell inducers via upregulation of the cell fate determinant Numb.

MATERIALS AND METHODS

Chemistry

All the tested compounds were synthesized, described and fully characterized according to previously reported procedures (16).

Biological Evaluation

Cell line and tissue culture

K562, THP-1 and U937 cell lines were purchased from the American Type Culture Collection. Cells were maintained in RPMI 1640 (Sigma), supplemented with 10% FBS (Lonza), 100IU/mL penicillin, 100mg/mL streptomycin and 2mmol/L L-glutamine (Sigma). Cell viability was assessed by trypan blue exclusion analysis. Cell numbers were determined by using a hemacytometer.

Side population staining by DyeCycle™ violet stain

For DCV staining, cells were pelleted and suspended in RPMI cell culture medium at a concentration of $1*10^6$ cells/mL. DCV (Invitrogen Molecular Probes®, Eugene, OR) was added at a final staining concentration of 10 μM, as this concentration gave optimal separation between SP and non-SP cells. PI stained was used to exclude dead cells. To gate only side population cells, a reference blocker Virapamil (100 μM) was used. All analyses were performed on a FACS LSRII (BD Biosciences). Debris and cell clusters were excluded during side-scatter and forward-scatter analyses.

WST-1 cell proliferation assay

Cells were seeded into 96-well plates at $0.4*10^4$/well and incubated overnight. The medium was replaced with a fresh one containing the desired concentrations of the compounds. After 48 h, 10 μL of the WST-1 reagent was added to each well and the plates were re-incubated for 4 h at 37°C. The amount of formazan was quantified using ELISA reader at 450 nm.

Apoptosis assay

Vybrant apoptosis assay kit (Annexin-V, APC conjugate; Molecular Probes™) was used to evaluate cell viability as per the manufacturer's recommendation. Briefly, both adherent and floating cells were collected. DAPI (4′,6-diamidino-2-phenylindole) was used as a viability dye. Fluorescence was analyzed on a total of 10^4 cells per sample using a flow cytometer and cells were considered viable if they were double negative for Annexin-V and DAPI.

Western blot

SDS-PAGE was performed using 12% separating mini gels, the protein load was 30 μ) for each sample. After separation the protein was transferred from the gel onto polyvinylidene difluroide membrane (PVDF). Next, the membrane was incubated overnight with the appropriate antibodies, ABCG2 (Aviva System Biology) Numb and GAPDH (Cell Signaling) then developed using Image Quant LAS-4010.

Immunofluorescence microscopy

K562 cells were cultured in 6-well plate and treated by Ni9 with various doses for 48 hours. The cells of treated and untreated wells were washed, dried and fixed in 4% formaldehyde. Cells were stained overnight with anti-Musashi1,2 and anti-Numb (Cell Signaling) at 1:100. Cells were washed and stained with secondary Abs FITC (Invitrogen). DAPI (Invitrogen) was added for 10 min to counterstain the nuclei. Slides were mounted and immunofluorescence was visualized using BD Pathway 855 system.

Differentiation analysis

The differentiation of K562 cells was followed by the increase in the expression of marker as follows: CD271 for dendritic cells differentiation, glycophorin GYPA for erythrocyte differentiation and CD15 for macrophage differentiation. Anti-CD34 (FITC), anti-CD271 (APC), anti-GYPA (FITC), anti-CD15 (FITC) were purchased from BD Pharmingen™. Cells were freshly stained and incubated for 45 min on ice in phosphate buffered saline with 2% FBS. Side scatter and forward scatter profiles were used to eliminate cell doublets and DAPI was used to eliminate dead cells. Flow cytometry was performed on a BD™ LSR II flow cytometer.

RESULTS

Chemistry

In the present work, originally, the isatin derivatives of nicotinic acid amide were designed based on the suggestion that the coupling of two heterocyclic compounds (nicotinic acid and isatin), *via* certain amino acid as a bridge, could result in producing small molecules with potent biological activity.

Side population inhibition effect of isatin derivatives of nicotinic acid amide

In order to find a series of compounds that showed activity to block the chemo resistance of leukemic cells, we used a dye-excluded side population technique. The percentage of SP cells of untreated and treated K562 cells was measured and the inhibition percentage was given for each derivative shown in Table I. The SP cell analysis showed a potent inhibition effect against leukemic SP cells compared with untreated cells as can be seen in Fig. 1, A and B. The target derivatives showed inhibition effect with more than 50% at 10 μM. Compared with reference SP cell inhibitor drug virapamil, the target derivatives showed a potent effect of at least 5-fold. The ranging effect of verapamil took a place between 50 to 200 μM. All the tested compounds showed > 50% inhibition effects on side population cells at 10 μM, except Nic2.

Cell proliferation inhibition and chemoresistance blocking effect of isatin derivatives of nicotinic acid amide

To test whether these compounds may have activity on the bulk of tumor cells, we performed cell proliferation WST-1 assay by using three different leukemic cell lines, K562, THP-1 and U937. All the tested compounds showed inhibitory effect on these cell lines with IC_{50}> 10 μM, and the most active compound on K562 cells was Nic10 with IC_{50}=20μM, indicating the selectivity of these series toward SP cells, and the effect was cell proliferation and cell toxicity independent. *In vitro* cytotoxic activity of the prepared compounds against cancer cell lines were measured and recorded in Table II.

The cross talk between chemoresistance of leukemic cells and SP is very high, therefore, we hypothesized that the inhibition of side population cells by the target derivatives may increase the sensitivity of leukemic cells to chemotherapy. To test our hypothesis, we used the induction of apoptosis by chemotherapeutic agent Mitoxantrone at 100 nM alone or after one-day treatment by the most active compound Nic9 as test for increased chemo-sensitivity. The treatment by the mentioned compound, one day before the chemotherapy,

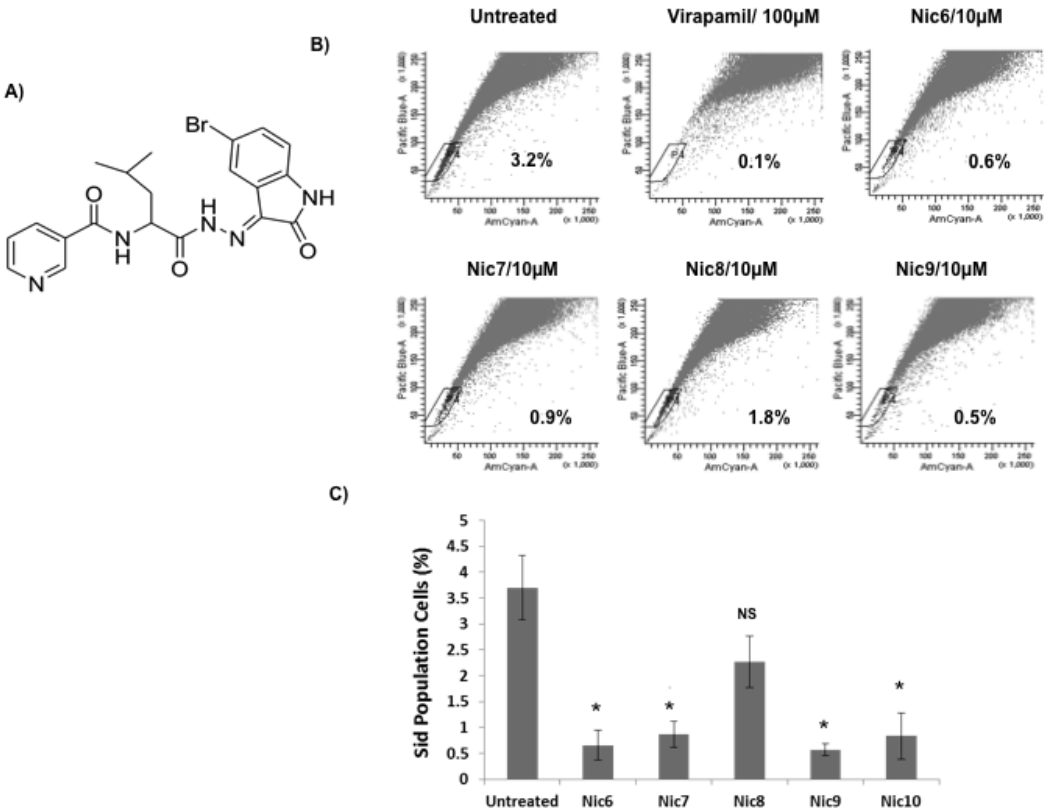

Fig. 1. ***A)*** *The chemical structure of the most potent member Nic9.* ***B)*** *DCV SP staining of K562 cells treated with Isatin derivatives of nicotinic acid amide Nic6-9 10 μM and SP inhibitor reference drug Verapamil 100 μM for 48 hrs.* ***C)*** *Bar graph showing SP% cells after treatment with Nic 6-10. Data represent the average ± SD (error bar) of three independent experiments.*

increased the sensitivity of leukemic cells to apoptosis as shown in Fig. 2, A and B. Mitoxantrone alone at 100 nM increased apoptosis by 25% while the combination therapy increased apoptosis by 50%, showed a synergistic effect in the combination therapy compared with chemotherapy alone.

ABCG2 inhibition effect of isatin derivatives of nicotinic acid amide

ATP-binding cassette sub-family G member 2 (ABCG2) is defined as specific marker for the SP in many tissues. Furthermore, it is highly expressed in SP cells and is responsible for the maintenance of SP phenotype (17). In order to test whether these derivatives inhibit the expression of ABCG2, we used Western blot technique to show the expression of ABCG2 protein in K562 cells treated with different doses of the most active compound Nic9. The treatment showed inhibition in the expression of ABCG2 level in 5 and 10 μM concentrations. However, the treatment with low dose 2.5 μM showed no effect in the expression suggesting that the effective low range of theses derivatives is 5 μM. Importantly, the treatment had no effect on internal protein control GAPDH, as seen in Fig. 3.

Isatin derivatives of nicotinic acid amide induced differentiation to leukemic cells through musashi/ numb pathway modulation

Recently, induced cell differentiation has been gaining major attention since CSCs are one of the major obstacles for cancer treatment. The target derivatives showed a potent inhibitory effect on SP cells, therefore, we hypnotized that the treatment may induce differentiation to leukemia cells given that SP cells are highly enriched by CSCs.

Table I. *Side Population (SP) % of K562 cells treated with compounds (1-10) and the inhibition % compared with untreated cells.*

Compounds	Side Population % [*]at 10 μM	Inhibition % [#]
1	3.23±**0.7**	12.61
2	4.86±**0.7**	-31.53[&]
3	2±**0.1**	45.94
4	3.53±**0.47**	4.50
5	2.4±**0.1**	35.13
6	0.65±**0.28**	82.25
7	0.86±**0.25**	76.57
8	2.26±**0.5**	38.73
9	0.56±**0.1**	84.68
10	0.83±**0.45**	77.47

[*] *Side population % as Mean*±**SD** *of three independent experiments.*
[#] *Inhibition % =100-(SP% of treated cells/SP% of untreated cells)*100.*
[&] *Minus sign indicated that the compound* ***2*** *increased SP%.*

Table II. *In vitro cytotoxic activity of the prepared compounds against cancer cell lines.*

Compounds	IC_{50} [a] (μM)		
	Histiocytic lymphoma U937	Acute monocytic leukemia THP-1	Chronic myelogenous leukemia K562
1	26.18±0.01	In[b]	84.92±0.05
2	47.78±0.28	39.77±0.26	45.68±0.05
3	13.82±0.37	26.40±0.17	22.15±0.07
4	16.81±0.08	17.22±0.36	28.36±0.07
5	27.20±0.29	127.30±0.08	70.70±0.06
6	53.58±0.44	45.40±0.59	58.20±0.02
7	84.89±0.22	57.42±0.38	46.41±0.04
8	11.90±0.09	24.87±0.47	21.65±0.2
9	16.63±0.36	21.19±0.25	24.16±0.04
10	18.70±0.06	18.99±0.17	20.11±0.02

[a] IC_{50}*: concentration of the compound (μM) producing 50% cell growth inhibition after 48 h of compound exposure.*
[b] *Inactive within 300 μM concentration range.*

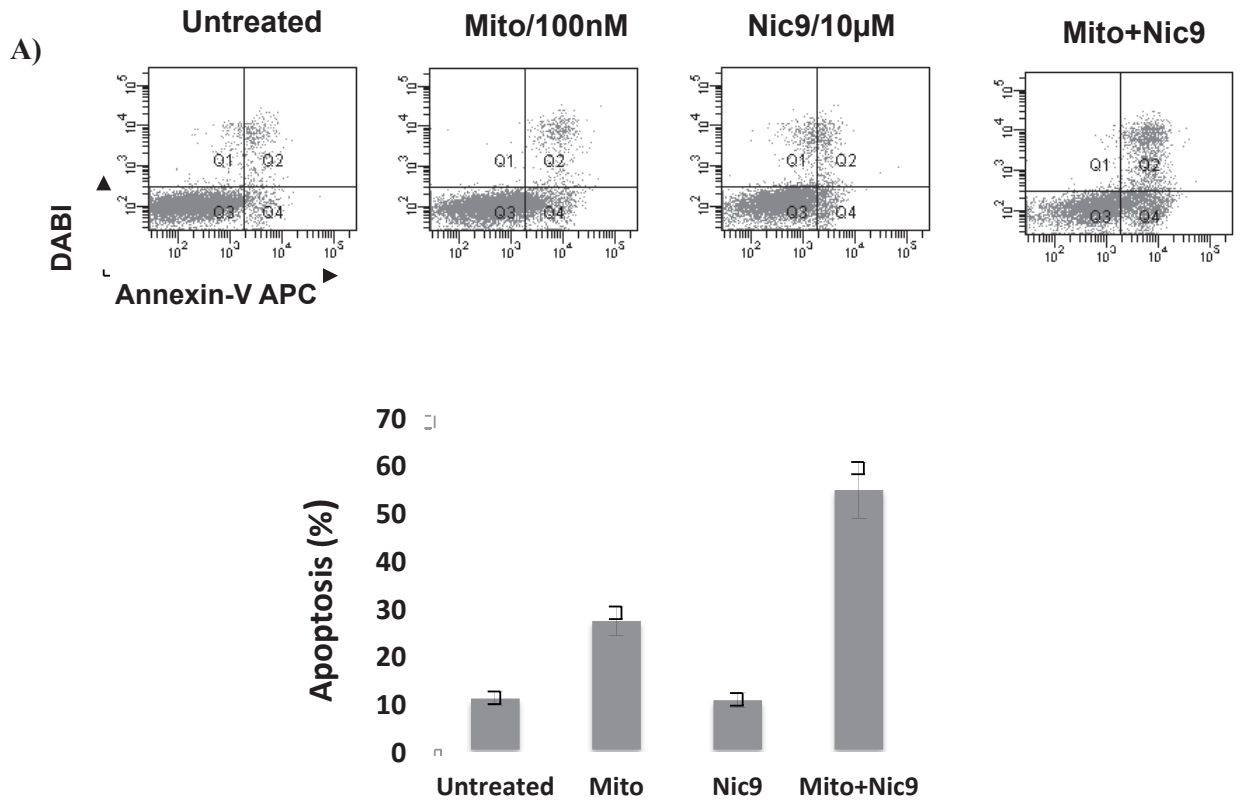

Fig. 2. ***A)*** *Dot plot of Annexin V and DABI staining following treatment of K562 cells with chemotherapeutic agent Mitoxantrone alone and Nic9 alone and the combination for 48 h.* ***B)*** *Bar graphs showing mean ± SD. apoptotic cells of chemotherapy alone and the combination with Nic9. The pretreatment of leukemic cells with Nic9 increased the killing effect of Mitoxantrone by 2-fold. Data represent the average ± SD (error bar) of three independent experiments.*

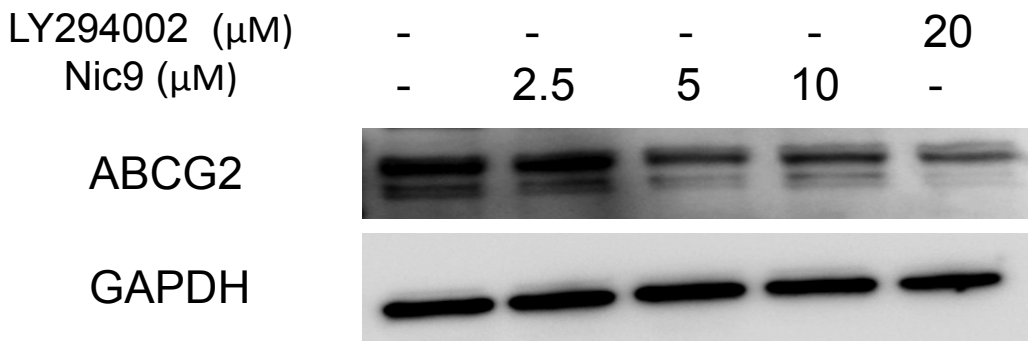

Fig. 3. *Western blot showing the expression levels of ABCG2 in K562 cells following treatment with various doses of Nic9 for 48 h. AKT pathway inhibitor LY294002 was used as positive control for ABCG2 inhibition.*

To examine our hypothesis, a panel of stem and differentiation markers, namely CD34 for leukemic CSCs, CD271 for dendritic cell differentiation, glycophorin GYPA for erythrocyte differentiation and CD15 for macrophage differentiation, were used. Flowcytometric analysis of K562 cells treated with Nic9 showed a decrease in the expression of leukemic cancer stem cell marker CD34. Accompanied with the decrease in the expression of stem cell marker, expression of CD271 increased by about one-fold in 5 and 10 μM concentrations. Increasing the concentration to 20 μM resulted in an approximate 4-fold increase of CD271 positive cells, as shown in Fig. 4, A and B. The increase in CD271 expression was concentration-dependent. The treatment also increased the expression of glycophorin GYPA. The increased in GYPA was in a concentration-independent manner in which the highest induction, about 3-fold, was detected in 5 μM. The lower induction of GYPA was detected in the higher concentration 20 μM. The treatment showed no increase in macrophage marker CD15. The results demonstrated that isatin derivatives of nicotinic acid amide induced erythrocyte and dendritic cell differentiation but not macrophages differentiation.

One of the main pathways that regulate stem/differentiation state of leukemic cells is Musashi/Numb pathway. Therefore, we asked whether the derivatives main effect is through the said pathway or not. In order to evaluate the effect of isatin derivatives of nicotinic acid amide on Musashi/Numb pathway, we used immunefluorescence microscopy to visualize both proteins in the treated and untreated K562 cells. As seen in Fig. 5A, inhibition in the expression of Musashi1 and 2 was observed. In contrast to inhibition of Musashi1and 2, a detectable increase in the expression of cell fate determined Numb protein in K562 cells treated with Nic9 compared with untreated cells, as shown in Fig. 5B. The increase in the expression was dose-dependent in which the highest induction was seen in 20 μM. The induction of expression was in both nucleus and the cytoplasm. For further confirmation, we used Western blot to detect the change on the expression of Numb protein after treatment. Nic9 treatment by the same protocol resulted in the increase in Numb protein expression in a dose-dependent manner, mimicking the results of immunofluorescence, as shown in Fig. 5C.

DISCUSSION

Chemoresistance remains the main reason for relapse and represents the most significant obstacle to successful chemotherapy for cancer and particularly for leukemia. The cross-talk between chemoresistance and cancer stem cells is very high. The SP cells are identified according to their ability to efflux the fluorescence dyes, and are responsible for chemoresistance in leukemia. In this manuscript, we report a novel activity of interested conjugation of nicotinic acid and isatin nucleus through amino bridge. The hybrid derivatives showed a potent inhibitory effect against leukemic side population SP cells. The target derivatives showed >50% inhibition activity at 10 μM, whereas the reference drug Virapamil showed >50% inhibition activity at 100 μM, demonstrating superior potency of these series. In agreement with previous reports demonstrating that SP cells are enriched by cancer stem cells CSCs, we provide proof of selective elimination of SP cell phenotype in K562 cells which may have application to overcome the chemoresistance and induce differentiation to leukemic cells. The pre-treatment sensitized leukemic cells to chemotherapy. Interestingly, the treatment with Nic9 alone, showed no increased in apoptosis suggesting that the target derivatives SP inhibition effect is through a therapeutic response and not through toxicity response, increasing the potential of the preclinical and clinical development of isatin nicotinic acid amides as SP inhibitor for the treatment of leukemia.

The role of ABCG2 in the regulation of SP cell phenotype is well characterized. Furthermore, ABCG2 is sharply down-regulated during hematopoietic stem cell differentiation and is expressed at a low level in mature cells compared with progenitor cells (18). The highly regulated expression of ABCG2 suggests that ABCG2 may play a regulatory role in maintaining stem cells in an undifferentiated state (19). CSCs are also supposed to be responsible for the acquisition of multi-drug

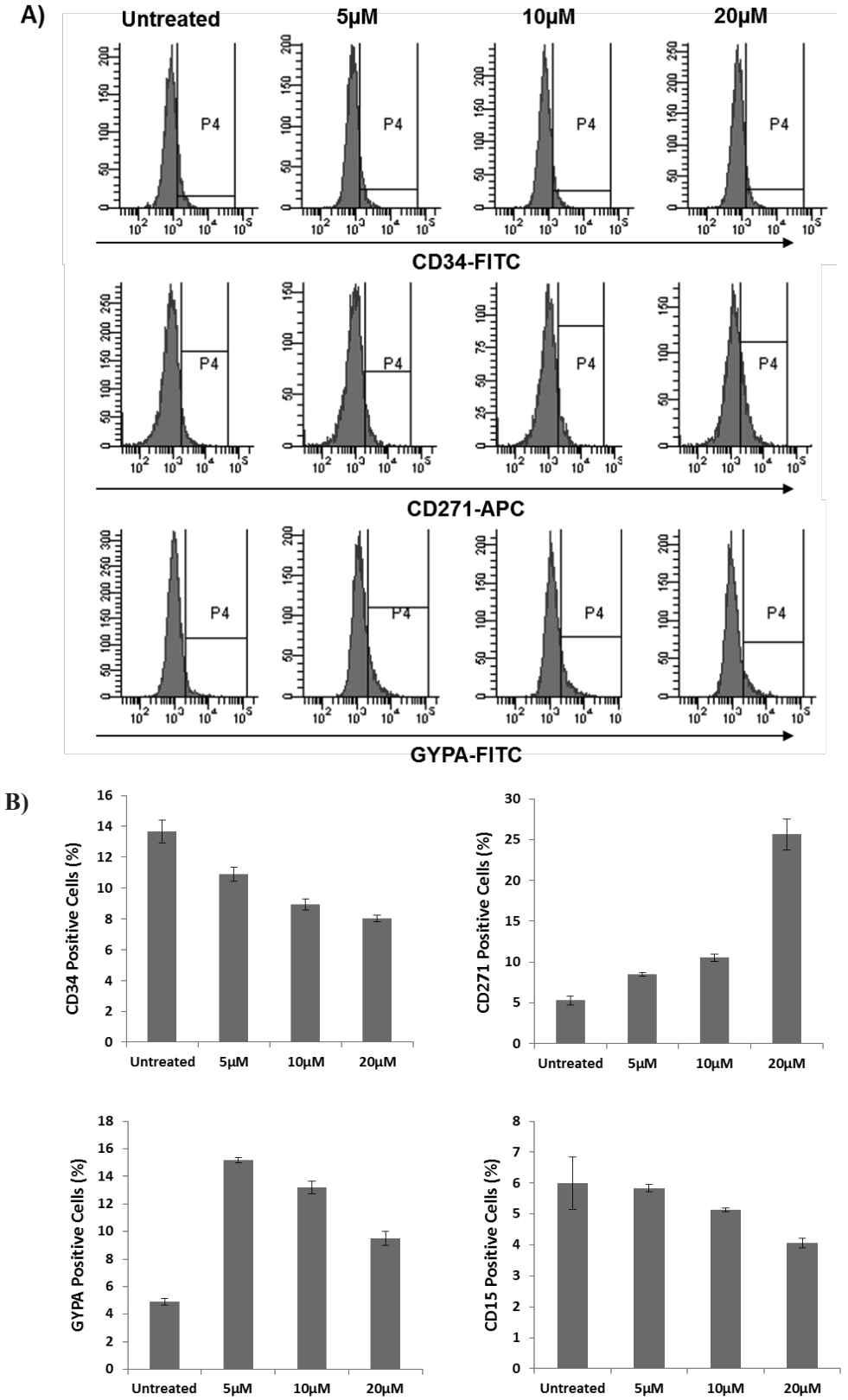

Fig. 4. ***A)*** *Histograms of different CD markers of K562 cells treated with Nic9 10 μM for 48 hrs.* ***B)*** *Bar graph showing positive cell percentage after treatment with Nic9. Data represent the average ± SD (error bar) of three independent experiments.*

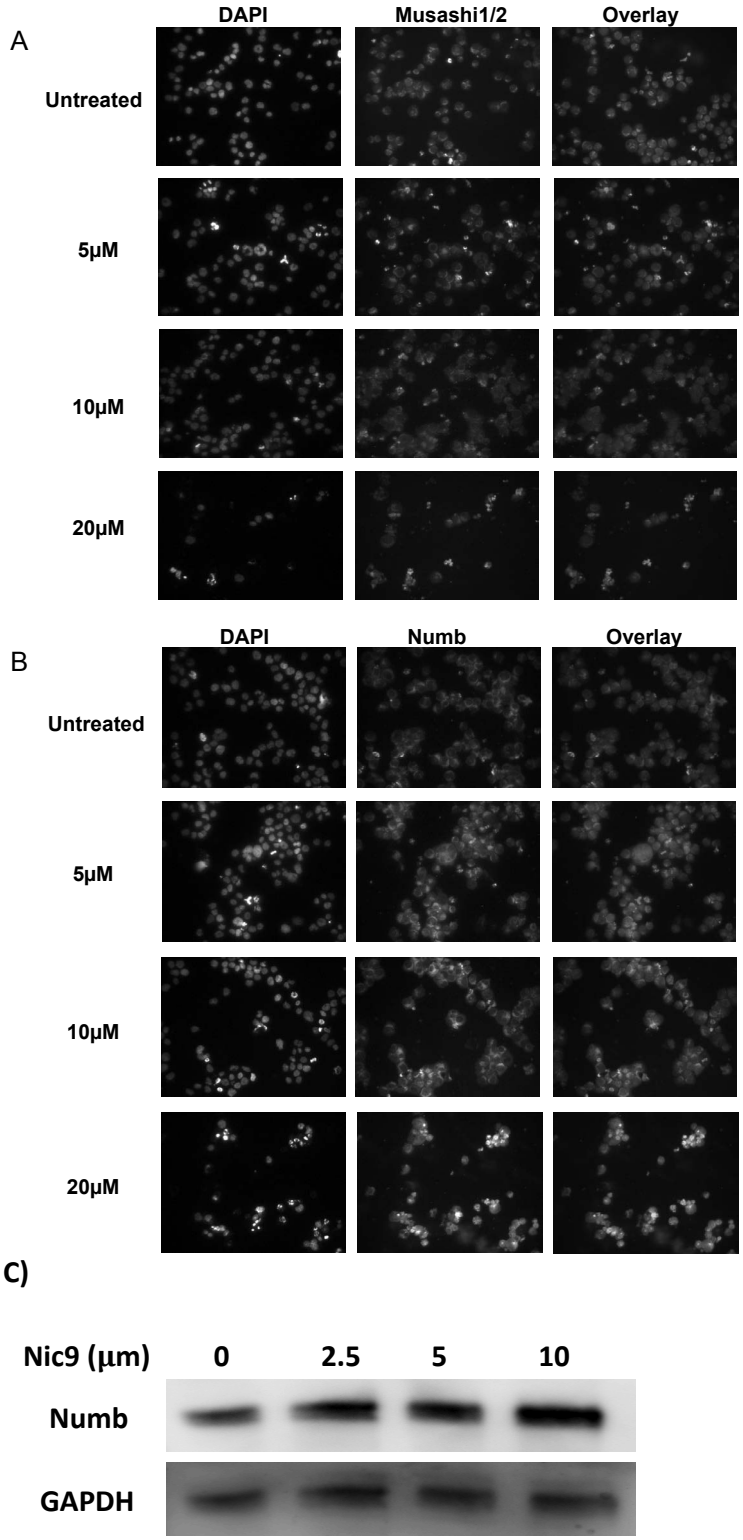

Fig. 5. *Using immunofluorescence staining for Numb and Musashi1,2 on K562 cells treated with different doses of Nic9 for 48 hrs.* ***A****) IF staining sowed decreased in the expression of Musash1,2 in a dose-dependent manner.* ***B****) In contrast of Musashi1,2 inhibition, the treatment by various doses of Nic9 increased the expression of Numb.* ***C****) Western blot showing the expression levels of Numb in K562 cells following treatment with various doses of Nic9 for 48 h.*

chemoresistance and lead to cancer relapse. Side population SP and chemoresistance suggest a close link between ABCG2 and CSCs. Targeting CSCs by the small molecule compound inhibitor of ABCG2 represents an attractive strategy because dual effect which reverses chemoresistance and induces differentiation to cancer cells. Therefore, we suggest that isatin derivatives of nicotinic acid amide had a dual targeted effect on leukemic stem cells via SP cells and ABCG2.

Induced cell differentiation is gaining major attention since CSCs are one of the major obstacles for cancer treatment. We demonstrated induction of leukemic cells to differentiate to erythrocyte and dendritic cells but not to macrophages. One of the main pathways that regulate stem/differentiation state of leukemic cells is Musashi/Numb pathway. The most potent member in this series, Nic9, inhibits the expression of stem cell driver Musashi1 and 2 proteins. The Musashi (Msi) family is a group of RNA-binding proteins characterized by two RNA recognition motifs (RRMs).(13) In mammals, the function of Msi has been found to activate Notch signaling through the translational repression of NUMB, which represses an intracellular Notch signaling by binding to the 3′ untranslated region (UTR) of the Numb mRNA and therefore activating self-renewal state (12). In myeloid leukemia cells, MSI2 is highly expressed, and depletion results in decreased proliferation and increased apoptosis (20); for this reason, we can indicate that isatin derivatives of nicotinic acid amide cell proliferation inhibition and chemotherapy sensitization effects are mainly through Msashi/Numb pathway modulation.

To our knowledge, this is the first report to demonstrate functional targeting of leukemic SP cells by using isatin derivatives of nicotinic acid amide, supporting the preclinical and clinical development to block the chemoresistance and induce differentiation to leukemic cells.

ACKNOWLEDGEMENTS

The authors would like to extend their sincere appreciation to the Deanship of Scientific Research at King Saud University for funding this work through Research Group no. (RG. 1436 - 015).

The authors (Z.S, M.A. and A.A.) would like to thank the research centre administration at King Faisal Specialized Hospital KFSHRC for their support.

REFERENCES

1. Passegue E, Jamieson CH, Ailles LE, Weissman IL. Normal and leukemic hematopoiesis: are leukemias a stem cell disorder or a reacquisition of stem cell characteristics? Proc Natl Acad Sci U S A 2003; 100:1842-49.
2. Bomken S, Fiser K, Heidenreich O, Vormoor J. Understanding the cancer stem cell. Br J Cancer 2010; 103:439-45.
3. Goodell MA, Rosenzweig M, Kim H, Marks DF, DeMaria M, Paradis G, Grupp SA, Sieff CA, Mulligan RC, Johnson RP. Dye efflux studies suggest that hematopoietic stem cells expressing low or undetectable levels of CD34 antigen exist in multiple species. Nat Med 1997; 3:1337-45.
4. Richard V, Nair MG, Santhosh Kumar TR, Pillai MR. Side population cells as prototype of chemoresistant, tumor-initiating cells. Biomed Res Int 2013:517237.
5. Gross E, L'Fagihi-Olive FE, Ysebaert L, et al. B-chronic lymphocytic leukemia chemoresistance involves innate and acquired leukemic side population cells. Leukemia 2010; 24:1885-92.
6. Lourenço MCS, d Souza MVN, Pinheiro AC, Ferreira Mde L, Onçalves RS B, Nogueira TCM, Peralta MA. Evaluation of anti-tubercular activity of nicotinic and isoniazid analogues. Arkivoc 2007; 15:181-91.
7. Chu W, Zhang J, Zeng Cet al. N-benzylisatin sulfonamide analogues as potent caspase-3 inhibitors: synthesis, in vitro activity, and molecular modeling studies. J Med Chem 2005; 48:7637-47.
8. Chu W, Rothfuss J, Chu Y, Zhou D, Mach RH. Synthesis and in vitro evaluation of sulfonamide isatin Michael acceptors as small molecule inhibitors of caspase-6. J Med Chem 2009; 52:2188-91.
9. Chohan ZH, Pervez H, Rauf A. Khan KM, Supuran CT. Isatin-derived antibacterial and antifungal compounds and their transition metal complexes. J Enzyme Inhib Med Chem 2004; 19:417-23.
10. Marchwicka A, Cebrat M, Sampath P, Snieżewski L, Marcinkowska E. Perspectives of differentiation

therapies of acute myeloid leukemia: the search for the molecular basis of patients' variable responses to 1,25-dihydroxyvitamin D and vitamin D analogs. Front Oncol 2014; 4:125.

11. Okano H, Imai T, Okabe M. Musashi: a translational regulator of cell fates. J Cell Sci 2002; 115(Pt 7):1355-59.
12. Imai T, Tokunaga A, Yoshida T, et al. The neural RNA-binding protein Musashi1 translationally regulates mammalian numb gene expression by interacting with its mRNA. Mol Cell Biol 2001; 21:3888-900.
13. Abdel-Aziz HA, Elsaman T, Al-Dhfyan A, Attia MI, Al-Rashood KA, Al-Obaid AR. Synthesis and anticancer potential of certain novel 2-oxo-N'-(2-oxoindolin-3-ylidene)-2H-chromene-3-carbohydrazides. Eur J Med Chem 2013;70:358-63.
14. Bhat MA, Al-Dhfyan A, Khan AA, et al. Targeting HER-2 over expressed breast cancer cells with 2-cyclohexyl-N-[(Z)-(substituted phenyl/furan-2-yl/thiophene-2-yl) methylidene]hydrazinecarbothioamide. Bioorg Med Chem Lett 2015; 25(1):83-7.
15. Abdel-Aziz HA, Ghabbour HA, Eldehna WM, et al. 2-((Benzimidazol-2-yl)thio)-1-arylethan-1-ones: Synthesis, crystal study and cancer stem cells CD133 targeting potential. Eur J Med Chem 2015; 104:1-10.
16. Naglah AM, Awad HM, Bhat MA, Al-Omar MA, Abd El Galil EA. Microwave-assisted synthesis and antimicrobial activity of some novel isatin schiff bases linked to nicotinic acid via certain amino acid bridge. J Chem 2015; 2015:8.
17. Zhou S, Schuetz JD, Bunting KD, et al. The ABC transporter Bcrp1/ABCG2 is expressed in a wide variety of stem cells and is a molecular determinant of the side-population phenotype. Nat Med 2001; 7:1028-34.
18. Scharenberg CW, Harkey MA, Torok-Storb B. The ABCG2 transporter is an efficient Hoechst 33342 efflux pump and is preferentially expressed by immature human hematopoietic progenitors. Blood 2002; 99:507-12.
19. Ding XW, Wu JH, Jiang CP. ABCG2: a potential marker of stem cells and novel target in stem cell and cancer therapy. Life Sci 2010; 86:631-37.
20. Kharas MG, Lengner CJ, Al-Shahrour F, et al. Musashi-2 regulates normal hematopoiesis and promotes aggressive myeloid leukemia. Nat Med 2010; 16:903-8.

INVASION AND METASTASIS ABILITY OF RENAL CANCER CELL STRAINS 786-0: UNDER THE INFLUENCE OF miR-141

Y. XU, LN. LV, ZY. GUO and W. ZHANG

Nephrology D, Shandong JiNing No.1 People's Hospital, Shandong, China

Received March 2, 2016 – Accepted May 16, 2016

The first two authors contributed equally to this work

This study aimed to explore the invasion and metastasis ability of miR-141 in 786-0 renal cancer tissue cells, as well as identify the key function of endogenous miR-141 in adjustment and control of malignant activities of renal cancer. The renal cancer cell strain with overexpression of miR-141 and its control renal cancer cell line were constructed; methyl thiazolyl tetrazolium (MTT) assay was adopted to measure proliferation of renal cancer cells; Transwell assay was performed to measure the invasion and metastasis ability of cells; MTT assay and fluorescence activated cell sorting (FACS) were used for measurement of cell apoptosis and drug susceptibility. Results indicated that the expression of miR-141 in 786-0 cells could be significantly increased 400-fold by slow viruses that contained miR-141; moreover, comprehensive functions showed that miR-141 inhibited the invasion and metastasis ability of renal cancer cells to a great extent ($p < 0.001$), partially inhibited cell growth ($p < 0.05$) and also induced cell cycle to be arrested in G0/G1 as well as reducing the number of cells in S phase (DNA replicative phase). Moreover, miR-141 could not induce morphologic changes of renal cancer cells, had no direct stimulating effect on cell apoptosis and could not improve the drug susceptibility of renal cancer cells to drugs such as cis-Dichlorodiamineplatinum (DDP), 5-fluorouracil (5-FU) and tumor-related apoptosis-inducing ligand (TRAIL). In conclusion, miR-141 can be considered an important cancer suppressor gene of renal cancer by inhibiting proliferation and metastasis of renal cancer cells.

Renal cell cancer (RCC), derived from the renal tubular epithelial cells, is a common renal malignant tumor that accounts for 2-3% of all adult malignant tumors, and 85-90% in renal primary malignant tumors (1-3). Types of renal carcinoma are varied, including clear cell carcinoma, corpora mammillaria renal cell carcinoma, chromophobe cell tumor, collecting duct carcinoma and unclassified renal cell carcinoma (4).

miR-141 consists of 22 basic groups (3'GGUAGAAAUGGUCUGUCACAAU5) and it locates in 12pl3.31 chromosome, which belongs to the miR-200 family; miR-141 is mainly expressed in epithelial cells and expressed at low level in fibroblasts or mesenchymal cells (5). Different kinds of tumors have different expression tendency of miR-141. For example, the expression of miR-141 is up-regulated in colorectal cancer cells (6), ovarian cancer, adrenocorticotrophic hormone pituitary tumor (7), nasopharynx cancer and bile duct cancer tissues, while it is down-regulated in renal cell cancer (8), breast cancer, pancreatic ductal adenocarcinoma

Key words: invasion and metastasis, apoptosis, proliferation, 786-0 cell strains

Mailing address:
Dr Wei Zhang,
No.6, Jiankang Road, Nephrology department,
Shandong JiNing, No.1 People's Hospital,
JiNing, Shandong, 272100, China
e-mail: xuxuyyan@163.com

0393-974X (2016)

(9), head and neck cancer, liver cancer, hormone refractory prostate cancer and gastric cancer tissues. Thus we know that expression of miR-141 may depend on source and progression of tumors. Current expression profile of miRNA reveals the significantly down-regulated expression of miR-141 in renal cancer; however, the clinical value of miR-141 in renal cancer remains unclear (10-12).

Relevant studies indicate that, according to clinicopathologic features and expression level of miR-16, no relevance between expression level of miR-16 and tumor node metastasis (TNM) staging or American Joint Committee on Cancer (AJCC) cancer staging has been found; expression level of miR-16 was regulated downwards in other tumors (13-14), while it was obviously regulated upwards in renal cancer, indicating that miR-16 accelerated the development and progression of renal cancer by inhibiting expression of cancer suppressor gene instead of accelerating expression of cancer gene. Therefore, taking miR-16 as the control, the invasion and metastasis ability of miR-141 in renal cancer cell strain 786-0 was explored in this study.

MATERIALS AND METHODS

Research materials

Human renal cancer cell strains 786-0 were purchased from Zheng-Neng Biotechnology Limited Liability Company (Chengtu, China) (article number: LC107); 786-0 cell culture fluid (about 100 ml a time) was collected by centrifugation over three days.

Experimental grouping

miR-41 group (experimental group) was further divided into two groups: miR-141 group (slow virus 786-0 cells that contained miR-141) and miR-NC group (slow virus 786-0 cells without miR-141);

The miR-16 group (control group) was further divided into two groups: miR-16 group (slow virus 786-0 cells that contained miR-16) and miR-NC group (slow virus 786-0 cells without miR-16).

Culture of 786-0 renal cancer cell strains in vitro

Human renal cancer 786-0 cells preserved in a refrigerator were taken out and put into a water bath at 37°C to melt; then cell suspension was drawn and added with culture solution in a 10-fold volume; the obtained mixture was centrifuged (1000 g) for 5 min, and cells were then collected. After that, cells were inoculated in 10% FBS RPMI1640 culture medium at 37°C, with 5% CO2; 0.25% pancreatin solution was used for digestion and passage. Cell culture supernatant (100 ml) over three days was collected and centrifuged (10000 g) for 30 min to eliminate cell debris; then it was kept at -20°C until use.

Construction of renal cancer cell strain with overexpression of miR-141

A lentiviral vector with overexpression of hsa-miR-141 was constructed; plasmid template structure was H1 promoter-miR-CMV-GFP. A 24-well plate was then inoculated with 4×10^4 cells per 400 μL, and Dulbecco's modified eagle medium (DMEM) high glucose and 10% fetal bovine serum (FBS) were used to culture cells in an incubator (5% CO_2) at room temperature. When cell confluence reached 40%, pGCsil-GFP-hsa-miR-141 and its blank control low virus liquid was added to the 24-well plate (multiplicity of infection (MOI) of 786-0 cells was 10); then polybrene (5 μg/ml) was added and the volume of final culture solution was 500 μL, after which the culture plate was returned to the incubator. After 12 hours, culture medium that contained viruses was replaced by fresh culture medium that contained DMEM+10% FBS. After 3 days of infection, the expression of green fluorescent protein (GFP) was observed under a microscope and cells were cultured continuously; after passage, the medium was changed and the cells were cryopreserved; ribonucleic acid (RNA) was extracted for detection of overexpression for follow-up functional study using quantitative real-time polymerase chain reaction (qRT-PCR).

Methyl thiazolyl tetrazolium assay

For the proliferation ability of cells, 0.25% pancreatin was used to digest 786-0 cells in logarithmic phase; then cells were centrifuged and resuspended to obtain single-cell suspension; 10% cell sap was added with 10 μL of Trypan blue for staining; the number of cells was counted using counting plate. Each well of a 96-well culture plate was inoculated with 3×10^3 cells; the number of duplication wells was 6 and there were four 96-well culture plates; culture plates were cultured in incubators for 1, 2, 3 and 4 days, respectively. The culture plates were then taken out

and each well was added with 20 μL of MTT (5mg/mL), and the plates were continually cultured for 4 h after which the culture solution was removed; each well as added with 150 μL of dimethylsulfoxide (DMSO) and plates were agitated at low speed for 10 min to thoroughly dissolve crystal substances; light absorption values of each well were measured at 490 nm wavelength using microplate reader, and proliferation curves were drawn.

For the drug susceptibility analysis, the cells were digested, centrifuged and counted and each well of a 96-well plate was cultured with 1×10^4 cells; DDP, 5-FU and TRAIL in different concentrations were added to process cells for 24 h or 48 h; after that, MTT was added and the culture plate was put into a microplate reader for measurement of light absorption values of each well at 490 nm wave length; then growth curves were drawn.

Invasion and metastasis experiment

786-0 cells were cultured with Roswell Park Memorial Institute (RPMI) 1640 culture solution overnight in vitro; after digestion using 0.25% pancreatin, cell suspension (1×10^4/200 μL) was obtained. Matrige in 50 mg/L (serum-free RPMI1640=1:8, coated on the upper surface of the Transwell was air dried at 4°C) was prepared; leftover liquid in the 24-well plate was removed and each well was added with 50 μL of serum-free RPMI1640 which contained 10g/L bovine serum albumin (BSA); then the plate was placed at 37°C for 30 min. An amount of 0.2 mL cell suspension was inoculated into the gelatinized Transwell which was then placed in the 24-well plate; the lower chamber of the Transwell was added with 600 μL of RPMI1640 complete culture medium and cultured at 4°C for 24 h. The Transwell was taken out and a cotton bud was used to wipe off the Matrigel and upper chamber cells; then it was washed by PBS and fixed by 95% ethyl alcohol; trypan blue was used for staining; the filter membrane of Transwell was taken out and observed under a light microscope; the numbers of cells in five random fields of view were counted and the average value was obtained.

Next, 60 μL of above Matrigel diluent was coated on the upper chamber of Transwell and air dried at 4°C; then the Transwell was transferred to an incubator at 37°C and cultured for at least 1 h. The upper chamber was then added with 2×10^4 786-0 cells and the follow-up processes were the same as above.

Statistical analysis

Experimental data were processed by SPSS 19.0 software and five samples at least were observed in each experiment; the results were presented by mean ± SD. Student's t-test was adopted for comparison among groups and $p < 0.05$ was considered to be statistically significant.

RESULTS

Inhibiting effect of miR-141 on invasion and metastasis ability of 786-0 cells

This study used miR-141 and its control 786-0 cells to construct renal cancer cells with stable high expression of miR-141; the results indicated that the expression level of miR-141 in 786-0 cells increased by about 400 times, while the control group had no significant change (Table I). In addition, renal cancer cells with overexpression of miR-141 had no significant morphological change.

Table I. *Analysis of expression level of miR-141 and miR-16 in 786-0 cells using qRT-PCR.*

Group	miR-141		miR-16	
	miR-141	miR-NC	miR-16	miR-NC
Expression level ($2^{-\Delta\Delta CT}$)	406.13±20.24* **	1.02±0.12	1.06±0.08	1.01±0.06

*$p < 0.001$

Table II. *Number of cells in arrest of cell cycles during the process of miR-141 overexpression inhibiting renal cancer cell growth.*

Group	miR-141			miR-NC		
Cycle	G0/G1	S	G2/M	G0/G1	S	G2/M
Percentage (%)	55.61±3.14*	32.06±0.87*	12.52±2.18	39.21±2.35	45.31±1.62	17.03±1.12

$*p < 0.05$

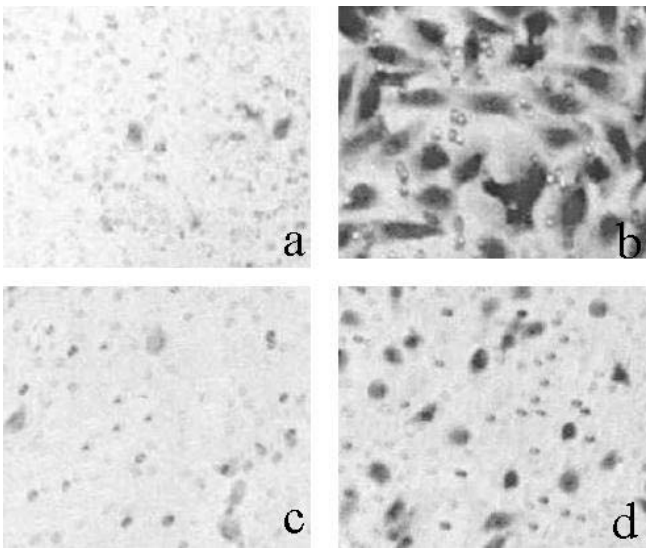

Fig. 1. *Inhibiting effect on invasion and metastasis ability of cells.* ***a*** *and* ***b****) Invasion ability of miR-141 and miR-NC, respectively, in experimental group.* ***c*** *and* ***d****) Metastasis ability of miR-141 and miR-NC, respectively, in the experimental group.*

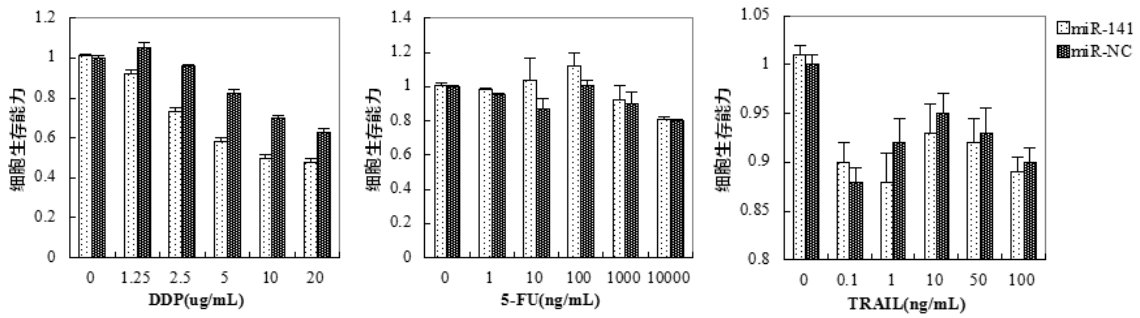

Fig. 2. *Analysis of drug susceptibility of overexpression miR-141 and its control 786-0 cells to DDP, 5-FU and TRAIL using MTT assay.*

MTT results showed that during the inhibition process of miR-141 overexpression to growth of renal cancer cells, arrest of cell cycle was in G0/G1 staging and the number of cells in S staging decreased (Table II). Moreover, overexpression of miR-141 significantly destroyed invasion and metastasis ability of 786-0 cells (Fig. 1), but it did not significantly increase the drug susceptibility of 786-0 cells to DDP, 5-FU and TRAIL (Fig. 2). It can therefore be hypothesized that miR-141 plays the

role of a cancer suppressor gene by inhibiting growth and movement of renal cancer cells

Expression of intracellular and extracellular miR-141

Condition medium of overexpressed miR-141 and its control cells cultured conventionally for 24 h, 48 h and 72 h, respectively, was collected, and RNA of cells in culture solution was extracted; expression level of extracellular miR-141 and miR-16 (control) was detected using qRT-PCR. As shown in Table III, the extracellular expression level of cells with overexpression of miR-141 was significantly higher than that of the control group, while miR-16 had no significant difference.

As shown in Fig. 3, the expression level of extracellular miR-141 was significantly lower than that of intracellular miR-141; specific value of extracellular and intracellular miR-141 of 786-0 cells was less than 2.2%. After cells in the control group were cultured using condition medium that contained extracellular miR-141 for 48 h, they were collected and RNA was extracted to detect changes of intracellular miR-141 and miR-16. Results showed that the condition medium of overexpressed miR-141 could improve intracellular expression level of miR-141 of renal cancer cells, which was in accordance with expected results.

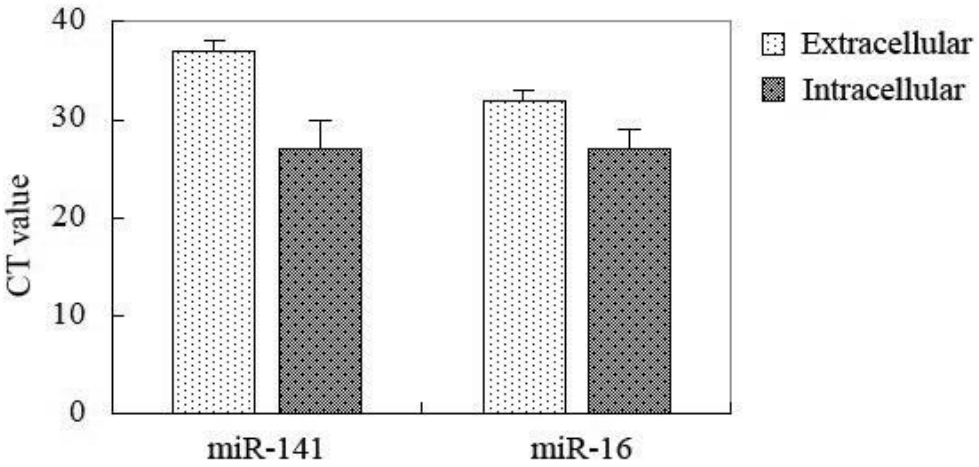

Fig. 3. *Expression level of intracellular and extracellular miR-141 and miR-16.*

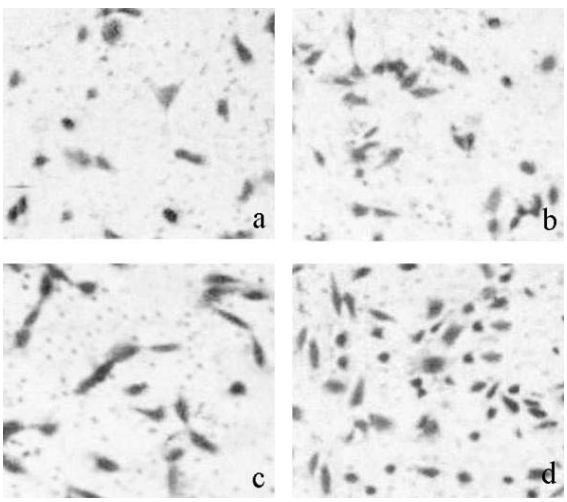

Fig. 4. *Effect of extracellular high expression miR-141 on invasion and metastasis ability.* ***a*** *and* ***d****) Invasion ability of miR-141and miR-NC, respectively.* ***c*** *and* ***d****) Metastasis ability of miR-141and miR-NC, respectively.*

Table III. *Inter-group comparison of expression level of cells.*

Group		24h	48h	72h
miR-141	miR-141	1.52±0.13**	7.34±1.61**	11.02±2.13***
	miR-NC	0.85±0.01	1.03±0.02	1.06±0.01
miR-16	miR-16	0.35±0.08	0.74±0.21	1.12±0.18
	miR-NC	0.36±0.12	0.87±0.17	1.03±0.01

Invasion and metastasis ability of miR-141 in renal cancer

In order to verify the effect of extracellular miR-141 on invasion and metastasis ability of cells, cells with overexpressed miR-141 were cultured in Transwell; the upper chamber was added with cells of the control group; after 24 h, the number of cells penetrating from the upper chamber to the lower chamber was observed. As shown in Fig. 4, extracellular miR-141 can inhibit invasion and metastasis ability of ccRCC cells to some extent, however, the effect of intracellular miR-141 was much stronger. Furthermore, the effect of extracellular miR-141 on proliferation and apoptosis of ccRCC cells was also analyzed, but the results showed no significant change.

DISCUSSION

Invasion and metastasis of tumor cells is a complicated and multi-step process, including degradation of extracellular matrix (ECM) and basilar membranes of tumor cells, changes of movement ability of cells and changes of adhesive ability of cells (15). Recent studies have verified that a large number of molecules are closely related to the invasion and metastasis of tumor cells. An increasing number of studies indicate that chemotactic factors and their receptors play an important role in metastasis of tumor cells (16).

Research in recent years has shown that miR-141 can be taken as a cancer suppressor gene as well as an oncogene, mainly depending on its expression level in tumor tissues (17-19). For example, high expression of miR-141 in ovarian cancer can accelerate the formation of tumors (20); high expression of miR-141 in nasopharynx cancer can not only improve the proliferation and invasion ability of 5-8F cells, but can also inhibit apoptosis of 5-8F cells (21); however, the expression of miR-141 in liver cancer shows a downward tendency, overexpression miR-141 can inhibit proliferation and invasion ability of HCCLM3 and inhibition of miR-141 can enhance the proliferation and invasion ability of MHCC97L cells (22). Expression of miR-141 in renal cancer (23-24) and gastric cancer (25) also shows a downward tendency and overexpression miR-141 can inhibit growth of tumor cells. The in-vitro cellular level experiment in this study showed that the main inhibition effect of miR-141 was on invasion and metastasis ability of renal cancer cells and the secondary effect was the regulation of proliferation ability and cell cycles. The effect of miR-141 on cellular morphology, apoptosis or drug resistance was not significant, indicating that miR-141 plays the role of inhibiting cancers by inhibiting invasion, metastasis and proliferation ability of renal cancer cells.

The study also discovered that miR-141 can be secreted by donor renal cancer cells to the outside of cells, and extracellular miR-141 can be taken in by recipient cells and thus play a certain inhibiting role. However, compared with the expression level of intracellular miR-141, the expression level of extracellular miR-141 was extremely low. Therefore, we hypothesize that secreting type miR-141 might be the by-product of life activities of cells.

This study was carried out on the basis of 786-0 renal cancer cells and the results showed that the anti-metastasis effect of miR-141 was no different from research results in recent years. The results obtained in this study were highly reliable. Moreover, the study defined the primary and secondary anti-

tumor effect of miR-141; miR-141 mainly inhibited invasion and metastasis ability of tumor cells, and secondarily, it inhibited the growth of cells, while it had no significant influence on cellular morphology and apoptosis of cells. These results provide a direction for future studies.

REFERENCES

1. Abdel-Rahman O, Fouad M. Efficacy and toxicity of sunitinib for non clear cell renal cell carcinoma (RCC): A systematic review of the literature. Crit Rev Oncol/Hematol 2015; 94(2):238-50.
2. Slovin SF, Motzer RJ, Jefferson M, et al. Phase I trial of a PSMA DNA vaccine for patients (pts) with good risk renal cell carcinoma(RCC). J Clin Oncol 2008; 26(15):431-36.
3. Borje L, Karim B, Steven C, et al. EAU Guidelines on Renal Cell Carcinoma: 2014 Update. Eur Urol 2015; 67(5):913-24.
4. Argani P, Hicks J, De Marzo AM, et al. Xp11 translocation renal cell carcinoma (RCC): Extended immunohistochemical profile emphasizing novel RCC markers. Am J Surg Pathol 2010; 34(9):1295-303.
5. Vrba L, Jensen TJ, Garbe JC, Heimark RL, Cress AE, Dickinson S, Stampfer MR, Futscher BW. Role for DNA methylation in the regulation of miR-200c and miR-141 expression in normal and cancer cells. Plos One 2010; 5(1):e8697.
6. Zhu W, Xu HG, Zhu DX, et al. miR-200bc/429 cluster modulates multidrug resistance of human cancer cell lines by targeting BCL2 and XIAP. Cancer Chemother Pharmacol 2012; 69(3):723-31.
7. Amaral FC, Torres N, Saggioro F, et al. MicroRNAs differentially expressed in ACTH-secreting pituitary tumors. J Clin Endocrinol Metab 2009; 94(1):320-23.
8. Nakada C, Matsuura K, Tsukamoto Y, et al. Genome-wide microRNA expression profiling in renal cell carcinoma: significant down-regulation of miR-141 and miR-200c. J Pathol 2008; 216(4):418-27.
9. Zhu ZM, Xu YF, Su QJ, et al. Prognostic significance of microRNA-141 expression and its tumor suppressor function in human pancreatic ductal adenocarcinoma. Mol Cell Biochem 2013; 388(1-2):39-49.
10. Yamamura S, Sharanjot S, Shahana M, et al. Abstract 3149: MicroRNA-141 inhibits proliferation and invasion by suppressing the Wnt signaling pathway in renal cell carcinoma. Cancer Res 2012; 72(8 S):3149-49.
11. Chen G, Zhang Y, Wu XH.786-0 Renal cancer cell line-derived exosomes promote 786-0 cell migration and invasion in vitro. Oncol Lett 2014; 7(5):1576-80.
12. Liu HQ, Brannon AR, Reddy AR, et al. Identifying mRNA targets of microRNA dysregulated in cancer: with application to clear cell Renal Cell Carcinoma. Bmc System Biol 2010; 4(9):51-51.
13. Zhang L, Deng T, Li X, et al. microRNA-141 is involved in a nasopharyngeal carcinoma-related genes network. Carcinogenesis 2010; 31(4):559-66.
14. Tan G, Tang X, Tang F. The role of microRNAs in nasopharyngeal carcinoma. Tumor Biolo 2014; 36(1):69-79.
15. Andre F, Schartz NE, Movassagh M, et al. Malignant effusions and immunogenic tumour-derived exosomes. Lancet 2002; 360(9329):295-305.
16. Zhang HG, Zhuang X, Sun D, Liu Y, Xiang X, Grizzle WE. Exosomes and immune surveillance of neoplastic lesions: a review. Biotech Histochem 2012; 87(3):161-68.
17. Senanayake U, Das S, Vesely P, et al. miR-192, miR-194, miR-215, miR-200c and miR-141 are downregulated and their common target ACVR2B is strongly expressed in renal childhood neoplasms. Carcinogenesis 2012; 33(5):1014-21.
18. Mahdavinezhad A, Mousavibahar SH, Poorolajal J, Yadegarazari R, Jafari M, Shabab N, Saidijam M. Association between tissue miR-141, miR-200c and miR-30b and bladder cancer: A matched case-control study. Urol J 2015; 12(1):2010-13.
19. Tanaka S, Hosokawa M, Yonezawa T, Hayashi W, Ueda K, Iwakawa S. Induction of epithelial-mesenchymal transition and down-regulation of miR-200c and miR-141 in oxaliplatin-resistant colorectal cancer cells. Biol Pharm Bull 2015; 38(3):435-40.
20. Mateescu B, Batista L, Cardon M, et al. miR-141 and miR-200a act on ovarian tumorigenesis by controlling oxidative stress response. Nature Med 2011; 17(12):1627-35.
21. Zhou XL, Wang YD, Shan BE, et al. The downregulation of miR-200c/141 promotes ZEB1/2 expression and gastric cancer progression. Med

Oncol 2014; 32(1):428-28.
22. Xue J, Niu YF, Huang J, Peng G, Wang LX, Yang YH, Li YQ. miR-141 suppresses the growth and metastasis of HCC cells by targeting E2F3. Tumor Biol 2014; 35(12):12103-7.
23. Yu XY, Zhang Z, Liu J, Zhan B, Kong CZ. MicroRNA-141 is downregulated in human renal cell carcinoma and regulates cell survival by targeting CDC25B. Oncotargets Ther 2013; 6(1):349-54.
24. Berkers J, Govaere O, Wolter P, et al. A possible role for microrna-141 down-regulation in sunitinib resistant metastatic clear cell renal cell carcinoma through induction of epithelial-to-mesenchymal transition and hypoxia resistance. J Urol 2013; 189(5):1930-8.
25. Du Y, Xu YJ, Ding L, et al. Down-regulation of miR-141 in gastric cancer and its involvement in cell growth. J Gastroenterol 2009; 44(6):556-61.

CO-SUPPRESSION OF VITAMIN C COMPOSITE NANO-DRUG CARRIER AND ITS DRUG DELIVERY TO NIDUS IN TUMOR CELLS

HZ. LIU[1], XM. LIU[2], XC. LIU[1], CZ. ZHANG[3] and HQ. LIU[1]

[1]Deparment of Pharmacy, Jining No.1 People's Hospital, Jining, China; [2]Department of Clinical Laboratory, Jining No. 1 People's Hospital, Jining, China; [3]Department of Pharmacy, Jining Municipal Authority Hospital, Jining, China

Received March 2, 2016 – Accepted May 18, 2016

The first two authors contributed equally to this work

This study aimed to discuss the co-suppression of vitamin C-contained composite nano-drug carrier and its drug delivery to nidus in tumor cells. Amphiphilic polymers PLA-block-PAAA and block polymer PLA-PEG4000-Maleimide, PLA-block-PAAA and PLA-PEG4000-Maleimide composite nano-micelles were prepared, and, PLA-block-PAAA polymer-coated Nile red nano-micelle, PLA-block-PAA and PLA-PEG4000-Maleimide composite nano-micelles as well as paclitaxel-carrying composite nano-micelle in different molar ratios were given stability tests. Lastly, PLA-block-PAAA and PLA-PEG4000-Maleimide composite nano-micelle cancer cells and paclitaxel-carrying composite nano-micelle cancer cells were given toxicity tests. Stability tests showed that self stability of PLA-block-PAAA (63/8) nano-micelle was not sufficient; the stability was good when the molar ratio of PLA-block-PAAA and PLA-PEG4000-Maleimide composite nano-micelle was 3:1; paclitaxel-carrying composite nano-micelle had good stability within 48 hours; PAAA segment had an inhibiting effect on C6 cancer cells and paclitaxel-carrying composite nano-micelle had a strong inhibiting effect also on tumors. After 24 hours, with the continuous release of paclitaxel, the tumor inhibiting effect of paclitaxel-carrying composite nano-micelle enhanced gradually, and the controlled-release of drugs had continuous inhibiting effect on tumor cells. Therefore, PAAA segment and paclitaxel had time-postponed synergistic effect. In conclusion, vitamin C-contained composite nanometer drug carrier materials can deliver anti-cancer drugs to nidus and thus inhibit tumor cells.

Cancer is one of the serious diseases that severely threaten human health. Although anti-cancer drugs are improved continuously and extensive progress has been achieved, the incidence rate of cancer is still increasing year by year and the cancer age tends to be younger. Thus, it is urgent to find a new effective method to treat cancer. Vitamin C, known as ascorbic acid, is an important biomolecule and antioxidant that is widely distributed in the organism which can protect cells from free radicals and oxidation of oxidizing agents (1). Vitamin C ramification can induce cancer cells to apoptosis, accelerate activities of macrophage and prevent lipid

Key words: Vitamin C, composite nano-drug carrier, anti-cancer drugs, inhibition of tumor cells

Mailing address:
Dr Hongzhang Liu
Deparment of Pharmacy,
Jining No.1 People's Hospital,
Jining, 272000, China
e-mail: liuhongzhang589@163.com

0393-974X (2016)

peroxidation of biological membrane. Thus, ascorbic acid shows hopeful efficacy in controlling cancer attack as well as treating cancer. Chen, et al. (2) performed an experiment on 9 types of cancer cells and 4 types of normal cells, and the results showed that the cancer cells had higher absorption of ascorbic acid compared with the normal cells. The lethal effect of ascorbic acid on cancer cells was selective and did not harm or influence normal cells or other tissues. However, the ascorbic acid concentration that was able to kill cancer cells could only be obtained by intravenous injection of ascorbic acid. As to the functional mechanism, with the help of sodium ascorbate and translocator, ascorbic acid could enter directly into certain cells, such as leukemia cell HL-60, while for most cells, it entered through glutamate transporters (GLUTS) (3). Another study verified that oxidative stress could make some anti-cancer drugs, such as paclitaxel, become toxic (4-5). Vitamin C could be used as an antioxidant and could have a synergistic anticancer effect when combined with paclitaxel. Other studies also verified that vitamin C could strengthen the efficacy of paclitaxel (6-9). Green, et al. (10) found that albumin nano-particle paclitaxel-carrying system had been successfully applied as breast cancer treatment; nano-drug carrier could warp drugs inside the carrier or had the drugs adsorbed on the surface of the carrier to deliver drugs. There were two ways to use polymers nano-micelles to wrap drugs: one was to encapsulate using physical acting force; the other one was to combine using chemical covalence (11). Multi-functional nano-micelles could be used in palladium ligand connection, tumor imaging research and anti-cancer reagent preparation, which became a main trend in the following studies of nano-micelles (12). Based on the characteristics and advantages of multi-functional drug delivery system, this study designed and compounded two kinds of amphipathic block polymer materials to form the composite paclitaxel-carrying nano-drug carrier and achieve the multi-function of nano-micelles, which could not only realize the cancer inhibiting effect of drugs, but also achieve the synergistic effect with paclitaxel to fight cancer.

MATERIALS AND METHODS

Preparation of amphipathic PLA-block-PAAA taking poly vitamin C as hydrophilic segment

Micromolecule vitamin C was used as the initial material. Firstly, benzyl bromide was used for benzyl protective response of enol-form hydroxyl to obtain benzyl-protected PAAA. Then a functional micromolecule initiator HEBP was used to have acylation reaction and obtain PAAA monomer. Polylactic acid homopolymer was obtained by using ring opening polymerization, and PLA-block-PAAA was prepared by atom transfer radical polymerization (ATRP). Finally, with the catalyzing of catalyst palladium as well as the participation of hydrogen, the benzyl protective group was removed and PLA-block-PAAA was finally obtained.

Stability test of PLA-block-PAAA polymer coated Nile red nano-micelle

A 25 ml round-bottom flask was used to volatilize dichloromethane of 60 μL of Nile red dichloromethane solution. Then 10 mg of PLA-block-PAAA polymer was added into the round-bottom flask and was dissolved by 4 ml of 1, 4-dioxane. Organic phases were taken out and put into a 4 ml centrifuge tube for latter application. Then 4 ml of deionized water was added to the 25 ml round-bottom flask and 1, 4-dioxane solution was slowly added dropwise to deionized water for self-assembly. After 2 h of continuous stirring, the solution was transferred to a dialysis bag with a molecular cut off of 3500. Phosphate buffered saline (PBS) (PH 7.4) was then added to the solution for dialysis, and the concentration of obtained nano-solution was 1.0 mg/ml.

PBS (PH 7.4) samples after dialysis were added into small centrifuge tubes (2 ml) respectively for three samples and were put into table concentrator for response at 37°C to simulate inner body environment to detect fluorescence intensity change of Nile red.

Composite block polymer PLA-PEG4000-Maleimide

A 25 ml Schlenk bottle was used and the inner oxygen was eliminated in vacuum state. Niitrogen was added to the bottle to eliminate oxygen and this process was repeated three times. Then, lactide (1.0 g, 0.7 mmol), initiator HO-PEG4000-Maleimide (194 mg, 0.0463 mmol), catalyst stannous octoate (9.4 mg, 0.0232 mmol), solvent anhydrous toluene (2 ml) and lactide were added to the bottle and

stirred; the molar ratio of lactide, HO-PEG4000-Maleimide and stannous octoate was 300:2:1. The reaction system was put into oil bath at the constant temperature of 94°C for 4 h. After reaction, a little trichloromethane dissolving reacting solution was added and the obtained solution was precipitated and centrifuged for three times using absolute methanol. An amount of 0.82 g of white flocculent solid was obtained and the productive rate was 75%.

Preparation of PLA-block-PAAA and PLA-PEG4000-Maleimide composite nano-micelle

A 25 ml round-bottom flask was used to volatilize acetone of 60 μL of Nile red acetone solution (1 mmol/L), and 4.2 mg of PLA-block-PAAA and 4.1 g of PLA-PEG4ooo-Maleimide were added to the flask and fully dissolved by 4 ml of 1, 4-dioxane. Organic phases were taken out and put into a 4 ml centrifuge tube for latter application. Then, 4 ml of deionized water was added to the 25 ml round-bottom flask and 1, 4-dioxane solution was slowly added to deionized water dropwise for self-assembly. After 2 h of continuous stirring, the solution was transferred to a dialysis bag whose molecular cut off was 3500. PBS (PH 7.4) was added to the solution for dialysis, and the concentration of obtained nano-solution was 1.0 mg/ml.

Stability test of PLA-block-PAAA and PLA-PEG4000-Maleimide composite nano-micelles in different molar ratios

Nano-micelle solution (polymer concentration was 1.0 mg/mL) was obtained through molar ratio adjustment of PLA-block-PAAA (63/8) and PLA-PEG4000-Maleimide, the molar ratios of which were 12:1, 8:1, 3:1, 1:1, 1:5 and 1:10. PBS (PH 7.4) samples after dialysis were placed in small centrifuge tubes (2 ml) respectively for three samples which were put into table concentrator for response at 37°C to simulate inner body environment, and the fluorescence intensity change of Nile red was detected.

Characteristics of PLA-block-PAAA and PLA-PEG4000-Maleimide composite nano-micelles

Composite nano-micelle carrier materials were prepared according to the optimal molar ratio (steps refer to preparation of PLA-block-PAAA and PLA-PEG4000-Maleimide composite nano-micelle) and the concentration of obtained nano-solution was 1.0 mg/ml. An amount of 3 ml of nano-solution was used for dynamic light scattering (DLS) test. A clean filter paper was put into a glass dish and then a carbon film copper net covered the filter paper. A pipette was used to draw a moderate amount of nano-solution and gently drip it on the copper net. After a period of time, the solution was volatilized and samples were fully dried, then transmission electron microscopy (TEM) characterization test was performed.

Cancer cells toxicity test of PLA-block-PAAA and PLA-PEG4000-Maleimide composite nano-micelles

C6 glioma cells were used for toxicity test of cancer cells. The substrate of C6 cells was F10 substrate, which was added with 10% fetal calf serum and 1% antibiotic. When cells were in good growing status, C6 cells were evenly planted in a 96-well plate; each well contained about 10,000 cells. After 24 h, the original substrate was removed. Film processed substrate nano-micelle solution (400 μg/mL) was added to the 96-well plate and co-cultured with cells. The experimental group was co-cultured nano-micelle and cells, while the control group had no nano materials and only used substrate to culture cells for 24 h, 48 h and 72 h. Then methyl thiazolyl tetrazolium (MTT) was used to detect activities of cells, and each concentration had three parallel samples. At the scheduled time of co-culture, each well was directly added with MTS reagent (20 μL) and put into an incubator at 37°C constant temperature for 4 h. Then the outside diameter (OD) value of each well was measured by a microplate reader at 490 mn wavelength.

Stability test on paclitaxel-loaded composite nano-micelle using dynamic light scattering test

Nano-micelle solution (1 mL) was added to a dialysis bag and the bag mouth was tightened. Then the bag was put into PBS (PH=7.4) (dissolving medium 6 ml). Samples after dialysis were put into a 37°C table concentrator for reaction. Each small centrifuge tube was wrapped with tinfoil to keep out light. Samples received DLS tests at 0 h, 24 h and 48 h, respectively. The amount of testing sample taken each time was 1.5 ml and the concentration of nano-micelles was 0.4 mg/mL

Cancer cells toxicity test on paclitaxel-carrying composite nano-micelle

Toxicity test of cancer cells was performed on C6 glioma cells. The substrate of C6 cells was F10 substrate,

and it was added with 10% fetal calf serum and 1% antibiotic. When cells were in good growing status, C6 cells were evenly planted in a 96-well plate, each well containing about 10,000 cells. After 24 h, the original substrate was removed. Film processed substrate nano-micelle solution (400 μg/mL) was added to the 96-well plate and co-cultured with cells. The experimental group was co-cultured nano-micelle and cells, while the control group had no nano material and only used substrate to culture cells for 24 h, 48 h and 72 h. Then the MTT method was used to detect activities of cells, and each concentration had three parallel samples. At scheduled time of co-culturing, each well was directly added with MTS reagent (20 μL) and put into an incubator at 37°C constant temperature for 4 h, after which the OD value of each well was measured by a microplate reader at 490 mn wave length.

RESULTS

Stability test of PLA-block-PAAA polymer coated Nile red nano-micelle

Hydrophilic segment and lyophobic segment of PLA-block-PAAA polymer were unbalanced and polymer was put in PBS; two hydroxyl of segments were affected by strong ions and lost activity, thus PLA-block-PAAA (63/8) nano-micelle was lack of stability. As shown in Fig. 1, the release rate of polymer PLA-block-PAAA (63/8) nano-micelle in PBS (PH=7.4) within 48 h was close to 70%, thus the release behavior was obvious.

Stability test of PLA-block-PAAA and PLA-PEG4000-Maleimide composite nano-micelles in different molar ratios

Different molar ratios of two polymers resulted in different stability of composite nano-micelles. The only thing in common was that stability of all kinds of composite nano-micelles was stronger than separate self-assembly of two polymers. After 48 h of observation, we found that when the molar ratio of PLA-block-PAAA and PLA-PEG4000-Maleimide was 3:1, the release rate of Nile red within 48 h was only about 10%. Thus composite nano-micelles had the best stability.

DLS characteristics of PLA-block-PAAA and PLA-PEG4000-Maleimide composite nano-micelles

As shown in Fig. 3, when a nano-micelle did not carry medicine molecules, its size was about 73 mn and polydispersity index (PDI) was narrow, indicating that the nano-micelle had a good application prospect. In a later cell experiment, its co-culture with cells could enter through apertures on cytomembrane, and if it carried drugs, it could also release drug efficacy in cells.

Cancer cells toxicity test of PLA-block-PAAA and PLA-PEG4000-Maleimide composite nano-micelles

The cancer cell toxicity test was carried out under the same conditions for the experimental group (PLA-block-PAAA) and the control group (PLA-

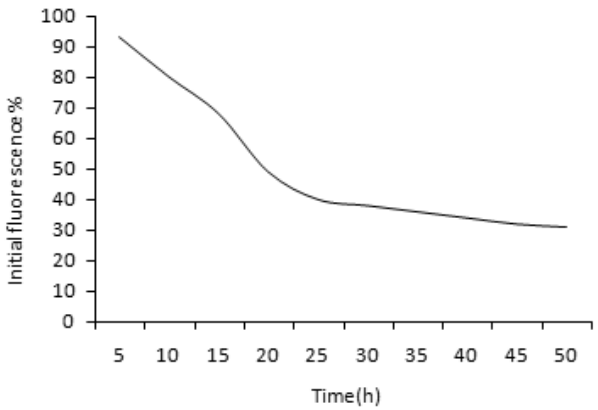

Fig. 1. *Stability test of polymer PLA-block-PAAA (63/8).*

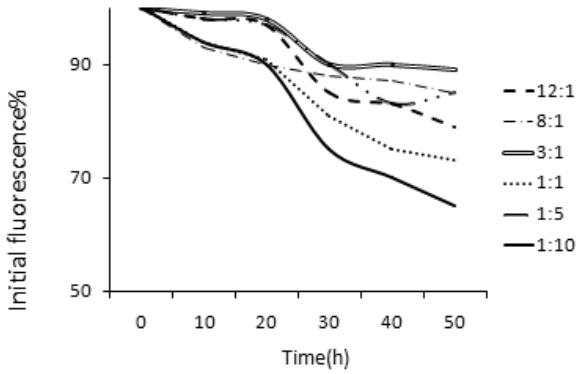

Fig. 2. *Stability tests of composite nano-micelles in different molar ratios.*

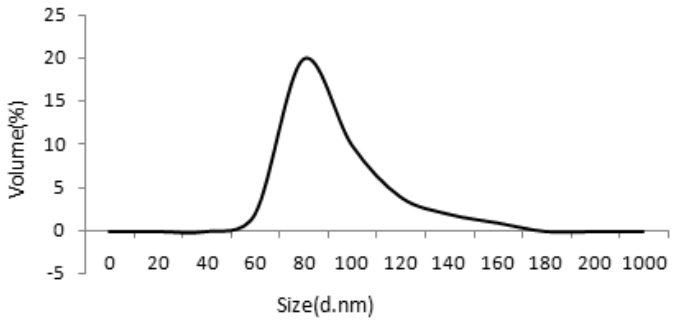

Fig. 3. *DLS characteristics of composite nano-micelle (Diameter=70.98 nm, PDI=0.132).*

PEG4000-Maleimide). After 24 h of co-culture, composite nano-particles (contained PLA-block-PAAA) showed strong cancer cell toxicity and the survival rate of cancer cells was approximately 79%. After 48 h of co-culture, the survival rate of cancer cells reduced to about 70%. However, the nano-particles formed by PLA-PEG4000-Maleimide individual self-assembly had no control on cancer cells. The only difference between these two nano materials was PAAA segment, and PLA and PEG were verified as having no cancer cell toxicity. Therefore, the control behavior on cancer cells was due to the PAAA segment (Fig. 4).

Stability test on paclitaxel-loaded composite nano-micelle using DLS

Size change of paclitaxel-loaded nano-micelle within 48 h is shown in Fig. 5. Within 48 h, paclitaxel-carrying nano-micelle was in good status and its particle size was maintained at 130~140 nm and no aggregation of nano-micelles was found. Thus paclitaxel-carrying nano-micelle had good stability within 48 h and could be applied to future cell and animal experiments.

Cancer cell toxicity test on paclitaxel-carrying composite nano-micelle

The comparison between paclitaxel-carrying composite nano-micelle and blank composite nano-micelle showed that in the earlier stage of co-culture (within 24 h), PAAA segment had obvious control on cancer cells, and the control rates of paclitaxel-carrying composite nano-micelle and blank composite nano-micelle on cancer cells were almost equal ($p > 0.1$), approximately 80%. In the later stage (after 24 h), the control effect of blank composite

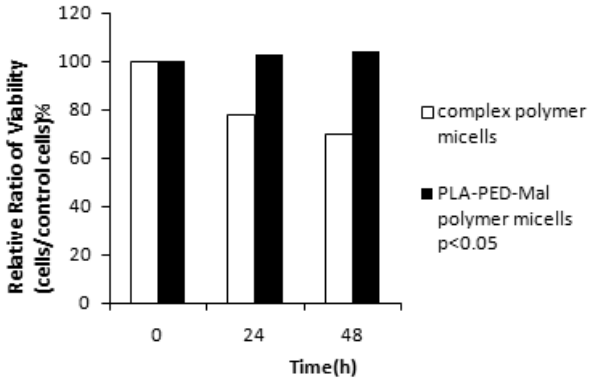

Fig. 4. *Comparison chart of cancer cell toxicity test.*

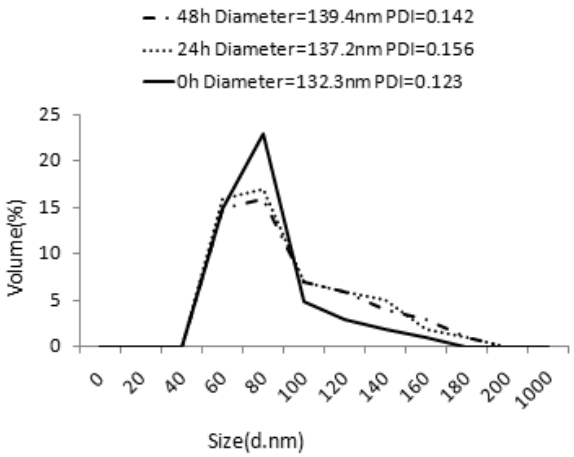

Fig. 5. *Stability test of paclitaxel-loaded nano-micelle.*

nano-micelles on cancer cells stopped increasing and maintained at 60~70%, while the paclitaxel-carrying composite nano-micelle continued to have a strong control effect on cancer cells. Within 24 h, paclitaxel did not release abundantly and it had no control effect on cancer cells when the concentration was in low level. Thus, the control effect on cancer cells at that time was due to PAAA segment, and two nano-micelles had no significant difference on the control rate of cancer cells. After 24 h, with the continuous release of paclitaxel, the control effect of paclitaxel-carrying composite nano-micelle on cancer cells began to enhance and the slow release of drugs had continuous control effect on cancer cells. At 72 h, the control rate on cancer cells was about 70%. Therefore, PAAA segment and paclitaxel had time-postponed synergistic effect.

DISCUSSION

Traditional therapeutic drugs are distributed in the human body non-specifically and have control effect on both cancer cells and normal cells, which greatly restricts drug efficacy. To overcome the disadvantages of traditional drugs on cancer specificity, molecular targeting treatment comes into being (13-14). Nano-drug carriers can not only avoid cytotoxicity of chemotherapeutics drugs to some extent, but can also effectively control the release of drugs, increase the ratio of drugs used and maintain optimal stability in blood circulation. When a nano carrier is connected with a specificity receptor to enter the cells, they can successfully avoid the recognition reaction of p-glucose protein through being encapsulated by cell nucleus endosome due to endocytosis of receptor-ligand, which is also

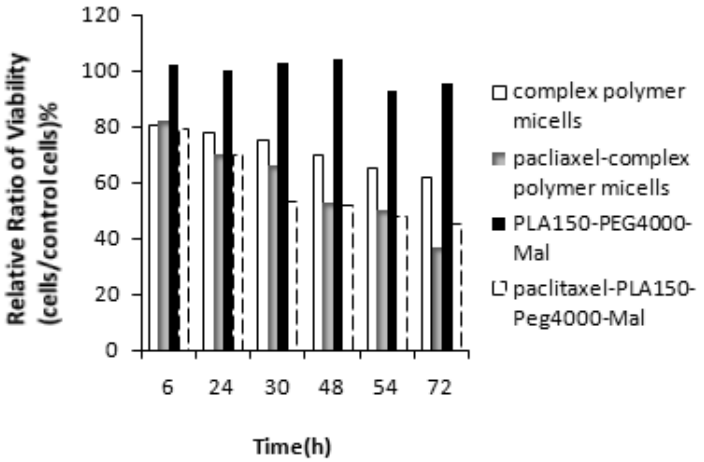

Fig. 6. *Toxicity tests comparison of glioma C6 cells.*

the mechanism of drug tolerance (15). Although using a nano-particle system as drug carrier has the above advantages, practical applications have many limitations, such as poor oral bioavailability, body circulation and toxicity, etc. Vitamin C is an important nutriment and powerful antioxidant, which can protect the body from free radicals. It also has good application potentials in controlling cancer cell growth, as it can transfer hydrogen peroxide to nidus. This study discussed a vitamin C-contained composite nano-drug carrier which could have both a control effect on cancer as well as deliver paclitaxel to nidus to control cancer cell growth. The study also improved polymer PLA-block-PAAA nano-micelle that was lacking stability and created another multi-functional PLA-PEG-Maleimide. With the self-assembly of PLA-block-PAAA and PLA-PEG-Maleimide, a stable composite nano-micelle was obtained and used as paclitaxel-carrying carrier. PLA-block-PAAA/PLA-PEG-Maleimide composite nano-micelle underwent tests to determine its particle size, form, drug release behavior, etc. MTT test was used to test the cell toxicity of PLA-block-PAAA /PLA-PEG-Maleimide composite nano-micelle. Various kinds of cancer cells were used to test the control effect of nano carrier materials on cancer cells as well as to find out whether nano carrier materials and paclitaxel had synergistic effects on controlling tumor growth.

In conclusion, this study describes amphiphilic polymers PLA-block-PAAA and block polymer PLA-PEG4000-Maleimide, PLA-block-PAAA and PLA-PEG4000-Maleimide composite nano-micelles. Based on the deficiency of PLA-block-PAAA stability, this study also uses functional polymer PLA-PEG4000-Maleimide recombination to obtain stable nano-micelle as well as a series of characterization tests. The results verify that paclitaxel-carrying composite nano-micelle has a longtime control effect on cancer cells. PAAA segment and released drug paclitaxel have time-postponed synergistic effect and can control cancer cell growth, thus it can be applied to cancer treatment.

REFERENCES

1. Verrax J, Calderon P B. The controversial place of vitamin C in cancer treatment. Biochem Pharmacol 2008; 76:1644-52.
2. Chen Q, Espey MG, Sun AY, et al. Ascorbate in pharmacologic concentrations selectively generates ascorbate radical and hydrogen peroxide in extracellular fluid in vivo. PNAS 2007; 104(21):8749-54.
3. Chen Q, Espey MG, Krishna MC, et al. Pharmacologic ascorbic acid concentrations selectively kill cancer cells: Action as a pro-drug to deliver hydrogen peroxide to tissues. PNAS 2005; 102(38):13604-9.
4. Ramanathan B, Jan KY, Chen CH, Hour TC, Yu

HJ, Pu YS. Resistance to paclitaxel is proportional to cellular total antioxidant capacity. J Cancer Res 2005; 65:8455-60.

5. Alexandre J, Batteux F, Nicco C, et al. Accumulation of hydrogen peroxide is an early and crucial step for paclitaxel-induced cancer cell death both in vitro and in vivo. Int J Cancer 2006; 119:41-48.
6. Grad J, Bahlis NJ, Reis I, Oshiro MM, Dalton WS, Boise LH. Ascorbic acid enhances arsenic trioxide-induced cytotoxicity in multiple myeloma cells. Blood 2001; 98:805-13.
7. Reddy V, Khanna N, Singh N. Vitamin C augments chemotherapeutic response of cervical carcinoma HeLa cells by stabilizing P53. Biochem Biopliys Res Commun 2001; 282:409-15.
8. Kassouf W, Highshaw R, Nelkin GM, Dinney CP, Kamat AM. Vitamins C K3 sensitize human urothelial tumors to gemcitabine. J Urol 2006; 176:1642-47.
9. Bahlis N, McCafferty-Grad J, Jordan-McMurry I, et al. Feasibility and correlates of arsenic trioxide combined with ascorbic acid-mediated depletion of intracellular glutathione for the treatment of relapsed/refractory multiple myeloma. Clin Cancer Res 2002; 8:3658-68.
10. Green MR, Manikhas GM, Orlov S, Afanasyev B, Makhson AM, Bhar P, Hawkins MJ. Abraxane, a novel Cremophor-free, albumin-bound particle form of paclitaxel for the treatment of advanced nonsmall-cell lung cancer. Ann Oncol 2006; 17:1263-68.
11. Nasonklda N, Bey E, Ren J, et al. Multifunctional polymeric micelles as cancer-targeted, MRJ-ultrasensitive drug delivery systems. Nano Lett 2006; 6:2427-30.
12. Kim TY, Kim DW, Chung JY, et al. Phase I and pharmacokinetic study of Genexol-PM, a cremophor-frec, polymeric micelle-formulated paclitaxel, in patients with advanced malignancies. Clin Cancer Res 2004; 10:3708-16.
13. Wang Y Z, Yang J J, Yang J. Synthesis and self-assembly of novel amphiphilic copolymers poly (lactic acid) - block-poly (ascorbyl actuate). Poly Chemistry, 2011, 49, 3988-3996.
14. Ross JS, Schenkein DP, Pietrusko R, et al. Targeted therapies for cancer. Am J Clin Pathol 2004; 122:598-609.
15. Rawat M, Singh D, Saraf S, Saraf S. Nanocarriers: promising vehicle for bioactive drugs . Biol Pharm Bull 2006; 29:1790-98.

REGULATORY EFFECT OF ESTROGEN RECEPTOR-α-MEDIATED Wnt/β-CATENIN SIGNALING PATHWAY ON OSTEOBLAST PROLIFERATION

XG. HAN[1], DW. WANG[1], ZG. BI[1] and F. GAO[2]

[1]Department of Orthopedics, First Affiliated Hospital of Harbin Medical University, Harbin, Heilongjiang, China; [2]Pharmacy Intravenous Admixture Service, First Affiliated Hospital of Harbin Medical University, Harbin, Heilongjiang, China

Received March 2, 2016 – Accepted May 10, 2016

This study was designed to investigate the regulatory effect of estrogen receptor-α (ERα)-mediated Wnt/β-catenin signaling pathway on osteoblast proliferation. Mc3T3-El cells were infected by ERα and ERβ small interfering ribose nucleic acid (siRNA) viruses and treated with estradiol 2 (E2) for 120 min after 24-h infection. Western blot was used to detect expressions of β-catenin, Gsk 3β, p-Gsk3β (Ser9) and CyclinDl; and methyl thiazolyl tetrazolium (MTT) was applied to detect osteoblast proliferation after interference by different ERs. Western blot results indicated that the expressions of β-catenin, p-Gsk3β (Ser9) and CyclinDl decreased after ERβ interference and ERα + ERβ joint interference, and a more obvious decrease was found after the joint interference. After ERβ interference, β-catenin, p-Gsk3β (Ser9) and CyclinDl were strongly expressed compared with expressions in the blank control group. MTT results demonstrated that the proliferation rate of osteoblast was lower after the joint interference than after ERβ interference, while a slight increase was found in the proliferation rate after ERβ interference in comparison with the blank control group. It can be concluded that estradiol is able to promote the proliferation of osteoblasts in mice by ERα-mediated Wnt/β-catenin signaling pathway.

In the microenvironment of bone metabolism, hormonal regulation, growth factor adjustment and nervous system jointly form a nerve-endocrine local growth factor regulating network involved in the whole process of bone growth and bone resorption. Estrogen plays an important role in regulating bone metabolism and maintaining normal bone mass (1). Many studies indicate that estrogen deficiency can lead to abnormal osteoblast formation and function (2-4). Osteoblast is a main functional cell in the process of bone formation. Signal transduction pathway, such as Wnt signal system, plays a vital role in the entire process of osteoblast differentiation and proliferation, of which, Wnt/β-catenin signaling pathway has become a hot topic in recent years (5).

Gary et al. (6) first discovered estrogen receptor (ER) on *in vitro* cultured osteoblasts and found estrogen had a direct effect on osteoblasts and can further act on osteoclast through regulating the generation of other cytokines. Kousteni et al. (7, 8) discovered that ER ligand could induce ER, protein kinase pathway, bone morphogenetic protein (BMP)-2 and Wnt signaling pathway to form a large signal group without affecting ER DNA binding activity, so as to jointly regulate osteoblast differentiation and maturation. Tan et al. (9) speculated that ERα showed

Key words: estradiol, osteoblast precursor cells in mice, Wnt signaling pathway, estrogen receptor

Mailing address:
Dr Feng Gao,
Pharmacy Intravenous Admixture Service,
First Affiliated Hospital, Harbin Medical University,
Number 23, Youzheng Street, Nangang district, Harbin,
Heilongjiang, 150001, China
e-mail: gf04518@163.com

0393-974X (2016)

a great promo effect on osteoblast differentiation on the 7th day and 14th day of bone mesenchymal stem cells (BMSCs) induced osteogenic differentiation. Gabriel et al. (10) considered that β-catenin protein could provide a molecular induction signal for osteogenic differentiation of MSCs. Experiments verified that β-catenin induced the osteogenic differentiation of MSCs by enhancing the response of MSCs to BMP-2, ROS17/2.8 cell and was capable of significantly up regulating Wnt pathway-mediated β-catenin and alkaline phosphatase, and ER modulators (I-C1182780 and tamoxifen) and ERα knockouts could terminate the situation.

This study aims to explore the regulation of osteoblast proliferation via ERα-mediated Wnt/β-catenin signaling pathway.

MATERIALS AND METHODS

Experimental materials

Mice osteoblast strain Mc3T2-E1 (Shanghai Beinuo Biotech. Co., Ltd., China), Dulbecco's modified eagle medium (DMEM) (Beijing Chenglin Biotech. Co., Ltd., China), fetal bovine serum (FBS) (100 ml) (Shanghai Kanglang Biotech. Co., Ltd., China), pancreatin (Shanghai Guangrui Biotech Co., Ltd., China), ethylene diamine tetraacetic acid (EDTA) (Shanghai Liaoqi Biotech. Co., Ltd., China), dimethylsulfoxide (DMSO) (20 ml) (Shanghai Yanhui Biotech. Co., Ltd., China), methyl thiazolyl tetrazolium (MTT) (Shanghai Shingene Molecular Biotech. Co., Ltd., China), β-estradiol (Dalian Meilun Biotech. Co., Ltd., China), Wnt signaling pathway key protein antibody (Shanghai Wancheng Medical Instrument Co., Ltd., China), ERα and ERβ antibodies (Shenyang Wanlei Biotech. Co., Ltd., China) as well as ERα and ERβ ribose nucleic acid interference (RNAi) lentiviral vectors (Shanghai Junrui Biotech. Co., Ltd., China) were used in this experiment (Table I).

ERα and ERβ RNAi chronic virus infection

Mc3T3-E1 cells were taken out of liquid nitrogen container and inoculated into a 24-well plate (2×10^4 cells/well) and the plate was put into an incubator (37°C, 5% $CO_{2)}$ for cell culture. Then 12 mL of liquid containing five kinds of virus suspensions with a titer of 1×10^{11} TU·L^{-1} (2 mL for each suspension) and 2 mL of Mc3T3-El culture medium was poured into each well and mixed. Polybrene was added to adjust the concentration to 8 μg/mL. The medium containing virus solution was abandoned and each well was added with 500 mL of fresh complete medium (the medium was changed every two days), and the plate was placed into an incubator (37°C, 5% $CO_{2)}$ for cell culture. The medium was changed every day and infection rate was observed on the 4th day of infection, i.e., the ratio of green fluorescent protein (GFP) positive cells was observed under a fluorescence microscope.

Protein expression of Wnt pathway signal molecule after ERα and ERβ RNAi interference

The negative control group was packaged with viruses. The virus combining ERα and ERβ RNAi and small interfering ribose nucleic acid (siRNA) of two receptors were used to infect Mc3T3-E1 cells. After 24-h infection, the Mc3T3-E1 cells were treated with β-estradiol. Seventy-two hours later, protein was extracted from the cells and detected by Western blot.

A 6-well plate was taken and washed with phosphate buffer solution (PBS) once. Then cells were collected using a cell scraper. Each well was added with lysate and then the plate was put on ice for lytic reaction. Ten

Table I. *Oligonucleotides of siRNA.*

pll3.7-ERα siRNA	F: 5'-tGTCTCTGGAAGAGAAGGACTTCAAGAGGTCCTTCTCTTCCAGAGACTTTTTTGGAAAc-3'
	R: 5'-TCGAGTTTCCAAAAAAGTCTCTGGAAGAGAAGGACCTCTTGAAGTCCTTCTCTTCCAGAGACa-3
pll3.7ERβ siRNA	F: 5'-tGTAGGAATGGTCAAGTGTGTTCAAGAGACACACTTGACCATTCCTACTTTTTTGGAAAc-3'
	R: 5'-TCGAGTTTCCAAAAAAGTAGGAATGGTCAAGTGTGTCTCTTGAACACACTTGACCATTCCTACa-3'

minutes later, the cells were centrifuged at 12000 rmp for 20 min. The supernate obtained was transferred to another centrifuge tube. The concentration of protein was measured using the Bradford method. Protein split product in a certain volume was taken and boiled for 5 min. The incubation of first antibody started after 10% SDS-PAGE gel electrophoresis, transfer membrane (4°C, 100 V, 1.5 h), 1-h sealing with skim milk powder at room temperature and three times of membrane cleaning. Primary antibody which had been diluted with 5% Bull Serum Albumin was added with Polyvinylidene Fluoride (PVDF) membrane and then incubated at 4°C overnight. The following day, after three times of membrane washing (10 min each time), it was incubated with second antibody dilute for one hour. After another three times of membrane washing, color development was performed. Target protein was detected through electrochemiluminescence color development.

Growth curve of E2 processed Mc3T3-E1 cells after ER interference

The negative control group was packaged with viruses. The virus combining ERα and ERβ RNAi and small interfering ribose nucleic acid (siRNA) of two receptors were used to infect Mc3T3-E1 cells. After one-day infection, the culture medium was abandoned and a fresh culture medium containing E2 (10^{-7} m) was added into each well for cell incubation for 1, 3, 5, 7 and 9 days, respectively. New culture medium of the same concentration is needed to replace the old one once a day. Mc3T3-E1 cells in the logarithmic phase were digested with trypsin and inoculated into a 96-well plate, 200 μL for each well, with the density of 10^4/mL, and then cultured in an incubator (37°C, 5% CO_2). Twenty-four hours later, the culture medium was abandoned and a fresh culture medium containing 1 mL of E2 was added to each well for cell incubation for 1, 3, 5, 7 and 9 days, respectively. New culture medium of the same concentration replaced the old once a day. Additionally, 20 μL of MTT (5 mg/mL) was poured into the wells for another 4-h culture, and 150 μL of DMSO was then added into the wells and shaken for 15 min after supernatant liquor was removed. After intensive dissolution, the crystal was put on an enzyme-linked immune tester for the measurement of optical density (OD) at the wavelength of 490 nm. Finally, results were recorded and a cell growth curve was drawn, taking time and OD value as x axis and y axis, respectively.

Statistical analysis

GraphpadPrism5 software was used to process and analyze experimental data. Enumeration data were processed by non-parametric test and expressed as mean ± standard deviation (SD). Analysis of variance was performed for pairwise comparison, and the difference was considered to be statistically significant if $p < 0.05$.

RESULTS

Viral packaging of 293FT cells and infection of Mc3T3-E1 cells

293FT cells were transfected by PlentiLox3.7 plasmid and packaging cell system. Mc3T3-E1 cells were collected 24 h and 48 h after virus infection and rate of green fluorescent protein (GFP) positive cells was observed on the 4th day (Fig. 1). After 48-h infection, the morphology of Mc3T3-E1 cell changed dramatically and a lot of small spots appeared on the cell surface (Fig. 2B).

Protein expression of ERα + ERβ and key molecules expressions of Wnt signaling pathway after ER interference

The negative control group was packaged with viruses. The virus combining ERα and ERβ RNAi and small interfering ribose nucleic acid (siRNA) of two receptors were used to infect Mc3T3-E1 cells. Twenty-four hours later, Mc3T3-E1 cells were treated with β-estradiol (10^{-7} m). Two hours later, protein was extracted for measuring expressions of ERs, GSK-3β, β-catenin and Cyclin D1 by Western blot. As shown in Fig. 3, ER siRNA was effective in reducing expressions of ERα + ERβ. ERα showed a lower expression after ERα siRNA interference compared with p-GSK-3β, β-catenm and Cyclm D1 in the control group based on equal conditions, while it showed a higher expression after ERβ siRNA interference compared to the control group; among Wnt signaling pathways, P-GSK-3β, β-catenin and Cyclin D1 demonstrated higher expressions after ERβ siRNA interference compared to the normal control group, while their expressions reduced when ERα and ERβ interfered at the same time.

Fig. 1. *Mc3T3-E1 cells infected by GFP virus.*

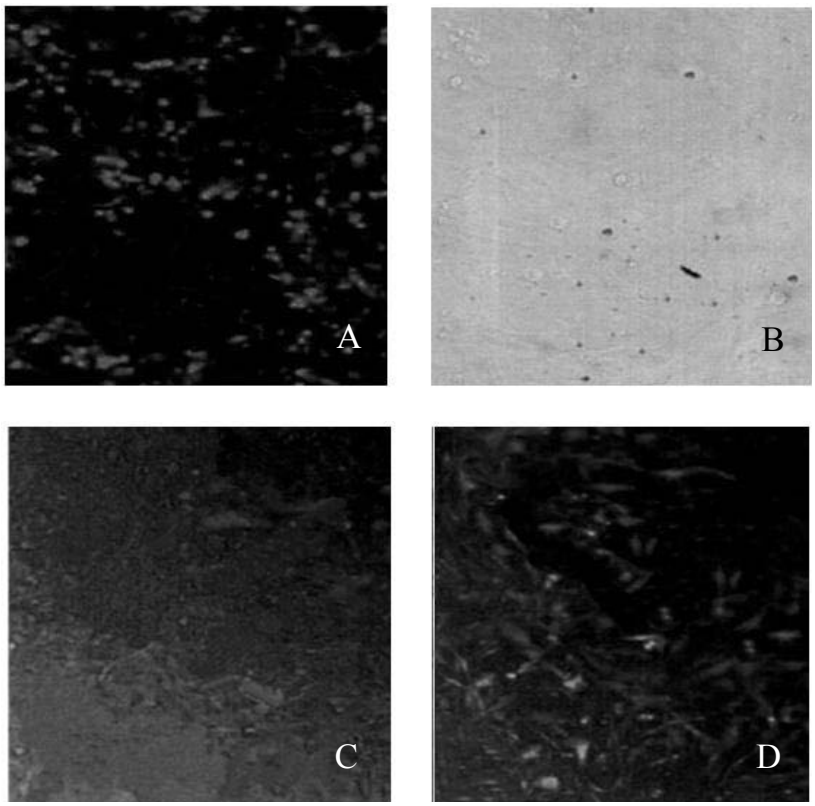

Fig. 2. *Viral packaging and infection of Mc3T3-E1 cells (100×).* ***A)*** *Transfection efficiency in 293FT viral packaging.* ***B)*** *Mc3T3-E1 cells after lentivirus infection.* ***C)*** *Efficiency of lentivirus infection.* ***D)*** *Efficiency of GFP virus infection.*

Mc3T3-E1 cell growth after ER interference

MTT was applied to detect 4 groups of cells (DMSO, E2, E2 + ERα RNAi, E2 + ERβ RNAi). Samples in each group were inoculated into 6 wells in each plate and moreover, 6 blank control wells were also set up. One 96-well plate was selected from 5 plates on the 1st, 3rd, 5th, 7th and 9th days, respectively, after the transfection. OD values of cells in each group were detected using an automatic enzyme-linked immunosorbent assay system and the values of A490 are shown in Table II. On the 1st day after the transfection, there was no statistically significant difference in each group ($p > 0.05$); but an obvious remarkable difference was observed between four groups on the 5th day ($p < 0.05$) (Table II and Fig. 4).

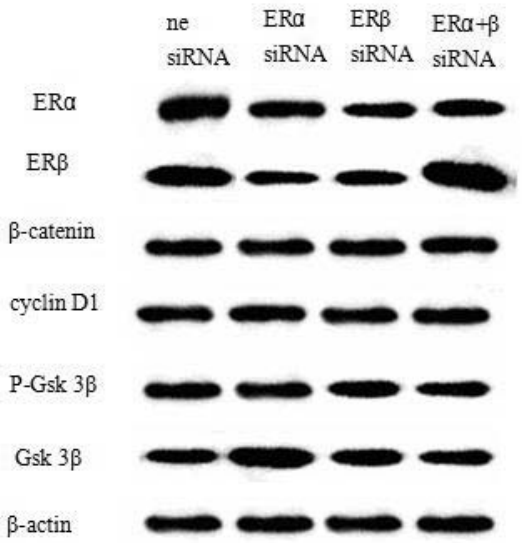

Fig. 3. *Expressions of Wnt pathway signaling molecules and ERs after ER interference.*

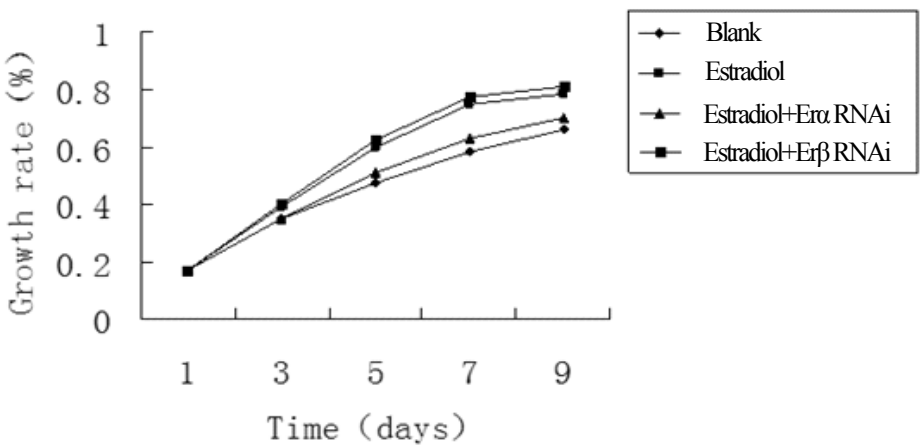

Fig. 4. *Growth curve of Mc3T3-E1 cell after ER interference.packaging.* ***B****) Mc3T3-E1 cells after lentivirus infection.* ***C****) Efficiency of lentivirus infection.* ***D****) Efficiency of GFP virus infection.*

Table II. *A490 values of cells in each group at different time points.*

Groups	Blank control group	Estradiol (10^{-7}M)	ER + ERα RNAi	ER + ERβ RNAi
1d	0.1726±0.0076	0.1767±0.0079	0.1749±0.0069	0.1742±0.0098
3d	0.3445±0.0106	0.3844±0.0093	0.3457±0.0076	0.3947±0.0103
5d	0.4536±0.0166	0.6024±0.0137	0.5043±0.0135	0.6272±0.0182
7d	0.5755±0.0185	0.7453±0.0147	0.6327±0.0123	0.7787±0.0164
9d	0.6535±0.0095	0.7818±0.0168	0.6944±0.0123	0.8084±0.0319

DISCUSSION

Currently, there are two key techniques for studying gene function, i.e., gene knockout and gene interference (11). Gene knockout is realized through destroying a gene or specific genome sequence (12). However, gene knockout technique is lack of cell models (13). RNAi, which can be used to explore the expression function of gene in a certain age stage or specific site, is featured by high efficiency in inhibiting expression of target gene, good specificity of target shooting and simple operation (14). PlentiLox3.7 lentiviral vector (15), a highly efficient gene transduction tool, was used in this study. Compared to psuper retroviral vector previously used (16), plentiLox3.7 lentiviral vector can prepare virus with high titer.

Estrogen plays a role in regulating cell differentiation by transferring signals to the nucleus via ERs (17). Recently, T Okamoto et al. (18) found highly expressed ERβ in the site of active bone formation. ERβ was capable of enhancing the expression of bone formation-related genes as well as osteoblast functions; however, the specific mechanism is not known. Bone growth and sexual maturation are also affected by the gene polymorphisms of ERs. Gene mutation can result in abnormal bone growth and bone loss (19). The gene polymorphisms of ERα and ERβ are closely related to scoliosis, osteoporosis and osteoarthritis of adolescents induced by bone growth and metabolic disorders (20). Comparing ASPP049 estrogen analogs with estradiol, it is found that ASPP049 can promote the proliferation of Mc3T3-E1 cells and activate β-catenin signaling pathway by Era/Akt/Gsk 3β (21). Estrogen can independently promote β-catenin transcriptional expression in N2a-m neuron cells, instead of relying on IGF-1 and Wnt signaling pathways (22). In this study, RNAi technology (23) was applied to interfere ER expression and it was found that estrogen affected osteoblast proliferation by regulating β-catenin expression through ERα receptor.

This study applied the cell biology method (24) to detect the expression of Wnt/p-catenint signaling pathway key factors CyclinDl and p-gsk3β as well as endonuclear β-catenin in Mc3T3-E1 cells after being processed by ER, and moreover determined the influences of Wnt signaling pathway on the proliferation of osteoblast precursor cells in mice by activating Wnt signaling pathway with Wnt 3a. Based on the experimental results, the conclusion is drawn that estradiol can regulate osteoblast proliferation via ERα/Gsk3β/β-catenin-mediated Wnt signaling pathway.

ACKNOWLEDGEMENTS

This work was supported by the science and technology projects of Heilongjiang Province Health Department, number: 2013005

REFERENCES

1. Vilhelmiina P, Peng ZQ, Teuvo H, Juha R, Teresa E, Kalervo HV, Pirkko H. Estrogen responsiveness of bone formation in vitro and altered bone phenotype in aged estrogen receptor-alpha-deficient male and female mice. Eur J Endocrinol 2005; 152(2):301-14.
2. Hoffman-Goetz L, Duerrstein L. The effect of chronic and acute exercise on thymocyte apoptosis and necrosis in ovariectomized mice given dietary genistein. J Sports Med Phys Fitness 2004; 44(3):281-87.
3. Méndez-Dávila C, García-Moreno C, Turbì C, Piedral CDL. Effects of 17beta-estradiol, tamoxifen and raloxifene on the protein and mRNA expression of interleukin-6, transforming growth factor-beta1 and insulin-like growth factor-1 in primary human osteoblast cultures. J Endocrinol Invest 2004; 27(10):904-12.
4. Fua SW, Zeng GF, Zong SH, et al. Systematic review and meta-analysis of the bone protective effect of phytoestrogens on osteoporosis in ovariectomized rats. Nutr Res 2014; 34(6):467-77.
5. Xie X, Shenghua LI, Zhao Y. Research progress of the mechanisms of Wnt signaling pathway in the differentiation of osteoblasts by bone mesenchymal stem cells. Chin J Osteoporos 2011; 17(12):1103-1094.
6. Gray TK, Flynn TC, Gray KM, Nabell LM. 17 beta-estradiol acts directly on the clonal osteoblastic cell line UMR106. Proc Nat Acad Sci 1987; 84(17):6267-71.

7. Kousteni S, Chen JR, Bellido T, et al. Reversal of bone loss in mice by nongenotropic signaling of sex steroids. Obstetr Gynecol Surv 2003; 58(3):843-46.
8. Kousteni S, Han L, Chen JR, Almeida M, Plotkin LI, Bellido T, Manolagas SC. Kinase-mediated regulation of common transcription factors accounts for the bone-protective effects of sex steroids. J Clin Invest 2003; 111(11):1651-64.
9. Tan HB, Giannoudis PV, Boxall SA, McGonagle D, Jones E. The systemic influence of platelet-derived growth factors on bone marrow mesenchymal stem cells in fracture patients. BMC Med 2015; 13(1):1-11.
10. Gabriel M, Sharmin S, Joseph PS, Valerie SS, Cheng SL, Chen D, Roberto C. Beta-catenin and BMP-2 synergize to promote osteoblast differentiation and new bone formation. J Cell Biochem, 2005; 94(2):403-18.
11. Kai S, Tillmann W, Ariana F, et al. Dysfunctional finance: positive shocks and negative outcomes. Policy Res Working Paper Series 2010; 1(1):4-4.
12. Li G, Chunxu Y, Guisheng L. Efficient p53 gene targeting by homologous recombination in rat-induced pluripotent stem cells. Cell Prolifer 2012; 46(1):1-9.
13. Hayashi T, Horiuchi A, Sano K, et al. Molecular approach to uterine leiomyosarcoma: LMP2-deficient mice as an animal model of spontaneous uterine leiomyosarcoma. Sarcoma 2011; 476498 doi: 10.1155/2011/476498.
14. Bian ZQ, Sun LL, Chen WZ, et al. C gene-targeting short hairpin RNA suppresses the replication and expression of hepatitis B virus in BHK-21 cells. Nat Med J Chin 2010; 90(39):2776-81.
15. Song Y, Xu T, Yang MK, Sheng WB. Construction of targeting short hairpin RNA plasmid vector expressing TERT gene. Chin J Tissue Eng Res 2014; 18(7):1057-62.
16. Aliya, Lin W, He Q. Construction of FAK- shRNA retroviral vector and screening of stable HCC-LM3 cell line with persistent knockdown of FAK. Chin J Pathophysiol 2011; 27(4):688-94.
17. Hwang PY, Liufang J, Hoffman BD, Setton LA. The role of extracellular matrix elasticity and composition in regulating the nucleus pulposus cell phenotype in the intervertebral disc: a narrative review. J Biomech Eng 2014; 136(2):40-48.
18. Okamoto T, Kodama S, Nomi N, Umemoto S, Suzuki M. Expression of bone morphogenic protein in sinonasal inverted papilloma with new bone formation. Allergy Rhinol 2011; 2(1):16-20.
19. Rebelo AC, Verlengia R, Kunz V, et al. Lack of association of estrogen receptor alpha gene polymorphisms with cardiorespiratory and metabolic variables in young women. Int J Mol Sci 2012; 13(10):13691-703.
20. Amor IMB, Edouard T, Glorieux FH, et al. Low bone mass and high material bone density in two patients with Loeys-Dietz syndrome caused by transforming growth factor receptor 2 mutations. J Bone Miner Res 2012; 27(3):713-18.
21. Bhukhai K, Suksen K, Bhummaphan N, et al. A phytoestrogen diarylheptanoid mediates estrogen receptor/Akt/glycogen synthase kinase 3β protein-dependent activation of the Wnt/β-catenin signaling pathway. J Biol Chem 2012; 287(43):36168-78.
22. Sharma A, Hu XT, Napier TC, Al-Harthi L. Methamphetamine and HIV-1 Tat Down Regulate β-catenin Signaling: Implications for Methampetamine Abuse and HIV-1 Co-morbidity. J Neuroimmune Pharmacol 2011; 6(4):597-607.
23. Pan Q, Ramakrishnaiah V, Henry S, et al. Hepatic cell-to-cell transmission of small silencing RNA can extend the therapeutic reach of RNA interference (RNAi). Gut 2012; 61(9):1330-39.
24. Lindström M, Thornell L E. New multiple labeling method for improved satellite cell identification in human muscle: application to a cohort of power-lifters and sedentary men. Histochem Cell Biol 2009; 132(2):141-57.

ACTIVATION OF PROTEIN PHOSPHATASE 2A IS RESPONSIBLE FOR INCREASED CONTENT AND INACTIVATION OF RESPIRATORY CHAIN COMPLEX I INDUCED BY ALL-TRANS RETINOIC ACID IN HUMAN KERATINOCYTES

F. PAPA[1], N. SARDARO[1], R. LIPPOLIS[2], D. PANELLI[1] and S. SCACCO[1]

[1]Department of Basic Medical Sciences, Neurosciences and Sense Organs. University of Bari "Aldo Moro", Bari, Italy; [2]Institute of Bioenergetics and Biomembranes (IBBE) of the Italian National Council of Researches (CNR), Bari, Italy

Received April 17, 2015 – Accepted October 27, 2015

This study presents the effect of all-trans retinoic acid (ATRA) on cell growth and respiratory chain complex I in human keratinocyte cultures. Keratinocyte treatment results in increased level of GRIM-19 and other subunits of complex I, in particular of their carbonylated forms, associated with inhibition of its enzymatic activity. The results show that in keratinocytes ATRA-promoted phosphatase activity controls the proteostasis and activity of complex I.

All-trans retinoic acid (ATRA), a vitamin A metabolite, exerts diverse effects on cell growth, differentiation and transformation (1). More than five hundred genes have been put forward as ATRA targets (2). Several ATRA responsive genes are associated with retinoid-interferon-induced mortality (3), one of which is GRIM-19 (NDUFA13) encoding a protein of 16 kDa (4), evolutionary conserved in most eukaryotes (5, 6, 7). GRIM-19 promotes cell death and appears to function as a tumor suppressor. GRIM-19 protein was initially detected in the nucleus as inhibitor of the transcription factor STAT3 (8, 9), but it was subsequently found to be essentially localized in mitochondria where it appears as a constituent subunit (subunit B16.6) of complex I of the respiratory chain (10). GRIM-19 is essential for the assembly and function of complex I, but its biological role is still to be fully understood. Several tumors show down regulation of GRIM-19 (11); overexpression of GRIM-19 was, on the other hand, found to enhance death of HeLa cells and other lines of cancer cells (12, 13). Transfection of cell lines with vectors expressing antisense GRIM-19 results in enhancement of cell growth rate (14). It has been shown that the cytostatic action of ATRA in ovarian carcinoma cells was associated with promotion of PP2A phosphatase, which resulted in dephosphorylation of the Rb/p130 tumor suppressor and prevention of its degradation (15). Our group previously found that ATRA inhibition of the growth of human keratinocyte cultures was associated with increased level of GRIM-19 and other subunits of complex I, but inhibition of the respiratory activity of the complex (16). The present work shows that ATRA effects on complex I are mediated by promotion of keratinocyte phosphatase activity.

MATERIALS AND METHODS

Normal human keratinocytes from Clonetics (NHEK,

Key words: all-trans retinoic acid, human keratinocytes, GRIM-19, mitochondria, cell growth, NADH ubiquinone oxidoreductase

Mailing address: Prof. Salvatore Scacco,
Department of Basic Medical Sciences,
Neurosciences and Sense Organs
University of Bari "Aldo Moro",
P.zza Giulio Cesare, 11,
70124, Bari, Italy
e-mail: salvatore.scacco@uniba.it

0393-974X (2016)

CC-2501, BioWhittaker Inc., Walkersville, MD, USA) were tested for keratin production and contact-inhibited growth. KGM2 basal medium was from Clonetics; Phosphate Buffered Saline (PBS), Trypsin (0.05%) - EDTA (0.02%), penicillin, streptomycin and fetal bovine serum were from EuroClone; All-trans retinoic acid was from SIGMA; mouse monoclonal antibodies against 20 kDa and 39 kDa of complex I, core II of complex III, β-subunit of complex V and subunit IV of complex IV, were from Molecular Probes; Anti GRIM-19 was from Mitosciences: Annexin-V test from BioVision; Apoptotic DNA Ladder detection assay was from Promega. Horseradish peroxidase conjugate goat anti-mouse IgG antibody was from Calbiochem; Western blot enhanced chemiluminescence reagent (ECL) was from NEN Life Science; Bradford assay was from Bio-Rad; all other chemicals were of the highest purity available.

Apoptosis assays

For Annexin V-FITC apoptotic assay, the fluorescence microscopy analysis was performed according to the manufacturer (BioVision). For analysis of apoptotic DNA fragmentation, handling of samples for DNA preparation was performed according to the protocol indicated by the manufacturer of the Apoptotic DNA Ladder detection assay (Promega) which also provided, as positive control, samples of apoptotic fragmented DNA.

Immunofluorescence in keratinocyte cultures

For histological preparations, keratinocytes were grown on polylysine coverglasses on the bottom of six-well plates under standard medium conditions and fixed 20 min with 100% methanol and permeabilized 10 min with 0.1% Triton in PBS. The cells were then incubated overnight in a cold room in a PBS solution with 1% BSA and 1:200 primary mouse monoclonal antibody for GRIM-19. The primary antibody was washed with PBS and incubated for 4 h with FITC-conjugated rabbit anti-mouse antibody (Invitrogen). After PBS washing, the coverglasses were mounted on a microscope slide with a 1:1 glycerol-PBS drop and the fluorescence was read with a Leica TCS (Leica Microsystems Heidelberg GMBH, Germany) confocal microscope, under laser argon-krypton Innova 310, 75 mW, ultraviolet source.

Cell culture and mitoplast preparation

Normal human keratinocytes were maintained in culture with KGM2 medium with 10% fetal bovine serum at 37°C (17) and, where indicated, treated with 20 μM all-trans retinoic acid from a 20 mM stock solution in DMSO. To examine the effects of RA on the cell growth, cells were seeded in multi-wells flask and treated with 20 μM RA, using DMSO in controls, and on the indicated days the cells were harvested and counted. For mitoplast preparation, keratinocytes were harvested with 0.05% trypsin and 0.02% EDTA and washed in phosphate buffered saline pH 7.4 (PBS), with 5% FBS. Cells in PBS, were exposed 10 min on ice to 0.5 mg digitonin/mg cellular protein. Mitoplasts were pelleted at 14000g x 10 min and exposed to 10W ultrasound energy for 5 s x 3 times. The protein concentration was determined by the Bradford assay using bovine serum albumin as standard.

Real-time PCR

Total RNA was treated with DNAase RNAase free (Roche) and then 1 μg of RNA was reverse transcribed with 0.5 μg of oligo dT18 or 0.5 μg of random hexamers and 200 U of M-MLV Reverse Transcriptase, RNase H Minus, Point Mutant (Promega). Quantitative real-time PCR experiments were performed by IQ Sybr Green super mix (Biorad), and 40 ng cDNA were used to measure β-actin and GRIM-19 (NDUFA13). In each amplification 200 nM of specific primers (NDUFA13, Fw 5′ - ATC GAC TAC AAA CGG AAC TTG CCG - 3′; Rw 5′ - GTA ACA GTG GCA ACA GCG CGAT - 3′) were used. Relative RNA levels were calculated from CT values according to the ΔCT method (Biorad) and relative levels were normalized in respect to the β-actin. The PCR conditions were: 20″ at 94°C, 30″ at 59.5°C, 45″ at 72°C for 45 cycles, followed by a melt curve cycle.

Electrophoresis and immunoblotting

Forty to forty-five μg per lane of proteins were electrophoresed on a 12% Tricine/SDS PAGE according to Shagger (18). Samples were re-suspended with Lysis buffer 3X (12% SDS, 150 mM Tris Cl, 6% β-mercaptoethanol, 30% glycerol, pH 6.8 and transferred onto nitrocellulose membrane (1 h) by Western blotting. Membranes were blocked with TTBS + 5% milk overnight at 4°C. Afterward the blots were treated with primary monoclonal antibodies diluted in TTBS supplemented with 5% milk at 4°C using the following dilutions: cytochrome c 1:2000; GRIM-19 1:1500. After rinsing three times with TTBS the blots were incubated 1 h with secondary antibody peroxidase conjugated. Specific detection of the secondary antibody was obtained with the chemiluminescent Western blotting detection system (Amersham). Semi-quantitative densitometry analysis of immunodetected bands was performed with Versa-Doc gel analyzer (Bio-Rad). Two-dimensional gel analysis (Blue Native PAGE/SDS-PAGE) of mitoplasts from keratinocytes was carried out as described by Scacco et al. (19). After the second dimension (SDS-PAGE), gels were transferred onto nitrocellulose for immunoblotting of subunits of complexes as described by Iuso et al. (20).

Enzymatic assays

Protein phosphatase (PP2A type) activity on total cell lysate was assayed photometrically using a Ser/Thr phosphatase assay kit (Upstate Biotechnology). The NADH–UQ oxidoreductase activity: Vmax and Km were determined on 70 μg sonicated mitoplasts (16). The non-significant changes of Km (15-25 μM) were not, consequently, reported. Cytochrome c oxidase activity was determined on 20 μg mitoplasts in 700 μl 25 mM phosphate buffer, 5 mM $MgCl_2$, pH 7.4, following the oxidation of 10 μM ferrocytochrome c (16). Citrate synthase activity was used as mitochondrial matrix enzymatic marker. Thirty μg mitoplasts, 0.5 mM acetyl CoA, 0.5 mM DTNB were added to 700 μl 100 mM Tris-Cl buffer, pH 8.0; the reaction was started by the addition of 0.5 mM oxalacetate (17).

Carbonylation of Complex I subunits

Four hundred μg protein mitoplasts from human keratinocytes were loaded on 4 separated gel lines and submitted to Blue Native-PAGE. The band corresponding to complex I was excised from gel and electroelution was performed. 0.1 mg of electroeluted subunits of complex I were incubated for 1 h at 25°C in 5 mM DNPH in 2 N HCl. The proteins were then precipitated with 10% TCA (w/v) and centrifuged at 10,000 g for 5 min. The proteins were separated by 12% SDS-polyacrylamide gel electrophoresis and transferred to a nitrocellulose membrane. The membrane was blocked with 5% nonfat dry milk in TTBS for 2 h at 4°C and probed with antibody against the anti-DNPH (Invitrogen) (1:3000). After being washed in TTBS, the membrane was incubated for 60 min with anti IgG peroxidase-conjugated antibody (1:5000). Immunodetection was then performed, after further TTBS washes, with ECL (Euroclone).

Statistical analysis

Differences in growth curves in standard conditions or in the presence of RA, differences in specific subunits expression after 72 hours of treatment with RA and differences in the effect of RA treatment on NADH ubiquinone oxidoreductase (complex I), cytochrome c oxidase (complex IV) and citrate synthase activities in mitoplasts were tested by using the Student's *t*-test. Values of $P < 0.05$ were considered statistically significant.

RESULTS

ATRA added at a concentration of 20 μM to NHEK cell cultures suppressed cell growth (Fig. 1). Annexin-V immunofluorescence of the NHEK cultures and the DNA ladder test showed that ATRA induced growth suppression without triggering apoptotic cell death (Fig. 2). Confocal microscope analysis of NHEK cultures revealed a marked increase in the ATRA-treated cells of the GRIM-19 protein, revealed by immunofluorescence with monoclonal specific antibody. Magnification of the

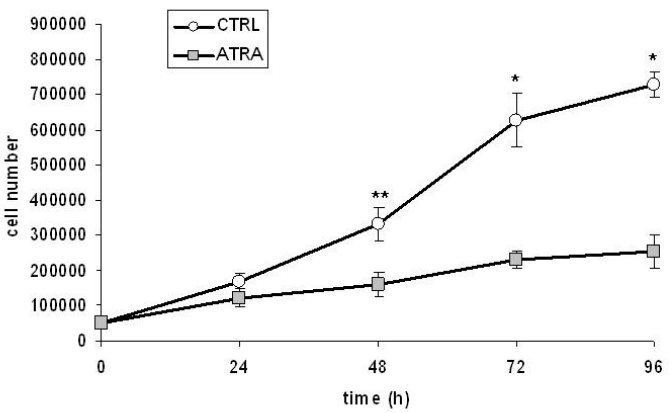

Fig. 1. *Effect of ATRA on NHEK cell growth rate. Growth curves in normal human keratinocytes (NHEK) cultured in KGM-2 basal medium (circles) and in presence of all-trans retinoic acid (ATRA) 20 μM (squares) are shown. The cell growth rate was evaluated by daily cell count after the initial seeding of 10,000 cells/well in a six-well petri dish. (*) P<0.001; (**) P<0.01; (***) P<0.05.*

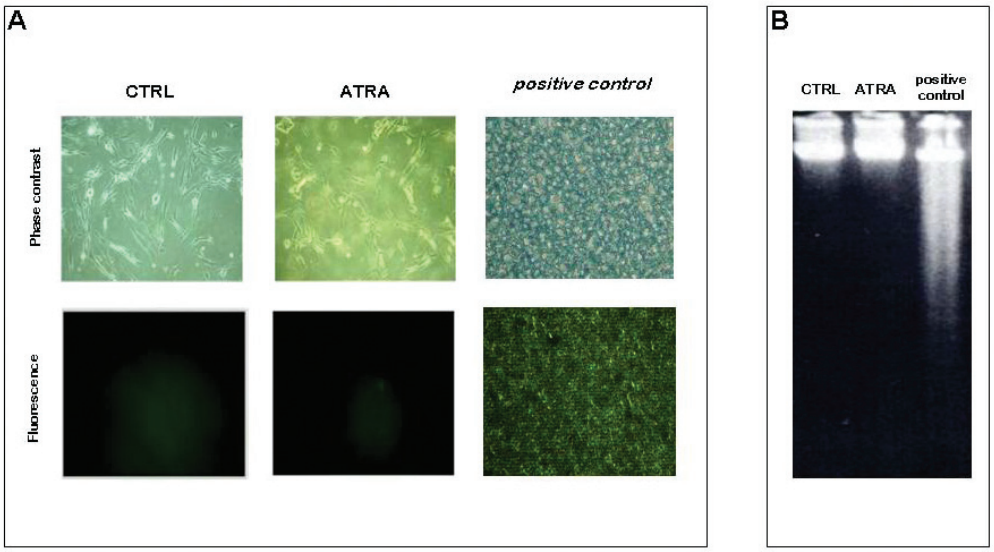

Fig. 2. *Tests for apoptosis.* ***A****) Annexin-V immunofluorescence detection in cultures of human keratinocytes (CTRL) and after 72-h treatment with all-trans retinoic acid (ATRA). After ATRA treatment no signal is detected, indicating that it does not induce apoptosis. UV exposed cultured slices from mice cerebellum, which exhibits a signal for Annexin-V, was used as "positive control". Upper lines show the aspect of the cultures under visible light; lower lines, same fields under UV light.* ***B****) DNA ladder test on nuclear extracts from cultures of human keratinocytes (CTRL), after 72-h treatment with all-trans retinoic acid (ATRA) and apoptotic fragmented DNA (standard positive control). Absence of genomic DNA degradation indicates that ATRA treatment suppress cell growth without inducing apoptosis.*

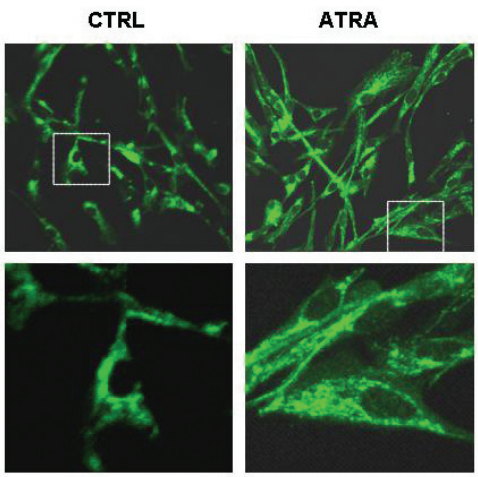

Fig. 3. *FITC-anti GRIM-19 immunofluorescence in keratinocyte cultures. Human keratinocytes were grown on polylisine coverglasses on the bottom of six-well plates under standard medium conditions (Ctrl) and treated 72 h with all-trans retinoic acid (ATRA). For histological preparation, the cells were fixed 20 min with 100% methanol and permeabilized 10 min with 0.1% Triton in PBS. The cells were then incubated overnight in cold room in a PBS solution with 1% BSA and 1:200 primary mouse monoclonal antibody for GRIM-19. The primary antibody was washed with PBS and incubated 4 h with FITC-conjugated rabbit anti-mouse antibody (Invitrogen). After PBS washing, the coverglasses were mounted on a microscope slide with a 1:1 glycerol-PBS drop and the fluorescence was read with a Leica TCS (Leica Microsystems Heidelberg GMBH, Germany) confocal microscope, under laser argon-krypton Innova 310, 75 mW, ultraviolet source.*

confocal microscope images showed that GRIM-19 was essentially localized in the mitochondrial cellular network (Fig. 3).

Keratinocyte treatment with ATRA had no significant effect on the level of its messenger RNA (Fig. 4A), under the conditions in which it resulted in an increase of the cellular level of GRIM-19 protein (Fig. 4B). Thus the increase in the GRIM-19 protein cellular level induced by ATRA, is due to post-transcriptional increase of the protein level.

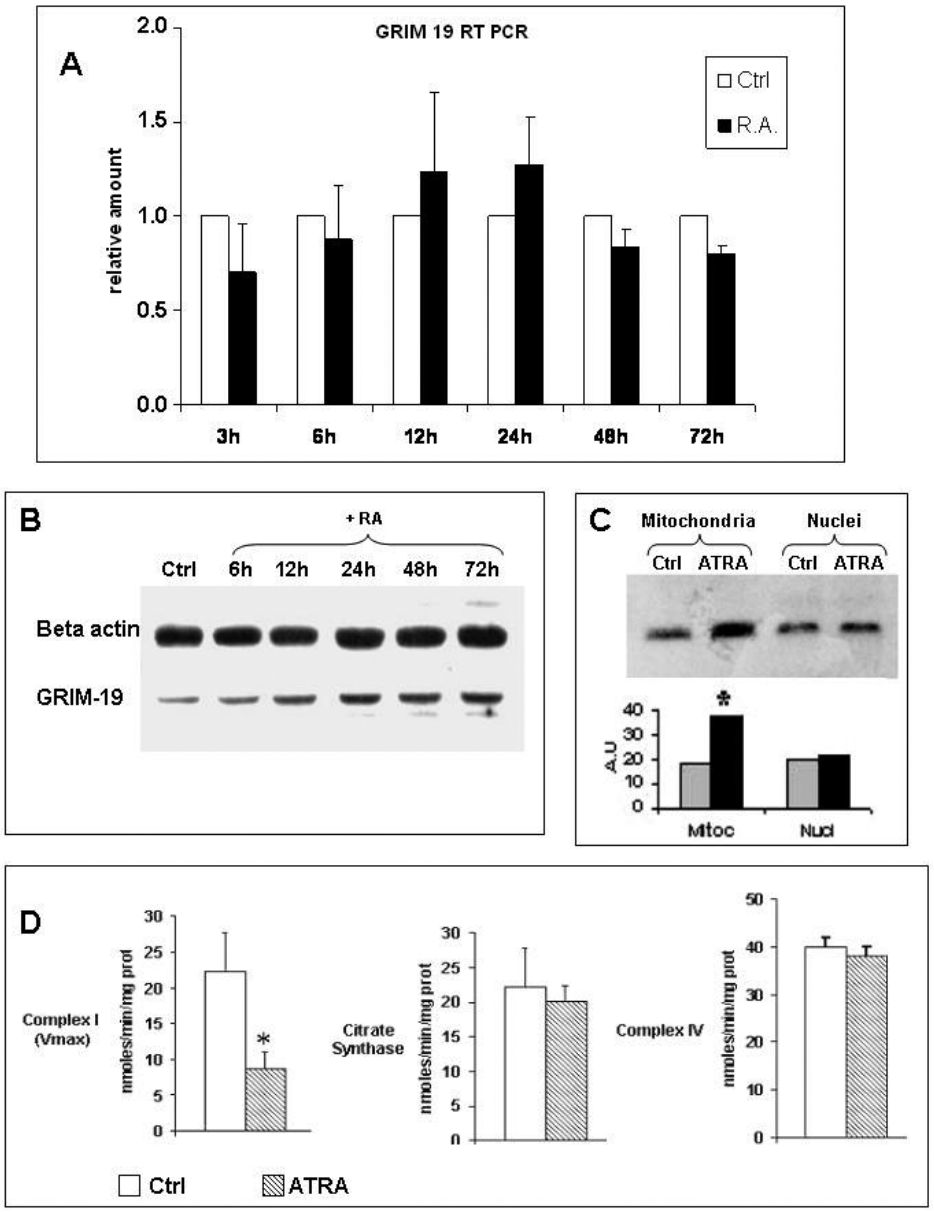

Fig. 4. *Effect of ATRA on cellular expression of GRIM-19.* ***A)*** *Real-time PCR quantification of GRIM-19 mRNA from human keratinocytes (CTRL, white bars) and after 3 h, 6 h, 12 h, 24 h, 48 h and 72-h treatment with 20 μM ATRA (black bars). Beta-actin mRNA was used to normalize the reaction and values are shown as relative ratio to control cell cultures. P values were not significant at each time point.* ***B)*** *Total cell extract Western blot with mouse monoclonal antibody for GRIM-19 and beta-actin. Forty* μg *protein samples from human keratinocytes (CTRL) and after 6 h, 12 h, 24 h, 48 h and 72 h treatment with 20 μM ATRA were separated by SDS-PAGE and blotted onto nitrocellulose membrane for immunodetection. Western blots of three different experiments showed similar results.* ***C)*** *Mitochondrial and nuclear fraction Western blot with mouse monoclonal anti GRIM-19. Forty* μg *protein samples from human keratinocytes (CTRL) and after 72-h treatment with all-trans retinoic acid (ATRA) were separated by SDS-PAGE and blotted onto nitrocellulose membrane for immunodetection. Densitometric analysis of two fractions is shown. Determinations were made on three different experiments. (*) P<0.001; (**) P<0.01; (***) P<0.05.* ***D)*** *Mitochondrial enzyme activities in mitoplast preparations from human keratinocytes (CTRL) and after 72-h treatment with 20 μM ATRA. Activities of rotenone sensitive NADH-UQ oxidoreductase (Vmax) (Complex I), citrate synthase and cytochrome c oxidase (Complex IV) are shown. Determinations were made on three different experiments. (*) P<0.001; (**) P<0.01; (***) P<0.05.*

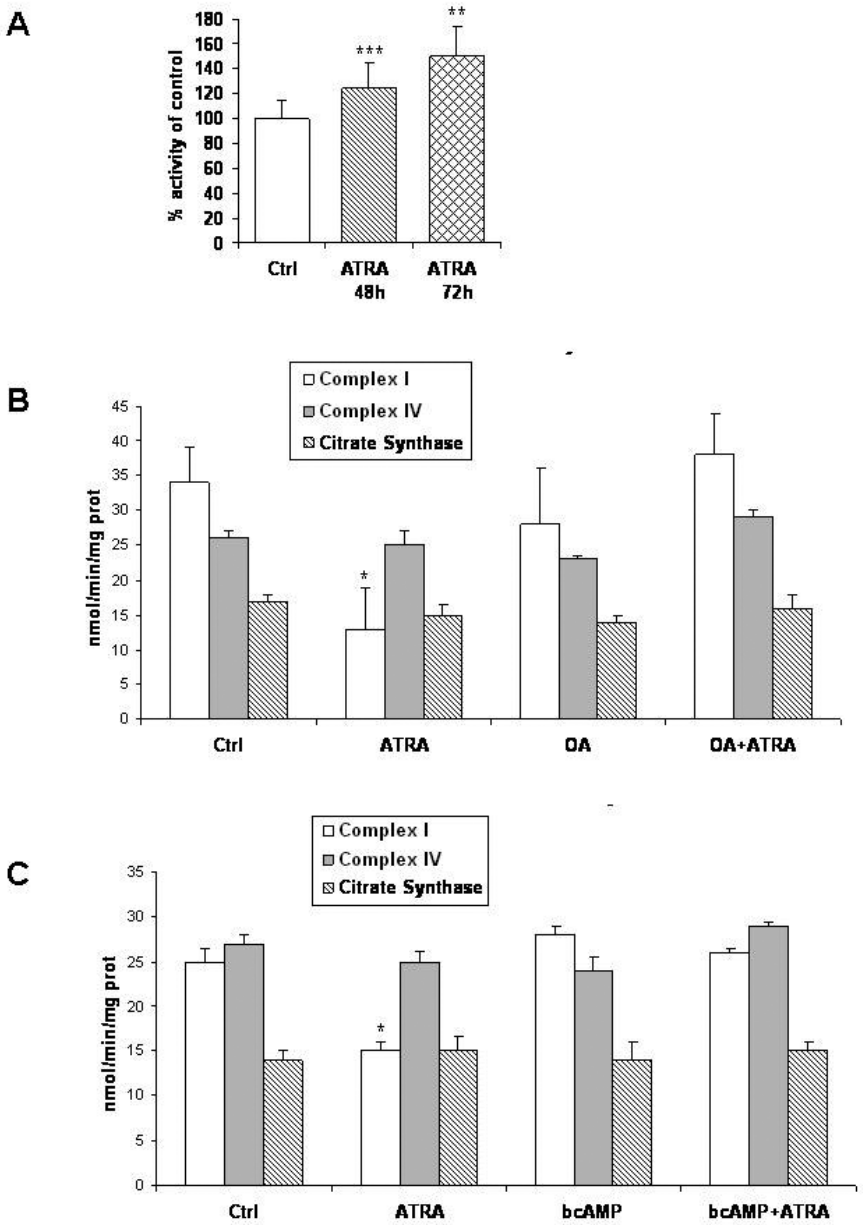

Fig. 5. *Enzymatic activity of respiratory complexes and PP2A and after ATRA treatment.* ***A)*** *Protein Phosphatase 2A activity in total cell extracts of cultures of human keratinocytes (CTRL) and after 48-h and 72-h treatment with 20* μM ATRA. ***B)*** *NADH-UQ oxidoreductase (Vmax) (CI), cytochrome c oxidase (COX) and citrate synthase (CS) activities were measured in mitoplast fraction from control human keratinocytes (CTRL) and after 72-h treatment with 20 μM ATRA (RA). The supplementation with 100 nM okadaic acid 1 h, after 72-h ATRA treatment, reversed significantly CI inhibition (OA+RA). No significant effect of okadaic acid alone (OA) was observed.* ***C)*** *NADH-UQ oxidoreductase (Vmax) (CI), cytochrome c oxidase (COX) and citrate synthase (CS) activities were measured in the mitoplast fraction from control human keratinocytes (CTRL) and after 72-h ATRA treatment (RA). After 72-h ATRA treatment, supplementation with 100* μM *dibutyryl cyclic AMP for 1 h, reversed significantly CI inhibition (RA+dbAMPc). No significant effect of dibutyryl cyclic AMP alone (dbcAMP) was observed. All determinations were made on three different experiments. (*) P<0.001; (**) P<0.01; (***) P<0.05.*

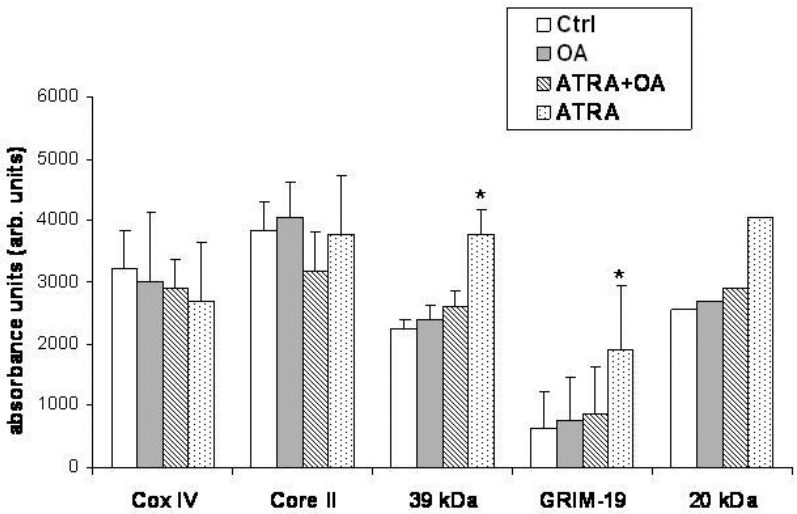

Fig. 6. *Level of subunits of respiratory complexes after ATRA and okadaic acid treatment. Eighty µg protein mitoplasts from control human keratinocytes (CTRL) and after 72-h 20 µM ATRA treatment, 1 nM okadaic acid, or ATRA plus okadaic acid, were subjected to 2D-BlueNative-SDS PAGE, blotted onto nitrocellulose and specific subunits of Complex IV (Cox IV), complex III (Core II) and complex I (39kDa, GRIM-19, 20 kDa) were immunodetected by monoclonal antibodies. All determinations were made on five different blots, except for 20 kDa which was analysed in two experiments. (*) P<0.001; (**) P<0.01; (***) P<0.05.*

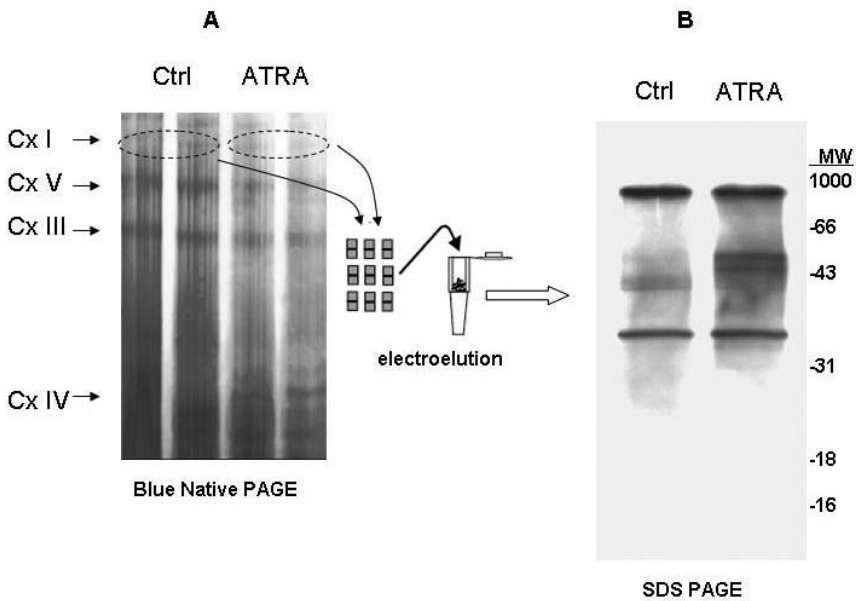

Fig. 7. *Detection of oxidized subunits of complex I from keratinocytes. Protein mitoplasts from control human keratinocytes (CTRL) and after 72-h treatment with 20 µM ATRA, were submitted to Blue Native-PAGE (**A**). The bands corresponding to Complex I were excised from gel, collected, electroeluted and DNPH crosslinked to carbonylic groups of oxidized proteins. The products were applied to SDS PAGE, blotted onto nitrocellulose and immunodetected with anti-DNPH antibody and anti-NDUFS3 antibody (**B**). All determinations were made on three different blots.*

Immunoblot analysis of keratinocyte subcellular fractions showed that ATRA treatment of the cultures increased specifically the mitochondrial level of GRIM-19, where the protein was practically confined as a constituent subunit of complex I (10, 14). The small amounts of GRIM-19 detected in the nucleus were practically unaffected by ATRA (Fig.4C). The ATRA-induced increase of the content of complex I GRIM-19 was, however, associated with depression of the NADH-ubiquinone oxidoreductase activity (expressed as Vmax) of the complex (Fig. 4D). No significant modification of complex I Km was detected (see under Materials and Methods).

Treatment of keratinocyte cultures with ATRA resulted, within the same time range in which it increased the GRIM-19 level, in stimulation of the activity of protein phosphatase A2 (Fig. 5A) (18).

The inhibition of complex I activity caused by ATRA treatment of keratinocyte cultures, was rescued by the addition of the protein phosphatase inhibitor okadaic acid (Fig. 5B) or dibutyryl cyclic AMP (Fig. 5C). It can be noted that the activity of cytochrome c oxidase and citrate synthase were both unaffected by the above treatments (Fig. 5 B-C).

Extensive two dimensional blue-native/SDS gel electrophoresis followed by immunoblotting with specific antibodies showed that the ATRA-induced increase in the level of GRIM-19 was associated with similar increase in the level of other constitutive subunits of complex I, i.e. 39 kDa and 20 kDa subunits (Fig. 6). The ATRA-induced increase of complex I subunits was prevented by the presence of okadaic acid, which per se had little or no effect on the level of complex I subunits (Fig. 6). It can be noted that ATRA and okadaic acid had no effect on the level of subunit IV of cytochrome c oxidase (complex IV) and core II subunit of ubiquinone cytochrome c oxidoreductase (complex III), thus eliminating any false change of complex I subunits due to differences in protein loading on the gels used for the protein analysis.

There is evidence showing that oxidative damage of complex I subunits results in inhibition of its catalytic activity (21). Direct anti-DNP analysis of the keratinocyte complex I subunits, separated by 2D Blue Native/SDS gel electrophoresis, show that ATRA treatment of the keratinocyte cultures increased the level of carbonylated subunits of complex I (Fig. 7).

DISCUSSION

Treatment of keratinocyte cultures with ATRA, under conditions in which it suppresses cell growth, is associated with enhanced content but inactivation of respiratory chain complex I (14). The present work shows that these effects of ATRA on complex I are associated with ATRA-induced promotion of the functional capacity of protein phosphatase A (PP2A type). The ATRA effects on complex I were, in fact, prevented or reversed by the phosphatase inhibitor okadaic acid or by dibutyryl cAMP.

These findings show that in keratinocytes the balance between phosphatase and protein kinase controls proteostasis and activity of complex I. Previous findings from our laboratory (15, 22, 23) and others (13) suggest that these effects of ATRA-promoted phosphatase result from dephosphorylation of complex I subunits. This remains to be directly verified and other mechanism(s), cannot at present be excluded.

Mass spectrometric analyses have shown that GRIM-19 is present in complex I both in non-phosphorylated and threonine-phosphorylated forms (21). This indicates that GRIM-19 undergoes a dynamic condition of phosphorylation/dephosphorylation which can regulate the role of these subunits in the assembly and stability of complex I and cell growth control. Deletion of the C-terminus of GRIM-19, where the threonine phosphorylation site is located, has been found to suppress its cell death promoting effects (4). It can be argued that ATRA-dephosphorylation of GRIM-19, inhibits its proteolytic degradation, in a similar way as shown for the growth suppressor Rb/p130 in ovarian carcinoma cells (13).

Increased level of GRIM-19, which promotes complex I assembly is accompanied by increased level of other complex I subunits. Besides GRIM-19 (B16.6), other subunits of complex I have been found to undergo dynamic phosphorylation, i.e. subunits 42 kDa , B14.5a, B14.5b and NDUFS4 (18, 21). In particular, phosphorylation of the NDUFS4 subunit by cAMP-dependent protein kinase plays a critical role in promoting the activity of the complex and preventing oxygen free radical production (24).

It is conceivable that conditions under which complex I subunits are dephosphorylated because of phosphatase activation, a vicious cycle is set-up in which subunits of the inactivated complex undergo oxidative damage with further depression of its catalytic activity (19, 25). The mechanism by which the ATRA-induced accumulation of GRIM-19 and of the overall complex I results in suppression of cell growth remains to be clarified. The finding that ATRA treatment did not lead to increase of the nuclear content of GRIM-19, would exclude the possibility that the inhibition of cell growth is, in the present case, due to ATRA-induced translocation of GRIM-19 from mitochondria to the nucleus.

It can be noted that AIF, a mitochondrial flavoprotein which, upon induction of apoptosis, translocates to the nucleus where it activates chromatinolysis, has been detected in the serine phosphorylated form in complex I (18). Furthermore, the oncogene STAT-3, besides being localised in the nucleus, has also been found in mitochondria where it interacts with GRIM-19 (26). Thus, perturbation of the interplay of GRIM-19 with these other factors, associated with complex I, can be involved in the ATRA suppression of keratinocyte growth.

ACKNOWLEDGEMENTS

This work was supported by: University of Bari Research Grant, 2009 to F. Papa. National Project, "Progetto FIRB Rete Nazionale per lo Studio della Proteomica Umana (Italian Human ProteomeNet)", Ministero dell'Istruzione, dell'Università e della Ricerca (MIUR), [RBRN07BMCT_014]. Progetto Strategico Ric.002, Cip PS 101, POR 2000/06.

REFERENCES

1. Love JM, Gudas LJ. Vitamin A, differentiation and cancer. Curr Opin Cell Biol 1994; 6:825-31.
2. Balmer JE, Blomhoff R. Gene expression regulation by retinoic acid. J Lipid Res 2002; 43:1773-808.
3. Kalvakolanu DV. The GRIMs: a new interface between cell death regulation and interferon/retinoid induced growth suppression. Cytokine Growth Factor Rev 2004; 15:169-94.
4. Angell JE, Lindner DJ, Shapiro PS, Hofmann ER, Kalvakolanu DV. Identification of GRIM-19, a novel cell death-regulatory gene induced by the interferon-beta and retinoic acid combination, using a genetic approach. J Biol Chem 2000; 275:33416-26.
5. Huang G, Lu H, Hao A, Ng DC, Ponniah S, Guo K, Lufei C, Zeng Q, Cao X. GRIM-19, a cell death regulatory protein, is essential for assembly and function of mitochondrial complex I. Mol Cell Biol 2004; 24:8447-56.
6. Fearnley IM, Carroll J, Shannon RJ, Runswick MJ, Walker JE, Hirst J. GRIM-19, a cell death regulatory gene product, is a subunit of bovine mitochondrial NADH:ubiquinone oxidoreductase (complex I). J Biol Chem 2001; 276:38345-8.
7. Lai CH, Chou CY, Ch'ang LY, Liu CS, Lin W. Identification of novel human genes evolutionarily conserved in *Caenorhabditis elegans* by comparative proteomics. Genome Res 2000; 10:703-13.
8. Lufei C, Ma J, Huang G, Zhang T, Novotny-Diermayr V, Ong CT, Cao X. GRIM-19, a death-regulatory gene product, suppresses Stat3 activity via functional interaction. EMBO J 2003; 22:1325-35.
9. Syed Z, Cheepala SB, Gill JN, et al. All-trans retinoic acid suppresses Stat3 signaling during skin carcinogenesis. Cancer Prev Res (Phila) 2009; 2:903-11.
10. Carroll J, Fearnley IM, Shannon RJ, Hirst J, Walker JE.Analysis of the subunit composition of complex I from bovine heart mitochondria. Mol Cell Proteomics 2003; 2:117-26.
11. Alchanati I, Nallar SC, Sun P, et al. A proteomic analysis reveals the loss of expression of the cell death regulatory gene GRIM-19 in human renal cell carcinomas. Oncogene 2006; 25:7138-47.
12. Hao M, Shu Z, Sun H, Sun R, Wang Y, Liu T, Ji D, Cong X. GRIM-19 expression is a potent prognostic marker in colorectal cancer. Hum Pathol 2015; (Aug 4, Epub ahead of print).
13. Moreira S, Correia M, Soares P, Máximo V. GRIM-19 function in cancer development. Mitochondrion 2011; 11:693-9.
14. Zhang J, Yang J, Roy SK, Tininini S, Hu J, Bromberg JF, Poli V, Stark GR, Kalvakolanu DV. The cell death regulator GRIM-19 is an inhibitor of signal transducer and activator of transcription 3. Proc Natl Acad Sci USA 2003; 100:9342-7.
15. Vuocolo S, Purev E, Zhang D, Bartek J, Hansen K,

Soprano DR, Soprano KJ. Protein phosphatase 2A associates with Rb2/p130 and mediates retinoic acid-induced growth suppression of ovarian carcinoma cells. J Biol Chem 2003; 278:41881-9.

16. Papa F, Delia M, Trentadue R, et al. Differential effects of all-trans retinoic acid on the growth of human keratinocytes and mouth carcinoma epidermoid cultures. Involvement of GRIM-19 and complex I of the respiratory chain. Int J Immunopathol Pharmacol 2007; 20:719-29.
17. Srere PA. Controls of citrate synthase activity. Life Sci 1974; 15:1695-710.
18. Papa S, Scacco S, De Rasmo D, et al. cAMP-dependent protein kinase regulates post-translational processing and expression of complex I subunits in mammalian cells. Biochim Biophys Acta 2010; 1797:649-58.
19. Scacco S, Vergari R, Scarpulla RC, Technikova-Dobrova Z, Sardanelli A, Lambo R, Lorusso V, Papa S. cAMP-dependent phosphorylation of the nuclear encoded 18-kDa (IP) subunit of respiratory complex I and activation of the complex in serum-starved mouse fibroblast cultures. J Biol Chem 2000; 275:17578-82.
20. Iuso A, Scacco S, Piccoli C, et al. Dysfunctions of cellular oxidative metabolism in patients with mutations in the NDUFS1 and NDUFS4 genes of complex I. J Biol Chem 2006; 281:10374-80.
21. De Rasmo D, Signorile A, Larizza M, Pacelli C, Cocco T, Papa S. Activation of the cAMP cascade in human fibroblast cultures rescues the activity of oxidatively damaged complex I. Free Radic Biol Med 2012; 52:757-64.
22. De Rasmo D, Palmisano G, Scacco S, et al. Phosphorylation pattern of the NDUFS4 subunit of complex I of the mammalian respiratory chain. Mitochondrion. 2010; 10:464-71.
23. Palmisano G, Sardanelli AM, Signorile A, Papa S, Larsen MR. The phosphorylation pattern of bovine heart complex I subunits. Proteomics 2007; 7:1575-83.
24. Papa S, De Rasmo D. Complex I deficiencies in neurological disorders. Trends Mol Med 2013; 19:61-9.
25. Signorile A, Sardaro N, De Rasmo D, Scacco S, Papa F, Borracci P, Carratù MR, Papa S. Rat embryo exposure to all-trans retinoic acid results in postnatal oxidative damage of respiratory complex I in the cerebellum. Mol Pharmacol 2011; 80:704-13..
26. Wegrzyn J, Potla R, Chwae YJ, et al. Function of mitochondrial Stat3 in cellular respiration. Science 2009; 323:793-7.

Wnt SIGNALING PATHWAY INHIBITORS AS PROMISING DIAGNOSTIC SERUM MARKERS OF OSTEOLYTIC BONE METASTASIS

E. GALLIERA[1,2], M.G. MARAZZI[3], L. DRAGO[1,3], G. BANFI[1], A. LUZZATI[1] and M.M. CORSI ROMANELLI[3,4]

[1]IRCCS Galeazzi Orthopedic Institute, Milan, Italy; [2]Department of Biomedical, Surgical and Oral Science, University of Milan, Milan, Italy; [3]Department of Biomedical Sciences for Health, University of Milan, Milan, Italy; [4]U.O.C SMEL-1 Patologia Clinica IRCCS Policlinico San Donato, San Donato (Milan) Italy

Received September 3, 2015 – Accepted April 14, 2016

Despite the clinical importance of bone metastases, we still know little about their onset and progression and current diagnostic tools lack the sensitivity and specificity required for clear early diagnosis. We therefore need to continue studying the pathogenesis of bone metastatic invasion in order to improve diagnosis. The Wnt pathway has been described as having an important role in bone carcinogenesis and metastatic progression. This study investigated the diagnostic potential of the two main Wnt inhibitors, sclerostin and DKK-1, to improve the detection of osteolytic bone metastases. We measured sclerostin and DKK-1, MMP-2 and MMP-9, the bone resorption marker TRAP5b and the metastatic marker survivin in a control group of healthy patients, in patients with primary tumors and in a group with metastasis. Sclerostin and DKK-1 were clearly high in primary tumor patients and even higher in metastatic patients, compared to controls. The close correlations with metastatic markers and bone resorption markers make sclerostin and DKK-1 promising as new biomarkers in the diagnosis of bone osteolytic metastases.

Skeletal metastases are a major problem in the management of advanced cancer, because they cause a range of adverse skeletal events (bone pain, hypercalcemia, spinal cord compression and fractures) (1, 2). The disordered regulation of bone turnover induced by metastatic spread can lead to two different types of metastasis: osteoblastic metastases, typical of prostate cancer, where the bone disruption is due to an increase of both bone formation and resorption, and the more common osteolytic metastases, typical of breast cancer and multiple myeloma, where there is a prevalence of bone erosion, leading to local bone destruction and fracture (3).

It is essential to investigate bone metastasis for cancer staging as it influences therapeutic and clinical decisions. Nevertheless, these metastases are still difficult to diagnose without radiology (4). However, the current diagnosis based on X-rays and scintigraphy often lacks specificity (5). Better diagnostic tools are therefore still needed for early detection and monitoring of bone metastases.

Bone metastasis results from the disruption of physiological bone turnover, and recent findings by our group and others suggest that biochemical markers of bone turnover could help in the diagnosis and follow-up (4-6). Cancer diseases establish bone

Key words: Wnt signaling, bone metastasis, diagnostic markers

Mailing address:
Dr. Emanuela Galliera, PhD
Clinical Pathology,
Department of Biomedical, Surgical and Oral Science,
University of Milan, Via festa del Perdono, 7, 20122 Milan, Italy
Tel.: +39 02 50315354 - Fax:+39 02 50315338
e-mail: emanuela.galliera@unimi.it

0393-974X (2016)

DISCLOSURE: ALL AUTHORS REPORT NO CONFLICTS OF INTEREST RELEVANT TO THIS ARTICLE.

metastasis through their ability to convert the normal bone turnover of resorption and formation into metastatic progression.

Growing understanding of the interaction between cancer and bone has led to the identification of innovative new diagnostic tools (7). An emerging family of molecules with a pivotal role in bone tumor progression and metastasis is the Wnt gene family (8). Wnts are a large family of small secreted morphogenic proteins heavily involved in bone development, and they contribute to maintaining the homeostasis of bone mass.

The Wnt canonical signaling pathway is mediated by the inhibition of β-catenin degradation. Briefly, when Wnt binds to its membrane receptor, a member of the Frizzled family (FRZ), low-density lipoprotein is formed which, in turn, stabilizes β-catenin, which can translocate into the nucleus and activate the transcription of genes controlling osteoblast and osteoclast differentiation, thus promoting bone formation. Wnt function is balanced by a variety of secreted endogenous inhibitors, such as the Dikkopf family, secreted FRZ-related proteins and sclerostin. By inhibiting Wnt signaling, these molecules reduce osteoblast activity. The Dikkopf family comprises four secreted proteins (DKK-1,-2,-3,-4), produced by osteoblasts and osteoclasts. The main Wnt antagonist is DKK-1, which blocks the interaction of Wnt with β-catenin, leading to β-catenin degradation.

Sclerostin (also known as SOST) is an osteocyte-soluble factor that negatively regulates osteoblast activity by binding lipoprotein receptor 5, an essential cofactor of Wnt signaling, preventing the Wnt interaction (9). DKK-1 and sclerostin have been described as having an important role in bone cancer progression and metastasis development (9-12), particularly in myeloma (13-14) and prostate cancer (10,15).

To date, these molecules have been examined mainly as new potential therapeutic targets (12), and there is little evidence suggesting their use as a diagnostic tool in cancer (9). In this study we analyzed two groups of patients, one with primary tumors and the other with metastasis, and measured the serum sclerostin and DKK-1, correlating them to a panel of established metastatic bone turnover and metastasis markers, such as survivin. Since the metastases analyzed were mainly osteolytic, in order to evaluate bone resorption we assayed serum levels of TRAP5b and the two main bone-related metalloproteinases MMP-2 and MMP-9.

The aim of the study was to assess the diagnostic potential of the two main Wnt inhibitors, sclerostin and DKK-1, with a view to their clinical use to improve the detection of osteolytic bone metastases.

MATERIALS AND METHODS

Patients

Forty selected patients (20 female and 20 male, age 58.42 SD 21.14 years) were enrolled at the Oncological Orthopedic Surgical Unit, at Galeazzi Hospital, Milan, and divided into two groups: 20 had metastatic bone tumors, confirmed by bone scan and biopsy, and 20 had primary tumors (chordoma, primitive fibrous tumor, sarcoma, hematological tumors) without metastatic spread. To examine the concentrations of the bone markers in a healthy population, we enrolled a control pool of 15 healthy subjects without skeletal disease, matched for age and gender. We checked the medical records of all participants to make sure they were not taking any medication known to interfere with bone turnover, such as calcium supplementation or bisphosphonates.

All procedures followed were in accordance with the Helsinki of Declaration of 1975, as revised in 2000 and 2008. Informed consent was obtained from all individual participants included in the study. The study was in line with the guidelines for experimental studies on humans applicable within the Galeazzi Orthopaedic Institute and approved by the Local Ethics Committee.

Serum Wnt inhibitors (sclerostin, DKK-1), survivin, MMP-2, MMP-9, TRAP5b

Blood samples were taken from all patients and sera were separated from whole blood after complete coagulation, by centrifugation at 3000 rpm for 10 min. Sera were stored at -70°C until analyses, which were carried out in a single batch.

Levels of soluble sclerostin, DKK-1, MMP-2, MMP-9, TRAP5b and survivin in serum were determined by commercial assays, according to the manufacturer's instructions (Quantikine ELISA Human DKK-1, Human SOST (sclerostin), Human Survivin, Human MMP-2 and Human MMP-9 immunoassay, R&D Systems, Minneapolis, Minnesota, USA; TRAP5b EIA Kit, METRA, Hannover, Germany). For the survivin assay, the sensitivity was 4.44 pg/mL, and intra- and inter-assay coefficients of variation were 5.5% and 5.6%, respectively. For DKK-1, the sensitivity was 4.2 pg/mL, with intra- and inter-assay coefficients of variation 4.2% and 6%. For sclerostin, the sensitivity was 1.74 pg/mL, and intra- and

inter-assay coefficients of variation were 1.8% and 8.2%. For MMP-2, the sensitivity was 33 pg/mL, with intra- and inter-assay coefficients of variation 3.6% and 6.5%. For MMP-9, the sensitivity was 156 pg/mL, and intra- and inter-assay coefficients of variation were 1.9% and 6.9%. For TRAP5b, the sensitivity was 0.2 U/L, and intra- and inter-assay coefficients of variation were 1.9% and 2%.

Statistical analysis

For all parameters, the normality of distribution of the three groups was verified by KS normality. Statistical analysis was carried out using one-way ANOVA, $p<0.05$ being considered significant and $p<0.001$ highly significant. Correlation analysis was measured using PRISM 5.0 software, by linear regression analysis between the different groups of data and calculating the 95% confidence interval of the regression line.

Statistical analysis of Receiver Operating Characteristic (ROC) curves and Area Under the Curve (AUC) was performed by PRISM 5.0 software

RESULTS

Serum levels of Wnt inhibitors sclerostin and DKK-1

Serum levels of the Wnt inhibitors sclerostin and DKK-1 are shown in Fig. 1. Sclerostin (Fig. 1 A) in the control group (137.37±29.18 pg/mL) was in the physiological range (67.0-200 pg/mL), but was significantly higher in primary tumor patients (237.81±87.31 pg/mL) and even higher (with a significant difference) (3329.26±88.21 pg/mL) in metastatic patients ($p<000.1$ in both cases). In metastatic patients, sclerostin was highly significantly elevated compared to primary tumor patients ($p<0.01$).

Similarly, DKK-1 in serum (Fig. 1 B) was within the normal range (172-1488 ng/mL) in control patients (202.32±28.21 pg/mL) but was much higher - significantly so - in primary tumor patients (358.46±80.21 pg/mL, $p<0.001$). It was even higher in metastatic patients (466.7±76.21 pg/mL) and the difference from primary tumor cases was highly significant. In this case the physiological range is very wide, so even if the DKK-1 levels in the different groups do not exceed the upper limit of normal, the increases reach significance.

To better depict the patterns of increase of the two Wnt inhibitors in primary and metastatic patients, we carried out a linear regression analysis of DKK-1 and sclerostin in the two groups; there was a good positive correlation in primary tumors ($r^2=0.685$) and a more significant correlation in metastatic patients ($r^2=0.859$).

In order to evaluate the diagnostic value of sclerostin and DKK-1, a ROC curve and Area Under the Curve was calculated for both the markers, and the AUC resulted 0.913 (Fig. 1 D) and 0.898 for sclerostin and DKK-1 (Fig. 1 E), respectively.

Serum levels of bone metalloproteinases MMP-2 and MMP-9

Serum levels of MMP2-and MMP-9 are shown in Fig. 2. MMP-2 (Fig. 2A) was markedly and significantly higher in patients with primary tumors than in healthy controls (118.15±51.13 and 43.24±20.12 ng/mL, $p<0.0001$). In metastatic patients, MMP-2 serum levels were even higher (149.48±74.21 ng/mL), the difference being highly significant compared to healthy controls ($p<0.0001$) and significant compared to primary tumor patients ($p<0.001$).

Similarly, MMP-9 was highly significantly elevated in primary tumors compared to controls (1459.35±325.56 and 345.25±17.25 ng/mL respectively, $p<0.0001$) with an even greater increase in metastatic patients (1736.23±221.56 ng/mL); this was slightly but significantly different from the primary tumor levels ($p<0.05$).

Correlations between DKK-1 and sclerostin and bone metabolic/metastatic serum markers

To evaluate the clinical importance of DDK-1 and sclerostin in the diagnosis of bone osteolytic metastasis, we employed linear correlation analysis in the two distinct groups of primary and metastatic tumors, between DKK-1 and sclerostin and a panel of metabolic and metastatic markers. MMP-2 and MMP-9 were measured as markers of bone matrix remodeling, while survivin, a metastatic marker, and TRAP5b, a canonical marker of bone resorption, had already been measured in this set of patients, as reported in our previous study, Galliera et al. (6).

Fig. 3 shows the correlation for DKK-1 (Fig. 3 A): there was a weak correlation ($r^2=0.661$) with MMP-2 in primary tumors but a very good one in metastases ($r^2=0.848$). The correlation was similar between DKK-1 and MMP-9 in primary and metastatic tumors ($r^2=0.833$ and 0.958) (Fig. 3 B). Similarly, there was a good correlation between DKK-1 and TRAP5b in primary tumors ($r^2=0.847$) and it was even more

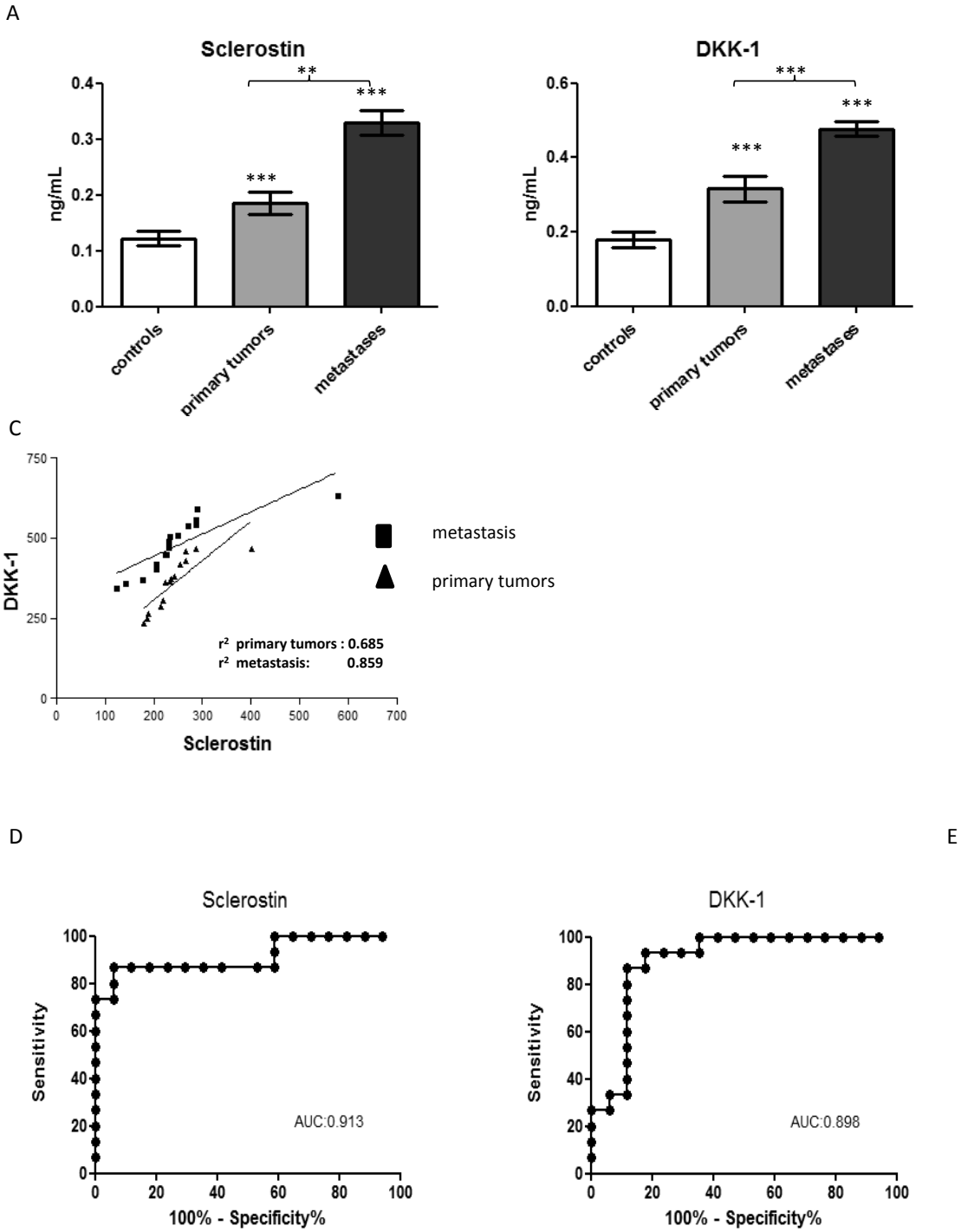

Fig. 1. *Wnt inhibitors in primary tumors and bone metastasis.* ***A)*** *Sclerostin serum levels in healthy patients without skeletal disease (white bar), primary tumor (light gray bar), and metastatic patients (dark gray bar).* ***B)*** *DKK-1serum levels in healthy patients without skeletal disease (white bar), primary tumor (light gray bar), and metastatic patients (dark gray bar).* ***C)*** *linear correlation between Sclerostin and DKK-1 serum levels in metastatic (black square) and primary tumors (black triangle).* ***D)*** *ROC curve and Area Under the Curve (AUC) of Sclerostin.* ***E)*** *ROC curve and Area Under the Curve (AUC) of DKK-1*

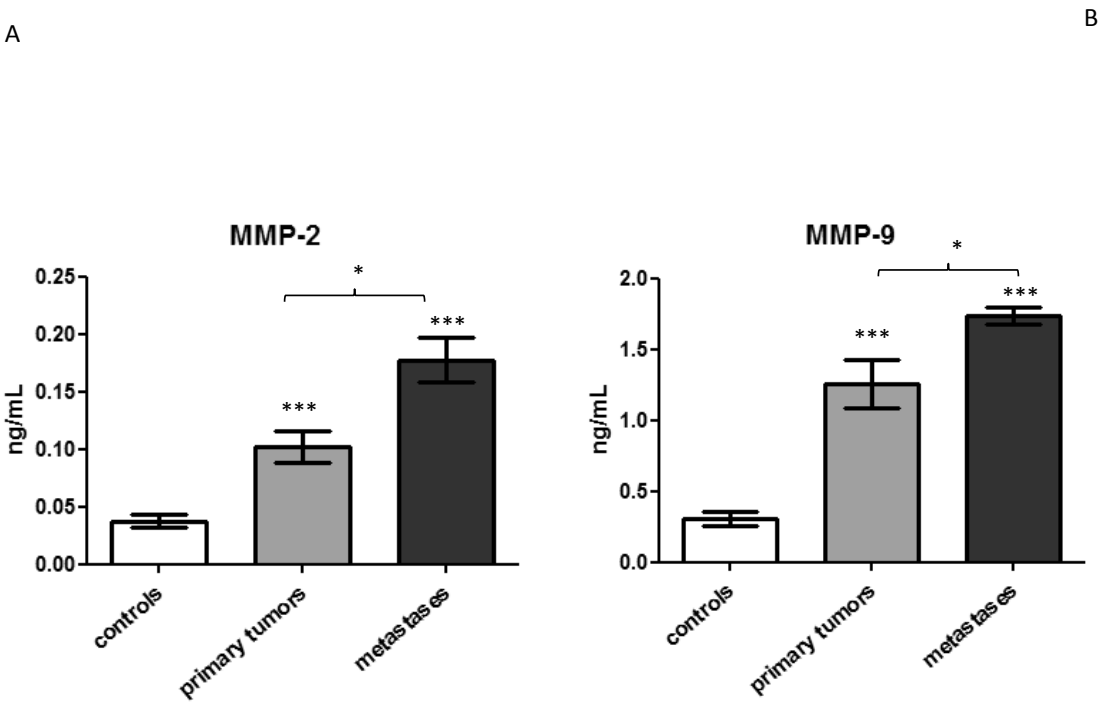

Fig. 2. *Wnt inhibitors in primary tumors and bone metastasis. MMP-2 (**A**) and MMP-9 (**B**) serum levels in healthy patients without skeletal disease (white bar), primary tumor (light gray bar), and metastatic patients (dark gray bar)*

significant in metastasis patients (r^2=0.939). DKK-1 had a very different correlation with the metastatic marker survivin in the two groups: the correlation was weak in primary tumors (r^2=0.747) but more significant in metastases (r^2=0.851, Fig. 3 C).

Fig. 4 A and B show the clear differences in the correlation of sclerostin with both MM-2 and MMP-9 in primary and metastatic tumors. In primary tumors sclerostin had little or no correlation with MMP-2 (r^2=0.383) and MMP-9 (r^2=0.526), while in metastatic patients it showed good positive correlations with both (respectively r^2=0.738 and 0.689). This difference was confirmed in the linear correlation analysis with survivin, where sclerostin had a correlation of r^2=0.779 with survivin in primary tumors and a more significant positive correlation of r^2= 0.945 in metastatic cases. A similar but smaller difference between the two groups was also confirmed by linear correlation analysis between sclerostin and the resorption marker TRAP5b: in primary tumors sclerostin had an adequate correlation with TRAP5b (r^2=0.681), while in metastatic patients it was more strongly positive (r^2=0.789).

DISCUSSION

Bone metastases are the main cause of morbidity and ultimately mortality in cancer patients (7). Despite their clinical importance, however, metastatic onset and progression are still poorly understood and the current diagnostic tools lack sensitivity and specificity to obtain a clear early diagnosis. We therefore still need more knowledge on the mechanism(s) of bone metastatic invasion in order to improve the diagnostic process.

Bone turnover markers have recently proved useful for the early diagnosis and monitoring of bone metastases (4, 6, 16), but the panel of diagnostic tools for detection still needs to be improved. The morphogenetic Wnt pathway has been described as vital in bone carcinogenesis and metastasis progression (8, 17). Wnt signaling stimulates osteoblast activity, leading to bone formation, while the endogenous negative regulators of Wnt signaling, sclerostin and DKK-1, block osteoblast activity and induce osteoclast-mediated bone resorption, leading to bone erosion (18, 19). Bone metastases differ in different

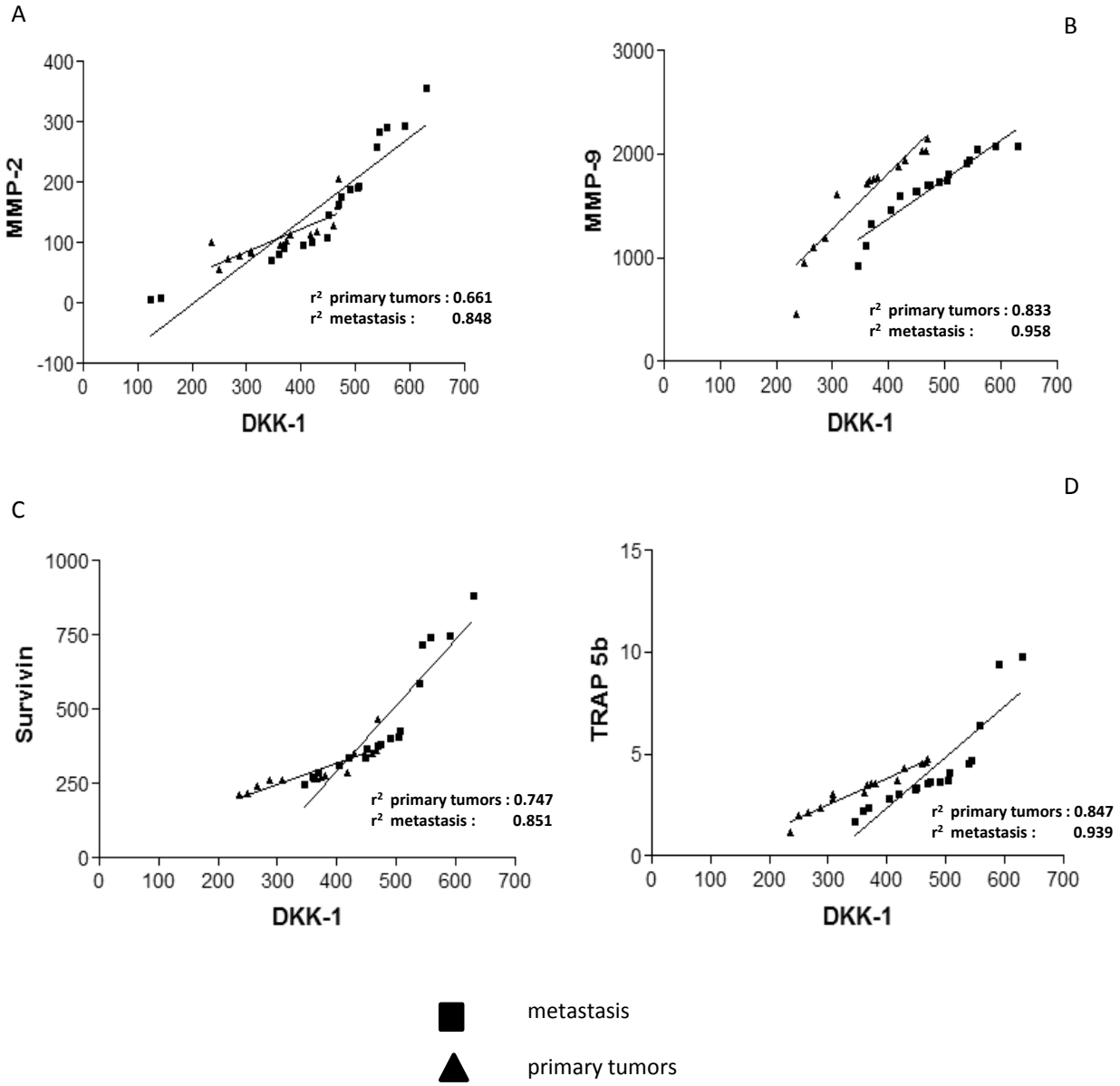

Fig. 3. *Correlation between DKK-1 and bone metabolic/metastatic markers. Linear correlation between DKK-1 and MMP-2 (**A**), MMP-9 (**B**), surviving (**C**) and TRAP5b (**D**) serum levels in metastatic (black square) and primary tumors (black triangle).*

cancer types, and may cause bone formation - as in prostate cancer - though in most cancers metastatic spread leads to bone erosion and ultimately osteolysis and fracture (3). The clinical presentation of these two kinds of bone metastases differs, as indicated by bone remodeling markers, therefore they require a specific panel of diagnostic tools.

We investigated the potential diagnostic role of two main inhibitors of Wnt signaling, DKK1 and sclerostin, in the osteolytic form of metastasis. To distinguish the roles of these two inhibitors in tumor onset and bone metastasis progression, we analyzed two groups of patients, one with primary tumors and one with established bone metastasis, compared to a control group without any malignancies or skeletal disease. This approach should bring to light the clinical ability of these markers, not only to distinguish tumor patients from healthy controls, but also to stratify primary tumor and metastatic cases.

Firstly, serum levels of DKK-1 and sclerostin were

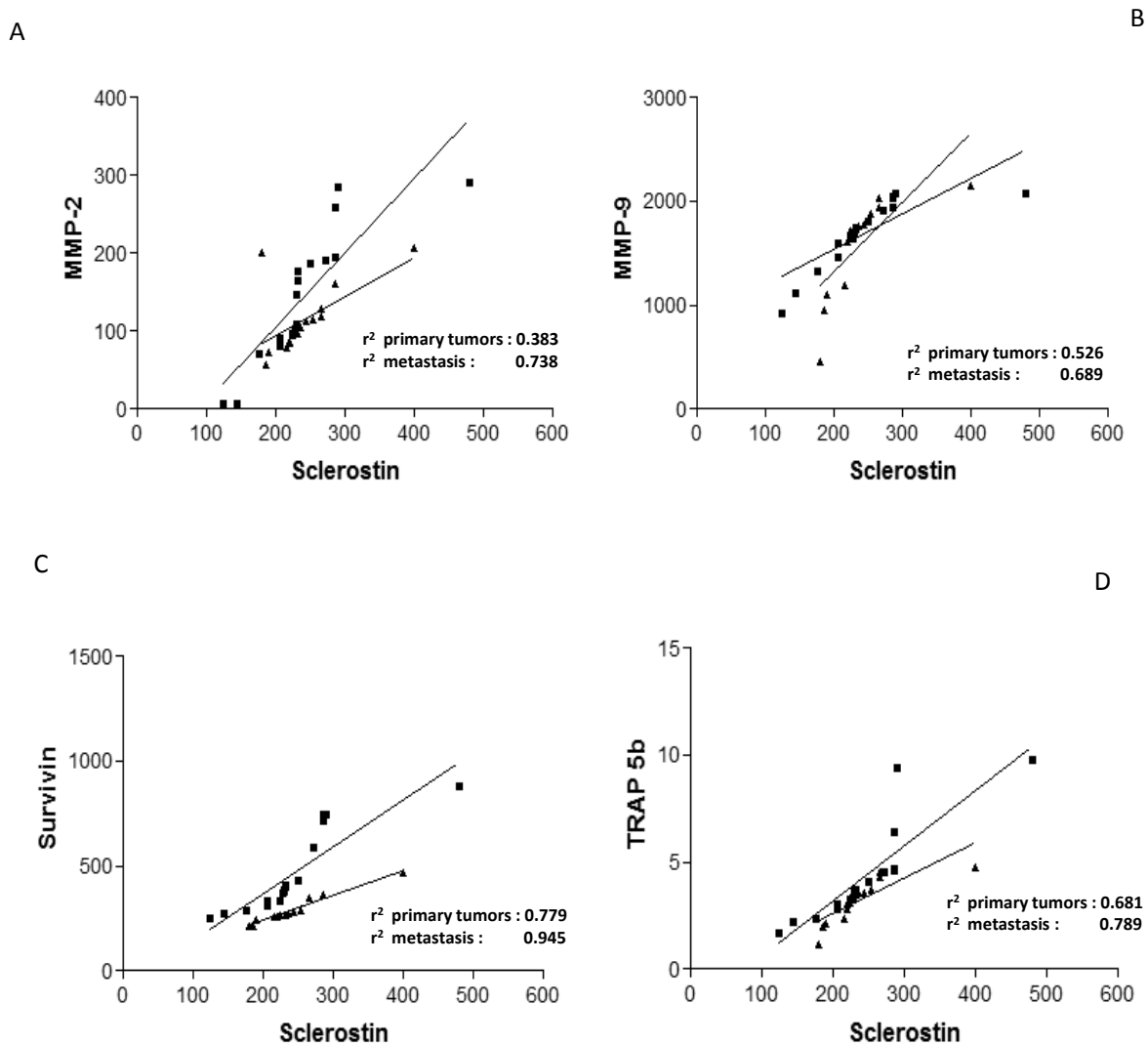

Fig. 4. *Correlation between DKK-1 and bone metabolic/metastatic markers. Linear correlation between Sclerostin and MMP-2 (**A**), MMP-9 (**B**), survivin (**C**) and TRAP5b (**D**) serum levels in metastatic (black square) and primary tumors (black triangle).*

significantly higher in tumor patients than healthy controls. Moreover, sclerostin and DKK-1 displayed a very good AUC (0.913 and 0.898 for sclerostin and DKK-1 , respectively), indicating that these two Wnt pathway inhibitors can be considered promising serum markers for the diagnosis and follow-up of bone metastases**.**The elevations of both sclerostin and DKK-1 also differed highly significantly in primary and metastatic patients, indicating that the serum levels of these two markers can distinguish patients with or without bone metastasis; this was confirmed by the good linear correlation between sclerostin and DKK-1, which was particularly significant in metastatic patients. This aspect is of extreme clinical importance for the prognosis because, while a primary tumor can be treated with a therapeutic or surgical approach, metastases can only be treated palliatively. Therefore, it is extremely important to detect metastases as early as possible, by constant monitoring of primary tumor patients. A serum marker would be very useful for

monitoring primary tumor patients in order to take early action to prevent bone metastases, as it would be less invasive than radiography or scintigraphy (commonly used for skeletal monitoring), and could allow more frequent follow-up (20, 21).

One of the main steps in tumor progression and metastatic spread is breakdown of the extracellular matrix (22). Since osteolytic lesions involve extensive extracellular matrix remodeling, we measured the serum levels of the two main matrix metalloproteases associated with bone metastases, MMP-2 and MMP-9. Both were much higher than in healthy controls, but the changes differed in primary and metastatic tumors. While MMP-2 serum levels were clearly different in the two groups, with a significant increase in metastatic patients compared to primary tumors, MMP-9 reached very high but only slightly significantly different levels in metastatic patients and primary tumors. This can be explained by the different temporal regulation of MMP-2 and MMP-9 extracellular matrix remodeling, indicating that MMP-9 expression and function take place earlier than MMP-2 (23). This reflects the different functions of the two MMPs in tissue remodeling and healing: MMP-2 is involved in the degradation of basement membrane and matrix, which is vital for cell migration, while MMP-9 controls fibronectin degradation. MMP-9 plays a large part in bone development (24), and a high serum level of MMP-9 has been described in advanced colon-rectal cancer and melanoma (25). The high levels of MMP-9 also agree with a recent report of higher MMP-9 in serum than in plasma (26). We made all our measurements in serum to maintain uniformity with the other marker, and probably the particularly high level of MMP-9 reflects this to some extent.

MMP-9, which has an early role in metastasis progression, promptly reached its peak in both primary and metastases patients, while MMP-2, which acts in a later step, can still distinguish primary from metastatic tumors. The combined use of the serum levels of metalloproteinases could be useful for following the timing of tumor progression and bone metastasis onset.

These two metalloproteinases also correlated well with the two Wnt inhibitors, sclerostin and DKK-1 (Fig. 3). DKK-1 showed a good positive correlation with MMP-9 in both primary and metastatic tumors, but the difference was more significant in metastatic patients. Correlation analysis with MMP-2 showed a clear difference between primary tumors, where DKK-1 poorly correlates with MMP-2, and metastatic tumors, where the correlation is closer. This was even more evident with sclerostin, which gave little or no correlation with MMP-9 and MMP-2 in primary tumors, but in metastatic patients there was a good positive correlation with both MMPs.

This clearly indicates that DKK-1 and sclerostin are positively correlated with bone resorption parameters and the link is particularly strong in metastatic patients. Therefore, both these markers can distinguish between primary and metastatic tumors on the basis of metastatic bone resorption. In order to confirm this, we correlated DKK-1 and sclerostin with a canonical bone resorption marker, TRAP5b, already measured together with survivin in these patients in our previous study (6). As expected, sclerostin and DKK-1 showed a good positive correlation with TRAP5b, with higher positivity in metastatic patients, particularly for DKK-1 (Fig. 3D). This confirms the close relationship between the level of metastatic bone resorption and the serum concentrations of sclerostin and DKK-1, signifying that these two molecules can be considered good markers of metastatic osteolysis.

To further test the diagnostic value for the detection of bone metastasis, we correlated the serum levels of sclerostin and DKK-1 with the metastatic marker survivin (Figs. 3 and 4), which is involved in the control of both cell growth and survival (27). Survivin is over expressed in many tumors, and is closely involved in tumor development, metastatic onset and progression (28, 29). We found a good correlation with survivin for DKK-1, and even higher for sclerostin, particularly in metastatic patients, definitely confirming the importance of these two Wnt inhibitors as diagnostic markers of bone metastases.

Understanding the mechanism of bone metastasis would offer a great opportunity for diagnosis and therapy. Particular attention is needed for micro metastatic disease and changes in bone turnover before bone metastasis is clinically measurable with instrumental approaches (X-ray or scintigraphy) (9). Advances in our knowledge on the role of Wnt signaling in bone metastases has led to this pathway being targeted for the development of new therapeutic approaches aimed at these metastases

(7, 13, 30). However, to our knowledge, there is as yet no description of the clinical combined use of the Wnt inhibitors sclerostin and DKK-1 in the diagnostic steps of tumor patients and particularly in metastasis diagnosis. We believe that this is the first study describing the potential value of Wnt inhibitors as a diagnostic tool for metastasis detection.

In conclusion, the possibility of measuring sclerostin and DKK-1 as circulating serum molecules and the good correlation with metastatic and bone resorption markers make them promising new biomarkers for the diagnosis of bone osteolytic metastases.

ACKNOWLEDGEMENTS

We acknowledge the Italian Ministry of Health for supporting this study by "Ricerca Corrente " Grant.

REFERENCES

1. Fohr B, Dunstan CR, Seibel MJ. Clinical review 165: Markers of bone remodeling in metastatic bone disease. J Clin Endocrinol Metab 2003; 88:5059-75.
2. Dougall WC, Chaisson M. The RANK/RANKL/OPG triad in cancer-induced bone diseases. Cancer Metastasis Rev 2006; 25:541-9.
3. Guise TA, Mohammed KS, Clines G, et al. Basic mechanisms responsible for osteolytic and osteoblastic bone metastases. Clin Cancer Res 2006; 12:6213s-6s.
4. Joerger M, Huober J. Diagnostic and prognostic use of bone turnover markers. Recent Results Cancer Res 2012; 192:197-223.
5. Fontana A, Delmas PD. Markers of bone turnover in bone metastases. Cancer 2000; 88:2952-60.
6. Galliera E, Luzzati A, Perrucchini G, Gagliano F, Colloredo Mels L, Banfi G, Corsi Romanelli MM, Drago L. Bone formation and resorption markers as diagnostic tools for bone metastases evaluation. Int J Biol Markers 2012 ;27(4):e395-9
7. Santini D, Galluzzo S, Zoccoli A. et al. New molecular targets in bone metastases. Cancer Treat Rev 2010 ;36 Suppl 3:S6-S10.
8. Hall CL, Keller ET. The role of Wnts in bone metastases. Cancer Metastasis Rev 2006; 25:551-58.
9. Sottnik JL, Hall CL, Zhang J, Keller ET. Wnt and Wnt inhibitors in bone metastasis. Bonekey Rep 2012 Jul 4;1:101
10. Hall CL, Kang S, MacDougald OA, Keller ET. Role of Wnts in prostate cancer bone metastases. J Cell Biochem 2006; 97:661-72.
11. Cai Y, Cai T, Chen Y. Wnt pathway in osteosarcoma, from oncogenic to therapeutic. J Cell Biochem 2014 ;115(4):625-31.
12. Yao H, Ashihara E, Maekawa T. Targeting the Wnt/beta-catenin signaling pathway in human cancers. Expert Opin Ther Targets 2011 ;15(7):873-87.
13. Gkotzamanidou M, Dimopoulos MA, Kastritis E, Christoulas D, Moulopoulos LA, Terpos E. Sclerostin: a possible target for the management of cancer-induced bone disease. Expert Opin Ther Targets 2012 ;16(8):761-69.
14. Terpos E, Christoulas D, Katodritou E, et al. Elevated circulating sclerostin correlates with advanced disease features and abnormal bone remodeling in symptomatic myeloma: reduction post-bortezomib monotherapy. Int J Cancer 2012 ;131(6):1466-71.
15. Dai J, Hall CL, Escara-Wilke J, Mizokami A, Keller JM, Keller ET. Prostate cancer induces bone metastasis through Wnt-induced bone morphogenetic protein-dependent and independent mechanisms. Cancer Res 2008; 68:5785-94.
16. Demers LM, Costa L, Lipton A. Biochemical markers and skeletal metastases. Cancer 2000; 88:2919-26.
17. Dong LL, Qu LY, Chu LY, Zhang XH, Liu YH. Serum level of DKK-1 and its prognostic potential in non-small cell lung cancer. Diagn Pathol 2014; 9:52.
18. Bu G1, Lu W, Liu CC, Selander K, Yoneda T, Hall C, Keller ET, Li Y.. Breast cancer-derived Dickkopf1 inhibits osteoblast differentiation and osteoprotegerin expression: implication for breast cancer osteolytic bone metastases. Int J Cancer 2008; 123:1034-42.
19. Pinzone JJ, Hall BM, Thudi NK, Vonau M, Qiang YW, Rosol TJ, Shaughnessy JD Jr.. The role of Dickkopf-1 in bone development, homeostasis, and disease. Blood 2009; 113:517-25.
20. Coleman RE. The role of bone markers in metastatic bone disease. Cancer Treat Rev 2006; 32(Supp)1:1-2.
21. Palma MA, Body JJ. Usefulness of bone formation markers in breast cancer. Int J Biol Markers 2005; 20:146-55.
22. Stamenkovic I. Matrix metalloproteinases in tumor invasion and metastasis. Semin Cancer Biol 2000; 10:415-33.

23. Rengel Y, Ospelt C, Gay S. Proteinases in the joint: clinical relevance of proteinases in joint destruction. Arthritis Res Ther 2007; 9:221.
24. Luo XH, Guo LJ, Shan PF et al. Relationship of circulating MMP-2, MMP-1, and TIMP-1 levels with bone biochemical markers and bone mineral density in postmenopausal Chinese women. Osteoporos Int 2006; 17:5212-6.
25. Kostova E, Slaninka-Miceska M, Labacevski N. et al. Expression of matrix metalloproteinases 2, 7 and 9 in patients with colorectal cancer. Vojnosanit Pregl 2014 ;71(1):52-59.
26. Thrailkill K, Cockrell G, Simpson P, Moreau C, Fowlkes J, Bunn RC. Physiological matrix metalloproteinase (MMP) concentrations: comparison of serum and plasma specimens. Clin Chem Lab Med 2006; 44:503-4.
27. Capalbo G, Rödel C, Stauber RH, Knauer SK, Bache M, Kappler M, Rödel F.. The role of survivin for radiation therapy. Prognostic and predictive factor and therapeutic target. Strahlenther Onkol 2007; 183:593-99.
28. Yie SM, Luo B, Ye NY, Xie K, Ye SR. Detection of Survivin-expressing circulating cancer cells in the peripheral blood of breast cancer patients by a RT-PCR ELISA. Clin Exp Metastasis 2006; 23:279-89.
29. Zohny SF, El-Shinawi M. Significance of survivin and Bcl-2 homologous antagonist/killer mRNA in detection of bone metastasis in patients with breast cancer. Med Oncol 2011; 28(Suppl 1):S108-14.
30. Neth P, Ries C, Karow M, Egea V, Ilmer M, Jochum M. The Wnt signal transduction pathway in stem cells and cancer cells: influence on cellular invasion. Stem Cell Rev 2007; 3:18-29.

HYALURONAN SCAFFOLD SUPPORTS OSTEOGENIC DIFFERENTIATION OF BONE MARROW CONCENTRATE CELLS

C. CAVALLO[1], G. DESANDO[1], A. FERRARI[2], N. ZINI[3], E. MARIANI[1,4,5] and B. GRIGOLO[1,4]

[1]SSD Laboratory RAMSES Rizzoli Orthopedic Institute, Bologna, Italy; [2]Laboratory of Musculoskeletal Cell Biology, Rizzoli Orthopedic Institute, Bologna, Italy; [3]IGM- CNR c/o Rizzoli Orthopedic Institute, Bologna, Italy; [4]SC Laboratory of Immunorheumatology and Tissue Regeneration, Rizzoli Orthopaedic Institute, Bologna, Italy; [5]Department of Medical and Surgical Sciences, University of Bologna, Bologna

Received October 15, 2015 – Accepted April 26, 2016

Osteochondral lesions are considered a challenge for orthopedic surgeons. Currently, the treatments available are often unsatisfactory and unable to stimulate tissue regeneration. Tissue engineering offers a new therapeutic strategy, taking into account the role exerted by cells, biomaterial and growth factors in restoring tissue damage. In this light, Mesenchymal Stem Cells (MSCs) have been indicated as a fascinating tool for regenerative medicine thanks to their ability to differentiate into bone, cartilage and adipose tissue. However, in vitro-cultivation of MSCs could be associated with some risks such as de-differentiation/reprogramming, infection and contaminations of the cells. To overcome these shortcomings, a new approach is represented by the use of Bone Marrow Concentrate (BMC), that could allow the delivery of cells surrounded by their microenvironment in injured tissue. For this purpose, cells require a tridimensional scaffold that can support their adhesion, proliferation and differentiation. This study is focused on the potentiality of BMC seeded onto a hyaluronan-based scaffold (Hyaff-11) to differentiate into osteogenic lineage. This process depends on the specific interaction between cells derived from bone marrow (surrounded by their niche) and scaffold, that create an environment able to support the regeneration of damaged tissue. The data obtained from the present study demonstrate that BMC grown onto Hyaff-11 are able to differentiate toward osteogenic sense, producing specific osteogenic genes and matrix proteins.

Osteochondral defects are associated with mechanical instability of the joint and severe pain, therefore with an increased risk of developing osteoarthritis (1). These lesions, which involve both the articular cartilage and the subchondral bone, remain a challenge for orthopedic surgeons, especially for the poor self-healing ability of cartilage (2). Several treatments are available to promote an adequate restoration of cartilage and bone structures, however, only the microfracture technique and Autologous Chondrocyte Implantation (ACI) have shown good clinical outcomes (3, 4). Unfortunately, long-term results of these surgical techniques are unsatisfactory, due to the formation of a fibrous

Key words: orthopaedics, bone, transplantation, biomaterial, cells, histochemistry

Mailing address:
Dr Brunella Grigolo,
SSD Laboratory RAMSES;
SC Laboratory of Immunorheumatology
and Tissue Regeneration, Rizzoli Orthopedic Institute
Via di Barbiano 1/10, 40136 Bologna, Italy
Tel.: +39 051 6366803/6366802 - Fax: +39 051 6366807
e-mail: brunella.grigolo@ior.it

0393-974X (2016)

tissue which is not capable of supporting mechanical properties of the hyaline cartilage and protecting the subchondral bone (5, 6). Recently, promising approaches have been developed to improve the regeneration of full-thickness cartilage thanks to the advancements in the field of regenerative medicine, through the use of different combinations of cells, biocompatible scaffolds and growth factors. In particular, the appropriate choice of both cells and biomaterials represents one of the most important aspects of cell-based engineering (7). Furthermore, autologous chondrocytes, Mesenchymal Stem Cells (MSC) are an attractive cell source for osteochondral tissue engineering; MSC can be harvested in a less invasive manner, easily isolated, and have a high capacity to proliferate and to differentiate into several cell lineages such as osteoblasts, adipocytes, muscle and chondrocytes (8). Moreover, MSC are key elements for tissue homeostasis due to their trophic, paracrine and immunomodulatory properties which render them ideal candidates for the treatment of pathologic processes (9). However, there are some limitations related to their use due to the *in-vitro* manipulation that could lead to an increased risk of infection and contamination (10). To overcome these problems, the use of autologous Bone Marrow Concentrate (BMC), surrounded by their native microenvironment, which provides a suitable behavior for stem cell self-renewal, proliferation, differentiation, mobilization and homing, has been advocated by several authors (11, 12), and recent clinical studies reported encouraging results by using BMC to treat bone injuries (13, 14). The beneficial effects reported following BMC implantation are likely due its heterogeneity of cell population. The bone marrow is an architecturally complex tissue that houses cells of the haematopoietic and endothelial lineages. These cells support angiogenesis and vasculogenesis by producing several growth factors which stimulate the bone marrow release of progenitor stem cells for purposes such as wound healing (15, 16).

However, although we accept that a suitable cell population is a mandatory first element for an unimpaired bone repair process, tissue regeneration often requires the use of scaffolds to achieve sufficient mechanical function and to favor cell attachment especially in the musculoskeletal system (17). Hyaluronic acid (HA), is widely used in tissue engineering due to its physical and biological functions in many tissues, including cartilage (18). Thus, its use could be recommended to hold BMC, cytokine and blood, providing not only a bio-mechanical support, but also an appropriate microenvironment for stem cell differentiation. Some Authors have demonstrated an important role of hyaluronan in triggering endochondral bone formation in several *in vitro/vivo* preclinical studies (19-20). In a previous work, we demonstrated that BMC seeded onto a hyaluronan derivative named Hyaff-11 was able to differentiate toward chondrogenic lineage reporting the expression of specific cartilaginous genes and cartilage matrix proteins (21). The aim of the present study is to elucidate by an *in vitro* study the osteogenic potential of BMC grown onto Hyaff-11 to support its use for the treatment of osteochondral lesions.

MATERIALS AND METHODS

Biomaterial

The scaffold used in this study (provided by Anika Therapeutics, Bedford, MA, USA) was made of Hyaff-11, a polymer derived from the total esterification of sodium hyaluronate (80–200 kDa) with the benzyl alcohol on the free carboxyl groups of glucuronic acid along the polymeric chain. The configuration used in this study was a pad of nonwoven mesh composed of a random array of polymer fibers having a diameter of 10 mm, sterilised by γ-irradiation.

Bone marrow harvesting and concentration

Bone marrow was obtained from the iliac crest of 10 patients (mean age 25.20±10.0; 5 females and 5 males) who underwent bone marrow concentrate transplantation for the treatment of osteochondral lesions. The Ethics Committee of the Institution approved the human protocol for this study (Protocol n° 00081310, March 2013). All investigations were conducted in conformity with ethical principles of research, and written informed consent was signed by all the patients enrolled in this research.

As previously reported (14), bone marrow was aspirated

in small fractions from different points of the posterior iliac crest in a sterile regimen, with the patient in prone decubitus and in general or spinal anesthesia. The harvested bone marrow was reduced in volume by removing most of the red cells and plasma, directly in the operating theater. Thus, it was possible to obtain a concentrate of nucleated cells including stem cells, monocytes, lymphocytes and other bone marrow resident cells.

The bone marrow was concentrated with a suitable device (Smart PReP®, Harvest Technologies Corp., Plymouth, MA, USA), through a sterile and disposable dedicated kit (BMAC®, Harvest Technologies Corp., Plymouth, MA, USA) following the manufacturer' s instructions.

Colony-forming units-fibroblast (CFU-F) assay

To test the clonogenic ability of BMC, CFU-F assays were performed as previously reported (21). Briefly, BMC was seeded in Petri dishes in minimum essential medium eagle alpha modification (α-MEM, Gibco, Invitrogen, Carlsbad, CA, USA) supplemented with 15% of fetal bovine serum (FBS, Life Technologies). At 7 and 14 days, cells were washed twice with phosphate-buffered saline (PBS), fixed in methanol and subsequently stained with a 0.1% crystal violet solution (Sigma, St. Louis, MO, USA). An aggregate of 50 cells was classified as a colony.

Osteogenic differentiation of BMC

0.1 ml of BMC (approximately $15x10^6 \pm 3x10^6$ mononuclear cells), was seeded onto Hyaff-11 (size 0.5x0.5 cm) and incubated for 1 h at RT to allow a good adhesion of the cells to the scaffold. α-MEM (Gibco) with 15% FBS was successively added. After 24 hours, medium was replaced with α-MEM (Gibco) supplemented with 15% FBS containing the osteogenic factors; ascorbate-2 phosphate (Sigma, 75 μg/mL), β-Glicerol Phospate (GP) (Sigma, 0.01 mM) and dexamethasone (Sigma, 10^{-7} M). The medium was changed twice a week and the constructs were evaluated by immunohistochemistry at 0, 40 and 52 days to analyze the production of Collagen type I (Coll I), alkaline posphatase (ALP), bone morphogenetic protein (BSP) and osteopontin (OPN). A number of specific osteogenic markers such as Coll I, ALP, BSP, osteocalcin (OC), OPN, Runt-related transcription factor-2 (RUNX-2) and osterix (OSX) were evaluated after RNA extraction from the scaffolds by Real-Time PCR.

Cellular viability and proliferation evaluation

Cell viability and proliferation of constructs were analyzed at days 0, 40 and 52 by Alamar blue test (22). Samples were incubated with 10% Alamar blue (AbD Serotec, UK) for 4 hours and then the fluorescence was read at 490ex–540em nm wavelength, using a microplate-reader (CytoFluorTM 2350, Millipore, Bedford, MA, USA). The Alamar blue was converted to fluorescent dye via a redox reaction of metabolically active cells and the results were expressed as percentage of Alamar blue reduction following the manufacturer' s instructions.

Histological evaluations

To assess general morphology and osteogenic differentiation of BMC grown onto hyaluronan scaffold, histological stainings were performed on days 0, 40 and 52. Slides were thawed, air-dried and fixed in Buffered Formalin for 10 min. Successively, samples were stained for hematoxylin-eosin and Von Kossa and analyzed by a light microscope (Nikon Eclipse 90i).

Light microscopy and transmission electron microscopy (TEM) analyses.

Toluidine blue staining was performed on semithin sections to assess cell biodistribution within Hyaff-11 by light microscopy. On days 0, 40 and 52, constructs were fixed in 2.5% glutaraldehyde in 0.1 M cacodylate buffer pH 7.4 for 3 h at 4°C, postfixed with 1% osmium tetroxide, dehydrated in a graded series of ethanol, and embedded in Epon. Cross-sections of each sample were cut perpendicularly in respect to the biomaterial surface to allow internal analysis.The ultra-structural interactions between BMC and scaffold were performed on thin sections stained with tannic acid, uranyl acetate and lead citrate and observed with a Zeiss EM 109 transmission electron microscope (Carl Zeiss, Oberkochen, Germany).

Immunoistochemical analyses

Coll I, ALP, BSP and OPN were analized on Hyaff-11 constructs. Slides were air-dried for two hours at RT following by specific un-masking procedures and blocking steps. Samples were then incubated with the primary antibodies: mouse monoclonal anti-human Coll I (Chemicon International, Temecula, CA, USA) diluted 1:40; mouse monoclonal anti-human ALP (Hybridoma Bank, Department of Biological Sciences, (DSHB), Iowa

City, IA, USA) diluted 1:40; mouse monoclonal anti-BSP (DSHB) diluted 1:40 and mouse monoclonal anti-OPN (DSHB) diluted 1:10. Subsequently, a Biotinylated secondary antibody followed by an alkaline-labelled streptavidin (Biocare Medical, Walnut Creek, CA, USA) was added. The reaction was developed using Fast red substrate (Biocare Medical). Negative controls were performed either by omitting the primary antibodies or using an isotype-matched control. Slides were observed with an Eclipse 90i microscope (Nikon).

Analysis of mRNAs expression by real-time PCR

A number of specific osteogenic markers such as Coll I, ALP, BSP, OC, OPN, RUNX-2 and OSX was used to assess the osteogenic differentiation of BMC within Hyaff-11 by Real-Time RT-PCR.

On days 0, 40 and 52, constructs were lysed with 0.5 ml TRIzol reagent (Invitrogen, Life Technologies). Successively, RNA was recovered by precipitation with isopropyl alcohol and treated with DNase I (DNAfree Kit, Ambion, Austin, TX, USA). Total RNA was reverse transcribed using the Multiscribe reverse transcriptase (Applied Biosystems, Courtaboeuf, France), according to the manufacturer's protocol. Real time PCR was run in a LightCycler Instrument (Roche Molecular Biochemicals, Mannheim, Germany) using the SYBR Premix Ex Taq (TaKaRa Biomedicals, Tokyo, Japan) following previously described protocols (21). mRNA levels were calculated for each target gene and normalized using the reference gene GAPDH according to the formula $2^{\Delta Ct}$ and expressed as a percentage of the reference gene. PCR primers for the selected genes, obtained from published references (23) or designed using PRIMER3 software (24) are listed in Table I.

Table I. *List of primers used in Real-Time RT-PCR.*

RNA template	Primer sequences (5'-3')	Annealing temperature (°C)	References*
Collagen type I	5'- AGG TGC TGA TGG CTC TCC 3'- GGA CCA CTT TCA CCC TTG T	60	24
ALP	5'- GGAAGACACTCTGACCGT 3'- GCCCATTGCCATACAGGA	60	24
BSP	5'- CAGTAGTGACTCATCCGAAG 3'- CATAGCCCAGTGTTGTAGCA	60	24
OC	5'- GCAGCGAGGTAGTGAAGA 3'- TCCTGAAAGCCGATGTGG	60	24
OPN	5'- ATGATGGCCGAGGTGATAG 3'- GCTTTCCATGTGTGAGGTG	60	24
RUNX-2	5'- GGAATGCCTCTGCTGTTATG 3'- AGACGGTTATGGTCAAGGTG	60	24
OSX	5'- TGCTTGAGGAGGAAGTTCACTATG 3'- AAAGGTCACTGCCCACAGA	60	24
GAPDH	5'-TGGTATCGTGGAAGGACTCATGAC 3'-ATGCCAGTGAGCTTCCCGTTCAGC	60	23

**Primer sequences were obtained from published references where indicated or designed using PRIMER3 software.*

Statistical analyses

All the statistical tests were non-parametric and performed by Exact methods. Data were expressed in terms of mean±Standard Deviation (SD). The Kendall W test was performed to assess the ordinal correlation between the follow-up times and the gene expression. The Friedmann test, followed by Wilcoxon post hoc pairwise comparison with the Sidak correction for multiple tests, was performed to assess differences in gene expression among the different follow-ups. $P<0.05$ was considered significant. Statistical analyses were carried out by the Statistical Package for the Social Sciences (SPSS) software version 19.0 (IBM, USA).

RESULTS

Colony-forming units-fibroblast (CFU-F) assay

Colony formation assays showed the presence of small colonies on day 7. An increase of the number and size of colonies was observed at day 14. Data are in agreement with our previous findings (21).

Cellular viability and proliferation evaluation

Cells from BMC grown onto Hyaff-11 were viable at all the experimental times analyzed. In particular, BMC showed a high increase in their proliferative capacity from day 0 to day 40 followed by a slight decrease until day 52 (Fig. 1).

Histological evaluation

Hematoxylin-eosin staining showed the scaffold totally colonized by cells with a fibroblastic morphology especially at day 52, which reported a far higher cell concentration (Fig. 2a,b). A negative staining for Von Kossa was observed on day 0 (data not shown). On day 40, the presence of dark mineral nodules, sign of the production of calcium ions was evident, and on day 52 black metallic deposits were also detected in Hyaff-11 fibers (Fig. 2c,d).

Light microscopy and transmission electron microscopy (TEM) analyses.

On day 0, we observed the presence of many blood cell precursors and erythrocytes within the scaffold fibers (data not shown). Toluidine blue staining showed the presence of cells with a fibroblastic morphology completely embedded in extracellular matrix detectable within the Hyaff-11 fibers at days 40 and 52. Some calcified areas were evident inside the scaffold (Fig. 3a,b). Electron microscopy allowed to better assess the interactions between cells and the biomaterial. On days 40 and 52 constructs showed

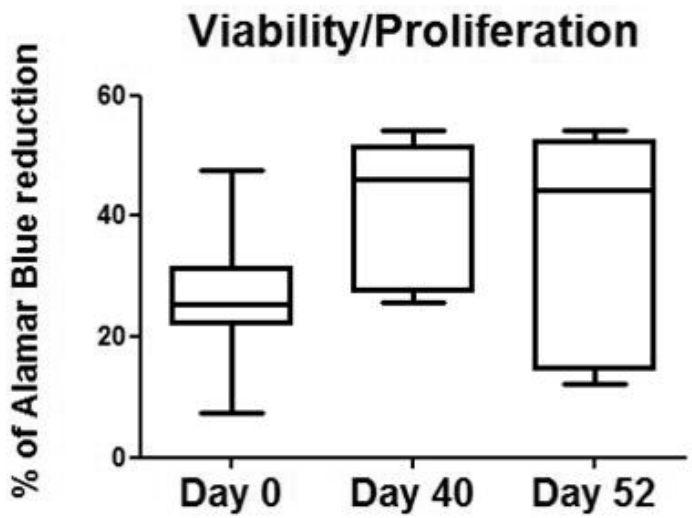

Fig. 1. *Proliferation of BMC seeded onto Hyaff-11 scaffold on days 0, 40 and 52. Data are expressed as % of Alamar blue reduction.*

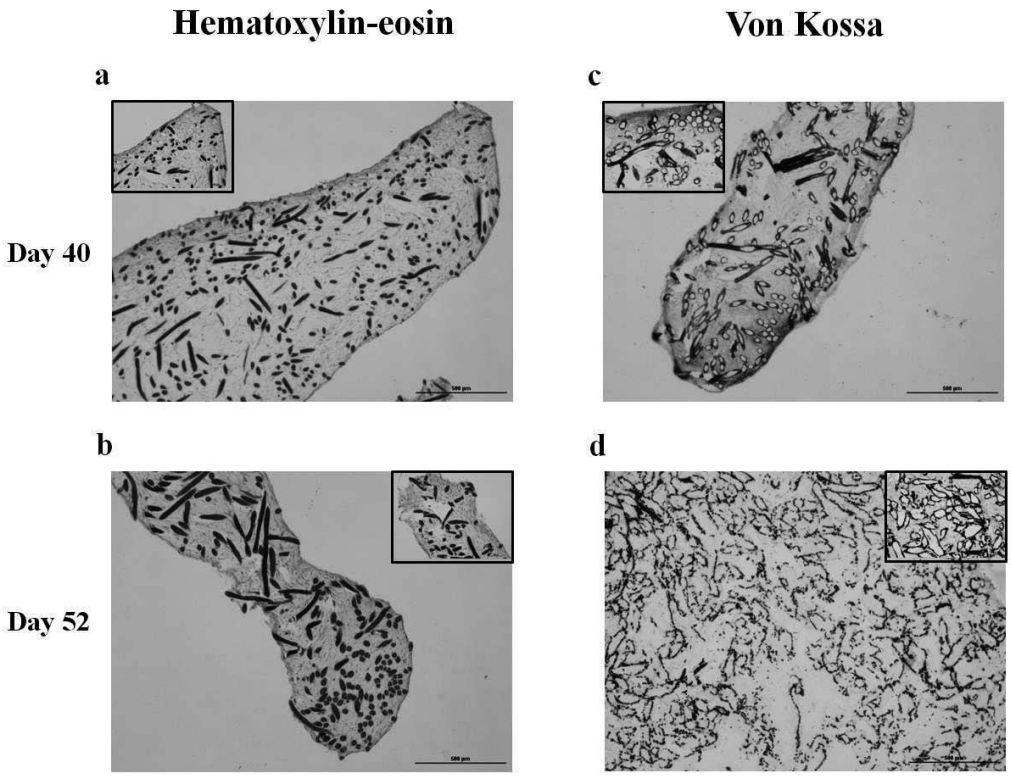

Fig. 2. *Histological analysis of BMC seeded on Hyaff-11 scaffold. Ematossilin-Eosin (**a-b**) and Von Kossa (**c-d**) staining were performed on days 40 and 52. The insets indicate the areas enlarged. Scale bars: 500 µm, insets 100 µm.*

similar characteristics, cells were elongated and located in the empty areas within the fibers. Some fibrils and granules resembling extracellular matrix component were evident (Fig. 3c,d).

Immunohistochemical analyses

Iimmunohistochemical evaluations, performed on BMC grown onto Hyaff-11 and differentiated towards osteogenic pathway, confirmed the production of extracellular matrix mentioned above. On day 0, all markers evaluated showed a negative staining (data not shown). Collagen type I, was expressed from cells starting from day 40, and on day 52 the majority of the extracellular matrix was positive (Fig. 4a,b). By contrast, cells showed a higher positivity for ALP on day 40 compared to day 52 (Fig. 4c,d). For BSP and OPN, similar findings were noted, reporting a strong positivity at cellular and extracellular level at day 40 and 52 (Fig. 4e,h).

Analysis of mRNAs expression by Real-Time PCR

Collagen type I and BSP mRNA expression, which were not or slightly expressed at day 0, increased from day 40 and significantly at day 52 ($p<0.05$) in respect to day 0 (Fig. 5a,b). mRNA ALP levels were detectable at day 0, increased at day 40 but progressively decreased up to day 52 (Fig. 5c). OC mRNA was expressed starting from day 0 with a slightly increase until day 52 (Fig. 5d). OPN mRNA did not show a regular trend, it was detectable at day 0 and decreased during the culture period evaluated (Fig.5e). Runx-2 mRNA levels decreased significantly from day 0 to day 52, while OSX mRNA, which was not detectable at day 0 increased significantly up to day 52 ($p<0.05$) (Fig. 5 f,g).

DISCUSSION

Osteochondral injuries can cause pain, swelling

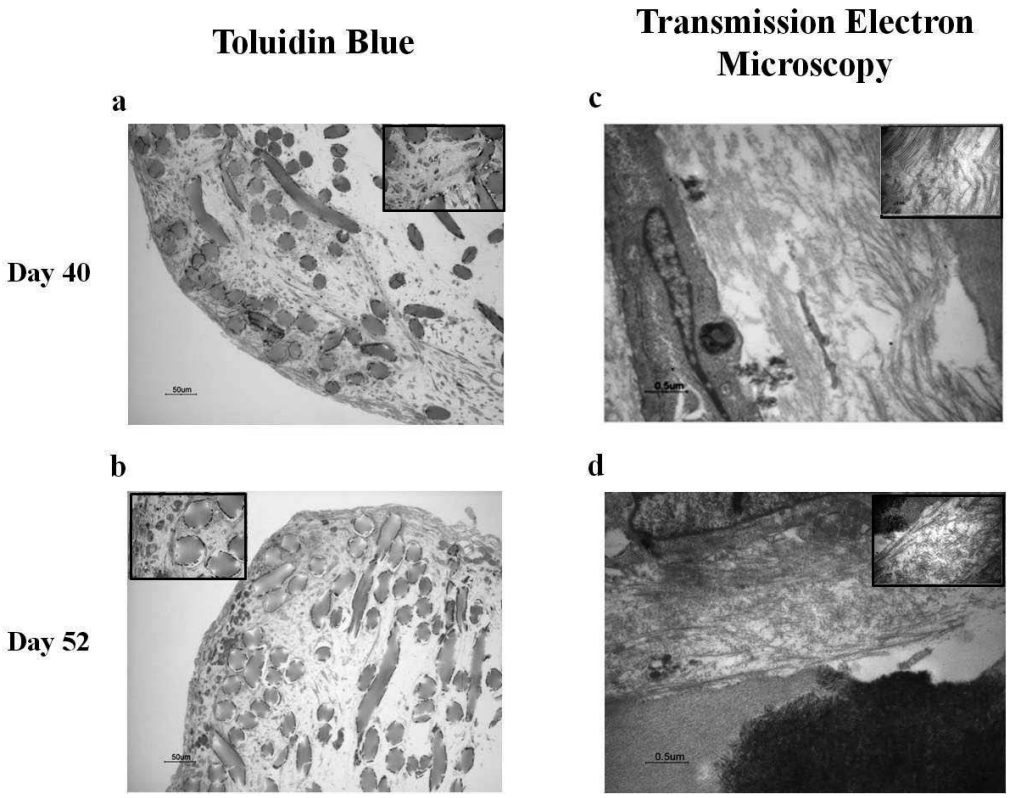

Fig. 3. *Toluidine blue staining of BMC seeded onto Hyaff-11 at different experimental times. At day 40 scaffold was colonized by cells in particular on the superficial layer, which in some areas gave rise to structures that resembled bone matrix (**a**). After 52 days of culture, cells showed a similar appearance, cells were completely surrounded by extracellular matrix (**b**). Electron microscopy images, showed the presence of extracellular matrix between cells and the Hyaff-11 fibers on day 40 (**c**). On day 52, collagen fibrils were detected in the extracellular matrix (**d**). The insets indicate the areas enlarged. Scale bars: 50 µm (a-b), 10 µm (insets); 0.5 µm (c-d), 0.1 µm (insets).*

and decrease function of the joints and, in some cases, lead to osteoarthritis (25). Although several surgical procedures are available to treat osteochondral defects, there is not an ideal therapeutic solution (26). Recently, the use of MSC combined with different types of biomaterials, seems to be one of the most appealing approaches for the treatment of these lesions with promising results (27, 28). However, MSC as osteoprogenitor cells represent only a small fraction (0.001–0.01%) within the whole population of nucleated cells, and in order to increase their concentration, several techniques have been developed, above all the *ex vivo* cultivation of mesenchymal progenitor cells from bone marrow (29). However, this bears several disadvantages, such as the problems of sterility during the cell culture, long times of cultivating that make an operation process in two stages necessary, but also high costs and the questionable use of foetal bovine serum in connection with cell expansion (30). An enrichment of progenitor cells by means of density gradient centrifugation of bone marrow could be seen as a possible solution in the daily clinical routine overcoming all the risks related to *in vitro* cultures, and permits to implant cells surrounded by their niche (11, 12). Generally, a niche is identified as a physical site in adult tissues that provides a microenvironment in which several molecules and different cell types regulate and modulate stem cell fate. The importance of microenvironment and the crosstalk between the cells, has been demonstrated by several authors who showed how the presence of HSCs influences the osteoblastic differentiation of progenitors cells (31, 32). Thus, the presence of the

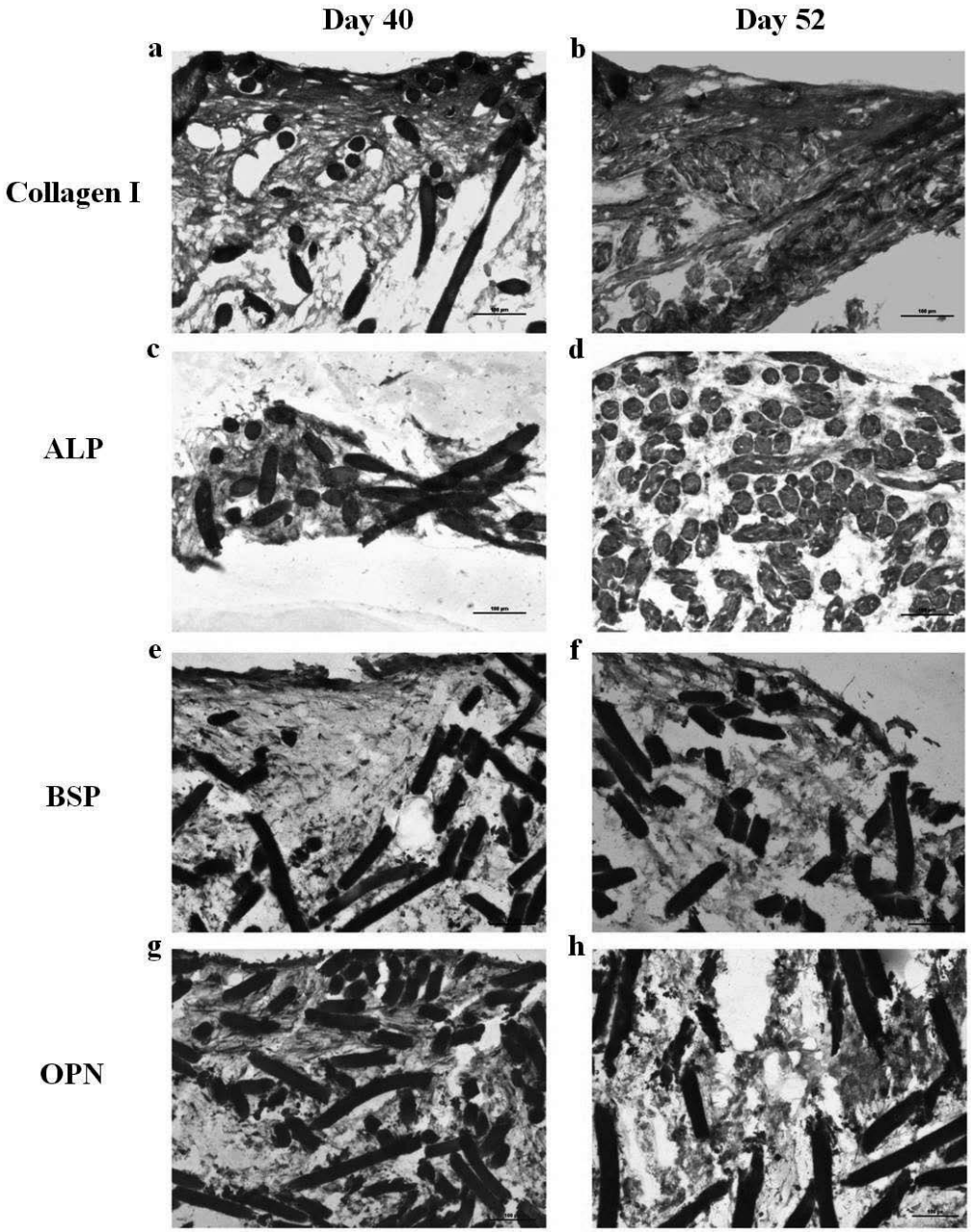

Fig. 4. *Immunohistochemical analysis of Collagen type I (**a-b**), alkaline phosphatase (**c-d**), bone sialon protein (**e-f**) and osteopontin (**g-h**) performed on BMC seeded onto Hyaff-11 scaffold at different experimental times. Scale bars: 100 µm.*

niche, in which cells and growth factors work together to support the differentiation, the proliferation and the survival of stem cells, could favor the natural regeneration of tissue. Despite the choice of the cellular component being one of the crucial steps for regenerative medicine, the use of an ideal support is needed. Scaffolds can provide an adequate milieu and a tridimensional structure to support cell growth and differentiation. Our previous study (21) gave evidence that BMC seeded onto Hyaff-11 was able to differentiate into a cartilage-like tissue, indicating how the interaction between cells and scaffold is crucial for an adequate tissue engineering device. In the present work, we evaluated whether the

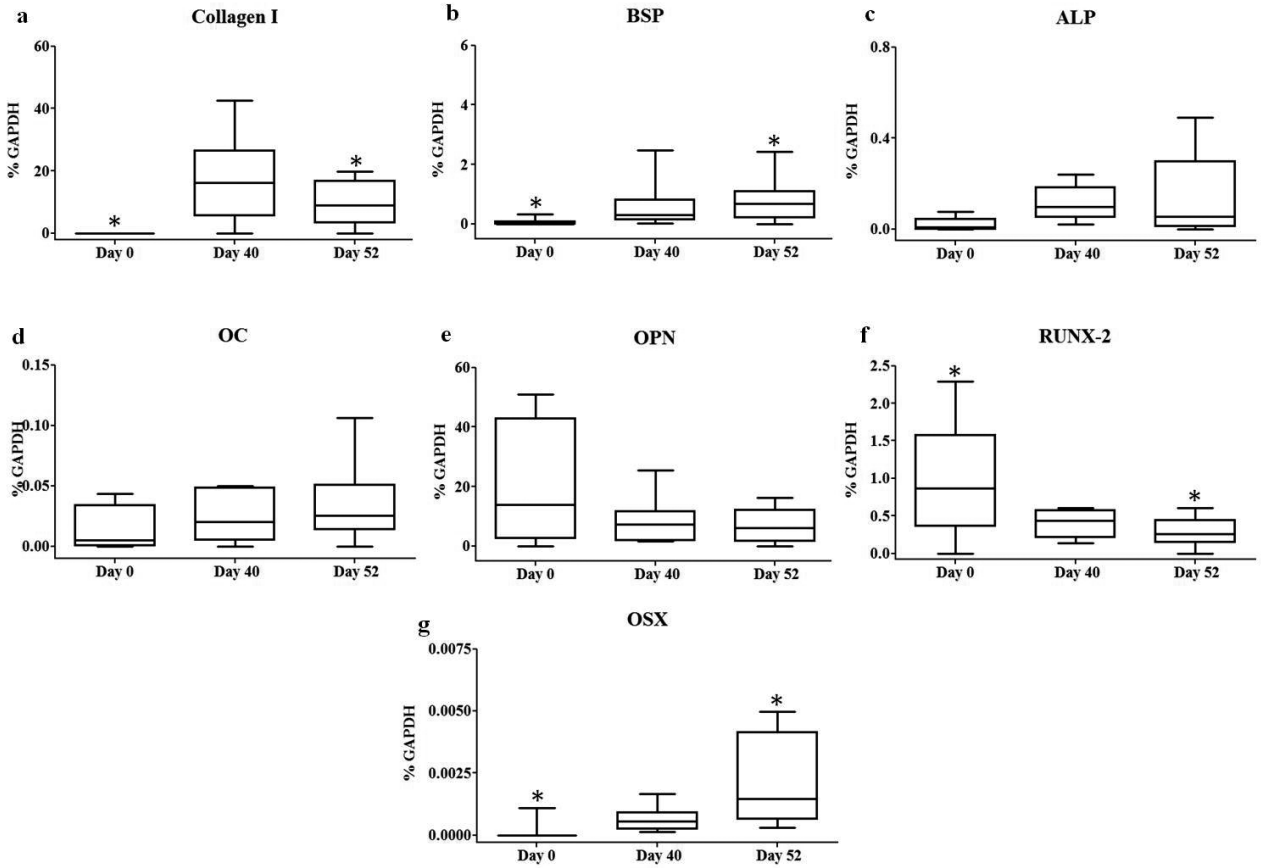

Fig. 5. *Messenger RNAs expression in BMC grown onto Hyaff-11 scaffolds on days 0, 40 and 52. Kinetics for osteogenic markers:* ***a****) Collagen type I;* ***b****) bone sialon protein;* ***c****) alkaline phosphatase;* ***d****) osteocalcin;* ***e****) osteopontin;* ***f****) Runx-2 and Osterix g). Data were normalized to GAPDH and expressed as a percentage of the reference gene. Data are expressed as mean ± Standard Deviation (SD). $p<0.05$*

combination of BMC with Hyaff-11 was able to form a bone-like tissue for the treatment of osteochondral lesions in the orthopedic field. Our data showed how BMC seeded onto Hyaff-11 is able to differentiate in an osteogenic sense with the production of mineralized extracellular matrix. Osteocalcin, osteopontin, collagen type I, alkaline phosphatase, Runx-2 and osterix are a few of the markers related with matrix maturation at different stages during MSC differentiation toward bone tissue (33, 34). Histological and immunohistochemical evaluations demonstrated that after 40 days all the stages occurring during bone differentiation were evident, not only with the presence of mineral deposits, but also with calcification areas within the biomaterial. These findings validate the hypothesis of Solchaga et al., who reported that Hyaff-11 is able to create an environment that supports the recapitulation of embryonic-like events that could lead to the regeneration of damaged tissue (20). Moreover, electron microscopy analysis showed the presence of an extracellular matrix constituted of fibrils, granules and a significant mineralization of biomaterial that could be useful to create a bone-like tissue suitable for cell differentiation. Taking into account that the commitment of BMC toward an osteogenic lineage occurs through different stages that involve the activation and the production of different sets of genes and proteins, the expression of the principal genes and proteins involved in MSC differentiation and function was evaluated. Our experiments demonstrated that BMC grown onto Hyaff-11 was able to stimulate the production of collagen type I mRNA, alkaline phosphatase, osteocalcin,

osteopontin, and bone sialoprotein. Moreover, we analyzed the major transcription factors involved in osteoblastogenesis; Runx-2 that promotes the early stage of MSC differentiation toward osteogenic sense and osterix which induces the terminal one. Our data demonstrated a down-regulation of Runx-2 and an up-regulation of osterix on the constructs during the experimental times planned. The presence of both osterix and Runx2 was necessary to enhance the osteogenic potential of MSC; indeed they were able to regulate the expression of osteoblast specific genes, including alkaline phosphatase, osteocalcin, osteopontin, and bone sialoprotein, by cooperating with various co-factors (35). Data from molecular biology were confirmed by the production of collagen I, ALP, OP and BSP, typical bone proteins that were normally expressed during formation and maturation of osteogenic matrix.

Our *in vitro* study demonstrates that BMC seeded onto Hyaff-11 is able to differentiate into osteoblast-like cells, and considering also its ability to differentiate toward chondrocytes, it can represents an appropriate and suitable biological compound to be used for the repair of osteochondral defects.

However, despite the potential use of BMC and its efficacy in regenerating musculo-skeletal tissue, there are some limitations that have to be taken into account and which are related to: i) the inherent variability of bone marrow ii) differences in marrow architecture within the iliac crest at different sites that could lead to different numbers and activity of the injected cells; iii) the variability in the osteogenic potential from patient to patient that could represent a limitation of the technique *in vivo*.

ACKNOWLEDGEMENTS

We thank the II Orthopedic and Traumatologic Clinic of our Institute for providing us with Bone Marrow Concentrate samples. ALP hybridoma surnatant developed by J.A. Katzmann, osteopontin and bone sialon proteine hybridoma surnatant developed by M. Solursh and A. Franzen, was obtained from the Developmental Studies Hybridoma Bank.

We thank Patrizia Rappini and Graziella Salmi for their assistance in the preparation of the manuscript and Luciano Pizzi for his technical assistance. We also thank Dr Elettra Pignotti for statistical analysis. This work was partially supported by grants from Progetto Regione Emilia-Romagna Università 2010-2012 “Regenerative medicine of cartilage and bone”.

REFERENCES

1. Martin I, Miot S, Barbero A, Jakob M, Wendt D. Osteochondral tissue engineering. J Biomech 2007; 40:750-65.
2. Buckwalter JA, Mankin HJ. Articular cartilage repair and transplantation. Arthritis Rheum 1998; 41:1331-42.
3. Steadman JR, Rodkey WG, Rodrigo JJ. Microfracture: surgical technique and rehabilitation to treat chondral defects. Clin Orthop Relat Res 2001; 391:S362-69.
4. Brittberg M. Autologous chondrocyte transplantation. Clin Orthop Relat Res 1999; 367:S147-55.
5. Ochi M, Uchio Y, Tobita M, Kuriwaka M. Current concepts in tissue engineering technique for repair of cartilage defect. Artif Organs 2001; 25:172-79.
6. Kreuz PC, Steinwachs MR, Erggelet C, Krause SJ, Konrad G, Uhl M, Südkamp N. Results after microfracture of full-thickness chondral defects in different compartments in the knee. Osteoarthritis Cartilage 2006; 14:1119-1125.
7. Giannoudis PV, Einhorn TA, Marsh D. Fracture healing:the diamond concept. Injury 2007; 38:S3-6.
8. Pittenger MF, Mackay AM, Beck SC, et al. Multilineage potential of adult human mesenchymal stem cells. Science 1999;284:143-147.
9. Murphy MB, Moncivais K, Caplan AI. Mesenchymal stem cells: environmentally responsive therapeutics for regenerative medicine. Exp Mol Med 2013; 45:e54.
10. Herberts CA, Kwa MS, Hermsen HP. Risk factors in the development of stem cell therapy. J Transl Med 2011; 22:9-29.
11. Bianco P, Riminucci M, Gronthos S, Robey PG. Bone marrow stromal stem cells: nature, biology, and potential applications. Stem Cells 2001; 19:180-192
12. Block JE. The role and effectiveness of bone marrow in osseous regeneration. Med Hypotheses 2005; 65:740-47.
13. Hernigou P, Guissou I, Homma Y, Poignard A, Chevallier N, Rouard H, Flouzat Lachaniette CH. Percutaneous injection of bone marrow

mesenchymal stem cells for ankle non-unions decreases complications in patients with diabetes. Int Orthop 2015; 39(8):1639-43.
14. Giannini S, Buda R, Vannini F, Cavallo M, Grigolo B. One-step bone marrow-derived cell transplantation in talar osteochondral lesions. Clin Orthop Relat Res 2009; 467:3307-20.
15. Velazquez OC. Angiogenesis and vasculogenesis: inducing the growth of new blood vessels and wound healing by stimulation of bone marrow-derived progenitor cell mobilization and homing. J Vasc Surg 2007; 45:A39-47.
16. Hisatome T, Yasunaga Y, Yanada S, et al. Neovascularization and bone regeneration by implantation of autologous bone marrow mononuclear cells. Biomaterials 2005; 26:4550-56.
17. Hosseinkhani M, Mehrabani D, Karimfar MH, Bakhtiyari S, Manafi A, Shirazi R. Tissue engineered scaffolds in regenerative medicine. World J Plast Surg 2014; 3:3-7.
18. Yoo HS, Lee EA, Yoon JJ, Park TG. Hyaluronic acid modified biodegradable scaffolds for cartilage tissue engineering. Biomaterials 2005; 26:1925-33.
19. Lisignoli G, Fini M, Giavaresi G, Nicoli AN, Toneguzzi S, Facchini A. Osteogenesis of large segmental radius defects enhanced by basic fibroblast growth factor activated bone marrow stromal cells grown on non-woven hyaluronic acid-based polymer scaffold. Biomaterials 2002; 23:1043-51.
20. Solchaga LA, Yoo JU, Lundberg M, Dennis JE, Huibregtse BA, Goldberg VM, Caplan AI. Hyaluronan-based polymers in the treatment of osteochondral defects. J Orthop Res 2000; 18:773-80.
21. Cavallo C, Desando G, Columbaro M, Ferrari A, Zini N, Facchini A, Grigolo B. Chondrogenic differentiation of bone marrow concentrate grown onto a hylauronan scaffold: rationale for its use in the treatment of cartilage lesions. J Biomed Mater Res A 2013; 101:1559-70.
22. Ahmed SA, Gogal RM Jr, Walsh JE. A new rapid and simple non-radioactive assay to monitor and determine the proliferation of lymphocytes: an alternative to [3H]thymidine incorporation assay. J Immunol Methods 1994; 170:211-24.
23. Blanco FJ, Geng Y, Lotz M. Differentiation-dependent effects of IL-1 and TGF-beta on human articular chondrocyte proliferation are related to inducible nitric oxide synthase expression. J Immunol 1995; 154:4018-26.
24. Rozen S, Skaletsky H. Primer3 on the WWW for general users and for biologist programmers. Methods Mol Biol 2000; 132:365-86.
25. Mankin HJ. The response of articular cartilage to mechanical injury. Bone Joint Surg Am 1982; 64:460-66.
26. Sharma L. Osteoarthritis year in review 2015: clinical. Osteoarthritis Cartilage 2016; 24:36-48.
27. Marcacci M, Kon E, Moukhachev V, Lavroukov A, Kutepov S, Quarto R, Mastrogiacomo M, Cancedda R. Stem cells associated with macroporous bioceramics for long bone repair: 6- to 7-year outcome of a pilot clinical study. Tissue Eng 2007; 13:947-55.
28. Matsumoto T, Okabe T, Ikawa T, Iida T, Yasuda H, Nakamura H, Wakitani S. Articular cartilage repair with autologous bone marrow mesenchymal cells. J Cell Physiol 2010; 225:291-95.
29. Gan Y, Dai K, Zhang P, Tang T, Zhu Z, Lu J. The clinical use of enriched bone marrow stem cells combined with porous beta-tricalcium phosphate in poste-rior spinal fusion. Biomaterials 2008; 29:3973-82.
30. Jager M, Jelinek EM, Wess KM, Scharfstadt A, Jacobson M, Kevy SV, Krauspe R. Bone marrow concentrate: a novel strategy for bone defect treatment. Curr Stem Cell Res Ther 2009; 4:34-43.
31. Blair H, Sun L, Kohanski RA. Balanced regulation of proliferation, growth, differentiation, and degradation in skeletal cells. Ann N Y Acad Sci 2007; 116:165-73.
32. Kacena MA, Gundberg CM, Horowitz MC. A reciprocal regulatory interaction between megakaryocytes, bone cells, and hematopoietic stem cells. Bone 2006; 39:978-84.
33. Shang XL, Tao HY, Chen SY, Li YX, Hua YH. Clinical and MRI outcomes of HA injection following arthroscopic microfracture for osteochondral lesions of the talus. Knee Surg Sports Traumatol Arthrosc 2016; 24:1243-49.
34. Marijanović I, Jiang X, Kronenberg MS, Stover ML, Erceg I, Lichtler AC, Rowe DW. Dual reporter transgene driven by 2.3 Col1a1 promoter is active in differentiated osteoblasts. Croat Med J 2003; 44:412-17.

35. Schroeder TM, ED Jensen, Westendorf JJ. Runx2: A master organizer of gene transcription in developing and maturing osteobasts. Birth Defects Res 2005; 75:213-25.

VASCULAR ENDOTHELIAL GROWTH FACTOR AND NITRIC OXIDE SYNTHASE EXPRESSION IN HUMAN TOOTH GERM DEVELOPMENT

F. MASTRANGELO[1], M.T. SBERNA[1], L. TETTAMANTI[2], G. CANTATORE[1], A. TAGLIABUE[2] and E. GHERLONE[1]

[1]Department of Oral Science Ateneo Vita e Salute, University of S. Raffaele, Milan Italy; [2]Department of Medical and Morphological Science, University of Insubria, Varese, Italy

Received November 26, 2015 – Accepted April 21, 2016

Vascular Endothelia Growth Factor (VEGF) and Nitric Oxide Synthase (NOS) expression, were evaluated in human tooth germs at two different stages of embryogenesis, to clarify the role of angiogenesis during tooth tissue differentiation and growth. Seventy-two third molar germ specimens were selected during oral surgery. Thirty-six were in the early stage and 36 in the later stage of tooth development. The samples were evaluated with Semi-quantitative Reverse Transcription-Polymerase chain Reaction analyses (RT-PcR), Western blot analysis (WB) and immunohistochemical analysis. Western blot and immunohistochemical analysis showed a VEGF and NOS 1-2-3 positive reaction in all samples analysed. VEGF high positive decrease reaction was observed in stellate reticulum cells, ameloblast and odontoblast clusters in early stage compared to later stage of tooth germ development. Comparable VEGF expression was observed in endothelial cells of early and advanced stage growth. NOS1 and NOS3 expressions showed a high increased value in stellate reticulum cells, and ameloblast and odontoblast clusters in advanced stage compared to early stage of development. The absence or only moderate positive reaction of NOS2 was detected in all the different tissues. Positive NOS2 expression showed in advanced stage of tissue development compared to early stage. The action of VEGF and NOS molecules are important mediators of angiogenesis during dental tissue development. VEGF high positive expression in stellate reticulum cells in the early stage of tooth development compared to the later stage and the other cell types, suggests a critical role of the stellate reticulum during dental embryo-morphogenesis.

Many studies have shown a possible genetic influence of intracellular and intercellular action proteins as key regulators of physiological and pathological tissues development (1). Nitric oxide (NO) and Vascular Endothelial Growth Factor (VEGF) play active roles during many phases of tissue differentiation and proliferation. Recent studies have shown that NO produces a post-translational modification of proteins (2). NO is produced by three distinct genes: neuronal and endothelial nitric oxide synthases (nNOS and eNOS) and inducible nitric oxide synthases (iNOS) (3-4).

In contrast to the activities of nNOS and eNOS,

Key words: angiogenesis, human tooth development, nitric oxide synthase, stellate reticulum, vascular endothelial growth factor

Mailing address:
Filiberto Mastrangelo MD,DDS,PhD
Ateneo Vita e Salute,
University of S. Raffaele,
Via Olgettina, 60
20132 Milano, Italy
Tel.: +3902.26432921
e-mail: filibertomastrangelo@hotmail.com

0393-974X (2016)

which are strictly regulated by calcium-dependent calmodulin binding, iNOS does not require calcium ions or post-translational modification for its activities. Therefore, iNOS expression is associated with a prolonged NO generation compared with nNOS and eNOS (5-6). iNOS expression is increased by various stimuli, including acute and chronic inflammatory processes, and is expressed even in normal conditions in many tissues during angiogenesis and vasculogenesis (7-8). In normal or pathological tissues, numerous studies reported that endogenous NO promotes oncogenesis and angiogenesis in various forms of cancer (9-10). In contrast, other in vitro and in vivo studies have shown that NO inhibits cell proliferation and induces apoptosis in many cells including cancer ones (11-12).

The VEGF family consists of VEGF-A, -B, -C, -D, c-fos-induced growth factor (FIGF), placenta growth factor-1(PIGF-1), -2 and -3, including additional angiogenic factors having the ability to promote growth of vascular endothelial cells (12). VEGF-A is a key regulator of blood vessel growth (subsequently referred to as VEGF) and expressed not only in organ development and differentiation during embryogenesis (13) but also in angiogenesis and wound healing (12). VEGF acts as a paracrine factor, the signals of which are mediated by two type III tyrosine kinase receptors: VEGF receptor-1 (VEGFR-1) and VEGF receptor-2 (VEGFR-2).

During the development of tooth germs, dental epithelial cells produce different tissues: inner enamel epithelium, stratum intermedium, stellate reticulum, and outer enamel epithelium (1-14). At the cap stage, tooth shape formation begins from the enamel epithelium in the enamel organ, and following the bell stage, enamel formation begins in the enamel organ and the dentin formation begins from the odontblasts. In these cap and bell stages, enamel epithelium differentiates into ameloblasts, which form enamel, while dentinogenesis starts by odontoblast formation of dentin tubes, which, in turn, cover the odontoblast process (2). In rat embryo, an increased level of VEGF mRNA expression was seen in the inner enamel epithelium, and different VEGF mRNA expression levels were found at each stage (15). Immunohistochemical expression of VEGF was marked in tooth germ and mesenchyme only during the initial stages of crown mineralization (1-16).

Blood vessels appear early in the dental papilla and grow to provide nutrition to odontoblasts in the periphery of dental papilla during the bell stage (17). In adults, the VEGF gene in dental pulp is induced by cariogenic bacteria and the VEGF produced may influence a developing pulpal inflammation (18). However, little is known about the role of VEGF and VEGFR-2 expression in dental papilla, ameloblasts and odontoblasts in the developing tooth germ. In literature, the highly hydrated intercellular space between the stellate reticulum cells, which contains a special network of different extracellular matrix molecules (17-18), is considered to have a specific role in maintaining normal tooth shape development and to control the nutritional exchange when the dental papilla is not fully vascularized (2).

In mice, several studies on the mechanisms of continuous incisor growth suggest that the stellate reticulum cells, which express Notch-1-receptors, could represent a complex model associated with early tooth morphogenesis and cell differentiation in ameloblast lineage cells (19-20). Angiogenesis is considered a complex mechanism of postnatal blood vessel formation with the formation of new capillary structures from pre-existing vasculature. It requires a series of cellular events in which endothelial cells locally degrade their basement membrane, proliferate and migrate into the stroma, to form a capillary sprout, then elongate and organize into capillary loops with a lumen. These events occur in response to angiogenic stimuli, polypeptide growth factors which can have either a positive or negative regulatory effect (21). They may act either directly to regulate endothelial cell function or indirectly to regulate growth-factor expression by other cell types. During dentinogenesis, a rich vasculature network develops around a dentine-pulp complex area, and shows an increased vessel fenestration for the odontoblast cell nutrition and growth. Then, at the end of dentine formation it is possible to observe a fenestration decrease and a withdrawal of vessels from the odontoblast layer.

The purpose of this study was to evaluate the VEGF and nitric oxide synthesis enzymatic activity in different tissues during embryogenesis of the human tooth germ center.

MATERIALS AND METHODS

Tissue preparation

Sixteen patients (7 Female and 9 Male) between the ages of 10 and 20 years (average age 12) were selected at the Department of Oral Science, University G. d'Annunzio, Chieti. All subjects were in orthodontic treatment for II and III class malocclusion, hyperdivergence (SN^GoGn value 38.5°) and overcrowding. After an accurate anamnesis, an objective examination and informed consent, 72 third molar germs (36 mandibular and 36 maxillary) were surgically obtained. Thirty-six germs (18 mandibular and 18 maxillary) were extracted in the early stage of tooth development (when initial tissue mineralization was seen by orthopantomograph). Thirty-six germs (18 mandibular and 18 maxillary) were extracted in the later stage of enamel organ, when the dental hard tissue was starting to develop. All samples were fixed in nitrogen liquid and maintained at -80°C.

Western blot analysis

Determination of VEGF and eNOS, nNOS and iNOS proteins was performed by Western blotting (WB) of total protein extracts. Fifty g cytoplasmatic proteins, quantified by spectrophotometric assay (HP 8452A, California, USA) using the Lowry method, were separated by electrophoresis in a 7.5% sodium dodecyl sulfate-polyacrylamide gel (SDS-PAGE (BIO-RAD), Hercules, California, USA) and transferred at 4°C to nitrocellulose membrane (BIO-RAD, Hercules, California) in glycine-methanol buffer. Nitrocellulose was then blocked in Tris-Buffered Saline (TBS)-milk and incubated overnight with various primary antibodies: anti human-eNOS, nNOS, iNOS (Santa Cruz Biotech, Inc. Santa Cruz, California, USA). The nitrocellulose was then washed in TBS, incubated with a secondary antibody conjugated with alkaline phosphatase for 2 h, washed again, and developed in an alkaline buffer with nitrobluetetrazolium (NBT) as substrate (Alkaline Phosphatase Conjugate Substrate Kit, BIO-RAD, Hercules, California). β-actin (Sigma, 1/10.000) was used as an internal standard. The densitometric analysis of Western blots was performed using a computerized densitometric system (Bio-Rad Gel Doc 1000, Milan, Italy).

Semi-quantitative reverse transcription-polymerase chain reaction analysis

Total RNA was extracted using 1 ml ULTRASPEC-RNA (Biotech, Lab., Inc. Huston, TX, USA), as recommended by the manufacturer. RNA was dissolved in diethyl pyrocarbonate (DEPC)-treated water and quantified spectrophotometrically at 260 nm. First-strand cDNA was generated by adding RNA (1 μg) to a mixture containing 1 mM deoxy-nucleoside- triphosphates (d-NTP), 1U/μl RNase inhibitor, 2.5 U/ μl moloney murine leukemia virus reverse transcriptase, 2.5 μM oligo-dt, 5 mM $MgCl_2$, and 10x PCR buffer in a final volume of 20 μl. Reverse transcription was performed at 42°C for 1 h followed by heat inactivation of reverse transcriptase at 92°C for 10 min. 18S was amplified from the same amount of RNA to correct for variation of the different samples. PCR amplification was performed using a Programmable Thermal Controller (MJ Research, Inc. Massachusetts, USA) at the following annealing temperatures: 58°C for 60 s for eNOS, 56°C for nNOS and 55°C for iNOS. The PCR solution contained 10 μl of first-strand cDNA, 4 μl 10x PCR buffer, 2 mM $MgCl_2$. The following primer pairs were used: sense 5'-CTC TCC AGG CAC TTC AGG C-3' and antisense 5'-TGT CTG TCT GCT GCT CCT AG-3' for human eNOS, sense 5'-CGT TTG GCA TGG GGG AGT GAG C-3' and antisense 5'-TTG GGG GCC TGG GAT TTC TGG-3' for human nNOS, sense 5'-CGT AAA GAC CTC TAT GCC AA-3' and antisense 5'-AGC CAT GCC AAA TGT CTC AT-3' for human iNOS and 5'-TCGGGCCTCCGAAACCATGA-3' (sense) and 5'-CCTGGT GAGAGATCTGGTTC-3' (antisense) for human VEGF. The β-actin was included as an internal control with the forward primer: 5'-GTGGGGCGCCCCAGGCACCA-3' (sense) and 5'-CTCCTTAATGTCACG-CACGATTTC-3' (antisense). 2U Termophylus Acquaticus (Taq) DNA polymerase (Celbio, Milan, Italy), and water to a final volume of 50 μl. PCR products were run on 2% agarose gel electrophoresis and photographed after ethidium bromide staining under UV light. Bands on the gel were scanned using a computerized densitometric system (Bio-Rad Gel Doc 1000, Milan, Italy).

Immunohistochemistry

The samples were fixed in 10% formalin for 1 day and embedded in paraffin, by using Tissue-Tex VIP E 150. Serial sections 3-μm thick were taken from the tissue blocks by using rotatory microtomes (Leitz 1512, Heidelberg, Germany). The sections were demineralized in a 3.7% EDTA solution containing 7 cc of Hcl for 60 days. The specimens were then dehydrated by immersion in ethanol solution and embedded in liquid paraffin and incubated with phosphate buffered saline (PBS) (ph 7.4) for 10 min. For antigen retrieval, the samples in antigen immunostaining were treated by microwave boiling in 2.1% citrate acid (pH 6.0) for 2 periods of 5 min and stained with Optimax® Plus Consolidated Staining System (Biogenex, San Ramon, CA, USA). They were then incubated with 3% hydrogen peroxide solution, rinsed and, after a reaction with antibodies for 30 min at room temperature, washed in PBS and treated with the Super Sensitive Immunodetection system (Biogenex, San Ramon, CA, USA) at room temperature, including a multi-link secondary biotinylated antibody (Super Sensitive Multilink ® Biogenex, San Ramon, CA, USA) and streptavidin-biotin-peroxidase (strep-ABC – peroxidase) (Super Sensitive Label®, Biogenex, San Ramon, CA, USA). Reaction products were visualized by immersing the sections in 3% diaminobenzidine (DAB) (Biogenex, San Ramon, CA, USA) solution containing 2 nM hydrogen peroxide for 3 to 5 min. Nuclei were lightly counterstained with hematoxylin of Mayer (Bio-optica, Milano, Italy); the sections were finally dehydrated by immersion in ethanol solution and observed through Leica DMRB microscope (Leica, Heidelberg, Germany). The applied antibodies were: anti- vascular endhotelial growth factor (anti-VEGF) (Santa Cruz Biotechnology, Inc, Santa Cruz, CA, USA; diluted at 1:100) and anti- nitric oxide synthase (anti-NOS) (anti-NOS1, anti-NOS2 and anti-NOS3) (Santa Cruz Biotechnology, Inc, Santa Cruz, CA, USA).

Data analysis

The Statistical Package for Social Sciences software (SPSS® Inc., Chicago, Ill) was used to perform the data analysis. In each of the two groups the statistical significance of difference in the percentages of reactivity levels for VEGF, NOS-1, NOS-2 and NOS-3 were analyzed by Pearson's ^{2}-test. For all the VEGF, NOS-1, NOS-2 and NOS-3 immune reactions, the Wilcoxon paired sign rank sum test was used to evaluate the significance of the differences in the IOD scores between the data obtained in the early and the later development groups. P-values less than 0.05 were considered to indicate statistical significance.

RESULTS

VEGF

RT-PCR analysis

The RT-PcR analysis showed a typical expression of VEGF in all samples examined in both stages of tooth germ development (early stage vs advanced stage). However, different expressions were found. In stellate reticulum cells it was possible to notice a significant decrease of VEGF expression in the early stage compared to cells of advanced tooth development. In all samples of ameloblasts and odontoblasts, VEGF showed a slight decreased expression in the early stage compared to advanced tooth development, while in the endothelial cells the VEGF value appeared comparable between the two different stages of tissue development (Table I and Fig. 1).

Western blot analysis

The VEGF protein Western blot analysis showed high levels in all samples of both stages of tooth development. However, it was possible to observe different expressions in all the tissues. A strong decrease showed in stellate reticulum in the early stage compared to advanced stage cells. While a slightly decreased VEGF value was observed in both ameloblast and odontoblast cells in early to advanced stage development. Comparable VEGF values were observed in early and advanced endothelial cells (Table II and Fig. 2).

Immunoreactivity

VEGF and NOS1-2-3 expressions were quantified using photo analysis computer software (Scion Image, Beta 4.03, Frederick, MD, USA) and classified as follows: (-) negative (less than 10% of blood vessel endothelium intensity), (-/+) moderately positive (10-30% of blood vessel

Table I. *RT-PcR expression of VEGF and NOS1-2-3(nNOS-iNOS-eNOS).*

	Stage of tooth development	VEGF	NOS1	NOS2	NOS3
Endothelial cells	Early	20%	30%	10%	50%
	Advanced	40%	60%	30%	70%
Stellate reticulum	Early	*60%	*20%	10%	60%
	Advanced	10%	90%	10%	90%
Odontoblasts	Early	30%	*30%	20%	60%
	Advanced	20%	90%	20%	80%
Ameloblasts	Early	*50%	*30%	10%	*50%
	Advanced	10%	80%	10%	90%

RT-PcR VEGF and NOS1-2-3 expression: (+/−) weakly less or equal than 10% of positive cells, (+) moderately 10−50% of positive cells, (+ +) strongly more than 50% of positive cells, (*) Significant difference between the two groups (early stage of development and advanced stage of development)

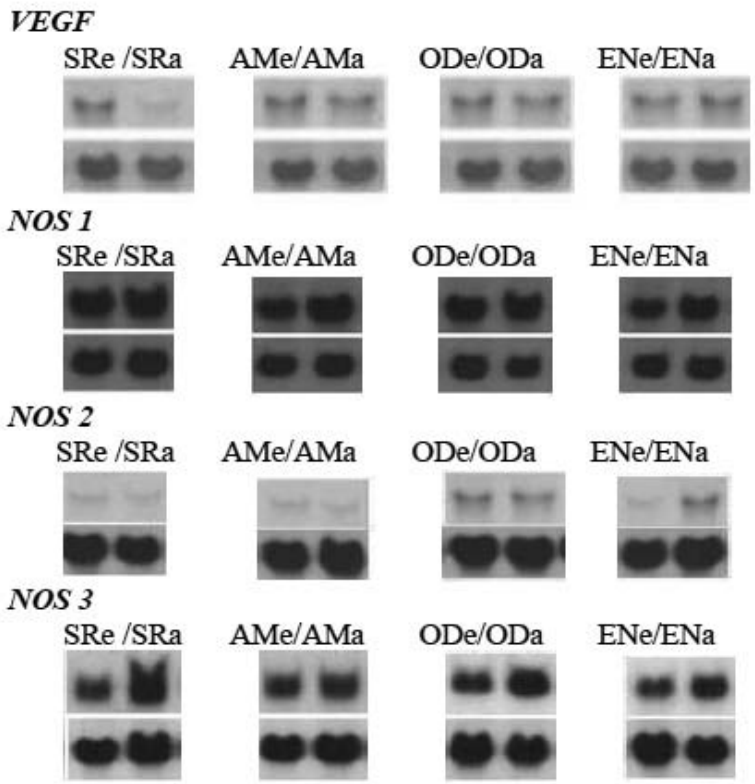

Fig. 1. *Semi-quantitative Reverse transcription-Polymerase Chain Reaction (RT-PcR) analysis.*
RT-PcR analysis: VEGF and NOS1-2-3 expression: SRe: Stellate reticulum cells Early stage of tooth development; SRa: Stellate reticulum cells Advanced stage of tooth development; AMe: Ameloblasts Early stage of tooth development; AMa: Ameloblasts Advanced stage of tooth development; Ode: Odontoblasts cells Early stage of tooth development; Oda: Odontoblasts cells Advanced stage of tooth development; ENe: Endothelial cells Early stage of tooth development; ENa: Endothelial cells Advanced stage of tooth development.

Table II. *Western blot expression of VEGF and NOS 1-2-3 (nNOS-iNOS-eNOS).*

	Stage of tooth development	VEGF	NOS1	NOS2	NOS3
Endothelial cells	Early	10%	*50%	10%	30%
	Advanced	40%	90%	30%	70%
Stellate reticulum cells	Early	*70%	*20%	10%	*10%
	Advanced	10%	80%	10%	70%
Odontoblasts	Early	50%	60%	30%	*30%
	Advanced	50%	90%	20%	70%
Ameloblasts	Early	50%	*50%	10%	*20%
	Advanced	20%	90%	20%	70%

WB VEGF and NOS1-2-3 expression: (+/−) weakly less or equal than 10% of positive cells, (+) moderately 10−50% of positive cells, (+ +) strongly more than 50% of positive cells, (*) Significant difference between the two groups (early stage of development and advanced stage of development)

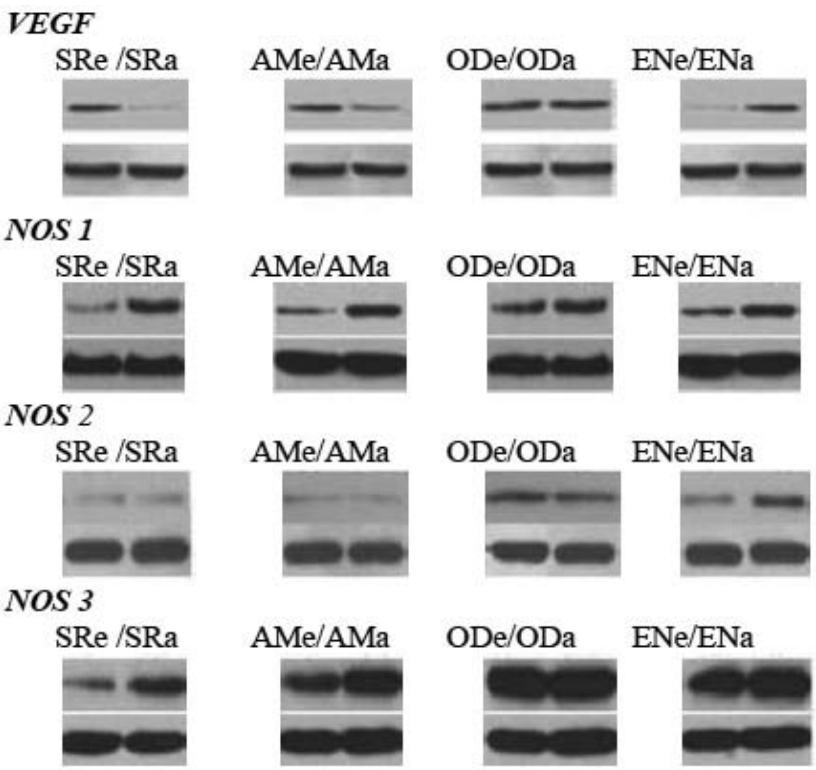

Fig. 2. *WB analysis. VEGF and NOS1-2-3 expression: SRe: Stellate reticulum cells Early stage of tooth development; SRa: Stellate reticulum cells Advanced stage of tooth development; AMe: Ameloblasts Early stage of tooth development; AMa: Ameloblasts Advanced stage of tooth development; Ode: Odontoblasts cells Early stage of tooth development; Oda: Odontoblasts cells Advanced stage of tooth development; ENe: Endothelial cells Early stage of tooth development; ENa: Endothelial cells Advanced stage of tooth development.*

endothelium intensity), (+) positive (10–50% of blood vessel endothelium intensity), and (++) strongly positive (more than 50% of blood vessel endothelium intensity). The levels of reactive intensity for immunohistochemical staining for VEGF and NOS1-2-3 in the blood vessel endothelium at 16 weeks were considered positive controls. Statistical significance: *P-0.001. P-values from G-tests were less than 0.001 for all columns in each subject, and were considered as statistically significant. The quantitative evaluation of the VEGF immunoreaction showed a decreased value of VEGF in all samples of stellate reticulum. In stellate reticulum early stage samples, an intense positive expression was observed compared to advanced stage cells indicating a statistical significance ($p<0.05$). In early stage samples of ameloblast and odontoblast, strongly positive expression was noticed, compared to positive/ moderately positive expression in the advanced stage of tooth development ($p<0.005$). A positive expression showed in all samples of endothelial cells in both stages of tooth growth (Fig. 3).

NOS-1 and NOS-3

RT-PCR analysis

NOS1 and NOS3 expression were detected in all samples with different expressions. A high increased expression of NOS1-3 showed in stellate reticulum cells in the early stage compared to the advanced tooth germ stage with statistical significance. The same behavior was observed in odontoblast and ameloblast samples. A moderate increase of NOS1-3 expression showed in early vs advanced endothelial cells. (Table I)

Western blot analysis

NOS1 and NOS3 expression values showed a similar behavior in all samples analyzed. In the stellate reticulum specimens a high increased expression in the advanced compared to the early stage of tooth development was found with statistical significance. The same values were observed in odontoblast and ameloblast samples with statistical significance of variation for NOS1. A moderate/positive increase of NOS1-3 expression was observed in early vs advanced endothelial cells (Table II).

Immunoreactivity

The immunohistochemical analysis showed strong expression levels of NOS1 and NOS3 in stellate reticulum cytoplasm in advanced stage of tooth development compared to the early stage with a statistical significance ($p<0.05$). High levels of immunoreactivity for NOS-1 and NOS-3 were detected in the cytoplasm of cellular components in odontoblast and ameloblast cells in later stage germ development compared to early stage ones with a statistical significance ($p<0.05$). NOS1 and NOS3 positive expressions were observed in endothelial cells in the later advanced stage compared to the early stage (Fig. 3).

NOS-2

RT-PCR analysis

The RT-PcR analysis detected NOS2 in all the samples, however, it was possible to observe different expressions in all the tissues. High positive expressions were evaluated in ameloblast, odontoblast and stellate reticulum cells of the advanced stage of tooth development compared to the early stage. Positive expression was observed in the advanced stage endothelial cells compared to early stage ones (Table I).

Western blot analysis

The NOS2 Western blot expression showed increased levels of cytoplasm protein. Moderate positive intensity was detected in all tissues. High positive NOS2 expression it was evaluated in all the specimens analyzed (Table II).

Immunoreactivity

The NOS2 immunoreaction showed a low value expression in all samples. In stellate reticulum and ameloblast samples, a low positive expression in both early and advanced stage cells was observed. In both stages of tooth development, the odontoblast samples showed a low or positive expression of NOS2 ($p<0.005$). A low value of NOS2 expression was detected in all samples of endothelial cells in

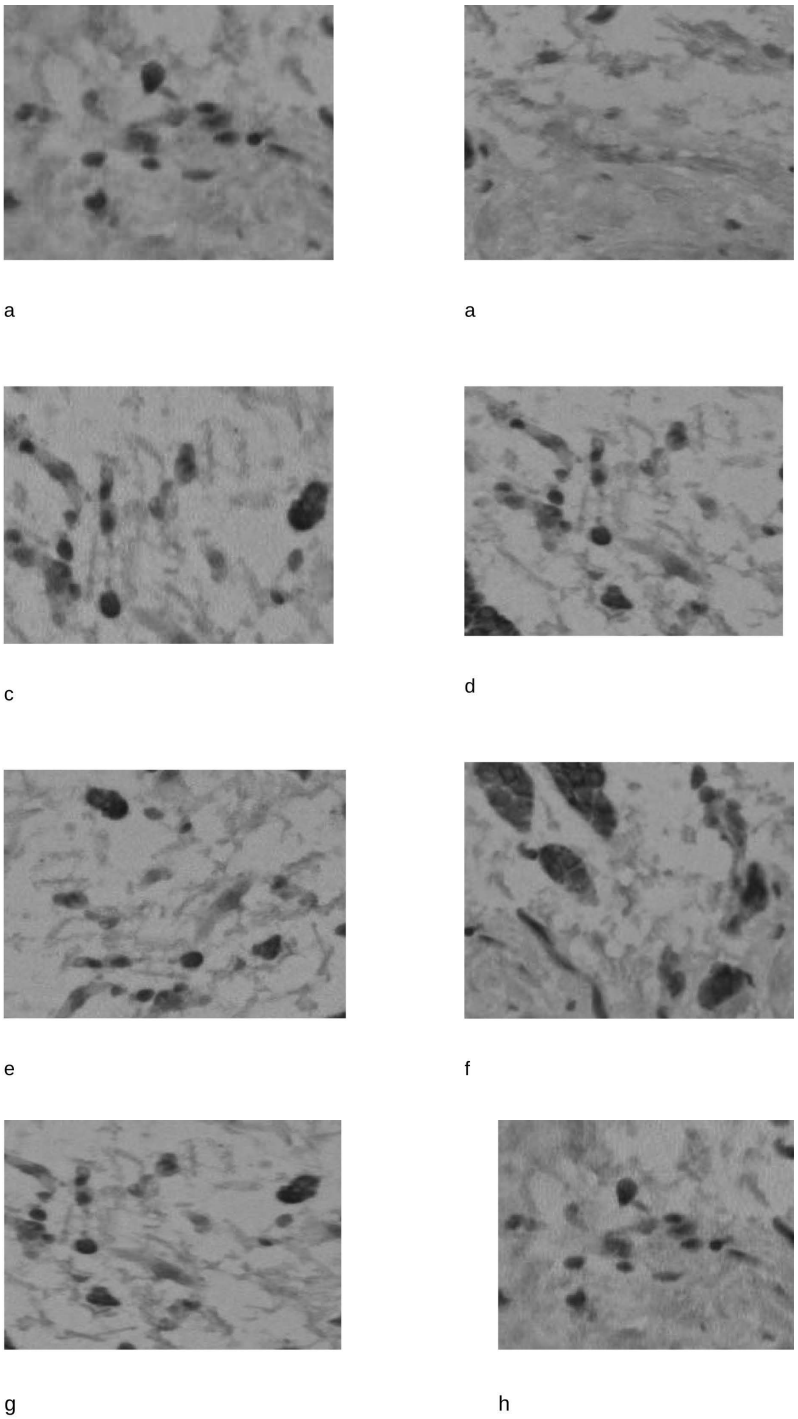

Fig. 3. *Immunohistochemical expression.* ***a)*** *VEGF immunohistochemical expression in stellate reticulum cells in early stage of tooth development;* ***b)*** *VEGF immunohistochemical expression in stellate reticulum cells advanced stage of tooth development;* ***c)****nos1immunohistochemical expression in stellate reticulum cells in early stage of tooth development;* ***d)*** *nos1immunohistochemical expression in stellate reticulum cells in advanced stage of tooth development;* ***e)*** *nos2immunohistochemical expression in stellate reticulum cells in early stage of tooth development;* ***f)*** *NOS2 immunohistochemical expression in stellate reticulum cells in advanced stage of tooth development;* ***g)*** *NOS3immunohistochemical expression in stellate reticulum cells in early stage of tooth development;* ***h)*** *nos3immunohistochemical expression in stellate reticulum cells in advanced stage of tooth development.*

both stages of tooth growth, indicating no statistical significance (Fig. 3).

DISCUSSION

Physiological and pathological events of tissue development, show a possible genetic influence at the tissue origin which is regulated by both intracellular and intercellular action proteins (1). These genes are able to produce proteins which produce intracellular and extracellular actions that act as key regulators of the cellular cycle and tissue development (14). Vascularization is essential for organ and tissue development and is required for maintaining metabolic homeostasis by supplying oxygen and nutrients as well as excreting metabolized products (7, 9-22).

It is known that neovascularization of the embryonic organs occurs through vasculogenesis or angiogenesis or both (23, 24). Vasculogenesis is an in situ process by which progenitor cells differentiate and give rise to capillaries (25), while angiogenesis refers to the formation of new capillaries from pre-existing ones, comprising endothelial sprouting and intussusceptive microvascular growth (IMG): a mechanism of capillary growth (25). Teeth develop through interactions between epithelium and mesenchyme. The developing capillaries in the enamel organ and the dental epithelial structure occur simultaneously by mechanisms of vasculogenesis and angiogenesis at the onset of dentinogenesis (26). The vascular neoformation in the dental mesenchyme has been reported to start from the cap stage. However, the mechanisms of vascularization in the dental mesenchyme remain unknown.

Teeth develop as a result of sequential and reciprocal interactions between epithelium and cranial neural crest-derived mesenchyme (26-27). In a rat model, when the enamel organ of the rat tooth germ is fully developed at the tip of the prospective cusp, amelogenesis begins, and at this site the overlaying stellate reticulum begins its involution (25). During the involution process, there is a gradual decrease in intercellular spaces, invasion by blood vessels, appearance of macrophage-like cells and reduction in the number of stellate reticulum cells (26). In the mouse, the development of the incisors is a continuous process and all morphological events during the late prenatal period (bell stage), continue throughout life. In the human model, tooth development proceeds in an established sequential cascade of events beginning in the oral ectodermal derived odontogenic placode through bud, cap and bell stages and culminating in the formation of the mineralized enamel extracellular matrix.

Development of the teeth is characterized by the in-growth of induced ectoderm into the mesoderm, which is derived from neural crest cells of the isthmus region, and subsequent reciprocal interactions between the cells located at the epithelial-mesenchymal interface. It is well known that the dental epithelium (inner dental epithelium; IDE) and dental mesenchyme play important roles in morphogenesis and inductive tissue interactions (25-27). Corresponding regulatory processes of tooth formation are being disclosed by the correlation with tooth development of the expression patterns of various genes, such as cell and substrate adhesion molecules of the mesenchymal extracellular matrix (19), carbohydrate residues, growth factors and their receptors including IGF-I receptor, neurotrophins, and both aFGF and bFGF (28), among others (3, 27). Nitric oxide synthase (NOS) is a small, high reactive radical protein, produced from the amino acid l-arginine by the enzyme nitric oxide synthase (29-30) in three different isoforms; two constitutively produced (NOS-1 and NOS-3), and one inducible (NOS-2) from three distinct genes (9, 30). The constitutive forms (endothelial, NOS-1, and neuronal, NOS-3) both calcium- and calmodulin-dependent, contribute to the maintenance of normal nervous and cardiovascular systems physiology (16). The inducible form (NOS-2) both calcium and calmodulin-independent, is principally involved in inflammation and carcinogenesis (30). In neoplastic tissues, NO was implicated in tumour growth, mutagenicity, angiogenesis and metastasis, although it has also been implicated in the cytotoxicity of macrophages toward tumour cells and in immunosuppression (9). Furthermore, nitric oxide reacts with the superoxide anion to form a peroxynitrite anion, a highly toxic molecule, causing

DNA damage and protein modifications (32).

Vascular Endothelial Growth Factor (VEGF) is an endothelial-specific growth factor that induces angiogenesis, i.e., sprouting of capillaries from preexisting vessels in vivo. Endothelial nitric oxide synthase (eNOS-NOS1) is an essential molecule in mediating VEGF-A-induced angiogenesis and endothelial function via production of nitric oxide (NO). Moreover, the protein level of eNOS is upregulated in response to VEGF-A. While VEGF-A-induced NO release in human trophoblast cells appears to be initiated via VEGF receptor-1, it is not clear which of the VEGF-receptors mediates the signal for induction of eNOS protein expression. In addition, it is unclear whether other NOS isoforms are upregulated in response to VEGF-A stimulation (1, 32). In an eNOS knock-out rat model the angiogenesis and the permeability inhibition induced from VEGF action were observed. In a VEGFR-1 knock-out rat model, during embriogenesis, it was shown that endothelial cells do not control proliferation (33). In an adult model VEGFR-1 induced growth signals (PLC-, MAPKs) to endothelial cells and pericytes, and to macrophage migration (12, 34). VEGF-A165 peptide increases the number of proliferating cells without inducing differentiation of endothelial lineage. Additionally, exposure of human dental pulp stem cells (hDPSC) cultured in osteogenic medium to VEGF-A165 showed an increase of ALP and osteogenic differentiation and proliferation (14). In a rat model, an increased level of VEGF mRNA expression was seen in the outer enamel epithelium in comparison to inner enamel epithelium, stellate reticulum and dental papilla at the cap stage. From the early to late bell stages, there was increased VEGF mRNA expression predominantly in the inner enamel epithelium (15). These variations in expression between human tooth germ and rats may result from the changes in inner enamel epithelium such as ameloblasts at the human bell stage of tooth development (34). The expression of VEGF and VEGFR-2 in inner enamel epithelium (ameloblasts) is dependent upon the differentiation stage, leading us to propose that VEGF and its receptor are expressed in tooth germ and influence, not only vascularization, but also the activation of inner enamel epithelium in tooth shape formation at the cap and bell stages. In addition to endothelial cells, VEGF receptor expressing cells contribute to the formation of hard tissue, osteoblasts, osteoclasts and chondrocytes (7-14). In the human tooth germ at the late bell stage, the expression of the VEGF and VEGFR-2 is almost constantly positive in human ameloblasts. In addition to epithelium-derived enamel epithelium and ameloblasts, immunohistochemical localization of VEGF was also detected in the mesenchyme-derived odontoblasts in human third molar teeth germ at the initial stage of crown mineralization (1,14).

Our research data, showed VEGF expression in all samples examined in both stages of tooth germ development (early stage vs advanced stage). Moreover, in stellate reticulum cells a significant decrease of VEGF level was detected between the early stage compared to cells of advanced tooth development, showing a statistical significance ($p<0.05$). In all the samples of ameloblasts and odontoblasts, the expression of VEGF showed a slightly decreased expression between the early stage compared to advanced tooth development ($p<0.005$), while, a positive expression showed in all samples of endothelial cells in both stages of tooth growth. The NOS 1 and NOS 3 expression, in all samples had different behavior. A highly increased expression of NOS1-3 showed in stellate reticulum cells between the early stage compared to the advanced tooth germ stage with statistical significance ($p<0.05$). The same behavior, was observed in odontoblast and ameloblast samples with a statistical significance ($p<0.05$). A moderate increase of NOS 1-3 expression showed in both early and advanced endothelial cells. Moreover, NOS2 positive expression was evaluated in ameloblast, odontoblast and stellate reticulum cells at advanced stage of tooth development in comparison to the early stage. It was possible to observe by immunodetection moderately positive NOS 2 in advanced endothelial cells compared to early stage.

In our investigation, the VEGF and NOS 1-3 positive expression in all samples examined suggests a critical role of angiogenesis gene proteins action during all phases of tooth embryogenesis. The high levels of VEGF expression in early stage tissues and

the significant decrease of this key regulator in the advanced stage of tissue development could confirm the crucial role of angiogenesis during tooth germ tissue differentiation and growth. In accordance with the literature, the NOS1-3 increased expression in the advanced stage compared to the early stage of tooth development, confirmed an important role of these key regulators during tissue growth.

The different intensity of protein expression, associated to the two stages of germ development, in ameloblast, odontoblast and endothelial cells, seems to suggest a different energetic need during the two stages of development related to the gene. The NOS2 lower or moderate positive reaction in all samples could suggest an indirect action as key modulator protein during dental differentiation and growth.

Also, the particular stellate reticulum cell behaviour, with a significant decrease of VEGF action between the early stage compared to later stage tooth development, in addition to the high increased NOS1-3 expression in these tissues between the advanced phase compared to the early stage of tissue growth, suggests their possible crucial role in promoting and maintaining an adequate energy supply to the tissues during the differentiation and proliferative phases of the initial period of tooth development.

In conclusion, further research is required to learn the delicate biological control mechanisms responsible for cellular activity and tissue survival and growth. Moreover, the angiogenesis gene expression could represent a functional tool for investigating the mechanisms involved in embryogenesis evolution, human dental tissue differentiation and progression in physiological and pathological conditions, offering exciting opportunities for a new tissue engineering approach for novel treatments and clinical techniques for dental tissue restoration.

REFERENCES

1. Mastrangelo F, Piccirilli M, Dolci M, et al. Vascular endothelial growth factor (VEGF) in human tooth germ center. Int J Immunopathol Pharmacol 2005; 18(3):587-94
2. Ten Cate AR. Development of the tooth and its supporting tissues; oral histology; development, structure and formation. fifth ed. London: Mosby, St. Louis, 1998 78—103.
3. Thesleff I. Epithelial—mesenchymal signalling regulating tooth morphogenesis. J Cell Sci 2003; 116:1647-48.
4. Kollar EJ, Baird GR. The influence of the dental papilla on the development of tooth shape in embryonic mouse tooth germs. J Embryol Exp Morphol 1969; 21:131-48.
5. Ohshima H, Wartiovaara J, Thesleff I. Developmental regulation and ultrastructure of glycogen deposits during murine tooth morphogenesis. Cell Tissue Res 1999; 297:271-81.
6. Felszeghy S, Modis L, Tammi M, et al. The distribution pattern of the hyaluronan receptor CD44 during human tooth development. Arch Oral Biol 2001; 46(10):939-45.
7. Tetè S, Zara S, Vinci R, et al. Vascular endothelial growth factor and e-nitric oxide synthase-mediated regenerative response occurring upon autologous and heterologous bone grafts. Int J Immunopathol Pharmacol 2009; 22(4):1105-16.
8. Haradaa H, Kettunena P, Junga H-S, et al. Localization of Putative Stem Cells in Dental Epithelium and Their Association with Notch and FGF Signaling. J Cell Biol 1999; 147:105-20.
9. Speranza L, Pesce M, Franceschelli S, et al. The role of inducible nitric oxide synthase and haem oxygenase 1 in growth and development of dental tissue'. Cell Biochem Funct 2012; 30(3):217-23.
10. Mitsiadis TA, Henrique D, Thesleff I, et al Mouse Serrate-1 (Jagged-1): expression in the developing tooth is regulated by epithelial-mesenchymal interactions and fibroblast growth factor-4. Development 1997; 124:1473-83.
11. Hattori R. Structure and function of nitric oxide synthases. Int J Cardiol 1994; (Suppl.)S71-S75.
12. Ferrara N, Gerber HP, LeCouter J. The biology of VEGF and its receptors. Nat Med. 2003; 9(6):669-76.
13. Carmeliet P, Mackman N, Moons L, et al. Role of tissue factor in embryonic blood vessel development. Nature 1996; 383(6595):73-75.
14. D' Alimonte I, Nargi E, Mastrangelo F, et al. Vascular endothelial growth factor enhances in vitro proliferation and osteogenic differentiation of human

dental pulp stem cells. J Biol Regul Homeost Agents 2011; 25(1):57-69.
15. Aida M, Irié T, Aida T, et al. Expression of protein kinases C betaI betaII, and VEGF during the differentiation of enamel epithelium in toot development Dent Res 2005; 84(3):234-39.
16. Kumamoto H, Suzuki T, Ooya K. Immunohistochemical analysis of inducible nitric oxide synthase (iNOS) and heat shock proteins (HSPs) in ameloblastomas. J Oral Pathol Med 2002; 31:605-15.
17. Avery S, Inniss K, Moore H. The regulation of self-renewal in human embryonic stem cells. Stem Cells Dev 2006; 15(5):729-40.
18. Felszeghya Sz, Mészarb Z, Prehmc P, et al. The expression pattern of hyaluronan synthase during human tooth development. Arch Oral Biol 2005; 50:175-79.
19. Mitsiadis TA, Hirsinger E, Lendahl U, et al. Delta-Notch signaling in odontogenesis: correlation with cytodifferentiation and evidence for feedback regulation. Dev Biol 1998; 204:420-31.
20. S. Kawano, M. Saito, K. Handa, et al. Characterization of dental epithelial progenitor cells derived from cervical-loop epithelium in a rat lower incisor. J Dent Res 83(2):129-33, 2004
21. Folkman J, Klagsbrun M. Vascular physiology. A family of angiogenic peptides. Nature 1987; 329(6141):671-2.
22. Arfuso F. A study of physiologic angiogenesis in the human using the dental pulp as an in vivo model. Endothelium 2006; 13(5):359-63.
23. Patan S. Vasculogenesis and angiogenesis. Cancer Treat Res 2004; 117:332.
24. Ratajska A, Czarnowska E. Vasculogenesis of the embryonic heart: contribution of nucleated red blood cells to early vascular structures. Cardiovasc Hematol Disord Drug Targets 2006; 6(3):219-25
25. Yuan G, Zhang L, Yang G, et al. The distribution and ultrastructure of the forming blood capillaries and the effect of apoptosis on vascularization in mouse embryonic molar mesenchyme. Cell Tissue Res 2014; 356(1):137-45.
26. Baratella L, Arana-Chavez VE, Katchburian E. Apoptosis in the early involuting stellate reticulum of rat molar tooth germs. Anat Embryol (Berl) 1999; 200(1):49-54.
27. Thesleff I. Current understanding of the process of tooth formation: transfer from the laboratory to the clinic. Aust Dent J 2014; 59(S)1:48-54.
28. Bredt DS, Snyder SH. Isolation of nitric oxide synthase, a calmodulin-requiring enzyme. Proc Natl Acad Sci USA 1990; 87:682-85.
29. Nathan C, Xie Q-W. Nitric oxide synthases: roles, tolls and controls. Cell 1994; 78:915-918
30. Knowles SM, Moncada S. Nitric oxide synthases in mammals. Biochem J 1994; 298:249-58.
31. Palmer RM, Ashton DS, Moncada S. Vascular endothelial cells synthesize nitric oxide from l-arginine. Nature 1998; 333:664-66.
32. Kroll J, Waltenberger J. A novel function of VEGF receptor-2 (KDR): rapid release of nitric oxide inresponse to VEGF-A stimulation in endothelial cells. Biochem Biophys Res Commun 1999; 265(3):6363.
33. Shibuya M, Claesson-Welsh L. Signal transduction by VEGF receptors in regulation of angiogenesis and lymphangiogenesis. Exp Cell Res 2006; 312(5):549-60.
34. Miwa Y, Fujita T, Sunohara M, et al. Immunocytochemical localization of vascular endothelial growth factor and vascular endothelial growth factor receptor-2 of the human deciduous molar tooth germ development in the human fetus. Ann Anat 2008; 190(3):246-51.

LETTER TO THE EDITOR

THE PREVALENCE OF CHLAMYDIA PNEUMONIAE IN THE AORTIC WALL AND IN PERIPHERAL BLOOD OF PATIENTS SCHEDULED FOR CORONARY ARTERY BYPASS GRAFTING

A. KUCZAJ[1], P.J. STRYJEWSKI[2], M. FUDAL[1], D. DOMAL-KWIATKOWSKA[3], B. RYFIŃSKI[4], E. SLIUPKAS-DYRDA[5], S. SMOLIK[3], L. WĘGLARZ[3], U. MAZUREK[6] and E. NOWALANY-KOZIELSKA[1]

[1]2nd Department of Cardiology, Zabrze, Medical University of Silesia, Katowice, Poland [2]Department of Cardiology, City Hospital, Chrzanow, Poland; [3]Department of Biochemistry, Medical University of Silesia, Katowice, Poland; [4]Clinical Ward of Cardiac Surgery, Silesian Center for Heart Diseases, Zabrze, Poland; [5]Department of Cell Biology, Medical University of Silesia, Katowice, Poland; [6]Department of Molecular Biology, Medical University of Silesia, Katowice, Poland

Received November29, 2015 – Accepted February 22, 2016

Some reports confirm a potential role of Chlamydia pneumoniae (ChP) in atherogenesis. In order to explore possible association between ChP and atherosclerosis, investigations were carried out in which the frequency of ChP in the arterial wall and peripheral blood was assessed in a group of patients with chronic coronary artery disease (CAD). Fifty-seven patients were enrolled in the study, 13 women and 44 men aged 61.8±6.5 (47-74), with previously diagnosed CAD, scheduled for planned coronary artery bypass grafting due to clinical indications. Vessel specimens retrieved from the ascending aorta (as a part of routine proximal venous graft development procedure) and peripheral blood mononuclear cells (PBMCs) from venous blood were evaluated for the presence of ChP DNA. Genomic DNA was extracted from PBMCs and vessel specimens. Quantitative real-time polymerase chain reaction (qPCR) was performed to detect ChP DNA. A statistically more frequent occurrence of ChP was observed in aortic tissues compared to blood samples (70.2% vs 56.1%, respectively). Similarly, the number of ChP DNA genomic copies [n/1µg genomic DNA] was significantly higher in tissue specimens compared to blood samples (89±91 vs 41±77, respectively; p=0.0046). In patients without ChP in blood specimens, we observed significantly higher amounts of ChP in tissue specimens compared to patients with ChP in blood specimens (156±71 vs 107±88, respectively; p=0.0453). No correlation was found between the number of ChP DNA copies [n/1µg genomic DNA] in blood and in aortic specimens. The infection of ChP in the aortic wall was connected with hypercholesterolemia (p=0.029) and diabetes (p=0.03). We conclude that Chlamydia pneumoniae is a pathogen frequently occurring in the aortic wall of patients with CAD. The occurrence of ChP DNA in the aortic tissue is related to classic CAD risk factors such as diabetes and dyslipidemia.

The pathogenesis of coronary artery disease (CAD) has not been fully understood despite many years of investigations. It appears that there are a number of mechanisms and risk factors of CAD and atherosclerosis involved in this process which extend beyond traditional and accepted risk factors such

Key words: aortic wall, Chlamydia pneumoniae (ChP), coronary artery bypass grafting (CABG), coronary artery disease (CAD)

Mailing address:
Piotr Jozef Stryjewski MD, PhD
City Hospital, Department of Cardiology,
Topolowa 16 st., 32-500 Chrzanow, Poland
Tel.: +48 509 59 89 59 - Fax: + 32 624 72 58
e-mail: pstryjewski@o2.pl

0393-974X (2016)

as lipid profile, hypertension, cigarette smoking, diabetes and family history.

The majority of investigators agree that inflammatory markers and autoimmune processes may play a very significant role in the development of CAD. It is all the more important due to the fact that some results obtained from large epidemiological studies concerning the prevalence of CAD cannot be explained using traditional risk factors only (1).

Currently, according to the theory proposed by Ross in The New England Journal of Medicine (1999), local inflammatory processes may play a significant role in atherogenesis (2).

For many years considerable attention has also been paid to a role of infectious agents in the etiology and pathogenesis of CAD (3-6). In some studies the presence of genetic material of pathogens, such as *Chlamydia pneumoniae* (*ChP*), was found in atheromatous changes in patients with CAD (4, 7).

The majority of available studies are based on indirect evidence such as antibodies against previously described pathogens. It is also confirmed that in some populations the results of immunological assessments are positive in over 50% of investigated subjects without concomitant symptoms and are not necessarily related to the current clinically overt infection (8).

The life cycle of *ChP* comprises elementary bodies (extracellular infectious form) and reticular bodies (intracellular, replicable form). A metabolically inactive, but living spore form may occur in unfavorable conditions. Due to this fact, *Chlamydiae* are good candidates for causing chronic intracellular infections (9). After primary respiratory tract infection, *ChP* may migrate from the circulation to peripheral tissues, such as vessel walls and previously existing atheromatous plaques. The migration is possible due to peripheral blood monocytes (10).

The pathogen was detected for the first time in atheromatous plaques by Kuo et al. (11). In microscopic preparations it is also detected in smooth muscle cells, foam cells, areas of fibrosis, lipid bodies and in the extracellular matrix (12).

It is postulated that penetration of an infectious agent into cells connected with atheromatous plaque increases the production of inflammatory cytokines and smooth muscle proliferation. The pathogen may provoke dysfunction of epithelial cells and metalloproteinase secretion, degrading the extracellular matrix, which in consequence destabilizes the extracellular matrix (13).

It is suggested that *ChP* may be related to atherogenesis, particularly in the cases where classic risk factors do not explain the presence of CAD.

The aim of the study was to assess the prevalence of the infectious agent *(ChP)* in the arterial wall and in peripheral blood of patients with chronic CAD scheduled for coronary artery bypass grafting (CABG).

MATERIALS AND METHODS

The investigated group comprised 57 patients with previously diagnosed CAD scheduled for planned CABG due to clinical indications. The study was approved by the Bioethics Committee of the Medical University of Silesia (No. KNW /0022 /KB1 /29 /I /10 of 27th April 2010). All the investigated patients gave a written consent for participation.

The inclusion criteria were angiographically confirmed CAD scheduled for cardiac surgery due to clinical indications, written informed consent for the participation in the study, age >18 years.

The exclusion criteria were age <18 years, pregnancy, severe concomitant systemic disease, lack or withdrawal of the consent.

A detailed history was obtained and physical examination was performed on each patient after admission to the ward.

Routine additional investigations were performed. These included laboratory tests (complete blood count with blood smear, electrolytes, lipid profile, serum creatinine, urea, uric acid, liver function test, blood glucose), ECG and transthoracic echocardiography. Subsequently, coronary angiography was performed after excluding contraindications.

Patients with diagnosed chronic CAD established on the basis of coronary angiography were enrolled in the study after cardiac surgeon consultation. Patients were scheduled for planned CABG within 3-6 months from the date of qualification for surgery.

On the day of the surgical procedure (CABG), peripheral blood samples were collected for basic laboratory tests and for the assessment of *ChP*.

During CABG, tissue samples from the ascending aorta (as a part of routine aortic window excision) were taken and sent for molecular studies (within 24 h after procedure at the temperature of -20°C). The samples were later stored at -70°C until the time of analysis. The assessment of *ChP* genetic material was performed using quantitative real-time polymerase chain reaction (qPCR) detection method.

Genomic DNA was isolated from aortic samples and from peripheral blood. Blood samples were collected with anticoagulant. The obtained nucleic acid isolates were used as a template in *ChP* DNA qPCR reaction.

DNA extraction was performed using Genomic DNA Prep Plus kit (A&A Biotechnology). Isolated extracts of nucleic acids were stored at the temperature of -70°C until the time of analysis.

Quantitative and qualitative assessment of the obtained extracts

DNA extracts obtained in the course of isolation were analyzed qualitatively with the use of agarose gel electrophoresis and quantitatively with the use of spectrophotometry.

Isolated DNA concentration and the purification grade were assessed based on spectrophotometric measurements (Pharmacia Biotech GeneQuant RNA/DNA Calculator). DNA concentration was estimated with the presumption that 1.0 OD260 = 50 μg dsDNA in 1 ml of the extract. On the basis of the obtained results we calculated the number of extracted μg DNA from 1 ml of blood plasma.

DNA extracts were assessed qualitatively with the use of 0.8% ethidium bromide (0.5 μg/ml) agarose gel electrophoresis. Electrophoresis was performed in SUBMINI apparatus (Kucharczyk). The extract samples mixed with loading solution (0.05% bromophenol blue, 60% glycerol) were analyzed electrophoretically. The obtained electropherogram was analyzed with the application of UV transilluminator (λ = 260 nm).

Estimation of the number of ChP DNA particles

The estimation of the number of *ChP* DNA particles was performed on the basis of PCR kinetic analysis with the application of ABI PRISM™ 7000, Applied Biosystems sequence detector and with the use of QuantiTect SYBR Green RT–PCR kit.

Q-PCR and starter sequence design

Oligonucleotide sequences for the reaction were designed with the use of Primer ExpressTM Version 1.0 ABI PRISM based on sequences of the investigated genes (available at www.ncbi.nlm.nih.gov).

Specificity of the designed oligonucleotide sequences was checked in the BLAST software (www.ncbi.nlm.nih.gov/BLAST) for complementarity to human genome loci. The quantitative assessment of *ChP* genetic material was performed with the use of qPCR.

In order to establish the optimal reaction temperature, a series of reactions were performed using the following thermal conditions: polymerase activation (94ºC, 15 min), 40 two-step cycles comprising denaturation (94ºC, 15 s) and variable primer-template hybridization temperature (ranging from 53ºC to 68ºC, 30 s) and terminal elongation (72ºC, 600 s).

In order to establish the calibration curve, amplification of commercially available β–actin gene was performed with simultaneous sample investigation (TaqMan® DNA Template Reagents Kit and β–actin Control Reagent Kit - Applied Biosystems) in five dilutions (from 1 to 10000 copies cDNA/μl). The composition of reaction mixture was the same as in the case of the investigated samples. Table I shows primer sequences for the investigated gene fragments used in qPCR.

Each assay was performed in three replicates. Samples with deionized water instead of DNA template were used as the negative control. Molecular assays were conducted in the Departments of Biochemistry and Molecular Biology at the School of Pharmacy with the Division of Laboratory Medicine of Medical University of Silesia, Katowice, Poland.

Statistical analysis

The obtained results were collected in Excel spreadsheet and were subsequently exported to Statistica to perform statistical analysis. The following were calculated: mean values, standard deviations, median value, minimum and maximum of the investigated parameters.

The Kolmogorov–Smirnov test was used for the assessment of normal distribution. Non-parametric tests were used in the further analysis due to the lack of

Table I. *Primer sequences used in Q–PCR.*

Gene primers	Name	Sequence
Chlamydia pneumoniae	F	5'- TCCGCATTGCTCAGCC -3'
	R	5'-AAACAATTTGCATGAAGTCTGAGAA -3'
β–actin gene - exon 4	F	5'-TCACCCACACTGTGCCCATCTACGA-3'
	R	5'-CAGCGGAACCGCTCATTGCCAATGG-3'

Table II. *The number of DNA copies in peripheral blood and in tissue (part of ascending aorta) [n/1μg DNA genomic].*

		Chlamydia pneumoniae	Comparison (Wilcoxon test)	p
		PERIPHERAL BLOOD	**TISSUE**	
Investigated group	N	57	57	**p=0.0046**
	mean value ± SD	**41 ± 77**	**89 ± 91**	
	Median value	9	48	
	Min-Max	0 –313	0 – 274	

normal distribution of the investigated parameters. The non-parametric Mann–Whitney U test was used in the comparison between groups The relationship between parameters was verified using Spearman's rank correlation coefficient.

The frequency of the occurrence of the investigated pathogen was calculated. The frequencies were compared, depending on the subgroup size and the expected values with the use of *chi*-squared test, *chi*-squared test with Yates' correction or Fisher's exact test. A $p<0.05$ was considered statistically significant.

RESULTS

Fifty-seven patients were enrolled in the study (13 women and 44 men aged 61.8±6.5 (47-74). In the investigated group 70.2% were hypertensive, 38.6% had diabetes, 54.4% hypercholesterolemia,

31% hypertriglicerydemia, 24.6% were obese (BMI ≥ 30.0 kg/m^2), and 47.4% were cigarette smokers. Impaired renal function defined as GFR < 60 [ml/min/1.73m^2] was observed in 28.1% of patients, advanced non-coronary arteriosclerosis in 36.8%. Single-vessel CAD was observed in 1.8%, two-vessel in 31.5%, three-vessel in 66.7%. Positive family history of CAD existed in 47.4% of the investigated group.

Quantitative and qualitative assessment of ChP occurrence

A significantly higher occurrence of *ChP* was observed in aortic samples when compared to peripheral blood. Similarly, the number of *ChP* DNA copies [n/1µg of genomic DNA] was significantly higher in tissue samples when compared to blood samples (Table II).

A significantly higher number of *ChP* DNA copies was observed in tissue samples in patients without the presence of *ChP* in blood samples when compared to patients with *ChP* presence in blood samples. Similar differences were not demonstrated in the number of *ChP* DNA copies in blood between patients with and without *ChP* presence in tissue samples (Table III).

No correlation was demonstrated between the number of *ChP* DNA copies (n/1µg genomic DNA) in blood samples and in aortic tissue samples (Fig. 1).

A significantly more frequent occurrence of *ChP* was observed in patients with diabetes 86.4% *vs* 60% p=0.0342 and hypercholesterolemia 84.6% *vs* 58.1% p=0.0291.

Results obtained for hypertriglyceridemia were at the limit of statistical significance: 78.9% *vs* 55%, p=0.656. Similar relationships were not observed for CAD risk factors such as hypertension, obesity, reduced glomerular filtration rate and cigarette smoking.

DISCUSSION

In the investigated material, *ChP* assessed by PCR occurred in 70.2% of aortic samples. The obtained result is consistent with the analyses of other authors. The pathogen was detected in atheromatous plaques of

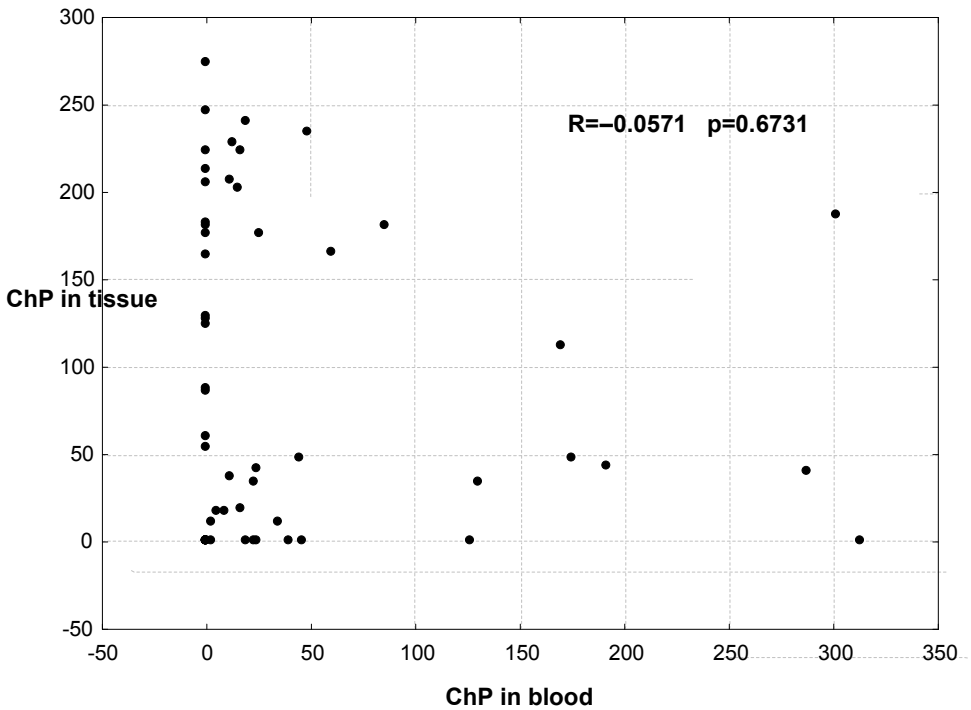

Fig. 1. *Correlation between number of Chlamydia pneumoniae (ChP) DNA copies in blood and number of DNA copies in aortic tissue samples.*

Table III. *The number of ChP DNA copies in peripheral blood samples and in aortic samples.*

Chlamydia pneumoniae	**Investigated group**	**Group of patients with *ChP* presence in tissue samples**	**Group of patients without *ChP* presence in tissue samples**	**Comparison of groups (Mann-Whitney U test)**	**p**
Number of *ChP* DNA copies in blood samples [*n*/1µg genomic DNA]	N	32	24	8	NS (p=0.7773)
	mean value ± SD	72 ± 91	72 ± 89	74 ± 104	
	Median value	25	25	32	
	Min – Max	2 – 313	3 – 301	2 – 313	
Chlamydia pneumoniae	**Investigated group**	**Group of patients with *ChP* presence in blood samples**	**Group of patients without *ChP* presence in blood samples**	**Comparison of groups (Mann-Whitney U test)**	**p**
Number of *ChP* DNA copies in tissue samples [*n*/1µg genomic DNA]	N	40	24	16	**p=0.0453**
	mean value ± SD	126 ± 84	107 ± 88	156 ± 71	
	Median value	128	48	170	
	Min – Max	11 – 274	11 – 241	34 – 274	

coronary arteries, carotid arteries, lower limb arteries, abdominal aortic aneurysms, atheromatous heart valves and atrial tissues derived from heart donors.

The investigation results for the presence of *ChP* in the examined samples differ, depending on the study, ranging from 0% to 100%. In a study by Hedayat et al. the presence of *ChP* was confirmed in the fragments of coronary arteries in 23% of 102 patients scheduled for CABG (14). In a study by Maass et al. (7) the presence of *ChP* was detected in 30% of the investigated atheromatous plaques. The review of the investigations assessing the occurrence of this pathogen with the use of PCR prepared by Maraha et al. (15) showed that *ChP* occurred, on average, in 31% of the investigated samples. In the meta-analysis by Ieven et al. (12) assessing 3,551 samples analyzed by PCR, 2,688 samples were *ChP*-negative and only 863 *ChP*-positive. On the other hand, in the meta-analysis performed by Kalayoglu et al. (16), the pathogen occurred in 46% of 1,852 samples of arteries with atheromatous changes.

In the current investigation, the analyzed group with a high percentage of *ChP* occurrence was constituted only by patients with angiographcally confirmed arteriosclerosis. Therefore a relationship may be suspected between *ChP* and arteriosclerosis. Some authors (e.g. Banach et al.) (17) draw far-reaching conclusions and are of the opinion that detection of *ChP* or its antigens in the arterial wall should be the basis for connecting this pathogen with the development of arteriosclerosis.

The presence of *ChP* in peripheral blood varies considerably, depending on reports (10, 12, 18-20). A high percentage of *ChP* occurrence in the presented results may be related to the fact that patients with confirmed multivessel CAD were enrolled in the study, which may be connected with a higher prevalence of the pathogen. Based on the current analyses performed by other authors (10, 21), the relationships between *ChP* in arteriosclerotic plaques and *ChP* located in PBMCs are not completely clear. In the present investigation neither quantitative nor qualitative correlation was observed between the occurrence of *ChP* in peripheral blood and in aortic samples.

Some authors suggest that *ChP* assessment in peripheral blood may be useful for the detection of the pathogen in arterial walls (34). However, it was not confirmed in the current study. On the other hand, in our study a higher amount of *ChP* genetic material was detected in the tissue as compared to blood samples. A higher number of *ChP* in the tissue in a group of patients without evidence of infection in blood may be explained by the course of the infection (10, 13).

In patients with *ChP* in ascending aorta samples, the presence of diabetes and elevated cholesterol concentration was more frequently observed. However, the results for triglycerides were at the limit of statistical significance. The above observation is consistent with the study results of many authors (14, 22). A higher percentage of infections in patients with diabetes may be explained by lowered cellular immunity in this group of patients, and thus a higher susceptibility to bacterial infections. The presented result is consistent with the study by Mendis et al. (23).

Mechanisms and causes of CAD development have remained unrecognized despite many years of trials. It seems that the role of *ChP* and other pathogens has not been determined and it cannot be simply eliminated from the list of potential causes of arteriosclerosis. In the context of the presented study results, further investigation assessing the relation of pathogens with the development of CAD appears to be reasonable.

REFERENCES

1. Hunik MG, Goldman L, Tosteson AN, Mittleman MA, Goldman PA, Williams LW, Tsevat J, Weinstein MC. The recent decline in mortality from coronary heart disease, 1980-1990: the effect of secular trends in risk factors and treatment. JAMA 1997; 277:535-42.
2. Ross R. Atherosclerosis – an inflammatory disease. N Engl J Med 1999; 340:115-26.
3. Chandra HR, Choudhary N, O'Neill C, Boura J, Timmis GC, O'Neill WW. Chlamydia pneumoniae exposure and inflammatory markers in acute coronary syndrome (CIMACS). Am J Cardiol 2001; 88:214-18.
4. Horvath R, Cerny J, Bendik JJr, Hökl J, Jelínková I, Benedík J. The possible role of human

cytomegalovirus in the origin of atherosclerosis. J Clin Virol 2000; 16:17-24.
5. Zhu J, Nieto FJ, Horne BD, Anderson JL, Muhlestein JB, Epstein SE. Prospective study of pathogen burden and risk of myocardial infarction or death. Circulation 2001; 103(1):45-51.
6. Hsich E, Zhou YF, Paigen B, Johnson TM, Burnett MS, Epstein SE. Cytomegalovirus infection increases development of atherosclerosis in apolipoprotein-E knockout mice. Atherosclerosis 2001; 156(1):23-28.
7. Maass M, Bartels C, Engel PM, Mamat U, Sievers HH. Endovascular presence of viable Chlamydia pneumoniae is a common phenomenon in coronary artery disease. JACC 1998; 31:827-32.
8. Danesh J, Collins R, Peto R. Chronic infections and coronary heart disease: is there a link? Lancet 1997; 350:430-36.
9. Anderson JL, Muhlestein JB, Carlquist J. Randomized secondary prevention trial of azithromycin in patients with coronary artery disease and serological evidence for Chlamydia pneumoniae infection. Circulation 1999; 99:1540-47.
10. Berger M, Schröder B, Daeschlein G, Schneider W, Busjahn A, Buchwalow I, Luft FC, Haller H. Chlamydia pneumoniae DNA in non-coronary atherosclerotic plaques and circulating leukocytes. J Lab Clin Med 2000; 136(3):194-200.
11. Kuo C, Shor A, Campbell LA, Fukushi H, Patton DL, Grayston JT. Demonstration of Chlamydia pneumoniae in atherosclerotic lesions of coronary arteries. J Infect Dis 1993; 167 (4):841-49.
12. Ieven MM, Hoymans VY. Involvement of Chlamydia pneumoniae in atherosclerosis: more evidence for lack of evidence. J Clin Microbiol 2005; 43(1):19-24.
13. Berg HF, Maraha B, Zee A, Gielis SK, Roholl PJ, Scheffer GJ, Peeters MF, Kluytmans JA. Effect of clarithromycin treatment on Chlamydia pneumoniae in vascular tissue of patients with coronary artery disease: a randomized, double-blind, placebo-controlled trial. J Clin Microbiol 2005; 43(3):1325-29.
14. Hedayat DK, Jebeli M, Mendegar MH, et al. The association between Chlamydia pneumoniae DNA in atherosclerotic plaque and major risk factors in patients undergoing coronary artery bypass grafting. Kardiol Pol 2009; 67(9):981-86.
15. Maraha BH, Berg GJ, Scheffer A, van der Zee A, Bergmans A, Miseré J, Kluytmans J, Peeters M. Correlation between detection methods of Chlamydia pneumoniae in atherosclerotic and non-atherosclerotic tissues. Diagn Microbiol Infect Dis 2001; 39:139-43.
16. Kalayoglu MV, Libby P, Byrne GI. Chlamydia pneumoniae as an emerging risk factor in cardiovascular disease. JAMA 2002; 288:2724-31.
17. Banach M, Markuszewski L, Zasłonka J, Grzegorczyk J, Okonski P, Jegier B. Rola zakażenia w patogenezie miażdżycy. Przegl Epidemiol 2004; 58:671-76.
18. Smieja S, Mahoney J, Petrich A, Boman J, Chernesky M. Association of circulating Chlamydia pneumoniae DNA with cardiovascular disease: a systematic review. BMC Infect Dis 2002; 2:21.
19. Cannon CP, Braunwald E, McCabe C, et al. Antibiotic treatment of Chlamydia pneumoniae after acute coronary syndrome. N Engl J Med 2005; 352:1646-54.
20. Wang SS, Tondella ML, Bajpai A, et al. Circulating Chlamydia pneumoniae DNA and advanced coronary artery disease. Int J Cardiol 2007; 118(2):215-19.
21. Blasi F, Boman J, Esposito G, et al. Chlamydia pneumoniae DNA detection in peripheral blood mononuclear cells is predictive of vascular Infection. J Infect Dis 1999; 180(6):2074-76.
22. Kaperonis EA, Liapis CD, Kakisis JD, Perrea D, Kostakis AG, Karayannakos PE. The association of carotid plaque inflammation and Chlamydia pneumoniae infection with cerebrovascular symptomatology. J Vasc Surg 2006; 44(6):1198-204.
23. Mendis S, Arseculerante YM, Withana N, Samitha S. Chlamydia pneumoniae infection and its association with coronary heart disease and cardiovascular risk factors in a sample South Asian population. Int J Cardiol 2001; 79(2-3):191-96.

LETTER TO THE EDITOR

ARTICULAR CAPSULE REPAIR IN INITIAL ARTIFICIAL HIP REPLACEMENT VIA ANTEROLATERAL APPROACH TO THE HIP JOINT

B.L. ZHANG, F. WANG, M.B. TIAN, W.L. YIN, X.Y. YOU, D. LI, L.G. MA and L.Q. XING

Department of Orthopedics, People's Hospital of Zhengzhou, Zhengzhou, Henan, China

Received August 14, 2015 – Accepted March 29, 2016

This study was carried out to explore articular capsule repair in first artificial hip replacement (AHR) via anterolateral approach and its influence on postoperative dislocation. A total of 292 patients who received AHR via anterolateral approach and had the articular capsule repaired in People's Hospital of Zhengzhou (Henan, China) from February 2008 to February 2014 were selected and divided into total hip replacement (THR) group (group A1) and artificial femoral head replacement (AFHR) group (group A2). Five hundred and five cases in the control group treated using the same approach but receiving no articular capsule repair were divided into THR group (group B1) and AFHR group (group B2). Condition of postoperative dislocation was compared between the two groups. All cases were followed up for 6 months to 5 years (average: 3.75 years); it was noted that the difference in average age, gender, disease constitution and follow-up time in the two groups was not significant (P>0.05). Moreover, groups A1 and B1 were found with 1 case of early hip joint dislocation (0.73%) and 13 cases of hip joint dislocation (5.24%) respectively post-operatively, and the comparison between the two groups was statistically significant (P<0.05). One case of hip joint dislocation (0.65%) was found in group A2 and 5 cases (1.95%) in group B2 in early post operation and the difference between two groups had no statistical significance (P>0.05). Neither the repair group nor the control group developed late-onset dislocation after the operation. Thus, we can state that articular capsule repair is feasible during the first AHR via anterolateral approach, which decreases the occurrence of early hip joint dislocation after operation and proves that repairing articular capsule during AFHR via anterolateral approach is unnecessary.

Artificial hip replacement (AHR) is one of the most widely used operations in orthopedics as artificial joint material and operation techniques develop continuously (1). AHR, which is divided into total hip replacement (THR), artificial femoral head replacement (AFHR), has various postoperative complications, and hip joint dislocation as one of the serious complications is only second to aseptic loosening of artificial joint (2). It is reported that the incidence of prosthetic dislocation after AHR operation reaches 3.2% to 6.5% in the first replacement and nearly doubles during revision (3). One in three patients suffering from re-dislocation undergoes revision surgery and only 60% of these become stable after surgery (4).

Artificial prosthesis dislocation occurs most frequently when posterolateral approach is widely applied. Hence, Chinese and western scholars (5,

Key words: artificial hip replacement, articular capsule repair, dislocation, anterolateral approach

Mailing address:
Dr Baolong Zhang,
No.33, Yellow River Road, Department of Orthopedics,
People's Hospital of Zhengzhou,
Zhengzhou, Henan, 450000, China
e-mail: zhangbaolong3768@163.com

0393-974X (2016)

6) focus on the correlation between the repair of the rear joint capsule and extorter as well as artificial prosthesis dislocation. Blom et al. (7) reported that the first THR dislocation rate was 2.81% and Parvizi et al. (8) considered it between 0.3% and 10.0%. According to studies, artificial prosthesis anterior dislocation is a form of complication rarely connected to the repair of anterior soft tissues (9). This study analyzed patients who received AHR via anterolateral approach in People's Hospital of Zhengzhou to evaluate the effect of articular capsule repair for the prevention of postoperative joint dislocation.

MATERIALS AND METHODS

Research subjects

Patients undergoing AHR via anterolateral approach in People's Hospital of Zhengzhou (Henan, China) from February 2008 to February 2014, were divided into repair group (292 patients) and control group (505 patients) based on whether their articular capsules were repaired during surgery. All research projects were approved by the medical ethics committee of People's Hospital of Zhengzhou and verified by pathologists. All patients signed informed consent.

According to the surgery methods used, the repair group was subdivided into THR group (group A1, 137 cases) and AFHR group (group A2, 155 cases). According to preoperative hip joint lesion in group A1, 103 cases developed fresh femoral neck fracture, 6 cases obsolete femoral neck fracture, 20 cases femoral head necrosis, 5 cases hip joint osteoarthritis and 3 cases congenital hip dysplasia. Only one patient received bilateral artificial joint replacement using Pinnacle and Corail AMT HA uncemented biological hip joint prosthesis (De Puy Company, Shanghai, China). In group A2, 120 cases developed fresh femoral neck fracture, 5 cases due to obsolete femoral neck fracture, 28 cases due to femoral head necrosis and 2 cases due to hip joint osteoarthritis. Only one patient was treated with bilateral artificial joint replacement using Corail AMT uncemented biological bipolar partial hip joint prosthesis (De Puy Company, Shanghai, China).

The control group was also divided into THR control group (group B1, 248 cases) and AFHR control group (group B2, 257 cases). According to preoperative hip joint lesion in group B1, 183 cases developed fresh femoral neck fracture, 6 cases due to obsolete femoral neck fracture, 48 cases due to femoral head necrosis, 6 cases due to hip joint osteoarthritis and 5 cases due to congenital hip dysplasia. Two patients received bilateral artificial joint replacement using Pinnacle and Corail AMT HA uncemented biological hip joint prosthesis. In group B2, 206 cases developed fresh femoral neck fracture, 9 cases due to obsolete femoral neck fracture, 36 cases due to femoral head necrosis and 6 cases due to hip joint osteoarthritis. Two patients were treated with bilateral artificial joint replacement using Corail AMT uncemented biological bipolar partial hip joint prosthesis.

Inclusion criteria

Patients were included if they had avascular necrosis of the femoral head (ANFH) and acetabulum in good condition, if they had unilateral ANFH or developed Ficat III and IV stage disease in affected hip and Ficat III lower stage in lateral hip, if they had no surgical contraindication in preoperative examination and if they agreed to a one year follow up.

Exclusion criteria

Patients were excluded if there were contraindications to surgery and had heart, lung or other malfunctions, if they could not tolerate surgery or if they suffered from unstable diseases that might significantly increase the risk of death.

Preoperative preparation

Medical history was noted and patients received relevant preoperative routine inspections as well as hip joint imaging examination. Patients with other underlying diseases received relevant processing and related departments assisted in the diagnosis and treatment if necessary.

Surgical method

Patients were generally narcotized by static absorption and anterior and posterior pelvises were fixed with holders when patients were in lateral position. Surgery was carried out with anterolateral approach (Watson-Jones incision). Hip joint was rotated outward

to tense the front joint capsule.

The front joint capsule was cut along the direction of the femoral neck and then horizontally from the superior border of acetabulum and basilar part of femoral neck to make an "I" shaped incision and the joint capsule was pulled open from both sides. Hip joint was rotated outwardly and slightly bent, femoral neck was cut with pendulum saw at about 1.5 cm on the top of the lower trochanter. Femoral head was then taken out by screwing into a device and stubs of round ligament inside of acetabulum were wiped.

Three Hohmann wire retractors were put in the acetabulum peripheral bone to fully display the whole acetabulum. The affected limb was abducted, drooped slightly and rotated outwards to drive the femur near-end up and marrow was expanded gradually with intramedullary broacher under a direct vision. Both repair group and control group were required to test the stability of hip joint which needed to remain stable when being rotated outwards to 40 degrees or bent to 90 degrees and rotated inwards to 40 degrees.

Joint capsule petal was circled to the front femoral neck and sutured with 7# stitches with an appropriate overlap. Incisal edge of joint capsule was sutured into an "8" with absorbable thread on the cancellous bone surface and its tendinous tissues, 2 to 3 stitches in general and about 3 to 4 cm long. Negative pressure drainage was placed to repair and stitch gluteus minimus, gluteus medius, vastus lateralis muscle as well as tensor fasciae latae. Finally, incisions were closed layer by layer.

Postoperative treatment

Patients in the two groups were treated with routine oxygen inhalation and monitored for a 24 h period after surgery to observe vital signs, sensorimotor of affected limb and changes of peripheral blood cycle. They were given second-generation cephalosporins for 48 to 72 h, low-molecular-weight heparin sodium (2500 IU) was injected subcutaneously 6 h after operation and 5000 IU from the next day, once a day for 7 to 14 days. On the 2nd day after surgery, routine blood, heart, liver and kidney electrolyte, together with brain natriuretic peptide (BNP) were reviewed. On the 2nd and 5th day, hip plain film was reviewed and the location of artificial joint was observed. Volume and color of drainage liquid were observed, and drainage tube was removed 24 to 48 h later. The condition of incision exudation was also closely observed and was cleaned every one to three days to keep wound dressing clean and dry. Stitches were generally removed after 14 days.

Follow-up and curative effect evaluations

All patients were followed up periodically at 1, 3, 6 and months after discharge. Harris hip function and pain score as well as pelvis normotopia and lateral hip X-ray examinations were performed to verify whether the prosthesis had loosened or dislocated.

Statistical methods

All data were analyzed statistically with SPSS19.0 software, measurement data were expressed as mean±SD and difference between groups was compared using *t*-test. Difference of enumeration data among groups adopted *chi*-square test for comparison and the difference was considered to be statistically significant if $p<0.05$.

RESULTS

Analysis of general material

All cases were followed up for 6 m to 5 years and no statistically significant difference was found in age, gender and disease constitution between groups ($p>0.05$). Therefore, they were comparable (Table I).

Comparison of early dislocation rate of patients in groups A1 and A2

Group A1 had one case of hip dislocation (0.73%) 6 months after surgery. This patient had muscle weakness in the lower affected limb, obviously atrophied, loosened muscles around hip joint and poor ability to walk as he suffered from multiple lacunar infarctions before surgery. Joint was dislocated during functional exercise. Large-area cerebral infarction then occurred, as well as semi paralysis on the affected side and family members gave up on continuous treatment. Thirteen cases of hip dislocation (5.24%) were also found in the B1 group and the differences of early dislocation rate between two groups had statistical significance (Table II).

Table I. *Comparison of difference in average age, gender and disease constitution in repair and control group.*

Factors		Group A1	Group B1	P	Group A2	Group B2	P
Gender	Male	65	121	0.645	74	123	0.724
	Female	72	127		81	134	
Age (year)		63.7±10.7	64.5±10.8	0.878	78.1±11.6	78.9±11.6	0.823
Pre-operative hip diagnosis	Femoral neck fracture	109	189	0.253	125	215	0.316
	Femur necrosis	20	48		28	36	
	Other diseases	8	11		2	6	

Table II. *Comparison of early dislocation rate in group A1 and A2.*

	Dislocation/case number	Normal/case number	Total/case number	Dislocation rate/%
Repair group (group A1)	1	136	137	0.73
Control group (group B1)	13	235	248	5.24
Total	14	371	385	3.64
	x^2=3.920		P<0.05	

Comparison of early dislocation rate of patients in group A2 and B2

Only one hip dislocation (0.65%) was discovered in group A2, 6 months after surgery. This patient had muscle weakness in the lower affected limb, obviously atrophied and loosened muscles around hip joint as he had cerebral infarction sequelae before surgery. After surgery, the anterior joint in anesthesia was dislocated.

Patients were restricted in their movements for 3 weeks and were able to go back to a normal routine 6 weeks after surgery.

Five cases of hip dislocation (1.95%) were found in the B2 group and the comparison of early dislocation rate between two groups were not statistically significant (Table III).

Analysis of typical cases

A male patient (case n. 1) was diagnosed at the age of 60 with left femoral neck fracture before operation (Fig. 1A). He then received left THR. Three days later, the prosthesis was in position

Table III. *Comparison of early dislocation rate in two groups.*

	Dislocation/case number	Normal/ case number	Total/ case number	Dislocation rate/%
Repair group (group A2)	1	154	155	0.65
Control group (group B2)	5	252	257	1.95
Total	6	406	412	1.46
	x^2=0.411		P<0.05	

Neither THR repair group nor ATHR control group were found with dislocation 6 months after operation.

(B), hip joint was dislocated due to improper body position in the process of postoperative functional recovery exercise (C). He was then treated with manual reposition immediately. After 3 weeks of skin traction, the image suggested that the prosthesis was in a good position (D).

A 70-year-old male patient (case n. 2) suffering from left femoral neck fracture (Fig. 2A) received left THR and joint capsule repair in January 2010. After surgery, the image indicated that the artificial joint was well located (B). AFHR was performed on the right side again in February 2013, but joint capsule was not repaired at that time. The postoperative image suggested that the prosthesis was in a good position (C).

DISCUSSION

Joint replacement has become an important method for the treatment of joint diseases in adults. Minimally invasive double incision technique has been used in other medical centers in America and has become increasingly popular worldwide since Berger et al (10, 11) finished the first THR operation in Chicago in 2001. To date, the most commonly used posterolateral approach (Moor incision) causes high dislocation rate, especially posterior dislocation. The Anterolateral approach, which features a low infection rate, little influence on hip joint function and small damage on joint stability, is often adopted. However, dislocation rate exists to some extent; anterior dislocation accounts for a relatively high proportion. Through observing 1910 patients who underwent AHR operation, some scholars (12) found a high dislocation rate by posterolateral approach, accounting for about 5.8%, which was the double of the lateral and anterior approach. Iorio (13) and Ji (14) et al. discovered that by strengthening the soft joint tissue in AHR, it decreased dislocation rate significantly. Traditional THR can cause deep venous thrombosis in lower limbs, weaken muscle strength and lead to poor gait (15), therefore, THR surgery can cause extensive trauma, especially for patients over 60-years-old (16).

A significant difference was found in the dislocation between group A1 and B1, suggesting that the repair was feasible and effective (Table II, P<0.05). Intra-operative inspection results indicated that prior to stitching the joint capsule, femoral head prosthesis slid within the acetabulum lining when hip joint was outreached and gently rotated outwards. Femoral head slid to the edge of the lining when it was rotated outwards to about 60 degrees, causing dislocation. In biomechanics, the strength of a repaired joint capsule is not strong enough to prevent hip joint dislocation, while stitched joint capsule can prevent the strength of femoral head prosthesis sliding. This proves that the repair method applied in this study is capable of reconstructing the integrity of joint capsule, increasing the immediate stability

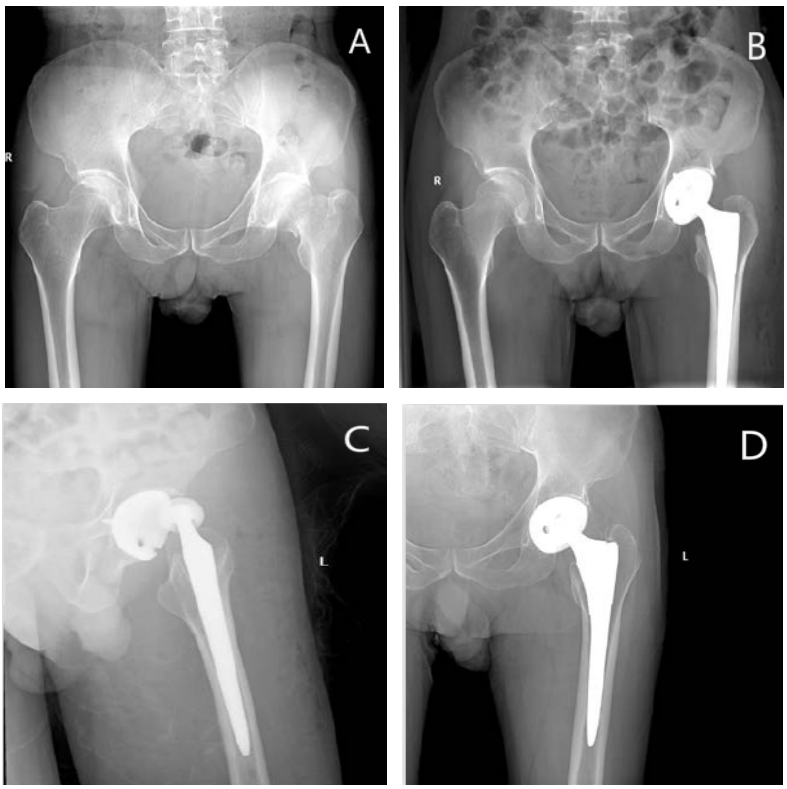

Fig. 1. *Disease condition of case n. 1 before and after operation.*

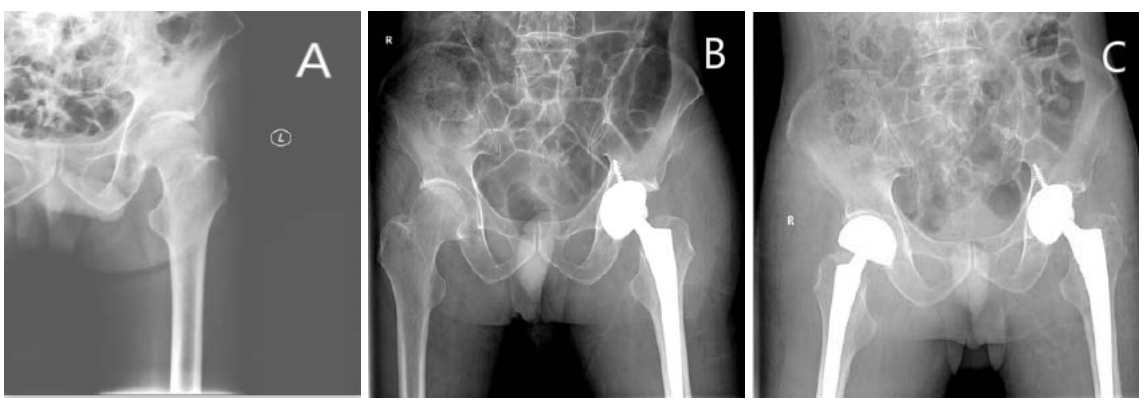

Fig. 2. *Disease condition of case n. 2 before and after operation.*

of joint prosthesis and decreasing the occurrence of early dislocation effectively.

Bipolar artificial femoral head prosthesis was used in AFHR in this study and its inner joints played a leading role in hip joint motion, similar to total hip prosthesis movement. Acetabular head joint (external joint) is involved only when the hip joint moves at a wide angle, thereby extending the range of normal movement of the hip joint after prosthesis replacement and reducing the risk of dislocation after surgery, delaying osseous acetabulum abrasion, prolonging the life of the prosthesis and enhancing the shock resistance effect of the hip joint.

These aspects make bipolar prosthesis better than monopole prosthesis. We also observed that bipolar femoral head prosthesis, matched with osseous

acetabulum, could form a certain degree of negative pressure, which made prosthesis dislocate through additional twisting force. The negative pressure increased the initial resistance of femoral head sliding out of acetabulum. In a sense, this negative pressure could replace stitched joint capsule in order to prevent the initial sliding effect of the femoral head as well as the occurrence of hip dislocation that was not caused by impact. This was consistent with our findings, and the comparison between group A2 and group B2 had no statistical significance (Table III, $P>0.05$). Therefore, bipolar artificial femoral head replacement had outstanding effects on aged patients who had sound acetabulum, did less activity and suffered from hip joint disease, but was of less significance in repairing hip joint during surgery.

In conclusion, the method of repairing articular capsule in AHR via the anterolateral approach is feasible, it features small incision, minimal trauma, fast recovery and satisfactory effects. This retrospective study is subject to restrictions, such as small sample size and errors caused by interference of other dislocation factors. The difference of long-term effect between the two groups cannot be confirmed due to lack of relevant research but further study will be carried out in the future.

REFERENCES

1. Drescher W, Pufe T, Smeets R, Eisenhart-Rothe RV, Jäger M, Tingart M. Avascular Necrosis of the Hip Diagnosis and Treatment. Z Orthop Unfall 2011; 149(2):231-40.
2. DeWal H, Su E, Di Cesare PE. Instability following total hip arthroplasty. Am J Orthop 2003; 32(8):377-82.
3. Demos HA, Rorabeck CH, Bourne RB, MacDonald SJ, McCalden RW. Instability in primary total hip arthroplasty with the direct lateral approach. Clin Orthop Relat Res 2001; 393:168-80.
4. SP White, Blom AW, Lee M, Smith EJ. The crescent sign: dissociation of the polyethylene liner from a modular acetabular component in total hip arthroplasty. Skeletal Radiol 2005; 34(10):620-4.
5. Sioen W, Simon J P, Labey L, et al. Posterior transosseous capsulotendinous repair in total hip arthroplasty: a cadaver study. J Bone Joint Surg Am 2002; 84-(10):1793-8.
6. James A, Browne MD, Mark W, et al. A simple soft tissue only repair of the capsule and external rotators in posterior-approach THA. Clin Orthop 2012; 470:511-5.
7. Blom AW, Rogers M, Taylor AH, et al. Dislocation following total hip replacement: the avon orthopaedic centre experience. Ann R Coll Surg Engl 2008; 90(8):658-62.
8. Parvizi J, Picinic E, Sharkey PF. Revision total hip arthroplasty for instability: surgical techniques and principles. J Bone Joint Surg Am 2008; 90(5):1134-42.
9. Masonis JL, Boume RB. Surgical approach, abductor function, and total hip arthroplasty dislocation. Chin Orthop 2002; 405:45-53.
10. Berger R. Grand rounds presentation. University of Pittsburgh, Pittsburgh, 2001.
11. Berger RA. The technique of minimally invasive total hip arthroplasty using the two-incision approach. Instr Course Lect 2004; 53:149-55.
12. Dudda M, Gueleryuez A, Gautier E, et al. Risk Factors for Early Dislocation after Total Hip Arthroplasty: a Matched Case-control Study. J Orthop Surg 2010; 18 (2):179-83.
13. Iorio R, Specht LM, Healy WL, et al. The Effect of EPSTR and Minimal Incision Surgery on Dislocation after THA. Clin Orthop Relat Res 2006; 447:39-42.
14. Ji HM, Kim KC, Lee YK, et al. Dislocation after Total Hip Arthroplasty: a Randomized Clinical Trial of a Posterior Approach and Modified Lateral Approach. J Arthroplas 2012; 3:378-85.
15. Waldman BJ. Advancements in Minimally Invasive Total Hip Arthroplasty. Orthopedics 2003; 26(8):833-6.
16. Bascarevic Z, Radojevic BB, Timotijevic SS, et al. Minimal Incision Total Hip Joint Arthroplasty. Acta Chir Iugosl 2006; 53(4):53-6.

LETTER TO THE EDITOR

PSYCHOLOGICAL STRESS MODERATES THE RELATIONSHIP BETWEEN RUNNING VOLUME AND CD4+ T CELL SUBPOPULATIONS

K.E. REHM[1,2], I. SUNESARA[1,2,3], M.T. TULL[1,4] and G.D. MARSHALL[1,2]

[1]Laboratory of Behavioral Immunology Research, Division of Clinical Immunology and Allergy, University of Mississippi Medical Center, Jackson, MS, USA; [2]Department of Medicine, University of Mississippi Medical Center, Jackson, MS, USA; [3]Center of Biostatistics and Bioinformatics, University of Mississippi Medical Center, Jackson, MS, USA; [4]Division of Psychology, Department of Psychiatry and Human Behavior, University of Mississippi Medical Center, Jackson, MS, USA

Received July 21, 2015 - Accepted March 2, 2016

Endurance-based exercise training can lead to alterations in components of the immune system, but it is unknown how psychological stress (another potent immunomodulator) may impact these changes. The purpose of this study was to determine the moderating role of psychological stress on exercise-induced immune changes. Twenty-nine recreational runners were recruited for this study four weeks before completing a marathon. Each subject reported: weekly training volume (miles/wk) for the week prior to the study visit; completed the Perceived Stress Scale (PSS), the state version of the State-Trait Anxiety Inventory (STAI) and the Penn State Worry Questionnaire (PSWQ); and donated blood for assessment of CD4+ T cell subpopulations and mitogen-induced cytokine production. Participants ran an average of 30 (±13.4) miles (1 mile=1.6 km) per week. Average values (SD) for immune biomarkers were: regulatory T cells (Treg), 3.2% (±1.2%); type 1 regulatory cells (Tr1), 27.1% (±8.3%); T helper 3 (Th3), 1.8% (±0.7%); interferon gamma (IFNγ), 3.1 pg/ml (±1.0); interleukin (IL)-4, 1.4 pg/ml (±1.1); IFNγ/IL-4, 8.6 (±1.2); IL-10, 512 pg/ml (±288). There was a significant relationship between running volume and both Treg cell numbers (slope of the regression line (β)=0.05, p<0.001) and IL-10 production (β=-10.6, p=0.002), and there was a trending relationship between running volume and Tr1 cell numbers (β=-0.2%, p=0.064). Perceived stress was a trending moderator of the running volume-Treg relationship, whereas worry was a significant moderator of the running volume-IFNγ and running volume-IFNγ/IL-4 relationships. These data indicate that various forms of psychological stress can impact endurance exercise-based changes in certain immune biomarkers. These changes may reflect an increased susceptibility to clinical risks in some individuals.

Endurance-based exercise training can have a significant impact on immunity (1), including decreased lymphocyte proliferation (2), increased antigen-stimulated interleukin (IL)-10 production (3), and decreased salivary IgA production (4). These changes may increase the risk for clinical disease, such as upper respiratory infections and/or exacerbations of existing inflammatory-based diseases such as allergic rhinitis (5).

We recently reported that there were significant changes to T helper 1 (Th1), Th2, and IL10+ cell populations and mitogen-induced production of

Key words: immune, cytokine, stress, anxiety, worry, exercise

Mailing address:
Kristina E. Rehm, Ph.D.,
Division of Clinical Immunology and Allergy,
Department of Medicine, University of Mississippi Medical Center,
2500 North State Street - N416, Jackson, MS 39216, USA
Tel.: +1 601 815 5527 - Fax: +1 601 815 4770
e-mail: krehm@umc.edu

0393-974X (2016)

interferon (IFN)-γ, IL-4, IL-10, and the IFNγ/IL-4 ratio from peripheral blood mononuclear cells (PBMC) obtained during the final four weeks of marathon training in a group of recreational runners and that some of these immune changes were enhanced by higher levels of psychological stress (6). Interestingly, the relationship between stress and immune biomarkers (specifically regulatory T cells (Treg), IL-4 and IL-10 production, and the IFNγ/IL-4 ratio) was significantly different four weeks before the marathon when participants were running significantly higher mileage compared to 24 hours before the marathon when participants were at an overall lower weekly mileage. These data suggested that levels of both psychological and physical stress (such as exercise) could play a major (albeit variable) role in individual immune balance. There are relatively little data available about how existing psychological stress levels may influence, or moderate, exercise-induced immune changes. The purpose of this study was to examine the relationship between running volume and immune biomarkers in a group of recreational runners and then determine whether psychological stress operated as a moderator in these immune relationships.

MATERIALS AND METHODS

Participants

Twenty nine healthy recreational runners from the Jackson, MS, metropolitan area were recruited for this study. Data were obtained from 19 participants that were reported in a previous study (6) plus an additional 10 participants subsequently recruited training in the same local environment for a different marathon. All recruited participants were recreational runners training for a marathon that was 4 weeks away from the study visit. Participants were recruited after obtaining written informed consent according to a University of Mississippi Medical Center IRB-approved protocol and were excluded for any past medical history of smoking, psychiatric illnesses, cardiovascular diseases, autoimmune diseases, or recent medical use of systemic glucocorticoids, catecholamines, and/or adrenergic antagonists. Study visits were conducted during the same four span of the day (7:30-11:30AM) to control for diurnal variations in immune measures.

Blood collection and PBMC isolation

Venous blood was collected into heparinized tubes for PBMC isolation. PBMC were isolated using a Ficoll-Hypaque gradient as previously described (6). Briefly, cells were centrifuged at 650 x *g* for 30 min, washed twice in Hank's Balanced Salt Solution (HBSS), and then resuspended in 1 ml HBSS. Cell counts were obtained using a Scepter Handheld Automated Cell Counter (Millipore).

Flow cytometry

T cell populations in PBMC were analyzed by flow cytometry according to previously described methods (6). Briefly, 1 x 10^6 PBMC were incubated with the manufacturer's recommended amount of surface antibodies for cluster of differentiation 4-(CD4)-ECD (Beckman Coulter; Miami, FL) and CD25-PECy7 (eBioscience; San Diego, CA). Cells were then washed, fixed with 0.5% paraformaldehyde (PFA) for 10 min at room temperature (RT), followed by an additional wash. Fixed cells were then permeabilized with 0.5% saponin in phosphate buffered saline (PBS) and incubated with antibodies for the following intracellular antigens: FoxP3-PECy5 (eBioscience), IL-10-FITC (R&D Systems; Minneapolis, MN), or transforming growth factor beta (TGFβ)-PE (R&D Systems). Appropriate isotype controls were used to define positive and negative staining during the initial set-up of the T cell profiles of interest. Gates for the isotype controls were set at 10%. Forward and side scatter were used to define the lymphocyte population. Data (at least 150,000 events) were collected and analyzed using the Beckman Coulter Cytomics FC500 flow cytometer. Cell populations were defined as follows, Treg: $CD4^+CD25^{hi}FoxP3^+$; Tr1: $CD4^+IL\text{-}10^+$; Th3: $CD4^+TGF\beta^+$. For all cell populations, we are reporting percentage of total lymphocytes.

Mitogen cultures and ELISA

1 x 10^6 PBMC were cultured in 1 ml cRPMI media and stimulated with 10 μg/ml phytohemagglutinin (PHA; Sigma) and 1 ng/ml phorbol myristate acetate (PMA; Sigma) for 72 h as previously described (6). Supernatants were harvested and stored at -80°C. The amount of IFNγ, IL-4, and IL-10 in the supernatant was determined using commercially available Ready-Set-Go! ELISA kits (eBioscience) per the manufacturer's

instructions. ELISAs were prepared with a standard curve and were read on a Coulter Microplate Reader at 450 nm. Coefficient of variation for the duplicate ELISA samples was less than 20%. The lower limits of detection for IFNγ, IL-4, and IL-10 were 4, 2, and 2 pg/ml, respectively. Concentrations were calculated from the standard curve using the SoftMax Pro 5.4 software. IFNγ/IL-4 ratio was determined as an indicator of the Th1/Th2 cytokine shift.

Measurement of psychological stress

To measure levels of perceived stress, state anxiety, and worry, participants completed a battery of questionnaires at each visit. The Perceived Stress Scale (PSS) was used to measure perception of acute stress over the last month and has a range of 0-40 (7). PSS is not a diagnostic instrument and has no standards or cutoff score. Instead, researchers are instructed to make comparisons within their own sample (7). The State Trait Anxiety Inventory (STAI) was used to assess the severity of acute (i.e., at this moment) anxiety and has a range of 20-80 (8). A score of 39-40 has been suggested to be indicative of clinical symptoms (9). The Penn State Worry Questionnaire (PSWQ) was used to measure tendencies to experience excessive and uncontrollable worry and has a range of 16-80 (10). The PSWQ has a cutoff score of 50 that is indicative of generalized anxiety disorder (11). All measures have extensive support for their validity and reliability (12).

Training volume

To measure training volume, each participant was asked to record the number of miles that they ran for the seven days leading up to the study visit (1 mile = 1.6 km). The average number of miles ran in that time period was used as the running volume (13-15).

Statistical analyses

Descriptive statistics were computed as mean (standard deviation) and frequencies (percentages) for continuous and categorical variables respectively (Table I). The relationship between outcomes of biomarkers and predictors of running volume, PSS, STAI and PSWQ was evaluated using simple linear regression (Table II). Median split was used to dichotomize PSS, STAI and PSWQ for better interpretability of the results (16). Participant's characteristics (Table III) were compared using Fisher exact test and Mann Whitney U test where appropriate. Linear regression was used to test the main effects and interaction between the outcomes of biomarkers and running volume for high-low psychological stress (PSS, STAI and PSWQ). Huber-White robust standard errors were computed. Slopes of the regression lines (β), difference of slopes and 95% confidence intervals are reported (Table IV). Analyses were performed after log transformations were applied to skewed data (Th3, IFNγ, IL-4, and IFNγ/IL-4) based on exploratory data analyses. Normality was assessed using visual inspection of q-q plots. A p-value of <0.05 was considered statistically significant. Statistical analysis was performed using STATA (version 13; StataCorp, College Station, TX, USA).

RESULTS

Participant characteristics

The characteristics of the study population are described in Table I. Participants were predominantly white (97%) and male (62%). The average age was 37.6 (±9.3) years and the average BMI was 23.1 (±2.1) kg/m^2. Participants ran an average of 29.8 (±13.4) miles per week. Average values (SD) for the immune biomarkers were: Treg, 3.2% (±1.2%); Tr1, 27.1% (±8.3%); Th3, 1.8% (±0.7%); IFNγ, 3.1 pg/ml (±1.0); IL-4, 1.4 pg/ml (±1.1); IFNγ/IL-4, 8.6 (±1.2); IL-10, 512 pg/ml (±289).

Correlation of running volume with immune biomarkers

There was a significant relationship between running volume and several of the immune biomarkers measured (Table II), including the percentage of peripheral Treg cells ($p<0.001$) and IL-10 secretion from mitogen-stimulated PBMC ($p=0.002$). In addition, there was a trending relationship between running volume and the percentage of Tr1 ($CD4^+IL\text{-}10^+$) cells ($p=0.064$). The percentage of peripheral Treg cells increased by 0.05% ($p<0.001$) while IL-10 production from mitogen-stimulated PBMC decreased by 10.6 pg/ml ($p=0.002$) for every one mile increase in weekly running volume. In addition, the percentage of Tr1 cells had a tendency to decrease by 0.2% ($p=0.064$) for every one mile increase in weekly running

Table I. *Participant characteristics.*

Characteristics	Total
Age	37.62 ±9.28
Gender	
Female	11 (38%)
Male	18 (62%)
Race	
Non White	1 (3%)
White	28 (97%)
BMI	23.06 ±2.15
Running Volume	29.8 ±13.4
PSS	32.8 ±13.3
STAIS	40.6 ±16.6
PSWQ	29.83 ±13.39
Treg: CD4+CD25hiFoxP3+, %	3.23 ±1.23
Tr1 cells: CD4+IL-10+, %	27.12 ±8.33
Th3: CD4+TGFß+, %[1]	1.75 ±0.73
sIFNγ (×1,000), pg/ml[1]	3.05 ±1.03
sIL-4, pg/ml[1]	1.35 ±1.13
sIFNγ/IL-4 ratio[1]	8.61 ±1.24
sIL-10, pg/ml	512.4 ±288.7

Footnote: Mean and standard deviations for age, BMI, running volume, stress measures, and immune biomarkers are reported
[1] Log transformed

volume. There were no significant relationships between running volume and any of the remaining immune biomarkers (Th3 (CD4+TGFβ+), IFNγ, IL-4, and IFNγ/IL-4).

Stress levels and immune biomarkers

To determine whether stress levels impacted immune biomarkers in this group of recreational marathoners, we performed a median split and grouped individuals into LOW and HIGH groups on the basis of scores on the PSS (perceived stress), STAI (state anxiety), and PSWQ (worry) (Table III). There were no significant differences in any of the demographic (gender, race, and age) or anthropometric (BMI) variables or in the weekly running volume (miles/wk) when comparing the LOW and HIGH PSS, STAI, and PSWQ groups. For the immune biomarkers, the HIGH PSWQ group had significantly greater levels of IL-10 production from mitogen-stimulated PBMC compared to the LOW PSWQ group (LOW, 351 pg/ml (±191) vs. HIGH, 644 pg/ml (±292); p=0.005). No other immune measures were significantly different between the LOW and HIGH PSS, STAI, or PSWQ groups.

Stress levels moderate the relationship between running volume and immune biomarkers

PSS level had a trending effect on the relationship between Treg and running volume (p=0.059) (Table IV). For the LOW PSS group, there was a significant positive relationship between running volume and Treg levels - Treg increased by 0.07% for every one mile increase in running volume (p<0.001). For the HIGH PSS group, there was only a trending positive relationship between running volume and Treg levels - Treg increased by only 0.03% for every one

Table II. *Relationship of running volume and biomarkers.*

Biomarkers	Running Volume (β, p value 95% CI)
Treg: CD4+CD25hiFoxP3+, %	0.05 p<0.001 (0.03,0.08)
Tr1 cells: CD4+IL-10+, %	-0.20 p=0.064 (-0.41,0.01)
Th3: CD4+TGFß+, %[1]	-0.01 p=0.14 (-0.03,0.00)
IFNγ (×1,000), pg/ml[1]	0.00 p=0.85 (-0.03,0.03)
IL-4, pg/ml[1]	0.00 p=0.98 (-0.02,0.02)
IFNγ/IL4 ratio[1]	0.00 p=0.88 (-0.03,0.03)
IL-10, pg/ml	-10.57 p=0.002 (-16.84,-4.31)

[1] *Log transformed; n=29*
CI=Confidence Interval

mile increase in running volume (p=0.076). Level of worry as assessed by the PSWQ had a significant effect on the relationship between running volume and both IFNγ production (p=0.008) and the IFNγ/IL-4 ratio (p=0.028) (Table IV). For the LOW PSWQ group, there was not a significant relationship between running volume and IFNγ production (β=-0.03 pg/ml; p=0.138). In contrast, there was a significant positive relationship between running volume and IFNγ in the HIGH PSWQ group. In this group, IFNγ production increased by 0.04 pg/ml for every one mile increase in weekly running volume (p=0.02). PSWQ level also had a significant effect on the relationship between running volume and the IFNγ/IL-4 ratio (p=0.028). For the LOW PSWQ group, there was a trending negative relationship between running volume and the IFNγ/IL-4 ratio (β=-0.03 pg/ml; p=0.066). Running volume was not significantly associated with the IFNγ/IL-4 ratio in the HIGH PSWQ group (β=0.04 pg/ml; p=0.130).

DISCUSSION

We measured the association between running volume and $CD4^+$ T cell subpopulations in recreational runners. We also examined whether psychological stress levels may have affected this association. Running volume was associated Treg, IL-10 and Tr1 levels. Perceived stress levels may moderate the relationship between running volume and Treg levels. Worry level moderated the relationship between both IFNγ and the IFNγ/IL-4 ratio. To our knowledge, this is the first study to show the moderating role of psychological stress on the relationship between weekly running volume and immune measures in a group of recreational runners.

Table III. *Stress levels and immune biomarkers.*

	PSS			STAIS			PSWQ		
Characteristics	Low (41%)	High (59%)	P-value	Low (48%)	High (52%)	P-value	Low (45%)	High (55%)	P-value
Age	35.75 ±8.14	38.94 ±10.03	0.45	37.79 ±9.26	37.47 ±9.61	0.97	38.62 ±8.91	36.81 ±9.77	0.57
Stress Measure	7.3 ±2.2	16.7 ±5.4	<0.001	24 ±5	43.2 ±12.5	<0.001	26 ±3.9	55 ±11.7	<0.001
Gender									
Female	5 (42%)	6 (35%)	0.99	5 (36%)	6 (40%)	0.99	3 (23%)	8 (50%)	0.25
Male	7 (58%)	11 (65%)		9 (64%)	9 (60%)		10 (77%)	8 (50%)	
Race									
Non White	0 (0%)	1 (6%)	0.99	0 (0%)	1 (7%)	0.99	0 (0%)	1 (6%)	0.99
White	12 (100%)	16 (94%)		14 (100%)	14 (93%)		13 (100%)	15 (94%)	
BMI	22.89 ±2.05	23.18 ±2.27	0.77	22.81 ±1.96	23.29 ±2.35	0.63	22.61 ±1.62	23.42 ±2.49	0.48
Running Volume	27.20 ±15.65	31.69 ±11.69	0.49	30.69 ±16.9	29.03 ±9.45	0.91	34.53 ±14.94	26.01 ±11.03	0.11
Treg: CD4+CD25hiFoxP3+, %	3.18 ±1.44	3.26 ±1.10	0.61	3.44 ±1.28	3.03 ±1.18	0.37	3.66 ±1.20	2.88 ±1.17	0.091
Tr1 cells: CD4+IL-10+, %	30.17 ±10.32	24.97 ±6.04	0.17	28.66 ±9.27	25.68 ±7.38	0.43	26.69 ±8.84	27.47 ±8.17	0.59
Th3: CD4+TGFß+, %[1]	1.77 ±0.75	1.73 ±0.73	0.91	1.86 ±0.74	1.65 ±0.73	0.68	1.89 ±0.90	1.63 ±0.55	0.68
IFNγ (×1,000), pg/ml[1]	2.71 ±1.09	3.29 ±0.95	0.14	2.75 ±1.08	3.33 ±0.93	0.14	3.07 ±1.00	3.03 ±1.08	0.99
IL-4, pg/ml[1]	1.28 ±0.84	1.41 ±1.32	0.79	1.15 ±0.70	1.55 ±1.41	0.51	1.21 ±0.76	1.47 ±1.37	0.83
IFNγ/IL-4 ratio[1]	8.34 ±1.03	8.79 ±1.37	0.27	8.52 ±1.11	8.69 ±1.39	0.49	8.77 ±0.88	8.47 ±1.49	0.59
IL-10, pg/ml	521.22 ±281	506.2 ±301.8	0.86	437.3 ±258.2	582.5 ±306	0.19	350.8 ±190.8	643.7 ±292.3	0.005

Footnote: Mean and standard deviations for Age,BMI, running volume, stress measure, and immune biomarkers are reported

Table IV. *Stress level moderates the relationship between running volume and immune biomarkers.*

	PSS			STAIS			PSWQ		
Biomarkers	**Low** (β, p value 95% CI)	**High** (β, p value 95% CI)	**Diff** (β, p value 95% CI)	**Low** (β, p value 95% CI)	**High** (β, p value 95% CI)	**Diff** (β, p value 95% CI)	**Low** (β, p value 95% CI)	**High** (β, p value 95% CI)	**Diff** (β, p value 95% CI)
Treg: CD4+CD25hiFoxP3+, %	0.07 p<0.001	0.03 p=0.076	-0.04 p=0.059	0.05 p=0.001	0.04 p=0.083	-0.01 p=0.75	0.05 p=0.025	0.05 p=0.012	0.00 p=0.88
	(0.04,0.10)	(-0.00,0.06)	(-0.08,0.00)	(0.02,0.08)	(-0.01,0.09)	(-0.07,0.05)	(0.01,0.08)	(0.01,0.09)	(-0.05,0.06)
Tr1 cells: CD4+IL-10+, %	-0.22 p=0.12	-0.11 p=0.35	0.11 p=0.53	-0.41 p=0.20	-0.40 p=0.057	-0.26 p=0.26	-0.08 p=0.64	-0.39 p=0.011	-0.31 p=0.19
	(-0.50,0.06)	(-0.34,0.13)	(-0.25,0.48)	(-0.36,0.08)	(-0.82,0.01)	(-0.73,0.21)	(-0.45,0.28)	(-0.69,-0.10)	(-0.78,0.16)
Th3: CD4+TGFß+, %[1]	-0.01 p=0.41	-0.02 p=0.18	-0.01 p=0.45	-0.01 p=0.22	-0.02 p=0.45	-0.01 p=0.82	-0.02 p=0.14	-0.02 p=0.38	0.00 p=0.91
	(-0.02,0.01)	(-0.05,0.01)	(-0.05,0.02)	(-0.03,0.01)	(-0.06,0.03)	(-0.06,0.05)	(-0.04,0.01)	(-0.05,0.02)	(-0.04,0.05)
IFNγ (×1,000), pg/ml[1]	0.00 p=0.89	-0.01 p=0.73	-0.01 p=0.74	-0.01 p-0.71	0.03 p=0.085	0.04 p=0.11	-0.03 p=0.14	0.04 p=0.020	0.07 p=0.008
	(-0.03,0.04)	(-0.04,0.03)	(-0.06,0.04)	(-0.03,0.02)	(-0.00,0.07)	(-0.01,0.08)	(-0.06,0.01)	(0.01,0.08)	(0.02,0.12)
IL-4, pg/ml[1]	-0.01 p=0.59	0.01 p=0.81	0.01 p=0.66	-0.00 p=0.96	0.01 p=0.86	0.01 p=0.86	0.01 p=0.57	0.00 p=0.98	-0.00 p=0.87
	(-0.02,0.01)	(-0.04,0.05)	(-0.04,0.06)	(-0.02,0.02)	(-0.07,0.08)	(-0.07,0.08)	(-0.01,0.03)	(-0.06,0.06)	(-0.07,0.06)
IFNγ/IL-4 ratio[1]	0.01 p=0.67	-0.01 p=0.67	-0.02 p=0.55	-0.00 p=0.79	0.03 p=0.43	0.03 p=0.41	-0.03 p=0.066	0.04 p=0.13	0.07 p=0.028
	(-0.03,0.05)	(-0.06,0.04)	(-0.08,0.04)	(-0.04,0.03)	(-0.04,0.09)	(-0.05,0.11)	(-0.06,0.00)	(-0.01,0.10)	(0.01,0.14)
IL-10, pg/ml	-12.42 p=0.001	-8.76 p=0.19	3.66 p=0.62	-12.49 p<0.001	-3.6 p=0.72	8.89 p=0.39	-10.72 p<0.001	-3.56 p=0.60	7.16 p=0.31
	(-19.10,-5.74)	(-22.20,4.68)	(-11.34,18.67)	(-16.58,-8.39)	(-24.03,16.83)	(-11.95,29.73)	(-13.80,-7.64)	(-17.35,10.22)	(-6.97,21.28)

dark shading, p<0.05

light shading, 0.05<p<0.1

There are several limitations to this study that warrant mention. Firstly, we did not directly measure levels of cortisol and catecholamines and instead used self-report stress measures; however, these measures have been previously correlated with stress hormone levels (17-20). Secondly, we did not collect occupational data which may have affected the stress measures (21). Thirdly, we did not assess whether the immune differences were biologically meaningful and correlated with clinical symptoms. Finally, we had a small sample size which likely reduced power to obtain significant findings and increase risk for Type II error. Replication of our findings are needed within a larger sample.

Overall, our data suggest an important moderating role for psychological stress in exercise immunology studies. Various types of stress likely interact to influence individual susceptibility to altered immune status and possible adverse clinical outcomes. Psychological-based interventions may be an important approach to mitigate risk for adverse outcomes and thus enhance athletic performance. Further studies are needed to validate our initial findings and determine their potential clinical applications.

ACKNOWLEDGEMENTS

The authors would like to acknowledge both Scotty Taylor and Denise Montgomery for their technical assistance and the University of Mississippi Medical Center Department of Medicine for the funds to complete the study.

REFERENCES

1. Walsh NP, Gleeson M, Shephard RJ, et al. Position statement. Part one: Immune function and exercise. Exerc Immunol Rev 2011; 17:6-63.
2. Lancaster GI, Halson SL, Khan Q, Drysdale P, Wallace F, Jeukendrup AE, Drayson MT, Gleeson M. Effects of acute exhaustive exercise and chronic exercise training on type 1 and type 2 T lymphocytes. Exerc Immunol Rev 2004; 10:91-106.
3. Handzlik MK, Shaw AJ, Dungey M, Bishop NC, Gleeson M. The influence of exercise training status on antigen-stimulated IL-10 production in whole blood culture and numbers of circulating regulatory T cells. Eur J Appl Physiol 2013; 113:1839-48.
4. Gleeson M, Bishop N, Oliveira M, McCauley T, Tauler P, Muhamad AS. Respiratory infection risk in athletes: Association with antigen-stimulated IL-10 production and salivary IgA secretion. Scand J Med Sci Sports 2012; 22:410-17.
5. Gleeson M, Bishop NC. Uri in athletes: Are mucosal immunity and cytokine responses key risk factors? Exerc Sport Sci Rev 2013; 41:148-53.
6. Rehm KE, Elci OU, Hahn K, Marshall GD, Jr. The impact of self-reported psychological stress levels on changes to peripheral blood immune biomarkers in recreational marathon runners during training and recovery. Neuroimmunomodulation 2013; 20:164-76.
7. Cohen S, Kamarck T, Mermelstein R. A global measure of perceived stress. J Health Soc Behav 1983; 24:385-96.
8. Julian LJ. Measures of anxiety: State-trait anxiety inventory (STAI), Beck anxiety inventory (BAI), and hospital anxiety and depression scale-anxiety (HADS-A). Arthritis Care Res 2011; 63 Suppl 11:S467-72.
9. Knight RG, Waal-Manning HJ, Spears GF. Some norms and reliability data for the State-Trait Anxiety Inventory and the Zung Self-Rating Depression scale. Br J Clin Psychol 1983; 22(Pt 4):245-49.
10. Meyer TJ, Miller ML, Metzger RL, Borkovec TD. Development and validation of the Penn State worry questionnaire. Behav Res Ther 1990; 28:487-95.
11. Wuthrich VM, Johnco C, Knight A. Comparison of the Penn State Worry Questionnaire (PSWQ) and abbreviated version (PSWQ-A) in a clinical and non-clinical population of older adults. J Anxiety Disord 2014; 28(7):657-63.
12. Roemer L. Measures for anxiety and related constructs. In: Antony MM, Orsillo SM, Roemer L, editors. Practitioner's guide to empirically based measures of anxiety. New York: Guilford Publications; 2001. p. 49-83.
13. Kokkinos PF, Holland JC, Narayan P, Colleran JA, Dotson CO, Papademetriou V. Miles run per week and high-density lipoprotein cholesterol levels in healthy, middle-aged men. A dose-response relationship. Arch Intern Med 1995; 155:415-20.
14. Kiernan M, Rodin J, Brownell KD, Wilmore JH, Crandall

C. Relation of level of exercise, age, and weight-cycling history to weight and eating concerns in male and female runners. Health Psychol 1992; 11:418-21.
15. Williams PT, Wood PD, Haskell WL, Vranizan K. The effects of running mileage and duration on plasma lipoprotein levels. JAMA 1982; 247:2674-79.
16. Iacobucci D, Posavac S, Kardes FR, Schneider MJ, Popovich DL. Toward a more nuanced understanding of the statistical properties of a median split. J Consum Psychol 2015; 25(4): 652-65.
17. Mantella RC, Butters MA, Amico JA, Mazumdar S, Rollman BL, Begley AE, Reynolds CF, Lenze EJ. Salivary cortisol is associated with diagnosis and severity of late-life generalized anxiety disorder. Psychoneuroendocrinology 2008; 33:773-81.
18. Keenan K, Hipwell AE, Bortner J, Hoffmann A, McAloon R. Association between fatty acid supplementation and prenatal stress in African Americans: A randomized controlled trial. Obstet Gynecol 2014; 124:1080-87.
19. Coco M, Fiore AS, Perciavalle V, Maci T, Petralia MC, Perciavalle V. Stress exposure and postural control in young females. Mol Med Rep 2015; 11:2135-40.
20. Newham JJ, Wittkowski A, Hurley J, Aplin JD, Westwood M. Effects of antenatal yoga on maternal anxiety and depression: A randomized controlled trial. Depress Anxiety 2014; 31:631-40.
21. Kivimäki M, Singh-Manoux A, Nyberg S, Jokela M, Virtanen M. Job strain and risk of obesity: systematic review and meta-analysis of cohort studies. Int J Obes (Lond) 2015; 39(11):1597-600.

LETTER TO THE EDITOR

ASSESSMENT OF MAGNESIUM INFLUENCE ON FATTY ACID CONTENT IN ISOLATED RAT HEPATOCYTES SUBJECTED TO INCUBATION

B. CAŁYNIUK[1], E. GROCHOWSKA-NIEDWOROK[1], M. KARDAS[2], M. MUC-WIERZGOŃ[3] and E. NOWAKOWSKA-ZAJDEL[4]

[1]Department of Human Nutrition, School of Public Health in Bytom, Medical University of Silesia, Zabrze, Poland; [2]Department of Food Technology and Quality Evaluation, School of Public Health in Bytom, Medical University of Silesia, Zabrze, Poland; [3]Department Internal Medicine, School of Public Health in Bytom, Medical University of Silesia, Bytom, Poland; [4]Department of Nutrition Related Prevention, School of Public Health in Bytom, Medical University of Silesia, Bytom, Poland

Received January 20, 2016 – Accepted March 10, 2016

Magnesium salts are components of many dietary supplements used in treatment or prevention of magnesium deficiency. Hypomagnesemia usually results from an improper lifestyle, including unbalanced diet. Isolated hepatocytes of animals or humans are the preferred model used to study the *in vitro* effects of exogenous factors on cellular metabolic changes. The aim of this study was to evaluate the content of saturated, monounsaturated and polyunsaturated fatty acids and their esters in isolated rat hepatocytes influenced by different magnesium concentrations. The isolated rat hepatocytes were used as the test material. Hepatocytes were prepared in culture medium (Hepatocyte Medium) + $MgCl_2$ solutionto concentrations of 2 mM/dm^3 $MgCl_2$, 4 mM/dm^3 $MgCl_2$. After incubation with different concentrations of magnesium ions, changes in the content of fatty acids and their esters were found for the whole hepatocytes and hepatocyte membranes. Despite changes in the fatty acid content in the whole hepatocytes and their membranes, there were no changes in the coefficient of degree of saturation of fatty acids when different concentrations of MgCl2 were used.

Magnesium salts are components of many dietary supplements used in treatment or prevention of magnesium deficiency. Hypomagnesemia usually results from an improper lifestyle, including unbalanced diet (1, 2). Solid oral dosage forms are classical and often contain vitamin B_6 in its composition. Magnesium salts (organic and inorganic) are rarely added to food products. They are dietary supplements, which are an independent group of foodstuffs according to the pending legislation.

Numerous studies have centred on the problem of endogenous and exogenous factors interfering with the basic biochemical processes in the cells. The exogenous factors include magnesium ions, which are provided as deliberately administered dietary supplements. Studies indicate disadvantageous effects of both high and low concentrations of magnesium. There is also a relationship between mortality and magnesium concentration (3-5). High magnesium concentration affects kidney filtration and

Key words: magnesium ions, fatty acids, hepatocytes

Mailing address:
Dr Beata Całyniuk,
Department of Human Nutrition, Faculty of Public Health in Bytom,
Medical University of Silesia in Katowice,
Jordana 19, 41-808 Zabrze, Poland
Tel.: +48 32 2755195 - Fax: +48 32 3976527,
e-mail: wiosenna8@poczta.onet.pl

0393-974X (2016)

DISCLOSURE: ALL AUTHORS REPORT NO CONFLICTS OF INTEREST RELEVANT TO THIS ARTICLE.

development of various diseases (6).

Isolated hepatocytes of animals or humans are the preferred model used to study the *in vitro* effects of exogenous factors on cellular metabolic changes (7-10). The analyzed changes at the cellular level include, in particular, maintenance of homeostasis in terms of the possible peroxidation process.

The aim of this study was to evaluate the content of saturated (SFA), monounsaturated (MUFA) and polyunsaturated fatty acids (PUFA) and their esters in isolated rat hepatocytes influenced by different magnesium concentrations.

MATERIALS AND METHODS

Isolated rat hepatocytes were used as the test material. Liver hepatocytes were isolated from male Wistar rats aged ±3 months with a body weight of approximately 300 g. The animals originated from the Central Experimental Animal House of the Medical University of Silesia. The research obtained the approval of the Bioethics Committee of the Medical University of Silesia.

Hepatocytes were isolated by enzymatic digestion with collagenase according to the Selgena method (11). Numbers and viability of isolated hepatocytes were determined, hepatocytes were prepared in culture medium (Hepatocyte Medium) + $MgCl_2$ solution, so that their concentrations were as follows: 2 mM/dm^3 $MgCl_2$, 4 mM/dm^3 $MgCl_2$. The concentrations used were selected according to the states of hypermagnesemia. Methodology of hepatocyte isolation, cell membrane isolation and analytical tests have been described in earlier publications (12, 13). 1 cm^3 of hepatocyte suspension containing exactly, if possible, $1.3x10^7$ cells was added to the culture media containing appropriate amounts of magnesium chloride. The tested samples were placed in an incubator. Experiments with *in vitro* cell cultures were carried out for 5 hours. This time is necessary to observe changes in hepatocytes caused by external factors. After 5 hours of incubation, the following biochemical tests in hepatocytes were performed: the total content of fatty acids, saturated, monounsaturated and polyunsaturated fatty acids and ester-linked fatty acids in the whole hepatocytes and hepatocytes membranes (14). Results are the means of three repeats.

It was assumed that there are differences in the volume of samples to be tested in comparison to the control volume. Therefore, the area under the chromatographic peaks of tested samples was normalised in order to compare with the control surface.

Statistical evaluation of the *in vitro* experiments was carried out by comparing the normalized area for fatty acids in hepatocytes incubated for 5 hours with the test substances. The differences in volume of the samples as compared with the volume control were taken into consideration. Therefore, in order to compare the obtained results, standardized surface of the chromatographic peaks of the samples in relation to the surface control was used.

RESULTS

Table I shows the results for the saturated, mono- and polyunsaturated fatty acids and their esters in the incubated hepatocytes.

Upon addition of 2 mM/dm^3 or 4 mM/dm^3 $MgCl_2$ to the incubation medium (full hepatocytes), the content of saturated, monounsaturated and polyunsaturated was decreased in comparison to the control group. The saturation factor slightly decreased its value, and in both trials it was 1.20. In contrast, after adding 2 mM/dm^3 $MgCl_2$ to the hepatocytes, the ratio of ester-linked saturated fatty acids to unsaturated did not change. After addition of 4 mM/dm^3 $MgCl_2$, this factor slightly decreased, it was 0.50 and lower than the control sample (Table I).

Table II presents the results for the saturated, mono- and polyunsaturated fatty acids and their esters in the membranes of hepatocytes subjected to incubation.

Upon addition of 2 mM/dm^3 or 4 mM/dm^3 $MgCl_2$ to the incubation medium (hepatocyte membranes), the content of saturated and polyunsaturated fatty acids decreased, while the content of monounsaturated fatty acids increased in comparison to the control group. The saturation factor increased its value (1.40) for the sample containing 2 mM/dm^3 $MgCl_2$ as compared to the control. For the sample with 4 mM/dm^3 $MgCl_2$, the saturation factor was significantly decreased (0.93). The content of ester-linked fatty acids in the membranes of hepatocytes after addition of 2 mM/dm^3 and 4 mM/dm^3 $MgCl_2$ was increased in comparison to the control group. After addition of 2 mM/dm^3 $MgCl_2$, the ratio of ester-linked saturated to

unsaturated fatty acids in the hepatocyte membranes was 0.92 and lower than the control sample. After addition of 4 mM/dm^3 $MgCl_2$, it was 1.39 and higher than in the control sample (Table II).

DISCUSSION

The study was conducted by analyzing changes in whole hepatocytes and their membranes, because properties of cell membranes depend mainly on the composition and the type of fatty acids. Saturated fatty acids are responsible for cell membrane rigidity while unsaturated fatty acids increase its flexibility and permeability.

It has long been known that membranes with a high content of monounsaturated fatty acids are much more resistant to oxidation caused by free radicals and this leads to inhibition of this process is atherosclerosis, aging, and tumorigenesis (15). It was confirmed that peroxidation of essential fatty acid (EFA) present in cell membranes changes the properties of the lipid bilayer (16). These changes are often irreversible.

The process of cellular lipid peroxidation, its mechanism, as well as the resulting products of this process are the subjects of study in many research centres. Many authors believe lipid peroxidation to be a major cause of dangerous cellular damage and even cell death (17, 18). Particular attention is paid to its role in initiating the process of free radical peroxidation (RFT- free radical oxygen). Aldehydes are a large group of lipid peroxidation products.

Determination of the content and quantity of cellular fatty acids allows to assess whether their metabolism is proper. As the components of cell membranes and cellular organelles fatty acids determine their properties, and especially permeability to nutrients.

Table I. *The content of saturated, mono- and polyunsaturated fatty acids and their esters in whole hepatocytes subject to incubation (total area under chromatographic peaks).*

	4 mM $MgCl_2$	**2 mM $MgCl_2$**	**Control**
The content of fatty acids in whole hepatocyte after incubation			
SFA	400.0	361.0	416.3
MUFA	36.3	35.2	38.3
PUFA	297.3	266.8	316.5
MUFA +PUFA	333.6	302.0	354.8
Total FA	733.6	663.0	771.1
*SFA / UFA	1.20	1.20	1.17
The content of fatty acids ester bound in whole hepatocyte after incubation			
SFA	161.8	212.1	215.8
MUFA	33.4	42.4	40.3
PUFA	288.8	326.7	339.7
MUFA +PUFA	322.2	369.1	380.0
Total FA	484.0	581.2	595.8
*SFA / UFA	0.50	0.57	0.57

**SFA/UFA coefficient of degree of saturation of fatty acids as ratio summarized AUPs of saturated fatty acids to*

Table II. *The content of saturated, mono- and polyunsaturated fatty acids and their esters in hepatocyte membranes subject to incubation (total area under chromatographic peaks).*

	4 mM $MgCl_2$	**2 mM $MgCl_2$**	**Control**
The content of fatty acids in hepatocyte membranes after incubation			
SFA	224.4	341.1	348.7
MUFA	188.0	195.3	187.9
PUFA	54.1	48.4	72.1
MUFA +PUFA	242.1	243.7	260.0
Total FA	466.5	548.8	608.7
*SFA / UFA	0.93	1.40	1.34
The content of fatty acids ester bound in hepatocyte membranes after incubation			
SFA	196.7	169.6	115.0
MUFA	106.9	138.7	77.5
PUFA	35.1	45.8	26.5
MUFA +PUFA	142.0	184.5	104.0
Total FA	338.7	354.1	219.0
*SFA / UFA	1.39	0.92	1.11

**SFA/UFA coefficient of degree of saturation of fatty acids as ratio summarized AUPs of saturated fatty acids to summarized AUPs of unsaturated fatty acids*

Monitoring liver efficiency by assessing the changes occurring in hepatocytes makes it possible to specify the energy reserves that determine the compensatory and regenerative potential of the liver.

Common access to the classic drug forms and uncontrolled supplementation with magnesium ions can lead to changes in the cellular homeostasis and development of metabolic disturbances (3, 5). Analyses of changes in the cellular homeostasis caused by magnesium ions are of multifactoral character.

The experiments here assessed the kind of *in vitro* changes in hepatocytes under hypermagnesemia conditions. To develop the experimental hypermagnesemia, 2 and 4 mM $MgCl_2$ solutions were added to the cell culture of isolated hepatocytes.

When analysing the influence of magnesium ions on the content of fatty acids in complete hepatocytes, we found a decreased content of total fatty acids, which was larger with lower concentrations of $MgCl_2$. Higher $MgCl_2$ concentrations in the medium increased the content of fatty acids.

An inverse relationship was observed in the hepatocyte membranes - upon addition of 2 mM/

dm^3 or 4 mM/dm^3 $MgCl_2$, SFA and PUFA content was reduced as compared to the control group. On the other hand, the MUFA content was increased compared to the control group. However, in the membranes of hepatocytes, an inverse relationship between concentration of added $MgCl_2$ solution was found. The higher concentration of $MgCl_2$, the lower the content of the fatty acids. This study showed that addition of the varying concentrations of $MgCl_2$ solution decreased the pool of polyunsaturated fatty acids. This fact can be explained by a progressive peroxidation. In the whole hepatocytes, mainly the free polyunsaturated fatty acids are exposed to the activity of free radicals.

Performed experiments confirmed the effect of magnesium ions on the fatty acid content in the whole hepatocytes and their membranes. Changes in the fatty acid profile will result in changes in the properties of the cell membranes of hepatocytes. This will apply to the change of membrane fluidity and permeability. However, an important result of the study is confirmation that within 5 hours of the experiment, no changes in the value of the coefficient of saturation in fatty acid profile was found, which may be the evidence of a quest to preserve the integrity of the cells.

Probably, malondialdehyde (MDA) produced during peroxidation of polyunsaturated fatty acids, consisting of the part of membrane phospholipids, has a high reactivity with proteins and nucleic acids. MDA easily penetrates into distant tissues and there, thanks to the possibility of forming covalent bonds with many compounds, it may modify their structure and properties (19, 20). The resulting modified physical properties of cell membranes lead to the loss of the cellular integrity (21). This in turn leads to disruption of cellular normal functions, and results in dysfunction of various organs (22).

In both tests, the ester content of polyunsaturated fatty acids in the hepatocyte membranes was higher than in the membranes of control hepatocytes. This confirms the observation that no peroxidation of polyunsaturated fatty acids released from phospholipids took place in this group of fatty acid esters.

After incubation with different concentrations of magnesium ions, changes in the content of fatty acids and their esters were found for the whole hepatocytes and hepatocyte membranes. Despite changes in the fatty acids content in the whole hepatocytes and their membranes, there were no changes in the coefficient of degree of saturation of fatty acids when different concentrations of MgCl2 were used.

REFERENCES

1. Grőber U, Schmidt J, Kisters K. Magnesium in prevention and therapy. Nutrients 20015; 7(9):8199-226.
2. Niedworok E, Całyniuk B, Szczepańska E. Assessment of some macro and microelements daily intake of two groups of women from Silesia region. Proceedings of 9 Symposium Vitamine und Zusatzstoffe in der Ehnarung von Mensch und Tier. Jena 2003; 164-67.
3. Cheungpasitporn W, Thongprayoon C, Ericson SB. Admission hypomagnesemia and hypermagnesemia increase the risk of acute kidney injury. Ren Fail 2015; 37(7):1175-79.
4. Cheungpasitporn W, Thongprayoon C, Qian Q. Dysmagnesemia in hospitalized patients: prevalence and prognostic importance. Mayo Clin Proc 2015; 90(8):1001-10.
5. Haider DG, Lindner G, Ahmad SS, et al. Hypermagnesemia is a strong independent risk factor for mortality in critically ill patients: results from a cross-sectional study. Eur J Intern Med 2015; 26(7):504-7.
6. Horibata K, Tanoue A, Ito M, Takemura Y. Relationship between renal function and serum magnesium concentration in elderly outpatients treated with magnesium oxide. Geriatr Gerontol Int 2015; doi: 10.1111/ggi.12530.
7. Bader A, Zech K, Crome O, Christians U, Ringe B, Pichlmayr R, Sewing K-Fr. Use of organotypical cultures of primary hepatocytes to analyse drug biotransformation in man and animals. Xenobiotica 1994; 24(7):623-33.
8. Gomez-Lechon MJ, Lopez P, Donato P, Montoya A, Larrauri A, Gimenez P, Trullenque R, Fabra R, Castell JV. Culture of human hepatocytes from small surgical liver biopsies. Biochemical characterization

and comparison with in vivo. In Vitro Cell Dev Biol 1990; 26:67-74.
9. Chen HL, Wu HL, Fon CC, Chen PJ, Lai MY, Chen DS. Long-term culture of hepatocytes from human adults. J Biomed Sci 1998; 5:535-40.
10. Mitaka T. The current status of primary hepatocyte culture. Int J Exp Path 1998; 79:393-409.
11. Seglen P. Preparation of isolated rat liver cells. Methods Cell Biol 1976; 13:29-83.
12. Niedworok E, Muc-Wierzgoń M, Nowakowska-Zajdel E, Nowak A, Kokot T. Ethanol induced changes in profile of fatty acids in isolated rats hepatocytes and influence of magnesium ions. J Biol Regul Homeost Agents 2008; 22(2):105-8.
13. Niedworok E, Muc-Wierzgoń M, Nowakowska-Zajdel E. Influence of magnesium on fatty acids and their esters in isolated rat hepatocytes. J Biol Regul Homeost Agents 2010; 24(3):377-80.
14. Wollenweber H, Rietschel E. Analysis of lipopolysaccharide /lipid A/ fatty acids. J Microbiol Methods 1990; 11(3):195-211.
15. Pamplona R, Barja G, Portero-Otin M. Membrane fatty acid unsaturation, protection against oxidative stress and maximum life. Ann N Y Am Sci 2002; 959:475-90.
16. Nakamura M, Cho H, Xu J, Tang Z, Clarke S. Metabolism and functions of highly unsaturated fatty acids: an update. Lipids 2001; 36(9):961-64.
17. Siu GM, Draper HH. Metabolism of malonaldehyde in vivo and in vitro. Lipids 1982; 17(5):349-55.
18. Spiteller G. Lipid peroxidation in aging and age-dependent diseases. Experimental Gerontology 2001; 36(9):1425-57.
19. Marnett LJ. Oxy radicals, lipid peroxidation and DNA damage. Toxicology 2002; 181/182:219-22.
20. Blair IA. Lipid hydroperoxide-mediated DNA damage. Exper Geront 2001; 36(9):1473-81.
21. Esterbauer H, Schaur RJ, Zollner H. Chemistry and biochemistry of 4-hydroxynonenal, malonaldehyde and related aldehydes. Free Rad Biol Med 1991; 11(1):81-128.
22. Szymańska JA, Bruchajzer E, Piotrowski JK. Malondialdehyde levels in rat liver and kidney under the influence stress. Acta Pol Toxicol 1996; 4:1-9.

LETTER TO THE EDITOR

INSULIN PUMP FOR THE TREATMENT OF DIABETES IN COMBINATION WITH ULCERATIVE FOOT INFECTIONS

HJ. FAN, JH. YU, GM. CUI, WY. ZHANG, X. YANG and QJ. DONG

Department of Endocrinology, People's Hospital of Zhengzhou, Zhengzhou, China

Received September 1, 2015 – Accepted March 29, 2016

Ulcerative foot infection is a chronic complication frequently seen in diabetic patients, and can result in disability. To evaluate insulin pump treatment for type 2 diabetes in combination with ulcerative foot infection, we selected 168 diabetic patients who developed foot ulcers and received treatment from April 2012 to April 2014 in the People's Hospital of Zhengzhou, Henan, China. The patients were divided into a treatment group and a control group, 84 in each group. Besides anti-infection treatment, patients in the control group were given multiple subcutaneous insulin injection (MSII), while patients in the treatment group were given continuous subcutaneous insulin infusion (CSII). Ulcer area, fasting plasma glucose (FPG), C-reactive protein (CRP) and count of white blood cells (WBC) were recorded before treatment, one week after treatment, two weeks after treatment and four weeks after treatment; moreover, ulcer healing condition was recorded four weeks after treatment and the related factors were analyzed. Patients in the treatment group showed an obviously narrowed ulcer area two and four weeks after treatment ($P<0.05$) and significantly lowered levels of FPG, CRP and WBC in the 1st, 2nd and 3rd weeks after treatment ($P<0.05$); four weeks after treatment, 88.1% of patients in the treatment group and 66.7% in the control group had healed well, and the difference between two groups was statistically significant ($\chi 2=5.509$, $P=0.019$). Multi-factor logistic regression analysis indicated that levels of FPG, CRP and WBC at baseline and four weeks after treatment had a positive correlation to ulcer healing ($P<0.05$). All the above findings suggest that insulin pump can improve ulcer healing of patients suffering from diabetic foot ulcers as it effectively controls blood glucose level, restrains inflammatory reaction and prevents spreading of infection.

Diabetic foot ulcer, a commonly seen chronic complication in diabetes patients, on shallow or deep tissues of the foot is induced by local neurological abnormality or microangiopathy of the lower limbs (1, 2). Patients usually suffer from local infection, which aggravates damage on foot tissue and delays healing of ulcers, leading to a high disability rate; the risk of amputation for these patients is 30 times that of patients without diabetes (3, 4). Thus, it is of great significance to control blood glucose level and infection as well as accelerate ulcer healing. The current treatment mode for diabetes in clinical practice (5) is diet and exercise treatment first, then oral administration of hypoglycemic drugs, and eventually insulin treatment. Insulin pump treatment which simulates insulin physiological secretion mode can rapidly control blood glucose level and thus reverse toxicity effect caused by high blood

Key words: diabetic foot ulcers, insulin pump, C-reactive protein, fasting plasma glucose level

Mailing address:
Dr Qijuan Dong,
Department of Endocrinology,
People's Hospital of Zhengzhou,
No.3 3 Huanghe Road, Zhengzhou,
Henan, 450000, China
e-mail: qjddongqj@163.com

0393-974X (2016)

DISCLOSURE: ALL AUTHORS REPORT NO CONFLICTS OF INTEREST RELEVANT TO THIS ARTICLE.

glucose level. But treating diabetic foot ulcer patients with insulin pump has not been extensively studied (6). On this basis, we retrospectively analyzed 84 diabetic foot ulcers patients who received insulin pump treatment in the Zhengzhou People's Hospital, Henan, China and then compared the curative effect with 84 other patients who underwent multiple subcutaneous insulin injections (MSII).

MATERIALS AND METHODS

One hundred and sixty-eight patients who suffered from diabetic foot ulcers and received treatment in the People's Hospital of Zhengzhou, Henan, China, between April 2012 and April 2014 were selected. Diagnosis of diabetes referred to diabetic diagnostic criteria released by the World Health Organization (WHO) in 1999; diagnosis of diabetic foot referred to relevant criteria in Hemadenology (2002); diagnosis of infection referred to Nosocomial Infection Diagnostic Criteria formulated by the Ministry of Health (2001). All patients signed informed consent before the treatment and this study was approved by the Medical Ethics Committee of the People's Hospital of Zhengzhou, Henen, China. All patients were confirmed with Wagner grade I ~ III and 1 ~ 21 cm^2 ulcer area (average 8.3±2.4 cm^2). They were evenly divided into a treatment group and a control group according to diagnostic sequence. Of 84 cases in the control group, 44 were males and 40 were females, with an average age of (57.2±7.2) years, average diabetes course of (9.1±2.4) years, average ulcer course of (29.8±6.1) days, average glycosylated hemoglobin (HbAlc) level of (10.7±1.9)% and average polymorphonuclear (PMN) level of (0.82±0.2)%. In the treatment group, 46 were males and 38 were females, with an average age of (56.8±7.4) years, average diabetes course of (9.3±2.6) years, average ulcer course of (9.3±2.6) days, average glycosylated hemoglobin level of (HbAlc) (10.9±2.1)% and average PMN level of (0.84±0.2)%. No statistically significant differences were found in age, gender composition, course of ulcer and PMN between the two groups ($P>0.05$); therefore, results were comparable.

All patients received regular dressing change and anti-bacterial treatment after being admitted to hospital. The wound was washed by normal saline and then bound with gauze which contained 0.1% ethacridine lactate solution, once each day generally and twice or thrice for wounds with extensive seepage. Furthermore, patients were given nutritional support and diabetic diet. Insulin pump treatment was carried out referring to the Chinese Insulin Pump Treatment Guide (2010). Patients were continuously pumped with Novolin R insulin (Novo Nordisk, China) through the abdomen using Minimed712 insulin pump (Medtronic, Inc., USA). The needle head was fixed 4 ~ 5 cm from the navel. The needle was replaced at an interval of 5 ~ 7 days. The initial dosage of insulin was half of the total dosage, and the other half was pumped before three meals. Patients in the control group were subcutaneously injected with insulin before meals and before sleep. Dosage of insulin could be adjusted according to physiological and dietary status and monitoring results of blood glucose until the level of blood glucose reached the standard (FBG<7.0 mmol/L, 2h<10.0 mmol/L).

Observation index

Ulcer area, fasting plasma glucose (FPG) level, C-reactive protein (CRP) level and white blood cell (WBC) level of all patients were examined before treatment, then in the 2^{nd}, 4^{th} and 8^{th} weeks after treatment. The level of CRP was detected using immune turbidity technique. Blood routine indexes were detected with Mindray-5500 fully automatic hematology analyzer.

Time taken for reaching glucose standard, length of hospital stay, dosage of insulin and incidence of hypoglycemia (with clinical symptoms of low blood glucose and (or) level of glucose<3.9 mmol/L) of the two groups were recorded.

Determination of curative effect

Determination criteria for the curative effect were as follows. Patients were determined as being cured when the ulcer was totally healed in the 8^{th} week after treatment. Disease condition was determined as being improved if the ulcer area reduced by 50-75% eight weeks after treatment. Narrowed ulcer area of no more than 50% four weeks after treatment was considered to be no significant change. If patients were found with unchanged or enlarged ulcer area eight weeks after treatment, the disease condition was considered to be deteriorative. The formula of overall good healing rate was: overall good healing rate=(number of cured cases+number of cases with improved condition)/ total number of patients×100%.

Statistical analysis

SPSS ver. 19.0 statistics software package was used to process data. Quantitative data were expressed as mean±standard deviation (SD). Comparison between groups was performed using *t*-test. Qualitative data were processed by *chi*-squared test. Repeatedly measured data were processed by analysis of variance for repeated data. Multiple factor correlation analysis was performed using logistic regression. Difference was considered to be statistically significant if $P<0.05$.

RESULTS

Comparison of various indexes between the two groups

The treatment group took less time to reach glucose standard and less dosage of insulin compared to the control group ($P<0.05$); incidence of hypoglycemia of the treatment group was much lower than that of the control group ($P<0.05$); length of hospital stay of the treatment group was lower than that of the controls, but there was no statistical significant difference ($P>0.05$) (Table I).

Table I shows that both methods were both effective in controlling high blood glucose level of patients with diabetes and ulcerative foot infection, but the treatment group took less time for reaching glucose standard and had much lower incidence of hypoglycemia and much less dosage of insulin compared to the control group. Half dosage of insulin was pumped as a basis using insulin pump in the treatment group, which significantly reduced dosage of insulin before meals and lowered risks of whole-day hyperinsulinemia and hypoglycemia after meals. Moreover, insulin absorption rate changed slightly when an insulin pump was used, which could keep application of a relatively stable daily insulin dosage and thus lower incidence of hypoglycemia.

Comparison of ulcer area and levels of FPG, CRP and WBC between the two groups before and after treatment

Ulcer area in the treatment group significantly narrowed in the 4th and 8th weeks after treatment ($P<0.05$). Levels of FPG, CRP and WBC of the treatment group obviously declined in 2nd, 4th and 8th weeks after treatment, and there were statistically significant differences ($P<0.05$). Detailed data are shown in Table II.

Comparison of curative effect between groups in the 8th week after treatment

In the 8th week after treatment, good healing rates in the treatment group and the control group were 88.1% and 66.7% respectively; difference between two groups was statistically significant ($\chi^2=5.509$, $P=0.019$) (Table III).

Logistic regression analysis on ulcer healing of patients with diabetic foot ulcers

Well healing, i.e., cured or improved, was taken as dependent factor and factors such as age, PMN, HbALc as well as levels of FPG, CRP and WBC before and after treatment were taken as independent variances. Multi-factor logistic regression analysis suggested that age, HbAlc, and levels of FPG, CRP

Table I. *Comparison of various indexes between two groups.*

Group	N	Time taken for reaching standard glucose (d)	Length of hospital stay	Incidence of hypoglycemia (%)	Dosage of insulin (μ/d)
Treatment group	84	3.2±1.6	17.9±2.1	3.6	38.4±7.9
Control group	84	8.3±2.2	18.8±2.0	20.2	55.8±12.4

Table II. *Comparison of ulcer area and levels of FPG, CRP and WBC before treatment and at different time points after treatment.*

Group	N	Ulcer area (cm^2)				FPG (mmoL/L)			
		Before	In the 2nd week	In the 4th week	In the 8th week	Before	In the 2nd week	In the 4th week	In the 8th week
Treatment group	84	8.25±2.37	7.81±2.19	5.22±1.51[ab]	2.34±0.82[ab]	10.11±1.62	7.53±1.63[ab]	6.52±1.14[ab]	6.03±0.91[ab]
Control group	84	8.41±2.50	8.03±2.20	6.72±1.90[a]	4.13±1.34[a]	10.32±1.73	8.47±1.43[a]	7.63±1.25[a]	7.14±1.03[a]

Group	N	CRP(mg / L)				WBC ($\times 10L^{-1}$)			
		Before	In the 2nd week	In the 4th week	In the 8th week	Before	In the 2nd week	In the 4th week	In the 8th week
Treatment group	84	8.74±2.27	6.62±1.84[ab]	4.43±1.20[ab]	2.51±0.52[ab]	11.80±3.23	8.31±1.73[ab]	6.22±1.11[ab]	4.33±0.51[ab]
Control group	84	8.51±2.04	7.67±2.13[a]	5.64±1.51[a]	3.73±0.81[a]	11.54±2.81	9.43±2.03[a]	7.51±1.50[a]	5.44±1.12[a]

[a] $P<0.05$ compared to before treatment; [b] $P<0.05$ compared to control group

Table III. *Comparison of curative effect between groups in the 8th week after treatment*

Group	N	Cure	Improved	No significant change	Worsen	Good healing rate (%)
Treatment group	84	28	46	6	4	88.1*
Control group	84	20	36	18	10	66.7

** $P<0.05$ ($\chi^2 = 5.509$, $P=0.01$) compared to control group*

Table IV. *Multi-factor logistic regression analysis on factors influencing ulcer healing.*

Variable	B	SE	Wald X^2	df	P value	OR	%CI
Constant term	-8.632	2.472	39.429	1	0.000		
Age	1.023	0.185	17.930	1	0.000	2.782	1.667~2.943
CRP at baseline	0.249	0.094	7.287	1	0.008	1.284	1.135~1.643
CRP after treatment	1.323	0.399	9.305	1	0.001	3.756	2.583~12.381
FPG at baseline	0.857	0.129	23.014	1	0.000	2.356	1.749~2.905
FPG after treatment	0.662	0.262	6.569	1	0.012	1.938	1.352~3.783
WBC at baseline	0.704	0.489	7.882	1	0.005	2.022	1.635~4.321
WBC after treatment	0.400	0.179	5.011	1	0.026	1.492	1.258~2.541
PMN	0.758	0.502	2.511	1	0.131	2.134	0.763~ 5.552
HbA1c at baseline	0.124	0.384	32.650	1	0.000	1.733	1.023~4.023

and WBC at baseline as well as levels of FPG, CRP and WBC in the 8th week after treatment were in a positive correlation with ulcer healing ($P<0.05$). Details are presented in Table IV.

DISCUSSION

In recent years, the number of patients with diabetes-induced foot ulcers has grown. Diabetic patients with weak immunity are difficult to heal once a local wound surface is infected; what is worse, they have a higher risk of amputation due to worsening infection, increased ulcer area and more invaded tissues (7, 8). It has been reported that diabetes and foot ulcer promote each other (9). Thus measures for controlling infection, inhibiting inflammation and accelerating ulcer healing are being constantly explored. However, multiple factors contribute to healing diabetes-induced foot ulcer (10, 11). The results of the present study demonstrate that levels of FPG, CRP and WBC at baseline and four weeks after treatment were in an independent positive correlation with ulcer healing ($P<0.05$). Moreover, FPG has been confirmed as one of the high-risk factors.

It has been proved that continuous insulin resistance and constantly decreased function of β cells have obvious influence on sugar tolerance

abnormality evolving into diabetes and progress of diabetes (12). Chronic hyperglycemia and blood fat abnormality, especially glucose toxicity and lipotoxicity caused by increased free fatty acid, contribute to progressively decreased β cells and aggravated insulin resistance. Insulin pump as a model simulating physiological secretion of insulin (13) can realize basic secretion of insulin and pulsatile release of insulin after meals. Continuously pumped insulin can not only relieve fluctuation of blood sugar but can also reduce insulin resistance. In addition, insulin treatment can restrain fat decomposition and thus reduce lipotoxicity (14). In this study, levels of FPG, CRP and WBC in the treatment group were significantly lower than those of the control group in the 2^{nd}, 4^{th} and 8^{th} weeks after treatment ($P<0.05$), indicating insulin pump could control blood sugar and restrain inflammatory reaction. In addition, the ulcer area in the treatment group obviously narrowed four weeks and eight weeks after treatment ($P<0.05$) and the good healing rate of the treatment group (88.1%) was much higher than that of the control group (66.7%) in the 8^{th} week after treatment, suggesting that an insulin pump can also accelerate the healing of ulcers.

REFERENCES

1. Hanaire H, Lassmann-Vague V, Jeandidier N, et al. Treatment of diabetes mellitus using an external insulin pump: the state of the art. Diabet Metab 2008; 34(4):401-23.
2. Raymond A. Plodkowski, Steven V. Edelman. Chapter 32-Physiologic insulin replacement with continuous subcutaneous insulin infusion: insulin pump therapy. Clin Diabet 2006:429-41.
3. Jeandidier N, Riveline JP, Tubiana-Rufi N, Vambergue A, Catargi B, Melki V, Charpentier G, Guerici B. Treatment of diabetes mellitus using an external insulin pump in clinical practice. Diabet Metab 2008; 34(4):425-38.
4. Ikura K, Hanai K, Shinjyo T, Uchigata Y. HDL cholesterol as a predictor for the incidence of lower extremity amputation and wound-related death in patients with diabetic foot ulcers. Atherosclerosis 2015; 239(2):465-69.
5. Haas LB. Optimizing insulin use in type 2 diabetes: role of basal and prandial insulin in long-term care facilities. J Am Med Dir Assoc 2007; 8(8):502-10.
6. Richter WO, Schneidewind JM, Ramlow W, et al. Extracorporeal fibrinogen adsorption-efficacy, selectivity and safety in healthy subjects and patients with foot ulcers. Transfus Apher Sci 2002; 26(1):15-27.
7. Garg R, Williams ME. Diabetes management in the kidney patient. Med Clin North Am 2013; 97(1):135-56.
8. Huynh K, Bernardo BC, McMullen JR, Ritchie RH. Diabetic cardiomyopathy: mechanisms and new treatment strategies targeting antioxidant signaling pathways. Pharmacol Ther 2014; 142(3):375-415.
9. Bharucha AE, Batey-Schaefer B, Cleary PA, et al. Delayed gastric emptying is associated with early and long-term hyperglycemia in type 1 diabetes mellitus. Gastroenterology 2015; 149(2):330-39.
10. Hanas R, Ludvigsson J. Side effects and indwelling times of subcutaneous catheters for insulin injections: a new device for injecting insulin with a minimum of pain in the treatment of insulin-dependent diabetes mellitus. Diabet Res Clin Pract 1990; 10(1):73-83.
11. Alonso-Fernández M, Mancera-Romero J, Mediavilla-Bravo JJ, Comas-Samper JM, López-Simarro F, Pérez-Unanua MP, Iturralde-Iriso J. Glycemic control and use of A1c in primary care patients with type 2 diabetes mellitus. Prim Care Diabet 2015; (5):385-91.
12. Koopal C, van der Graaf Y, Asselbergs FW, Westerink J, Visseren FL. Association between CETP gene polymorphism, insulin resistance and risk of diabetes mellitus in patients with vascular disease. Atherosclerosis 2015; 242(2):605-10.
13. Vedhara K, Dawe K, Wetherell MA, et al. Illness beliefs predict self-care behaviours in patients with diabetic foot ulcers: A prospective study. Diabet Res Clin Pract 2014; 106(1):67-72.
14. Tallis A, Motley T, Wunderlich RP, Dickerson J, Waycaster C, Slade HB. Clinical and economic assessment of diabetic foot ulcer debridement with collagenase: results of a randomized controlled study. Clin Ther 2013; 35(11):1805-20.

JOURNAL OF BIOLOGICAL REGULATORS & HOMEOSTATIC AGENTS Vol. 30, no. 2, 471-476 (2016)

LETTER TO THE EDITOR

CONTINUOUS PLASMA FILTRATION ADSORPTION IN TREATMENT OF SEVERE INFECTION-INDUCED MULTIPLE ORGAN DYSFUNCTION SYNDROME

SL. YIN, C. LAN, H. PEI and ZQ. ZHU

Emergency Department, the First Affiliated Hospital of Zhengzhou University, Zhengzhou, China

Received September 10, 2015 – Accepted April 8, 2016

Multiple organ dysfunction syndrome (MODS), a high-risk disease, has a fatality rate of 70%. To improve treatment of this disease, in recent years many scholars have explored the pathological and physiological changes of MODS. To observe the curative effect of continuous plasma filtration adsorption (CPFA) in the treatment of MODS, we selected 96 patients who were diagnosed with severe infection-induced MODS and were treated in the First Affiliated Hospital of Zhengzhou University between February 2012 and October 2014 and divided them into an observation group and a control group. Besides conventional treatment, the observation group was also given CFPA in combination with high volume hemofiltration (HVHF), while the control group only received HVHF. Changes of blood routine index, balance of electrolyte and acid-base as well as vital signs were observed before and after treatment. Also, blood, kidney and blood gas were examined. For all patients, tumor necrosis factor-α (TNF-α), interleukin-6 (IL-6) and C-reactive protein (CRP) were recorded at the start of treatment (0 h), and 5 h and 10 h after treatment. It was found that both therapies could lower blood urea nitrogen (BUN) and creatinine levels and maintain balance of electrolyte and acid-base, but had no obvious influence on leukocyte, blood platelet and hematocrit. In the observation group, PaO2/FiO2 and mean arterial pressure (MAP) were significantly improved after surgery (P<0.05), while Acute Physiology and Chronic Health Evaluation (APACHE) II score had an obvious decrease (P<0.05). In contrast, the control group was observed with insignificantly changed PaO2/FiO2, MAP and APACHE II score (P>0.05). TNF-α, IL-6 and CRP levels of the two groups had no statistically significant difference at the start of treatment (P>0.05), but TNF-α, IL-6 and CRP levels of the observation group became remarkably lower than those of the control group 5 h and 10 h after treatment (P<0.05). Therefore, CPFA is proved to be safe and effective in treating patients with severe infection-induced MODS as it can lower the level of proinflammatory cytokines and improve the level of anti-inflammatory cytokines; thus, it is worthy of clinical promotion.

Multiple organ dysfunction syndrome (MODS), a highly fatal disease, is mostly induced by serious trauma, shock or severe infection and involves multiple organs or systems, which can lead to death in a short time (1, 2). Severe infection-induced MODS reflecting as systemic inflammatory response syndrome (SIRS) in the early stage is treated with a therapeutic schedule targeted at lowering the level of proinflammatory cytokines and improving the ratio of anti-inflammatory cytokines to proinflammatory

Key words: multiple organ dysfunction syndrome, continuous plasma filtration adsorption, vital signs, inflammatory cytokines

Mailing address:
Dr Shenglu Yin,
Emergency Department,
the First Affiliated Hospital of Zhengzhou University,
Zhengzhou, Henan, 450052, China
Tel.: +86 15393702252
e-mail: yslyinsl@163.com

0393-974X (2016)

DISCLOSURE: ALL AUTHORS REPORT NO CONFLICTS OF INTEREST RELEVANT TO THIS ARTICLE.

cytokines. As blood purification treatment is often recommended for severe infection- induced MODS, continuous blood purification methods, such as high volume hemofiltration (HVHF), have been developed. HVHF is effective in reducing the level of inflammatory mediators such as interleukin-6 (IL-6) and maintaining stability of haemodynamics (3-5). However, the scavenging effect of HVHF is still restrained by the size of aperture of the filter membrane. Even medium with molecular weight less than 30KD can lower the scavenging effect due to the form of polymers (for example, TNF-α in form of trimer), generation of protein membrane on the surface of filter membrane, etc (6). Continuous plasma filtration adsorption (CPFA), currently, has been widely recognized in many countries. CPFA as a novel CBP method integrates multiple mechanisms of blood purification treatment, which shows a good application prospect in treatment of MODS (7-9). However, studies on these aspects are still in the initial stage, therefore, we selected 96 patients for a comparative study of CPFA for the treatment of MODS patients.

MATERIALS AND METHODS

Ninety-six patients who developed severe infection-induced MODS and received treatment in the Emergency Department of the First Affiliated Hospital of Zhengzhou University between February 2012 and October 2014 were selected as research subjects. Systemic Inflammatory Response Syndrome (SIRS) of all patients conformed to the diagnostic criteria of SIRS released by the American College of Chest Physicians (ACCP)/Society of Critical Care Medicine (SCCM) (10) in 1991; MODS conformed to the diagnostic criteria released in the Academic Conference of Chinese Critical Care Medicine (11). The patients included had at least 8 points of Acute Physiology and Chronic Health Evaluation (APACHE) II score and had no contraindication to renal replacement therapy. They were divided into an observation and a control group. In the observation group, there were 48 patients (36 males and 12 females) aged from 18 to 71 years (average 45.1±2.1 years); and the average time from onset of disease to hospitalization was (7.1±2.4) h. The control group was composed of 48 patients (38 males and 10 females) with ages ranging from 19 to 77 years [average (44.2±1.9) years] and average time from onset of disease to hospitalization was (6.3±2.8) h. Difference of general data between the two groups was not statistically significant ($P>0.05$), thus the results were comparable. This study was approved by the ethics committee of the First Affiliated Hospital of Zhengzhou University and all patients signed an informed consent.

Inclusion criteria

Patients who were confirmed with MODS by Marshall scoring criteria, conformed to SIRS diagnostic criteria recommended by ACCP/SCCM and had APACHE II score equal to or over 8 points were included in the study. Those who could not receive renal replacement therapy were excluded.

Treatment

Both groups were initially given conventional treatment. The observation group was given CPFA in combination with HVHF, while the control group only received HVHF.

The main instruments used in CPFA included ACH-10 multi-functional blood purification machine (Asahi Kasei Corporation, Japan), PN2000N blood separator with a membrane area of 0.35 m^2 (GAMBRO, Sweden), F6 dialyzer with polysulfone membrane area of 1.3 m^2 and plasma separation speed of 30 ~ 40 m/min (Fresenius Company, Germany) and HA300-I adsorber (Lizhu Company, China). Before blood separation, liquid composing of 1000 ml of glucose (5%), 1000 ml of normal saline and 40 mg of ordinary heparin were used for preflushing for 30 min. Adsorber was exchanged with a new one every five hours; and the flow of dialyzate was 2L/h.

The main instruments used for HVHF included Diapact multi-functional blood purification machine (Braun Medical Co., Ltd, Germany) and AV600 blood hemofiltration machine with polysulfone membrane area of 1.3 m^2 (Fresenius Company, Germany). Displacement liquid was prepared using a Jinbaochao 200 hematodialysis and hemofiltration machine. Flow rate was 6 L/h, 60 L each time.

Observation index

Heart rate (HR) and mean arterial pressure (MAP) were recorded during treatment. Venous blood was

collected from patients at the start of treatment (0h) and 10 h after treatment to detect the total number of white blood cells (WBC), platelets (PLT), hematokrits (HCT), blood urea nitrogen (BUN), creatinine level, potassium (K), sodium (Na), chlorine (CL) and calcium (Ca). Also, PH value, concentration of bicarbonate radical (HCO^{3-}) as well as oxygen partial pressure (PaO_2) were recorded by performing blood gas analysis. PaO_2/FiO_2 was calculated.

APACHE II scores were recorded before and after treatment. Levels of inflammatory factors including tumor necrosis factor-α (TNF-α), interleukin-6 (IL-6) and C-reactive protein (CRP) were detected at the start of treatment, and 5 and 10 hours after treatment, respectively.

Statistical analysis

SPSS 19.0 statistics software was used to process data. Measurement data were expressed by mean ± SD. Comparison between the two groups was performed using *t*-test. Values obtained before and after treatment were compared using paired *t*-test. $P<0.05$ indicated that difference was statistically significant.

RESULTS

Comparison of vital sign and APACHE II score between two groups

In the control group, MAP was (80.29±7.06) mmHg before treatment and rose to (88.57±9.73) mmHg after treatment, but the difference had no statistical significance ($P>0.05$); APACHE II score was 24.29±6.47 points before treatment and 19.43±5.32 points after treatment, but there was no statistically significant difference ($P>0.05$). In the observation group, MAP was (96.00±13.84) mmHg after treatment, much higher than MAP before treatment (79.20±13.14) mmHg; furthermore, APACHE II score was 26.20±5.36 points before treatment and 14.20±2.78 points after treatment, and there was a remarkable difference ($P<0.05$). Both therapies were found to be effective in slowing HR ($P<0.05$).

Changes of blood routine, hepatic and renal function and electrolytes

Blood routine indexes such as WBC, PLT and HCT all had no obvious variation in the two groups after treatment. Patients in the observation group and the control had abnormally high levels of BUN and Cr before treatment (33.20±12.56 mmol/L *vs* 40.59±9.43 mmol/L; 285.40±133.53 μmol/L *vs* 486.71±173.11 μmol/L, respectively). However, values of these two indexes in the two groups declined significantly after treatment ($P<0.05$); BUN level and Cr level of the observation group decreased to 18.30±9.43 mmol/L and 129.40±66.83 μmol/L, respectively, and BUN level and Cr level of the control group decreased to 22.53±9.97 mmol/L and 276.57±89.88 μmol/L, respectively; the decrease in the observation group was more obvious than that of the control group. Before treatment, 2 cases in the observation group had hyperkalemia, while in the control group, there were 2 cases of hyperkalemia and 1 case of hypokalemia; but all of them recovered after treatment. One patient in the control group and one patient in the observation group developed hepatic failure but the other patients had normal liver function. We found the influence of the two therapies on liver function was not obvious.

Results of blood gas analysis

PaO_2/FiO_2 was low in both groups before treatment and the difference between two groups was not statistically significant ($P>0.05$). But after treatment, it improved significantly in the observation group ($P<0.05$). PaO_2/FiO_2 of the control group had a rising tendency, but the difference was not statistically significant ($P>0.05$). Additionally, both therapies could maintain acid-base balance. Detailed data are given in Table I.

Comparison of level of inflammatory factors of the two groups at different stages

At the start of treatment, the difference of TNF-α, IL-6 and CRP levels between the two groups had no statistical significance ($P>0.05$). Five and 10 hours after treatment, TNF-α and CRP levels had a remarkable decline ($P<0.05$). Five and 10 hours after treatment, TNF-α, IL-6 and CRP levels in the observation group was much lower than that of the control group ($P<0.05$). Detailed data are shown in Table II.

In recent years, treatment of MODS has

Table I. *Changes of indexes relating to blood gas analysis before and after treatment in the two groups.*

	Observation group	Control group		
Observation index	0 h	10 h	0 h	10 h
PH	7.47±0.06	7.41±0.04	7.35±0.04	7.35±0.03
HCO^{3-}(mmol/L)	21.31±7.74	23.52±2.31	22.16±7.55	23.27±4.18
BE(mmol/L)	-3.37±6.27	1.45±2.42	-1.56±5.27	2.47±0.55
PaO_2/FiO_2	187.80±58.33	297.4037.87*	192.43±34.78	234.28±46.60

(Mean ± SD) * *P<0.05 compared to before treatment*

Table II. *Comparison of level of inflammatory factors of the two groups at different stages.*

Group	TNF-α (pg/ml)	IL-6 (pg/ml)	CRP (mg/l)
Observation gorup (N=48)			
0 h	345.50±107.80	177.20±92.70	22.70±3.70
5 h	280.70±122.20[ab]	163.20±82.50[b]	11.80±2.20[ab]
10 h	199.70±97.10[ab]	142.50±92.50[b]	15.20±4.70[ab]
Control group (N=48)			
0 h	350.80±97.50	168.10±72.20	23.80±5.20
5 h	339.70±120.10	206.40±100.70	20.90±3.30
10 h	372.50±112.30	182.20±82.70	21.50±4.10

(Mean ± SD) [a] *P<0.05 compared to at the time when the treatment started within group;* [b] *P<0.05 compared to control group after treatment*

concentrated on elimination of inflammatory factors such as TNF-α, IL-6 and CRP. CRP is an acute phase protein synthesized by liver, has a molecular weight of 115000. In addition, CRP, which is a non-specific marker reflecting acute injury, bacterial infection and inflammatory reaction, can reflect the severity of inflammatory reaction induced by trauma, infection and necrosis (12). TNF-α generated by mononuclear phagocytes plays inducing and regulatory functions in involvement of other cytokines in inflammatory reaction. TNF-α, the level of which rose at first, plays a core role and, moreover, can induce waterfall-like release of other cytokines such as IL-6 and IL-8 (13). Table II shows that levels of TNF-α, IL-6 and CRP declined significantly at different treatment stages, suggesting cytokine elimination effect of HVHF alone was not so satisfactory but the application of CPFA could make up the shortcoming.

DISCUSSION

To lower its fatality rate, experts and scholars from different countries are dedicated to exploring the pathological mechanism of MODS. Many animal experiments have verified that inflammatory response out of control is the leading cause for severe infection-induced MODS (14, 15), and the process is considered to be in positive correlation with overexpression of inflammatory factors. Karasek and Theorell (16) proposed the hypothesis of peak concentration. They thought that removing a large number of pro-inflammatory and anti-inflammatory mediators from blood could weaken the toxic effect and thus relieve distant organ injury. In recent decades, many clinical tests (17) verified that, HVHF, the improved mode of continuous hemofiltration technology, could relieve clinical

symptoms of sepsis by eliminating inflammatory mediators, which promoted the wide application of HVHF in treatment of sepsis. However, HVHF is also restrained by narrow mediator elimination scope and demands a large amount of replacement fluid, which causes difficulty for clinical operation.

Compared to HVHF, CPFA integrates multiple effects of blood purification, especially the introduction and enhancement of absorption mechanism (18). In this study, levels of TNF-α, IL-6 and CRP of the observation group all showed significant decline at different treatment stages; maintenance of hemodynamic stability and improvement in liver function of the observation group were superior to those of the control group, and improvement in vital signs, biochemical index and APACHE II score of the observation group were improved compared to the control group, suggesting that CPFA is a safe and effective treatment method for MODS.

In conclusion, HVHF in combination with CPFA treatment can effectively improve severe infection-induced MODS as the therapy can significantly improve hemodynamic index, lower APACHE II score and eliminate inflammatory mediators. This study only explored the clinical effects of single treatment; therefore, whether patients need CPFA or not and the determination of treatment time remain to be further discussed. Furthermore, the sample size of this study was small; clinical tests with a large sample size is needed.

REFERENCES

1. Zhou N, Li J, Zhang Y, et al. Efficacy of coupled low-volume plasma exchange with plasma filtration adsorption in treating pigs with acute liver failure: A randomised study. J Hepatol 2015; 63(2):378-87.
2. Schiffer CA, Buchholz DH, Aisner J, Betts SW, Wiernik PH. Clinical experience with transfusion of granulocytes obtained by continuous flow filtration leukopheresis. Am J Med 1975; 58(3):373-81.
3. Combes A, Solignac M. Hémofiltration à haut volume (HVHF) dans le syndrome de réponse inflammatoire systémique (SIRS) en post-chirurgie cardiaque. Réanimation 2010; 19(5):H2-H6.
4. Hites M, Dell'Anna AM, Scolletta S, Taccone FS. The challenges of multiple organ dysfunction syndrome and extra-corporeal circuits for drug delivery in critically ill patients. Adv Drug Deliv Rev 2014; 77(20):12-21.
5. Tateishi Y, Oda S, Sadahiro T, Nakamura M, Hirayama Y, Abe R, Hirasawa H. Continuous hemodiafiltration in the treatment of reactive hemophagocytic syndrome refractory to medical therapy. Transfus Apher Sci 2009; 40(1):33-40.
6. Choudhuri AH, Tyagi R, Tyagi R, Agarwal D, Uppal R. Early use of ulinastatin reduces Multiorgan Dysfunction (MODS) in septic shock following anastomotic failure. Clin Ther 2015; 37(8):112.
7. Guillevin L, Lhote F. Treatment of polyarteritis nodosa and Churg-Strauss syndrome: Indications of plasma exchanges. Transfus Sci 1994; 15(4):371-88.
8. Mao HJ, Yu S, Yu XB, et al. Effect of coupled plasma filtration adsorption on endothelial cell function in patients with multiple organ dysfunction syndrome. Int J Artif Organs 2011; 34 (3):288-294.
9. Ban Y, Shen H, Li TS. An experimental study of a rat model with MODS as a result of trauma induced infection. Zhongguo Wei Zhong Bing Ji Jiu Yi Xue 2008; 20(1):41-44.
10. Bone RC, Sibbald WJ, Sprung CL. The ACCP-SCCM consensus conference on sepsis and organ failure. Chest 1992; 101:1481-83.
11. NIOSH Working Group. Stress at work. NIOSH Publication 1999; 99-101.
12. Matsuda K, Moriguchi T, Harii N, Goto J. Comparison of efficacy between continuous hemodiafiltration with a PMMA membrane hemofilter and a PAN membrane hemofilter in the treatment of a patient with septic acute renal failure. Transfus Apher Sci 2009; 40(1):49-53.
13. Du XG, Chen XM, Gan H, Wang XC. Continuous blood purification ameliorates Rho A·mediated endothelial permeability in severe acute pancreatitis patients with lung injury. Int J Artif Organs 2011; 34(4):348356.
14. Hu D, Sun S, Zhu B, Mei Z, Wang L, Zhu S, Zhao W. Effects of coupled plasma filtration adsorption on septic patients with multiple organ dysfunction syndrome. Renal Fail 2012; 34 (7):834-839.
15. Mao HJ, Yu S, Yu XB, Zhang B, Zhang L, Xu

XR, Wang XY, Xing CY. Effects of coupled plasma filtration adsorption on immune function of patients with multiple organ dysfunction syndrome. Int J Artif Organs 2009; 32 (1):31-38.

16. Karasek RA, Theorell T. Healthy Work: Stress, Productivity, and the Reconstruction of Working Life. New York: Basic Books 1990, p.89-103.
17. Lu J, Chen MQ, Geng YX, Cheng L, Lu H, Jiang H, Zhou J, Wang X. Effect of qi benefiting stasis removing method on systemic inflammatory response and coagulation function in MODS patients. Zhongguo Zhong Xi Yi Jie He Za Zhi 2014; 34 (1):35-38.
18. 18. Brophy PD. Renal supportive therapy for pediatric acute kidney injury in the setting of multiorgan dysfunction syndrome/sepsis. Semin Nephrol 2008; 28(5):457-69.

LETTER TO THE EDITOR

VENA-VENOUS HEMOFILTRATION IN TREATING SEVERE INJURY-INDUCED MULTIPLE ORGAN DYSFUNCTION SYNDROME

Y. FANG[1,2], H.L. ZONG[2], L. ZHANG[1,3], Z.H. WANG[2], L.M. SUN[2] and R.F. ZHANG[2]

[1]Key-Disciplines Laboratory Clinical-Medicine Henan, Zhengzhou, China; [2]Department of Intensive Care Unit, The First Affiliated Hospital of Zhengzhou University, Zhengzhou, China; [3]Department of Neurology, The First Affiliated Hospital of Zhengzhou University, Zhengzhou, China

Received February 7, 2016 – Accepted April 21, 2106

Yu Fang and Lu Zhang contributed equally to this work

Severe multiple injury (SMI) can induce multiple organ dysfunction syndrome (MODS) and easily result in complications, as well as having a high mortality rate. To explore the curative effect of continuous vena-venous hemofiltration (CVVH) in treating MODS and its effect on serum tumor necrosis factor (TNF)-α, interleukin (IL)-10 and nitric oxide (NO), we selected 200 patients who suffered from SMI and received treatment in the First Affiliated Hospital of Zhengzhou University between April 2012 and April 2014 as research subjects. All patients were treated with CVVH. Vital signs, blood oxygen pressure (PaO2) and oxygenation index (OI) of artery, electrolyte and acid-base balance were observed before and after treatment. Before treatment, 1 h and 12 h after the start of treatment, and at the end of treatment, TNF-α and IL-10 concentrations in serum and ultrafiltrate were tested using enzyme linked immunosorbent assay, and NO concentration in serum and ultrafiltrate was detected using nitrate reduction method. After treatment, heart rate and respiratory rate of patients had significant decline (P<0.05) and average arterial pressure rose remarkably (P<0.05); blood urea nitrogen and creatinine decreased (P<0.05 or 0.01); PaO2 and OI were both significantly increased (P<0.01); hyperkalemia and acidosis were effectively corrected (P<0.01); but differences of Na+, Ca2+ and Cl- before and after treatment had no statistical significance (P>0.05). Serum IL-10 concentration had a significant increase after treatment, while TNF-α and NO concentrations had a significant decline after treatment. A small quantity of IL-10, but not of TNF-α, was detected from ultrafiltrate. Concentration of NO in ultrafiltrate was higher. It can be concluded that CVVH can effectively relieve clinical symptoms of MODS patients, improve function of organs, correct electrolyte disturbance and acid-base imbalance and eliminate TNF-α and NO in serum, which is effective in improving the ratio of successful rescue of patients developing MODS.

Multiple organ dysfunction syndrome (MODS) refers to concurrent or sequential dysfunction or failure of two or more organs after severe trauma or infection. Prognosis of patients developing MODS is poor if no positive targeted treatment is performed. Risk of MODS on human health is increasingly frequent and has become one of the major causes leading to death (1, 2). The pathogenesis of MODS

Key words: severe multiple injury, multiple organ dysfunction syndrome, continuous vena-venous hemofiltration, vital sign

Mailing address:
Dr Yu Fang,
No.1 East Jianshe Road,
Department of Intensive Care Unit,
First Affiliated Hospital of Zhengzhou University,
Zhengzhou, Henan, PR China
e-mail: fyufangy@163.com

0393-974X (2016)

is not yet known (3), although hypotheses on its mechanism are diverse, but the theory that MODS is induced by imbalanced systemic inflammatory response syndrome (SIRS) and compensatory anti-inflammatory response syndrome (CARS) attributable to infection factors and non-infection factors, such as severe trauma, shock and ischemia/reperfusion injury, has been widely accepted. Hence, most scholars consider that the key to treatment of MODS in the early stage is to eliminate residual inflammatory media (6, 7). In recent years, studies in China and abroad have focused on pro-inflammatory mediators such as tumor necrosis factor (TNF)-α, interleukin (IL)-1 and IL-6, with few concerns about anti-inflammatory mediators. IL-10, an important anti-inflammatory mediator, can inhibit macrophages to secrete IL-1 and TNF-α, therefore, it plays an important role in restricting inflammatory reactions in MODS (6). In recent years, continuous veno-venous hemofiltration (CVVH) has been considered an effective method for treating MODS (7). As MODS is correlated to the uncontrollable release of inflammatory mediators, CVVH, which can eliminate those mediators, is believed to be a feasible treatment measure for MODS, however, its effectiveness is still controversial (8, 9). This work applied CVVH to treat MODS patients and carefully analyze the effects of CVVH on TNF-α, IL-10 and NO, to study the clinical effect of the treatment and its relevant mechanisms.

MATERIALS AND METHODS

General data

Two hundred patients who developed severe multiple injury (SMI) and received treatment between April 2012 and April 2014 were included in this study. The patients conformed to MODS staging and diagnostic standards proposed in the National Academic Conference on Critical Care Medicine of 1995. Of 200 patients, 152 cases were males and 48 cases were females, aged from 17 to 82 years (average 56.6 years). As to primary disease, there were 104 cases of mine gas explosion, 56 cases of traffic accidents, 20 cases of fire accidents and 20 cases of others. Their scores of Acute Physiology and Chronic Health Evaluation (APACHE) II was (27.4±8.6) points and the average number of the failed organs was (3.2±0.1). All patients gave their informed consent to participate in the study.

Main instruments

The instruments used included NO kit (Nanjing Jiancheng Bioengineering Institute, China), TNF-α kit (Shanghai Sengxiong Biotech Co., Ltd., China), IL-10 kit (Shanghai Sengxiong Biotech Co., Ltd., China), 721 spectrophotometer (Sichuan Ninth Instrument Factory, China), three-use thermostatic water bath box (Beijing Changan Scientific Instrument Factory, China), 3HELL/JB incubator (Sheldon Company, USA), high-speed centrifuge (Shanghai Anting Scientific Instrument Factory, China), DG3002A enzyme-linked immunometric meter (East China Electronic Tube Factory, China), vortex oscillator (Beijing Jingke Weiye Experiment Equipment Co., Ltd., China) and sample injector (Nichiryo Corporation, China).

Treatment protocol

Patients were treated with CVVH. Continuous renal replacement instrument (Braun Company, Germany) and Frensius AV 600S polymers polysulfone membrane filters were used. The replacement liquid was made up of 3000 mL sodium chloride solution (0.9%), 1000 mL glucose (5%), 8 mL magnesium sulfate (10%), 20 mL calcium chloride (5%), 8 mL potassium chloride (10%) and 200 mL sodium bicarbonate (5%). The content of electrolyte and dosage of sodium bicarbonate in the replacement liquid needed to be adjusted according to results of blood gas analysis and biochemical tests. Patients without tendency of bleeding were given 0.5 ~ 1 mg/kg first and then 5 ~ 10 mg/h, while those who had tendency of bleeding were given 0.3 ~ 0.4 mL low molecular heparin at first and then 0.2 mL more every 4 to 6 hours. The filter was washed with 20 mg heparin for 30 min before treatment. During CVVH, pre-dilution method was used; the flow of the replacement liquid was kept between 2000 and 4000 ml/h; the blood flow was controlled between 150 and 250 mL/min; the other drugs were administered using post-dilution method. Patients were treated for 18 ~ 36 h each time, for 1 to 8 times. The duration of CVVH was no shorter than 18 h or no longer than 284 h. Treatment time of CVVH was determined by stability of vital signs such as blood pressure and heart

rate, normality of central venous pressure, clearance rate of blood urea nitrogen (BUN), serum creatinine (Scr) and serum potassium (K^+) and amount of dehydration. Dosage of drugs used in CVVH was determined by Scr clearance rate, drug screening coefficient and the dose recommended by the manufacturer.

Detection of inflammatory mediators

Before CVVH, 5 mL of arterial blood sample was preserved. One hour after beginning the treatment, two hours after, and at the end of the treatment, 3 mL samples of arterial blood and venous blood were taken, respectively, as well as 5 mL of ultrafiltrate. The blood samples were centrifuged at 3000 r/min for 5 min. The upper-layer serum was taken and loaded with EP tube. The serum and ultrafilrate were preserved at -26 °C.

Detection of TNF-α

The serum, ultrafiltrate and TNF-α were cooled to room temperature. In a reaction plate, eight standard wells were established; each well was added with 100 μl of sample diluent. Then, 100 μl of liquid was absorbed from the first well and transferred to the second well by the sample injector. The doubling dilution was performed from the first well to the seventh well. Finally, 100 μl of liquid was taken out of the seventh well and discarded. The eighth well was taken as blank control. Wells for testing were added with samples, 100 μl for each well, and kept at 37°C. Two hours later, the plate was washed for four to six times, and after drying with filter paper was added with enzyme conjugate, 100 μl for each well, and maintained at 37°C. One hour later, the plate was fully washed for four to six times, and after drying with filter paper, the plate was again added with enzyme conjugate, 100 μl for each well and maintained at 37°C in the dark for 5 ~ 10 min. After the reaction, each well was added with one drop of blocking solution. Absorbance was detected the wavelength of 492 nm. Standard curve was drawn on a semilogarithmic paper using optical density (OD) value of standard samples (1000, 500, 250, 125, 62.5, 32, 16 and 0 pg/mL). Then the content of TNF-α was obtained from the curve graph using the OD value of the sample.

Detection of IL-10

The detection of IL-10 was carried out using the same method as for TNF-α.

Detection of NO

Nitrate reduction method was used. Nitrate reductase was used to specifically restore NO-3 to NO-2. The level of NO in body was represented by the sum of serum NO-3 and NO-2. Colorimetric assay was performed at the wavelength of 540 nm. Extinction values of the testing tube and standard tube were recorded. Then the content of NO (μmol/L) was calculated using the formula of A of testing tube/A of standard tube×100. The NO kit used (enzymic method) was produced by Nanjing Jiancheng Bioengineering Institute. Colorimetric determination was performed using 721 spectrophotometer.

Observation indexes

Vital signs were measured before and after treatment. BUN, Scr and electrolyte were detected using fully automatic biochemical instruments (Shenzhen Mindray Co., Ltd., China). Blood oxygen pressure (PaO_2), oxygenation index (OI) and acid-base balance were also detected, as well as inflammatory mediators TNF-α, IL-10 and NO.

Statistical analysis

Data were processed using SPSS19.0. Measurement data were expressed as mean±SD and processed with *t*-test. Enumeration data were processed by *chi*-squared test. Comparison between groups was carried out using single factor variance analysis. The correlation of NO concentration with PaO_2 and mean artery pressure (MAP) was analyzed with linear correlation regression. Difference was considered to be significant if $P<0.05$.

RESULTS

Vital signs before and after CVVH

Body temperature decreased from 37.8±0.4°C before treatment to 36.8±1.0°C after treatment; heart rate decreased from 115±23 time/min to 94±12 time/min; and respiratory frequency decreased from 31±6 time/min to 20±4 time/min; MAP increased from 58.2±15.2 mmHg to 101.9±6.5 mmHg; the differences had statistical significance ($P<0.05$).

Laboratory indexes before and after CVVH treatment

BUN level decreased from 410.3±180.6 μmol/L

before treatment to 218.3±107.5 μmol/L after treatment; Scr level decreased from 28.5±10.1 μmol/L to 21.5±9.3 μmol/L; the differences were statistically significant (P<0.05); hyperkalemia and acidosis were corrected; levels of Na^+, $Ca2^+$ and Cl^- before and after treatment had no significant differences (145.8±11.6 mmol/LVS 142.3±6.5 mmol/L, 2.1±0.4 mmol/L VS 2.1±0.8 mmol/L, 101.6±10.3 mmol/LVS 98.6±9.7 mmol/L). These results indicate that CVVH could effectively improve blood biochemical indexes, and control azotemia as well as adjust water-electrolyte and acid-base disturbance. The level of hemobilirubin had no obvious decline, probably because CVVH is weak in eliminating molecular substances in bilirubin when molecular weight is lower than 50 kD (unconjugated bilirubin: 548 kD; conjugated bilirubin: 800 kD) and could influence the prognosis.

Impact of CVVH on PaO_2 and SaO_2

The level of PaO_2 was 89.7±19.2 mmHg at the end of CVVH, much higher than the level before treatment (56.9±16.8 mmHg), and the difference had statistical significance (q=3.83, P<0.05); the level of SaO_2 was 93.5±12.3% at the end of CVVH, much higher than before treatment (70.5±9.8%); and the difference was significant (q=4.1, P<0.05).

Clinical outcome

A total of 200 patients underwent CVVH; 112 patients survived and 88 patients died, with a survival rate of 56.0%.

Variation of TNF-α, IL-10 and NO concentrations in serum and ultrafiltrate

One hour after CVVH treatment, TNF-α concentration in venous blood was much lower than that in arterial blood (t=2.68, P<0.05); 12 h after commencing treatment, the difference was no longer significant. At the end of CVVH treatment, the concentration of venous blood TNF-α was much lower than that of arterial blood TNF-α (t=2.13, P<0.05) and much lower than before treatment (q=4.1, P<0.05); TNF-α was not detected in ultrafiltrate (Table I).

IL-10 concentration of arterial blood at the end of CVVH treatment was much higher and the difference had statistical significance (q=4.11, P<0.05); one hour and twelve hours after CVVH and at the end of CVVH treatment, IL-10 concentration of arterial blood and venous blood had no significant difference. A small quantity of IL-10 was detected in ultrafiltrate (Table II).

One and 12 h after CVVH and at the end of CVVH, NO concentration of venous blood was much lower than that of arterial blood and the difference was significant (p<0.05); arterial blood NO concentration at the end of CVVH was much

Table I. *Comparison of TNF-α in serum and ultrafiltrate (pg/mL).*

Time point	Serum		Ultrafiltrate	Sieve coefficient	Scavenging coefficient
	Artery	Vein			
0	97±31	/	/	/	/
1h after the starting of CVVH	89±27	75±24[a]	0	0	25±12
12 h after the starting of CVVH	73±21[*]	69±18	0	0	7±3
At the end	51±13[*]	42±11[a]	0	0	-15±7

[a]: P<0.05 compared to artery; [*]:P<0.05

Table II. *Comparison of IL-10 concentration of serum and ultrafiltrate (pg/mL).*

Time point	Serum		Ultrafiltrate	Sieve coefficient	Scavenging coefficient
	Artery	Vein			
0	174±29	/	/	/	/
1h after the starting of CVVH	185±35	178±33	8±4	0.04±0.01	4±7
12h after the starting of CVVH	233±27*	237±44	10±5	0.03±0.03	-3±5
At the end	314±39*	318±31	7±3	0.02±0.03	-2±3

**: P<0.05*

Table III. *Comparison of NO concentration of serum and ultrafiltrate (μmol/L).*

Time point	Serum		Ultrafiltrate	Sieve coefficient	Scavenging coefficient
	Artery	Vein			
0	189±25	/	/	/	/
1 h after starting CVVH	178±27	151±31[a]	31±10	0.23±0.05	21±8
12 h after starting CVVH	144±32*	122±19[a]	27±8	0.26±0.11	19±9
After CVVH	113±21*	94±23[a]	25±4	0.21±0.09	23±12

*[a]: P<0.05; *: P<0.05*

lower than the concentration before treatment and the difference had statistical significance (q=3.89, P<0.05); a relatively high level of NO was detected in the ultrafiltrate (Table III).

Correlation regression analysis on NO concentration of artery, MAP and PaO_2

A negative linear correlation was found between NO concentration of artery and MAP (r=-0.83030; y=155.35603-0.49333x; coefficient of determination R2=0.6894) (Fb=b177.57, P<0.01) (Fig. 1).

NO concentration of arterial blood was in a negative linear correlation with MAP, indicating that NO is an important mediator for low blood pressure. Hence CVVH which can effectively eliminate NO may be one of mechanisms for the increase of MAP (Fig. 1).

NO concentration of arterial blood was in a negative linear correlation with PaO_2 (r=-0.7777, y=121.21081-0.31705x, coefficient of determination R2=122.50) (F=122.5, P<0.01) (Fig. 2).

NO concentration tended to decrease while PaO_2 increased as the treatment time prolonged and they were in an obvious negative linear correlation,

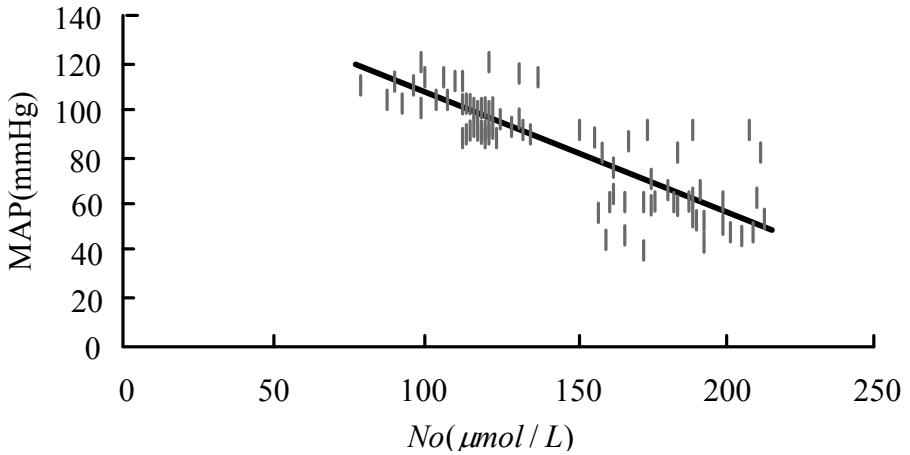

Fig. 1. *Correlation between the concentration of NO and MAP of arterial blood.*

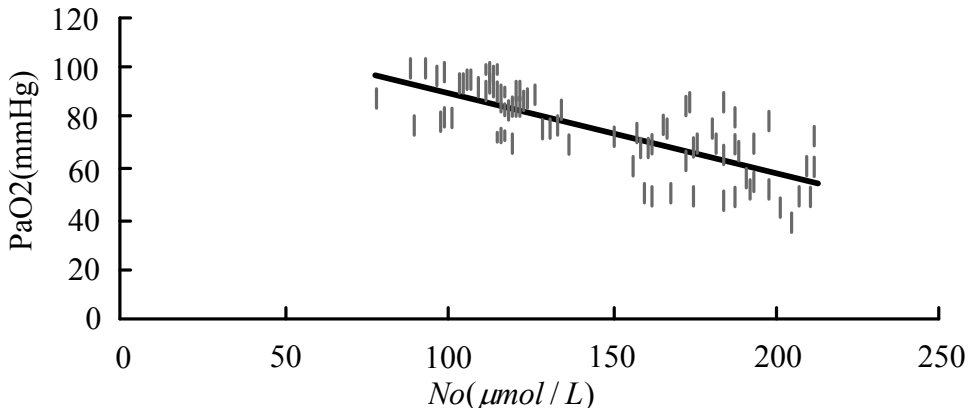

Fig. 2. *Correlation between NO concentration and PaO_2 of arterial blood.*

indicating that elimination of NO with CVVH might be one of the mechanisms for improving respiratory functions (Fig. 2).

DISCUSSION

Pathogenesis of MODS is quite complex (10, 11). Generally, inflammatory reaction has protective effects, but when it becomes very severe or out of control, the inflammatory reaction transforms from protective to harmful, which may result in necrosis and rapid failure of cells and organs. MODS patients usually suffer from severe complications, such as acute renal failure as well as water-electrolyte and acid-base balance disorders. Therefore, many scholars consider eliminating excessive inflammatory mediators as the key of MODS treatment. However, in recent years, CVVH has been extensively applied for treating MODS.

TNF-α, as one of the key pro-inflammatory mediators for MODS, plays a core role in chain reaction induced by inflammatory mediators. After application of endotoxin, the level of TNF-α increased first, which can promote the release of anti-inflammatory mediators such as IL-10 and IL-4 as well as pro-inflammatory mediators such as IL-1 and IL-6 (12). TNF-α as an endogenous pyrogen can induce fever and malnutrition (13). NO, as one of

the mediators, can lower blood pressure (14). IL-10, an important immune negative regulatory factor and anti-inflammatory mediator, can inhibit the secretion of IL-1 and TNF-α.

The results demonstrate that serum TNF-α concentration decreased after treatment, but was not detected in filtrate, suggesting that it was eliminated through absorption rather than convection. Serum IL-10 level at the end of treatment was significantly higher than the level before treatment, which might be because of the generation of a large amount of IL-10 caused by activation of Th2 cells. IL-10 levels of venous blood and arterial blood had no remarkable difference. IL-10 could be detected from the filtrate but the level was low, therefore, CVVH was considered with low effectiveness in eliminating IL-10. NO concentration had a significant decrease; NO concentration in venous blood was much lower than that in the arterial blood. However, high-concentration NO could be detected in the filtrate, which may be because it had a small molecular weight and can be eliminated by CVVH through convection.

Furthermore, the study also found that heart rate and respiratory frequency of patients had significant decline after treatment ($P<0.01$); MAP had significant increase ($P<0.01$); BUN and Scr had remarkable decrease ($P<0.05$ or 0.01); PaO_2 and SaO_2 had apparent increase ($P<0.01$); and hyperkalemia and acidosis were both corrected ($P<0.01$), suggesting CVVH could effective improve rescue achievement ratio of MODS and positively prolong survival period of patients.

ACKNOWLEDGEMENTS

This work was supported by Zhengzhou Science & Technology Basic Research Program (No.340600531794) and by Henan Science & Technology Basic Research Program (No.122300410365).

REFERENCES

1. Vincent JL, Nelson DR, Williams MD. Is worsening multiple organ failure the cause of death in patients with severe sepsis? Crit Care Med 2011; 39(5):1050-55.
2. Schmidt H, Lotze U, Ghanem A, et al. Relation of impaired interorgan communication and parasympathetic activity in chronic heart failure and multiple-organ dysfunction syndrome. J Crit Care 2014; 29(3):367-73
3. Nardocci G, Martin A, Abarzúa S, et al. Sepsis progression to multiple organ dysfunctions in carotid chemo/baro-denervated rats treated with lipopolysaccharide. J Neuroimmunol 2015; 278(15):44-52
4. Pu YC, Yang DK, Mao YQ, Zhang Y, Chen KH. Therapeutic effects of blood purification in treatment of fulminant hepatic failure. Brazilian J Infect Dis 2013; 17(4):427-30.
5. Samue D, Idier I, Mimoz O, Saliba F, Castaing D, Bismuth H. Hemodialysis (HD) and continuous veno-venous hemofiltration (CVVH) in liver transplantation of patients with fulminant hepatitis (FH). J Hepatol 1991; 13:S68.
6. Cole L, Bellomo R, Hart G, Ranco C. A phase II randomized, controlled trial of continuous hemofiltration in sepsis. Crit Care Med 2002; 30:100-106.
7. Smail N, Messiah A, Edouard A, Samii K. Role of systemic inflammatory response syndrome and infection in the occurrence of early multiple organ dysfunction syndrome following severe trauma. Intens Care Med 1995; 21(10):813-16.
8. Sun IF, Lee SS, Lin SD, Lai CS. Continuous Arteriovenous Hemodialysis and Continuous Venovenous Hemofiltration in Burn Patients with Acute Renal Failure. Kaohsiung J Med Sci 2007; 23 (7):344-51.
9. Tegeder I, Neumann F, Bremer F, Brune K, Lötsch J, Geisslinger G. Pharmacokinetics of meropenem in critically ill patients with acute renal failure undergoing continuous venovenous hemofiltration. Clin Pharmacol Therap 1999; 65 (1):50-57.
10. Diltoer M, Laureys M, Huyghens L, Schueren G. Intermittent hemodialysis in critically ill patients with multiple organ dysfunction syndrome is associated with intestinal intramucosal acidosis. Intens Care Med 1996; 22 (8):747-51.
11. Zhu QL, Qian XS, Wang SW, Xu B. A comparison of elderly and adult multiple organ dysfunction

syndrome in the rat model. Experim Gerontol 2006; 41(8):771-77.
12. Hommel D, Hulin A. Cytokine kinetics (TNF, IFN, IL-6) in patient with multiple organ dysfunction syndrome (MODS) treated by continuous veno-venous hemofiltration (CVVH). Réanimation Urgences 1999; 8(3):209-13.
13. Li Ag, Xiong JJ, Chen ZY. IL-6, TNF-α, and iNOS is associated with decreased colonic contraction in rats with multiple organ dysfunction syndrome. J Surg Res 2012; 178(2):e51-e57.
14. Van Dissel JT, Groereveld PHP, Maes B, Feuth HD. Nitric Oxide: a predictor of morbidity in postoperative patients. Lancert 1994; 343:1579-83.

LETTER TO THE EDITOR

BLCA-4 AND UBC COMBINED DETECTION FOR EARLY DIAGNOSIS OF BLADDER CANCER

L. CUI[1], M.M. SUN[2], Z.H. ZHAO[1], J.P. YANG[1], Y.P. ZHENG[1], L.L. HE[1], K.S. CHEN[1] and Q.X. FAN[3]

[1]Department of Pathology, The First Affiliated Hospital of Zhengzhou University, Zhengzhou city, PR China; [2]Department of Pathology, Henan Cancer Hospital, Zhengzhou city, PR China; [3]Medical oncology, The First Affiliated Hospital of Zhengzhou University, Zhengzhou city, PR China

Received November, 17, 2015 – Accepted March 29, 2016

The objective of the present study was to report the clinical significance of bladder cancer specific nuclear matrix protein 4 (BLCA-4) and urinary bladder cancer (UBC) on early diagnosis of bladder cancers. Enzyme-linked immunosorbent assay (ELISA) was used to detect BLCA-4 and UBC of 56 bladder cancer patients and 26 patients with urinary tract benign diseases, serving as controls. Urine exfoliated cell test was performed, and then the significance of BLCA-4 and UBC on the diagnosis of bladder cancers was analyzed. The sensitivity of BLCA-4 and UBC of the bladder cancer patients was significantly higher than that of the urine exfoliated cell test ($P < 0.05$). The difference of BLCA-4 and UBC was not significant ($P > 0.05$). The difference of BLCA-4 and UBC in the tumors with different gradings and stagings was not significant ($P > 0.05$). Combined detection of BLCA-4 and UBC could improve the diagnosis sensitivity and specificity of bladder cancers with the advantages of high maneuverability, repeatability and objective results.

Bladder tumor is one of the most common tumors in the genitourinary system. The incidence of bladder cancer is 7.49 in 100,000 in China, accounting for 2.5% of the malignant tumor onsets. In the last 10 years, the incidence of bladder cancer in China has shown an increasing trend (1). Early diagnosis is a key for the treatment, and the existing standards include urine exfoliated cytology examination, cystoscopy and biopsy. However, the sensitivity of the urine exfoliated cell detection is low, and the invasive cystoscopy inevitably is painful, with risk of infection or hemorrhage (2). Therefore, it is very important to find a non-invasive index for the early diagnosis of bladder cancers. This study applied enzyme-linked immunosorbent assay (ELISA) to detect bladder cancer specific nuclear matrix protein 4 (BLCA-4) and Urinary Bladder Cancer (UBC) of bladder cancer patients.

MATERIALS AND METHODS

Inclusion criteria

Bladder cancer patients were diagnosed and confirmed by cystoscope biopsy and postoperative pathological slice. The patients had not undergone any bladder cancer surgery, radiation therapy, chemotherapy or other related

Key words: bladder tumor, BLCA-4, UBC, combined detection

Mailing address:
Dr Q.X. Fan,
The First Affiliated Hospital,
Zhengzhou University, No. 1, East Jianshe Road,
Zhengzhou City,
450052, People's Republic of China
e-mail: cuili1117@sina.com

0393-974X (2016)

DISCLOSURE: ALL AUTHORS REPORT NO CONFLICTS OF INTEREST RELEVANT TO THIS ARTICLE.

treatments. Patients had no severe functional disorders of heart, lung, liver or kidney. The ethics committee of the First Affiliated Hospital of Zhengzhou University approved the study. An informed consent to participate in the study was signed by each patient. Patients were voluntarily enrolled in the project which conformed to the Declaration of Helsinki.

Study subjects

In this study, there were 82 patients (58 males and 24 females), ages ranging from 32 to 81 years, among whom there were 56 cases of bladder cancer (39 male and 17 female) with ages ranging 46-75 years, average 65 years. Patients were confirmed as having bladder cancer through cystoscopy and postoperative pathological diagnosis, including 8 cases of patients with G1, 32 cases with G2, 16 cases with G3, 2 cases with pTis, 28 cases with pTa, 12 cases with pT1, and 14 cases with pT2. Twenty-six patients (19 males and 7 females; ages 32 to 81 years, average 48 years) had benign urinary diseases. Twelve patients had benign prostatic hyperplasia, 6 had urinary calculi, 4 had urinary tract infection, 2 had neurogenic bladder and 2 had urethral stricture.

Samples and detection

One hundred ml of urine were collected in the morning before cystoscopy testing. Each urine sample was divided into three parts, which were used in the detection of BLCA-4 and UBC and the urine exfoliated cell test. Regular cystoscopy test was employed to observe tumors and biopsies. Tumors were graded based on the surgical sample pathology and imaging.

BLCA-4

BLCA-4 (Catalogue number: CSB-E14959h, Wuhan Huamei Biological Co., Ltd) was detected by ELISA. The cut-off value was 13.0A/μg protein, as described previously (1). One ul protein was incubated for 10 min and the detection absorption wavelength was 490 nm.

UBC

UBC (Catalogue number: IDL-201502, Branch Company of Sweden IDL Biotech) was detected by ELISA. Positive predictive value of UBC diagnosis was based on the instruction and value of 12 μg/L. One ul protein was incubated for 10 min and the detection absorption wavelength was 490 nm.

Urine exfoliated cell test

Acridine Orange and HE staining was employed for observation. The acridine orange staining stages of III to V were taken as positive controls, and the HE staining with medium nuclear heterogeneous, severe heterogeneity and tumor cells were taken as positive controls (3-5).

Statistical analysis

SPSS 16.0 statistical software was used for analysis. Fisher exact probability test was applied for the analysis of the data in the tables. Non-parametric Kruskal-Wallis test was employed for the analysis of the differences between groups.

RESULTS

Comparisons of BLCA-4 and UBC between bladder cancer patients and patients with urinary tract benign diseases

Comparisons between the two groups were calculated, and the positive rates of BLCA-4, UBC test and urine exfoliated cell test in the bladder cancer patients were 87.5% (49/6, 80.4% (45/56) and 42.6% (24/56), respectively. The results from the patients with urinary tract benign diseases were 3.8% (1/26), 11.5% (3/26) and 8.3% (2/26), respectively. The tests of BLCA-4, UBC and urinary tract benign diseases were helpful for the diagnosis of bladder cancers. The BLCA-4 and UBC positive rates were significantly higher than those in the urinary tract benign diseases, as shown in Table I.

Comparisons of sensitivity, specificity, accuracy, positive predictive value and negative predictive values of BLCA-4, UBC and urinary tract benign diseases

The sensitivity, specificity and accuracy were calculated and defined as described previously (8, 11). The sensitivities of BLCA-4 and UBC of bladder cancer patients were significantly higher than those in the urinary tract benign disease patients ($P < 0.05$). However, the differences detected of BLCA-4 and UBC were not significant ($P > 0.05$). There was no significant difference in the three methods on the

specificities. However, the detection accuracies of BLCA-4 and UBC were significantly higher than those in the urine exfoliated cells test patients Table II)

Sensitivity comparisons of bladder cancer different grades and stages from three detection methods

The sensitivities of BLCA-4 and UBC in different grades and stages of bladder cancers were significantly higher than those in the urine exfoliated cell tests. The detection differences of BLCA-4 and UBC in different gradings and stagings were not significant, ($P > 0.05$). The detection sensitivity of the urine exfoliated cells increased with the increasing of the tumor classification, but there were no significant differences in different tumor staging ($P > 0.05$) (Table III).

DISCUSSION

BLCA-4 is a tumor marker for bladder cancer. In 1996, Getzenbery et al. investigated nine kinds of bladder nuclear matrix proteins, of which six kinds of bladder nuclear matrix proteins (BLCA-1,

Table I. *Comparison of BLCA-4, UBC and urine exfoliated cells between the two groups.*

Group	Case	BLCA-4		UBC		Urine Exfoliated Cells Test	
		≥13.0	13.0	≥12	12	Positive	Negative
Bladder Cancer	56	49	7	45	11	24	32
Urinary Tract Benign Disease	26	1	25	3	23	2	24

Table II. *Comparison of sensitivity, specificity, accuracy, positive predictive value and negative predictive value of the three groups.*

Item	BLCA-4	UBC	Urine Exfoliated Cell Test
Sensitivity	87.5 (49/56)	80.4 (45/56)	42.9 (24/56)
Specificity	96.2 (25/26)	88.5 (23/26)	92.3 (24/26)
Accuracy	61.0 (50/82)	58.5 (48/82)	31.7 (26/82)
Positive Predictive Value	98.0 (49/50)	93.8 (45/48)	92.3 (24/26)
Negative Predictive Value	78.1 (25/32)	67.6 (23/34)	42.9 (24/56)

Table III. *Sensitivity comparison of bladder cancer different grading and staging from three detections.*

	Case	BLCA-4 (%)	UBC (%)	Urine Exfoliated Cell Test (%)
Tumor Grading				
G1	8	75.0 (6)	62.5 (5)	12.5 (1)
G2	32	93.8 (30)	87.5 (28)	43.8 (14)
G3	16	81.2 (13)	75 (12)	56.3 (9)
Tumor Staging				
pTis	2	100.0 (2)	100.0 (2)	0 (0)
pTa	28	92.8 (26)	85.7 (24)	42.9 (12)
Pt1	12	83.3 (10)	75.0 (9)	50.0 (6)
≥pT2	14	78.6 (11)	71.4 (10)	57.1 (8)

BLCA-2, BLCA-3, BLCA-4, BLCA-5 and BLCA-6) existed only in the bladder cancer tissues but not the normal bladder tissues. This study laid a basic theory and experiment to explore the significance of BLCA in the diagnosis of bladder cancer (6). Van et al. found that BLCA-4 was one of the important members of the ETS transcription factor family (7). ETS transcription factors were involved in cell apoptosis, carcinogenesis, expression of vascular endothelial growth factor, angiogenesis and local diffusion and metastasis (7). Through the dot immunochro-matography assay, the prepared BLCA-4 antibodies were applied to detect the BLCA-4 expression in bladder cancer tissues and bladder cancer surrounding tissues. The sensitivity was 96.4% and the specificity was 100%. It could be used as a marker of bladder cancer (8). In addition, another study indicated that urine BLCA-4 could not be interfered by other benign diseases, such as benign prostatic hyperplasia, urolithiasis and urinary

tract infection, which could be applied in the normal bladder cancer screening (9). This study showed that the sensitivity of BLCA-4 was 87.5% and its specificity was 96.2% (25/26) in the diagnosis of bladder cancers.

UBC is actually the soluble CK8 and CK18 fragment of the bladder tumor tissues. CK is a sign of epithelial differentiation. Different types of epithelial cells have their particular types of CK expression. CK7, CK8, CK18, CK19 and CK5 were expressed in the normal urinary transitional epithelial cells and the urinary tract epithelial tumors (10).

Shoshtari MA etal. (11) found that the differences of the UBC concentrations between the bladder cancer patients, patients with benign urinary tract diseases and healthy volunteers were significnt. TBoth the dectedion sensiti2.0% its specificity of C wa82.6%high □(11). At the same time, the sensitivity of exfoliative urine cytology test was 60.7% and its specificity was 86.9%. The comparative differences were significant ($P < 0.05$). More importantly, for the low differentiation of the bladder cancer patients, the detection sensitivity of UBC was significantly higher than that in the urine cytology examination. Konkialas et al. also found that the detection sensitivity of UBC was higher than that in the urine cytology test, while the specificity was basically similar (12). In this study, the results showed that the urinary UBC value in the bladder cancer patients was higher than that in the patients without bladder cancer, and the sensitivity and specificity were similar.

Although Feng CC et al. (8) and Shoshuster e et al. (11) have already demonsd ththe useapplication of these two markers of BLCA4 and UBC for the diagnosis of bladdercas, and the combined detection method of BLCA-4 and UBC used in this study could improve the sensitivity and specificity of the diagnoof the bladder resl as. ItitThe method in thisudy hadillustrates high clinical significan the diagnosis low-upss.

At present, there are a few clinical comparative studies of BLCA-4 and UBC in China. This study shows that both have high sensitivity, while there was no statistically significant differences between them. BLCA-4 and UBC detection were better than urine exfoliated cell test. However, there was no statistically significant differences between the gradings and stagings. Combined detection could improve the diagnosis sensitivity and specificity of bladder cancers.

There are some limitations to the study. First of all, the number of bladder cancer cases in this study was limited, and the results need to be further confirmed by larger cohorts. Furthermore, the detection method of ELISA was time-consuming and laborious. Finally, whether BLCA-4 and UBC can serve as a biomarker of bladder cancer still needs to be investigated.

Due to the shortages of the tumor marker itself, single detection of some markers for tumor diagnosis had more defects. Two or more markers of the combined detection were better (12-15). The urinary tumor markers could not completely replace cystoscopy. The combined detection of the markers could improve the accuracy of diagnosis and minimize the quantity of cystoscopy applications or the extension of the periods between cystoscopies. It could monitor recurrence of bladder cancer and screen hematuria or bladder cancer with bladder irritation, which was the objective of the study on bladder tumors. Combined detection of BLCA-4 aity andcan provide objective results, and it had promising clinical significance in the diagnosis of bladder cancer and follow-up.

REFERENCES

1. Liu Z, Tian Q, Xia S, Yin H, Yao D, Xiu Y. Evaluation of the improved tubeless cutaneous ureterostomy technique following radical cystectomy in cases of invasive bladder cancer complicated by peritoneal metastasis. Oncol Lett 2016; 11:1401-05.
2. Dey P. Urinary markers of bladder carcinoma. Clin Chim Acta 2004; 340:57-65.
3. Henry CJ, Tyler JW, McEntee MC, et al. Evaluation of a bladder tumor antigen test as a screening test for transitional cell carcinoma of the lower urinary tract in dogs. Am J Vet Res 2003; 64:1017-20.
4. Eissa S, Kassim S, El-Ahmady O. Detection of bladder tumours: role of cytology, morphology-based assays, biochemical and molecular markers. Curr Opin Obstet Gynecol 2003; 15:395-403.

5. Otto W, Denzinger S, Fritsche HM, et al. Introduction and first clinical application of a simplified immunohistochemical validation system confirms prognostic impact of KI-67 and CK20 for stage T1 urothelial bladder carcinoma: single-center analysis of eight biomarkers in a series of three hundred six patients. Clin Genitourin Cancer 2013; 11:537-44.
6. Getzenberg RH, Konety BR, Oeler TA, Quigley MM, Hakam A, Becich MJ, Bahnson RR. Bladder cancer-associated nuclear matrix proteins. Cancer Res 1996; 56:1690-94.
7. Van Le TS, Myers J, Konety BR, Barder T, Getzenberq RH. Functional characterization of the bladder cancer marker, BLCA-4. Clin Cancer Res 2004; 10 :1384-91.
8. Feng CC, Wu Z, Jiang HW, Wen H, Guan M, Ding Q. Urinary BLCA-4 level is useful to detect upper urinary tract urothelial cell cancinoma. Actas Urol Esp 2012; 36:597-602.
9. Konety BR, Nguyen TS, Brenes G, Sholder A, Lewis N, Bastacky S, Potter DM, Getzenberg RH. Clinical usefulness of the novel marker BLCA-4 for the detection of bladder cancer. J Urol 2000; 164:634-39.
10. Silen A, Rizvi SS, Letocha H, Lennernas B, Wiklund B. Evaluation of the UBC test in the urine of healthy individuals, patients with benign disorders and urinary bladder cancer. Oncol Rep 2000; 7:1269-74.
11. Shoshtari MA, Soleimani M, Moslemi M. Comparative evaluation of urinary bladder cancer antigen and urine cytology in the diagnosis of bladder cancer. Urol J 2005; 2:137-40.
12. Konety BR, Nguyen TS, Brenes G, Sholder A, Lewis N, Bastacky S, Potter DM, Getzenberg RH. Clinical usefulness of the novel marker BLCA-4 for the detection of bladder cancer. J Urol 2000; 164:634-39.
13. Eissa S, Swellam M, Sadek M, Mourad MS, EI Ahmady O, Khalifa A. Comparative evaluation of the nuclear matrix protein, fibronectin, urinary bladder cancer tumor. J Urol 2002; 168: 465-69.
14. Saint-Jacques N, Lee JS, Brown P, Stafford J, Parker L, Dummer TJ. Small-area spatio-temporal analyses of bladder and kidney cancer risk in Nova Scotia, Canada. BMC Public Health 2016; 16:175.
15. Lee MH, Thomas JL, Chang YC, Tsai YS, Liu BD, Lin HY. Electrochemical sensing of nuclear matrix protein 22 in urine with molecularly imprinted poly(ethylene-co-vinyl alcohol) coated zinc oxide nanorod arrays for clinical studies of bladder cancer diagnosis. Biosens Bioelectron 2016; 79:789-95.

LETTER TO THE EDITOR

THROMBIN IN COMBINATION WITH INTENSIVE NURSING IN TREATING UPPER GASTROINTESTINAL BLEEDING IN CHILDREN

F. YANG, ML. XIANG and YM. LIU

Second Ward of Pediatric Medicine Department, the First Affiliated Hospital of Zhengzhou University, Zhengzhou, China

Received September 10, 2015 – Accepted April 13, 2016

Pediatric upper gastrointestinal bleeding, a commonly seen pediatric emergency, needs timely symptomatic treatment to avoid a worse outcome. To discuss the clinical effect of thrombin treatment in combination with intensive nursing on pediatric upper gastrointestinal bleeding, this study analyzed 128 children who were treated in the second ward of the Children's Internal Medical Department in the First Affiliated Hospital of Zhengzhou University between February 2012 and December 2014. The patients were divided into two groups, an experimental group and a control group. Besides thrombin, the experimental group was given intensive nursing, consisting of regular nursing and targeted nursing, while the control group was given regular nursing only. Clinical indexes of the two groups, such as effective rate, nursing satisfaction and side effect rate, were compared. Relevant clinical indexes such as duration of hospital stay, time to stopping of bleeding and Self-Rating Anxiety Scale (SAS) score, as well as overall satisfaction level of the observation group were all better than those of the control group and differences between the two groups had statistical significance (P<0.05). Furthermore, difference of overall effective rate between the experimental group (90.63%) and the control group (68.75%) was significant. Difference of incidence of side effects between the two groups was statistically significant. Thus thrombin treatment in combination with intensive nursing proved to have a remarkable clinical effect and high safety level in treating pediatric upper gastrointestinal bleeding and, moreover, it shortens treatment time and enhances the patients' quality of life.

Upper gastrointestinal bleeding, a critical pediatric disease, results from peptic ulcer and acute erosive gastritis (1). As children have poor local defense functions due to their immature digestive tract, they are easily injured by digestive tract damage and ulcer caused by invasion of pepsase, gastric acid and *Helicobacter pylori*. Once ulcerative blood vessels are invaded, upper gastrointestinal bleeding will occur, and delayed treatment can even threaten patients' lives (2-4). To date, the disease is mainly treated with hemostats and antacids in the clinic (5). For example, thrombin extracted from pig blood can shorten blood coagulation time by quickening transformation of contractinogen into fibrae sanguis or stopping bleeding by filling the hemorrhagic spot. However, its curative effect is not satisfactory due to poor prognosis.

Therefore, children suffering from upper

Key words: thrombin, upper gastrointestinal bleeding, intensive nursing, overall effective rate

Mailing address:
Dr Yanmian Liu,
Second Ward,
Pediatric Medicine Department, First Affiliated Hospital,
Zhengzhou University, No. 1, Jianshe East Road,
Zhengzhou, 450052, China
e-mail: ymliuliuym@163.com

0393-974X (2016)

gastrointestinal bleeding should be given more careful clinical nursing besides emergency treatment. Intensive nursing refers to performing etiological treatment and symptomatic nursing, carefully monitoring conditions of patients including temperature, blood pressure, urine volume, pulse, melena and haematemesis and strengthening diet. Upper gastrointestinal hemorrhage, a serious disease, is aggravated due to patients' feeling of fear; at that moment, compliance of patients to treatment can be treatment can be improved if mental nursing is strengthened to relieve anxiety emotion of patients (6, 7).

Hence we carried out an analysis on data of 128 children who developed upper gastrointestinal bleeding and received treatment in the First Affiliated Hospital of Zhengzhou University, comparing nursing strategies for those children and providing a clinical basis for curative effect improvement.

MATERIALS AND METHODS

General information

One hundred and twenty-eight children who developed upper gastrointestinal bleeding and were treated in the First Affiliated Hospital of Zhengzhou University between February 2012 and December 2014 were selected. The patients were presented symptoms of coffee-like vomiting fluid and melenaand were diagnosed with upper gastrointestinal bleeding through gastroscopy. Those who had severe basic diseases, coagulation disorders and bleeding disorders, or were difficulty to undergo gastroscopic examination were excluded. The patients were divided into two groups. The experimental group included 64 patients, including 50 males and 14 females, with ages ranging from 1 to 6 years, average (3.52±2.01) years, and weight ranging from 8 to 21 kg, average (14.51±3.2) kg. The causes of bleeding for these patients included gastric ulcer (8 cases), erosive gastritis (16 cases), duodenal ulcer (20 cases), and duodenal gastritis (20 cases). Of the 64 patients in the control group, 48 were males and 16 were females, with ages ranging from 1 to 7 years, average (4.01±2.35) years, and weight ranging from 9 to 21 kg, average (15.22±4.01) kg. Causes of bleeding in the control group included 6 cases of gastric ulcer, 16 of erosive gastritis, 22 of duodenal ulcer, and 20 of duodenal gastritis. The parents or guardians of all the patients signed informed consent before the study. There was no statistically significant difference in general data between the two groups, therefore, the results were comparable.

Thrombin delivery pattern

Patients were intravenously injected with 2 mg/kg diprivan whilst undergoing gastroscopy and being supplied with oxygen (8). After eyelash reflex, patients were inserted with a gastroscope so that the operator could determine the ulcer bleeding area; then local lesions were washed by icy physiological saline. Once the succus gastricus was completely absorbed, patients were injected locally with 400 U thrombin in the bleeding areas. The gastroscope was removed when bleeding stopped. Patients were forbidden to eat within 24 h after treatment.

Nursing pattern

Patients in the control group were given regular clinical nursing, such as observation of disease conditions, evaluation of bleeding volume and quality of life indexes (9). On the basis of regular nursing, patients in the experimental group were treated with additional nursing as follows. The first was mental nursing. Clinical performances caused by acute hemorrhage of the digestive tract have a negative effect on patients' psychology, resulting in passive treatment due to lack of confidence; therefore, paramedics are required to provide patients with psychological service and instruction of disease-related knowledge. Moreover, paramedics can introduce ward-mates who obtain satisfying results with other patients as they help to increase their confidence. Haematemesis and melena needed to be timely cleared to avoid malignant effects and feeling of fear. Next was particular nursing for bleeding. After drugs were applied to stop bleeding, side effects and severity were closely observed to prevent local pain caused by medicine exosmosis; when somatostatin was applied to stop bleeding, blood pressure was closely monitored. Hemostatics were forbidden to be used since they may cause severe side effects. In addition, blood volume was supplemented in time to create venous channels; and blood transfusion was also needed. If the disease condition worsens, plasma is necessary. In cases of emergency, blood should be transfused immediately; blood transfusion can be slowed down if the disease condition is relieved. The next step was nursing for cases of shock. It is important to supply blood for patients, which should be given immediately in cases of emergency. In

addition, indexes, such as blood pressure, pulse and urinary production (UPD) must be intensely monitored to adjust infusion speed, in order to prevent side effects such as heart failure, pneumonedema and elevation of blood pressure caused by high speed infusion. Diet nursing was also required. Patients were not allowed to eat when they were bleeding to reduce gastric acid, slow down peristole and avoid more severe bleeding caused by food stimulus. Liquid diet (base-forming food, such as milk and rice-water) was allowed 24 hours after bleeding stopped, and soft diet was available when the disease condition became stable. To be more specific, patients needed digestible foods with high calories, protein and vitamins, and avoided pungent and rough foods, and strong tea. The final step was decubation nursing. During decubation, patients ate a healthy and reasonable diet without rough and spicy foods (more meals a day but less food each time) and drank more water. Family members were advised to prepare rational and nutritional diets for the patients.

Curative effect standards

Treatment was considered to be significantly effective if fecal occult blood and gastric occult blood drainage appeared to be negative within 48 hours after the clinical intervention; treatment was determined as effective if active hemorrhage remained within 48 hours after the clinical intervention, defection frequency and nasogastric tube drainage reduced, and fecal occult blood and gastric occult blood drainage was negative within 96 hours after clinical intervention. Treatment was considered as ineffective if active hemorrhage continued within 96 hours after clinical intervention, and defection frequency and nasogastric tube drainage remained unchanged.

Statistical analysis

SPSS ver. 19.0 was used to process and analyze data. Enumeration data was expressed as number of cases (n); comparison between groups was performed using *chi*-squared and *t*-test, and average value was expressed as Mean ± SD. Difference was considered to be statistically significant if $P<0.05$.

RESULTS

Comparison of clinical indexes

In the clinical index changes before and after the treatment, the nursing effect of the experimental group was much better than that of the control group, and the difference between them was statistically significant (Table I).

Table I. *Comparison of clinical indexes.*

Group	SAS (Self-Rating Anxiety Scale) score	Time to stopping of bleeding (d)	Duration of hospital stays (d)	
	Admission	After intervention		
Experimental group	46.3±9.5	26.5±4.5	2.5±0.53	7.0±8.0
Control group	46.0±9.4	32.5±5.0	3.8±0.75	9.8±1.3
P	>0.05	<0.05	<0.05	<0.05

[n (%); Mean ± SD; 64 cases in each group]

Note: experimental group: thrombin+intensive nursing; control group: thrombin+conventional nursing

Table II. *Comparison of clinical nursing satisfaction.*

	Admission	After intervention		
Experimental group	46.3±9.5	26.5±4.5	2.5±0.53	7.0±8.0
Control group	46.0±9.4	32.5±5.0	3.8±0.75	9.8±1.3
P	>0.05	<0.05	<0.05	<0.05

[n(%); 64 cases in each group]
Note: experimental group: thrombin+intensive nursing; control group: thrombin+conventional nursing

Comparison of clinical nursing satisfaction

Table II shows that nursing satisfaction of the experimental group (98.5%) was much higher than that of the control group (83%) (Table II).

Comparison of clinical effective rate between the two groups

Comparison of curative effects between two groups suggested that treatment of 38 patients in the observation group achieved a remarkable effect, 20 patients achieved effective treatment and treatment of 6 patients was ineffective (overall effective rate: 90.63%); in the control group, the corresponding number of patients was 18, 26 and 20, respectively, (overall effective rate: (68.75%). The difference of overall effective rate between the two groups had no statistical significance (χ^2=6.35, P<0.05).

Comparison of side effects between the two groups

Incidence of side effect in the control group reached 6.25% (2 cases of vomiting and 2 cases of dysphoria); while only 1 case in the experimental group suffered vomiting. Thus there was no statistically significant difference.

DISCUSSION

Acute hemorrhage of the upper gastrointestinal tract, a common pediatric internal medicine disease, involves bleeding caused by lesions in the oesophagus, stomach, pancreas, biliary passage and duodenum; its incidence and fatality rate both tend have risen in recent years (10, 11). Pediatric upper gastrointestinal bleeding shows no typical clinical symptoms (12). Children cannot describe their conditions in an accurate way, leading to difficulties for clinical diagnosis, including misdiagnosis and missed diagnosis. The disease condition is worse and even threaten patients' lives if there is a great amount of bleeding (13). Currently, treatment for pediatric upper gastrointestinal tract mainly focuses on drug intervention using medicines for vasoconstriction and anapetia (14, 15). However, because of poor prognosis, clinical nursing is indispensable to guarantee curative effects, besides necessary emergency measurements. In this study, satisfaction on nursing of the control group was 83% since patients could not receive perfect nursing, while that of the experimental group reached 98.5% because of the intensive and all-round nursing service (intensive nursing). With regard to the clinical effect, relevant clinical indexes such as SAS score, time to stop bleeding and duration of hospital stays in the experimental group were all better than those of the control group. Moreover, the experimental group had an overall effective rate of 90.63%, which was much higher than 68.75% in the control group.

To sum up, treating pediatric upper gastrointestinal bleeding with thrombin in combination with intensive nursing proved to be safe and effective,

providing powerful evidence for its promotion in clinical application.

REFERENCES

1. Yeom HJ, Shim KN, Kim SE, et al. Clinical characteristics and predisposing factors of complications of caustic injury of the upper digestive tract. Gastrointest Endosc 2005; 61(5):AB158.
2. Derkay CS, Lefebvre SM, ST George MR. Retrieving foreign bodies from upper aerodigestive tracts of children. AORN J l 1994; 60(1):53-61.
3. Prandi D, Rueff B, Roche-Sicot J, Sicot C, Maillard JN, Benhamou JP, Fauvert R. Life-threatening hemorrhage of the digestive tract in cirrhotic patients: An assessment of the postoperative mortality after emergency portacaval shunt. Am J Surg 1976; 131(2):204-9.
4. Yin JJ, Zhang AD, Dong CQ, Ren JC. An aptamer-based single particle method for sensitive detection of thrombin using fluorescent quantum dots as labeling probes. Talanta 2015; 144(1):13-19.
5. Greenspoon J, Barkun A, Bardou M, et al. Management of patients with nonvariceal upper gastrointestinal bleeding. Clin Gastroenterol Hepatol 2012; 10(3):234-239.
6. Fernández de Sevilla E, Echeverri JA, Boqué M, et al. Life-threatening upper gastrointestinal bleeding due to a primary aorto-jejunal fistula. Int J Surg Case Rep 2015; (8):25-28.
7. Cesaroa P, Kohn A, Petruziello L, et al. A survey on mortality from non-variceal upper gastrointestinal bleeding: is the emergency referral system adequate? Dig Liver Dis 2013; 45(11):953-56.
8. Crooks CJ, West J, Card TR. Comorbidities affect risk of nonvariceal upper gastrointestinal bleeding. Gastroenterology 2013; 144(7):1384-93.
9. Parikh K, Ali MA, Wong RC. Unusual causes of upper gastrointestinal bleeding. Gastrointest Endosc Clin N Am 2015; 25(3):583-605.
10. Buscarini E, Conte D, Cannizzaro R, et al. White paper of Italian gastroenterology: delivery of services for digestive diseases in Italy: weaknesses and strengths. Dig Liver Dis 2014; 46(7):579-89.
11. Duncan EM, Cuthbertson BH, Prior ME, et al. The views of health care professionals about selective decontamination of the digestive tract: An international, theoretically informed interview study. J Crit Care 2014; 29(4):634-40.
12. Swain P. Gastrointestinal bleeding: endoscopic treatment of peptic ulcer haemorrhage. Baillieres Clin Gastroenterol 1991; 5(3):537-61.
13. Miyake K, Akimoto T, Hanada Y, et al. Proton pump inhibitors are associated with lower gastrointestinal tract bleeding in low-dose aspirin users with ischaemic heart disease. Dig Liver Dis 2015; 47(9):757-62.
14. Miller DT, Roque DM, Santin AD. Use of Monsel solution to treat obstetrical hemorrhage: a review and comparison to other topical hemostatic agents. AM J Obstet Gynecol 2015; 212(6):725-35.
15. Eren E, Başoğlu MS, Kulduk E, Şimsek F, İnan S. Mucosal trauma induced apoptosis in guinea pig middle ear: Comparision of hemostatic agents. Int J Pediatr Otorhinolaryngol 2014; 78(12):2222-28.

JOURNAL OF BIOLOGICAL REGULATORS & HOMEOSTATIC AGENTS Vol. 30, no. 2, 497-504 (2016)

LETTER TO THE EDITOR

ELEVATED EXPRESSION OF RUNT-RELATED TRANSCRIPTION FACTORS IN HUMAN ABDOMINAL AORTIC ANEURYSM

J. DUBIS[1], M. LITWIN[1], D. MICHALOWSKA[1], N. ZUK[1], A. SZCZEPANSKA-BUDA[1], R. GRENDZIAK[1,2], D. BACZYNSKA[3], P. BARC[4] and W. WITKIEWICZ[1,2]

[1]Wrovasc – Integrated Cardiovascular Centre, Regional Specialist Hospital in Wroclaw, Research and Development Centre, Wroclaw, Poland; [2]Department of Vascular Surgery, Regional Specialist Hospital in Wroclaw, Research and Development Centre, Wroclaw, Poland; [3]Molecular Techniques Unit, Department of Forensic Medicine, Wroclaw Medical University, Wroclaw, Poland; [4]Department of Vascular Surgery, General and Transplantation in Wroclaw University Hospital, Wroclaw, Poland

Received July 10, 2015 – Accepted April 20, 2016

Abdominal aortic aneurysm (AAA) is a multifactorial disease of unknown etiology. AAA is caused by segmental weakening of the aortic walls and progressive aortic dilation leading to the eventual rupture of the aorta, accompanied by intense inflammation. Additionally, studies have indicated a close relationship between the pathogenesis and progression of AAA and cellular immune responses in aneurysm wall tissue. The Runt-related genes (RUNX) encode multifunctional mediators of the of intracellular signal transduction pathways in vascular remodeling, endothelial function, immune response and inflammation. The aim of this study was to evaluate the expression level of RUNX regulatory genes in AAA tissues and to assess the correlations between them. The study was performed on AAA wall-tissue samples obtained from patients with AAA during open aneurysm repair and normal aortic tissues collected from healthy organ donors. There are no proven clinical management strategies or pharmaco-therapeutics to prevent AAA progression once an AAA has been detected. Moreover, so far no biomarkers have been established to indicate the disease status of AAA. Hence, understanding the pathogenesis of AAA has recently become an increasing priority in basic and translational vascular research. We identified significantly higher mRNA and protein level of all of three Runt-related genes in aneurysmal aorta compared to a normal aorta. Increased expression of RUNX2 was demonstrated for the first time in abdominal aortic aneurysm tissue. Additionally, relationships between the activity of RUNX genes in the pathological tissue were identified. The results of elevated expression of RUNX genes and their relationships in the AAA tissues suggest the involvement of conserved Runt-related genes in the pathophysiology of AAA development.

The pathophysiology of AAA is complex and involves abnormalities related to extracellular matrix remodeling, degradation and thinning of the vessel wall, resulting in widening of the aortic diameter and sometimes its rupture (1, 2). AAA development is marked by intensified immune response and dominant role of the cellular immune response processes, e.g., involving cytotoxic

Key words: abdominal aortic aneurysm, Runt-related genes, gene expression, signaling pathways

Mailing address:
Joanna Dubis, PhD
Regional Specialist Hospital in Wroclaw
Research and Development Centre
Kamienskiego 73a, 51-124 Wroclaw, Poland
tel +48713270538
e-mail: dubis@wssk.wroc.pl

0393-974X (2016)

DISCLOSURE: ALL AUTHORS REPORT NO CONFLICTS OF INTEREST RELEVANT TO THIS ARTICLE.

natural killer cells (NK). A significant risk factor for developing an aneurysm is atherosclerosis and aortic endothelial dysfunction which occurs as a result of its development (2-5). The Runt-related genes (RUNX1, RUNX2, RUNX3) encode evolutionarily conserved transcription factors that play an essential role in diverse intracellular signaling pathways (6, 7). RUNX proteins are integral components of signaling cascades mediated by transforming growth factor-β (TGFβ) and mainly regulate Wnt signal transduction pathway (6, 8, 9). Wnt is involved in fundamental processes of cells. It affects endothelial function, vascular smooth muscle cell proliferation, cell migration, formation of foam cells, immune response and angiogenesis (8). *RUNX1* and *RUNX3* are important regulators of the immune processes, mainly those related to T-cell immunity (10). *RUNX2* regulates the endothelial function (11, 12). Aberrant activity of *RUNX* genes induces neoplasts, and recently their role in atherosclerosis has been described (6, 13).

Disrupted regulation of the Wnt pathway causes intensification of the inflammation processes, thinning of vessels and atherosclerotic plaque development (8). The subject literature lacks comprehensive information on disruption of the regulatory mechanisms of Wnt pathways involved in the pathophysiology of vascular disease, including AAA. Therefore, the aim of our study was to determine the expression level of *RUNX* regulatory genes in AAA tissue and to define relationships between them.

MATERIALS AND METHODS

Patients and clinical sample collection

The study was conducted in accordance with the Helsinki Convention and approved by the local Ethics Committee of Wroclaw Medical University. Written informed consent was obtained from all the patients before enrolment in the study. Samples of abdominal aortic aneurysm were obtained from 64 patients operated on at the Department of Vascular, General and Transplantation Surgery, Wroclaw Medical University, between 2009 and 2012. Subjects comprised 54 males and 10 females, with ages ranging from 60 to 80 years. The control group consisted of 12 healthy donors aged 30-45. All tissues samples were collected in RNAlater solution (Sigma, USA), frozen and stored at -20°C until use. Characteristics of patients with AAA are presented in Table I.

Quantitative real-time RT-PCR assay

Total RNA was extracted from tissues using Trizol reagent (Sigma, USA) and RNeasy Tissue Mini Kit (Qiagen, Netherlands) following the manufacturer's instructions. DNase digestion (Qiagen, Netherlands) was performed to remove genomic DNA. Concentration and quality of isolated RNA was measured in the NanoDrop 2000 spectrophotometer. For reverse transcription reaction, 1 µg of RNA was used. Reverse transcription reaction was performed using High Capacity cDNA Reverse Transcription Kit (Life Technologies, USA) according to the instructions of the manufacturer. The transcribed cDNA was used for the subsequent real-time PCR using TaqMan Fast Universal PCR Master Mix and TaqMan Gene Expression Assays (Life Technologies, USA): Hs00257856_s1 specific for human *RUNX1*, Hs00231692_m1 for *RUNX2*, Hs00231709_m1 for *RUNX3* and Hs039299097_g1 for GAPDH. All target genes and a housekeeping gene (*GAPDH*) were run simultaneously and reactions were carried out in triplicate wells on a 96-well optical reaction plate in 25 µl reaction volume, using the StepOnePlus Real-Time PCR System (Applied Biosystems, USA). The reactions were conducted in defined conditions: preliminary denaturation at 95°C for 20 s, denaturation at 95°C for 1 s, annealing of primers and probes and synthesis at 60°C for 20 s, for 40 cycles. For quantification, the samples were normalized against the expression of *GAPDH* mRNA. Relative quantification (RQ) of mRNA for the examined genes was calculated using the $^{\Delta\Delta}$Ct method.

Isolation of tissue extracts

For Western blotting analysis, aortic biopsies were snap frozen in liquid nitrogen and ground under liquid nitrogen using a cryogenic mixer ball mill (MM400, Retsch, Germany). Total proteins were extracted using T-per Buffer (Thermo Scientific, USA) containing protease inhibitor cocktail (Sigma, USA). Tissue homogenates were obtained by vortexing samples for 30 min at 4°C and centrifugating at 12,000 rpm for 15 min at 4°C. Supernatants were pooled, portioned and stored at -70°C until analysis.

Total protein concentrations in tissue extracts were determined using a bicinchoninic acid (BCA) protein assay method, according to the manufacturer's instructions (Sigma, USA). Samples of an identical amount of protein (30 μg) were separated by 12.5% polyacrylamide gel electrophoresis in the presence of sodium dodecyl sulfate (SDS-PAGE) according to Laemmli (38), followed by transfer to nitrocellulose membrane, using the procedure described by Towbin et al. (39). Monoclonal, mouse anti-RUNX1, anti-RUNX2 and anti-RUNX3 antibodies (Santa Cruz Biotechnology, USA) were used for RUNX1, RUNX2 and RUNX3 identification, respectively. GAPDH, labeled by mouse anti-GAPDH antibody (Santa Cruz Biotechnology, USA), was used as an internal loading control. Goat anti-mouse antibodies conjugated to horseradish peroxidase (HRP) were applied according to the manufacturer's protocols. Immunoblots were developed using the Western blotting Luminol Reagent (Santa Cruz Biotechnology, USA) and scanned using the imaging system Stella (Raytest, Germany). All experiments were carried out in triplicate.

Statistical analysis

Statistical analyses were performed and graphs plotted using STATISTICA software, version 9 (StatSoft, Poland). Data were evaluated using the Mann-Whitney U-test. The correlations between variables (expression of *RUNX1*, *RUNX2*, *RUNX3*) were calculated by Spearman correlation coefficients. The results were considered as statistically significant at p values < 0.05.

RESULTS

Elevated erexpression of Runx1, Runx2 and Runx3 in AAA tissues

Real-time PCR analysis was performed to quantify the expression level of *RUNX1*, *RUNX2* and *RUNX3* genes in the artery from abdominal aortic aneurysm patients. As presented in Fig. 1, *RUNX* mRNA expression was significantly up-regulated in the AAA tissues examined compared to control aortas. Statistical analysis using the Mann–Whitney U-test revealed that the observed change

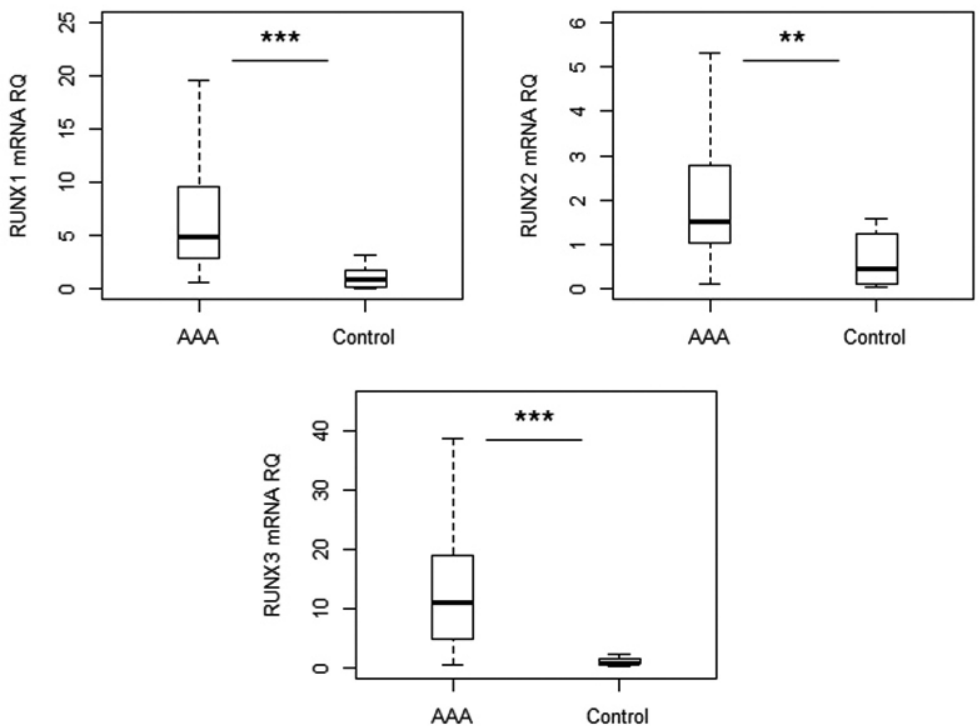

Fig. 1. *Relative quantification (RQ) of mRNA for the examined genes. (** p ≤0.001, *** p≤ 0.0001).*

in mRNA expression was statistically significant. Higher mRNA levels of *RUNX1*, *RUNX2* and *RUNX3* were observed in tissues from patients with AAA as a whole (n=64) compared to the control group (n=12). The mean values ±SD of the relative *RUNX1*, *RUNX2* and *RUNX3* mRNA levels in tissues from patients with AAA compared to the control group were 7.07±6.568 *vs* 1.046±0.988 (p=0.0001), 2.597±4.14 *vs* 0.957±1.2984 (p=0.0038) and 16.243±17.19 *vs* 1.138±0.6074 (p=0.0001), respectively. Furthermore, the material collected and the results obtained were divided into two groups: small AAAs with a diameter less than 45 mm (n=3) and large AAAs with a diameter greater than 65 mm (n=47). Analysis of the results showed that in the group of large AAAs the *RUNX1* and *RUNX2* gene expression is greater than in the whole group when compared with the control group: respectively, 9.52 (p=0.0001) *vs* 7.07 (p=0.0001) and 4.46 (p=0.01) *vs* 2.6 (p=0.004) for *RUNX1* and *RUNX2* genes. In the analyzed groups, no change was observed in the expression of *RUNX3* gene; 16.55 (p=0.0001) *vs* 16.24 (0.0001). Unfortunately, due to the lack of small AAAs, statistical analysis was not possible.

Following expression analysis at the mRNA level, we determined the expression of the analyzed factors in the AAA tissue samples at the protein level. Western blot assay was carried out using normal aortic tissue and AAA tissue specimens with known levels of *RUNX1*, *RUNX2* and *RUNX3* expression by quantitative real-time RT-PCR analysis (n=12). Results showed that the examined factors were commonly expressed in normal aortas but overexpressed in all analyzed AAA tissues (Fig. 2).

Relationship between gene expression of RUNX1, RUNX2 and RUNX3

Significant positive correlations between the mRNA expression of *RUNX1* and *RUNX2* (R=0.768, p≤0.0001), *RUNX1* and *RUNX3* (R=0.472,

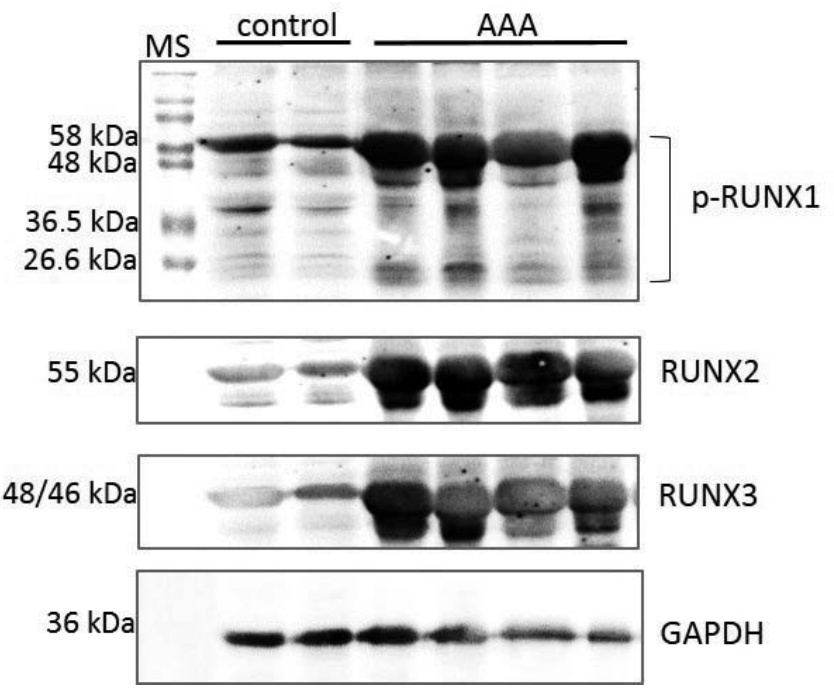

Fig. 2. *Expression of Runx1, Runx2, Runx3 proteins detected by Western blot analysis. Representative immunoblot of Runx1, Runx2 and Runx3 level in abdominal aneurysm aorta and control aortic samples. Equal amount of tissue extracts was separated on SDS-PAGE followed by Western blot analysis. Monoclonal anti-Runx1, 2, 3 and anti-GAPDH antibodies were used for Runx1, 2, 3 and GAPDH identification, respectively. GAPDH was used as the internal loading control.*

Table I. *Clinical characteristics of patients with AAA.*

Characteristic	Mean ± SD (Range) or Number of Patients (%) n=64
Age (years)	66.5 ± 8.1 (52–84)
Male	52 (81%)
BMI (kg/m^2)	28.7 ± 5.5 (17.0–38.9)
Smoking	
Current	21 (33%)
Exsmoker	33 (52%)
Nonsmoker	10 (16%)
Underlying disease	
Hypertension	33 (52%)
MI	3 (5%)
IHD	16 (25%)
Diabetes mellitus	7 (11%)
Dyslipidemia	39 (61%)
Kidney disease /uremia	9/4 (14%/6%)
Preoperative medication	
Calcium channel antagonists	25 (39%)
Statins	20 (31%)
Beta-blockers	16 (25%)
Laboratory tests	
White blood cell count (K/uL)	7.80 ± 2.92 (2.03-16.74)
APTT (s)	32.63 ± 5.43 (27.0–48.0)
INR	1.06 ± 0.20 (0.90–1.49)
Creatinine (mg/dL)	1.18 ± 0.39 (0.8–1.75)
Serum urea level (mg/dL)	37.4 ± 19.5 (16.0–112.0)
Glucose (mg/dl)	116.9 ± 35.9 (59.0–239.0)
Morphological characteristics of aneurysms	
The largest diameter (mm)	69.0 ± 27.1 (42–125)

BMI: body mass index; MI: myocardial infarction; IHD: ischaemic heart disease; APTT: activated partial thromboplastin time; INR: international normalized ratio

$p \leq 0.0001$) as well as *RUNX2* and *RUNX3* (R=395, $p \leq 0.00012$) were found in the AAA group using Spearman's correlation analysis. There were no correlations between the expression of genes studied in the control group.

DISCUSSION

This study presents the results of an analysis focusing on the activity of Runt-related genes involved in intercellular signal transduction

pathways, and mediating key processes related to vascular pathophysiology. We showed that the mRNA expression of *RUNX* genes is at a relatively high level in an aneurysmal aorta compared to a normal vessel. We demonstrated an increase in mRNA expression accompanied by a high level of RUNX proteins in AAA tissues. This is the first time the expression of *RUNX2* in the AAA tissue has been described. Results evaluating the mRNA expression of *RUNX1*, *RUNX3* genes were obtained in a group of 65 patients and they confirmed the data published by other authors but in smaller groups of patients, i.e., $n \leq 10$ (16, 17). Additionally, our results reveal the links between the expression of the investigated regulatory Runt-related genes and indicate their importance in the AAA pathophysiology. No correlations between the activity of the analyzed genes were observed in the control tissues.

RUNX genes encode multifunctional proteins that are integral components of intracellular signal transduction cascades, involving TGF-β and control specific gene expressions during tissue homeostasis. TGF-β signaling regulates molecular processes significantly implicated in pathogenesis of vascular remodeling as: cell differentiation, proteolysis, apoptosis, cell proliferation and vascular inflammation (6, 9, 13). Disruption of TGF-β in smooth muscle cell prevents elastase-induced AAA in mouse model (18). Genetic studies have shown that mutations in TGF-β signaling components are associated with the development of human aortic aneurysm (19, 20). The major vascular complication of Marfan syndrome (MFS) is aortic dissection and aneurysm formation. In human, TGF-β is one of the main factor involved in MFS and causes abnormal structure dysfunction of vascular smooth muscle and reduced integrity of the extracellular matrix (20).

Alterations of *RUNX* gene functions were reported in human pathologies, underscoring the roles of these genes in the regulation of proliferation and differentiation of epithelia and immune cells. The decrease or loss of *RUNX3* expression is a common finding in many human epithelial cancers, including pancreatic cancer (21), whereas, overexpression *RUNX2* is associated with advanced tumor progression and poor prognosis in epithelial ovarian cancer (12). RUNX2 transcription factor is known to be expressed in the vascular endothelium and to be involved in the cell migration processes (11). Endothelium plays an important role in AAA formation, as it directly affects the vessel remodeling processes (5). Given the above, it may be expected that the endothelial molecular signal involving RUNX2 could affect inflammatory processes, and thus participate in the pathophysiology of AAA.

Once of the defining characteristics of AAA is activation of the immune system accompanied by a cellular infiltrate of aneurysmal wall. Many different immune cells in the AAA tissue including NK cells, B- and T- lymphocytes produce cytokines and enzymes promoting inflammatory and extracellular matrix degradation, thereby contributing to aortic dilatation and progression of AAA (2-4, 22). Critical molecular pathways involved in AAA pathogenesis include immune processes involving cellular-mediated cytotoxicity. In patients with AAA there is increased percentage of natural killer cell and a rare subpopulation of $CD4^+$T cells deprived of $CD28^+$ expression (4, 22). *RUNX1* and *RUNX3* are involved in the differentiation of hematopoietic cells such as granulocytes or macrophages, and in the transition of $CD4^+$ T cells into $CD8^+$ T cells during thymopoesis (7, 10). It known that the transcription factor RUNX3 controls the activity of RUNX1, and it mediates RUNX1 repression in B cells (23).

Understanding of the activity of Runt-related factors will develop new strategies for the treatment of AAA. Further studies are necessary to determine the role of *RUNX* genes in the pathophysiology of AAA.

ACKNOWLEDGEMENTS

This publication is part of the project “Wrovasc – Integrated Cardiovascular Centre”, co-financed by the European Regional Development Fund, within Innovative Economy Operational Program, 2007-2013, implemented in the Regional Specialist Hospital, Research and Development Centre in Wroclaw.

REFERENCES

1. Sakalihasan N, Limet R, Defawe OD. Abdominal aortic aneurysm. Lancet 2005; 365:1577-89.
2. Pearce WH, Shively VP. Abdominal aortic aneurysm as a complex multifactorial disease: interactions of polymorphisms of inflammatory genes, features of autoimmunity, and current status of MMPs. Ann N Y Acad Sci 2006; 1085:117-32.
3. Chan WL, Pejnovic N, Hamilton H, Liew TV, Popadic D, Poggi A, Khan SM. Atherosclerotic abdominal aortic aneurysm and the interaction between autologous human plaque-derived vascular smooth muscle cells, type 1 NKT, and helper T cells. Circ Res 2005; 96:675-83.
4. Forester ND, Cruickshank SM, Scott DJ, Carding SR. Increased natural killer cell activity in patients with an abdominal aortic aneurysm. Br J Surg 2006; 93:46-54.
5. Siasos G, Mourouzis K, Oikonomou E, et al. The Role of Endothelial Dysfunction in Aortic Aneurysms. Curr Pharm Des 2015; 21(28):4016-34.
6. Miyazono K, Maeda S, Imamura T. Coordinate regulation of cell growth and differentiation by TGF-beta superfamily and Runx proteins. Oncogene 2004; 23:4232-37.
7. Lai CB, Mager DL. Role of runt-related transcription factor 3 (RUNX3) in transcription regulation of natural cytotoxicity receptor 1 (NCR1/NKp46), an activating natural killer (NK) cell receptor. J Biol Chem 2012; 287:7324-34.
8. Tsaousi A, Mill C, George SJ. The Wnt pathways in vascular disease: lessons from vascular development. Curr Opin Lipidol 2011; 22:350-57.
9. Slattery ML, Lundgreen A, Herrick JS, Caan BJ, Potter JD, Wolff RK. Associations between genetic variation in RUNX1, RUNX2, RUNX3, MAPK1 and eIF4E and riskof colon and rectal cancer: additional support for a TGF-β-signaling pathway. Carcinogenesis 2011; 32(3):318-26.
10. Woolf E, Xiao C, Fainaru O, et al. Runx3 and Runx1 are required for CD8 T cell development during thymopoiesis. Proc Natl Acad Sci USA 2003; 100:7731-36.
11. Qiao M, Shapiro P, Fosbrink M, Rus H, Kumar R, Passaniti A. Cell cycle-dependent phosphorylation of the RUNX2 transcription factor by cdc2 regulates endothelial cell proliferation. J Biol Chem 2006; 281(11):7118-28.
12. Li W, Xu S, Lin S, Zhao W. Overexpression of runt-related transcription factor-2 is associated with advanced tumor progression and poor prognosis in epithelial ovarian cancer. J Biomed Biotechnol 2012; 2012:456534.
13. Chuang LS, Ito K, Ito Y. RUNX family: Regulation and diversification of roles through interacting proteins. Int J Cancer 2013; 132(6):1260-71.
14. Laemmli UK. Cleavage of structural proteins during the assembly of the head of bacteriophage T4. Nature 1970; 15:680-85.
15. Towbin H, Staechelin T, Gordon J. Electrophoresis transfer of proteins from polyacrylamide gels to nitrocellulose sheets: procedure and some applications. Proc. Natl Acad Sci USA 1979; 76:4350-55.
16. Lenk GM, Tromp G, Weinsheimer S, Gatalica Z, Berguer R, Kuivaniemi H. Whole genome expression profiling reveals a significant role for immune function in human abdominal aortic aneurysms. BMC Genomics 2007; 8:237.
17. Nischan J, Gatalica Z, Curtis M, Lenk GM, Tromp G, Kuivaniemi H. Binding sites for ETS family of transcription factors dominate the promoter regions of differentially expressed genes in abdominal aortic aneurysms. Circ Cardiovasc Genet 2009; 2:565-72.
18. Gao F, Chambon P, Offermanns S, Tellides G, Kong W, Zhang X, Li W. Disruption of TGF-β signaling in smooth muscle cell prevents elastase-induced abdominal aortic aneurysm. Biochem Biophys Res Commun 2014; 454(1):137-43.
19. Biros E, Walker PJ, Nataatmadja M, West M, Golledge J. Downregulation of transforming growth factor, beta receptor 2 and Notch signaling pathway in human abdominal aortic aneurysm. Atherosclerosis 2012; 221(2):3838-6.
20. Bertoli-Avella AM, Gillis E, Morisaki H, et al. Mutations in a TGF-β ligand, TGFB3, cause syndromic aortic aneurysms and dissections. J Am Coll Cardiol 2015; 65(13):1324-36.
21. Wada M, Yazumi S, Takaishi S, et al. Frequent loss of RUNX3 gene expression in human bile duct and pancreatic cancer cell lines. Oncogene 2004; 23(13):2401-7.
22. Duftner C, Seiler R, Klein-Weigel P, Göbel H,

Goldberger C, Ihling C, Fraedrich G, Schirmer M. High prevalence of circulating CD4+CD28- T-cells in patients with small abdominal aortic aneurysms. Arterioscler Thromb Vasc Biol 2005;25(7):1347-52.

23. Brady G, Farrell PJ. RUNX3-mediated repression of RUNX1 in B cells. J Cell Physiol 2009; 221:283-87.

LETTER TO THE EDITOR

EFFECT OF EMBOLIC MICROSPHERES IN THE TREATMENT OF PRIMARY HEPATIC CARCINOMA

K.B. WANG[1], H. SUI[2], W. LI[3], LM. CUI[1] and B. BAI[1]

[1]Interventional department, the Second Hospital Affiliated Harbin Medical University, Harbin, China;
[2]Department of Medical Oncology, Harbin Medical University Cancer Hospital, Harbin, China;
[3]Department of Radiology, the Second Hospital Affiliated Harbin Medical University, Harbin, China

Received March 16, 2016 – Accepted April 27, 2016

The first two authors contributed equally to this work.

The purpose of this study was to evaluate the clinical effect of embolic microspheres in the treatment of primary hepatic carcinoma. Fifty-eight patients who were confirmed with primary hepatic carcinoma by imaging were retrospectively analyzed. They were firstly perfused with 50 mg of oxaliplatin and 40 mg of epirubicin. Embolic microspheres were then injected into the distal end of targeted blood vessels. After this procedure, dynamic observation was carried out until tumor stain disappeared. Liver function and blood indexes were reexamined on days 5, 6, 7 and 28 after treatment, and moreover, the liver was examined with Magnetic Resonance Imaging (MRI) or computed tomography (CT). Compared to traditional lipiodol embolization, embolic microspheres did not aggregate the damage on liver function and the imaging examination suggested necrosis of some tumor tissues. Embolic microspheres proved to be effective in treating primary hepatic carcinoma. It produces no damage on liver function and can lead to significant shrinkage of hepatic carcinoma and necrosis of some tumor tissues. Embolic microspheres, which merely block distal branches of tumor-feeding artery, can avoid collateral circulation induced by permanent blocking, thus achieve a good treatment effect.

Embolization is the major interventional treatment method for primary hepatic carcinoma. Previously, iodinated oil injection and gelatin sponge were frequently used as traditional embolic agents. Embolic microsphere as a novel embolic agent has been gradually applied in embolization treatment for tumor because of its smooth and hydrophilous surface and small aggregation property. Theoretically, microsphere particles can embolize distal tumor vessels for a longer time due to their non-absorbable properties. In this study, we evaluated the feasibility and advantages of applying embolic microspheres in the interventional treatment of primary hepatic carcinoma by comparing liver function before and after treatment and evaluating disease control with imaging (1).

MATERIALS AND METHODS

Fifty-eight patients with primary hepatic carcinoma who were treated with embolic microspheres from August 2014 to February 2015 were selected as research subjects. Of 58 patients, 38 were males and 20 were females. They were aged from 35 to 72 years-of-age (average 47.5 years).

Key words: primary hepatic carcinoma, embolic microspheres, embolization

Mailing address:
Dr Bin Bai,
Interventional Department,
The Second Hospital Affiliated Harbin Medical University,
246 Xue Fu Road, Harbin, Heilongjiang, 150086, China
e-mail: baibin314@163.com

0393-974X (2016)

DISCLOSURE: ALL AUTHORS REPORT NO CONFLICTS OF INTEREST RELEVANT TO THIS ARTICLE.

All patients signed informed consent to participate in the study.

Selection of cases

Patients were selected according to nodular-type or massive-type hepatic carcinoma (one or more lesions) and rich blood supply. The patients included had Child-Pugh grade A or B liver function and controllable ascites, but had not developed portal vein tumor thrombus. The patients recruited underwent liver computed tomography (CT) or enhanced Magnetic Resonance Imaging (MRI) examination, alpha fetal protein (AFP) examination, biochemical test, coagulogram test and blood routine examination before treatment. Levels of alanine aminotransferase (ALT) and aspartate amino transferase (AST) were equal to or lower than 2.5 times of the upper normal limits, the level of albumin (ALB) was no less than 33 g/L and the level of bilirubin was equal to or lower than 2 times the normal value. Levels of white blood cells and hemoglobin were within the normal scope and the level of platelets was at least 50x109/L.

Embolic microspheres

Embolic microspheres diameter, 100-300 μm (Merit Medical System Inc., USA), were selected. The diameter of embolic microspheres used should be small enough to block the distal branch of tumor-feeding artery and ensure the smooth of blood-supply artery.

Therapeutic method

Transcutaneous hepatic arterial embolization using embolic microspheres combined with chemotherapy was performed with digital subtraction angiography (DSA) machine (Angio Zee Plus, Siemens Company, Germany) using Seldinger technology. Firstly, the location and number of tumors were confirmed by coeliac arteriography, common hepatic angiography and superior mesenteric arteriography. The dosage of embolic microspheres was determined according to the size of tumor and blood supply. After superselective embolization was put in place, epirubicin and oxaliplatin were perfused, followed by embolic microspheres. The perfusion was dynamically observed until tumor staining completely disappeared. On day 5, either CT or MRI was performed and the level of AFP was measured to estimate the necrosis degree of tumor. On day 28, the liver was reexamined with CT or enhanced with MRI. If the imaging examination suggested there was an enhancement in hepatic carcinoma, interventional embolization treatment needed to be performed again and 1 month after the second treatment, liver CT or enhanced MRI was again carried out to evaluate whether a third treatment was necessary. If there was no enhancement, liver CT or enhanced MRI and AFP measurement were performed after 3 months to evaluate whether interventional embolization treatment was needed. If liver function of patients weakened and portal vein tumor thrombus was detected with imagining evaluation or ascites were found uncontrollable, the treatment terminated and patients were followed up until death.

Observation indexes

All patients were followed up for at least three months. Levels of total bilirubin (TBIL), direct bilirubin (DBIL), indirect bilirubin (IBIL), ALB, globulin (GLB), ALB/GLB, ALT and AST as well as tumor size (cm) were observed. Untoward reactions and complications were evaluated according to Common Terminology Criteria for Adverse Events (CTCAE) 4.0 formulated by National Cancer Institute (NCI).

Statistical analysis

SPSS ver. 19.0 was used for data analysis. Data were expressed as mean±SD. Changes of liver functions before and after treatment were processed by Wilcoxon's signed rank test. Difference of $p<0.05$ had statistical significance.

RESULTS

The technical success rate of the treatment was 100%. After the application of embolic microspheres, levels of TBIL and ALT showed slight increases, but the change of ALB level was not obvious (Table I). The size of tumor and serum AFP level both showed significant decrease after treatment. The AFP level of 28 patients decreased to a normal range and, moreover, tumors of 13 patients completely necrotized. One month after treatment, CT or enhanced MRI demonstrated obvious necrosis of tumor tissues and obviously decreased tumor blood supply (Fig. 1, 2). Postoperative reactions mainly included mild nausea and vomiting, fever, abdominal pain and discomfort. Thirty-four patients

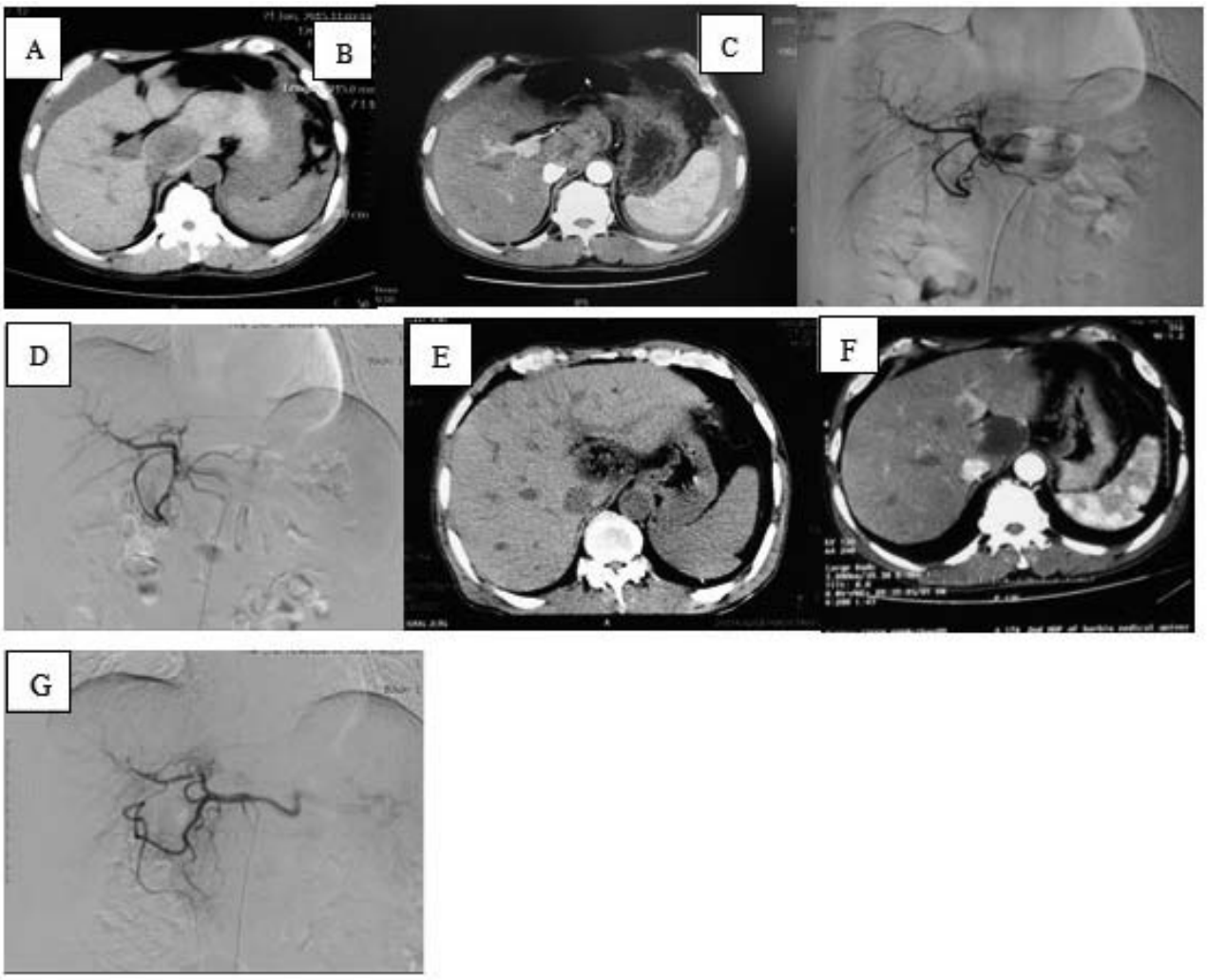

Fig. 1. *CT results of liver caudal lobe rupture and bleeding before and after microsphere embolization treatment.* ***A****) liver caudate lobe (S1) broke and bled, demonstrating low-density lesion and ascites in plain scanning;* ***B****) uneven enhancement of caudate lobe (S1) in enhancement scanning;* ***C****) before the first embolization, branches of tumor-feeding artery could be observed after staining;* ***D****) after embolization with embolic microspheres, staining disappeared from the caudate lobe and peripheral tumor-feeding artery branches;* ***E****) plain CT performed five days after operation suggested necrosis of tumor in caudate lobe and the absorption of ascites;* ***F****) liver enhanced CT performed one month later suggested necrosis of a large part of tumor in caudate lobe and enhancement of the margin;* ***G****) hepatic angiography performed one month later suggested deficiency of staining in most parts of liver caudate lobe and staining of margin.*

were observed with medium grade fever, i.e., Grade 1 fever, according to Common Terminology Criteria for Adverse Events (CECAE) 4.0 and the fever lasted for one week. Ten patients had a symptom of emesis immediately after surgery. Four patients showed relatively serious abdominal pain (Visual Analogue Scale (VAS) score: 5 points) on the day of surgery and required pethidine hydrochloride for pain relief. Three patients had abdominal pain scored as 3 points and the other patients had abdominal pain scored as less than 3 points. The symptoms disappeared after symptomatic treatment. Severe complications such as liver-renal dysfunction, bile leakage combined with infection, hepatapostema,

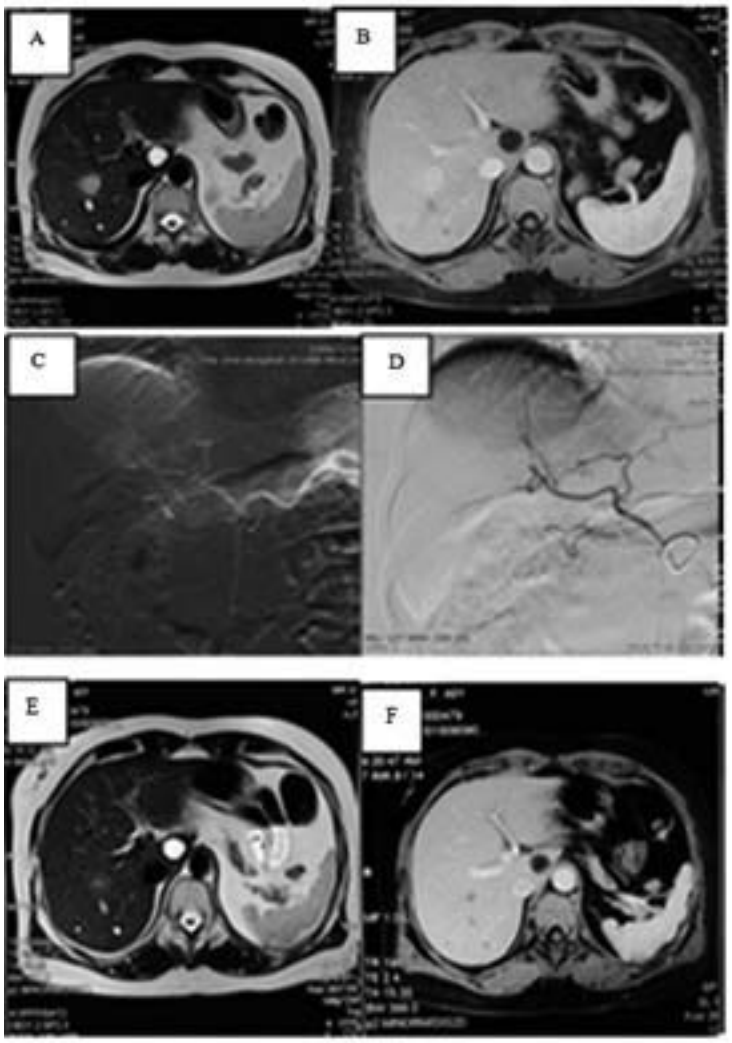

Fig. 2. *MRI before and after hepatic carcinoma operation and microsphere embolization treatment.* ***A)*** *MRI performed before the first interventional treatment suggested tumor in the right lobe of liver;* ***B)*** *enhanced MRI suggested obvious enhancement of tumor;* ***C)*** *radiography performed before the first interventional embolization suggested obvious staining of hepatic carcinoma;* ***D)*** *radiography after embolization suggested that staining disappeared from tumor and peripheral tumor-feeding artery, but reserved at major tumor-feeding artery;* ***E)*** *plain MRI performed one month later suggested remarkable shrinkage of tumor;* ***F)*** *enhanced MRI performed one month later suggested no enhancement of hepatic carcinoma.*

intra-abdominal hemorrhage, tumor rupture and bleeding, gastrointestinal bleeding, bone marrow suppression and cardiotoxicity were not observed in any cases.

DISCUSSION

The key point of interventional treatment for primary carcinoma lies in super-selective embolization of the tumor-feeding artery, which can induce necrosis (2). Most tumors are still alive after transhepatic arterial chemotherapy and embolization, which is mainly associated with the formation of collateral circulation of tumor-feeding artery in addition to incomplete embolization of multiple tumor-feeding blood vessels.

Tumor tissues become ischemic and hypoxic after patients undergo transhepatic arterial chemotherapy and embolization which can promote

Table I. *Comparison of liver function of patients before and after treatment.*

Liver function index	Before treatment (p value)*	One month after treatment (p value)#
ALB/(g/L)	40.8±3.76	38.7±4.59(0.19)
ALT/U/L)	31.9±12.4	33.7±10.3(0.15)
AST/(U/L)	39.4±17.4	42.3±15.6(0.12)
TBIL/(μmol/L)	13.6±4.53	14.3±6.53(0.11)

**: p value was obtained by comparing liver functions examined before treatment and three days after treatment; #: p value was obtained by comparing liver functions examined before treatment and one month after treatment.*

tumor cells, while adjacent normal cells could secrete proangiogenic substances, such as vascular endothelial growth factor and basic fibroblast growth factor, as well as the formation of collateral circulation of tumor blood vessels in order to lower the effect of transhepatic arterial chemotherapy and embolization (3). Therefore, a permanent embolic agent that can embolize peripheral artery is the best choice for embolization treatment for hepatic carcinoma. Embolic microsphere, a kind of peripheral embolization agent, can embolize blood vessels that are as big as the embolic microspheres. If no blood passes through the distal end of the target artery after blood vessels are embolized with the microspheres, we achieve targeted embolization. Permanent peripheral embolization can effectively prevent the formation of collateral circulation and block the blood flow of the liver artery more completely and effectively. Compared to traditional transhepatic arterial chemotherapy and embolization that applies iodipin, embolic microspheres show a higher response rate and delay disease progression.

In this study, no patient presented pulmonary embolization or esophagus venous bleeding, indicating that applying embolic microspheres with a diameter of 100-300 μm is safe (4-6). After treatment, tumor size and serum AFP level of all patients showed significant decline and the level of AFP of 28 patients lowered to the normal level, while tumors of 13 patients completely necrotized, suggesting embolic microspheres had a remarkable embolization effect.

We also found that patients developing a single tumor with a diameter of less than 3 cm obtained better effects and recovered. For patients with multiple lesions, treatment with embolic microspheres can be used for tumor which is supplied by single liver artery while the other lesions can be embolized using iodinated oil injection first and then embolic microspheres, which can reduce the damage on liver function.

REFERENCES

1. Rand T, Loewe C, Schoder M, et al. Arterial embolization of unresectable hepatocellular carcinoma with use of microspheres, lipiodol, and cyanoacrylate. Cardiovasc Intervent Radiol 2005; 28:313-8.
2. Ishida K, Hirooka M, Hiraoka A, Kumagi T, Uehara T, Hiasa Y. Treatment of hepatocellular carcinoma using arterial chemoembolization with degradable starch microspheresand continuous arterial infusion of 5-fluorouracil. Jpn J Clin Oncol 2008; 38(9):596-603.
3. Bonomo G, Pedicini V, Monfardini L, Vigna PD, Poretti D, Orgera G, Orsi F. Bland Embolization in patients with unresectable hepatocellular carcinoma using precise, tightly size-calibrated, anti-inflammatory microparticles: first clinical experience and one-year follow-up. Cardiovasc Intervent Radiol 2010; 33:552-9.
4. Nikhil B. Amesur Albert B. Zajko Brian I. Carr. Chemo-embolization for unresectable hepatocellular

carcinoma with different sizes of embolization particles. Dig Dis Sci 2008; 53:1400-4.
5. Huppert P. Current concepts in transarterial chemoembolization of hepatocellular carcinoma. Abdom Imaging 2011; 36(6):677-83.
6. Furuse J, Ishii H, Satake M, et al. Pilot study of transcatheter arterial chemoembolization with degradable starch microspheres in patients with hepatocellular carcinoma. J Am J Clin Oncol 2003; 26(2):159-64.

LETTER TO THE EDITOR

COMPUTED TOMOGRAPHY DIAGNOSIS OF NEONATAL HYPOXIC ISCHEMIC ENCEPHALOPATHY COMBINED WITH INTRACRANIAL HEMORRHAGE AND CLINICAL NURSING TREATMENT

Y. ZHANG[1], J.L. ZHANG[2] and Y. LI[3]

[1]NICU, Binzhou People's Hospital, Shandong, China; [2]Pediatrics Department, Binzhou People's Hospital, Shandong, China; [3]Emergency Department, Binzhou People's Hospital, Shandong, China

Received August 6, 2015 – Accepted April 20, 2016

Hypoxic ischemic encephalopathy (HIE), one of the common causes of newborn invalidism, is likely to induce nervous system-associated sequelae and even intracranial hemorrhage in severe cases. The incidence rate of HIE has been rising in recent years. In order to study the clinical nursing effect for HIE combined with intracranial hemorrhage, 76 newborns diagnosed with HIE combined with intracranial hemorrhage by spiral computed tomography (CT) from the of Binzhou People's Hospital, Shandong, China were selected. They were divided into a control group and an intervention group. The control group received routine nursing, while the intervention group received comprehensive nursing intervention. The experimental results suggested that the mental developmental index (MDI) value and the psychomotor developmental index (PDI) value of patients in the intervention group were much higher than those of the control group and the difference was significant ($p<0.05$). The curative effect of the intervention group was remarkably better than that of the control group and the difference was also statistically significant ($p<0.05$). Moreover, the intervention group had a lower incidence rate of untoward reactions. All the findings suggest that comprehensive nursing intervention can help newborns diagnosed with HIE combined with intracranial hemorrhage recover more effectively, therefore is worth applying.

Neonatal HIE is a dangerous disease with high incidence and refers to hypoxic-ischemic brain damage induced by perinatal asphyxia. Patients with severe HIE also develop permanent brain damage and nervous system associated sequelae (1, 2). Newborns with HIE usually display intracranial hemorrhage (ICH), one of the major causes leading to the high mortality rate of HIE. Spiral Computed Tomography (CT) is frequently used to confirm HIE in the early stages (3) and patients are mainly treated and nursed through rehabilitation. However, some newborns do not recover well after receiving treatment (4). To further analyze the curative effect of clinical nursing for HIE patients, this study randomly selected 76 HIE newborns who received hyperbaric oxygen therapy in the People's Hospital of Binzhou, Shandong, China and compared the curative effect of comprehensive nursing intervention and routine nursing in the treatment of HIE based on the precise analysis of spiral CT test results.

Key words: hypoxic ischemic encephalopathy, intracranial hemorrhage, computed tomography, comprehensive nursing

Mailing address:
Dr Ying Zhang,
NICU, Binzhou People's Hospital, No.515, Huanghe 7th Road,
Binzhou, Shandong, 256600, China
Tel.: +81 18654350090
e-mail: zyzhangbz@163.com

0393-974X (2016)

MATERIALS AND METHODS

General data

Seventy-six HIE newborns (42 males and 34 females) who received hyperbaric oxygen therapy in the Binzhou People's Hospital, Shandong, China from June 2012 to June 2013 were selected and divided into a control group and an intervention group according to the nursing method. Parents of all newborns signed an informed consent and the study was approved by the ethics committee of the People's Hospital of Binzhou, Shandong. In the control group, which received conventional nursing, there were 38 patients (22 males and 16 females), with ages ranging from 1 to 72 h (average 26.8±4.6 h), body mass ranging from 2.5 to 3.8 kg (average 3.1±0.9 kg) and average Apgar score of 4.2±1.3 points. With regard to the induction factor, there were 2 cases of amniotic fluid pollution, 5 cases of premature rupture of membranes, 4 cases of placenta previa, 3 cases of nuchal cord, 10 cases of intrauterine distress and 14 cases of premature delivery. In the intervention group, where the subjects received comprehensive nursing, there were 38 patients (20 males and 18 females), with ages ranging from 2 to 73 h (average 27.2±4.5 h), body mass ranging from 2.5 to 3.8 kg (average 3.1±0.9 kg), and average Apgar score of 4.1±1.1 points. Regarding the induction factor, there were 3 cases of amniotic fluid pollution, 3 cases of premature rupture of membranes, 5 cases of placenta previa, 11 cases of intrauterine distress and 16 cases of premature delivery. All patients were confirmed with intracranial hemorrhage by computed tomography (CT). For clinical performance, 53 cases were observed with irritation, 18 cases with convulsions and 5 cases with coma. Results were comparable as no statistically significant difference was found in the general data of the two groups (p>0.05).

Diagnosis with CT

A 16-slice spiral CT machine (GE, USA) was used to scan heads of patients, taking superior orbitomeatal line as base line (tube voltage: 120 kV; tube current: 50 mA; layer thickness: 5~10 mm; layer space: 5~10 mm; scanning layers: ~10 layers). CT examination was carried out after the newborns fell asleep.

Clinical diagnostic criteria

Diagnostic criteria and clinical grading of neonatal hypoxic ischemic encephalopathy proposed in a conference held in Hangzhou, China, in 1996 was used (5). HIE occurring in newborns can be divided into three levels based on the condition of disease (6). Newborns who were easily irritated or presented hyperarousal, shaking, fremitus, excitement or active embrace reflex were determined to have mild HIE. Those who were found with weak muscular tension, insomnia or light coma state and suffered from convulsions, apnea, weak embrace and sucking reflex within 6~12 h after birth were diagnosed with medium HIE. Patients who presented symptoms such as weakened or lack of muscular tension, no reflex, coma and continuous convulsions in 12 h after birth were diagnosed with serious HIE.

Treatment and nursing

Patients in the control group were given conventional nursing. Detailed operations of holistic nursing were as follows: body temperature and various vital signs were closely monitored; the patient was kept warm to prevent disturbance of blood circulation and promote blood supply. Ideal body temperature was established at 36-37°C which was maintained through the use of an incubator. Besides conventional nursing, patients in the intervention group also received health education for family members, in order to comprehend and control convulsions, sensory irritation, blood glucose and oxygen flux. This was deemed necessary because family members of patients might not follow the guidance of medical staff due to a state of anxiety, depression and fear. Massages were performed on the back, chest, abdomen, limbs, fingers and toes on a daily basis to stimulate perception of sensory nerves. Patients were also provided with glucose to maintain blood glucose levels between 3.9-6.1 mmol/L. Oxygen concentration was kept between 30% and 40%. Patients with mild HIE were fed six hours after birth and breast milk was advocated. For patients with middle or severe HIT, nutrition support was provided and pumped continuously until hypoxia symptoms were significantly relieved and intracranial hemorrhage acquired effective control, after which nutrition support was gradually replaced by lactation. Droppers could be used for feeding if children presented problems with suckling or deglutition.

Observation index

Mental developmental index (MDI) scale and psychomotor developmental index (PDI) scale were used. Higher score indicated good development of intelligence

and athletic ability. Curative effects of the two groups were evaluated according to the following criteria (7): treatment was considered significantly effective if clinical symptoms disappeared and development quotient was at a normal level; treatment was effective if clinical symptoms relieved to some extent and development quotient had remarkable improvement; treatment was considered ineffective if no remarkable improvement was observed in clinical symptoms and development quotient.

Statistical analysis

SPSS 19.0 software was used for statistical analysis. Measurement data were expressed as Mean±SD. Data of two groups were compared using *t*-test. Enumeration data was processed by *chi*-squared test. Difference was considered as statistically significant if $p<0.05$.

RESULTS

Diagnostic results of CT

Of 76 newborns, there were 53 cases of mild HIE (Fig. 1A), 18 cases of medium HIE (Fig. 1B) and 5 cases of severe HIE (Fig. 1C). Seventy-six newborns with different severity of HIE were all observed with different levels of ICH (Table I).

MDI and PDI of two groups

MDI and PDI values of newborns in the intervention group were much higher than those of the control group, and the difference was statistically significant ($p<0.05$) (Table II).

Improvement of encephalopathy

In the control group, 12 cases were significantly improved, 17 cases showed signs of improvement and the remaining 9 cases had no improvement. Total effective rate was 76.3%. The corresponding number of cases in the intervention group was 16, 20 and 2 and the total effective rate was 94.7%. The curative effect of hyperbaric oxygen therapy of the two groups was significantly different.

Comparison of incidence rate of untoward reactions

Eight cases in the control group showed untoward reactions during oxygen therapy (21.1%), while in the intervention group, only two cases were observed with untoward reactions (5.3%). Therefore, the incidence rate of untoward reactions was statistically significant between the two groups ($p<0.05$).

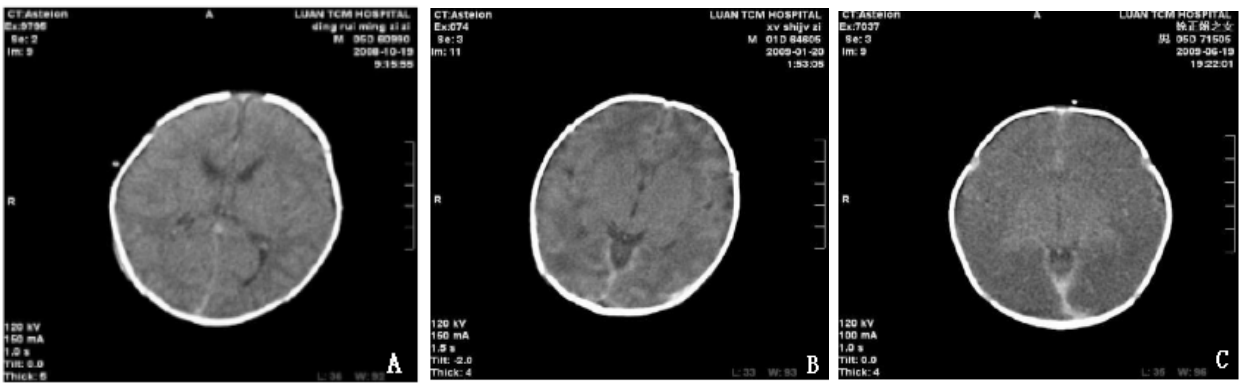

Fig. 1. *CT diagnostic results.* ***A)*** *mild hypoxic ischemic encephalopathy: local low-density area in the left frontal lobe; normal ventricle, but with little subarachnoid hemorrhage;* ***B)*** *medium hypoxic ischemic encephalopathy combined with subarachnoid hemorrhage: focal low-density area in the bilateral frontal lobes and temporal lobes; fuzzy boundary between brain gray matter and white matter; subarachnoid hemorrhage; surrounding sulus and fissures are narrowed;* ***C)*** *severe hypoxic ischemic encephalopathy: diffusive low-density area in lobes of brain solid; fuzzy boundary between brain gray matter and white matter; normal density of basal ganglia and dorsal thalamus; compressed paracele; disappearance of sulus and fissures.*

Table I. *CT results.*

Grade	Type of hemorrhage				
	SAH	IVH	SDH	IPH	SEH
Mild (53)	53	0	0	0	0
Medium (18)	16	4	2	3	1
Serious (5)	5	1	1	0	1

Among 76 cases, 65 cases developed SAH only, 1 case was observed with IVH only and 10 cases developed hemorrhage (SAH+IVH: 3 cases; IVH+IPH: 1 case; SAH+ IPH: 2 cases; SAH+SHE: 2 cases; SAH+SDH: 2 cases).
SAH: Subarachnoid hemorrhage; IVH: Intraventricular hemorrhage; SDH: Subdural hemorrhage; IPH: Intraparenchymal hemorrhag; SEH: Subependymal haemorrhage.

Table II. *Comparison of mental developmental index value and psychomotor developmental index values between two groups after treatment.*

Group	N	MDI	PDI
Intervention group	38	88.2±12.4	85.7±10.6
Control group	38	78.7±9.9	73.1±9.1
t		3.304	4.781
p		<0.05	<0.05

MDI: mental developmental index; PDI: psychomotor developmental index (mean ± SD).

DISCUSSION

Neonatal HIE is one of the major causes of neonatal brain damage. A large amount of studies have proved that the incidence mechanism of HIE is a pathological process involving multiple factors such as metabolic disturbance, vascular regulating mechanism disorder, cellular damage and intrapartum or birth asphyxia. Most patients present pathological symptoms such as intracranial hemorrhage, encephaledema and malacia (8, 9). Currently, prevention is the preferred clinical treatment for HIE (10). What should be pointed out is that CT diagnosis plays an important role in prevention treatment. It has been found that CT diagnosis is effective in accurately analyzing early ICH and providing detailed data on the severity and scope of brain damage (11, 12). All cases in this study were confirmed through CT to have ICH, among which 65 cases had SAH, 1 case was observed with IVH and 10 cases developed hemorrhage. For children with confirmed HIE, the degree of disability can be lowered by performing early treatment and monitoring various complications after the onset of symptoms. In this study, intelligence and motory ability of patients in the intervention group were much higher than those of patients in the control group. The effective rate and adverse reaction rate of the intervention group were 94.7% and 5.3% respectively, both better than the control group, which suggests that the application of comprehensive nursing is better than conventional nursing.

In conclusion, comprehensive nursing can

significantly lower the mortality rate and incidence of complications in newborns with HIE. Effective nursing is the basis for successful treatment of HIE, hence comprehensive nursing is worth being promoted in newborns with HIE.

REFERENCES

1. Zhou WH, Cheng GQ, Shao XM, et al. Selective head cooling with mild systemic hypothermia after neonatal hypoxic-ischemic encephalopathy: a multicenter randomized controlled trial in China. J Pediatr 2010; 157(3):367-72.
2. Ma J, Wang Y, Yang JH, et al. Treatment of hypoxic-ischemic encephalopathy in mouse by transplantation of embryonic stem cell-derived cells. Neurochem Int 2007; 51(1):57-65.
3. Shi Y, Zhao JN, Liu L, Hu ZX, Tang SF, Chen L, Jin RB. Changes of positron emission tomography in newborn infants at different gestational ages, and neonatal hypoxic-ischemic encephalopathy. Pediatr Neurol 2012; 46(2):116-23.
4. Ma QY, Zhang LB. Epigenetic programming of hypoxic-ischemic encephalopathy in response to fetal hypoxia. Prog Neurobiol 2015; 124:28-48.
5. Wang X, Meng FS, Liu ZY, Fan JM, Hao K, Chen XQ, Du JZ. Gestational hypoxia induces sex-differential methylation of Crhr1 linked to anxiety-like behavior. Mol Neurobiol 2013; 48(3):544-55.
6. Lin ZL, Yu HM, Lin J, Chen SQ, Liang ZQ, Zhang ZY. Mild hypothermia via selective head cooling as neuroprotective therapy in term neonates with perinatal asphyxia: an experience from a single neonatal intensive care unit. J Perinatol 2006; 26(3):180-4.
7. Qin M, Wang XH, Chen L, Fan SZ. Protective effects of hypothermia in hypoxic-ischemic brain injury in newborn rats. Pediatr Res 1998; 44:421.
8. Massaro AN, Evangelou I, Brown J, Fatemi A, Vezina G, McCarter R, Glass P. Neonatal neurobehavior after therapeutic hypothermia for hypoxic ischemic encephalopathy. Early Hum Dev 2015; 91(10):593-9.
9. Lei Z, Li B, Yang ZS, Fang HS, Zhang GM, Feng ZH, Huang B. Regulation of HIF-1alpha and VEGF by miR-20b tunes tumor cells to adapt to the alteration of oxygen concentration. PLoS One 2009; 4(10):e7629.
10. Giovanni GL, Diana LC, Mark SS. Brain lesions of fetal onset in encephalopathic infants with nonimmune hydrops fetalis. Pediatr Neurol 1994; 11(1):15-22.
11. Winkler MA, von Herrmann P, Penticuff RH, Majmudar PM, Plaisance BR, Hobbs SB, Brooks MA. A potential role of ECG-gated CT for the diagnosis of pulmonary vein thrombus: an illustrative case report. Clin Imaging 2015; 39(3):513-5.
12. Lu Q, Harris VA, Rafikov R, Sun XT, Kumar S, Black SM. Nitric oxide induces hypoxia ischemic injury in the neonatal brain via the disruption of neuronal iron metabolism. Redox Biol 2015; 6:112-21.

LETTER TO THE EDITOR

CHANGES IN PHAGOCYTOSIS AND EXPRESSION OF MICROGLIAL CELLS IN CRANIOCEREBRAL INJURY MICE MODELS

FY. GUO, T. LIU, JJ. CHEN, W. GAO, F. YANG, XY. ZHOU and YL. LIAO

Department of Traumatic Surgery, Tongji Hospital, Tongji Medical College of Huazhong University of Science and Technology, Wuhan, PR China

Received September 12, 2015 – Accepted March 30, 2016

The objective of this study was to investigate the changes in phagocytic function and expression quantities of CD11b and tumor necrosis factor-α (TNF-α) among microglia cells of craniocerebral injury mice. Modified Feeney method was used to establish the craniocerebral injury mice models. Twenty-one male SPF mice were divided into a control group and a trauma group. The scalp was incised and a bone window was opened in the control group without cerebral injury. In the trauma group, the mice were sacrificed after the craniocerebral injury at 1, 3, 6, 12, 24 and 48 h to make frozen sections of cerebral tissues. The phagocytic rate of microglia cells was observed by using fluorescent microsphere. The changes in the expression quantities of CD11b and TNF-α were detected by enzyme-linked immuno sorbent assay (ELISA). The phagocytic ability of the microglia cells after the craniocerebral injury increased at 1 h after injury compared with that of the control group (P<0.01). The expression of surface antigen CD11b of the microglia cells and the expression of TNF-α increased at 1, 3, 6, 12, 24 and 48 h after the injury compared with those of the control group (P<0.01). The phagocytic ability of the microglia cells increased. The expressions of CD11b and TNF-α were also gradually enhanced in the acute phase after craniocerebral injury, and then gradually decreased to the normal level. The expressions of CD11b and TNF-α indicated a high consistency with the changing trend of the phagocytic ability, suggesting that the microglia cells may participate in the regulation of the inflammatory process of the central nervous system through absorbing apoptotic cells and increasing and secreting inflammatory and anti-inflammatory factors.

Traumatic brain injury (TBI) is one of the common acute and severe diseases in neurosurgery. Craniocerebral injury cases caused by traffic accidents, falling or incidents of violence show a gradually rising trend. WHO points out that traffic-induced injury will be in the third place among all the global ailments in 2020 (1). Cerebral injury is divided into primary and secondary cerebral injuries (2).

Microglia cells, universally acknowledged as central nervous effector cells, are extensively spread. Cajal classified the neurogliocyte into three categories, two categories were equal to astrocytes and the third one was called "the third component", probably including oligodendrocytes and microglia (3). Oligodendrocyte and microglia cells are considered as macrophages (4).

Craniocerebral injury enables microglia to rapidly activate, and their activation and proliferation are the vital representation of the inflammatory reaction of the central nervous system (CNS). When the CNS

Key words: craniocerebral injury, microglia cells, phagocytic function, CD11b, TNF-α

Mailing address:
Dr YL. Liao, No.1095, Jeifang Avenue,
Wuhan City, Hubei Province, 430030, China
Tel.: +86 027 83665306
Fax: +86 027 83665346
e-mail: liaoyl228@163.com

0393-974X (2016)

DISCLOSURE: ALL AUTHORS REPORT NO CONFLICTS OF INTEREST RELEVANT TO THIS ARTICLE.

is damaged, local anemia and inflammation stimuli cause microglia cells to have a rapid response and they become activated (5). Microglia cells are able to clear up the apoptotic cells during the remodeling and maturity process of brains.

When the CNS is injured, the dormant microglia cells are activated into macrophages, swallowing debris and degenerating myelin sheath together with blood circulation-immersed monocytes. After the injury heals, they are again transformed into microglia cells. The common variation on formation in Nissl staining and HE staining sections are mainly related to their movements and swallowing foreign bodies.

MATERIALS AND METHODS

Twenty-one healthy male SPF mice (25±1) g were purchased from the Animal Experimental Center of Zhengzhou University. The mice were randomly divided into a traumatic group and a control group. The traumatic group was divided into 6 subgroups according to the time of sacrifice, with 3 mice in each subgroup. The establishment of the craniocerebral injury mice models was conducted by using the modified Feeney method as described previously (6).

Detection of the phagocytic function of the microglia cells

Twenty-four mice were randomly divided into a traumatic group and a control group. In accordance with the different scarifying time after trauma, the traumatic group was divided into several subgroups of 1, 3, 6, 12, 24 and 48 h, with 3 mice in each group. The mice were sacrificed at different times after trauma and the brain tissues in the trauma sections were collected for detection of the phagocytic function of the microglia cells by flow cytometry.

The mice in the trauma group were sacrificed at 1, 3, 6, 12, 24 and 48 h, respectively, after trauma. The brain tissues in the trauma sections were collected. The brain tissues were put into the complete medium and they were cut into pieces. 0.25% amylopsin was used for digestion of the materials for 10 min. Phagocytic index (PI) was analyzed, as described previously (7). PI = cell population of phagocytic fluorescent microsphere/ total cell count ×100%; High PI suggests strong phagocytic activity of cells (7).

Detection of the expression of CD11b of the microglia cells by flow cytometry

1×10^6 cells were collected, and incubated with the FITC-CD11b antibody for 30 min at 4°C in the dark. After they were resuspended with 300 ml PBS solution (containing 1% fetal calf serum), and flow cytometry was used for detection of the expression of CD11b of the microglia cells.

Expression analysis of TNF-α of the microglia cells by ELISA

Cell sap collected from the brain tissues of the sacrificed mice at 1, 3, 6, 12, 24 and 48 h, respectively, after trauma was centrifuged for 5 min at 1000 r/min and ELISA was adopted to detect TNF-α.

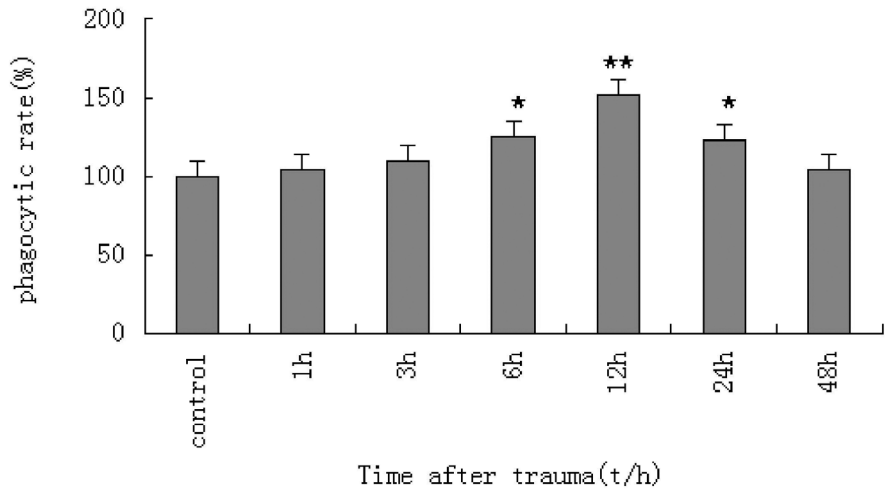

Fig. 1. *Changes of the phagocytic function of the microglia cells for mice after craniocerebral injury.*

Statistical analysis

SPSS 19.0 software was used for data analysis. $\bar{x} \pm s$ was used to represent the data with homogeneity test of variance and *t*-test. $P<0.05$ was considered statistically significant.

RESULTS

Detection on the phagocytic function of the microglia cells

The phagocytic rate of the microglia cells at different time points after trauma in the traumatic group was higher than that in the control group. The phagocytic ability of the microglia cells increased 1 h after trauma; There was a significant increase 6 h, 12 h and 24 h after trauma ($P<0.05$) (Fig. 1).

Expressions of CD11b and TNF-α of the microglia cells

The expressions of CD11b and TNF-α at different time points after trauma in the traumatic group were higher than those in the control group. The expressions of CD11b and TNF-α of the microglia cells 1 h after trauma were enhanced, but there was no statistical significance ($P>0.05$). The expressions of CD11b and TNF-α 6 h after trauma were significantly enhanced ($P<0.05$). The expression of CD11b in 24 h after trauma was significantly reduced ($P<0.05$) (Table I, Figs. 2 and 3). The expressions of CD11b and TNF-α indicated a high consistence with the change trend of the phagocytic ability.

DISCUSSION

The activated microglia cells in the CNS are able to ingest the inflammatory cells and the apoptotic cells by transference and transformation. The phagocytosis of the microglia cells on the apoptotic cells mainly depends on the specifically recognized valgus phosphatidylserine (PS) of the apoptotic cells (8). CD11b is the receptor of the complement activation fragment iC3b (9). This experiment showed that the normal microglia cells express CD11b, and the expression of CD11b of the activated microglia cells was enhanced under the craniocerebral injury conditions.

TNF-α is produced by the activation of the mononuclear cells and macrophages. After tissue injury, TNF-α can activate and recruit microglia cells. After nerve tissue injury, mature myelin sheath cells in the injured sections can inhibit the regeneration of axon. However, the activated macrophages can swallow the damaged myelin sheath and neuron pieces, and stimulate the proliferation of the Schwann cells to produce numerous nutrition supporting molecules to promote the repair and regeneration of axon at the same time. After the chronic stage of spinal cord injury, the activated microglia cells play a certain role in the neurotrophy and neuroprotection. TNF-α at low concentration can induce the synthesis

Table I. *Dynamic changes in the expressions of CD11b and TNF-α of microglial cells.*

Time	CD11b	TNF-α
Control group	6.31±0.82	145.64±3.15
1h after trauma	7.38±0.83	157.16±8.81
3h after trauma	15.67±0.72	
6h after trauma	19.02±0.74	
12h after trauma	38.07±0.82	212.18±24.84
24h after trauma	19.27±0.55	188.26±15.41
48h after trauma	9.39±1.00	169.29±11.25

(pg/ml)

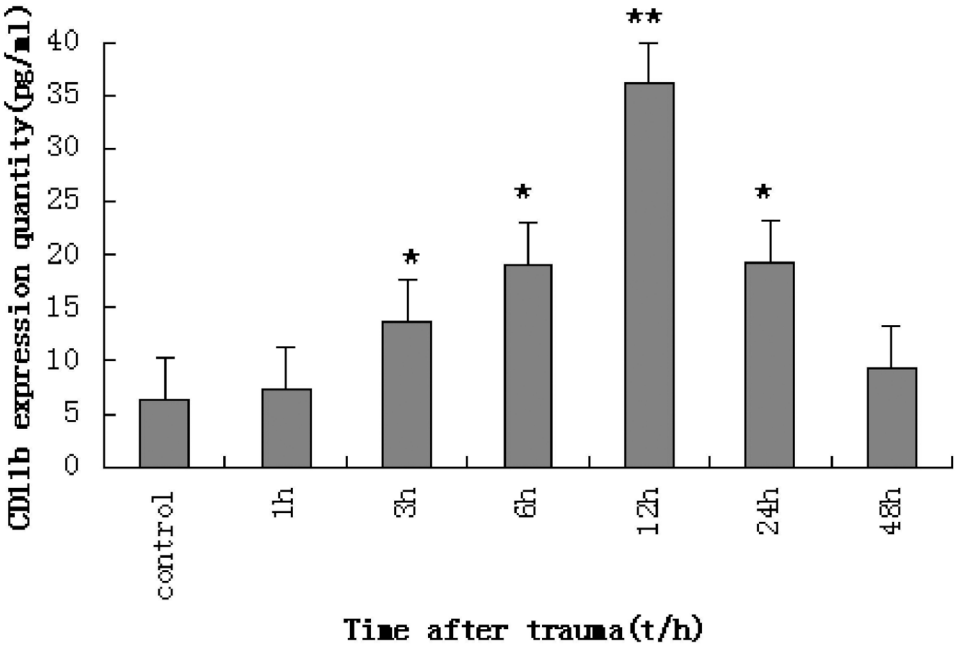

Fig. 2. *Changes of the expression of CD11b of the microglia cells from the mice after craniocerebral injury.*

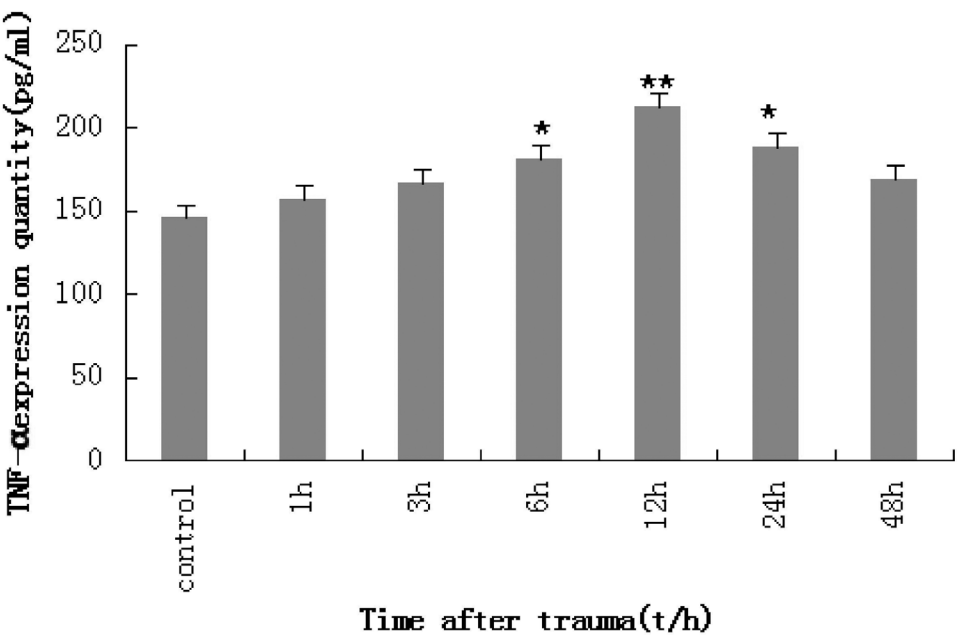

Fig. 3. *Changes of the expression of TNF-α of the mice after craniocerebral injury.*

of various growth factors (10). The neurotrophy affects TNF-α in the process of promoting neuron and repair and regeneration of axon. TNF-α can induce the regeneration of blood capillary and revascularization is the requirement of the survival of the residual tissues as well as the repair and regeneration of tissues (11).

In our study, the phagocytic ability of microglia cells was gradually enhanced, and then gradually decreased. The expressions of CD11b and TNF-α were also gradually enhanced and then gradually decreased. Further studies need to be carried out to confirm these results.

REFERENCES

1. Feeney DM, Boyeson MG, Linn RT, Murray HM, Dail WG. Responses to cortical injury: I. Methodology and local effects of contusions in the rat. Brain Res 1981; 211:67-77.
2. Grassi F, Mileo AM, Monaco L, Punturieri A, Santoni A, Eusebi F. TNF-alpha increases the frequency of spontaneous miniature synaptic currents in cultured rat hippocampal neurons. Brain Res 1994; 659(1-2):226-30.
3. Masuda T, Iwamoto S, Mikuriya S, Tozaki-Saitoh H, Tamura T, Tsuda M, Inoue K. Transcription factor IRF1 is responsible for IRF8-mediated IL-1β expression in reactive microglia. J Pharmacol Sci 2015; 8:216-20.
4. Rezaie P, Male D. Mesoglia & microglia--a historical review of the concept of mononuclear phagocytes within the central nervous system. J Hist Neurosci 2015; 11:325-99.
5. Bonardi JP, da Costa FH, Stabile GA, Pereira-Stabile CL. traumatic dysgeusia, an unusual complication of facial trauma: a case report. J Oral Maxillofac Surg 2016; pii: S0278-2391(16)00129-4.
6. Kapoor K, Bhandare AM, Farnham MM, Pilowsky PM. Alerted microglia and the sympathetic nervous system: A novel form of microglia in the development of hypertension. Respir Physiol Neurobiol 2015; pii: S1569-9048(15)30087-2.
7. Muessel MJ, Harry GJ, Armstrong DL, Storey NM. SDF-1α and LPA modulate microglia potassium channels through Rho GTPases to regulate cell morphology. Glia 2013; 61:1620-8.
8. Schrijvers DM1, Martinet W, De Meyer GR, Andries L, Herman AG, Kockx MM. Flow cytometric evaluation of a model for phagocytosis of cells undergoing apoptosis. J Immunol Methods 2004; 287:101-8.
9. Tooyama I, Bellier JP, Park M. Morphologic study of neuronal death, glial activation, and progenitor cell division in the hippocampus of rat mothods of epilepsy. Epilepsia 2002; 43(Suppl 9):39-43.
10. Xu B, Yu DM, Liu FS. Effect of siRNA–induced inhibition of IL6 expression in rat cerebral gliocytes on cerebral edema following traumatic brain injury. Mol Med Rep 2014; 10:1863-8.
11. Stover JF, Sakowitz OW, Schöning B, Rupprecht S, Kroppenstedt SN, Thomale UW, Woiciechowsky C, Unterberg AW. Norepinephrine infusion increases interleukin 6 in plasma and cerebrospinal fluid of brain injured rats. Med Sci Monit 2003; 9:3822-81.

LETTER TO THE EDITOR

LACTULOSE ORAL SOLUTION FOR THE TREATMENT OF POSTPARTUM CONSTIPATION

P. HUANG[1], WL. GOU[1], XT. WANG[2], YL. DING[3], J. HE[4] and CH. WANG[5]

[1]Department of Obstetrics and Gynecology, The First Affiliated Hospital of Medical College of Xi'an Jiaotong University, Xi'an, Shanxi, China; [2]Department of Obstetrics, Provincial Hospital Affiliated to Shandong University, Jinan, Shandong, China; [3]Department of Obstetrics and Gynecology, The Second Xiangya Hospital of Central South University, Changsha, Hunan, China; [4]Department of Obstetrics, Women's Hospital School of Medicine Zhejiang University, Hangzhou, Zhejiang, China; [5]Department of Obstetrics, Shenzhen Maternal & Health Hospital, Shenzhen, Guangdong, China

Received December 5, 2015 – Accepted May 10, 2016

The purpose of this study is to explore the effectiveness and safety of lactulose oral solution in treating puerperal constipation. The lactulose group was given lactulose, 15 ml once a day, and then given a maintenance dose of 5 ~ 15 ml/time according to defecation condition of patients. Maintenance treatment lasted for one week if the symptoms were relieved; but once symptoms recurred, the medication was restored. Patients in the control group were blank controls. The treatment lasted for six weeks. The conditions of patients, adverse events and combined medication were recorded every day. Patients were evaluated with SF-36 scale before and after treatment. Two hundred and eleven patients with postpartum constipation were selected from five research institutes and they were divided into lactulose group (n=106) and control group (n=105). The curative effect and the improvement of symptoms of the lactulose group were much better than those of the control group ($p < 0.01$). Constipation in the lactulose group relieved faster compared to the control group ($p < 0.05$). Number of days without constipation in the lactulose group was much more than that of the control group ($p < 0.05$). Defecation time in the lactulose group was shorter than that of the control group ($p < 0.05$). Dose of lactulose in the lactulose group reduced week by week. Differences of general physical conditions in SF-36 scale between two groups were statistically significant ($p < 0.05$). Various vital signs of the two groups had no significant changes after treatment. It can be concluded that, lactulose is an effective and safe drug for treating postpartum constipation.

Postpartum constipation is a commonly seen puerperal disease. An epidemiological investigation demonstrates that, 40% of pregnant women develop postpartum constipation in one month after delivery, and 2 to 5 days after delivery is the peak period of constipation occurrence. Constipation is usually accompanied by abdominal distension, abdominal pain, headache, insomnia, irritable mood, inappetence and even haemorrhoids and rectocele and can induce heart disease and cerebral hemorrhage in severe cases, which can influence diet, sleep, milk-secretion and recovery and thus affect living quality (1). Therefore, postpartum constipation should be attached importance. Lactulose is a synthesized

Key words lactulose, constipation, Bristol stool scale, clinical test

Mailing address:
Ms Wenli Gou,
No. 277, Western Yanta Road,
Department of Obstetrics and Gynecology
The First Affiliated Hospital, Medical College,
Xi'an Jiaotong University, Xi'an, Shanxi, 710061, China
e-mail: gouwenli215@163.com

0393-974X (2016)

disaccharide which has been applied for treating constipation in foreign countries for forty years. Lactulose will not cause risks to fetus or newborn because human body is lack of enzyme that can hydrolyze lactulose and moreover lactulose cannot be absorbed by intestinal tract, enter maternal blood or be secreted through milk (2). We carried out a clinical random-controlled study to observe clinical effect of lactulose in treating postpartum constipation and its side effects, aiming to provide an evidence-based medical basis for correct and reasonable use of lactulose in treating postpartum constipation.

MATERIALS AND METHODS

A multi-center clinical random-controlled research was carried out on two hundred and eleven patients with postpartum constipation selected from five research institutes who were divided into a lactulose group (n=106) and a control group (n=105).

Inclusion criteria

Subjects who had undergone caesarean section and had at least 2 points of constipation score and category III below stool type for at the last four weeks of gestation were included in the study. Pregnant women who developed galactosemia, diabetes, severe heart, liver andrenal dysfunction, severe anemia, severe hypertension, allergy or secondary constipation, who took other drugs that could influence this test in the previous three days, who could not understand or complete the test, who joined other clinical drug tests, or who had other factors that could influence the results of the test or was considered unadvisable to join the test by the researchers were excluded.

The study was approved by the medical ethics committee of the First Affiliated Hospital of Medical College of Xi'an Jiaotong University, Shanxi, China, and all participants signed informed consent.

Grouping and medication method

The participants were randomly divided into a lactulose group (n = 106) and a control group (n = 105).

Lactulose oral solution (Lidong) (Beijing Hanmi Pharmaceutical Co., Ltd.) was used as medication. The drug was stored in the pharmacies of the research centers where the patients could get the medication with a doctor's prescription. All subjects in the lactulose group were given lactulose postoperatively, first orally administrated 15 ml each time, once each day, then the dose was adjusted 5-15 ml daily, according to defecation condition (e.g. diarrhea). They were asked to do out of bed activity, strengthening exercises and pay attention to diet. If the symptoms relieved (stool type: category IV; constipation score: 0 point), then the treatment stopped after one week; but patients had to retake lactulose if the symptoms reappeared. The patients returned to the hospital for follow-up examination 42 days after delivery. Patients in the control group were advised to do out of bed bed activities and more exercises and they were given psychological and dietary interventions. They were asked to remain calm and to eat a healthy diet (crude fiber food, more vegetables, fruits and juice). The treatment lasted for six weeks.

Observation index

An observation diary was written for each case every day annotating the drug dose, Bristol stool type (3) (classification criteria: category I: isolated hard mass; category II: mass; category III: dried allantoids stool; category IV: soft allantoids stool; category V: soft mass; category VI: muddy stool; category VII: watery stool), time taken for defecation, defecation frequency, constipation degree (classification criteria: no difficulty: 0 point; hard defecation: 1 point; mass or harden stool, very hard: 2 points; incomplete defecation or anal obstruction or rectal obstruction: 3 points; need external force such as massage and even manual removal), abdominal distension condition, hemafecia or not, and haemorrhoids prolapse or not. The incidence of adverse events and concomitant medication were recorded. SF-36 scale was used both before and after treatment. SF-37 scale, a commonly used method for evaluating quality of life, includes 8 dimensions (physical component scale: physical function (PF), role - physical (RP), body pain (BP), and general health (GH); mental component scale: vitality (VT), social function (SF), role - emotional (RE), mental health (MH)) and 36 items. All patients were graded. A high score indicates milder damage on the corresponding function and a better quality of life. During the entire study, the safety of the subjects was monitored and an overall evaluation was made on curative effects.

Indexes of curative effects

The main indexes of the curative effects were evaluated based on defecation frequency, stool property as well as clinical condition (abdominal distension condition, hemafecia or not, haemorrhoids prolapsed or not). The curative effect can be divided into significantly effective, effective and ineffective. If defecation habit recovered, then treatment was determined as remarkably effective; if the patient defecated for more than 2 times each week, then treatment was considered as effective. When there was no improvement compared to before treatment, then the treatment was considered as ineffective. The calculation formula of overall effective rate was: overall effective rate = (number of cases of remarkable effect + number of cases of effective effect) / total number of cases × 100%. Patients in the lactulose group were forbidden to take other drugs of the same kind, purgative prescription, laxative, lubricant, etc. When use of the drugs mentioned above could not be avoided because of severe symptoms, treatment was considered as ineffective.

Secondary indexes of the curative effects were constipation relief time, dose and living quality score (SF-36 scale).

Safety evaluation

The incidence of adverse reactions was monitored during the entire study time. Blood routine indexes, blood biochemical indexes, urine routine indexes and stool routine indexes were examined at the beginning of the study and in the 6th week.

Statistical analysis

Statistical analysis software was used. The main curative effects were evaluated using Cochran-Mantel-Haenszel (CMH) *chi*-squared test. Constipation relief time in the evaluation of the secondary curative effects was processed by the Kaplan-Meier method. Comparison between the two groups was performed using log-rank test. Dose and medication days were processed by *t*-test or rank sum test. Score of living quality (SF-36 scale score) was tested with analysis of covariance (ANCOVA). Bristol stool type, defecation time, defecation frequency and constipation degree were compared between groups using rank sum test. All statistical tests were bilateral. Difference was considered to be statistically significant if $p < 0.05$.

RESULTS

General data

In the study, 221 patients who conformed to the inclusive criteria were selected from five research centers from November 2013 to April 2014 and were randomly divided into a lactulose group (n = 106) and a control group (n = 105). All cases finished the treatment. Demographic data, vital signs, medical history, quality of life scale and concomitant medication had no remarkable differences between the two groups, therefore the results were comparable.

Main indexes of curative effect

In the lactulose group, treatment for 103 cases was significantly effective or effective (97.11%) and treatment for 3 cases (2.83%) was ineffective; in the control group, the corresponding number of cases was 21 (20%) and 84 (80%), respectively. Difference between the two groups was remarkable ($p < 0.01$). The lactulose group had a higher total effective rate compared to the control group.

Secondary indexes of curative effect

Defecation frequency, stool property and clinical conditions in the two groups had no significant differences. Improvement of symptoms in the lactulose group was more obvious than that of the control group. Details are shown in Table I.

Constipation relief time

Censoring rate in the lactulose group (5.66%) was much lower than that of the control group (11.43%). It meant that the proportion of patients whose symptoms had not improved in the control group was higher than that of the lactulose group. Median relief time in the lactulose group (7 days) was shorter than that of the control group (9 days). Log-rank based statistical analysis demonstrated that the statistics were 9.55 and p value was 0.002, suggesting there was a statistically significant difference between the two groups.

The number of days without constipation in the lactulose group was more than that of the control group; mean and corresponding 95% confidence interval in the lactulose group and control group were 30.96 (28.49, 33.43) and 24.96 (22.28, 27.64),

Table I. *Statistical analysis of clinical curative effects of lactulose.*

Item	Lactulose group	Control group	Statistics	p value
No. of cases (missing case)	106(0)	105(0)		
Defecation frequency			*Chi*-squared value =89.8811	<0.001
Not improved	13(12.26%)	81(77.14%)		
Improved	93(87.74%)	24(22.86%)		
Stool property			*Chi*-squared value=134.5016	<0.001
Not improved	4(3.77%)	87(82.86%)		
Improved	102(96.23%)	18(17.14%)		
Clinical condition			*Chi*-squared value =76.2397	<0.001
Not improved	3(2.83%)	61(58.1%)		
Improved	103(97.17%)	44(41.9%)		

Table II. *Comparison of scores of 37F scale.*

Item	Lactulose group	Control group	Statistics	p value
Difference of PCS score			WIL rank sum test value = 0.575	0.566
No. of cases (missing)	106(4)	105(1)		
Mean (standard deviation)	8.91(16.88)	7.15(16.16)		
Difference of GH score			WIL rank sum test value = 2.493	0.013
No. of cases (missing)	106(4)	105(1)		
Mean(standard deviation)	2.7(13.08)	-2.07(11.9)		
Difference of MCS score			WIL rank sum test value = 0.695	0.487
No. of cases (missing)	106(4)	105(1)		
Mean (standard deviation)	4.24(15.77)	1.33(14.66)		

respectively. Differences between the two groups were significant, suggesting the improvement of defecation in the lactulose group was better than that of the control group.

The results suggested that F statistics of group effect was 19.4 and p value was lower than 0.001, suggesting a significant difference between the two groups; F statistics of time effect was 26.1 and p value was lower than 0.001, suggesting a significant difference in time effect between the two groups; F statistics of interaction effect of time and group was 3.43 and p value was 0.025, suggesting there was a remarkable difference. Compared to the first week, defecation time in the 2nd, 3rd, 4th, 5th and 6th week was significantly different. In addition, average defecation time of the lactulose group was lower than that of the control group.

Drug dosage

The dosage of lactulose in the lactulose group reduced weely. Mean of dose from the 1st week to 6th week was 18.17(6.03), 14.96(5.25), 13.45(5.34), 12.14(4.59), 11.46(4.09) and 11.65(3.76) respectively. Mean (standard deviation) of the first three weeks and the last three weeks was 15.33(4.61) and 11.8(4.1) respectively.

36F scale

In the lactulose group, mean and standard deviation of differences of PCS score were 8.91 and 16.88, respectively, while in the control group, the values were 7.15 and 16.16, respectively. There was no significant difference between the two groups (rank sum test = 0.575, p = 0.566). Mean and standard deviation of differences of GH score in the lactulose group were 2.7 and 13.08, respectively; and in the control group, the values were -2.07 and 11.9, respectively, and the difference was significant (rank sum test = 2.493, p = 0.013); the improvement of GH score in the lactulose group was more obvious than that of the control group. Mean and standard deviation of difference of MCS score were 4.24 and 15.77 in the lactulose group and 1.33 and 14.66 in the standard deviation; there was no significant difference (rank sum test = 0.695, p = 0.487). Details are shown in Table II.

Safety index

Temperature, heart rate, systolic pressure, diastolic pressure and breath before and after treament as well as changes of differences of these indexes in the two groups had no significant difference ($p > 0.05$), indicating the drug had no adverse influence on vital signs. Moreover, neither of the groups was observed with adverse events.

DISCUSSION

For pregnant women undergoing caesarean section, conspitation can be induced by fear of pain of surgical wound. Lactulose has been approved for use in treating constipation by the Food and Drug Administration (USA) (4). Lactulose can soften stools, thus increasing the volume of enteric cavity and promoting the discharge of stools (5-8). A previous research (9) suggests that lactulose relieves defecation during pregnancy, but the effect of lactulose on constipation of females who undergo caesarean section has not been reported.

The curative effect of the lactulose group was obviously superior to that of the control group ($p < 0.001$). There was a marked improvement in frequency of defecation, stool property and clinical condition of the lactulose group ($p < 0.001$); constipation of the lactulose group was relieved much faster than that of the control group ($p < 0.05$). The number of days without constipation of the lactulose group was much higher than that of the control group ($p < 0.05$). The average time of defecation of the lactulose group was lower than that of the control group, and the defecation time of the lactulose group in the second, third, fourth, fifth and sixth weeks was remarkably different compared to that in the first week. Furthermore, the dose of lactulose of the lactulose group tended to decrease week by week. Differences of the general physical conditions between the two groups were statistically significant ($p < 0.05$). The changes of difference of various vital signs in the two groups had no statistically significant differences, suggesting the medication of lactulose had no adverse effects on vital signs. As no adverse events were recorded in the two groups, it can be concluded that lactulose

is an effective and safe drug for treating puerperal constipation.

REFERENCES

1. Dennison C, Prasad M, Lloyd A, Bhattacharyya SK, Dhawan R, Coyne K. The health-related quality of life and economic burden of constipation. Pharm Econom 2005; 23(5):461-76.
2. Cullen G, O'Donoghue D. Constipation and pregnancy. Best Pract Res Clin Gastroenterol 2007; 21(5):807-18
3. Lewis SJ, Heaton KW. Stool form scale as a useful guide to intestinal transit time. Scand J Gastroenterol 1997; 32(9):920.
4. Ramkumar D, Rao SS. Efficacy and safety of traditional medical therapies for chronic constipation: systematic review. Am J Gastroenterol 2005; 100(4):936-971.
5. Bouhnik Y, Attar A, Joly F, Riottot M, Dyard F, Flourié B. Lactulose ingestion increases faecal bifidobacterial counts: a randomised double-blind study in healthy humans. Eur J Clin Nutr 2004; 58(3):462-66.
6. Roberfroid, M. Prebiotics: the concept revisited. J Nutrit 2007; 137(3):830S-37S.
7. Aydin S. Lactulose in fat-free milk, rather than increased ghrelin and motilin level, might help for solving constipation: Author update. Nutrition 2011; 27(6):731.
8. Panesar PS, Kumari S. Lactulose: production, purification and potential applications. Biotechnol Adv 2011; 29(6):940-48.
9. Taylor RR, Guest JF. The cost-effectiveness of macrogol 3350 compared to lactulose in the treatment of adults suffering from chronic constipation in the UK. Aliment Pharmacol Ther 2010; 31(2):302-12

LETTER TO THE EDITOR

EFFECT OF OPCML GENE ON THE BIOLOGICAL BEHAVIOR OF GASTRIC CANCER CELL LINE AGS

LH. WANG, FF. CHU, DH. REN and XL. DU

Department of Gastroenterology, Zhengzhou Central Hospital of Zhengzhou University, Zhengzhou, Henan, China

Received December 18, 2015 – Accepted April 4, 2016

The objective of this investigation was to explore the association of OPCML with gastric cancer and its clinical significance. The expression of OPCML was detected by immunohistochemistry in 118 cases of gastric carcinoma. The OPCML expression in the normal tissues and 7 kinds of gastric cells was assessed by RT-PCR. The recombinant plasmid pcDNA3.1-OPCML was constructed and transfected into AGS cells. CCK8 and colony formation assay were employed to analyze the effect of OPCML on AGS. Immunohistochemistry results showed that the expression of OPCML in gastric cancer was 68.6%, and the expression of OPCML was negatively correlated with the depth of tumor invasion and tumor differentiation degree (P <005); OPCML expression, depth of tumor invasion, lymph node metastasis and distant metastasis were important factors affecting the prognosis of the survival of the patients (P <0.05). OPCML m-RNA expression in the gastric cancer cells was significantly lower than that in the normal gastric mucosa. RT-PCR showed that the expression of OPCML was aberrantly increased in the cells transfected with pcDNA3.1-OPCML. CCK8 and colony formation assay showed that OPCML significantly inhibited the growth, proliferation, and colony formation of the AGS cells. OPCML plays an important role in gastric cancer, and may be a new prognostic indicator of gastric cancer.

Gastric cancer is one of the most common human malignant tumors (1), and there is a high percentage annually of new cases and deaths worldwide, with 70% of these occurring in the developing countries (1-3). The research of gastric cancer is a hot topic and its occurrence and development and metastasis-related molecular markers still remain to be investigated (4-5).

Protein/cell adhesion Opioid-binding molecule-like (OPCML) is a receptor for the opium receptor, located in the human chromosome 11q25, expressed in the cell membrane (1).

The number of brain tissues of rats is about 60 kDa (6), and it was found that OPCML plays an important role in cell differentiation and cell membrane properties (7). Studies have found that the expression of OPCML was closely related to many types of tumors (8-13). The objective of this investigation was to explore the association of OPCML with gastric cancer and its clinical significance.

MATERIALS AND METHODS

Cells and tissues from 118 cases of gastric cancer and 18 cases of cancer

Informed consent was signed by the patients to participate in the study, and the patients were voluntarily

Key words: gastric cancer, OPCML expression, biological behavior

Mailing address:
Dr Lihong Wang,
Department of Gastroenterology, Zhengzhou Central Hospital of Zhengzhou University, No195, Tongbai Road
Zhengzhou City, Henan Province, 450001, China
e-mail: wanglihong1202w@163.com

0393-974X (2016)

DISCLOSURE: ALL AUTHORS REPORT NO CONFLICTS OF INTEREST RELEVANT TO THIS ARTICLE.

enrolled in the project. The ethics committee of the Hospital of Zhengzhou University approved this study which conformed to the declaration of Helsinki.

Tissues and normal gastric mucosa tissues were from 98 male and 20 female patients of the First Affiliated Hospital of Zhongshan University, China. Of these patients, gastric cancer TNM staging was as follows: 20 cases with stage of T1 + T2, 98 cases with stage T3 + T4; 37 cases with stage N0 + N1, 1 case with stage N3 + N4. In all the 118 cases, 69 patients had no distant metastasis and 49 patients had distant metastasis. Pathological type: 45 cases of high differentiation adenocarcinoma, 73 cases of poorly differentiated adenocarcinoma. All cases had not received radiotherapy or chemotherapy. Human gastric cancer line 7901, BGC823, MKN28, AGS, N87, KATO, ATCC cell line Rike were from A TCC (Japan) and SNU1 cells were from Tsukuba (Rockville, MD, USA). In addition to AGS cells containing 10% fetal bovine serum (Hyclone) DMEM medium (Hyclone), the other six contained 10% fetal bovine serum RPMI-1640 medium (Hyclone).

Plasmids and strains

1-OPCML recombinant plasmid, pcDNA3.1 vector was purchased from the pan Keno Technology Co., Ltd., Beijing, China. Competent *Escherichia coli* (*E.coli*) DH5 alpha was and *E.coli* DH5 were purchased from TaKaRa company.

Major reagents and tools

Lipofectamine 2000 transfection reagents, neomycin (G418), Opti-MEM and RNA extraction kit were purchased from Invitrogen. Reverse transcription kit was purchased from Fermentas. PCR kit was purchased fromTaKaRa, and Plasmid Extraction Kit from MN company. CCK-8 was purchased from Guangzhou Yi source Biotechnology Co. Ltd.

Immunohistochemistry

Immunohistochemical SP method was used for immunohistochemistry as described previously (8-13). Briefly, The first step was collecting the tissue sample. Fixatives were used to immobilize antigens while retaining cellular and subcellular structures through cross-linking methylene bridges and Schiff bases between basic amino acid residues of proteins. Paraffin was used for maximum tissue preservation and makes a stronger block for sectioning tissue. Immunostaining was the process of incubating the tissue/cells with antibodies to form the antigen-antibody complex for the detection/ signal of targeted antigen. Detection was achieved using a fluorescent signal generated from an ultraviolet source.

Cell culture

Cells were cultured as described previously (7). Briefly, the cells were seeded onto the culture medium of DMEM with 10% FBS at a density of 5×10^5 cells/mL. The cell culture conditions were 37°C, 5% CO_2. The cells were cultured for 48 h for further analysis including RT-PCR and MTT assay.

m-RNA expression of OPCML gene was detected by RT-PCR

The total RNA of normal gastric mucosa and gastric cancer cells was extracted with MN kit, the cDNA was used as template, and the S12 was amplified by PCR. Specific bands at 688bp showed that cDNA was of good quality. The RNA extraction and RT-PCR amplification reaction of gastric cancer cells were performed with reference to the kit manual for normal gastric mucosal tissues and 7 human gastric cancer cells. The RT-PCR reaction conditions were as follows: 95°C, 5 min for pre-denaturation, and in each cycle, first 95°C,1 min for denaturation, 60°C, 30 s for annealing, 72°C, 40 s for extending, after a total of 30 cycles, there was final extending at 72°C for 7 min.

pcDNA3.1

OPCML gene was cloned into the vector pcDNA3.1 as described previously (7). Briefly, the DNA segment of OPCML gene was obtained by PCR, as shown in the PCR part above. Then, the DNA segment of OPCML gene and the pcDNA3.1 were digested with EcoR I and Hind III at 37°C for 4 h. The digested OPCML gene and the pcDNA3.1 were purified and ligated by DNA Ligase according to the manufacturer's instructions. The ligate produced were transformed into *Escherichia coli* for amplification.

Cell transfection

Cell transfection was conducted as described previously (7). Briefly, the cells were initially incubated in 5% CO2 at 37°C. for 24 h. With this transfection method, cells

were grown in 10% volume FBS during the transfection procedure. The transfection reagents were mixed with the pcDNA3.1 OPCML gene. After incubation of the above mixture for 5 min, the mixture was added to the cell culture medium. Then, the cells with the DNA mixture were mixed fully and slowly. The transfected cells were cultured in 5% CO2 at 37°C. for 24 h.

Cell clone formation experiment

Gastric cancer cells AGS were transfected with the empty vector pcDNA3.1 or the recombinant vector with OPCML. Clone formation experiments were conducted as described previously (7) using the above transfected cells. Briefly, the cells were seeded at 106 cells/ml in a 6-well plate and allowed to grow for 48 h. Cells were then transiently transfected with 1 μg of pcDNA3.1 using LipofectAMINE 2000. At 48-h post-transfection, the transfected cells were seeded onto six-well plates at a density of 104 cells/well with G-418 selection (200 μg/ml). After 2.5 weeks, cells were stained with Gentian Violet and examined. Numbers of colonies (with >50 cells/colony) were counted and analysed.

Cell growth curve

Gastric cancer cells AGS were transfected with the empty vector pcDNA3.1 or the recombinant vector with OPCML. Cell growth experiments were conducted as described previously (7) by using the CCK8 kit. Briefly, at 48 h post-transfection, the transfection medium in each well was replaced with 100 μl fresh serum-free medium containing 0.5 g/l MTT. Subsequent to incubation at 37°C for 4 h, the MTT medium was removed by aspiration and 50 μl dimethylsulfoxide was added to each well. Following incubation at 37°C for a further 10 min, the optical density at 570 nm was measured using the Bio-Tek™ ELX-800™ Absorbance Microplate reader.

Statistical analysis

Using SPSS13.0 software for statistical analysis, the experimental data were compared with the standard deviation (SD), *t*-test, survival analysis using Log-Rank test; $P < 0.05$ for the difference was statistically significant.

RESULTS

Relationship between the expression of OPCML and gastric cancer

OPCML protein was mainly expressed in the cytoplasm and cell membrane with yellow and brown staining (Fig. 1).

In 118 cases of gastric cancer, 81 (68.6%) had low

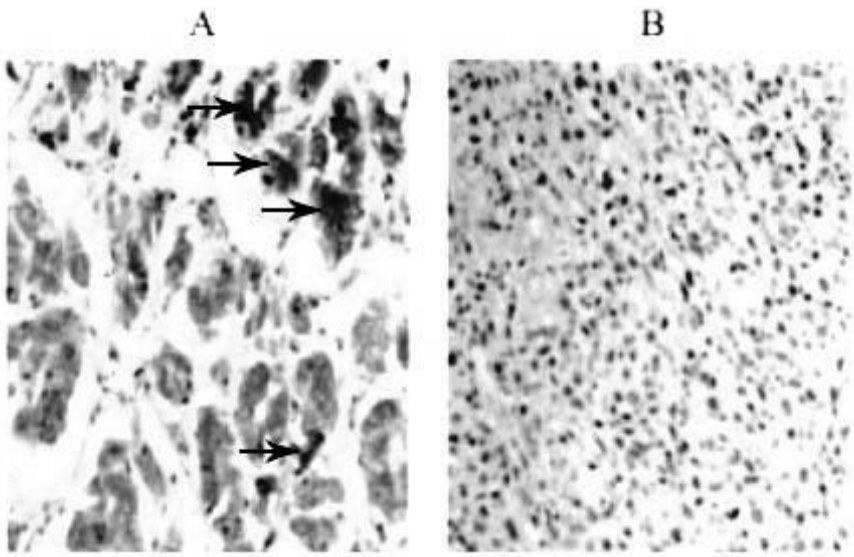

Fig. 1. *Representative images of OPCML protein expression in the gastric cancer tissues (**A**) and their adjacent non-tumour tissues (**B**) determined by immunohistochemistry. Arrows show positive expression of OPCML.*

Note: Both the gastric cancer tissues and their adjacent non-tumour tissues were collected and subjected to immunohistochemistry analysis. Representative images of OPCML protein expression are demonstrated.

expression of OPCML, and the expression of OPCML was related to the depth of invasion and differentiation of the gastric cancer. The expression rate of OPCML was 74.5% (73/98) and 40% (8 T_1) in /T4 T3 and /T_2 P, and the difference was significant ($P < 0.05$). The expression rate of OPCML in the poorly differentiated gastric cancer patients was 90.4% (66/73), which was significantly higher than that in the differentiation of 15 (33.3% /45), and the difference was significant ($P < 0.05$), and the expression of OPCML was not significantly related to gender, age, lymph node metastasis or distant metastasis ($P > 0.05$)

Relationship between OPCML expression and survival rate of the gastric cancer patients

The depth of invasion, lymph node metastasis, distant metastasis and OPCML expression are important factors affecting the prognosis of gastric cancer patients ($P < 0.05$). The average survival rates of the patients with T3/T4 and /T2 T1 were (26.0±2.7) and (49.8±8.4) months and the difference was significant ($P < 0.01$); /N3 N0 and /N1 N2 were (24.9±3.0) and (40.9±5.6) months, and the difference was significant. The survival rate of the patients without distant metastasis (38.4±3.7) was significantly higher than those of the distant metastasis (17.2±3.1) months ($P < 0.0001$). The survival rate of the patients with low expression of OPCML (25.7±2.9 months) was lower than that of the patients with high expression of OPCML (39.7±5.8 months) ($P < 0.05$). The survival rate of the patients had no significant relationship with age or differentiation degree ($P > 0.05$).

m-RNA expression of OPCML in normal gastric mucosa and gastric cancer cells

The expression of OPCML in the normal gastric mucosa was up-regulated after the transfection of OPCML, and the expression of AGS, BGC823, MKN28, N87, KATO, SNU1 was down regulated in the gastric cancer cell lines (Fig. 2).

Identification of OPCML transfection

After transfection of PcDNA3.1-OPCML and pcDNA3.1 vector into the gastric cancer cell line, RT-PCR results showed that OPCML was highly expressed (Fig. 3).

Inhibition of colony forming ability of AGS by OPCML

The number of colonies formed in the gastric cancer cells was small and the volume was small after transfection of OPCML gene (Fig. 4). The difference of the relative cloning formation rate of AGS cells was 72%. The difference was statistically significant ($P < 0.05$).

Inhibition of AGS cell proliferation by OPCML

Cell growth curve showed that the growth rate of AGS-OPCML group decreased significantly with the increase of time, while the growth curve of AGS-vector cells in the control group showed an increasing trend in 4 D, indicating that the cell proliferation of AGS cells transfected with OPCML gene was significantly decreased ($P < 0.05$) (Fig. 4).

DISCUSSION

The occurrence and development of gastric cancer is a multi-factor and multi-step process. It is closely related to the patients' environment, genetic factors and the infection of *H.pylori*. In addition, activation of oncogenes, inactivation of tumor suppressor genes, dysfunction of apoptosis genes, and activation of metastasis-related genes can lead to malignant transformation of cell proliferation, and participate in the development of tumor (14). McKie et al. (15) found in epithelial ovarian cancer cells that RTKs could bind specific receptor tyrosine kinase (RTKs) extracellular region, and regulate the receptor mediated endocytosis and poly-ubiquitin proteasome pathway.

OPCML is a broad tumor suppressor for multiple cancers, including gastric cancers (1, 10), supporting our data. The novelty of the study is that OPCML can be used as a biomarker for gastric cancer, since the expression level of OPCML is different at different stages of gastric cancer development.

In the present study, we did not use Western blot method to detect the expression of OPCML in cancer tissues because of the interference of other tissues. Therefore, Western blot may not a good method for

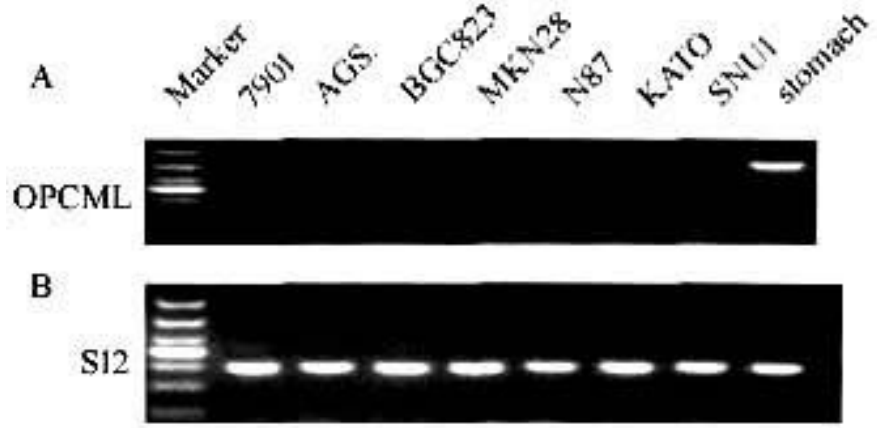

Fig. 2. *The expression of OPCML detected by RT-PCR.*
Note: The total RNA of normal gastric mucosa and gastric cancer cells was extracted with MN kit, the cDNA was used as template, and the S12 was amplified by PCR. Representative images of OPCML protein expression are shown.

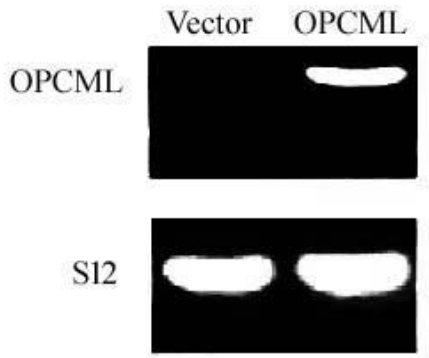

Fig. 3. *The expression of OPCML in the gastric cancer cell line.*
Note: PcDNA3.1-OPCML expression vector and pcDNA3.1 vector were transfected into the gastric cancer cell line, RT-PCR test showed that OPCML was highly expressed.

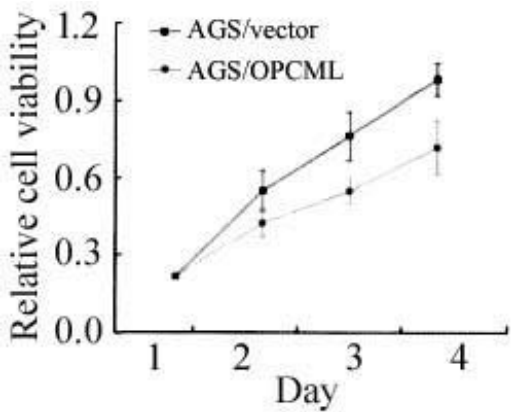

Fig. 4. *Effect of OPCML on the growth of gastric cancer cells (P < 0.05).*
Note: The growth rate of cells transfected with AGS-OPCMLand AGS-vector were analyzed, and there were significant differences in the cell proliferation of the two groups (P < 0.05). AGS-OPCML inhibited cell growth.

the detection of OPCML in cancer tissues. In addition, immunohistochemistry can not only analyze the expression quantity of OPCML of cancer tissues, but can also examine the distribution of OPCML in tumor tissues. Thus, immunohistochemistry is superior to the Western blot method.

In conclusion, the expression level of OPCML is different at different stages of gastric cancer development, therefore may be used as a biomarker for gastric cancer.

REFERENCES

1. Cui Y, Ying Y, van Hasselt A, et al. OPCML is a broad tumor suppressor for multiple carcinomas and lymphomas with frequently epigenetic inactivation. PLoS One 2008; 3:e2990.
2. Jemal A, Bray F, Center MM. Global cancer statistics. CA Cancer J Clin 2011; 61:9-90.
3. Ferlay J, Shin H R, Bray F. Estimates of worldwide burden of cancer in 2008: GLOBOCAN 2008. Int J Cancer 2010; 127:2893-917.
4. Liu HS, Xiao HS. Micro RNAs as potential biomarkers for gastric cancer. World J Gastroenterol 2014; 20:12007-17.
5. Hartgrink HH, Van de Velde CJ. Status of extended lymph node dissection: Locoregional control is the only way to survive gastric cancer. J Surg Oncol 2005; 90:153-65.
6. Schofield PR, McFarland KC, Hayflick JS. Molecular characterization of a new immunoglobulin superfamily protein with potential roles in opioid binding and cell contact. EMBO 1989; 8:489-95.
7. Sellar GC, Watt KP, Rabiasz GJ, et al. OPCML at 11q25 is epigenetically inactivated and has tumor-suppressor function in epithelial ovarian cancer. Nat Genet 2003; 34:337-43.
8. Zhou F, Ma M, Tao G. Detection of circulating methylated opioid binding protein /cell adhesion molecule-like gene as a bio-marker for ovarian carcinoma. Clin Lab 2014; 60:759-65.
9. Duarte-Pereira S, Paiva F, Costa V L. Prognostic value of opioid binding protein /cell adhesion molecule-like promoter methylation in bladder carcinoma. Eur J Cancer 2011; 47:1106-14.
10. Ye F, Zhang S F, Xie X. OPCML gene promoter methylation and gene expression in tumor and stroma cells of invasive cervical carcinoma. Cancer Invest 2008; 26:569-74.
11. Reed JE, Dunn JR, du Plessis DG. Expression of cellular adhesion molecule 'OPCML' is down-regulated in gliomas and other brain tumours. Neuropathol Appl Neurobiol 2007; 33:77-85.
12. Li C, Tang L, Zhao L, et al. OPCML is frequently methylated in human colorectal cancer and its restored expression reverses EMT via downregulation of smad signaling. Am J Cancer Res 2015; 5:1635-48.
13. Zhou F, Tao G, Chen X, Xie W, Liu M, Cao X. Methylation of OPCML promoter in ovarian cancer tissues predicts poor patient survival. Clin Chem Lab Med 2014; 52:735-42.
14. Dhar DK, Udagawa J, Ishihara S. Expression of regeneration gene I in gastric adenocarcinomas: correlation with tumor differentiation status and patient survival. Cancer 2004; 100:1130-36.
15. McKie A B, Vaughan S, Zanini E. The OPCML tumor suppressor functions as a cell surface repressor-adaptor, negatively regulating receptor tyrosine kinases in epithelial ovarian cancer. Cancer Discov 2012; 2:156-71.
16. Chen H, Ye F, Zhang J, Lu W, Cheng Q, Xie X. Loss of OPCML expression and the correlation with CpG island methylation and LOH in ovarian serous carcinoma. Eur J Gynaecol Oncol 2007; 28:464-67.

LETTER TO THE EDITOR

REACTIVITY OF PATIENTS WITH MAINTENANCE HEMODIALYSIS TO ERYTHROPOIETIN IN THE TREATMENT OF RENAL ANEMIA

JP. HU[1], X. CHENG[1], XF. XU[1], GJ. YU[2], F. LUO[3], GS. ZHANG[1], N. YANG[4], P. SHEN[1] and XY. YAN[5]

[1]Nephrology Division of Zhengzhou TCM Hospital, Zhengzhou, Henan, China; [2]Nephrology Division of the Affiliated Hospital of Henan Province Chinese Medicine Research Institute, China; [3]Endocrinology Division of Zhengzhou Central Hospital, Zhengzhou, Henan, China; [4]Science and Education Department of Zhengzhou TCM Hospital, Zhengzhou, Henan, China; [5]Vice President, Zhengzhou TCM Hospital, Zhengzhou, Henan, China

Received July 31, 2015 – Accepted April 14, 2016

To explore the reactivity of patients with renal anemia (MHD) to erythropoietin (EPO) in maintenance hemodialysis (HD), 31 patients were enrolled in this study. According to the level of serum ferritin (SF), they were divided into two groups; one group received treatment using recombinant human erythropoietin (rHuEPO) and the other group was given iron sucrose. Taking terminal EPO dosage, terminal erythropoietin resistance index (ERI) and rate of change of ERI (ΔERI) as target indexes, the influence of SF level on dosage of EPO was evaluated after usage conditions of relevant substances in a 3-month period. The results revealed that differences of dialysis age, albumin (ALB), blood calcium, initial and terminal SF, variable quantity of hemoglobin (Hb), terminal EPO and ERI between two groups had statistical significance. Furthermore, SF level and terminal EPO ($r = -0.37$, $P < 0.05$) as well as SF level and terminal ERI ($r = -0.39$, $P < 0.05$) were negatively correlated. Difference of terminal ERI between the two groups had statistical significance. It can therefore be summarized that supplementing an iron agent intravenously to maintain SF level between 500 ng/ml and 1200 ng/ml may improve reactivity of patients with MHD to EPO. In addition, rHuEPO therapy in treating anemia of patients with MHD has the same effect with intravenous drug delivery, less side effects and is easy to administer.

Renal anemia, one of the most common complications in patients with end-stage renal disease (ESDR) who receive maintenance hemodialysis (MHD), seriously affects patients' living quality and prognosis (1). Effective treatment of renal anemia is an important part of integrated treatment of patients with end-stage renal failure (2). To date, erythropoietin (EPO) has been advocated to correct anemia in China and overseas, but one study (3) found that large doses of EPO lead to risk of death rate, even in the premise of anemia correction (4, 5). Patients with MHD are prone to developing a large loss of iron in blood due to gastrointestinal bleeding and blood loss in the HD pipelines and dialyzer (6); and the use of EPO promotes bone marrow hematopoiesis, thereby increasing the requirement

Key words: erythropoietin, hemodialysis, renal anemia, serum ferritin, renal disease

Mailing address:
Dr Fang Luo,
Endocrinology Division, Zhengzhou Central Hospital,
Zhengzhou, Henan,
450000, China
e-mail: luoffan@163.com

0393-974X (2016)

of iron to the body. Hence, maintaining sufficient iron is likely to be an effective way to correct renal anemia of patients with MHD and reduce EPO dosage. In clinical practice, serum ferritin (SF) is usually considered as an index for evaluating iron, and high levels of SF may improve EPO reactivity, which has been pointed out by some scholars in recent years (7, 8).

One study (9) reveals that iron overload still does not occur in patients with MHD who received treatment for renal anemia with EPO when SF reaches 1,047±445 ng/ml. This study aimed to discuss the reactivity of patients with MHD to EPO when SF rises to 500 ~ 1,200 ng/ml, which provides a new treatment method for reducing dosage of EPO.

MATERIALS AND METHODS

Thirty-one patients who had no history of peritoneal dialysis (PD) and received HD at the blood purification department of the hospital of traditional Chinese medicine of Zhengzhou in Henan, China, from 2013 to 2015 were selected. The patients were 20 males and 11 females, with average age of 55±13 years (30-80 years), average weight of 59±10 kg and average dialysis treatment of 54±35 months. With regard to the causes of chronic kidney disease (CKD), there were 22 cases of chronic glomerulonephritis, 3 cases of hypertensive nephropathy, 3 cases of diabetic nephropathy (DN) and 3 cases of obstructive nephropathy (ON). According to the level of SF, the patients were divided into two groups: group A (100 ng/ml < SF < 500 ng/ml) including 13 males and 3 females (ages 32 to 80 years), and group B (500 ng/ml ≤ SF < 1,200 ng/ml) including 7 males and 8 females (ages 32 to 76 years). The study was approved by the ethics committees of the hospital of traditional Chinese medicine of Zhengzhou, and all patients signed informed consent.

Diagnostic standards

Patients were diagnosed with CKD-5 HD if they had had chronic kidney structural and functional disorders for over 3 months, had less than 15 ml/min glomerular filtration rate (GFR) and had received HD treatment; CKD-associated renal anemia was confirmed for CKD patients over 15 years and who on examination had 130 g/L (males) and 120 g/L (females) below hemoglobin (Hb) concentrations (6).

Inclusion criteria

Patients who were aged at least 18 years, had been undergoing dialysis for more than 3 months, suffered from CKD-5 HD, suffered from renal anemia and had previously received EPO therapy, undergone 4-hour HD three times every week and showed at least 1.2 urea clearance index, 10 mg/L higher C-reactive protein level (CRP) and SF level between 100 ng/ml and 1200 ng/ml, were included.

Exclusion criteria

Patients who had a history of blood transfusion, iron allergy, anemia related to malignant tumors, acute infection and anemia caused by other reasons (folic acid deficiency, systemic lupus erythematosus, hemorrhagic anemia or thalassemia) three months before the study were excluded.

Baseline indicators

Research data, such as basic clinical features, relevant HD data, biochemical and immune indexes, usage of statins and angiotensin converting enzyme inhibitor/angiotensin receptor blocker (ACEI/ARB), and dosage of recombinant human erythropoietin (rHuEPO), were collected from medical records and the database of the blood purification department of hospital of traditional Chinese medicine of Zhengzhou in Henan.

Measurement of biochemical and immune indexes

Hb was tested by LH780 five-classification automatic blood cell analyzer.

Albumin (ALB), blood calcium, serum phosphate, CRP and urea nitrogen were measured with bromocresol green (BCG), methyl-xylenol blue (MXB), ultraviolet light, immunoturbidimetry, urease continuous detection method and bathophenanthroline direct method, respectively, and iron and total iron saturation were tested with HITACHI automatic biochemical analyzer.

Intact parathyroid hormone (i-PTH) was measured with chemiluminescence immunoassay (CLIA) using LIAISON automatic chemiluminescence immune analyzer; and SF was tested with electrochemiluminescence (ECL) using Cobas e601.

Calculation formula

Transferrin saturation (TS) refers to the ratio of iron to total iron binding capacity (TIBC). The calculation formula for urine clearance index was as follows: urea clearance index = - In (R - 0.008 t) + (4 - 3.5 R) * (Δ B/W), in which t is dialysis duration, R refers to urea nitrogen after dialysis/ urea nitrogen before dialysis, AB represents ultrafiltration volume and W is weight after dialysis. Calculation formula for erythropoietin resistance index (ERI) was: ERI = weekly EPO usage / (weight after dialysis * Hb) * 100%.

Based on the above formulas, patients in the two groups were treated with iron sucrose and rHuEPO respectively, and the above observation indexes were collected and calculated; influence of SF levels on EPO reactivity were evaluated by taking terminal EPO usage, terminal ERI, and rate of change of ERI (ΔERI) as target indexes.

Statistical analysis

SPSS 17.0 statistical software was used for data analysis. Measurement data were expressed as mean±SD, and two groups of mean values with normal distribution and homogeneous variances were processed by independent sample *t*-test, while those not conforming to normal distribution were processed by rank sum test. Furthermore, enumeration data were expressed as percentage (N/%) and processed by *chi*-squared test, and correlation analysis was performed. Differences were considered as statistically significant if $P < 0.05$.

RESULTS

Analysis of basic clinical materials

In group A and group B, differences in age (54±14 years *vs* 56±12 years) , weight (58±7 kg *vs* 60±13 kg), gender (13/3 *vs* 7/8), dialysis period (28±10 months *vs* 80±70 months), chronic glomerulonephritis (11 cases *vs* 11 cases), hypertensive nephropathy (2 cases *vs* 1 case), DN (2 cases *vs* 1 case) and ON (1 case *vs* 2 cases) were obvious, especially dialysis age ($P < 0.05$), and the rest of features had no statistically significant differences ($P > 0.05$). Moreover, vascular accesses in group A and group B mainly included long-term catheter (9 cases *vs* 6 cases) and internal arteriovenous fistula (7 cases *vs* 9 cases), and the differences had no statistical significance ($P > 0.05$).

Biochemical and immunological indexes

Comparison of group A and group B showed that differences of levels of ALB (35.62±5.62 g/l *vs* 39.29±2.26 g/l) and blood calcium (2.08±0.21 mmol/L *vs* 2.32±0.30 mmol/L) were statistically significant ($P < 0.05$). However, levels of serum phosphate (1.89±0.61 mmol/L *vs* 1.82±0.42 mmol/L), i-PTH (339.9±275.4 pg/ml *vs* 613.9±317.8 pg/ml), CRP (6.6±4.5 mg/L *vs* 16±5.5 mg/L), TS (0.33±0.1 *vs* 0.3±0.09) had no statistically significant difference ($P > 0.05$), as well as terminal CRP (6.74±3.60 mg/L *vs* 5.50±5.11 mg/L).

Statins

In the two groups, differences of use of statins (1 case *vs* 1 case) and ACEI/ARB (11 cases *vs* 13 cases) had no statistical significance ($P > 0.05$).

Hemoglobin

Initial Hb (95.51±21.07 g/l *vs* 93.54±16.08 g/l) and terminal Hb (107.22±18.23 g/l *vs* 119.36±17.4 g/l) were not statistically significant in the two groups ($P > 0.05$); and difference of Δ Hb (11.67±5.75 g/l *vs* 24.36±13.22 g/l) had statistical significance ($P < 0.05$).

Serum ferritin

Initial SF (364.95±336.76 ng/ml *vs* 767.87±408.86 ng/ml) and terminal SF (291.67±109.2 ng/ml *vs* 833.15±169.05 ng/ml) of the two groups showed a statistically significant difference ($P < 0.05$).

Recombinant human EPO

Initial EPO of two groups were (146.58±27.23 U/Kg • W *vs* 121.1±56.6 U/Kg • W), Δ EPO was (-7.59±17.33 U/Kg • W *vs* -9.83±24.38 U/Kg • W), EPO amount was (112647.54±28117.28 *vs* 99557.0±40734.78)

ERI

Initial ERI of group A and B were (1.62±0.51 U/kg/Hb *vs* 1.29±0.66 U/kg/Hb) and Δ ERI was (-15.62%±11.78% *vs* -19.23%±16.88%); terminal ERI was (1.39±0.40 U/kg/Hb *vs* 1.02±0.50 U/kg/Hb); terminal ERI had a statistically significant difference ($P < 0.05$) while others had no statistical significance ($P>0.05$).

Table I. *Analysis of correlation between dosage of terminal EPO and E*

Index	Correlation coefficient		P value	
	Dosage of terminal EPO	Terminal ERI	Dosage of terminal EPO	Terminal ERI
Dialysis age	-0.04	0.85	-0.10	0.58
Blood calcium	-0.20	0.28	-0.21	0.27
Albumin	-0.19	0.29	-0.31	0.09
Serum ferritin	-0.37	0.04	-0.39	0.03

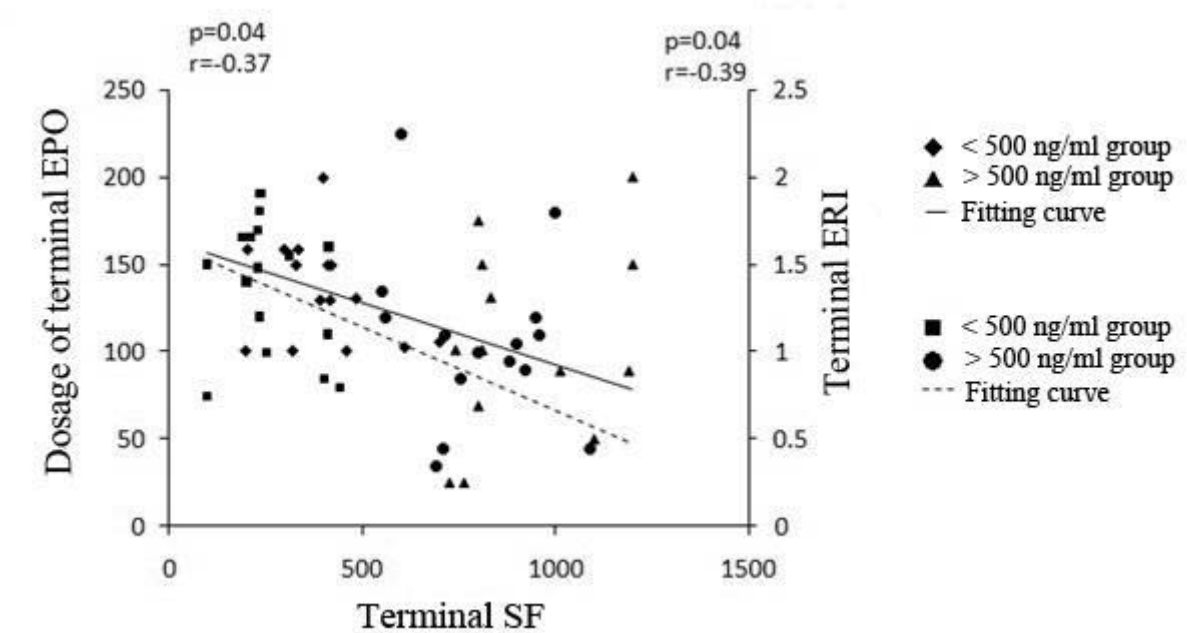

Fig. 1. *Correlation of terminal SF and terminal EPO dosage.*

Correlation analysis of independent variable and dependent variable

SF was negatively related to terminal EPO ($r = -0.37$, $P < 0.05$); terminal SF was in a negative correlation with ERI ($r = 0.39$, $P < 0.05$) (Table I and Fig. 1).

DISCUSSION

Recently, it was reported that renal anemia has great impact on quality of life and survival rate of patients with uremia, which can be compared to insufficient dialysis, malnutrition, infection, cardiovascular complications, etc. Not treating or treating renal anemia in an improper way always induces a series of complications that deteriorate the patient's prognosis (10, 11). Therefore, correct and timely treatment for renal anemia of CRF patients is of great importance. Kidney cannot be stimulated to produce sufficient EPO during CRF, as oxygen is poor because of anemia, hence

external supplement is necessary (12, 13).

Dialysis adequacy is believed to be an important independent factor predicting rHuEPO reactivity, and small molecule and medium molecular substances created by red blood cells are eliminated effectively through increasing dialysis dosage, which improves rHuEPO reactivity (14). Low EPO reactivity of patients with end-stage uremia is correlated to dialysis inadequacy, and haematocrit (HCT) rises obviously through increasing dialysis intensity. It is also reported that ACEI is able to induce red blood cell precursor apoptosis of patients with kidney transplant (15), lower the Hb level of patients undergoing HD, and increase the EPO dosage; and withdrawal of ACEI can result in the increase of HCT and the decrease of dosage of EPO.

Featured by definite curative effects and mild adverse reactions, EPO seems to be a good choice of treatment of chronic renal anemia. Blood transfusion has greater side effects than EPO, and is only suitable for a few patients with severe renal anemia when other therapies are not ideal or urgent blood transfusion is required to save lives.

ACKNOWLEDGEMENTS

This work is supported by the Scientific and technological key project of Henan, Project number: 142102310166.

REFERENCES

1. Du M, Cheng DM, Wei YL. Clinical observation of erythropoietin joint iron dextran treating chronic anemia of maintenance hemodialysis patients and nursing care. Pract J Clin Med 2011; (4):1-6.
2. Schneider A, Schneider MP, Scharnagl H, Jardine AG, Wanner C, Drechsler C. Predicting erythropoietin resistance in hemodialysis patients with type 2 diabetes. Nephrology 2013; 14(1):1-7.
3. Mehrotra A, Leung WY, Joson T. Erratum to: Nutritional vitamin D supplementation and health-related outcomes in hemodialysis patients: a protocol for a systematic review and meta-analysis. System Rev 2015; 4(1):143-49.
4. Gobin J, Cernii A, Mclean R, Finkelstein DFO, Simon DB. Conversion from epoetin alfa to darbepoetin alfa for management of anaemia in a community chronic kidney disease centre: a retrospective cohort study. Clin Drug Invest 2011; 31(2):113-20.
5. Pfeflfer MA, Burdmann EA, Chen CY, et al. A trial of darbepoetin α in type 2 diabetes and chronic kidney disease. N Engl J Med Overseas Ed 2009; 361 (21):2019-32.
6. Kidney Disease: Improving Global Outcomes (KDIGO) Anemia Work Group. KDIGO Clinical Practice Guideline for Anemia in Chronic Kidney Disease. Kidney Inters 2012; 2: 279-335.
7. Nagaraju SP, Cohn A, Akbari A, Davis JL, Zimmerman DL. Heme iron polypeptide for the treatment of iron deficiency anemia in non-dialysis chronic kidney disease patients: a randomized controlled trial. Nephrology 2013; 14(1):1-7.
8. Sedighi O, Makhlough A, Janbabai G, Neemi M. Comparative study of intravenous iron versus intravenous ascorbic acid for treatment of functional iron deficiency in patients under hemodialysis: a randomized clinical trial. Nephro-urol Mon 2013; 5(4):913-17.
9. El-Nakib GA, Mostafa T, Abbas TM, El-Shishtawy MM, Mabrouk MM, Sobh MA. Role of alpha-lipoic acid in the management of anemia in patients with chronic renal failure undergoing hemodialysis. Int J Nephrol Renovas Dis 2013; 6(default):161-68.
10. Gianella P, Martin PY, Stucker F. Management of renal anemia in 2013. Rev Med Suisse 2013; 9(375):462-67.
11. Liu S, Ren JA. Pathogenesis, diagnosis and treatment of anemia in inflammatory bowel disease. Chin J Gastrointest Surg 2013; 16(4):398-400.
12. Lovcić V, Vujić J, Basić-Jukić N, Janković RI, Kurtović I, Dzapo M, Lovcić P. Treatment of renal anemia with iron in hemodialysis patients in General Hospital Bjelovar. Acta Med Croat 2011; 65(3):49-53.
13. Kaushik T, Yaqoob MM. Lessons learned from peginesatide in the treatment of anemia associated with chronic kidney disease in patients on dialysis. Target Ther 2012; 7(default):243-46.
14. Gaweda AE, Goldsmith LJ, Brier ME, Aronoff GR. Iron, inflammation, dialysis adequacy, nutritional status, and hyperparathyroidism modify erythropoietic response. Clin J Ame Societ Nephrol 2010; 5(4):576-81.

15. Marziali M, Isgro A, Sodani P, Gaziev J, Fraboni D, Paciaroni K. Peripheral red blood cell split chimerism as a consequence of intramedullary selective apoptosis of recipient red blood cells in a case of sickle cell disease. Medit J Hematol Infect Dis 2014; 6(1):e2014066-e2014066.

JOURNAL OF BIOLOGICAL REGULATORS & HOMEOSTATIC AGENTS Vol. 30, no. 2, 541-545 (2016)

LETTER TO THE EDITOR

ROLE OF ANTI-INFLAMMATORY CYTOKINES IN PATHOGENESIS OF PEDIATRIC MYCOPLASMA PNEUMONIAE PNEUMONIA

T. YAN

Department of Pediatrics, the First Affiliated Hospital, and College of Clinical Medicine of Henan University of Science and Technology, Luoyang, China

Received January 29, 2016 – Accepted May 6, 2016

Through detection and analysis of the changes of interleukin (IL)-2 and IL-10 in children with mycoplasma pneumoniae pneumonia (MPP), this study aimed to explore the role of cytokines in the pathogenesis of pediatric MPP as well as immunological pathogenesis of MPP, to provide guidance for clinical diagnosis, assessment and treatment of MPP. Enzyme linked immunosorbent adsorption (ELISA) analysis was applied to determine the expression level of IL-2 and IL-10 in serum. According to the experimental results, we found that the expression levels of IL-2 and IL-10 changed significantly in different phases of MPP in comparison with a healthy control group and a case control group. The expression levels of IL-2 and IL-10 can be used as an important indicator for early diagnosis of MPP. Accordingly, detection of IL-2 and IL-10 is of great significance to the diagnosis of MPP and studies on their roles can provide guidance for treatment.

Mycoplasma pneumoniae pneumonia (MPP), the pathogen of which is mycoplasma pneumoniae (MP), is a common disease of the respiratory tract infection (RTI) among children (1). In recent years, the incidence of MPP has increased significantly, accompanied with onset at younger age and diversity of pulmonary complications (2). It has become an important pathogen of pediatric respiratory tract infection (3, 4). Cytokines (CK) can mediate and regulate the immune function and inflammatory reaction by specific binding with target cell surface receptors (5). MP infection can induce a variety of cells to produce and release cytokines, such as interleukin (IL)-2, IL-4, IL-5, IL-6, IL-8, IL-10 and TNF-α. It was considered that the change of these cytokines might be one of the pathogeneses of MP infection (6). Kammer et al. (7) found that in the case of MP infection with central nervous system symptoms, IL-18 level in serum and cerebrospinal fluid increased, accompanied with the rise of IL-6 and IL-8, indicating that IL-18 might be associated with severity of the disease. Some studies (8) found that IL-5 concentration in serum increased significantly in patients with MP infection during the acute phase; the increase of IL-5 concentration was more obvious among the patients with acute MP infection and wheeze, while the changes of IL-2, IL-4 and interferon-γ (IFN-γ) were not obvious; it was considered that IL-5 played an important role in the process of MP causing wheeze-related symptoms. Based on the above data, this paper studied the role of anti-inflammatory cytokines IL-2 and IL-10 in pathogenesis of pediatric MPP.

Key words: anti-inflammatory cytokines, pediatric mycoplasma pneumonia, IL-2, IL-10

Mailing address:
Dr Tang Yan, No 24, Jinghua Street, Jianxi District,
Department of Pediatrics,The First Affiliated Hospital,
and College of Clinical Medicine
of Henan University of Science and Technology,
Luoyang, 471003, China
e-mail: tangyantyan@163.com

0393-974X (2016)

DISCLOSURE: ALL AUTHORS REPORT NO CONFLICTS OF INTEREST RELEVANT TO THIS ARTICLE.

MATERIALS AND METHODS

Research subjects and grouping

The research subjects were divided into an MPP group, an MPP recovery group, non-MP infection pneumonia group (case control group) and a healthy control group.

The MPP group included acute-phase MPP patients who were hospitalized from December 2012 to December 2014 in the pediatric respiratory department of our hospital. A total of 45 (26 males,19 females) patients, ages 2-36 months (average 16.53±8.15 months), were selected. The 45 patients had follow-up visits and their blood in relieved phase was collected.

The MPP recovery group included the patients whose clinical symptoms disappeared, fever relieved, physical signs and chest X-ray manifestations disappeared or reduced significantly after 2 to 8 weeks of treatment after acute phase of MPP. All the patients in this group had regular follow-up for 3 to 6 months after discharge from hospital; the average follow-up period was (126±35.2) days.

The case control group included 45 randomly selected patients (24 males and 21 females) who were hospitalized in the same department during the same period; they were given definitive diagnosis of non-MP infection bronchial pneumonia; the patients ranged in age from 1-46 months, average (18.24±10.07) months.

Inclusion criteria for the healthy control group are as follows: 45 healthy children, with no history of immune diseases, no chronic diseases, no recent history of infection, no fever or cough, who underwent health check-ups in our hospital during the same period were selected as the control group,. They ranged in age from 2 to 40 months, with average of (21.12±7.86) months.

The parents or guardians of all the children involved in the study signed informed consent.

Specimen collection

Two ml samples of venous blood were taken from each child in each group; the venous blood was kept in test tubes without pyrogen or endotoxin; specimens with hemolysis or hyperlipidemia were excluded; then, the specimens were centrifuged at 3000 r/min for 10 min; and then serum was extracted and kept at -20°C until use.

Methods

Double antibody sandwich enzyme linked immunosorbent adsorption (ELISA) analysis was applied to determine IL-2 and IL-10 levels in the serum.

The first step was temperature recovery: the kit and specimens were taken out from the refrigerator in advance and balanced to room temperature after about an hour. Next, the serum was given two-fold dilution before testing; 200 µl of serum was added to 200 µl of sample dilution. The reference solution was diluted into different concentrations. Anti-human IL-10 and IL-2 monoclonal antibodies were coated onto the enzyme label plate; except for the blank well, specimens and standards of different concentrations (100 µl/well) were added into the corresponding wells and labeled and incubated in a 37°C incubator for 60 to 90 min. Except for the blank well, diluted antibody (50 µl/well) was added and mixed evenly, covered with closure plate membrane, and the specimens were incubated at 18~25°C for 2 h. Liquid was removed and 350 µl of washing liquid was added into each well; one minute later, the liquid was drained off. This step was repeated 3 times, after which it was dried on filter paper.

Except for the blank well, 100 µl of enzyme conjugate working solution was added in each well and was then covered with microplate sealer; it was incubated for 20 min at room temperature (18~25°C), followed by 30-min incubation in a 37°C incubator. Again, liquid in the well was removed; 350 µl of washing liquid was added in each well and one minute later the liquid was drained off. This step was repeated 3 times. 100 µl of chromogenic agent was added in each well; and was incubated away from light for 15 min at room temperature. Finally, 100 µl of blocking buffer was added quickly in each well to terminate the reaction; after blending, OD450 (optical density at 450 nm) value was measured within 5 min.

Determination of results

Optical density (OD) value of the zero well was subtracted from OD values of each standard and specimen. According to the standard curve, concentration of each sample was calculated, with dilution ratio of specimens multiplied.

Statistical analysis

Statistical package for social science (SPSS) 19.0 was used for the establishment of a database; through normality test, the data which accorded with normal distribution were compared using analysis of variance;

t-test was used for data measurement, while independent sample *t*-test was applied for data comparison between groups; paired samples *t*-test was used for the comparison between MPP acute phase and relieved phase.

RESULTS

Comparison of differences in age and gender of different groups

Pearson's χ^2 test was applied to analyze gender differences between groups and the results were as follows: MPP group and case control group (χ^2 = 0.269, p = 0.063 > 0.05); MPP group and healthy control group (χ^2 = 0.612, p = 0.434 > 0.05); case control group and healthy control group (χ^2 = 0.066, p = 0.798 > 0.05); accordingly, gender differences had no statistical significance, which was probably because gender composition was similar in the three groups. Independent sample *t*-test was applied to analyze age differences between groups:the MPP group and case control group (t = -0.697, p = 0.495 > 0.05); MPP group and healthy control group (t = -1.147, p = 0.261 > 0.05); case control group and healthy control group (t = -0.321, p = 0.748 > 0.05). Accordingly, age differences had no statistical significance, probably because there were no obvious differences in age among the three groups.

IL-2 and IL-10 level in serum of each group

In this study, it was found that IL-2 and IL-10 levels were in line with the normal distribution and met the homogeneity of variance; thus, IL-2 and IL-10 level in serum was expressed in the form of (mean ± SD). In the MPP group (acute phase), serum IL-2 level was (64.49±12.12) pg/ml, and IL-10 level was (22.79±10.05) pg/ml. In the relieved phase of MPP, IL-2 level in serum was (104.86±13.09) pg/ml, while IL-10 level was (21.65±9.49) pg/ml. In the case control group (non-MP infection pneumonia group), IL-2 level in serum was (108.31±11.33) pg/ml, while IL-10 level was (13±7.27) pg/ml. In healthy control group, IL-2 level in serum was (133.23±12.01) pg/ml, while IL-10 level was (10.46±2.33) pg/ml. The data are shown in Table I.

Comparison of IL-2 level between groups

In comparison with the healthy control group, IL-2 level in the acute-phase MPP group decreased, and the differences between them were significant (t = -25.413, p < 0.05). In comparison with case control group, IL-2 level in serum also decreased in the acute-phase MPP group, and the differences between them were significant (t = -16.523, p < 0.05). In comparison with the healthy control group, IL-2 level in relieved phase of MPP decreased, and the differences between the two were significant (t = -12.021, p < 0.05). In comparison with the case control group, IL-2 level in relieved phase of MPP decreased, but the difference was not significant (t = -1.104, p > 0.05).

Comparison of IL-10 level between groups

In comparison with the healthy control group, IL-

Table I. *IL-2 and IL-10 levels in serum of each group.*

Groups	n	IL-2	IL-10
Acute phase of MPP group	45	64.49±12.12	22.79±10.05
Relieved phase of MPP group	45	104.86±13.09	21.65±9.49
Case control group	45	108.31±11.33	13±7.27
Healthy control group	45	133.23±12.01	10.46±2.33

(pg/ml, mean ± SD)

.

10 level in the acute phase MPP group increased, and the difference was statistically significant ($t = 35.787$, $p < 0.05$). In comparison with the case control group, IL-10 level in serum of the acute phase MPP group also increased, and differences were significant ($t = 23.152$, $p < 0.05$). In comparison with the healthy control group, IL-10 level in serum of MPP relieved phase increased, and the difference was significant ($t = 34.681$, $p < 0.05$). In comparison with the case control group, IL-10 level of MPP relieved phase also increased, and the difference was significant ($t = 8.147$, $p < 0.05$).

DISCUSSION

IL-2 is capable of acting on various types of cells, with extensive biological effects. The most significant effect is to promote the proliferation of T lymphocytes and stimulate T-cell proliferation (9, 10). In this study, it was found that cellular immune function reduced, and IL-2 level in MPP acute phase decreased significantly in comparison with the case control group and healthy control group, indicating that pediatric MPP patients had lower cellular immune function. In the study, it was observed that IL-2 level showed gradient changes in different phases of MPP until it restored to normal level as that of healthy children, which also indicated the gradual recovery process of immune functions, and the changes helped the judgment of disease progress.

IL-10 is a recently discovered cytokine with extensive immunological effect. Its basic function is to inhibit Th1 cells from producing cytokines. Recent studies revealed that IL-10 had biological effects, mainly reflected in immune suppression and immune stimulation (11). In this paper, the study results showed that IL-10 level (either in MPP acute phase or relieved phase) was higher than that of the case control group and healthy control group, and the differences were statistically significant. High expression of IL-10 indicated disorder of body immune adjustment which might be associated with the onset of MPP. In the case of MPP, both pro-inflammatory response and anti-inflammatory reaction were intense when there was local and systemic inflammatory reaction.

In summary, based on this experimental study, it was found that combined detection of IL-2 and IL-10 in serum has a certain reference value to the diagnosis of MPP; it is likely that the expression of IL-2 and IL-10 can be used as an auxiliary diagnosis indicator, and the level changes of IL-2 and IL-10 can be used as important indicators for MPP staging and assessment of disease condition.

REFERENCES

1. Baum HV, Welte T, Marre R, Suttorp N, Lück C, Ewig S. Mycoplasma pneumoniae pneumonia revisited within the german Competence Network for Community-Acquired Pneumonia (CAPNETZ). Bmc Inf Dis 2009; 9(1):1-10
2. Li CM, Gu L, Yin SJ, Yang R, Xie Y, Guo XZ, Fu YX, Cheng D. Age-specific Mycoplasma pneumoniae pneumonia-associated myocardial damage in children. J Int Med Res 2013; 41(5):1716-23.
3. Qin Q, Xu B, Liu X, Shen K. Status of Mycoplasma pneumoniae Pneumonia in Chinese Children: A Systematic Review. Adv Micr 2014; 04(11):704-11.
4. Chen ZR, Ji W, Wang YQ, Yan YD, Zhu H, Shao XJ, Xu J. Epidemiology and associations with climatic conditions of Mycoplasma pneumoniae and Chlamydophila pneumoniae infections among Chinese children hospitalized with acute respiratory infections. Ital J Ped 2013; 39(2):34-34.
5. Sang HS, Hoffmann E, Webster RG. Addendum: Editorial note: Lethal H5N1 influenza viruses escape host antiviral cytokine responses. Nat Med 2012; 18:1592-92.
6. You-Cheol J, Mun-Soo Y, Joo-Hwa K, Ha-Baik L, Jae-Won O. Mycoplasma pneumoniae infection affects the serum levels of vascular endothelial growth factor and interleukin-5 in atopic children. Allergy Asthma Immunol Res 2012; 4(2):92-97.
7. Kammer J, Ziesing S, Davila LA, Illsinger S, Das AM, Hartmann H. OP82 – 2546: Neurological manifestation in children with Mycoplasma pneumoniae infection. Eur J Pediatr Neurol 2015; 19:S26.
8. Choi IS, Byeon JH, Yoo Y, Li KC, Ji TC. Increased serum Interleukin-5 and vascular endothelial growth factor in children with acute mycoplasma pneumonia

and wheeze. Ped Pulm 2009; 44(5):423-28.
9. Matsuda K, Narita M, Sera N, et al. Gene and cytokine profile analysis of macrolide-resistant Mycoplasma pneumoniae infection in Fukuoka, Japan. Bmc Inf Dis 2013; 13(6):1-7.
10. Shu LH, Shang YX, Cai XX, et al. Alterations of SP-A, SP-D and KL-6 in serum and bronchoalveolar lavage fluid in children with Mycoplasma pneumoniae pneumonia. Chin J Pediatr 2013; 51(10):779-82.
11. Orlandi C, Forlani G, Tosi G, Accolla RS. Molecular and cellular correlates of the CIITA-mediated inhibition of HTLV-2 Tax-2 transactivator function resulting in loss of viral replication. J Transl Med 2011; 9:106. doi: 10.1186/1479-5876-9-106.

LETTER TO THE EDITOR

FLOW CYTOMETER ANALYSIS OF CELL APOPTOSIS OF ENDOMETRIAL CARCINOMA WITH Wnt10b

Y. ZHOU[1], XL. ZHAO[1], RX. GUO[2], YH. QIAO[2], XY. ZHANG[1] and ZH. CHEN[2]

[1]Department of Obstetrics, the First Affiliated Hospital of Zhengzhou University, Zhengzhou, Henan, China; [2]Department of Gynecology, the First Affiliated Hospital of Zhengzhou University, Henan, China

Received February 2, 2016– Accepted May 10, 2016

The aim of this study is to analyze the cell apoptosis of endometrial carcinoma (EC) with Wnt10b by Fluorescence Activated Cell Sorting (FACS) technology. AN3CA cell lines and Ishikawa-H-12 cell lines were taken as the *in-vitro* cell models to observe the influence of Wnt10b on key factors of Wnt signal pathway. Methyl thiazolyl tetrazolium (MTT) was applied for the detection of cell proliferation while FACS was used for the detection of cell apoptosis. Data were analyzed using statistical software SPSS14.0. After the overexpression of Wntl0b in AN3CA cells, the apoptosis rate dropped significantly compared with the two control groups ($p < 0.05$); while the apoptosis rate increased significantly compared with the control groups ($p < 0.01$) after Wntl0b knock-off in Ishikawa3-H-12 cells. In normal endometrium, Wnt10b gene expression was negative, while that in EC cells was positive. It can be concluded that Wnt10b gene can promote EC cell proliferation and inhibit its apoptosis.

Annually, almost 200,000 new patients are diagnosed with endometrial carcinoma (EC), one of the most common tumors of the female reproductive system. EC is a common gynecologic malignant tumor which mainly results in death of patients, ranking only second to ovarian malignant tumor and cervical cancer. According to the American Cancer Society, the number of new EC cases in US increased to 46,470 in 2011, far higher than that of cervical and ovarian cancer, and 8,120 cases resulted in death (1). Gou et al. (2) reported that the rapid growth of EC cases in China was in line with other countries, which constituted a serious threat to women's health, with its pathogenesis remaining unclear. EC atypical hyperplasia process has the characteristics of early symptom appearance and good prognosis, therefore, early detection is the key to effective treatment (3). Chandra et al. (4) found that Wnt signal transduction pathway was associated with sexual hormone signal transduction during the process of carcinogenesis from normal endometrium to endometrial dysplasia and finally to cancer. The pathogenesis of EC is still not clear, and has long been a hot issue in the field. It may be associated with continued obesity, hypertension, heredity, diabetes, estrogen stimulation and other factors. Many studies have found that obesity and polycystic ovary syndrome (5) are commonly found in the development of EC. The overexpression of Wnt genes and their classic transduction pathway can refer to many human solid tumors. For example, an increasing number of studies focus on the mechanisms of gastric cancer, breast cancer, cervical cancer and ovarian cancer (6). Some studies have shown that key protein in

Key words: endometrial carcinoma, Wnt10b, EC cells, negative control, cell line knock down

Mailing address:
Dr Yan Zhou, NO.1, Jianshe East Road,
II Ward, Department of Obstetrical,
the First Affiliated Hospital,
Zhengzhou University,
Zhengzhou, Henan, 450052, China
e-mail: zhouyanzy5829@163.com

0393-974X (2016)

DISCLOSURE: ALL AUTHORS REPORT NO CONFLICTS OF INTEREST RELEVANT TO THIS ARTICLE.

the canonical Wnt signaling pathway is closely related to the development of EC, and inactivating mutations of key protein in the pathway account for approximately 10% to 45% in EC (7). This study found that Wnt10b protein DNA amplification was evident in Ishikawa cell lines while no amplification was found in AN3CA cell lines (8).

MATERIALS AND METHODS

Reagents and instruments

The materials and reagents included in this study were Ishikawa3-H-12 cell lines, AN3CA cell lines, cell culture media, methyl thiazolyl tetrazolium (MTT), protease inhibitor, phenylmethanesulfonyl fluoride (PMSF), ethylene diamine tetraacetic acid (EDTA), glycine, ammonium persulfate (AP), and diethylpyrocarbonate (DEPC).

The main instruments were horizontal electrophoresis apparatus, vertical electrophoresis apparatus, DDY-III 40B electrophoretic transfer trough, DDY-10 type (ECP-300 type), 1000inl\200ml\ 100 ml sample adding pipettor, ultra cold storage freezer, cell counting chamber, ordinary optical microscope.

Methods

AN3CA and Ishikawa3-H-12 cell lines were given adherent culture respectively in 50 ml culture flasks which were placed in the RPMI1640 culture medium, with10% of fetal bovine serum (FBS)) (37 ºC; 5% CO_2).

Cell recovery

Firstly, the frozen tube was removed from the liquid nitrogen and shaken in a water bath at 37ºC to melt. Then, 10 times the normal amount of 10% FBS culture solution was added immediately to the tube and the supernate was removed after centrifugation. Afterwards, 10% FBS culture solution was added again to the tube and fully mixed. Next, the mixed liquid was added to a culture flask and added once again with 10% FBS culture solution. Finally, the culture flask was placed under a 5%CO_2 environment (37ºC) (12).

Cell culture

Based on the conditions of the cells, the culture medium was changed every day. Firstly, the mouth of the culture flask was sterilized with an alcohol lamp. Then, the bottle cap was removed to pour out the old culture solution carefully. Afterwards, the flask was washed twice with Phosphate Buffer Solution (PBS). Finally, an appropriate amount of new 10% FBS DMEM culture medium was added to the flask (13).

Cell passage

When the cells grew by about 80 percent, the culture medium was removed and the culture flask was washed twice with PBS. Then, 0.25% trypsin and 0.25% EDTA solution were added to the culture flask. After three minutes, when the shape of the cells turned round, 10% FBS DMEM solution was used to end the reaction. Next, the cells were collected from the flask and cell suspension was moved to the centrifuge tube with a pipette for 5-min centrifugation at room temperature. Afterwards, the supernate was removed carefully and 10% FBS DMEM solution was added and mixed thoroughly. Finally, the cell suspension was uniformly assigned to a new culture flask, added with culture solution, for continuous culture in a cell incubator (14).

Cell freezing

Before freezing, the remaining culture solution was replaced with a fresh one. Then, primary cells and passage cells with one or two times of passage were added into the culture flask for digestion with 0.25% trypsin. After that, 10% FBS DMEM solution was used to adjust the cell density to 1×10^6-2×10^6/ml. Meanwhile, 10% dimethyl sulfoxide was added for rapid mixing. Then, the flask was placed in a frozen tube and sealed and marked. Afterwards, the tube was kept at -20ºC for 1-2 hours. Then, the temperature was adjusted to -40ºC for a night. Finally, the liquid was reserved in liquid nitrogen (15).

Cell count

The cells in logarithmic growth phase were made into single-cell suspension. Cells were seeded in a 96-well plate under 5% CO_2 environment (37ºC), with a density of $5x10^3$/well. Then, the culture medium was changed when there was cell attachment. The cells were divided into control group and experimental group. For the experimental group, three groups of cells were selected and added with 2.5, 5 and 10 ng/ml culture solution for further culture for 1 day, 2 days and 3 days, respectively. After that, 20 µl of 5mg/ml MTT solution was added and

the solution was then placed under 5% CO_2 environment (37 ºC) for 4 hours and the supernate was then removed. The 96-well plates were added with 200 µl of dimethyl sulfoxide, respectively, and shaken for 10 min. Finally, light absorption values of each well were measured by ELISA (wavelength of 490 nm, A490) and inhibition ratio was calculated. The above steps were repeated for three times, with 5 wells in each concentration group.

Detection of cell proliferation

MTT method was applied to carry out the colorimetric test. After the above processing, the cells were seeded onto a 6-well culture plate, 200 µl of each well (cell population of $5x10^5$), for culture under 5% CO_2 environment (37ºC). Three days later, each well was added with 20 µl of MTT 4 h before the termination of culture. After incubation, liquid in each well was removed. Then, 20 µl of DMSO was added to each well and shaken for 10 min. Finally, light absorption values of each well were measured by ELISA (wavelength of 570 nm), with 630 nm wavelength for calibration, ruling out the interference of background absorption of cell plates and cell debris. Cell vitality was expressed as OD570 ~ OD630. The above steps were repeated for three times to calculate the average value (16).

Detection of cell apoptosis

Annexin V-PITC/PI double staining method was applied in this section. Firstly, EDTA trypsin was used for digestive collection of cells. Then, the cells were washed with PBS for two times and $5xl0^5$ cells were collected. Afterwards, 500 ml of binding buffer suspension cells were added; 5 µl of Annexin V-FITC was added and mixed and then 5 µl of propidium iodide was added and mixed. Afterwards, the liquid was left for reaction for 5-15 min at room temperature away from light. Within one hour after the reaction, observation and detection was carried out by FACS. It was found through detection that excitation wavelength was Ex=488 nm, emission wavelength was Em=530 nm. The green fluorescence of AnnexinV-FITC was detected with FITC channel (FL1) and red sudden light of PI was detected with PI channel (FL2 or FL3).

Immunohistochemical analysis

Each tissue trimming was placed under the same environment while all the stained tissue trimmings were divided into positive and negative control group; existing positive biopsies included in the positive control group and negative control group were compared with PBS. The wax block specimen was made into 4-µm slices, after the diagnosis of haematoxylin eosin (HE) staining, immunohistochemical staining was carried out.

Statistical analysis

Data were analyzed and detected by SPSS 14.0 software and $p < 0.05$ was considered as the standard of significant difference.

RESULTS

Impact of Wnt10b genes on EC cell proliferation

Since Wnt10b is lowly expressed in AN3CA cell lines and highly expressed in Ishikawa3-H-12 cell lines, we used Ishikawa3-H-12 and AN3CA cell lines as the *in-vitro* models to observe the effect of Wnt10b on EC cell proliferation based on MTT method.

Wnt10b was applied to express plasmid transfection of AN3CA cell lines, and RT-PCR and Western blot were used to observe the transfection efficiency. Meanwhile, an empty plasmid transfection group and a blank control group were set up and MMT technology was used to observe cell proliferation in each group. After overexpression of Wnt10b in AN3CA cell lines, cell proliferation level increased significantly compared with the no-load group and the control group. To further confirm the impact of Wnt10b on EC cell proliferation, we selected specific siRNA to carry out gene knock-down of Wnt10b in Ishikawa3-H-12 cell lines, and knock-down efficiency was measured by RT-PCR and Western blot. A negative control group and a blank control group were set up and cell proliferation results of each group were measured by MTT method. The results revealed that the level of cell proliferation of Wntl0b knock-off group decreased significantly compared with the other two control groups. Therefore, this study suggests that Wnt10b genes can promote EC cell proliferation.

Impact of Wnt10b genes on EC cell apoptosis

As mentioned above, Ishikawa3-H-12 and AN3CA cell lines were also selected to observe the effect of Wnt10b genes on EC cell apoptosis.

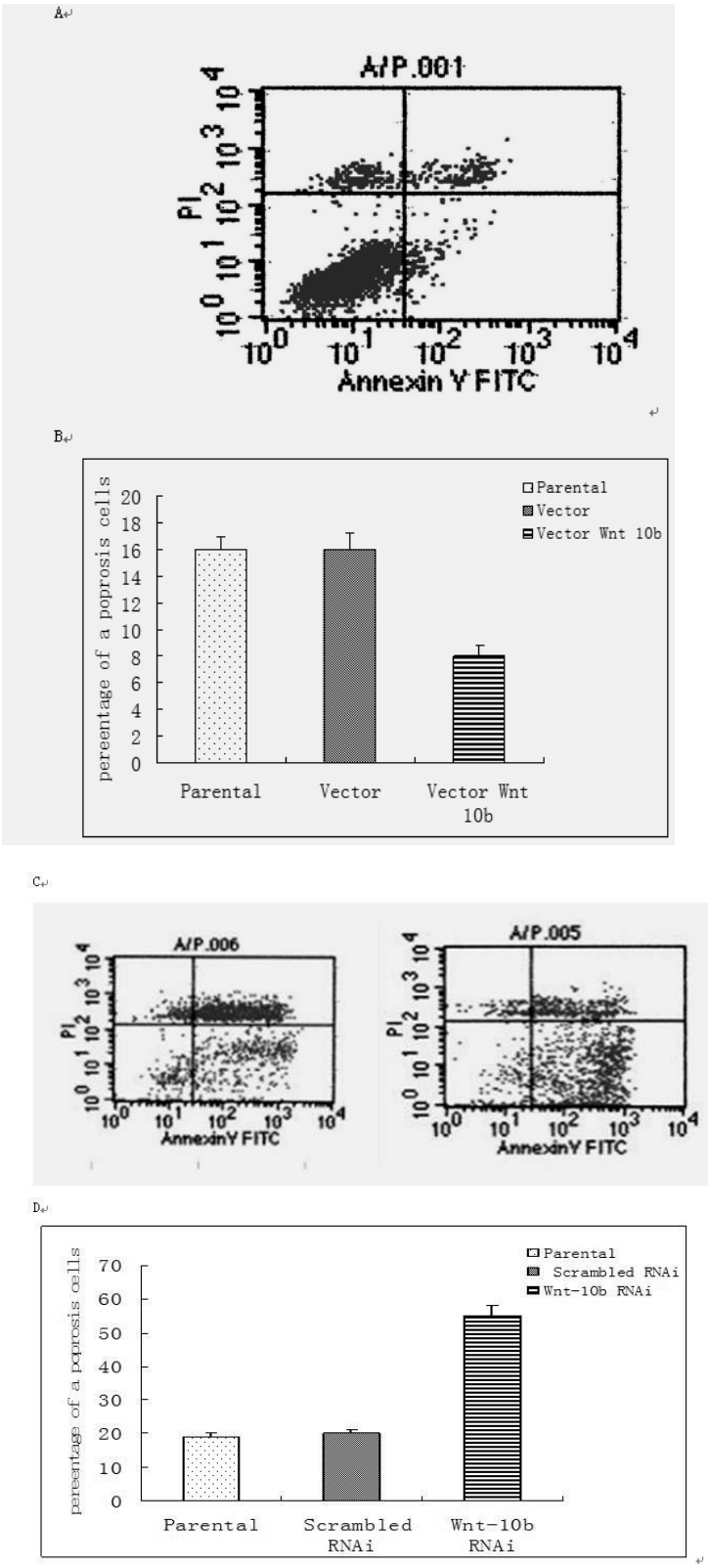

Fig. 1. *Impact of Wnt10b on cell apoptosis of ECAN3CA and ECIshikawa3-H-12 cells.*

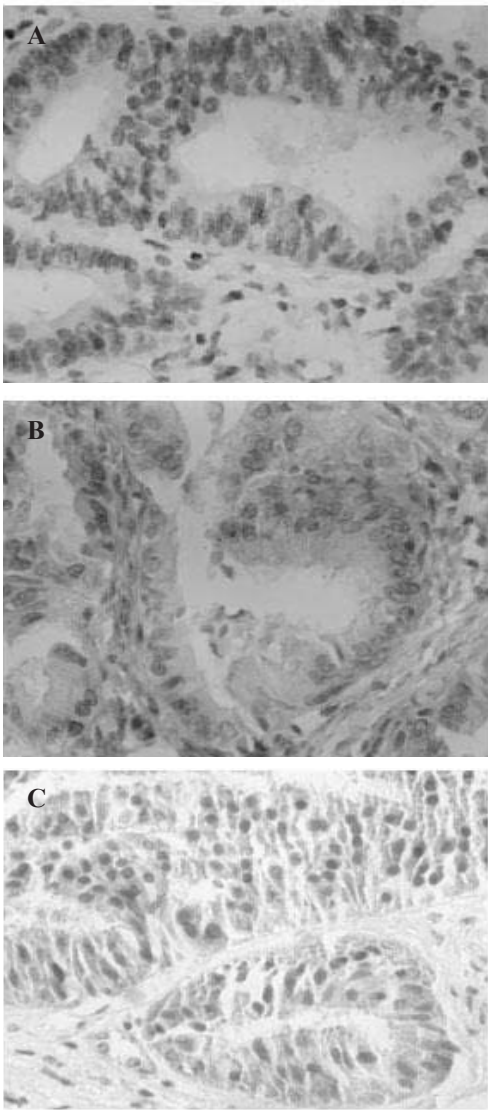

Fig. 2. *Wnt10b protein positive expression in various tissues.*

FACS was used for detection of apoptosis level in each group. The Wnt10b overexpression plasmid transfection of AN3CA cells and siRNA gene knock-down of Ishikawa3-H-12 cells were the same as that in the above section. The impact of Wnt10b genes on cell apoptosis of the two kinds of cells are shown in Fig. 1. As can be seen from Fig. 1A and 1B, after Wnt10b was expressed in AN3CA cells, the apoptosis rate dropped significantly compared to the negative control group and blank control group. Accordingly, after Wnt10b was knocked down in Ishikawa3-H-12 cells, the apoptosis rate went up significantly in contrast with the negative control group and blank control group, as shown in Fig. 1C and 1D.

Wnt10b protein expression in various endometrial tissues

This study applied immunohistochemistry method to detect the Wnt10b protein expression in EC simple, complex, atypical hyperplasia and normal endometrial tissues. The positive expression rate of Wnt10b protein in normal secretion phase was 27.78% (10/36) while that in normal proliferating phase was 33.33% (2/6); the positive expression rate of simple hyperplasia was 54.17% (26/48) while that of complex hyperplasia was 55.56% (10/18); the positive expression rate of atypical endometrial hyperplasia was 60% (18/30) while that of EC cell cytoplasm was 63.73% (65/102). This suggested that the positive rate of Wnt10b protein in each group went up gradually, with significant differences, $p < 0.05$ (x=8.12, p=0.02), as shown in Fig. 2.

DISCUSSION

During the development process from normal endometrium to EC, Wnt10b protein expression presents a significant increase trend, however, the specific mechanism needs to be further studied (9). There is an inverse linear relationship between the expression of Wnt10b protein in EC tissues and histological grade. There is no statistical difference on positive expression rate of Wnt10b protein in EC muscular infiltration in each subgroup (10), suggesting that Wnt10b gene is strongly linked with the occurrence and development of EC. This study also found that the predicted course and outcome of patients with positive Wnt10b expression was obviously better than that of patients with negative Wnt10b expression. The positive expression rate of Wnt10b increased gradually during the endometrial carcinogenesis process from normal tissues to proliferation at all levels and finally to cancerization, with statistically significant differences, indicating that Wnt10b gene can promote the development of EC. The results of this study show that after

Wnt10b was expressed in AN3CA cell lines, the cell proliferation level went up significantly in contrast with that in the no-load group and blank control group; Wntl0b knock down in Ishikawa3-H-12 cell lines by specific siRNA shows that the level of cell proliferation of Wntl0b knock-off group dropped significantly in contrast with that of the other two control groups, suggesting that Wnt10b gene can promote EC cell proliferation. After the overexpression of Wntl0b inAN3CA cells, the apoptosis rate dropped significantly compared with the other two control groups, while the apoptosis rate went up significantly compared with the other two control groups after Wntl0b knock-off in Ishikawa3-H-12 cells, suggesting that Wnt10b gene can inhibit EC cell apoptosis.

REFERENCES

1. Torres A, Torres K, Pesci A, et al. Deregulation of miR-100, miR-99a and miR-199b in tissues and plasma coexists with increased expression of mTOR kinase in endometrioid endometrial carcinoma. Bmc Cancer 2012; 12(4):369.
2. Gou HF, Chen XC, Zhu J, Jiang M, Yang Y, Cao D, Hou M. Expressions of COX-2 and VEGF-C in gastric cancer: correlations with lymphangiogenesis and prognostic implications. J Exp Clin Canc Res 2011; 30(1):1.
3. Hashimoto H, Kojima A, Sudo T, et al. Establishment and characterization of a human cell line derived from a uterine papillary serous carcinoma with wild-type p53 function. Hum Cell 2008; 21(3):64-69.
4. Chandra V, Fatima I, Manohar M, et al. Inhibitory effect of 2-(piperidinoethoxyphenyl)-3-(4-hydroxyphenyl)-2H-benzo(b)pyran (K-1) on human primary endometrial hyperplasial cells mediated via combined suppression of Wnt/-catenin signaling and PI3K/Akt survival pathway. Cell Death Dis 2014; 5: e1380-8.
5. Escobar-Morreale HF, Insenser M, Cortón M, Millan JLS, Peral B. Proteomics and genomics: A hypothesis-free approach to the study of the role of visceral adiposity in the pathogenesis of the polycystic ovary syndrome. Proteom Clin Appl 2008; 2(3):444-55.
6. Deng B, Zhang S, Miao Y, Zhang Y, Wen F, Guo K. Down-regulation of Frizzled-7 expression inhibits migration, invasion, and epithelial–mesenchymal transition of cervical cancer cell lines. Med Oncol 2015; 32(4):1-9.
7. Yi C, Saini S, Zaman M S, et al. Cytochrome P450 17 (CYP17) is involved in endometrial cancinogenesis through apoptosis and invasion pathways. Mol Carcinogen 2011; 50(1):16-23.
8. Wang Y, Yang D, Cogdell D, et al. Genomic characterization of gene copy-number aberrations in endometrial carcinoma cell lines derived from endometrioid-type endometrial adenocarcinoma. Technol Cancer Res T 2010; 9(2):179-8.
9. Xue SL, Su HF, Hu XQ, et al. Adjuvant combined systemic chemotherapy and intraperitoneal chemotherapy for locally advanced gastric cancer. Oncol Lett 2012; 4(6):1309-14.
10. Pei H P, Li X L, Zhu H, et al. Preliminary study on glucose regulated protein 78 kD and heat shock protein 20 differential expression between left-sided colon carcinoma and right-sided colon carcinoma. Chin J Gastrointest Surg 2013; 16(1):75-9.

JOURNAL OF BIOLOGICAL REGULATORS & HOMEOSTATIC AGENTS Vol. 30, no. 2, 553-558 (2016)

LETTER TO THE EDITOR

EFFECT OF X-RAY IRRADIATION ON EPITHELIAL-MESENCHYMAL TRANSITION OF COLORECTAL CANCER SW480 CELLS

WL. DIAO[1], L. LUO[2] and Q. LUO[1]

[1]Department of Radiology, Jining No.1 People's Hospital, Jining, Shandong Province, China;
[2]Department of Gynecology, Jining No.1 People's Hospital, Jining, Shandong Province, China

Received February 2, 2016 – Accepted May 9, 2016

The first two authors contributed equally to this work

This study was carried out to explore the effect of X-ray irradiation on epithelial-mesenchymal transition (EMT) of colorectal cancer SW480 cells. Human colorectal cancer SW480 cells used in this study were irradiated by X-rays in 0 Gy, 4 Gy and 8 Gy doses, respectively. Transwell method was adopted to detect the changes of invasion and migration ability of SW480 cells cultured for 24 h after being irradiated by X-rays in 0 Gy, 4 Gy and 8 Gy doses. After X-ray irradiation, invasion ability of cells in 4 Gy dose group and 8 Gy dose group strengthened significantly compared with that of the 0 Gy dose group ($p < 0.05$); invasion ability of cells in 8 Gy dose group also strengthened significantly compared to the 4 Gy dose group ($p < 0.05$). After X-ray irradiation, migration ability of cells also changed: migration ability of cells in 4 Gy dose group and 8 Gy dose group strengthened significantly compared with that of the 0 Gy group ($p < 0.05$). Results of QRT-RCR and Western blot detection showed that after X-ray irradiation, the expression of epithelial index E-cadherin in 4 Gy dose group and 8 Gy dose group decreased significantly compared with that of the 0 Gy dose group ($p < 0.05$); moreover, the higher the dose was, the more significantly the expression decreased. Therefore, X-ray irradiation-induced EMT is in positive correlation with the irradiation dose to some extent. Besides, X-ray irradiation can enhance the invasion and migration ability of human colorectal cancer cells.

Colorectal cancer is the most common malignant tumor of the digestive tract, and its incidence rate ranks only third after gastric cancer and esophagus cancer (1-3). Radiotherapy is a treatment that uses radioactive rays to kill cancer cells, and has become one of the three main treatment methods used to treat malignant tumors. X-ray therapy plays an important role in adjuvant therapy of colorectal cancer. However, radiotherapy can also cause side effects, such as bowel dysfunction and skin allergy, etc., and even cause changes of biological characteristics of cancer cells (4-6). Several studies indicated that X-ray therapy could lead to epithelial-mesenchymal transition (EMT) of cancer cells, such as breast cancer, nasopharynx cancer, cervical cancer and endometrial cancer, etc. Moreover, some researchers believed that radioactive rays could enhance invasion and migration abilities of human colorectal cancer cells *in vitro*, and EMT could also enhance the invasion and migration abilities of human colorectal cancer cells (7-9). X-ray therapy plays an important role in treatment of malignant tumors in that it can lead to changes of expression level of tumor-related genes. In radiation therapy, ionizing radiation reacts

Key words: X-ray, colorectal cancer, epithelial-mesenchymal transition, SW480 cells

Mailing address:
Dr Qian Luo,
Department of radiology, Jining No.1 People's Hospital,
No.6 Jiankang Road, Rencheng District,
Jining, Shandong, 272100, China
e-mail:luoqianlq702@163.com

0393-974X (2016)

DISCLOSURE: ALL AUTHORS REPORT NO CONFLICTS OF INTEREST RELEVANT TO THIS ARTICLE.

with the DNA in cells to cause double-strand break and single-strand break of DNA, thus killing tumor cells or changing biological characteristics of tumor cells (10). X-ray therapy and radiation therapy are similar in this regard. We therefore hypothesized that X-ray radiation affects the survival rate of patients with colorectal cancer by mediating EMT of human colorectal cancer cells and enhancing invasion and migration abilities of cancer cells. X-ray was used in this study to irradiate human colorectal cancer cells, and changes of EMT-related indexes were detected, which might be able to provide a theoretical basis and new thoughts for clinical intervention and treatment of progression and metastasis of human colorectal cancer.

MATERIALS AND METHODS

Experimental materials

The materials used in this study were human colorectal cancer SW480 cell strains, culture medium, fetal bovine serum (FBS), Transwell chamber, Matrigel, E-cadherin, polymerase chain reaction (PCR) primer, monoclonal antibody, vimentin monoclonal antibody, mouse-anti-human GAPHD monoclonal antibody, rabbit-anti-human K-ras monoclonal antibody, rabbit-anti-human Smad3 monoclonal antibody and a linear accelerator.

Cell culture

SW480 cells were cultured in RPMI1640 culture solution containing 10% FBS in an incubator (37°C, 5% CO2, saturated humidity); cells in logarithmic phase were used for the follow-up experiment. SW480 cells were divided into three groups, including a control group (without X-ray irradiation) and two experimental groups which received 4 Gy and 8 Gy irradiation doses, respectively.

Cell morphology

Human colorectal cancer SW480 cells in logarithmic phase were inoculated into a 6 cm deep culture dish; when 70% ~ 80% of the bottom of the culture dish was covered by cells, the cells were given isocenter irradiation of 6 MV X-rays; the irradiation dose for each single time was 4 Gy and the dose rate was 400 cGy/min. Different irradiation doses were marked and the culture dish was returned to the incubator (3°C, 5% CO2) for 48 h of culture; morphology of cells was then observed and photographed.

Transwell invasion

Matrigel which had been preserved at -20°C was then transferred to a 4°C refrigerator and preserved for 12 h; after the Matrigel transformed from semi-solid state to liquid state, it was placed on a surface of ice. Serum-free RPMI-1640 culture medium (360 µl) (precooled in the 4°C refrigerator) was added with 120 µl of Matrigel in 3:1; the mixture was fully blended to avoid bubbles. Then blended Matrigel diluent was poured onto the bottom of the inner chamber of a Transwell®, 50 µl in each well; then the Transwell chamber was incubated at 37° for 6 h for solidification of Matrigel. After that, redundant liquid in the Transwell chamber was removed; gel and the lower chamber was rinsed with serum-free RPMI-1640 culture solution; next, the Transwell chamber was put into the incubator at 37°C for 30 min for standby application.

Preparation of cell suspension: SW480 cells were digested using conventional method and centrifuged at 1000 r/min for 5 min; then cells were washed using PBS 1~2 times and serum-free culture solution that contained BSA was used to resuspend the cells; the concentration of cells was 1×10^5/ml.

Cell inoculation: 200 µl of cell suspension was added to the inner chamber of the Transwell and the lower chamber of a 24-well plate was added with 500 µl of culture medium that contained 5% FBS.

Cell culture: the culture plate was incubated at 37°C incubator for 24 h. Anchorage-dependent cells counting method was used for statistic results.

Transwell chamber migration

Procedures of the Transwell chamber migration experiment were basically the same as the Transwell chamber invasion experiment, but the differences were as follows: Matrigel was not needed in the migration experiment while it was needed in the invasion experiment; cell concentration was adjusted as 1×10^6/ml in preparation of cell suspension, while the cell concentration in the invasion experiment was 1×10^5/ml; after cell inoculation, the lower chamber of 24-well plate was added with RPMI-1640 culture medium containing 2.5% FBS, while the FBS concentration in the invasion experiment was 5%; in the migration experiment, cells

were continuously cultured in an incubator at 37°C for 18-20 h, while in the invasion experiment cells were cultured for 24 h.

Detection of E-cadherin and Vimentin mRNA

Human colorectal cancer SW480 cells in the logarithmic phase were inoculated in a 3-cm deep culture dish; when 70% of the bottom was covered by cells, the culture solution was replaced by fresh complete culture solution and the cells were continuously cultured for 24 h; the cells were then irradiated by X-rays and then cultured for another 48 h. Trizol one-step method was adopted to extract the total RNA of cells.

RNA spectral analysis and quantification

1 μl of extracted cell RNA sample was drawn from each tube and added with 1 ml of 1% diethyl pyrocarbonate·H2O (DEPC·H2O); OD260 and OD280 as well as the specific value and concentration values were measured by an ultraviolet spectrophotometer; if the specific value of OD260/OD280 was between 1.8-2.0, it indicated that the extracted total RNA was rarely contaminated by protein or other impurities, thus it had high purity.

Evaluation of RNA integrality through electrophoresis

The integrality of an RNA sample (5 μl) was evaluated by electrophoresis using prepared non-denaturing sepharose gel: 1 μl of bromphenol blue was added to the extracted RNA sample (5 μl); then the mixture was added to the 1.5% sepharose gel well; the voltage was designed as 110 mV and current was designed as 400 mA; buffer solution 1×TAE was added and electrophoresis was performed for 10-15 min; then gel-imaging system was used to analyze integrality of RNA. If the 28S and 18S of these two clear strips could be seen and the specific value 28S/18S was 2:1, then the extracted RNA had good integrality. Qualified RNA was preserved in a -80°C refrigerator for standby application.

Calculation of mRNA relative expression of target genes E-cadherin and vimentin

Calculation formula of mRNA relative expression of E-cadherin and vimentin was RQ=2^(-ΔΔCt); ΔΔCt=(ΔCt,Q-ΔCt,C)=(ΔCt,Q-Ct,GAPDH)-(ΔCt,C-Ct,GAPDH). In the equation, ΔCt, Q refer to genes to be tested, while ΔCt, C refer to genes in the control group. Western blot was used to detect expression of E-cadherin and vimentin before and after X-ray irradiation; bicinchoninic acid (BCA) protein quantification method was used to detect protein concentration.

Statistical analysis

Measurement data were presented by mean ± SD. SPSS19.0 software was used for analysis. Multi-sample homogeneity test of variance was adopted for comparison among groups; if variances were homogeneous, then *t*-test was adopted.

RESULTS

Colorectal cancer SW480 cells after X-ray irradiation at different doses

After X-ray irradiation and culture for 24 h, comparison between the 4 Gy dose group, 8 Gy dose group and 0 Gy dose group indicated that the invasion ability of cells in the 4 Gy and 8 Gy dose groups strengthened significantly ($p < 0.05$); moreover, the invasion ability of cells in the 8 Gy dose group increased significantly compared with that of the 4 Gy dose group ($p < 0.05$).

Colorectal cancer SW480 cells after X-ray irradiation in different doses

After X-ray irradiation and culture for 24 h, the migration ability of cells also changed. The migration ability of cells in the 4 Gy dose group strengthened significantly compared with that of the 0 Gy group ($p < 0.05$), and the migration ability of cells in the 8 Gy dose group strengthened significantly compared with that of the 0 Gy group ($p < 0.01$). However, the difference between the 4 Gy dose group and 8 Gy dose group had no statistical significance ($p > 0.05$).

Analysis of mRNA expression level of E-cadherin and vimentin in SW480 cells after X-ray irradiation

Ct values of target genes obtained through real-time PCR experiment were accurately recorded and calculated according to the equation $2^{-\Delta\Delta Ct}$; mRNA relative expression of target genes E-cadherin and vimentin and statistical results are shown in Fig. 1. Comparison results showed that the E-cadherin expression in both experimental groups was

significantly lower than in the control group ($p < 0.05$, $p < 0.01$); comparisons between the 4 Gy dose group and control group, and the 8 Gy dose group and control group were both $p < 0.01$. Expression of the 8 Gy group decreased most significantly and its comparison with 4 Gy dose group was $p < 0.01$ which was statistically significant. On the contrary, expression of vimentin in both experimental groups was significantly higher than that in the control group ($p < 0.01$), and the expression of vimentin in the 8Gy dose group was the highest; comparison between the 4 Gy dose group and 8 Gy dose group was $p < 0.01$.

Analysis of expression level of vimentin and E-cadherin in SW480 cells after X-ray irradiation

After X-ray irradiation and 48 h of continuous culture, Western-blot was used to detect the expression level of target gene proteins in cells of different groups, and the grey value of each group was calculated. As shown in Table I and Fig. 2, the 0 Gy control group had the highest E-cadherin expression and lowest vimentin expression. Compared with the control group, the E-cadherin protein expression in both experimental groups decreased significantly ($p < 0.01$). The difference between the 4 Gy group and 8 Gy group had statistical significance ($p < 0.05$); expression of E-cadherin decreased gradually with the increase of irradiation dose. However, compared with the control group, the Vimentin expression in the 4 Gy dose group increased significantly compared with the 0 Gy dose group ($p < 0.05$), while 8 Gy group increased even more significantly compared with the control group ($p < 0.01$). Significant difference could also be found between 4 Gy dose group and 8 Gy dose group ($p < 0.05$).

DISCUSSION

Excessive proliferation of epithelial cells and angiogenesis are signs of start and growth of primary tumors. Invasion ability (invasion of the basilar membrane) indicates the entering into the last stage of tumor progression, i.e., metastasis and spread, which can be life-threatening. At present, phenotypes of tumor cells obtaining invasion ability as well as latter widely disseminated inheritance and biochemical mechanism are extensively studied. In most studies, activation of EMT is considered to be one of the key mechanisms of epithelial tumor cells obtaining malignant phenotypes. Generation of EMT

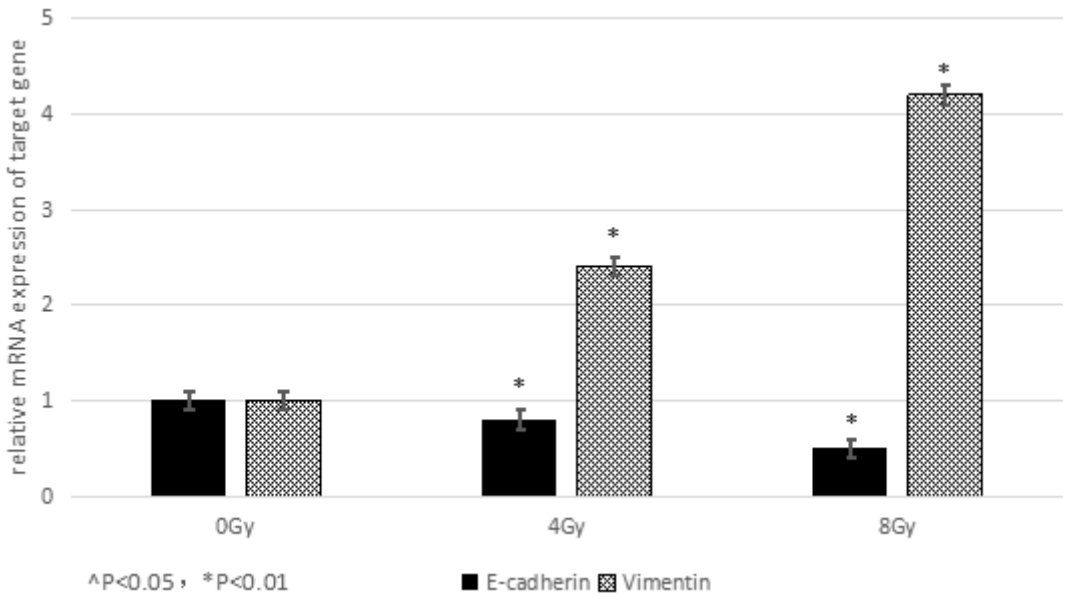

Fig. 1. *mRNA relative expression level of target genes E-cadherin and vimentin in experiment groups and the control group.*

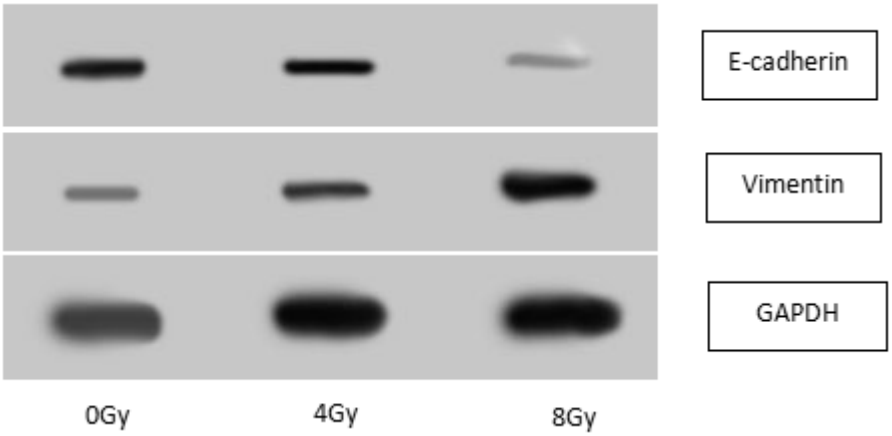

Fig. 2. *Western blot images of target genes in cells of different groups after X-ray irradiation. Note: 0 Gy refers to the control group.*

Table I. *Comparison of expression level of E-cadherin and vimentin protein in different dose groups.*

Group	Relative expression	
	E-cadherin	Vimentin
0 Gy dose	0.918±0.028	0.138±0.051
4 Gy dose	0.398±0.036*	0.291±0.065*
8 Gy dose	0.035±0.021*	0.905±0.329*

^ $p < 0.05$; * $p < 0.01$

is caused by biochemistry changes of cancer cells, and the reason X-rays can kill cancer cells is that the interaction between ionizing radiation and DNA can cause double-strand breaks or single-strand breaks of DNA, thus can kill tumor cells or change biological characteristics of tumors cells (11-12). Therefore, X-rays can cause changes of the molecular level of cancer cells. As mentioned previously, X-rays can mediate various kinds of cancer cells to have EMT, thus we hypothesized that X-rays can enhance the invasion and metastasis ability of human colorectal cancer cells because of EMT.

Human colorectal cancer SW480 cells which had high expression of epithelial indexes were used in this study. After X-ray irradiation in different doses, morphology of cells in experimental groups all changed compared with the 0 Gy control group; The cells became longer, and turned into fusiform shape from oval shape; moreover, cells began to be separated and typical EMT phenomena showed. Transwell chamber invasion and migration experiment indicated that, after X-ray irradiation, invasion and migration ability of cells in the experimental groups strengthened obviously compared with the control group; the invasion and migration ability increased more significantly with the increase of irradiation dose. Expression of E-cadherin in experimental groups decreased obviously, while the expression of mesenchymal index vimentin in the experiment groups increased significantly, as shown in Figs. 1 and 2 and Table I; the increase and decrease degree improved with the increase of irradiation dose. The

results verified that X-ray irradiation could mediate EMT of human colorectal cancer cells to improve invasion and metastasis ability of tumor cells. The phenotypic plasticity induced by EMT is reversible, that is to say, cells that already have mesenchymal characteristics can be reversed to epithelial state, which is called mesenchymal-epithelial transition (MET).

In conclusion, EMT of human colorectal cancer SW480 cells can be induced by X-ray irradiation, and it is possible that this is in positive correlation with the irradiation dose. Only a Cell Resource Center (CRC) cell line (SW480) was used *in vitro* and no further *in-vivo* or animal experiments were performed, thus the study was limited and further studies are needed.

REFERENCES

1. Gascun CFD, Bergin C, Regan CM, Coughlan SE, Powderly WG, Hall WW. Therapeutic strategy in unresectable metastatic colorectal cancer: an updated review. Ther Adv Med Oncol 2015; 7(3):75-89.
2. Nordholm-Carstensen A, Krarup PM, Morton D, Harling H. Mismatch repair status and synchronous metastases in colorectal cancer: A nationwide cohort study: Mismatch repair and colorectal cancer. Int J Cancer 2015; 137(2):2139-48.
3. Yao S, Zheng P, Wu H, et al. Erbin interacts with c-Cbl and promotes tumourigenesis and tumour growth in colorectal cancer by preventing c-Cbl-mediated ubiquitination and down-regulation of EGFR. J Pathol 2015; 236(1):65-77.
4. Chen Q, Wang J, Yang JH, et al. Association between adult weight gain and colorectal cancer: a dose-response meta-analysis of observational studies. Int J Cancer 2015; 136(12):2880-89.
5. Graveline M, Marti D, Thakur V, R Ruo, ET Soisson, H Patrocinio, D Roberge. 2061 POSTER Clinical evaluation of 6 degree-of-freedom X-ray image-guidance fusion algorithm and robotic positioning system for frameless cranial radiosurgery. Eur J Cancer 2011; 47(11):S206.
6. Lin MC, Lee CF, Lin CL, et al. Dental diagnostic X-ray exposure and risk of benign and malignant brain tumors. Ann of Oncol 2013; 24(6):1675-79.
7. Silva MP, Soave DF, Ribeiro-Silva A, Poletti ME. Trace elements as tumor biomarkers and prognostic factors in breast cancer: a study through energy dispersive x-ray fluorescence. Bmc Res Notes 2012; 5(1):194.
8. Ueki N, Ishihara Y, Matsuo Y, et al. Comparison of 4-dimensional doses and 3-dimensional doses in dynamic tumor tracking irradiation for lung tumor using a gimbaled x-ray head. Int J Radiat Oncol 2014; 90(1):S637.
9. Li R, Lewis JH, Jia X, et al. 3D tumor localization through real-time volumetric x-ray imaging for lung cancer radiotherapy. Med Phys 2011; 38(5):2783-94.
10. Li G, Liu Y, Su ZW, et al. Irradiation induced epithelial-mesenchymal transition in nasopharyngeal carcinoma in vitro. Chin J Otorhinolaryngol Head Neck Surg 2013; 48(8):662-67.
11. Yan S, Wang Y, Yang Q, et al. Low-dose radiation-induced epithelial-mesenchymal transition through NF-κB in cervical cancer cells. Int J Oncol 2013; 42(5):1801-6.
12. Frey B, Stache C, Rubner Y, et al. Combined treatment of human colorectal tumor cell lines with chemotherapeutic agents and ionizing irradiation can in vitro induce tumor cell death forms with immunogenic potential. J Immunotoxicol 2012; 9(3):301-13.

LETTER TO THE EDITOR

CORRELATION BETWEEN IL-6 AND INVASIVENESS OF ECTODERM CELLS OF EMBRYO IN EARLY PREGNANCY

XY. JIANG[1], TM. LU[1], WH. SHU[2] and HY. ZHOU[1]

[1]Gynecology and Obstetrics, People's Hospital of Liaocheng, Shandong, China; [2]Teaching and Research Office of Medical Science, Nursing Academy, Binzhou Polytechnic, Shandong, China

Received January 29, 2016 – Accepted May 17, 2016

This study aimed to explore the correlation between Interleukin-6 (IL-6) and invasiveness of ectoderm cells of embryo in early pregnancy, in order to further discuss whether IL-6 can enhance invasiveness of ectoderm cells. The study lays the foundation for determination of pathogenesis of some gestation period-related diseases. Differences in mRNA and protein expression of trophoblastic cell line JEG-3 cells in IL-6, matrix metalloproteinase-2 (MMP-2) and MMP-9 were analyzed; the regulating effect of different concentrations of IL-6 on invasive ability of trophoblast cells was studied by Transwell assay; the effect of IL-6 on proliferation of ectodermal cell line JEG-3 of embryo was analyzed by methyl thiazolyl tetrazolium (MTT) assay. The invasive number of JEG-3 cells incubated by IL-6 (10 ng/ml) was higher than that of the control group, and the difference had statistical significance ($p < 0.05$). Results of using MMT assay to detect the effect of IL-6 on proliferation of trophoblastic cell line JEG-3 showed that JEG-3 cells before and after processing had no significant difference from the control group ($p > 0.05$). Therefore, IL-6 can enhance invasiveness of ectoderm cells of embryo through activation of MMP-2.

Pregnancy refers to the physiological process from fertilization to parturition, in which the fertilized ovum enters the uterine cavity, and the embryo and its appurtenances grow rapidly until maturity; every gestational week is different, and the synergistic actions of cytokines, growth factors and hormones, etc., are needed for a successful pregnancy outcome. Ectoderm cells of embryo are also known as trophoblast cells which can differentiate into syncytiotrophoblast and cytotrophoblast (1-2) during the implantation of embryo. Trophoblast cells can invade the endometrial stroma and accomplish reconstruction of uterine spiral artery, thus enabling the fetus to receive sufficient blood flow from the matrix. A large number of studies verified that abnormal invasive function of trophoblast cells could lead to weak invasive ability of trophoblast cells in endometrium, resulting in reconstruction failure of the uterine spiral artery, anoxia and ischemia of placenta as well as damaging the vascular endothelial cells of the matrix's whole body, which could cause various pregnancy-related diseases (3).

To date, a number of scholars have made in-depth explorations on this problem. In 2011, Aspinall, et al. (4) discussed the molecular mechanism of IL-6 to trophoblast cells, indicating that the activation of MMP-2 was closely related to the regulatory effect of MMP-14 and tissue inhibitor of metalloproteinases-2

Key words: ectoderm cells of embryo (trophoblast cells), IL-6, JEG-3, transwell experiment

Mailing address:
Dr Xinyan Jiang
Gynecology and Obstetrics,
People's Hospital of Liaocheng,
Shandong, 25200, China
e-mail: jiangxinyan252@163.com

0393-974X (2016)

DISCLOSURE: ALL AUTHORS REPORT NO CONFLICTS OF INTEREST RELEVANT TO THIS ARTICLE.

(TIMP-2). In 2014, Volarevic, et al. (5) found that IL-6 was an important cytokine that participated in the immune response of embryo transplantation, which had two-way regulation. In 2014, Looijenga, et al. (6) discovered that IL-6 could enhance the tumor-cytotoxic effect of immune cells, accelerate development of hemocytes, induce expression of tumor necrosis factors and fibroblast growth factors as well as effectively regulate invasiveness of tumor cells. Therefore, it is possible that IL-6 can enhance invasiveness of trophoblast cells through activation of MMP-2.

MATERIALS AND METHODS

Experimental instruments

Common inverted microscope; pure water filter; fully-automatic equipment for rapid high temperature and high pressure sterilization; -80°C cryorefrigerator; -20°C refrigerator; micropipettor; electronic pipette; high speed refrigerated centrifuge; low speed centrifuge; low-temperature circulating water bath; microplate reader; optical microscope.

Experimental reagents

Dulbecco's modified eagle medium-high Gglucose (DMEM-H) complete medium; fetal bovine serum (FBS); SD-1008; Trypan blue; RNA extraction kit; cDNA reverse transcription kit; fluorescent quantitative polymerase chain reaction (PCR) kit; phosphate buffer saline (PBS); methyl thiazolyl tetrazolium (MTT) solution; phenylmethylsulfonyl fluoride, etc.

Transwell assay

After suspension using DMEM-H complete medium, JEG-3 cells were cultured in a constant temperature incubator and observed by inverted microscope every five hours; solution in the incubator was changed every two days. Then cells were observed by inverted microscope after culture; when cells covered 80% of the bottom, all experimental observation equipment was disinfected using alcohol wipes; then cells were cryopreserved. After that, precooled dimethylsulfoxide (DMSO) and FBS cryopreservation solution was mixed in 1:9 to resuspend cells; each cryogenic vial was added with 1 ml of cell suspension and sealed with sealing films and cryopreservation batches of vials were marked; then cryogenic vials were transferred to a nitrogen canister for cryopreservation. After cryopreservation, JEG-3 cells were taken out from the nitrogen canister and put into a 37°C water bath for instant melting; finally cells were revived.

Ice boxes needed for the experiment were prepared; matrigel was transformed into liquid state through temperature changes of environment. Then BD matrigel was diluted to an appropriate concentration by synthetic medium in 15:1; Transwell was put into a 24-well culture plate, and 100 µl of diluted matrigel was poured onto the surface of the Transwell which was then was cultured in an incubator (37°C). After that, serum-free medium that contained different concentrations of IL-6 was used for cell resuspension; then the 24-well culture plate was taken out from the incubator and resuspended cells were inoculated in a Transwell chamber; the whole chamber was then put back in to the culture well to culture cells.

MTT assay

An amount of 0.5 g of thiazolyl blue was dissolved by 100 ml of phosphate buffer; bacteria and impurities in the solution were filtered and the pure solution obtained was preserved at 4°C without light. Complete culture which contained IL-6 (10 ng/ml) was used to resuspend digested cells in growth phase; 200 µl of resuspended cells were inoculated onto a 96-well culture plate; each group of cells were placed into three repeated wells; then the plate was put into a constant temperature incubator (37°C, 5% CO_2 and saturated humidity) for two days; after two days, the culture plate was taken out and each well was added with 50 µl of MTT solution; after that, the plate was put back into the constant temperature incubator for further culture for 5 h. After cell culture, the culture solution in the plate was removed and 200 µl of DMSO was added to terminate the cell culture. A microplate reader was used to measure proliferation of cells.

Extraction of total cell protein

Protein extracting solution was prepared according to a certain proportion. The 6-well culture plate was processed again; culture medium was removed and the plate was washed gently using stroke-physiological saline solution for three times; each well was added with

a certain amount of protein extracting solution and cells were collected to a side of the culture well; homogenate was transferred to EP tubes and cells were split for 30 min in an ice box. After cell lysis, EP tubes were centrifuged at high speed at 4°C for 20 min. After the centrifugation, the supernate in EP tubes was transferred to new EP tubes and preserved in a cryogenic refrigerator (-80°C) for standby application.

Statistical analysis

Quantitative experiments were all repeated twice; SPSS19.0 software was used for data analysis; *t*-test was used to compare the difference of data between two groups; $p < 0.05$ indicated that the difference was statistically significant, while $p > 0.05$ indicated that the difference had no statistical significance; $\alpha=0.05$ was the inspection standard.

RESULTS

Effect of IL-6 on invasiveness of JEG-3 cells

Exogenous IL-6 (10ng/ml) was used in this experiment to process JEG-3 cells, thus to analyze the effect of IL-6 on invasiveness of ectoderm cells of embryo (20). After 36 h incubation using IL-6 (10ng/ml), the number of JEG-3 cells in the experimental group was significantly increased (72.4±17.3) compared to the control group (49.2±13.1) (Fig. 1).

Effect of IL-6 on proliferation ability of JEG-3 cells

Results of the MTT assay showed that the proliferation ability of JEG-3 cells processed by IL-6 was 0.41, while in the control group it was 0.36, thus the difference was not statistically significant ($p > 0.05$).

Effect of IL-6 on expression of matrix metalloproteinases mRNA in JEG-3 cells

After being incubated by IL-6, mRNA in JEG-3 cells of the control group and experimental group was extracted. The results showed that expression levels of MMP-2 mRNA and MMP-9 mRNA in JEG-3 cells of the IL-6 experimental group were not statistically different from that of the control group ($p > 0.05$).

Effect of IL-6 on expression of matrix metalloproteinases protein in JEG-3 cells

The results showed that the relative expression level of Pro-MMP-2 protein in the normal control group was (0.47±0.08); relative expression level of Pro-MMP-9 protein was (0.18±0.07); the relative expression level of Pro-MMP-2 in JEG-3 cells processed by IL-6 was (0.48±0.07), while the relative expression level of Pro-MMP-9 was (0.21±0.04). The differences in expression level of Pro-MMP-2 and Pro-MMP-9 in the experimental group and control group were not significant and had

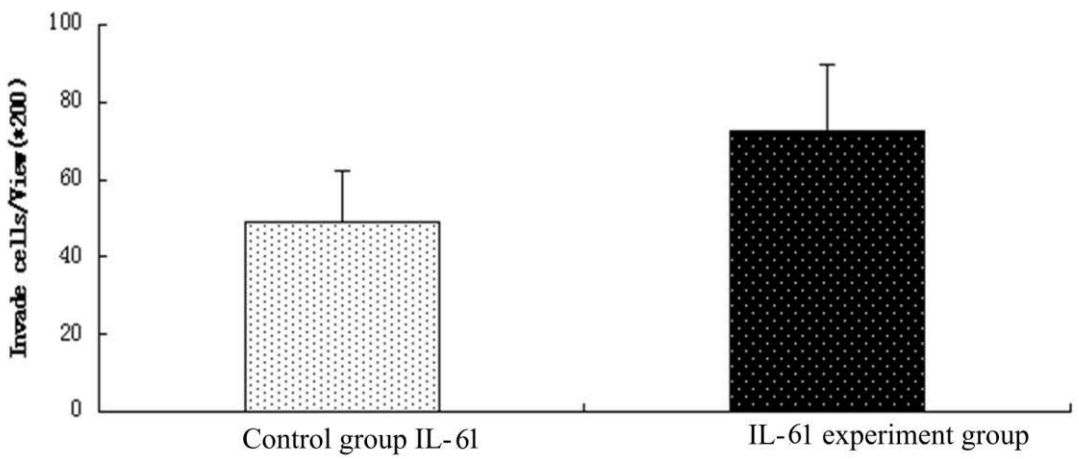

Fig. 1. *Effect of IL-6 on invasiveness of JEG-3 cells of embryo.*

Table I. *Effect of IL-6 on expression of MMPs mRNA in JEG-3 cells.*

Groups	Number of cases	Relative expression level of MMP-2 mRNA	Relative expression level of MMP-9 mRNA
Control group	24	1.1±0.2	1.0±0.1
IL-6 experiment group	24	0.9±0.1	1.2±0.2
t		-0.7	-0.9
p		0.5	0.4

no statistical significance ($p > 0.05$).

DISCUSSION

As a kind of heterogeneous cell, ectoderm cells of embryo in early pregnancy play a vital role in placentation. In the development process of embryo, ectoderm cells of embryo are also called trophoblast cells which can differentiate into syncytiotrophoblast and cytotrophoblast. Trophoblast cells can invade endometrium, muscular layer and spiral artery, thus form into circulation of uterine placenta (7-8). During pregnancy, ectoderm cells of embryo can invade uterus to deciduation and thus function properly. The expression level of IL-6 in placenta plays a vital role in successful pregnancy; it can stimulate growth of tumor cells through autocrine of tumor cells and paracrine of inflammatory cells; moreover, it has important regulatory effect on invasiveness of tumor cells (9).

By Transwell experiment and MTT assay, different concentrations of IL-6 were used to process JEG-3 cells as well as analyze the differences of expression levels of MMPs mRNA and pro-MMPs in JEG-3 cells, and to discuss whether molecular mechanism of IL-6 had effect on ectoderm cells of embryo and thus affect invasiveness of trophoblast cells (10). Transwell results indicated that the number of JEG-3 cells processed by IL-6 (10ng/ml) in the experimental group increased significantly compared with that of the control group, and the invasive ability of JEG-3 cells in the experiment group enhanced significantly; the difference had statistical significance ($p < 0.05$). This study adopted MTT experiment to detect the proliferation ability of cells. Results showed that the difference of proliferation ability of JEG-3 cells processed by IL-6 and JEG-3 cells in the control group had no statistical significance ($p > 0.05$), which excluded the effect of changes of proliferation ability of trophoblast cells on experiment of invasiveness. This study also explored the effect of IL-6 on expression of MMPs mRNA in JEG-3 cells; the results indicated that the expression level of MMP-2 mRNA and MMP-9 mRNA in JEG-3 cells processed by IL-6 had no statistical significance ($p > 0.05$). Finally, the effect of IL-6 on expression of MMP protein in JEG-3 cells was studied, and the results showed that the difference between IL-6 experiment group and control group had no statistical significance ($p > 0.05$) (11). In JEG-3 cells of the IL-6 experimental group, expression levels of activated MMP-2 and MMP-9 were significantly higher than those of the control group, which was closely related to the IL-- induced enhancement of invasiveness of JEG-3 cells (12).

In conclusion, IL-6 plays a vital role in successful pregnancy of humans; it can improve the invasiveness of trophoblast cells by stimulating activation of MMP-2, thus it lays the foundation for

determination of pathogenesis of relevant diseases during pregnancy therefore protecting the maternal and child health.

REFERENCES

1. Xie P, Zhou H, Zhou XY, Zhao XM, Du J, Lu GX, Lin G. Derivation of human embryonic stem cell from spinal muscular atrophy patient. Stem Cell Res 2016; 16(2):216-19.
2. Suman P, Godbole G, Thakur R, Morales-Prieto DM, Modi DN, Markert UR, Gupta SK. AP-1 transcription factors, mucin-type molecules and MMPs regulate the IL-11 mediated invasiveness of JEG-3 and HTR-8/SVneo trophoblastic cell. Plos One 2012; 7(1):e29745. doi: 10.1371/journal.pone.0029745.
3. Tessier DR, Yockell-Lelièvre J, Gruslin A. uterine spiral artery remodeling: the role of uterine natural killer cells and extravillous trophoblasts in normal and high-risk human pregnancies. Am J Reprod Immunol 2015; 74(1):1-11.
4. Aspinall R, Prentice AM, Ngom PT. Interleukin 7 from maternal milk crosses the intestinal barrier and modulates T-cell development in offspring. Plos One 2011; 6(6):e20812-e20812.
5. Volarevic V, Bojic S, Nurkovic J, et al. Stem cells as new agents for the treatment of infertility: current and future perspectives and challenges. Biomed Res Int 2014; 2014(2):164-65.
6. Looijenga LHJ, Stoop H, Biermann K. Testicular cancer: biology and biomarkers. Virch Arch: Int J Pathol 2014; 464(3):301-13.
7. Morelli M, Rocca ML, Mocciaro R, et al. Sonographic findings in postmenopausal women with a prior endometrial ablation: interpretation and management of women with endometrial thickening and bleeding. J Minim Invas Gynecol 2015; 22(3):489-94.
8. Naredi N, Sandeep K, Jamwal VDS. Interstitial implantation in a setting of recurrent ectopic pregnancy: A rare combination. MJAFI 2015; 71(2):194-96.
9. Takeda K, Kaisho T, Yoshida N, Takeda J, Kishimoto T, Akira S. Stat3 activation is responsible for IL-6-dependent T cell proliferation through preventing apoptosis: generation and characterization of T cell-specific Stat3-deficient mice. J Immunol 2015; 161(9):4652-60.
10. Barr TA, Shen P, Brown S, et al. B cell depletion therapy ameliorates autoimmune disease through ablation of IL-6-producing B cells. J Exp Med 2012; 209(5):1001-10.
11. Guiñazú N, Rena V, Genti-Raimondi S, Rivero V, Magnarelli G. Effects of the organophosphate insecticides phosmet and chlorpyrifos on trophoblast JEG-3 cell death, proliferation and inflammatory molecule production. Toxicol Vitro 2012; 26(3):406-13.
12. Yara M, Iwao B, Hara N, Yamanaka T, Uchino H, Inazu M. Molecular and functional characterization of choline transporter in the human trophoblastic cell line JEG-3 cells. Placenta 2015; 36(6):631-37.

JOURNAL OF BIOLOGICAL REGULATORS & HOMEOSTATIC AGENTS Vol. 30, no. 2, 565-569 (2016)

LETTER TO THE EDITOR

MECHANISM OF AGE-RELATED CHANGES OF BONE MARROW MESENCHYMAL STEM CELLS IN SENILE OSTEOPOROSIS

C. HUANG, G.F. ZHANG, J. HAN, G.J. LIAO and B.G. ZOU

Department of Orthopedic Surgery, Yan Tai Shan Hospital, Shandong, China

Received January 29, 2016 – Accepted April 27, 2016

This study was carried out to explore the age-related changes of bone marrow mesenchymal stem cells (BMMSCs) in mice as well as the influence of autophagy on the age-related changes of BMMSCs. BMMSCs aging-associated protein acetylation P53, P21 and P16 expressions in young and senile mice, protein expression of telomerase reverse transcriptase (TERT) as well as reactive oxygen species (ROS) level were detected and compared; the expression of BMMSCs autophagy associated gene, autophagy related protein molecule and LC3 molecule were detected; the influence of differently concentrated rapamycin and 3-MA on BMMSCs autophagy level was observed to select effective concentrations; the influence of rapamycin and 3-MA on BMMSCs cell cycle-related gene expression, apoptosis related gene expression and ROS level were discussed. Results revealed that the senile BMMSCs group had higher acetylation P53, P21 and P16 expression and fluorescence intensity than the young group, but its TERT expression, Beclin1 and LC3 gene expression and fluorescence intensity were lower than the young group. Both rapamycin and 3-MA inhibited CyclinD1 (CCND1) and CyclinD2 (CCND2) expression. Rapamycin promoted the expression of apoptosis-related genes Caspase3 and Caspase8 in the senile group, while 3-MA inhibited them in both the young and senile groups. It can therefore be concluded that senile BMMSCs have multiple age-related changes, performing as decrease of osteogenic capability and multiplication capacity, increase of acetylation P53, P21 and P16 protein expression, apoptosis and ROS level as well as decrease of telomerase activity. Furthermore, the autophagy level in senile BMMSCs reduced compared with young cells; autophagy activation can decrease ROS level and autophagy suppression improves ROS level; and autophagy regulation affects cell cycle and apoptosis.

With age, senile osteoporosis is featured by larger bone absorptive amount than osteogenesis amount, decreased proportion of cortical bone and cancellous bone amount, reduced bone strength and easily fractured bones (1-2).

Mesenchymal stem cells (MSCs) are stem cells with self-renewal and multi-directional differentiation ability existing around the blood vessel in bone marrow and a variety of organs (3). Bone marrow mesenchymal stem cells (BMMSCs) discussed in this study are the progenitor cells of mesenchymal stem cells, playing significant roles in the growth, development, metabolism and rebuilding of bone. Humans and rodents have been reported to have age-related changes of BMMSCs (4-5).

Autophagy, a conservative protein degradation process, is generally considered as a self protective mechanism, protecting some organic damage, such as liver, heart, nerve system and kidney, in animal models (6-7). Autophagy is usually divided into

Key words: senile osteoporosis, bone marrow mesenchymal stem cells, age-related changes

Mailing address:
Dr Chen Huang,
No.91 JieFang Road, Deartment of Orthopedic Surgery,
Yan Tai Shan Hospital, Yantai,
Shandong, 264001, China
e-mail: huangchen263@sina.com

0393-974X (2016)

three types - macroautophagy, microautophagy and chaperone-mediated autophagy (CMA). Autophagy in the present study mainly refers to macroautophagy. Meléndez et al. (8) hypothesized that insulin-like growth factor signal path inhibition and autophagy activation played an important role in prolonging the life of nematodes. Autophagy has a significant effect on the survival of stem cells as well as maintaining functional and biological characteristics, but the research is not conclusive. Based on this, the present study discusses the mechanism of age-related changes of BMMSCs in senile osteoporosis.

MATERIALS AND METHODS

Age-related changes of BMMSCs in senile mice

Specific pathogen free C57/BL6J mice aged one month and 12 months were raised under ordinary conditions; 2 ~ 4 and 16 ~ 18 months old mice were taken as a young group and a senescent group, respectively. Ten mice were randomly selected from the two groups. 1 ml injector was used to extract bone marrow; cells were blown and beaten gently and suspended in α-MEM culture medium containing 20% FBS; bone marrow of bilateral hind legs of each mouse was inoculated into two 90 mm culture dishes and then cultured in an incubator (37°C, 5% CO_2); half of the culture medium was changed every three days. Cells were passaged after covering 90% of the wall, and P3 cells were taken for the study.

Acetylation P53, P21 and P16 protein expression levelS in P3 BMMSCs in two groups were detected using Western blot and compared. Total protein was extracted from P3 cells and detected using Western blot, and TERT protein expression level in BMMSCs in two groups was compared. After tryptic digestion, the number of P2 BMMSCs was counted, and they were inoculated into a 24-well plate cover glass at the density of $3\times10^4/cm^2$ and mixed. Cells were cultured under routine conditions and stained as per the instruction of ROS detection kit after adhering to the wall.

Comparison of BMMSCs autophagy level in young and senescent mice

Total ribose nucleic acid (RNA) was extracted using spearhead and EP tube without RNA enzymes. RNA was reversely transcribed into cDNA on ice according to the manufacturer's instructions (TOYOBO RT-PCR kit) under 20 μl/2000ng RNA system. Then, cDNA was diluted 4 times in each group under reaction system, and BIO-RAD CFX96 real-time fluorescence quantification PCR instrument was used for real-time PCR reaction after samples were added.

Total protein was extracted from P3 cells, and Beclin1 and LC3 molecular expression levels were detected with Western blot. After pancreatic protein digestion, P2 cells were centrifuged at 800 rmp and washed for 3 times using phosphate buffer solution (PBS); cells were then stained after being fixed with 4% paraformaldehyde for 20 min. Afterwards, laser scanning confocal microscope (LSCM) was used to observe the fluorescence intensity of cells in each group. After pancreatic protein digestion, P3 cells were centrifuged at 1500 rmp for 15 min and washed twice with PBS. Then, samples were prepared after PBS was removed to observe with a transmission electron microscope the submicroscopic structure, and images were filmed.

Role of autophagy in the age-related changes of BMMSCs

P2 BMMSCs were taken from mice aged 2 months and counted after pancreatic protein digestion. Then, they were inoculated into 6 small bottles and cultured under routine conditions, with 1×10^6 cells in each bottle. When cells covered 90% of the bottle, they were divided into two groups. One group was added with 3 ml of normal culture solution and 3 ml of culture solution in different concentrations of 1 nM, 20 nM, 50 nM, 100 nM and 200 nM rapamycin, while the other group was added with 3 ml of normal culture solution, 3 ml of culture solution containing 0.1 mM 3-MA, 3 ml of culture solution containing 1 mM-3MA, 3 ml of culture solution containing 5 mM-3MA and 3 ml of culture solution containing 10 mM-3MA. Cells were washed twice with PBS 24 h later, and total protein was extracted and the expression of Beclin1 protein was detected with Western blot.

P2 BMMSCs taken from mice were inoculated into a 6-well plate at a density of 3×10^5 cell/well after pancreatic protein digestion, with 3 wells for each group, and cultured under routine conditions. The young group and senile group were divided into control group (routine culture solution), rapamycin group (100 nnM) and 3-MA group (5 mM) until cells covered 90% of the well plate. After 24 h the cells were washed twice with PBS, total protein

was extracted and the expression of cell cycle-associated gene CCND1, CCND2 and Caspase3 and Caspase8 was detected with RT-PCR.

P2 BMMSCs taken from mice were inoculated into a 24-well plate cover glass with at a density of 3×10^4 after pancreatic protein digestion, and cultured under routine conditions. The young group was divided into control group (routine culture solution), ROS group (10^{-4} M H_2O_2), ROS (10^{-4} M H_2O_2) + 100 nM rapamycin group and 5 mM 3-MA group until cells adhered to the wall; and the senescent group was divided into control group (routine culture solution) and 100 nM rapamycin group. Cells were inoculated into a 24-well plate and put into an incubator. ROS level in each group was observed with LSCM 24 h later.

Statistical analysis

SPSS17.0 software was applied to analyze data, comparison among groups was carried out using *t*-test and the difference was considered to be statistically significant if $p < 0.05$.

RESULTS

Age-related changes of BMMSCs in senile mice

Results of Western blot detection showed that the expression of acetylation P53, P21 and P16 protein molecules in the young group was found to be lower than in the senescent group, and the young group had a higher TERT protein molecular expression than the senescent group, i.e., telomerase activity was reduced in the senescent group.

Comparison of ROS level in BMMSCs in young and senescent mice

The young group was found with lower BMMSCs fluorescence intensity than the senescent group, i.e., ROS level in the young group was lower than in the senescent group.

Comparison of BMMSCs autophagy level in the young and senescent mice

Beclin1 and LC3 were lowly expressed in young mice compared with senescent mice ($p < 0.05$) as shown in Fig. 1. Western blot detection showed that Beclin1 and LC3II/LC3I protein were more highly expressed in young mice than in senescent mice. Observation using laser scanning confocal microscope indicated that young mice had higher BMMSCs fluorescence intensity than senescent mice, which explained that LC3 was more highly expressed in senescent mice. Transmission electron microscope examination showed that both two kinds of cells were observed with a typical autophagy structure, but the number of autophagosome in the senescent group was lesser than in the young group.

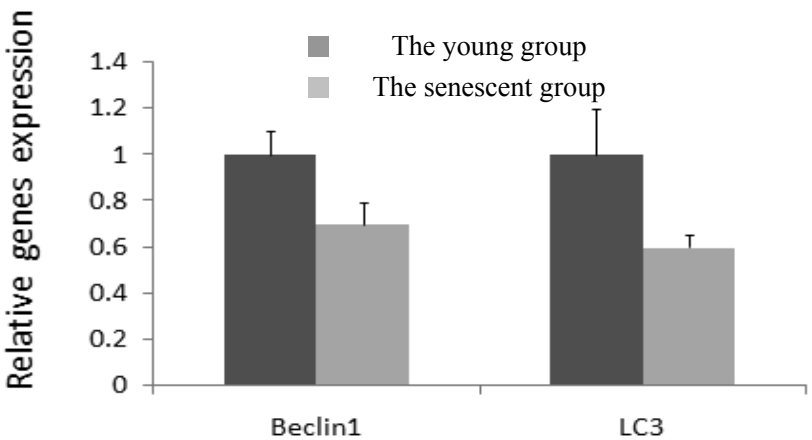

Fig. 1. *Comparison of BMMSC autophagy levels in the young and senescent mice detected by RT-PCR.*

Role and mechanism of autophagy in age-related changes of BMMSCs

As shown in Fig. 2, 100 nM rapamycin improving Beclin1 expression and 5 mM 3-MA decreasing Beclin1 expression to the greatest extent were considered as the best concentration. RT-PCR was adopted to detect the influence of rapamycin and 3-MA on cycle-associated genes of young and senescent BMMSCs and the results showed that CCND1 and CCND2 in the young and senescent mice were lowly expressed in the rapamycin and 3-MA stimulation group compared with the control group, which suggested that both drugs were able to inhibit the expression of cell cycle-associated genes. RT-PCR was used to detect the influence of rapamycin and 3-MA on apoptosis-related genes of young and senescent BMMSCs and the results showed that rapamycin had no obvious influence on cell apoptosis-associated gene expression, and promoted the expression of apoptotic gene in the senescent group; while 3-MA promoted the expression of apoptotic gene in both the young and senescent groups. Laser confocal scanning showed that the young group had stronger cell fluorescence intensity after being stimulated by 10^{-4}M H_2O_2 than the control group, indicating that H_2O_2 could enhance ROS level significantly. Cell fluorescence intensity was lower in the 100 nM rapamycin + 10^{-4}M H_2O_2 stimulation group than in the H_2O_2 stimulation group, which suggested that autophagy activation was effective in lowering ROS level resulting from H_2O_2 stimulation; cell fluorescence intensity in the senescent group after 100 nM rapamycin stimulation decreased obviously compared with the control group, which demonstrated that autophagy activation decreased ROS level in the senescent cells effectively. After 5 mM 3-MA stimulation, the young group had obviously higher cell fluorescence intensity than the control group, indicating that inhibiting autophagy could significantly improve ROS level of cells.

DISCUSSION

In this study, senescent BMMSCs presented a series of age-related changes, i.e., acetylation P53, P21 and P16 protein expressions were all higher than young cells, and TERT protein expression was lower than young cells while ROS level was high. These changes played significant roles in BMMSCs proliferation, apoptosis and differentiation.

Autophagy associated gene was in a downward trend in senile brain tissues and chondrocytes in

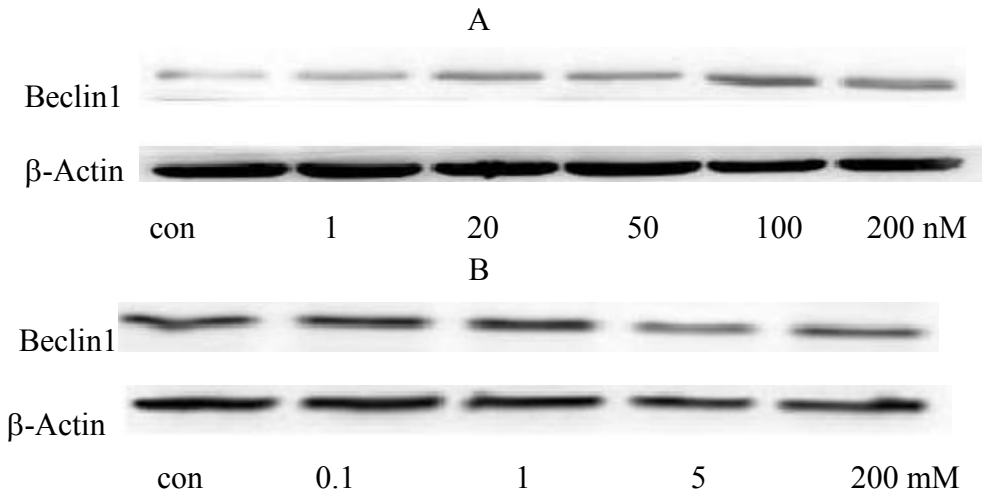

Fig. 2. *Detection of effective concentration of autophagy activation agent rapamycin and autophagy inhibitor 3-MA by Western blot.* ***A)*** *Rapamycin concentration screening.* ***B)*** *3-MA concentration screening*

senile patients with osteoarthritis (9). Through RT-PCR, Western blot, TEM and immunofluorescent staining, BMMSCs autophagy level in young and senile mice was detected, and the results verified that naturally aging mice had lower BMMSCs autophagy level than young mice, suggesting that autophagy had a certain effect on stem cell senescence.

Rapamycin and 3-MA were selected to activate and inhibit autophagy, and we found that CyclinD1 and CyclinD2 gene expressions in senile mice were slightly higher than in young mice, which was in accordance with reports that rapamycin was able to inhibit tumor growth (10).

In this study, rapamycin had different influences on young and senile BMMSCs apoptosis, which were likely to be related to the types of cells. 3-MA had been proved to induce a variety of cell apoptosis by inhibiting autophagy (11-12). However, this study discovered that it was capable of controlling Caspase 3 and Caspase 8 gene expression, indicating that the relationship between autophagy and Caspase 3 and Caspase 8 deserved further discussion. In this study, following the conclusions were drawn. Firstly, senile BMMSCs showed a series of age-related changes, including decrease of multiplication capacity, increase of apoptosis level, decrease of osteogenic capability and increase of adipogenesis capacity, protein expression of acetylation P53, P21 and P16 increases, telomerase activity decreases and ROS level increases. Secondly, autophagy level of senile BMMSCs was lower compared with young cells. Thirdly, activation of autophagy can lower the ROS level of BMMSCs, and inhibition of autophagy can enhance the ROS level of BMMSCs; regulation of autophagy can affect the cell cycle and cell apoptosis.

REFERENCES

1. Manolagas SC, Almeida M. Gone with the Wnts: beta-catenin, T-cell factor, forkhead box O, and oxidative stress in age-dependent diseases of bone, lipid, and glucose metabolism. Mol Endocrinol 2007; 21(11):2605-14.
2. Pearson KJ, Baur JA, Lewis KN, et al. Resveratrol delays age-related deterioration and mimics transcriptional aspects of dietary restriction without extending life span. Cell Metab 2008; 8(2):157-68.
3. Crisan M, Yap S, Casteilla L, et al. A perivascular origin for mesenchymal stem cells in multiple human organs. Cell Stem Cell 2008; 3(3):301-13.
4. Stolzing A, Jones E, Mcgonagle D, et al. Age-related changes in human bone marrow-derived mesenchymal stem cells: consequences for cell therapies. Mech Ageing Dev 2008; 129(3):163-73.
5. Sethe S, Scutt A, Stolzing A. Aging of mesenchymal stem cells. Ageing Res Rev 2006; 5(1):91-116.
6. Gottlieb RA, Mentzer RM. Autophagy during cardiac stress: joys and frustrations of autophagy. Annu Rev Physiol 2010; 72:45-59.
7. Jiang M, Liu K, Luo J, Dong Z. Autophagy is a renoprotective mechanism during in vitro hypoxia and in vivo ischemia-reperfusion injury. Am J Pathol 2010; 176(3):1181-92.
8. Meléndez A, Tallóczy Z, Seaman M, Eskelinen EL, Hall DH, Levine B. Autophagy genes are essential for dauer development and life-span extension in *C. elegans*. Science 2003; 301(5638):1387-91.
9. Marta ML, Bin Z, Tao L, et al Genome-wide analysis reveals mechanisms modulating autophagy in normal brain aging and in Alzheimer's disease. Proc Natl Acad Sci U S A 2010; 107(32):14164-14169.
10. Guba M, von Breitenbuch P, Steinbauer M, et al. Rapamycin inhibits primary and metastatic tumor growth by antiangiogenesis: involvement of vascular endothelial growth factor. Nat Med 2002; 8(2):128-35.
11. Jie L, Ni H, Ahmad F, Soichi T, Toshiyuki T, Hiroyuki K. Inhibition of autophagy by 3-MA enhances the effect of 5-FU-induced apoptosis in colon cancer cells. Ann Surg Oncol 2009; 16(3):761-71.
12. Jun H, Jingjie Y, Qing X, Lin W, Jenny ZZ, Lingzhi L, Binghua J. Downregulation of ATG14 by EGR1-MIR152 sensitizes ovarian cancer cells to cisplatin-induced apoptosis by inhibiting cyto-protective autophagy. Autophagy 2015; 11(2):373-84.

LETTER TO THE EDITOR

MULTICENTER STUDY OF AUTOVERIFICATION METHODS OF HEMATOLOGY ANALYSIS

X. ZHAO[1], XF. WANG[2], JB. WANG[2], XJ. LU[1], YW. ZHAO[3], CB. LI[1], BH. WANG[3], J. WEI[2], P. GUO[2], JP. XIAO[4], JH. WANG[4] and XL. YANG[3]

[1]Department of Laboratory Medicine, Beijing Hospital, Ministry of Health, Dongdan, Dongcheng District, Beijing, China; [2]Department of Laboratory Medicine, Ruijin Hospital, Shanghai Jiaotong University School of medicine, Shanghai, China; [3]Department of Laboratory Medicine, Armed Police General Hospital, Haidian District, Beijing, China; [4]Shenzhen Mindray Bio-medical Electronics Co. Ltd, Nanshan, Shenzhen, China

Received March 23, 2016 – Accepted May 10, 2016

The first five authors contributed equally to this paper

This study was designed to establish and validate a set of autoverification methods for hematology analysis. One thousand and twenty-four samples were selected from Shanghai Ruijin Hospital and 999 from Beijing Hospital, China. False positive, false negative and autoverification pass rates were verified and the rules were then adjusted and confirmed according to the verification results. After confirmation, at least 10,000 sample cases were selected from Shanghai Ruijin Hospital, Beijing Hospital and China Armed Police General Hospital and checked automatically. The differences in the autoverification pass rate and average report delivery time before and after the application of the autoverification methods were compared between the three hospitals. Preliminary validation results showed that the false negative rates of the Shanghai Ruijin Hospital and Beijing Hospital were less than 2%. The false positive rates of these two hospitals were high, close to 18%. After rule adjustment, the false negative rate was basically the same as before adjustment, but the false positive rate declined obviously while the pass rate of autoverification improved significantly. The autoverification pass rates of the three hospitals were 76.4%, 85.1% and 84.2%, respectively. The turnover time (TAT, time from receipt of sample to report of the result) of the three hospitals decreased by 4.1 min, 8.8 min and 10.2 min, respectively. Autoverification systems using a Mindray BC-6800 auto hematology analyzer and labXpert were confirmed as being effective in reducing TAT and enhancing working efficiency on the premise of ensuring low false negative rate.

Currently, a large-scale hospital is usually equipped with fully automated test equipment, thus the working efficiency is greatly improved compared to the past. To further save manpower cost, shorten turnaround time (TAT) and guarantee the quality of report, the method of analyzing results is especially important. Furthermore, the inconsistent quality of laboratory personnel can also affect the quality of report. The establishment of an autoverification method provides an effective way to solve the above problems, and currently autoverification is mostly adopted in biochemical, immune and blood coagulation analysis

Key words: hematology, autoverification, rules

Mailing address:
Dr Xiaoli Yang,
Department of Laboratory Medicine,
Armed Police General Hospital,
No.69 Yongding Road, Haidian District,
Beijing, 100039, China
e-mail: xiaoliyangxl@163.com

0393-974X (2016)

DISCLOSURE: ALL AUTHORS REPORT NO CONFLICTS OF INTEREST RELEVANT TO THIS ARTICLE.

in the department laboratory (1-3). One study (4) introduced a method to formulate and confirm an automatic biochemical analyzer autoverification system. However, the autovertification system to send reports is rarely adopted for hematology analysis, which may be related to the specificity of blood cell analytical results. In order to obtain high-quality blood cell analytical results, the following elements should be taken into consideration: property of sample (potential factors such as coagulation and hemolysis), instrument status (plugging the hole, abnormal channel), parameters and alarm, previous test results of certain patients (Delta check), labXpert is a software connecting routine hematology instruments with a laboratory information management system (LIMS) developed by Mindray Co., Ltd. Its autoverification path is designed according to the Clinical and Laboratory Standards Institute (CLSI) Auto 10-A (5). After the input of regulations, results of all the samples are determined according to the rules. Abnormal samples can be reviewed by microscopy in order to improve the checking efficiency. Autoverification can significantly improve working efficiency, but there are clinical risks. Hence, it is especially important to formulate scientific checking rules.

MATERIALS AND METHODS

Sample selection

Ethylene Diamine Tetraacetic Acid (EDTA)-K2 anticoagulant samples were selected from the outpatients and inpatients of the Ruijin Hospital affiliated to Shanghai Jiaotong University (1,024 samples) and the Beijing Hospital, (999 samples), including 80% of first-visit patients and 20% of re-visiting patients. Moreover, at least 10,000 cases of EDTA-K2 anticoagulant samples were selected from Shanghai Ruijin Hospital, Beijing Hospital and China Armed Police General Hospital.

All of the above samples were analyzed on CAL 8000 auto sample processing system (Mindray, Shenzhen, China) within 4 hours after collection.

Instruments and reagents

All three hospitals were equipped with CAL 8000 auto sample processing system (including two BC-6800 auto hematology analyzer and one SC-120 autoslide maker and stainer). Supplementary reagents, whole blood control and calibrators were provided by Mindray Co., Ltd (Shenzhen, China).

Autoverification system

Autoverification module is one of the most core modules of labXpert system. The module composes three parts, i.e., autoverification, manual verification and microscopic verification. Strict verification relationships consistent with the idea of manual verification are established.

Methods

All samples were strictly tested as per the operating instruction of CAL 8000 (6). The samples for the evaluation of autoverification rules were automatically dyed by SC-120 after detection by a blood analyzer and three blood smears were made for each sample. Referring to microscopic examination of CLSI H20-A2 (7), two experienced technicians microscopically examined all samples. After rule confirmation, at least 10,000 samples were selected from each hospital for analysis.

Formulation of preliminary rules

Based on "41 Items of International Consensus Review Rules" (8) and technological level of the BC-6800 hematology analyzer, preliminary rules for CAL 8000 blood cell analysis autoverification and microscopic examination conditions were formulated and the specific rules are shown in Table I.

Determination of positive criteria

Positive criteria for microscopic examination were determined by referring to the International Consensus Group for Hematology Review: medium or more significant morphological change of red blood cells (RBC); presence of plasmodium in blood smear; medium or more significant morphological change of platelet (PLT); more obvious platelet aggregation; presence of Dohle body, toxic change, medium or more significant morphological change of vacuolar granulocytes; primary cell ≥ 1; promyelocytic cell/metamyelocytes ≥ 1; metagranulocyte > 2; abnormal lymphocyte ≥ 5; nucleated red blood cell (NRBC) ≥ 1; plasmacyte ≥ 1.

The result was determined as positive if the sample result did not pass autoverification.

Table I. *Autoverification rules*

Category	Item	Validation standard
Specimen abnormality	1	Insufficient samples or insufficient sample collection/ abnormal samples
	2	RBC aggregation
Critical value (9)	WBC (adult)	$<2\times10^9$/L or $>37\times10^9$/L
	PLT (adult)	$<37\times10^9$/L or $>910\times10^9$/L
	HCT (adult)	<18% or >61%
	HGB (adult)	<66g/L or >199g/L
	WBC (child)	$<2.1\times10^9$/L or $>42.9\times10^9$/L
	PLT (child)	$<53\times10^9$/L or $>916\times10^9$/L
	HCT (child)	<20% or >62%
	HGB (child)	<69 g/L or >208g/L
Parameter range	WBC	$[4.0\text{-}30]\times10^9$/L
	RBC	$[0\text{-}8.2]\times10^{12}$/L
	HGB	[70-180]g/L
	MCV	[75 -105] Fl
	PLT	$[100\text{-}1000]\times10^9$/L
	RDW	≤22%
	MCHC	≤380g/L
	Neut#	$[1.0\text{-}20.0]\times10^9$/L
	Lym# (adult)	$\leq5.0\times10^9$/L
	Lym# (child)	$\leq6.0\times10^9$/L
	Mono# (adult)	$\leq1.5\times10^9$/L
	Mono# (child)	$\leq3.0\times10^9$/L
	Eos#	$\leq2.0\times10^9$/L
	Bas#	$\leq0.5\times10^9$/L
	NRBC#	≤0.01
	RET#	$\leq0.10\times10^9$/L
Alarming	NRBC	[NRBC?] OR [Presence of NRBC]
	Fragments	Fragments?
	Abnormal scatter diagram	[WBC Scattergram Abn.]OR[NRBC Scattergram Abn.]OR[PLT Scattergram Abn.]OR[RET Scattergram Abn.]
	PLT Clump	PLT Clump?
	Blast and Immature cell	[Blast ?]OR[Abn. Lymph/blast?]OR[Immature Gran?]
	Atypical Lymph	Atypical Lymph?
	Left Shift	Left Shift?
	Infected RBC	Infected RBC?
	Dimorphic Population	Dimorphic Population?
	Abnormal histogram	[RBC Histogram Abn.] OR [PLT Histogram Abn.]
	RBC Lyse Resistance	RBC Lyse Resistance?
	Turbidity /HGB interference	Turbidity /HGB interference?
Abnormal Delta Check	WBC Delta check	Recurred visit patients, relative deviation within 3 days > 20% or absolute deviation > 0.5×10^9/L
	MCV Delta check	Recurred visit patients, relative deviation within 3 days > 5% or absolute deviation > 5fL
	PLT Delta check	Recurred visit patients, relative deviation within 3 days > 20% or absolute deviation > 15×10^9/L
Normal Delta Check	MCV Delta check	Recurred visit patients, relative deviation within 3 days > 5% or absolute deviation > 5fL
	PLT Delta check	Recurred visit patients, relative deviation within 3 days > 20% or absolute deviation > 15×10^9/L
Additional rules	Newborn	0 – 28 days
	Low MCHC and normal or high MCV	MCHC<300g/L and MCV>80fl

Evaluation for autoverification rules

The microscopic review result was considered as "gold standard" for evaluating the preliminary verification rules. Referring to CLSI H20-A2 microscopic examination methods, each sample was microscopically examined by two technicians who each counted 200 white blood cells (WBC). Another technician participated in the verification if the microscopic review results of the first two technicians exceeded allowable range; and the average value of two similar results was taken as the final microscopic examination result. Based on these results and labXpert autoverification results, false positive rate, false negative rate, and autoverification pass rate were calculated and the composition of false positive and negative samples was analyzed. Autoverification rules were adjusted according to the analysis results.

Statistical analysis

The experimental data were processed by internal statistical functions of Microsoft Excel 2007 and labXpert and false positive and negative rates and pass rate of 2023samples were analyzed. After rule adjustment, the above data were recounted.

A sample was determined as false positive if the instrument suggested manual review or microscopic review but microscopic examination result was negative.

A sample was determined as false negative if the instrument suggested autoverification, but microscopic examination result was positive.

A sample was determined as true positive if instrument suggested manual review or microscopic review, and microscopic examination result was positive.

A sample was determined as true negative if instrument suggested autoverification, and microscopic examination result was negative.

Consistency was the sum of the number of true positive and true negative samples.

Autoverification pass rate was calculated using the formula: the number of samples passing autoverification / total number of samples * 100%.

The single rule trigger rate which reflects the operation and triggering conditions of rules was calculated by dividing the times of being operated and triggered by the total times of being operated.

Quality control

The Mindray BC-6800 auto hematology analyzer was calibrated and verified with the matched standard calibrator; before the experiment, whole blood quality control substance was detected.

RESULTS

Validation of preliminary autoverification rules

Beijing hospital and Ruijin hospital evaluated the effectiveness of preliminary autoverification rules by detecting 999 samples and 1,024 samples, respectively. False positive rate, false negative rate, consistency and autoverification pass rate were calculated and the distribution of samples with false negative or positive results was analyzed. Tables II shows the verification statistical results of autoverification rules. False negative samples mainly included abnormal RBC morphology, neutrophilic myelocytes (1%~2%), neutrophilic metamyelocytes (2%~3%), PLT aggregation and WBC toxic granulation. WBC < 4.0×10^9/L was taken as the determination criterion for false positive samples. The results indicated blast or immature cells, abnormal lymphocyte, high or low mean corpuscular volume (MCV), PLT < 100×10^9/L and other factors [hemoglobin (HGB) increase or decrease, PLT aggregation and abnormal RBC morphology alarms].

Adjustment and verification of autoverification rules

Autoverification rules were adjusted according to the above verification results. After analysis, it was found that the false negative rates of the two hospitals were less than 2%; low myelocyte and metamylocyte values (the ratio of blasts to promyelocytes less than 3%) and abnormal RBC and PLT morphologies were mainly found in false negative samples. No false negative sample was found with increased blasts or 3% higher blastic cell proportion. As microscopic positive standards mainly included the indexes of abnormal form rather than the increase or decrease of parameter count, the abnormity of parameter count of false positive samples accounted for a high proportion. Taking clinical risks and technological level of BC-6800 into consideration, we decreased WBC

Table II. *Statistics of preliminary autoverification rules.*

	Number of samples *(Beijing Hospital)*	Proportion *(Beijing Hospital)*	Number of samples *(Ruijin Hospital)*	Proportion *(Ruijin Hospital)*
True positive	54	5.41%	112	10.94%
True negative	748	74.87%	715	69.82%
False positive	181	18.12%	179	17.48%
False negative	16	1.60%	18	1.76%
Consistency	802	80.28%	827	80.76%
Number of samples failing autoverification	235	23.52%	291	28.42%
Number of samples passing autoverification	764	76.48%	733	71.58%
Total number of samples	999	/	1024	/

from (4.0~30)×10^9/L to (3.0~30)×10^9/L), PLT from (100~1000)×10^9/L to (80~1000)×10^9/L) and MCV from 75 ~105) Fl to (70 ~110) Fl). To lower clinical risks, we added the requirement of IMG % ≤ 0.8%

After rule adjustment, the new rules were rerun on 999 samples from Beijing Hospital and 1024 samples from Ruijin Hospital. False positive and negative rates, consistency and autoverification pass rate were recorded again according to the running results (Table III). It was found that false negative rate changed little compared with rules before adjustment (within 2%) and the clinical risk was small, but the false positive rate reduced obviously and the autoverification pass rate improved significantly.

Sample verification after rule adjustment

After rule confirmation, autoverification rules were uploaded into the labXpert system and a large number of samples were selected, from March 2014 to July 2014, for verification, involving 11,790 inpatient and outpatient samples from Ruijin Hospital, 15,421 inpatient and physical examination samples from Beijing Hospital, as well as 10,860 outpatient samples, from July 2014 to February 2015, from China Armed Police General Hospital. The autoverification pass rates of the three hospital were 76.4%, 85.1% and 84.2%, respectively.

Comparison of report delivery time applying, or not, the autoverification system

TAT (10, 11) was defined differently for laboratory workers and clinicians. For laboratory workers, TAT was the duration between the sign-in of samples and report delivery, while for the clinicians, TAT describes the duration between the issuing of the request note to the acquisition of reports. This clinical test mainly counted the time from the sign-in of samples to report delivery. One thousand samples were selected from each hospital to compare the difference of traditional sample verification means and labXpert software. The results demonstrated that after the application of autoverification, the TAT of Ruijin Hospital, China Armed Police General Hospital and Beijing Hospital was reduced by 4.1 minutes, 10.2 minutes and 8.8 minutes, respectively

Table III. *Statistical data after rule adjustment.*

	Number of samples *(Beijing Hospital)*	Proportion *(Beijing Hospital)*	Number of samples *(Ruijin Hospital)*	Proportion *(Ruijin Hospital)*
True positive	53	5.31%	110	10.74%
True negative	778	77.88%	781	76.27%
False positive	151	15.12%	113	11.04%
False negative	17	1.70%	20	1.95%
Consistency	831	83.18%	891	87.01%
Number of samples failing autoverification	204	20.42%	223	21.78%

DISCUSSION

LabXpert software, a sample verification system matched with automated hematology analyzer, was developed following the idea of manual sample verification. Preliminary validation rules were established in the first place based on "41 Items of International Consensus Review Rules" and instructions for Mindray BC-6800 auto hematology analyzer, and the rules were uploaded into the labXpert sample validation system. The false negative rate was less than 2% in both hospitals, but the false positive rate was relatively high, around 18%. The preliminary rules were adjusted based on the analysis of verification results. To lower the false negative rate of immature granulocyte, the percentage of IMG was taken as a verification criterion. The ranges of WBC, MCV and PLT were adjusted accordingly; after adjustment, the false negative rate remained below 2% and the false positive rate was significantly reduced.

Many samples were collected from the three hospitals to further verify the adjusted rules. The autoverification pass rates reported by Ruiju Hospital, Beijing Hospital and China Armed Police General Hospital were 76.4%, 85.1% and 84.2%, respectively.

One study in the literature (12) advocated using autoverification to improve efficiency, shorten TAT and reduce the number of employees. Our experimental results also showed that the application of autoverification could greatly shorten TAT. In summary, the application of an autoverification system in the verification of blood routine report can improve working efficiency on the premise of guaranteeing the quality of report, but the autoverification rates of different laboratories show certain disparities due to pathogenic differences. Therefore, we suggest that hospitals formulate a set of autoverification rules conforming to laboratory characteristics taking into consideration patients' features and technological levels of the instruments used. Furthermore, the rules should be optimized to be continuously efficient and reliable for application.

REFERENCES

1. Zhao Y, Yang L, Zheng G, Cai Y. Building and evaluating the autoverification of coagulation items in the laboratory information system. Clin Lab 2014; 60(1):143-50.
2. Gómez-Rioja R, Alvarez VA, Ventura M. Current status of verification practices in clinical biochemistry in Spain. Clin Chem Lab Med 2013; 51(9):1739-46.

3. Krasowski MD, Davis SR, Drees D, Morris C, Kulhavy J. Autoverification in a core clinical chemistry laboratory at an academic medical center. J Pathol Inform 2014; 5(1):13.
4. Shih MC, Chang HM, Ni T. Peng CT. Building and validating an autoverification system in the clinical chemistry laboratory. Lab Med 2011; 42:668-73.
5. Clinical and Laboratory Standards Institute (CLSI). Autoverification of clinical laboratory test results; approved guideline. Document AUTO 10-A. Wayne, PA: CLSI; 2006.
6. Shenzhen Mindray Medical Electronics Co., Ltd. Instructions for CAL 8000 auto sample processing system.
7. Clinical and Laboratory Standards Institute (CLSI). Reference Leukocyte Differential (Proportional) and Evaluation of Instrumental Methods, Approved Standard-Second Edition. Document H20-A2. USA, 2007.
8. Barnes PW, McFadden SL, Machin SJ, Simson E. The International Consensus Group for Hematology Review: suggested criteria for action following automated CBC and WBC differential analysis. Lab Hemato 2005; 11(2):83-90.
9. Kost GJ. Table of critical limits. Med Lab Obs 2004; 36(13 Suppl):6-7.
10. Pati HP, Singh G. Turnaround Time (TAT): difference in concept for laboratory and clinician. Indian J Hematol Blood Transfus 2014; 30(2):81-84.
11. Hawkins RC. Laboratory turnaround time. Clin Biochem Rev 2007; 28(4):179-94.
12. Torke N, Boral L, Nguyen T, Perri A, Chakrin A, Stronger JH. Process improvement and operational efficiency through test result autoverification. Clin Chem 2005; 51:2406-8.

LETTER TO THE EDITOR

EFFICACY AND SAFETY OF OMALIZUMAB IN PAEDIATRIC AGE: AN UPDATE OF LITERATURE DATA

N. MATIN[1], O. TABATABAIE[1], R. FALSAPERLA[2], P. PAVONE[2], A. SERRA[3], S. COCUZZA[3], P. DI MAURO[3], L. LICCIARDELLO[3], R. LUBRANO[4] and G. VITALITI[2]

[1]Teheran University of Medical Science, Teheran, Iran; [2]General and Acute Paediatric Operative Unit, Policlinico-Vittorio-Emanuele University Hospital, University of Catania, Italy; [3]ENT Department G.F. Ingrassia,Policlinico-Vittorio Emanuele University Hospital, University of Catania, Catania, Italy; [4]Pediatric Nephrology Operative Unit, Sapienza University of Rome, Rome, Italy

Received January 15, 2016 – Accepted March 11, 2016

Immunoglobulin E (IgE) was discovered in 1966 and was found responsible for immune defense against helminths, type I hypersensitivity and allergic diseases. IgE mediates allergic responses by binding to Fc receptors (the high affinity Fc-epsilon receptor I and the low affinity Fc-epsilon receptor II or CD23) expressed on tissue mast cells and blood basophils. This binding leads to degranulation and release of pro-inflammatory mediators. Considering the pivotal role of IgE in allergic diseases, antibodies against IgE potentiate an array of new therapeutic strategies and in this regard omalizumab (rhuMAb-E25, Xolair) has been developed as a monoclonal biologic drug to block serum IgEs. Although the use of omalizumab has been studied vigorously in many adult populations with allergic diseases, there are few heterogenous studies on children. There are very few ongoing clinical trials with omalizumab exclusively on children, although some adult studies have concluded pediatric patients as a part of their studies. Nevertheless, in pediatric clinical trials omalizumab has been demonstrated to be effective and safe also in this age group. Herein, the authors present a systematic review of extensive literature data on the use of omalizumab in children and adolescents.

Omalizumab (rhuMAb-E25, Xolair) is a humanized neutralizing monoclonal anti-IgE antibody that binds to free IgE and prevents its binding to Fc-epsilon receptor (FC-eR) I on mast cells and other responsible cells and inhibiting the allergic inflammatory cascade, thus decreasing serum free IgE levels. The drug is only used in allergic asthmatic patients with total plasma IgE levels from 30 to 1500 IU/mL (European Union) or 30 to 700 IU/mL (United States) (1-3).

Herein, the authors present an update of literature data on the use of omalizumab in allergic diseases of children.

Pediatric allergic asthma

The prevalence of asthma and allergic disorders has been increasing in the past decades among children and adults (4). In 2012, 6.8 million children had asthma (5-6), therefore, new therapeutic strategies have been proposed to invert this trend. In this regard, omalizumab phase I and II clinical trials were performed, respectively, in 1996 and in 1999, but they involved only adult patients, with some extension to adolescents (11 years of age and above). Literature data on children were provided after a few years in phase III studies, which consisted

Key words: allergic diseases, paediatric age, omalizumab, IgE, asthma, safety and efficacy

Mailing address:
Dr Giovanna Vitaliti,
AOU Policlinico-OVE,
Via Plebiscito n. 628
95100 Catania, Italy
Tel.: +39 0957435254
e-mail: giovitaliti@yahoo.it

0393-974X (2016)

DISCLOSURE: ALL AUTHORS REPORT NO CONFLICTS OF INTEREST RELEVANT TO THIS ARTICLE.

of three large multicenter studies both in the United States (US) and Europe. Among them only the third study of this group was addressed to pediatric age and it was a double-blind randomized controlled trial (RCT), carried out on 334 children aged 6 to 12 years with moderate to severe allergic asthma under inhaled CS treatment, 225 of whom were administered omalizumab subcutaneously, while the other 109 received placebo. As reported in that study, the main reduction in CS dosage was 100% in the omalizumab group and 66% in the control group. 18.2% of patients in the omalizumab group had asthma attacks during the steroid reduction phase in comparison to 38.5% in the placebo group. A statistically different reduction in rescue medication utilization was observed in the omalizumab group. The study did not report any severe adverse events (7).

In 2003, an open-label extension study evaluated the long-term effects of omalizumab on children. Omalizumab was prescribed for another 24 weeks and the one-year safety data was analyzed. No serious adverse event, anaphylaxis, serum sickness or immune complex formation was reported in this study (8).

Another double-blind multicenter RCT was performed on children aged 6 to 12 years, with moderate to severe persistent allergic asthma, uncontrolled with medium or high-dose inhaled CS. Six hundred and twenty-seven patients were included in this study, 421of whom were assigned to receive omalizumab (75 to 375 mg subcutaneously every 2 to 4 weeks) and 206 received placebo. Asthma attack rates were significantly reduced in the omalizumab group compared to the placebo group, representing a 31% reduction with omalizumab use [Relative Risk: 0.69 (0.53-0.90)]. Use of CS was reduced in omalizumab patients (-4%) and increased in the placebo group (+2), which was not significant. Incidence of adverse events between the two groups was not significant and upper respiratory tract infections were the most common ones (9)Marek</author><author>Taylor, Angel Fowler</author><author>Berhane, Indrias</author><author>Vidaurre, Carlos Fernandez</author></authors></contributors><titles><title>Omalizumab for the treatment of exacerbations in children with inadequately controlled allergic (IgE-mediated.

A subgroup analysis of this study evaluated the results of the use of omalizumab in children with severe allergic asthma, who were uncontrolled despite high-dose (fluticasone ≥500μg/day) inhaled CS and a long-acting β_2 agonist (LABA) administration. Two hundred and forty-six patients with severe asthma were considered: 134 from the omalizumab group and 64 from the placebo group completed the 52-week study. The rate of asthma attacks was significantly lower in the omalizumab group (0.42 *vs* 0.63), with an RR 0.662 [95% Confidence Interval (CI): 0.441-0.995] and 34% reduction. In the adjustable steroid phase, omalizumab was associated with 63% reduction in asthma exacerbation. Among the reported adverse events, upper respiratory tract infections were the most common ones and none of them were severe, with no statistically significant difference between adverse events in patients treated with omalizumab *vs* placebo (10, 11).

Later, in 2012, another observational study on paediatric age subjects evaluated the efficacy and safety of omalizumab as add-on therapy in 104 children with severe allergic asthma in a 52-week protocol of omalizumab therapy. None of the patients had good control of asthma at the beginning of the study, 53% reached it at week 20 and 67% at week 52. The mean rate of asthma exacerbations decreased from 4.4 per patient during the year before omalizumab therapy to 1.25 after receiving omalizumab for one year, equal to 72% reduction. Daily dosage of inhaled CS was also significantly decreased. At least one adverse event was reported in 47 patients of which the most commonly reported were pain and reaction at the injection site, headache, abdominal pain and malaise (12).

Another clinical trial was completed between 2010 and 2015 on 38 Japanese children, aged between 6 and 15 years. This study was a 24-week, open-label multi-center non-randomized interventional study. Efficacy of omalizumab by pulmonary function, asthma symptom score, asthma rescue medication and quality of life questionnaire score as well as safety were among the outcomes of this study. Asthma exacerbation rates were reduced by 69% and hospitalization rates were reduced by 78.2%. Quality of life was significantly improved in this study. No severe adverse event was reported and

all patients completed the study (13).

Finally, the PROSE (Preventative Omalizumab or Step-up Therapy for Severe Fall Exacerbations) study (NCT01430403) (14), started in 2011 and completed in August 2015, was a phase IV, double-blind randomized trial designed to compare the efficacy of 4-5 months of omalizumab, inhaled corticosteroid (fluticasone) therapy boost and placebo in reducing the fall exacerbations of asthma attacks in inner-city children and adolescents with allergic persistent asthma aged 6 to 17 years. Patients were recruited from different areas of the United States, and those in the omalizumab group received subcutaneous omalizumab every 2 or 4 weeks. Inhaled fluticasone was self-administered as much to deliver 200 or 500 mcg daily. Two hundred and fifty-nine patients were allocated to the omalizumab group and 130 were allocated to receive inhaled fluticasone. Eighty-nine patients were in the placebo group. Some of the primary outcomes have been published: The occurrence of one or more asthma exacerbations was 11.3 in the omalizumab group compared to 21 in the placebo group (percent of adjusted prevalence), showing a statistically significant difference. No serious adverse event was reported in the omalizumab group, one anaphylactic reaction was seen in inhaled fluticasone group and one case of 7th nerve paralysis was reported in the placebo group (14).

Pediatric atopic dermatitis

The effects of omalizumab in atopic dermatitis in children have been analyzed in a few studies. A double-blind randomized placebo controlled trial of omalizumab (150-376 mg administered subcutaneously every 2 or 4 weeks over 24 weeks) in eight children and adolescents (between 4 and 22 years) with atopic dermatitis (AD), resulted in significant decrease in IgE. Also, omalizumab was associated with improvement in severity of symptoms, shown as SCORAD (Index for severity scoring of AD) reduction of 45-80 % (15). One observational study in patients aged 6 to 19 years (5 children and 2 adolescents) with severe AD (high SCORAD), high serum IgE levels, reported a significant reduction of SCORAD index from 75.4 to 30 after 12 months of treatment with omalizumab (administered 225 mg to 375 mg every other week) (16).

Pediatric allergic rhinitis

The only randomized placebo-controlled double-blind trial on children (between 6-17 years of age) with allergic rhinitis was carried out in Germany. Two hundred and twenty-five patients with at least 2-year history of birch pollen–induced and grass pollen–induced seasonal AR were enrolled. All patients received specific immunotherapy (SIT) and were randomized to receive omalizumab or placebo at 2 to 4 week intervals. In both the birch and grass groups, median symptom load (sum of the mean daily symptom severity score reported by patients plus the mean daily rescue medication score) was significantly reduced (48%) by omalizumab from 0.82 to 0.43 and 0.6 to 0.31, respectively. Overall, omalizumab was associated with 50% reduction in symptom load. Median rescue medication score was reduced by 78% and 81% in SIT-birch group and SIT-grass group, respectively. No serious adverse events and no anaphylaxis were observed. Adverse events occurred in 25% of omalizumab-receiving group compared to 16% in the control group. Two cases of moderate urticaria were reported but were not related to omalizumab (17, 18).

Some other studies included pediatric and adolescent (over 12 years of age) patients among adult patients, but did not report exclusive data from use in children (19-22).

Pediatric chronic urticaria

There are no literature data on omalizumab use in chronic urticaria (CU) in pediatric age. The only phase II and III clinical trials were carried out on patients over 12 years of age, with promising results in terms of efficacy of the drug (23-25). To our knowledge, the only literature data published to date on pediatric age is a one case-series evaluating the use of omalizumab for three to 11 months on children with CU, showing a complete remission in the 4 studied patients (patients aged 4, 5, 10, 16 years, respectively) (26).

Pediatric food allergy

Omalizumab was first studied in children with

food allergy in combination with SIT in a pilot phase I study. Eleven children between 7 and 17 years of age with cow's milk allergy were included. Their immune reactions ranged from urticaria and nausea vomiting to anaphylaxis with total serum IgE levels of 148 to 2593 kilounits of antibody per liter. After nine weeks of omalizumab treatment (every 2 to 4 weeks, administered based on IgE levels), daily oral cow's milk desensitization was performed. Omalizumab was discontinued at week 16. Also, a double-blind, placebo-controlled food challenge (DBPCFC) was performed at week 24 of the study. One patient discontinued the study on the first day of desensitization due to abdominal migraine, and another patient discontinued the treatment due to allergic reactions. Nine of eleven patients tolerated desensitization to a dosage of 2000 mg/day in a period of 7 to 11 weeks. Also they began tolerating the normal amounts of milk in their diet (8000mg/day and more). The tenth delayed patient, reached a dose of 1000 mg/day bythe 7^{th} week of desensitization (27, 28). Another team performed a similar study on peanut allergic patients. In this study, 13 children were enrolled, with a median peanut-specific IgE level of 229 kU(A)/L and a median total serum IgE level of 621 kU/L who had failed DBPCFC at peanut flour doses of 100 mg or less. Omalizumab was started for patients, and at week 12 oral desensitization was started in eleven doses (rush) for the first day (cumulative dose equal to two peanuts). The dosage was increased until week 20 to a dose of 4000 mg peanut flour. Then omalizumab was discontinued. All 12 subjects successfully tolerated the amount of 8000 mg per day (equal to 20 peanuts) (29). Use of omalizumab was also successful in two cases of eosinophilic esophagitis: in an 18-year-old girl with history of severe atopic dermatitis, asthma and multiple food allergies. and a 9-year-old with limitation of daily activities and a history of Hirschprung's disease (30).

Other trials have been performed on the use of omalizumab in food allergy, but they included almost adult patients, with poor recruitment of children under 12 years of age, suggesting the lack of clinical trials in pediatric age.

CONCLUSIONS

Although the use of omalizumab has been studied vigorously in many adult populations with allergic diseases, there are few heterogenous studies on children. There are very few ongoing clinical trials with omalizumab exclusively in children, although some adult studies have included pediatric patients as a part of their studies. Also, among the few studies on children, different primary or secondary outcomes have been studied. This leads to the uncertain conclusions regarding the efficacy and safety of omalizumab in allergic disorders in children, highlighting the need of studies with a unique protocol performed simultaneously in connected pediatric research centers, also considering the easy manageability of the drug in pediatric age in those studies published to date.

REFERENCES

1. Pelaia G, Gallelli L, Renda T, et al. Update on optimal use of omalizumab in management of asthma. J Asthma Allergy 2011; 4:49.
2. Administration. FaD. Available from: http://www.accessdata.fda.gov/drugsatfda_docs/label/2014/103976s5211lbl.pdf
3. Information EMAEOXfp, (EU). 2007. Available from: http://www.ema.europa.eu/ema/index.jsp?curl=pages/medicines/human/medicines/000606/human_med_001162.jsp&mid=WC0b01ac058001d124. 6 Aug 2013.
4. Geneva WHO. Asthma 2006 (Fact sheet No. 307). Available from: http://www.who.int/mediacentre/factsheets/fs307/en/index.html.
5. Akinbami LJ, Bailey C, Zahran HS, King M, Johnson CA, Liu X. Trends in asthma prevalence, health care use, and mortality in the United States, 2001 2010-2012. Available from: http://www.cdc.gov/nchs/data/databriefs/db94.htm#x2013;2010%3C/a%3E.
6. Engelkes M, Janssens HM, de Ridder MA, de Jongste JC, Sturkenboom MC, Verhamme KM. Time trends in the incidence, prevalence and age at diagnosis of asthma in children. Pediatr Allergy Immunol 2015; 26:367-74.
7. Milgrom H, Berger W, Nayak A, Gupta N, Pollard

S, McAlary M, Taylor AF, Rohane P. Treatment of childhood asthma with anti-immunoglobulin E antibody (omalizumab). Pediatrics 2001; 108:e36-e.
8. Berger W, Gupta N, McAlary M, Fowler-Taylor A. Evaluation of long-term safety of the anti-IgE antibody, omalizumab, in children with allergic asthma. Ann Allergy Asthma Immunol 2003; 91(2):182-88.
9. Lanier B, Bridges T, Kulus M, Taylor AF, Berhane I, Vidaurre CF. Omalizumab for the treatment of exacerbations in children with inadequately controlled allergic (IgE-mediated) asthma. J Allergy Clin Immunol 2009; 124:1210-16.
10. Kulus M, Hebert J, Garcia E, Fowler Taylor A, Fernandez Vidaurre C, Blogg M. Omalizumab in children with inadequately controlled severe allergic (IgE-mediated) asthma. Curr Med Res Opin 2010; 26:1285-93.
11. Milgrom H, Fowler-Taylor A, Vidaurre CF, Jayawardene S. Safety and tolerability of omalizumab in children with allergic (IgE-mediated) asthma. Curr Med Res Opin 2010; 27:163-69.
12. Deschildre A, Marguet C, Salleron J, et al. Add-on omalizumab in children with severe allergic asthma: a 1-year real life survey. Eur Respir J 2013; 42:1224-33.
13. Odajima H, Ebisawa M, Nagakura T, et al. Omalizumab in Japanese children with severe allergic asthma uncontrolled with standard therapy. Allergol Int 2015; 64:364-70.
14. Limb SL, Starke PR, Lee CE, Chowdhury BA. Delayed onset and protracted progression of anaphylaxis after omalizumab administration in patients with asthma. J Allergy Clin Immunol 2007; 120:1378-81.
15. Iyengar SR, Hoyte EG, Loza A, Bonaccorso S, Chiang D, Umetsu DT, Nadeau KC. Immunologic effects of omalizumab in children with severe refractory atopic dermatitis: a randomized, placebo-controlled clinical trial. Int Arch Allergy Immunol 2013; 162:89-93.
16. Barrios JL, Bégin P, Paradis L, Hatami A, Paradis J, Des Roches A. Anti-IgE therapy and severe atopic dermatitis: a pediatric perspective. J Am Acad Dermatol 2013; 69:832-4.
17. Kuehr J, Brauburger J, Zielen S, et al. Efficacy of combination treatment with anti-IgE plus specific immunotherapy in polysensitized children and adolescents with seasonal allergic rhinitis. J Allergy Clin Immunol 2002; 109:274-80.
18. Rocklin Werninghaus C, Hamelmann E, Keil T, et al. The co-seasonal application of anti IgE after preseasonal specific immunotherapy decreases ocular and nasal symptom scores and rescue medication use in grass pollen allergic children. Allergy 2004; 59:973-9.
19. Casale TB, Condemi J, LaForce C, et al. Effect of omalizumab on symptoms of seasonal allergic rhinitis: a randomized controlled trial. JAMA 2001; 286:2956-67.
20. Chervinsky P, Casale T, Townley R, Tripathy I, Hedgecock S, Fowler-Taylor A, Shen H, Fox H. Omalizumab, an anti-IgE antibody, in the treatment of adults and adolescents with perennial allergic rhinitis. Ann Allergy Asthma Immunol 2003; 91:160-67.
21. Vignola A, Humbert M, Bousquet J, Boulet LP, Hedgecock S, Blogg M, Fox H, Surrey K. Efficacy and tolerability of anti immunoglobulin E therapy with omalizumab in patients with concomitant allergic asthma and persistent allergic rhinitis: SOLAR. Allergy 2004; 59:709-17.
22. Kopp M, Hamelmann E, Zielen S, et al; DUAL study group. Combination of omalizumab and specific immunotherapy is superior to immunotherapy in patients with seasonal allergic rhinoconjunctivitis and co-morbid seasonal allergic asthma. Clin Exp Allergy 2009; 39:271-79.
23. Bernstein JA, Saini SS, Maurer M, et al. Efficacy of omalizumab in patients with chronic idiopathic/spontaneous urticaria with different background therapy: post hoc analysis of Asteria I, Asteria II, and Glacial studies. J Allergy Clin Immunol 2014; 2:AB117.
24. Saini SS, Bindslev-Jensen C, Maurer M, et al. Efficacy and safety of omalizumab in patients with chronic idiopathic/spontaneous urticaria who remain symptomatic on H1 antihistamines: a randomized, placebo-controlled study. J Invest Dermatol 2015; 135:925.
25. Kaplan A, Ledford D, Ashby M, et al. Omalizumab in patients with symptomatic chronic idiopathic/spontaneous urticaria despite standard combination therapy. J Allergy Clin Immunol 2013; 132:101-9.
26. Netchiporouk E, Nguyen CH, Thuraisingham T, Jafarian F, Maurer M, Ben-Shoshan M. Management of pediatric chronic spontaneous and physical urti-

caria patients with omalizumab: case series. Pediatr Allergy Immunol 2015; 26:585-88.
27. Nadeau KC, Schneider LC, Hoyte L, Borras I, Umetsu DT. Rapid oral desensitization in combination with omalizumab therapy in patients with cow's milk allergy. J Allergy Clin Immunol 2011; 127:1622-24.
28. Vitaliti G, Pavone P, Guglielmo F, Falsaperla R. Sublingual immunotherapy in preschool children: an update. Expert Rev Clin Immunol 2013; 9:385-90.
29. Schneider LC, Rachid R, LeBovidge J, Blood E, Mittal M, Umetsu DT. A pilot study of omalizumab to facilitate rapid oral desensitization in high-risk peanut-allergic patients. J Allergy Clin Immunol 2013; 132:1368-74.
30. Rocha R, Vitor AB, Trindade E, Lima R, Tavares M, Lopes J, Dias JA. Omalizumab in the treatment of eosinophilic esophagitis and food allergy. Eur J Pediatr 2011; 170:1471-74.

LETTER TO THE EDITOR

PNEUMOMEDIASTINUM, SUBCUTANEOUS EMPHYSEMA AND PNEUMORRHACHIS IN ASTHMATIC CHILDREN

L. COLAVITA[1], C. CUPPARI[1], M.R. PIZZINO[1], M. STURIALE[1], B. MONDELLO[2], F. MONACO[2], M. BARONE[2] and C. SALPIETRO[1]

[1]Department of Genetics and Paediatric Immunology, University Hospital of Messina, Messina, Italy; [2]Unit of Thoracic Surgery, Department of Cardiovascular and Thoracic Sciences, University Hospital of Messina, Messina, Italy

Received December 14, 2015 – Accepted March 8, 2016

Pneumomediastinum (PM), subcutaneous emphysema (SE) and pneumorrhachis (also known as epidural air (EDA) or epidural emphysema) are very rare findings in children. PM is defined as the passage of air from intra-alveolar space to interstitium and, later, to the mediastinum. From the mediastinum, the air may catch up subcutaneous tissue (usually of the neck) and/or epidural space via the cervical fascial planes and neural foramina, forming respectively SE and EDA. The PM can be divided in spontaneous (or idiopathic) and secondary PM. Only few studies have evaluated the exact incidence of PM and its complications in children, and to define the correct diagnostic work up, treatment and outpatient follow-up. We report the case of a 9-year-old child with undiagnosed asthma that, during severe asthmatic flare secondary to acute infection of high airway, developed PM, SE and EDA.

Pneumomediastinum (PM), subcutaneous emphysema (SE) and pneumorrhachis (also known as epidural air (EDA) or epidural emphysema) are pathological very rare conditions in pediatric medicine and are characterized by inappropriate presence of free air in mediastinum, subcutaneous tissue and intraspinal space, respectively (1- 3). We report the case of a 9-year-old child with undiagnosed asthma which, during severe asthmatic flare secondary to acute infection of high airway, developed PM, SE and EDA.

A 9-year-old boy with attention deficit hyperactivity disorder after a few days of flu symptoms was admitted to the Pediatric Intensive Care unit for the appearance of thoracic pain, dyspnea, Chest X-ray (LL) (Fig. 1) evidence of SE and chest Computed Tomographic (CT) evidence of massive PM, EDA of the thoracis spine and SE (Fig. 2). Upon physical examination, diffuse crepitus was palpable at the base of the neck, and chest examination revealed bronchospasm. Diagnostic laboratory work-up showed elevation of white blood cell count (57% neutrophils) and of C-Reactive-Protein (2.4 mg/dl; normal values < 0.5 mg/dl). Intravenous antibiotic (ceftriaxone) and dexamethasone treatment were performed and associated with short-acting bronchodilator therapy (salbutamolo). For the improvement of his respiratory function and of radiologic imagines, he was admitted to our Inpatient Pediatric ward. Viral

Key words: pneumomediastinum, subcutaneous emphysema, pneumorrhachis, asthma, children

Mailing address:
Laura Colavita, MD
Department of Pediatric Sciences,
Unit of Genetics and Paediatric Immunology
University of Messina, University Hospital "Gaetano Martino",
Via Consolare Valeria 1, 98125 Messina, Italy
e-mail: lauracol85@gmail.com

0393-974X (2016)

(influenza A and B, parainfluenza, adenovirus) and some bacterial (*Mycoplasma* and *Chlamydia pneumoniae*) pathogens were ruled out. An in-depth medical history revealed exertional dyspnea. At further blood tests, total Immunoglobulins (Ig) E resulted very high (2651 UI/ml) and the specific IgE evaluation showed increased values of sIgE for dust mites (>100 KU/l). Because of these laboratory findings, the history of exertional dyspnea and the severe bronchospasm that characterized his recent chest objectivity, the child started asthma therapy with low-dose inhaled corticosteroid (budesonide; 400 mcg/day). After 2 months, a new chest X-ray and a spirometry were both normal.

Written informed consent for publication of clinical details was obtained from the patient's parent. A copy of the consent form is available.

DISCUSSION

PM is an uncommon finding in children, potentially life-threatening. It is commonly characterized by centrothoracic pain; dyspnea, SE and sometimes cough. Hamman's sign is a crunching sound synchronous with the heartbeat, in the precordial. It is pathognomonic of PM, consequence of heart beating against air-filled tissues, but not always found. Chest X-ray is the main diagnostic examination and shows the typical hyperclarity that surrounds the mediastinum outline (1-5).

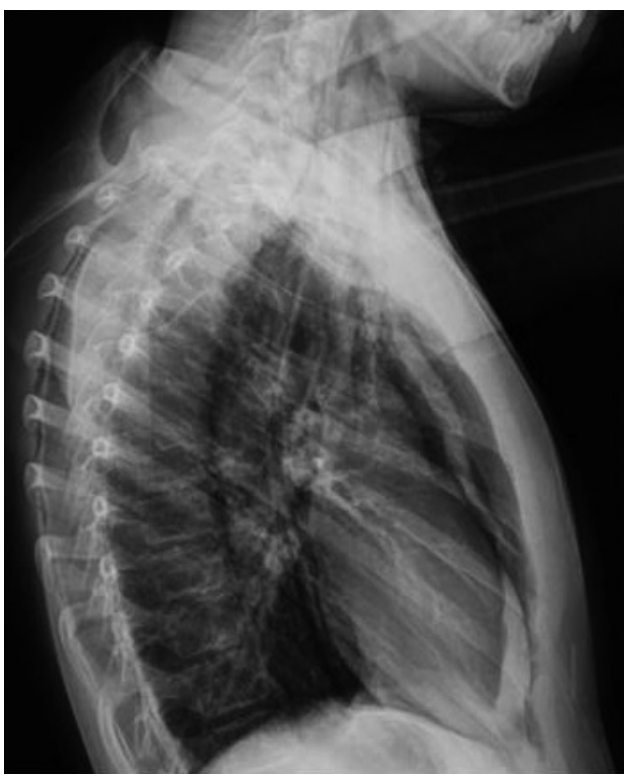

Fig. 1. *Chest X-ray (LL) demonstrating subcutaneous emphysema involving the cervical region and the retrosternal space.*

According to etiology, the PM can be divided into spontaneous and secondary PM. Spontaneous PM is more frequent in male adolescents (mostly with asthenic somatic type), without recognized causes. Secondary PM is caused by traumatic events, mechanical ventilation, endoscopic procedures, strong Valsalva manoeuvre, rupture of a hollow viscus or of spontaneous pneumothorax, gas-forming bacterial infection, diseases characterized by increased intra-alveolar pressure such as asthma or respiratory tract infections with bronchospasm (2, 3, 6). Only a few studies have been carried out to understand the exact incidence of PM and its complications in children, and to define the right diagnostic work up, treatment and outpatient follow-up. Freixinet et al. examined 32 adult patients: only 9 cases (28.1%) had a history of asthma (5). In another study, the estimated incidence in China of PM in pediatric patients was of 1:8.302 and the commonest cause was infection (8/18, 44.4%). Only 2 patients (11.1%) developed asthma later (7). A recent study reports a PM incidence of around 1 in 20,000 patients who arrive at the emergency ward with an asthma attack (4).

Some authors conclude that children with idiopathic PM should perform spirometry during their follow-up, to evaluate whether the patient has asthma and to reduce the risk of recurrence of PM. The exact time rate of spirometry is not well defined but the authors suggest that pulmonary function tests should be performed after acute episodes (8).

While SE is a common PM-related condition, EDA is very rare, without exact data on its incidence. In a study on 42 pediatric patients, only 4 patients had CT evidence of EDA. The commonest causes are traumatic events. Non-traumatic intraspinal air is described in various diseases, such as epidural

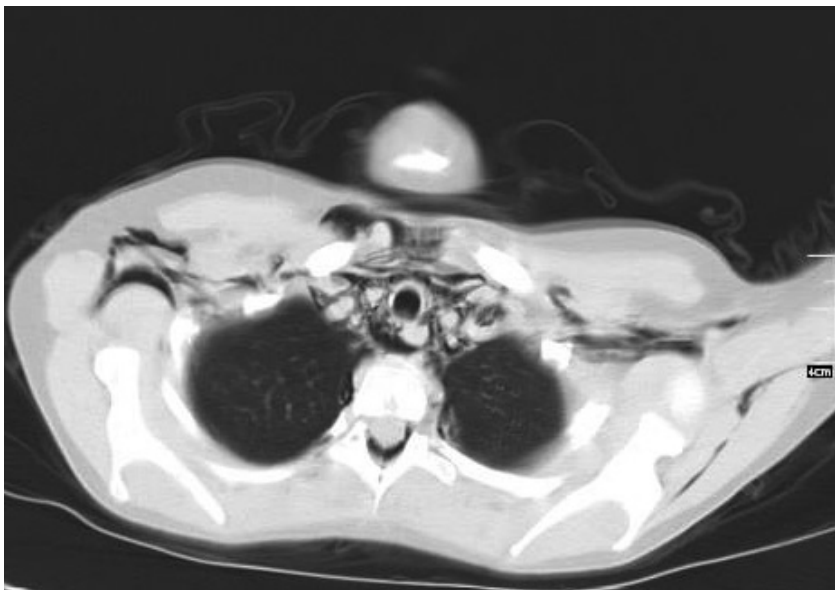

Fig. 2. *CT scan of the chest demonstrating air in the mediastinum, epidural space and subcutaneous tissue.*

abscess, anorexia nervosa, Crohn's disease, intestinal necrosis, intraspinal synovial cysts, disc herniation or degeneration, emphysematous pyelonephritis, pneumocephalus, pneumothorax and PM. EDA is the only type of pneumorrhachis in non-trauma patients. The low incidence of EDA, despite the higher incidence of PM, may be a consequence of the difficulty to see it using only chest X-ray (the gold-standard is chest CT). However, EDA can be visible also in chest X-ray but the spinal canal is not usually carefully studied in patients without neurological symptoms. In most of the literature, no significant neurological signs are associated with EDA but some authors report this possibility (9, 10). The problem of whether or not CT scanning should be performed routinely in neurologically asymptomatic patients with chest X-ray evidence of spontaneous PM to individuate EDA has not yet been resolved (9).

PM, SE and EDA usually disappear spontaneously or by treating only the underlying disease (in our case, asthma). A conservative management is usually recommended for the good prognosis with frequent spontaneous resolutions and the high risk of infection associated with surgical invasive treatments (1, 3, 4, 9-11).

With regard to the outpatients follow-up, we agree with some authors (8) for the need to investigate children with idiopathic PM with repeated pulmonary function tests (spirometry). The time rate of control spirometry in the follow-up of patients who have PM, with or without EDA, is not yet well defined. However, we believe that it would be advisable to perform a pulmonary function test every three months at first, and then based on the clinical trend and the results of the previous spirometry. The aim is to exclude asthma that sometimes (as in our case) can be a disease already present previously but never recognized, diagnosed and then treated. The initiation of adequate asthma therapy and regular clinical and spirometric checks may reduce the risk of recurrence of PM in asthmatic patients.

REFERENCES

1. Mondello B, Pavia R, Ruggeri P, Barone M, Barresi P, Monaco M. Spontaneous pneumomediastinum: experience in 18 adult patients. Lung 2007; 185(1):9-14.
2. Caceres M, Ali SZ, Braud R, Weiman D, Garrett HE Jr. Spontaneous pneumomediastinum: a comparative study and review of the literature. Ann Thorac Surg 2008; 86(3):962-66.

3. Chen IC, Tseng CM, Hsu JH, Wu JR, Dai ZK. Spontaneous pneumomediastinum in adolescents and children. Kaohsiung J Med Sci 2010; 26(2):84-88.
4. Giuliani S, Franklin A, Pierce J, Ford H, Grikscheit TC. Massive subcutaneous emphysema, pneumomediastinum, and pneumopericardium in children. J Pediatr Surg. 2010;45(3):647-9.
5. Freixinet J, García F, Rodríguez PM, Santana NB, Quintero CO, Hussein M. Spontaneous pneumomediastinum long-term follow-up. Respir Med 2005; 99(9):1160-63.
6. Mondello B, Barone M, Barresi P, Familiari D, Micali V, Nunnari F, Monici D, Monaco M. Etiology, pathophysiology and management of post-traumatic pneumomediastinum: our experience. G Chir 2009; 30(8-9):3656-8.
7. Lee CY, Wu CC, Lin CY. Etiologies of spontaneous pneumomediastinum in children of different ages. Pediatr Neonatol 2009; 50(5):190-95.
8. Chiu CY, Wong KS, Yao TC, Huang JL. Asthmatic versus non-asthmatic spontaneous pneumomediastinum in children. Asian Pac J Allergy Immunol. 2005; 23(1):19-22.
9. Kono T, Kuwashima S, Fujioka M, Kobayashi C, Koike K, Tsuchida M, Seki I. Epidural air associated with spontaneous pneumomediastinum in children: uncommon complication? Pediatr Int 2007; 49(6):923-27.
10. Karaoglan A, Cal MA, Orki A, Arpaozu BM, Colak A. Pneumorrhachis associated with bronchial asthma, subcutaneous emphysema and pneumomediastinum. Turk Neurosurg 2011; 21(4):666-68.
11. Mahajan PS, Al Maslamani NJ, Purayil NK. Rare case of pneumorrhachis, pneumomediastinum, pneumothorax, and surgical emphysema secondary to bronchial asthma. Int Med Case Rep J 2014; 6(7):35-39.

LETTER TO THE EDITOR

AN UNUSUAL CASE OF MAMMARY PAGET'S DISEASE IN A WOMAN WITH PSORIASIS

C. ALESSIO[1], E. SCALI[2], F. MANTI[1], G.F. AMORUSO[2], S. MARCHESE[1], B. RIGA[1], U. BOTTONI[2] and O. TAMBURRINI[1]

[1]Department of Experimental and Clinical Medicine-Radiology, University Magna Græcia, Catanzaro, Italy; [2]Department of Health Sciences, Operative Unit of Dermatology, University Magna Græcia, Catanzaro, Italy

Received September 24, 2015 – Accepted March 16, 2016

Mammary Paget's disease (MPD) is a malignant breast tumor, which is characterized by intraepidermal infiltration from malignant glandular epithelial cells. Often it may include an underlying ductal carcinoma in situ or an invasive ductal carcinoma. Clinically it appears as an erythematous patch, moist or crusted, with or without desquamation that in some cases becomes ulcerated, causing infiltration and inversion of the nipple. We report the clinical case of a 60-year-old woman, treated in our department for psoriasis, presenting with erythema of nipple and areola with nipple erosion, ulceration and poor secretion. Suspecting Paget's disease of the nipple, radiological exams (mammography and breast MRI) were performed. A biopsy for histological examination was carried out and confirmed the diagnosis of mammary Paget's disease. MPD is sometimes difficult to diagnose both clinically and radiologically, therefore it is important to distinguish from other conditions: in literature MPD is reported in differential diagnosis with psoriasis given its similar clinical features, and in some cases MPD has been treated with topical and systemic steroids due to a wrong diagnosis. However, the concomitance, in the same individual, of mammary Paget's disease and psoriasis has never been described.

The prevalence of psoriasis is high in the general Italian population, evaluated at approximately 1.5–1.8 million people (1); these data are of considerable importance as psoriasis is commonly a lifetime disorder. Many studies have shown that psoriasis is positively associated with increased risk of lymphoma and non-melanoma skin cancer (2). Some studies also investigated the association between psoriasis and solid organ cancers, but few studies have reported positive associations with lung, colorectal, breast and pancreas cancers. In the study of Prizment et al. the solid tumor that was found most associated with psoriasis was colorectal cancer. In that study the authors did not find any significant association between breast cancer and psoriasis. They found fewer patients with psoriasis and breast cancer and none of them had Paget's disease (3). Recently, we had the opportunity to study a psoriatic patient with Paget's disease. To the best of our knowledge in the literature no association between psoriasis and Paget's disease has been reported to date.

Case report

A 60-year-old woman, treated in the University

Key words: mammary Paget's disease, psoriasis, breast neoplasm, breast MRI

Mailing address:
Dr Caterina Alessio,
Department of Experimental and Clinical Medicine-Radiology,
University Magna Græcia, Viale Europa,
88100 Catanzaro, Italy
Tel.: +39 3202756231 - Fax: +39 09613647395
e-mail: alessio.caterina@libero.it

0393-974X (2016)

DISCLOSURE: ALL AUTHORS REPORT NO CONFLICTS OF INTEREST RELEVANT TO THIS ARTICLE.

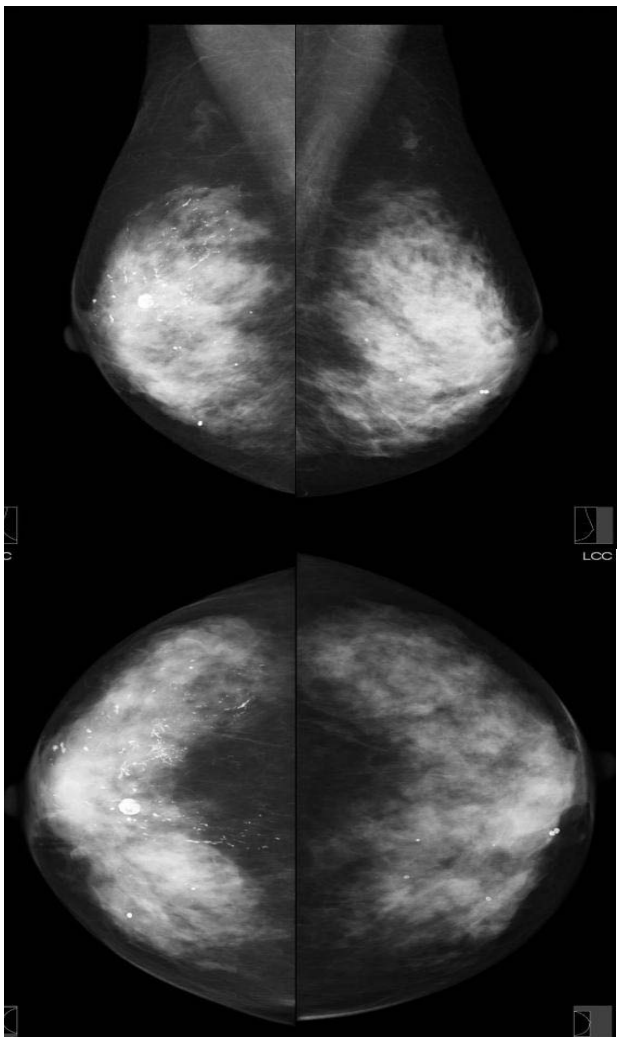

Fig. 1. *Mediolateral oblique and cranial-caudal mammograms show segmentally distributed fine polymorphic microcalcifications in the upper outer right breast.*

Magna Græcia, Catanzaro, Italy, for widespread psoriasis, presented eczema and itching of the right nipple which had appeared two months previously. The lesion was characterized by erythema with nipple erosion, ulceration and poor secretion. No palpable mass of the breast and no sign of any palpable swelling in the lymph nodes of the axilla or supraclavicular region were evident.

Right mammograms showed pleomorphic and branched microcalcifications in the upper outer right breast (Fig. 1) that were not present at the previous control. In addition, to evaluate the extent of disease, she underwent a breast MRI which showed differences and asymmetries in the characteristics of the nipple-areolar complex, in particular an abnormal right nipple enhancement (Fig. 2), with no other abnormalities in mammary glands.

Biopsy was then carried out on tissue of the right nipple. The histopathology showed epidermal cells with hyperchromatic and polymorphic nuclei, intraepithelial gland cells (Fig. 3) and a high expression of cytokeratin 7 so-called Paget's cells (Fig. 4). Cytokeratin 7 is a typical marker for glandular and transitional epithelia.

These results confirmed a diagnosis of Paget's disease of the nipple, and the patient was therefore scheduled for mastectomy and sentinel node biopsy. No complications occurred during or after surgery and she recovered well post-operatively. Histopathological diagnosis of the specimen was Paget's disease of the breast with no evidence of underlying invasive ductal carcinoma, DCIS of the breast tissue or lymph node invasion. Immunohistochemical staining showed a negative expression of estrogen and progesterone receptors. Ten months after surgery the patient was disease-free.

DISCUSSION

Paget's disease of the breast is uncommon, accounting for approximately 1–3% of all cases of breast carcinoma (4). It was described by James Paget in 1874 as a chronic eczematous or psoriasiform skin eruption on the nipple and areola associated with underlying breast carcinoma (5). The disease can be associated with either no underlying carcinoma, ductal carcinoma *in situ* (DCIS), or infiltrating ductal carcinoma. Recognition of the cutaneous finding is critical to early diagnosis and treatment of the underlying carcinoma.

The diagnosis of Paget's disease is often delayed for months because of its mistaken diagnosis for other dermatologic diseases involving the nipple. Both benign and malignant processes may produce visible changes in the skin of the nipple: eczema, allergic contact dermatitis, irritant dermatitis, lichen simplex chronicus, squamous cell carcinoma *in situ* (Bowen's disease), melanoma or psoriasis (6, 7).

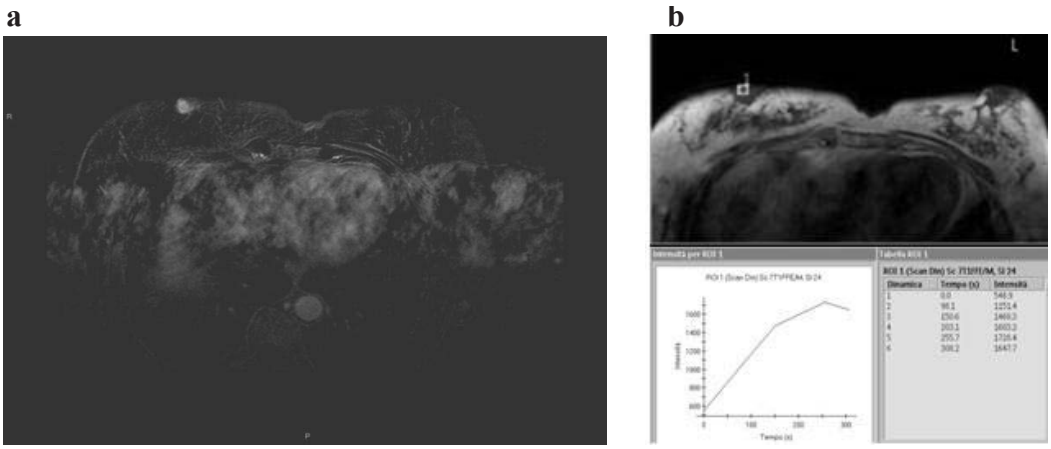

Fig. 2. ***a****) Axial contrast-enhanced fat-suppressed subtraction T1-weighted MR images show asymmetric nodular enhancement in the right nipple.* ***b****) The time-signal intensity curve appears slow and progressive.*

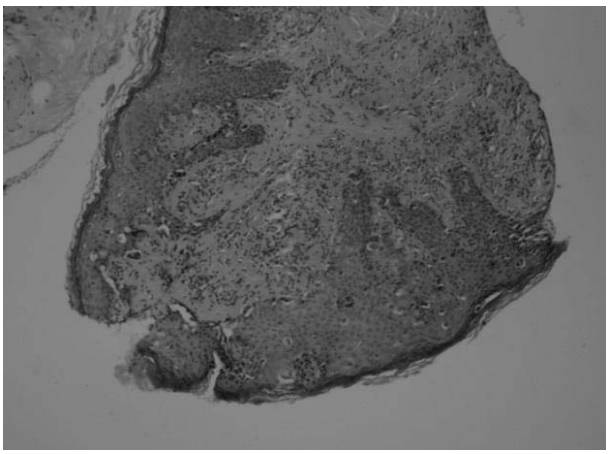

Fig. 3. *Histological mowing shows nests and groups of large, rounded, "acantholytic"* cells *predominantly involving the lower layers of the epidermis. Epidermis may be eroded and hyperplastic.*

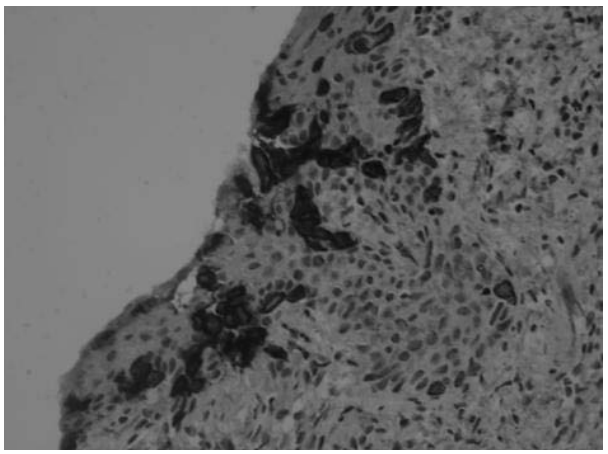

Fig. 4. *Histological mowing shows overexpression with low molecular weight cytokeratins (CKs), such as cytokeratin 7 (CK7). Immunohistochemical stain for CK7 highlights epithelial infiltration with Paget's disease cells.*

Psoriasis is a chronic, immune-mediated inflammatory skin disease. It may progressively worsen with age, or wax and wane in its severity; the degree of severity depends on inheritance and environmental factors (8). Clinical manifestations include few scattered red, scaly plaques up to most aggressive forms characterized by involvement of almost the entire body surface.

When psoriasis is localized to the thoracic region and involves the nipple and the breast area it is important to distinguish it from other dermatological diseases that can mimic this condition, such as mammary Paget's disease. In literature a case was reported of extramammary Paget's disease in the lateral part of the breast of a woman with known psoriasis treated incorrectly as psoriasis (9), but to date no case of association of nipple Paget's disease and psoriasis has been documented. We therefore describe the first case of a woman affected by psoriasis who had a concomitant nipple Paget's disease that was investigated by radiologic exams in order to evaluate the features and extent of the pathology.

Dermoscopy was not performed as, to our knowledge, it does not make a significant contribution to differential diagnosis between mammary Paget's disease and psoriasis.

A radiologic evaluation of the breast to detect an underlying malignancy should be performed (10) when mammary Paget's disease is suspected. Imaging evaluation of the breasts with at least mammography should preferably be performed before biopsy, with follow-up US and possibly MR imaging added in some cases even before performance of surgical biopsy (11, 12).

In this specific case, breast MRI excluded the presence of an underlying cancer, highlighting the exclusive interest of the nipple-areola complex which was later confirmed by histological examination. MRI, in fact, as known from the literature (13), has higher sensitivity than mammography in identifying the extent of the disease. MR imaging is useful in detecting both the involvement of the skin in Paget's disease and the underlying index cancer, and has proved to be more sensitive than other forms of imaging (14, 15).

REFERENCES

1. Colombo G, Altomare G, Peris K, et al. Moderate and severe plaque psoriasis: cost-of-illness study in Italy. Ther Clin Risk Manag 2008; 4(2):559-68.
2. Lee MS, Lin RY, Chang YT, Lai MS. The risk of developing non-melanoma skin cancer, lymphoma and melanoma in patients with psoriasis in Taiwan: a 10-year, population-based cohort study. Int J Dermatol 2012; 51(12):1454-60.
3. Prizment AE, Alonso A, Folsom AR, Ahmed RL, Virnig BA, Warshaw EM, Anderson KE. Association between psoriasis and incident cancer: the Iowa's Women's Health Study. Cancer Causes Control 2011; 22(7):1003-10.
4. Burke ET, Braeuning MP, McLelland R, Pisano ED and Cooper LL. Paget disease of the breast: a pictorial essay. Radiographics 1998; 18(6):1459-64.
5. Paget J. On disease of the mammary areola preceding cancer of the mammary gland. St Bartholomews Hosp Rep 1874; 10:87-89.
6. Nicholson BT, Harvey JA, Cohen MA. Nipple-areolar complex: normal anatomy and benign and malignant processes. Radiographics 2009; 29(2):509-23.
7. Geffroy D, Doutriaux-Dumoulins I, Labbe-Devilliers C, Meingan P, Houdebine S, Sagan C, Dejode M, Ricaud-Couprie M. Paget's disease of the nipple and differential diagnosis. J Radiol 2011; 92(10):889-98.
8. Parisi R, Symmons DP, Griffiths CE, Ashcroft DM. Identification and Management of Psoriasis and Associated Comorbidity (IMPACT) project team. Global epidemiology of psoriasis: a systematic review of incidence and prevalence. J Invest Dermatol 2013; 133(2):377-85.
9. Friis ML, Johansen T, Dahland E, Ejstrud P. Extramammary Paget's disease interpreted as psoriasis. Ugeskr Laeger 1999; 161(9):1276-7.
10. Günhan-Bilgen I, Oktay A. Paget's disease of the breast: clinical, mammographic, sonographic and pathologic findings in 52 cases. Eur J Radiol 2006; 60(2):256-63.
11. Ikeda DM, Helvie MA, Frank TS, Chapel KL, Andersson IT. Paget disease of the nipple: radiologic-pathologic correlation. Radiology 1993; 189(1):89-94.
12. Friedman EP, Hall-Craggs MA, Mumtaz H, Schneidau A. Breast MR and the appearance of the normal and abnormal nipple. Clin Radiol 1997; 52(11):854-61.
13. Lim HS, Jeong SJ, Lee JS, Park MH, Kim JW, Shin SS, Park JG, Kang HK. Paget disease of the breast: mammographic, US, and MR imaging findings with pathologic correlation. Radiographics 2011; 31(7):1973-87.
14. Kalli S, Freer PE, Rafferty EA. Lesions of the skin and superficial tissue at breast MR imaging. Radiographics 2010; 30(7):1891-913.
15. Frei KA, Bonel HM, Pelte MF, Hylton NM, Kinkel K. Paget disease of the breast: findings at magnetic resonance imaging and histopathologic correlation. Invest Radiol 2005; 40(6):363-67.

LETTER TO THE EDITOR

EFFICACY AND TOLERABILITY OF A COMBINED LIPID-LOWERING NUTRACEUTICAL ON CHOLESTEROLEMIA, hs-CRP LEVEL AND ENDOTHELIAL FUNCTION IN MODERATELY HYPERCHOLESTEROLEMIC SUBJECTS

A.F. CICERO, A. COLLETTI, M. ROSTICCI, E. GRANDI and C. BORGHI

Medical and Surgical Sciences Department, University of Bologna, Bologna, Italy

Received December 12, 2015 – Accepted March 7, 2016

Our aim was to test, by a double-blind, placebo-controlled randomized clinical trial, whether a short-term treatment with a combined lipid-lowering nutraceutical could improve endothelial function in a cohort of moderately hypercholesterolemic subjects. Thus, 80 healthy, moderately hypercholesterolemic subjects were consecutively enrolled and, after 4 weeks of stabilization diet, they were randomized to either the tested lipid-lowering nutraceutical or placebo for 8 weeks. At the beginning and end of treatment a complete lipid pattern, safety parameters, hs-CRP and endothelial function were measured. When compared to placebo, during nutraceutical treatment patients experienced a more favorable percentage change in total cholesterol (TC vs baseline: -17.9%; TC vs placebo: -5.6%), LDL-cholesterol (LDL-C vs baseline: -23.3%; LDL-C vs placebo: -2.8%), hs-CRP (hs-CRP vs baseline: -2.4%; hs-CRP vs placebo: -1.5%), and endothelial function (pulse volume displacement vs baseline: +17%; pulse volume displacement vs placebo treatment: -3.3%). No significant difference was observed in respect to effects on triglycerides, HDL-cholesterol and safety parameters. On the basis of our data, the tested lipid-lowering nutraceutical seems to significantly improve endothelial function in moderately hypercholesterolemic subjects. These results have to be confirmed on larger patient samples and over longer periods.

A great number of clinical trials have evaluated the lipid-lowering properties of dietary supplements and nutraceuticals and their combination (1). Among these, monacolin K aroused much interest: it acts as a reversible inhibitor of the 3-hydroxy-3-methyl-glutaryl-coenzyme A (HMG-CoA) reductase, a key enzyme in the cholesterol biosynthesis (2). Monacolin K is obtained from Chinese red yeast rice, which is gained by fermenting the yeast, *Monascus purpureus*, over rice (2). Many clinical trials have demonstrated that the consumption of red yeast rice was able to lower low-density lipoprotein cholesterol (LDL-C) concentrations by 33.6 mg/dL and triacylglycerol concentrations by 20.4 mg/dL (3). Considering the positive results reported in literature, the European Agency on Food Safety (EFSA) recognized that there is a cause and effect relationship between the consumption of monacolin K contained in red yeast rice and the maintenance of normal blood LDL-C concentration (4). In order to improve the cholesterol-lowering statin-like effect of red yeast rice, without increasing the related risk of side effects, it makes sense to administrate it in association with other lipid lowering nutraceuticals (5).

Key words: monacolins, LDL-cholesterol, metalloproteinases, high-sensitivity C-reactive protein, nutraceutical, clinical trial

Mailing address:
Arrigo F.G. Cicero, MD, PhD
Medical and Surgical Sciences Dept.
Via Albertoni 15, 40138 Bologna, Italy
Tel.: +39 512142224 - Fax: +39 51390646
e-mail: arrigo.cicero@unibo.it

0393-974X (2016)

DISCLOSURE: ALL AUTHORS REPORT NO CONFLICTS OF INTEREST RELEVANT TO THIS ARTICLE.

The guggul resin from *Commiphora mukul* interferes with lipid metabolism through the inhibition of the hepatic biosynthesis of cholesterol, the enhancement of the hepatic uptake of low-density lipoproteins (LDL) and very-low-density lipoproteins (VLDL) and the increase of the biliary excretion of cholesterol (6).

Octacosanols from *Saccharum officinarum* inhibit cholesterol biosynthesis through the indirect regulation of HMG-CoA reductase activity and increase LDL receptor-dependent processing, enhancing the catabolic rate of LDL (7). Silymarin from *Silybum marianum* has important anti-inflammatory properties; furthermore, it has demonstrated a significant lipid-lowering activity, however the mechanism of action is unclear (8).

Our current aim is to evaluate whether the lipid-lowering effect of this nutraceutical association translates into an improvement of endothelial function, with a further double-blind, randomized clinical trial.

MATERIALS AND METHODS

Study design

This double blind, placebo controlled, randomized clinical trial was carried out on 80 moderately hypercholesterolemic subjects, non-smokers, pharmacologically untreated, in primary prevention for cardiovascular diseases, consecutively enrolled in the ambulatory service of cardiovascular disease prevention in the Medical and Surgical Sciences Department of the University of Bologna.

Inclusion criteria were age between 18 and 70 and LDL-Cholesterol level between 130 and 190 mg/dL, confirmed in at least two sequential checks before signing the consent form.

Exclusion criteria were:

- Personal history of cardiovascular disease or risk equivalents
- TG>400 mg/dL and/or HDL-C<35 mg/dL
- Obesity (BMI>30 kg/m^2)
- Assumption of lipid-lowering drugs or drugs affecting lipid metabolism
- Known thyroid, liver, renal or muscle diseases.

The study was conducted in accordance with the Declaration of Helsinki, and the protocol was approved by the Ethics Committee of the University of Bologna. Informed consent was obtained from all patients before their inclusion in the study.

At baseline, patients were given standard behavioral and qualitative dietary suggestions to correct unhealthy habits. Standard diet advice was given by a dietitian and/or a specialist doctor, who periodically provided instructions on dietary intake recording procedures as part of a behavior modification program, and then later used the subjects' food diaries for counseling. In particular, the subjects were instructed to follow general indications of a Mediterranean diet, avoiding excessive intake of dairy and red meat-derived products, and maintaining overall constant dietary habits. Individuals were also generically encouraged to increase their physical activity by walking briskly for 20 to 30 minutes, 3 to 5 times per week, or by cycling.

Treatments

After 4 weeks of diet and physical activity, patients were allocated to treatment either with an indistinguishable tablet of placebo or with an active product containing 10 mg monacolins from *Monascus purpureus,*10 mg Guggulipids and 2.5 mg Guggulsterons from *Commiphora mukul* extract, 50 mg of octacosanols from *Saccharum officinarum*, and 150 mg of silymarin from *Silybum marianum* (kindly offered by Erbozeta SpA, Chiesanuova, San Marino, Italy). The doses of each component were chosen on the basis of the monacolin dose defined as efficacious and safe by the EFSA (5), that of policosanols on the basis of the one usually tested in clinical trials (7), and thoseof the other components mainly on the basis of technical tests on tablet stability. The patients were instructed to take 1 tablet each evening after dinner.

Clinical, instrumental and laboratory data were obtained at baseline and at the end of the 8-week period treatment.

Randomization was obtained by drawing envelopes containing randomization codes prepared by an independent statistician and specific software. The envelopes were then further mixed and distributed to the investigators who assigned the randomization code in a progressive way to the enrolled subjects. A copy of the code was provided only to the person responsible for carrying out the statistical analysis.

Table I. *Main characteristics of the investigated parameters at the baseline in patients treated with the tested nutraceutical or placebo.*

	Placebo (n.40; M:18, F: 22)		Active treatment (n. 40; M:19, F: 21)	
	Mean	**SD**	**Mean**	**SD**
Age (years)	49.8	7.2	49.5	7.7
Total Energy Intake (kcal)	2475	125	2396	144
Fat dietary intake (% on total energy)	27.8	3.2	27.5	3.8
Saturated fat intake (Fat dietary intake (% on total energy)	10.6	1.4	10.9	1.3
Protein intake (% on total energy)	16.7	1.9	16.6	1.7
Carbohydrate intake (% on total energy)	53.9	3.7	54.1	4.2
Cholesterol intake (mg)	205.6	11.8	206.9	12.1
BMI (kg/m2)	26.5	0.4	26.3	0.7
SBP (mmHg)	134.1	4.5	133.4	4.4
DBP (mmHg)	84.5	3.2	83.6	3.5
TC (mg/dL)	234.1	19.6	236.4	22.1
HDL-C (mg/dL)	41.2	3.7	41.7	4.0
LDL-C (mg/dL)	151.3	15.9	156.1	14.1
Tg (mg/dL)	139.4	36.9	132.4	37.5
FPG (mg/dL)	90.3	6.5	91.4	7.4
CPK (U/L)	124.6	27.0	130.2	26.3
AST (U/L)	21.7	3.9	21.3	3.6
ALT (U/L)	22.1	3.6	23.6	3.4
Hs-CRP (mg/L)	2.0	0.3	2.1	0.4
Pulse volume changes (%)	63.2	13.2	64.3	12.5

BMI: body mass index; SBP: systolic blood pressure; DBP: diastolic blood pressure; TC: total cholesterol; LDL-C: low-density lipoprotein cholesterol; HDL-C: high-density lipoprotein cholesterol; Tg: triglycerides; FPG: fasting plasma glucose; CPK: creatin-phosfo-kinase; AST: aspartate transaminase; ALT: alanine transaminase; hs-CRP: high sensitivity C-reactive protein

Descriptive values reported as mean and standard deviation. The subjects where cross-matched for all the tested variables.

Throughout the study, we instructed patients to take the first dose of the product on the day after they received it in a blinded box. At the same time, all unused products were retrieved for inventory. Product compliance was assessed by counting the number of product doses returned at the time of specified clinic visits.

Assessments

All plasma parameters were obtained after a 12-hour overnight fast. Venous blood samples were taken from all patients between 8:00 a.m. and 9:00 a.m. Plasma used was obtained by addition of Na_2EDTA (1 mg=mL) and centrifuged at 3,000 g for 15 min at 48°C. Immediately after centrifugation, plasma samples were frozen and stored at -80°C for no more than 3 months. The following parameters were evaluated via standardized methods (9, 10): total cholesterol (TC), high-density lipoprotein-cholesterol (HDL-C), triglycerides (TG),

Table II. *Changes in the investigated parameters after placebo and monacolin treatment.*

	Placebo (n. 40)			Active treatment (n. 40)		
Δ (T0-T1)	**Mean**	**SD**	**P *vs* Baseline**	**Mean**	**SD**	**P *vs* Baseline**
Δ TC (mg/dL)	-13.2	12.4	0.019	-42.4*	18.6	<0.001
Δ HDL-C (mg/dL)	+1.3	2.1	0.267	+1.5	2.4	0.244
Δ LDL-C (mg/dL)	-4.3	11.8	0.411	-36.4*	14.6	<0.001
Δ Tg (mg/dL)	-37.1	51.8	0.043	-42.7	38.7	0.032
Δ FPG (mg/dL)	-1.7	6.4	0.370	-2.3	6.5	0.278
Δ CPK (U/L)	+11.2	23.4	0.188	+25.6	34.1	0.191
Δ AST (U/L)	-3.5	4.2	0.138	-5.3	3.6	0.063
Δ ALT (U/L)	-3.3	4.6	0.141	-5.2	4.3	0.072
Δhs-CRP (mg/L)	-0.03	0.06	0.123	-0.05*	0.02	0.019
ΔPulse Volume (%)	-2.1	9.3	0.278	+10.9*	8.7	0.021

TC: total cholesterol; LDL-C: low-density lipoprotein cholesterol; HDL-C: high-density lipoprotein cholesterol; Tg: triglycerides; FPG: fasting plasma glucose; CPK: creatin-phosfo-kinase; AST: aspartate transaminase; ALT: alanine transaminase; hs-CRP: high sensitivity C-reactive protein

*All the data are expressed as mean and SD; *= P<0.01 vs placebo*

LDL-Cholesterol (LDL-C), glucose, liver transaminases, and Creatine-Phosfo-Kinase (CPK). All measurements were performed in the laboratory of our department.

High-sensitivity C-reactive protein (hs-CRP) was measured with the use of latex-enhanced immunonephelometric assays on a BN II analyzer (Dade Behring, Newark, Delaware, USA). The intra-assay and inter-assay coefficients of variation (CVs) were 5.7 and 1.3%, respectively (11).

Endothelial function was evaluated by Endocheck®, a method embedded within the Vicorder® device (Skidmore Medical Ltd, Bristol, UK), which records brachial pulse volume (PV) waveforms, at baseline and during reactive hyperemia. Reactive hyperemia was provoked through PV displacement, obtained by inflating a cuff positioned distally around the forearm. After a 10-min rest, brachial blood pressure was evaluated and PV waveforms were recorded at the baseline for 10 seconds. Then, the cuff was inflated to 200 mmHg for 5 min, and PV waveforms were recorded for 3 min after cuff release. PV displacement was then calculated as a percentage change in the PV waveform area, comparing waveforms during and before hyperemia through the equation $\sqrt{PV_2}/PV_1$, where PV_1 represents PV at the baseline and PV_2 represents PV during hyperemia (12).

Statistical analyses

Data were analyzed using intention-to-treat by means of the Statistical Package for Social Science (SPSS) 19.0, version for Windows. The sample size suggested to detect a mean difference of 10% in endothelial function between active treatment and placebo, with a power of

0.90 and an alpha error of 0.05, was of at least 30 subjects per group. Normally distributed baseline characteristics of the population were compared using Student's *t*-test and χ^2 test followed by Fisher's exact test for categorical variables. Between group difference was assessed by the ANOVA. All data are expressed as means and SD. A p level of <0.05 was considered significant for all tests.

RESULTS

Enrolled patients were age and sex matched. The baseline characteristics of patients assigned to placebo or nutraceutical were similar, and no significant differences were observed regarding the studied parameters (Table I).No patient dropped out from the study because of adverse events, even though one patient suffered from a mild tolerable myalgia in the nutraceutical treatment arm. From the randomization visit to the end of the study, the enrolled subjects maintained overall a similar dietary pattern, without significant change in total energy, total cholesterol and total saturated fatty acid intake.

When compared to the placebo, during nutraceutical treatment the patients experienced a more favorable percentage change in total cholesterol (TC *vs* baseline: -17.9%; TC *vs* placebo: -5.6%), LDL-cholesterol (LDL-C *vs* baseline: -23.3%; LDL-C *vs* placebo: -2.8%), hs-CRP (hs-CRP *vs* baseline: -2.4%; hs-CRP *vs* placebo: -1.5%), and endothelial function (pulse volume displacement *vs* baseline: +17%; pulse volume displacement *vs* placebo treatment: -3.3%). No significant difference was detected comparing pre- and post-treatment values with respect to effects on TG, HDL-C, glucose, transaminases, and CPK in both treatment groups (Table II).

DISCUSSION

Our clinical trial confirms the lipid-lowering activity of monacolins 10 mg, the results being in line with a recently published systematic review (13), as we recorded a decrease respectively of 17.9% for TC and 23.3% for LDL-C. We also evaluated the effect of monacolins on hs-CRP, an inflammation marker, which independently predicts myocardial infarction, stroke and peripheral artery disease (14, 15). Our results also show a reduction of hs-CRP with monacolins, in accordance with the conclusions of Liu et al. (16) on red yeast rice, and with another Italian study testing the same nutraceutical combination we tested (17). This effect is probably due to an indirect anti-inflammatory effect of monacolins, resulting from lipid-lowering and other processes that reduce triggers and stimulators, rather than a direct anti-inflammatory effect from the naturally occurring statin-like elements. Indeed, endothelial dysfunction is associated with a higher cardiovascular risk as demonstrated in various populations (18, 19). In our trial, subjects treated with monacolins presented greater changes in brachial PV waveform area during hyperemia than subjects treated with placebo (PV after monacolin treatment: +17%; pulse volume after placebo treatment: -3.3%). Previously, a similar effect was observed after the assumption of a compound containing red yeast rice, berberine and policosanols (20), where, however, the decrease in LDL-C was less impressive.

Nevertheless, our clinical trial has some limitations. First, the patient sample is quite small: however, the study strength is improved by a crossover design where subjects are all treated with both placebo and active treatment. Another limitation is the short duration of the trial, but our aim was to evaluate a short-term effect of the tested nutraceuticals on endothelial function.

In conclusion, based on our data, a nutraceutical containing 10 mg monacolins and guggul seems to be able to effectively improve endothelial function in moderately hypercholesterolemic subjects. These results have to be confirmed in longer studies.

ACKNOWLEDGEMENTS

This study was supported by University of Bologna institutional funding.

REFERENCES

1. Cicero AF, Ferroni A, Ertek S. Tolerability and safety of commonly used dietary supplements and nutraceuticals with lipid-lowering effects. Expert Opin Drug Saf 2012; 11:753-66.

2. Burke FM. Red yeast rice for the treatment of dyslipidemia. Curr Atheroscler Rep 2015; 17(4):495.
3. Li Y, Jiang L, Jia Z, Xin W, Yang S, Yang Q, Wang L. A meta-analysis of red yeast rice: an effective and relatively safe alternative approach for dyslipidemia. PLoS One 2014; 9:e98611.
4. European Food Safety Authority. Scientific Opinion on the substantiation of health claims related to monacolin K from red yeast rice and maintenance of normal blood LDL cholesterol concentrations (ID 1648, 1700) pursuant to Article 13(1) of Regulation (EC) No 1924/2006. EFSA Journal 2011; 9:2304-19.
5. Cicero AF, Colletti A. Combinations of phytomedicines with different lipid lowering activity for dyslipidemia management: The available clinical data. Phytomedicine 2015 Nov 10. [Epub ahead of print]
6. Deng R. Therapeutic effects of guggul and its constituent guggulsterone: cardiovascular benefits. Cardiovasc Drug Rev 2007; 25:375-90.
7. Castaño G, Más R, Fernández J, López E, Illnait J, Fernández L, Mesa M. Effects of policosanol on borderline to mildly elevated serum total cholesterol levels: a prospective, double-blind, placebo-controlled, parallel-group, comparative study. A Curr Ther Res Clin Exp 2003; 64:522-37.
8. Huseini HF, Larijani B, Heshmat R, Fakhrzadeh H, Radjabipour B, Toliat T, Raza M. The efficacy of Silybummarianum (L.) Gaertn. (silymarin) in the treatment of type II diabetes: a randomized, double-blind, placebo-controlled, clinical trial. Phytother Res 2006; 20:1036-39.
9. Cicero AF, Rosticci M, Parini A, Morbini M, Urso R, Grandi E, Borghi C. Short-term effects of a combined nutraceutical of insulin-sensitivity, lipid level and indexes of liver steatosis: a double-blind, randomized, cross-over clinical trial. Nutr J 2015; 14:30.
10. Cicero AFG, D'Addato S, Reggi A, Marchesini Reggiani G, Borghi C, on behalf of the Brisighella Heart Study. Hepatic Steatosis Index and Lipid Accumulation Product as middle-term predictors of incident metabolic syndrome in a large population sample: data from the Brisighella Heart Study. Intern Emerg Med 2013; 8:265-67.
11. Rifai N, Tracy RP, Ridker PM. Clinical efficacy of an automated high-sensitivity C-reactive protein assay. Clin Chem 1999; 45:2136-41.
12. Day LM, Maki-Petaja KM, Wilkinson IB, McEniery CM. Assessment of brachial artery reactivity using the Endocheck: Repeatability, reproducibility and preliminary comparison with ultrasound. Artery Res 2013; 7(3-4):119-20
13. Gerards MC, Terlou RJ, Yu H, Koks CH, Gerdes VE. Traditional Chinese lipid-lowering agent red yeast rice results in significant LDL reduction but safety is uncertain – A systematic review and meta-analysis. Atherosclerosis 2015; 240:415-23.
14. Zwacka TP, Hornbach V, Torzewski J. C-reactive protein mediated lipoprotein uptake by macrophages. Circulation 2001; 103:1194-97.
15. Medzhitov R, Janeway CA Jr. Innate immunity: impact on the adaptive immune response. Curr Opin Immunol 1997; 9:4-9.
16. Liu L, Zhao SP, Cheng YC, Li YL. Xuezhikang decreases serum lipoprotein(a) and C-reactive protein concentrations in patients with coronary heart disease. Clin Chem 2003; 49:1347-52.
17. Derosa G, Bonaventura A, Bianchi L, Romano D, D'Angelo A, Fogari E, Maffioli P. A randomized, placebo-controlled study on the effects of a nutraceutical combination of red yeast rice, silybum marianum and octacosanol on lipid profile, endothelial and inflammatory parameters. J Biol Regul Homeost Agents 2014; 28:317-24.
18. Van Sloten TT, Henry RM, Dekker JM, Nijpels G, Unger T, Schram MT, Stehouwer CD. Endothelial dysfunction plays a key role in increasing cardiovascular risk in type 2 diabetes: the Hoorn study. Hypertension 2014; 64:1299-305.
19. Hirata Y, Sugiyama S, Yamamoto E, et al. Endothelial function and cardiovascular events in chronic kidney disease. Int J Cardiol 2014; 173:481-86.
20. Affuso F, Ruvolo A, Micillo F, Saccà L, Fazio S. Effects of a nutraceutical combination (berberine, red yeast rice and policosanols) on lipid levels and endothelial function randomized, double-blind, placebo-controlled study. Nutr Metab Cardiovasc Dis 2010; 20:656-61.

LETTER TO THE EDITOR

DOES CYCLIC GUANOSINE MONOPHOSPHATE INDUCE AUTOPHAGY IN THYROID MALIGNANT CARCINOMA THROUGH DOWN-REGULATION OF CYCLIC GUANOSINE MONOPHOSPHATE PHOSPHODIESTERASE?

G. SPOTO[1], A. ESPOSITO[1], F. SANTOLERI[1], C. RUBINI[2], A.W.S. RUTJES[3], M. FIORONI[2], M. FERRANTE[1] and M. PETRINI[1]

[1]Laboratory of Medical Chemistry & Dental Materials, Department of Medical, Oral and Biotechnological Sciences, University "G. d'Annunzio", Chieti, Italy; [2]Anatomy and Histopathology, Dental School, Polytechnic University of Marche, Italy; [3]Institute of Social and Preventive Medicine, University of Bern, Bern, Switzerland

Received November 16, 2015 – Accepted April 14, 2016

The aim of this study was to evaluate whether or not the expression of cGMP- phosphodiesterases (cGMP-PDE) varies in different thyroid pathologies and to elucidate the relationship between the expression of cGMP-PDE, cGMP, and autophagy. Fifty-four thyroid biopsy samples, excised to perform the biopsy, were split into two parts and randomly assigned: one part was microscopically examined and histological classified, and the other was frozen and analysed in order to evaluate the cGMP-PDE activity. Intracellular cGMP was also measured. A strong expression of intracellular cGMP and cGMP-PDE activity was observed in carcinoma in respect to controls and benign pathologies. The level of cGMP-PDE in papillary carcinoma without lymph node involvement (N-) was approximately four-fold higher compared to those with lymph node invasion (N±). On the contrary, the cGMP was one and a half times higher in N± than N-. Our results are promising, although further epigenetical studies are needed to confirm this association. A correlation between the cGMP-degrading activity and the severity of thyroid pathology has been shown. The decrease of cGMP-PDE and the increase of cGMP in N± papillar carcinoma could be an autophagic stimulus, a defence mechanism of the body, against the cancer that is expanding and invading other tissues and organs.

A great variety of pathologies, comprehending benign nodules, thyroiditis, and benign and malign neoplasia can affect the thyroid and its enzymatic activity.

Most patients with thyroid nodules can be managed conservatively after malignancy is ruled out. To identify the minority of patients with thyroid cancer who need surgical treatment is a big challenge to clinicians, because most thyroid malignancies are clinically indistinguishable from benign loci (1).

The understanding of the mechanisms which regulate the growth and development of thyroid is fundamental both for the establishment of new diagnostic procedures, and for specific therapies. The cyclic nucleotides, cyclic adenosine monophosphate (cAMP) and cyclic guanosine monophosphate (cGMP), have long been recognized as important intracellular signal transduction molecules, acting as second messengers between an extracellular signal, such as a hormone, neurotransmitter or

Key words: thyroid, cGMP-Phosphodiesterase, cGMP, cAMP, carcinoma, autophagy

Mailing address:
Prof. Giuseppe Spoto,
Department of Medical, Oral and Biotechnological Sciences,
University of Chieti, Via dei Vestini 31, 66013 Chieti, Italy
Tel.: +39 0871 355 4066 - Fax: +39 0871 355 4375
e-mail: spoto@unich.it

0393-974X (2016)

DISCLOSURE: ALL AUTHORS REPORT NO CONFLICTS OF INTEREST RELEVANT TO THIS ARTICLE.

cytokine, and the elicited intracellular response (2). The cyclic nucleotides are very important for a great variety of transduction processes in human thyroid, and phosphodiesterases (PDEs) regulate their level (3). cGMP is formed through the activity of guanylyl cyclase (GC) enzymes from its precursor guanosine-5'-triphosphate (GTP). Hydrolysis of cyclic nucleotides is achieved by phosphodiesterases (PDEs), but the enzyme isoforms responsible for degrading cGMP in most cells have not yet been identified. Currently, it is widely accepted that there are 11 different families of PDEs comprising 21 different gene products (4). These unique PDEs differ in their three-dimensional structure, kinetic properties, mode of regulation, intracellular localization, cellular expression, and inhibitor sensitivities. They can be grouped into three categories based on their substrate specificity: cAMP- and cGMP-specific and dual specificity. However, to date, only PDE isoforms 8A, 10A and 11A normally have been described in thyroid. PDE 1, 2, 3, 5, 6, 9, 10 and 11 families are capable of hydrolyzing cGMP with PDE 5, 6, and 9 are selective for cGMP (5).

Because alterations in cyclic nucleotide signaling are common to a number of cancer types, which appear to occur early in the tumorigenic process, and correlate with stage and prognosis, these pathways could provide new molecular targets for cancer chemoprevention and/or chemotherapy (2).

The aim of this early phase study is to make a quantitative comparison of cGMP-PDE activity and intracellular cGMP in different samples of thyroid pathologies.

MATERIALS AND METHODS

The endocrinology specialists for biopsies of the thyroid referred 54 patients (mean age 46±12 years) to the Department of the Anatomy and Histopathology, Dental School, University of Ancona, Italy. All the 54 human thyroid biopsy samples (30 females and 24 males), excised to perform the biopsy, were microscopically and biochemically examined. After removal, the samples were randomly divided in two parts: one was sent for histological examination at the Section of Pathologic Anatomy of the same University and the other one was frozen and sent to the University of Chieti for cGMP and cGMP-PDE degrading activity evaluation.

Histopathological analysis

Tissue samples were fixed in 10% formalin for 24 h at room temperature and embedded in paraffin. Morphologic analysis was performed on 4-6-µm thick tissue sections stained with hematoxylin and eosin (H&E). The final diagnosis was based on histopathological criteria (6).

Partial purification of phosphodiesterases

The frozen samples were thawed and centrifuged for 10 min at 1000 rpm with a centrifuge model MIKRO22R (Hettich Zentrifugen) and then washed twice with isotonic PBS.

In order to purify the enzyme, the samples were homogenized with a phosphate buffer K1-K2 10 mM pH 7.00 in a 1:10 (w/v) ratio, using a Potter (T25 BASIC model - Ika Laborpechnik), three times for 20 swith 30 s pause; a progressive speed up gradually to red was used, always keeping test tubes on ice. The samples were then sonicated using an ultrasonic probe at 50 Hz power, to break the cell membranes, three times for 5 s with 1 m of rest in ice with a 2-mm-diameter probe (Model Labsonic M, B. Braun Biotech International; Melsungen, Germany). The homogenate was centrifuged for 30 s at 1000 rpm with a centrifuge model MIKRO22R (Hettich Zentrifugen). The withdrawn supernatant was then used for the phosphodiesterase analysis, for the protein determination and for the endogenous cyclic nucleotides evaluation (7).

cGMP-PDE assay

The enzymatic analysis was carried out using the method of Spoto et al. with minor modifications: 0.1 M TRIS-HCl buffer (pH 8.3), 10 mM of $MgCl_2$, 0.1 M of KCl at 37°C (7). The reaction was initiated by the addition of 44 µM of cyclic GMP. The mixture was incubated for 120 min at 37°C, after which the reaction was terminated by adding HCl 2M for a final concentration of 0.02 M and leaving the samples in a boiling water bath for 5 min. The samples were then centrifuged at 12000 rpm in a MIKRO 22R (Hettich Zentrifugen) model centrifuge and the supernatant was filtered through a nylon-66 0.22 µm filter (Rainin Corporation). The clear filtrate obtained was used for analysis in reverse phase HPLC. The HPLC system utilized during this experimentation

consisted of two pumps LC-9A model (Shimadzu), one spectrophotometer at variable wavelength SPD-10AV vp (Shimadzu) which measures at 254 nm, an autosampler SIL-10AXL (Shimadzu) and a LICHROSORB RP-18 (5 μM) column. The mobile phase used for the separation of the nucleotides consisted of 350 mM ammonium acetate (pH 6.0) with 0.6% of acetonitrile (v/v), previously degassed in an ultrasonic bath model SONIC 18-35 (Simply – Italia) in order to avoid bubbles.

Cyclic endogenous nucleotides evaluation

The determination of cGMP was obtained by HPLC method as described and was confirmed by the use of a Kit EIA from BIOMOL which uses a competitive immunoenzymatic analysis for the quantitative determination of these compounds, following the HPLC method previously described (7).

Protein-determination

A kit for protein determination with bicinchinonic acid (Sigma-Aldrich), with albumin of bovine serum as the standard of proteinic reference quantified the protein content in the sample. A spectrophotometric measurement at 280 nm and 350 nm was performed to determine the protein concentration of the supernatant, using a diluted 1:20.

Data processing

The World Health Organization (WHO) classification of thyroid disease (6) was used record and organise the data. The presence of statistically significant differences in the HPLC experimental data were tested with analyses of variance (ANOVA) applying the Bonferroni/Dunn correction for multiple testing (Stat View 4.0 software, Abacus Concepts, USA).

RESULTS

Based on WHO histopathological criteria the samples were classified as follows (7):

- 6 healthy thyroids;
- 38 benign samples: benign struma, adenomatous hyperplasia, chronic thyroiditis, benign adenoma;
- 10 malign samples: papillar carcinoma and

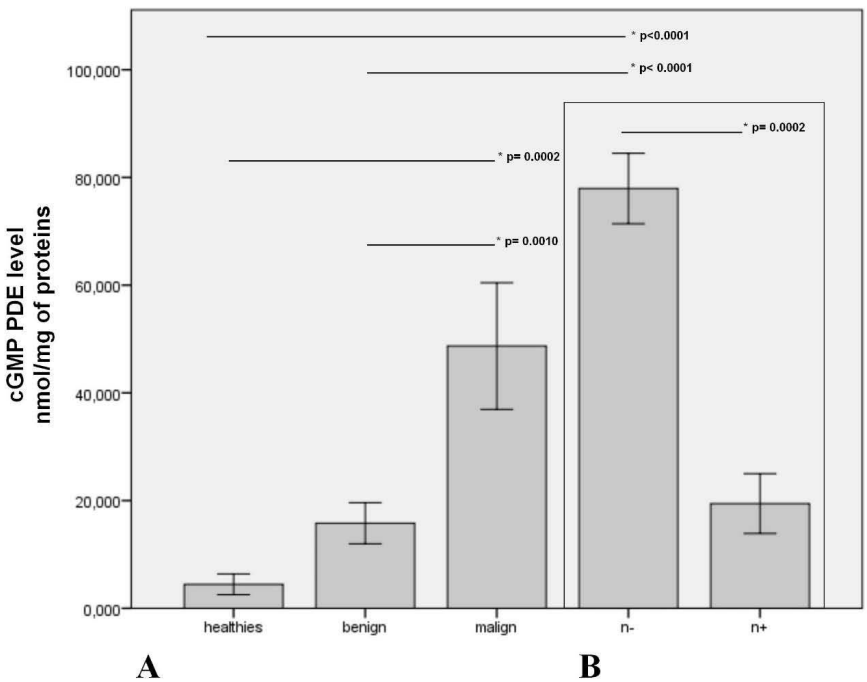

Fig. 1. ***A)*** *Levels of cGMP-PDE in different thyroid pathologies; these values are directly proportional to the severity of the pathologies: they are low in healthy samples, slightly increase in benign pathologies and higher in carcinoma. Bonferroni showed statistically significant differences among the groups.* ***B)*** *Level of cGMP-PDE activity in papillar carcinoma basing on the lymph node involvement: positive (N+) or negative (N-).*

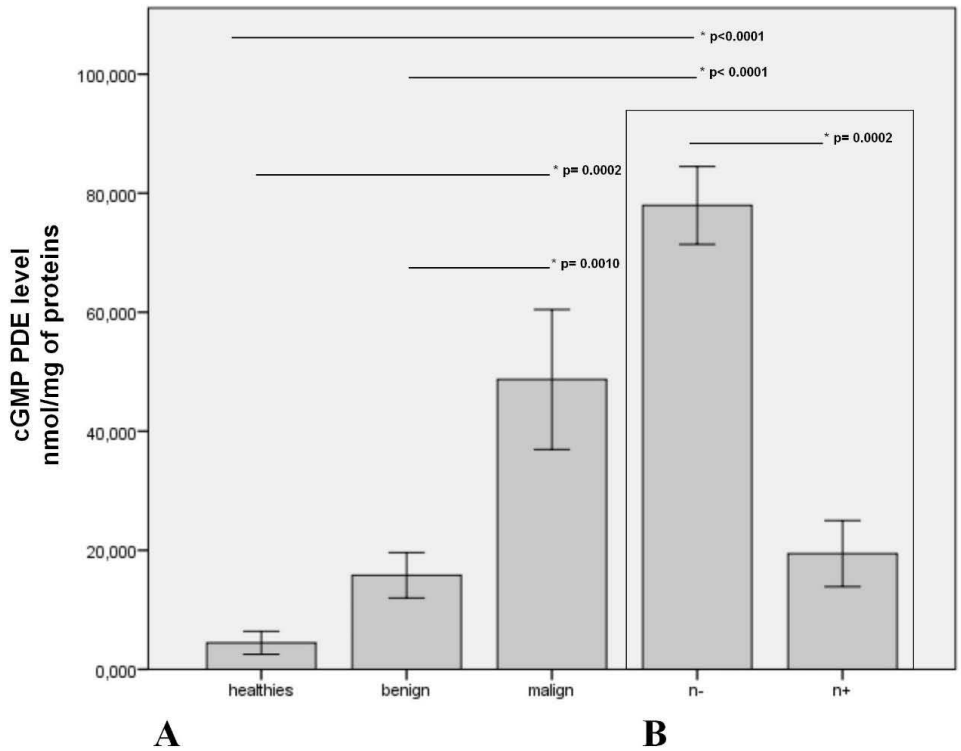

Fig. 2. ***A)*** *Level of intracellular cGMP; carcinoma were characterized by the higher cGMP levels (32.16±8.77 nmol/mg of protein). There were statistically significant differences between healthy samples 0.72 (±0.14) nmol/mg and malign samples, p=0.0038. The level of intracellular cGMP was 11.99±2.54 nmol/mg of protein in benign pathologies.* ***B)*** *Intracellular cGMP activity of the samples basing on lymph node involvment. N+ was about two-fold higher (38.12±16.06 nmol/mg) in respect to N- (24.22±5.73 nmol/mg). Healthy samples were characterized by an average cGMP 4.81±4.16 nmol/mg of protein.*

follicular carcinoma.

Average cGMP-PDE activity of all samples is summarized in Fig. 1. Phosphodiesterase activity in healthy samples and benign pathologies was 4.45 (±1.92) and 15.79±3.82 nmol/mg of protein, respectively. cGMP-PDE activity was in nmol/mg of protein.

The activity of cGMP-PDE of thyroid samples affected by non-neoplastic pathologies (benign struma, adenomatous hyperplasia and chronic thyroiditis), seemed higher in respect to healthy samples, and statistically significant differences were found (P=0.0002).

In particular, compared to healthy controls, thyroiditis were characterized by a light decrease of cGMP-PDE activity 1.22 (±0.96) nmol/mg. On the contrary a light increase of cGMP-PDE activity was found in benign struma 5.25 (±5.69) and adenomatous hyperplasia 5.11 (±4.1) nmol/mg. Samples of adenoma were characterized by a mean cGMP-PDE activity of 9.52 (± 9.26) nmol/mg. Mean values of cGMP-PDE activity from samples of papillar and follicular carcinoma were 40.43 (±29.67) and 69.05 (±15.61) nmol/mg of protein, respectively. The calculated ratio between cGMP-PDE activity in healthy samples versus benign neoplasia was 0.48; on the contrary the ratio between healthy and malignant ones was 0.0465.

The box in the right of Fig. 1 shows the level of cGMP-PDE activity in papillar carcinoma basing on the lymph node involvement: positive (N+) or negative (N-). N- (Fig. 1) was characterized by a cGMP-PDE of about three-fold higher (77.94±6.54

nmol/mg), compared to those N+ (19.44±5.56 nmol/mg). Healthy samples were characterized by an average cGMP-PDE of 2.55±2.38 nmol/mg of protein.

Fig. 2 shows the level of intracellular cGMP; carcinoma were characterized by the higher levels (32.16±8.77 nmol/mg of protein). There were statistically significant differences between healthy samples (0.72±0.14) nmol/mg and malign samples, p=0.0038. The level of intracellular cGMP was 11.99±2.54 nmol/mg of protein in benign pathologies.

The box in the right of Fig. 2 shows the intracellular cGMP activity of the samples basing on lymph node involvement. N+was about two-fold higher (38.12±16.06 nmol/mg) in respect to N- (24.22 ± 5.73 nmol/mg). Healthy samples were characterized by an average cGMP 4.81±4.16 nmol/mg of protein.

DISCUSSION

This research analysed the correlation between the concentrations of cGMP-PDE in relationship to the severity of thyroid pathology (inflammatory, benign and malignant neoplasia). Our results suggest that benign pathologies of thyroid are characterized by a fluctuation of cGMP-PDE activity, but the differences are not statistically significant. On the contrary, carcinoma are characterized by a cGMP-PDE activity higher in respect to healthy samples, and these results are in agreement with other studies that recorded an increment in cGMP-PDE activity in cancer of salivary glands, colon and gingiva (8-10). The correlation between cGMP and PDE in the malignant transformation is shown in Fig. 1B and Fig. 2B. The level of this enzymatic activity in papillar carcinoma was grouped basing on the lymph node involvement: positive (N+) or negative (N-). Surprisingly, the level of cGMP-PDE (Fig. 1B) is elevated in carcinoma without lymph node involvement (77.94±6.54 nmol/mg) in respect to N+ (19.44±5.56 nmol/mg). On the contrary, intracellular cGMP (Fig. 2B) is characterized by an inverse trend. Our results are in accordance with Bian et al. who found that by comparing with respective normal tissues, the expression of NO-cGMP signaling molecules in different human cancers varies significantly (11). Our hypothesis is that at first the increase of endogenous cGMP, induced by cGMP-PDE, in N- has the function to control the expansion of the pathology. However, with the severity and the spread of the carcinoma and the lymph node involvement, the ability is lost of cGMP-PDE to control the pathology, the ratio between cGMP and cGMP-PDE tend to normalize and the carcinoma can develop without control.

The decrease of cGMP-PDE and the increase of cGMP could be a defence mechanism of the body against the cancer that is expanding and invading other tissues and organs. In particular, we believe that an autophagic stimulus could induce the simultaneous increment of cGMP and the decrement of cGMP-PDE that is the unique degrading agent known. To confirm this hypothesis, the fact that various PDE1 to PDE5 selective inhibitors have also been reported to inhibit growth and induce apoptosis in many different cancer cell lines, suggests a potential role for this family of drugs also as antineoplastic agents (12). Cancer often occurs when several different pathways that regulate cell differentiation are disturbed. Autophagy plays an important role in cancer both in protecting against cancer and in potentially contributing to the growth of cancer (13). The deeper understanding of cyclic nucleotide signalling, down-stream factors, off-target effects and their roles in autophagy is critical for the development of cancer chemoprevention agents. This insight will allow for the development of safer and more efficacious drugs for both prevention and treatment of multiple types of cancer (6, 14).

REFERENCES

1. Shi L, Li Y, Guan H, Li C, Shi L, Shan Z, Teng W. Usefulness of serum thyrotropin for risk prediction of differentiated thyroid cancers does not apply to microcarcinomas: results of 1,870 Chinese patients with thyroid nodules. Endocr J 2012; 59(11):973-80.
2. Fajardo AM, Piazza GA, Tinsley HN. The role of cyclic nucleotide signalling pathways in cancer: targets for prevention and treatment. Cancers (Basel) 2014; 6(1):436-58
3. d'Alessandro L, Petrini M, Ferrante M, Di Marco S, Trubiani O, Spoto G. Cyclic nucleotide phosphodiesterase activity in stem cells of human periodontal ligament (PDL-MSCs) before and after

osteogenic induction. Oral Surg Oral Med Oral Pathol Oral Radiol 2013; 116(5):e317-23.
4. Bender AT, Beavo JA. Cyclic nucleotide phosphodiesterases: molecular regulation to clinical use. Pharmacol Rev 2006; 58(3):488-520.
5. Omori K, Kotera J. Overview of PDEs and their regulation. Circ Res 2007; 100:309-27.
6. DeLellis RA. Pathology and genetics of tumours of endocrine organs; International Agency for Research on Cancer; World Health Organization; International Academy of Pathology; International Association for the Study of Lung Cancer. Lyon : IARC Press, 2004.
7. Spoto G, Whitehead E, Ferraro A, Di Terlizzi PM, Turano C, Riva F. A reverse-phase HPLC method for cAMP phosphodiesterase activity. Anal Biochem 1991; 196(2):207-10.
8. Spoto G, Mariani A, Santoleri F, Fioroni M, Vitale D, Piatelli A, Di Nicola M, Rubini C. cGMP phosphodiesterase activity evaluation in human carcinoma of salivary glands. Int J Immunopathol Pharmacol 2004; 17(3 Suppl):25-9.
9. Spoto G, Fioroni M, Rubini C, Contento A, Di Nicola M, Forcella S, Piattelli A. Cyclic guanosine monophosphate phosphodiesterase activity in human gingival carcinoma. J Oral Pathol Med 2003; 32(4):189-94.
10. Savini F, Berardi S, Tatone D, Spoto G. Phosphodiesterase in human colon carcinoma cell line CaCo-2 in culture. Life Sci 1995; 56(22):421-5.
11. Bian K, SotolongoA, Lam H, Zhang D, Liu J, Murad F. NO-cGMP signalling and cancer therapy BMC Pharmacol Toxicol 2013; 14(Suppl 1):P9.
12. Maurice DH, Ke H, Ahmad F, WangY, Chung J, Manganiello VC. Advances in targeting cyclic nucleotide phosphodiesterases. Nat Rev Drug Discov 2014; 13(4):290-314.
13. Furuya N, Liang XH., Levin B. Autophagy and cancer. In Autophagy. D.J. Klionsky editor. Landes Bioscience. Georgetown, Texas, USA. 2004; p. 244-53
14. Morani F, Titone R, Pagano L, Galetto A, Alabiso O, Aimaretti G, Isidoro C. Autophagy and thyroid carcinogenesis: genetic and epigenetic links. Endocr Relat Cancer 2013; 21(1):R13-29.

LETTER TO THE EDITOR

ISOTONIC SALINE IN CHILDREN WITH PERENNIAL ALLERGIC RHINITIS

S. BARBERI[1], E. D'AURIA[2], L. BERNARDO[1], F. PINTO[1], B. PIETRA[2] and G. CIPRANDI[3]

[1]Department of Pediatrics, A.O. Fatebenefratelli, Milan, Italy; [2]Department of Pediatrics, San Paolo Hospital, University of Milan, Italy; [3]Department of Medicine, IRCCS-AOU San Martino, Genoa, Italy

Received December 30, 2015 – Accepted April 15, 2016

Children with HDM allergy suffer from perennial allergic rhinitis (PAR). The present pilot study evaluated nasal lavage with isotonic saline (0.9%) in 25 children (mean age 8.9 years; 13 males) with HDM-dependent PAR, assessing: nasal symptoms severity and parental perception of rhinitis control, sleep, and school performance. Nasal symptoms, rated by total symptom score, parental perception of PER control, sleep quality, and school performance, measured by visual analogue scale, were significantly improved by nasal lavage ($p<0.001$) after treatment. The effects tended to persist also during the follow-up. In conclusion, the present pilot study provides the first evidence that nasal lavage with isotonic saline relieved the nasal symptoms of children with PAR and improved the parental perception of the disease.

Allergic rhinitis (AR) is frequent in children, as its prevalence is up to 40% of the paediatric population, and has a relevant impact on school attendance and performance and sleep, as well as quality of life of both the children and their parents (1).

The AR immunopathology is characterized by a functional, potentially reversible, defect of allergen-specific T regulatory cells, promoting Th2 polarization and Th1 impairment. Allergic inflammation is closely dependent on allergen exposure (2). In this regard, house dust mites (HDM) are ubiquitous and perennially present in the home. Thus, children allergic to HDM have typically perennial allergic rhinitis (PAR). Moreover, there is evidence that children with PAR have more numerous and severe respiratory infections than non-allergic children (3). AR is also the main risk factor for asthma onset and worsening (4). Therefore, AR starts a vicious circle characterized by mucosal inflammation, nasal symptoms, respiratory infections, and bronchial involvement in predisposed subjects. Consequently, an adequate control of allergic inflammation in children with AR is an important strategy for improving symptom, including sleep and school performance, and saving drug use (1).

The treatment of PAR is usually based on medication, such as antihistamines and intranasal corticosteroids, which are customarily effective, but may have adverse events, including sedation, weight gain, and epistaxis, that may limit their use, and are rather expensive, mainly concerning the PAR duration. For these reasons, nasal irrigation may be an interesting alternative to drugs. Nasal irrigation is well known and popular, as nose rinsing has been used for centuries (5-7). However, the term 'nasal irrigation' is an "umbrella definition" that comprises different ways of administration (nasal irrigation, aerosol, spray) and different saline concentrations (isotonic, such as physiological, or hypertonic with

Key words: isotonic saline, perennial allergic rhinitis, children

Mailing address:
Giorgio Ciprandi, M.D.
Largo R. Benzi 10,
16132 Genoa, Italy
Tel.: + 39 10 35338120
e-mail: gio.cip@libero.it

0393-974X (2016)

saline content ranging from 1 to 6%).

To the best of our knowledge, only three studies have investigated the effectiveness of isotonic saline solution in children with AR (8-10), but no study directly considered children with PAR due to HDM mono-sensitization. On the basis of this background, the present pilot study aimed to evaluate whether isotonic saline (0.9%) nasal spray may be used as monotherapy to improve nasal symptom severity and parental perception of rhinitis control, sleep, and school performance in HDM-mono-sensitized children with PAR.

Globally, 25 consecutive children were enrolled in the study (mean age 8.9 years±2.2 years; 13 males). The inclusion criteria were: i) age range between 4-17 years; ii) PAR diagnosis based on the concordance between typical history of allergic symptoms and documented sensitization; iii) mono-sensitization to HDM; iv) presence of nasal symptoms (with moderate-severe obstruction and/or rhinorrhoea); v) written informed consent by parents. Exclusion criteria were: i) allergy to other allergens; ii) chronic illness; iii) immune deficiency; iv) continuous use of medications (e.g. antihistamines, corticosteroids) in the previous 4 weeks; and v) concomitant use of immune-stimulants.

The patients were treated by an isotonic saline solution and were instructed to assume 1 spray per nostril 3 times/day for 2 weeks. Cetirizine syrup (1 drop/3Kg/bw) was permitted as rescue medication during the treatment period.

The study was performed during the fall: the season usually characterized by worsening of allergic symptoms (because of high levels of exposure to mites).

Nasal symptoms (itching, sneezing, rhinorrhoea, and obstruction) were scored using a four-point scale (0=no symptom; 1=mild symptom; 2= moderate; 3= severe) assessed by a doctor. The sum of these symptoms was calculated and expressed as Total Symptom Score (TSS). In addition, a visual analogue scale (VAS) was used for assessing the parental perception of PAR control (VASa), sleep quality (VASb), and school performance (VASc).

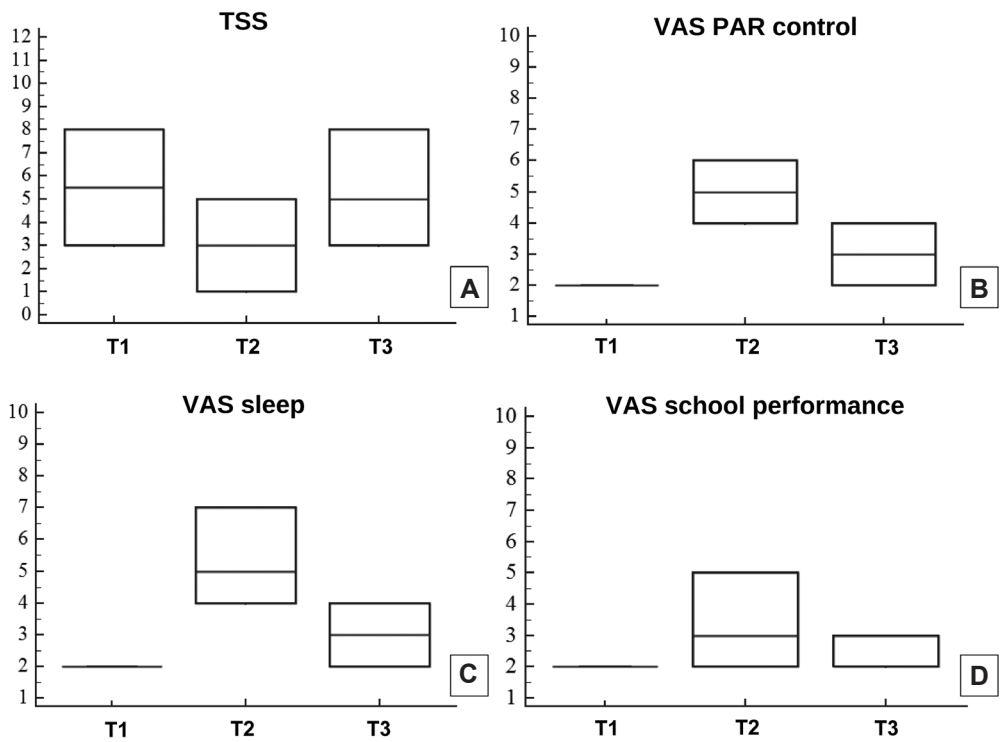

Fig. 1. ***A)*** *Total Symptoms Score (TSS) assessed before (T1) and after treatment (T2) and follow-up (T3).* ***B)*** *VASa assessed before (T1) and after treatment (T2) and follow-up (T3).* ***C)*** *VASb assessed before (T1) and after treatment (T2) and follow-up (T3).* ***D)*** *VASc assessed before (T1) and after treatment (T2) and follow-up (T3).*

The VAS is a segment of 10 cm where the parents indicate the actual perception of considered issues by marking a point (15). In this study, 0 implied the worst perception, while 10 corresponded to the optimal one.

The patients were visited at baseline (T1) and after treatment (T2), and after a 2-week follow-up (T3); all the above-mentioned parameters were evaluated during each visit. Symptomatic use of cetirizine was recorded as days. Adverse events were registered as usual.

Statistical analysis was performed by Friedman ANOVA and by post hoc assessment by Wilcoxon test. Data are expressed as median and percentiles (25^{th} and 75^{th}, IQR). A p-value ≤ 0.05 was considered statistically significant. All data were analyzed using the Stata statistical package, Release 13.1 Statistical Software (StataCorp, College Station, TX, USA).

All children completed the study and the treatment was well tolerated without significant adverse event. Fig. 1 reports the findings.

TSS significantly changed during the study ($p<0.001$): the basal values (M 5.5, IQR 3-8) significantly diminished ($p<0.0001$) after treatment (M 3, IQR 1-5), but significantly increased ($p<0.0001$) at follow-up (M 5, IQR 3-8), however a significant difference ($p<0.4$) remained between T1 and T3.

VASa significantly changed during the study ($p<0.001$): the basal values (M 2, IQR 2-2) significantly increased ($p<0.0001$) after treatment (M 5, IQR 4-6), but significantly decreased ($p<0.001$) at follow-up (M 3, IQR 2-4), however a significant difference ($p=0.03$) remained between T1 and T3.

VASb significantly changed during the study ($p<0.001$): the basal values (M 2, IQR 2-2) significantly increased ($p<0.0001$) after treatment (M 5, IQR 4-7), but significantly decreased ($p<0.0001$) at follow-up (M 3, IQR 2-4), however a significant difference ($p<0.04$) remained between T1 and T3.

VASc significantly changed during the study ($p<0.001$): the basal values (M 2, IQR 2-2) significantly increased ($p=0.003$) after treatment (M 3, IQR 2-5), but significantly decreased ($p<0.04$) at follow-up (M 2, IQR 2-3).

The mean number of days with antihistaminic use was 3.5 during the treatment period, and 4.4 during the follow-up.

The present study demonstrates that intranasal administration of isotonic saline is able to significantly reduce nasal symptoms in children with perennial allergic rhinitis due to mono-sensitization to HDM. In addition, this treatment was also able to significantly affect the parental perception of PAR control, sleep, and scholar performance. These findings support the concept that nasal lavage with saline solution may control allergic reaction, also improving the familiar AR burden. It must be underlined that the current treatment was administered as monotherapy: this aspect reinforces the effectiveness of nasal lavage in PAR.

The present study is also consistent with previous studies performed on children with seasonal allergic rhinitis (8, 10), and another study without clarification about the sensitization pattern (9).

The possible explanations of the efficacy of saline solution might depend on some mechanisms, such as removal of mucous containing pro-inflammatory mediators and allergens, and potential anti-inflammatory activity (5-7).

The main shortcoming of this study is the lack of a control group. However, it has to be considered that isotonic saline is *per se* capable of significantly improving nasal symptoms, as clearly demonstrated in previous studies (8-10). However, this study was designed to include a follow-up period to evaluate the time without treatment as a control of the active period. Further controlled studies should be performed to confirm this preliminary experience.

In conclusion, the present study provided the first evidence that isotonic saline monotherapy was able to relieve nasal symptoms and parental perception of PAR impact. Thus, this outcome could suggest that one course of this compound could be effective, thus reducing the use of pharmacological therapy.

REFERENCES

1. Bousquet J, Khaltaev N, Cruz AA, et al. Allergic Rhinitis and its Impact on Asthma (ARIA) 2008 Update (in collaboration with the World Health Organization, GA2LEN and AllerGen). Allergy 2008; 63(S86):8-160.

2. Barberi S, Villa MP, Pajno GB, et al. Immune response to sublingual immunotherapy in children allergic to mites. J Biol Reg 2011; 25:627-34.
3. Ciprandi G, Buscaglia S, Pesce GP, et al. Minimal persistent inflammation is present at mucosal level in asymptomatic rhinitic patients with allergy due to mites. J Allergy Clin Immunol 1995; 96:71-979.
4. Szefler SJ. Advances in pediatric asthma in 2013: coordinating asthma care. J Allergy Clin Immunol 2014; 133:654-61.
5. Brown CL, Graham SM. Nasal irrigation: good or bad? Curr Opin Otolaryngol Head Neck Surg 2004; 12:9-13.
6. Khianey R, Oppenheimer J. Is nasal saline irrigation all it is cracked up to be? Ann Allergy Asthma Immunol 2012; 109:20-28.
7. Hermelingmeier KE, Weber RK, Hellmich M, Heubach CP, Mosges R. Nasal irrigation as an adjunctive treatment in allergic rhinitis: a systematic review and meta-analysis. Am J Rhinol Allergy 2012; 26:e119-e125.
8. Garavello W, Di Berardino F, Romagnoli M, Sambataro G, Gaini RM. Nasal rinsing with hypertonic solution: an adjunctive treatment for pediatric seasonal allergic rhinoconjunctivitis. Int Arch Allergy Immunol 2005; 137:310-14.
9. Slapak I, Skoupa J, Stmad P, Hornik P. Efficacy of isotonic nasal wash (seawater) in the treatment and prevention of rhinitis in children. Arch Otolaryngol Head Neck Surg 2008; 134:67-74.
10. Marchisio P, Varricchio A, Baggi E, Bianchini S, Capasso M, Torretta S, et al. Hypertonic saline is more effective than normal saline in seasonal allergic rhinitis in children. Int J Immunopathol Pharmacol 2012; 25:721-30.

LETTER TO THE EDITOR

MANDIBULAR THIRD MOLAR DISPLACED IN THE SUBLINGUAL SPACE: CLINICAL MANAGEMENT AND MEDICOLEGAL CONSIDERATIONS

G. VARVARA[1], G. MURMURA[1], P. CARDELLI[1], D. DE ANGELIS[2], S. CAPUTI[1], B. SINJARI[1] and M. PIATTELLI[1]

[1]Department of Medical, Oral and Biotechnological Sciences, "G. d'Annunzio" University of Chieti–Pescara, Chieti, Italy; [2]Department of Biomedical Sciences, University of Milan, Italy

Received March 6, 2016 – May3, 2016

This paper describes the management of a failed mandibular third molar extraction, resulting in tooth displacement in the sublingual space, the discussion of the diagnosis, surgery and medico-legal considerations. A 28-year-old male patient underwent an unsuccessful attempt of the 4.8 tooth extraction. The clinician lost visual contact after luxation and the patient was nOt recalled for post-operative follow-up. After 24 hours, a severe trismus started. Ortopantomography and cone beam computer tomography revealed the displacement in the sublingual space. The tooth was removed under general anaesthesia with intraoral approach. The follow-up was uneventful and the paraesthetic area on the tongue did not enlarge after the retrieval. The displaced mandibular third molar is a rare but potentially serious complication of extraction. This event should be avoided with correct diagnosis and surgical technique. Cone beam computed tomography was useful to determine the three-dimensional position of the displaced tooth.

Mandibular third molar (MTM) removal is a common tooth extraction due to multiple possible indications: one or more episodes of symptomatic pericoronitis, periodontitis affecting the second molar; crown and/or root resorption of second molar; caries of third or second molars (1-3). The most common pre-operative complication is pericoronitis (1). However, when considering wisdom tooth removal, accurate diagnostic and surgical management are mandatory. This need derives from the anatomic location of the third molar. As for any surgical procedure, intra- and post-operative complications could occur; a recent review found incidence rates ranging from 2.6% to 30.9% (1). MTM intra-operative displacement into facial spaces is an unusual complication (less than 1% of cases), the most frequent areas are the submandibular space, sublingual space, pterygomandibular space, and lateral cervical area; displacement in the infratemporal space has been recently reported (2-4). The displacement is usually related to a lingual tooth position, associated with a fenestrated lingual cortical plate, combined with a not optimized diagnosis and surgical technique (5). This complication can be asymptomatic or determine adjacent soft tissue damage, lingual nerve (LN) paresthesia, pain, swelling, trismus and foreign body reaction, along with medical-legal implications (6). Lingual sensory impairment remains a clinical problem in oral surgery and has important medical and legal implications. In fact, the damage to the LN is a common cause of litigation in dentistry (6). MTM extractions should

Key words: accidental displacement; mandibular third molar; cone-beam computed tomography; medicolegal considerations

Mailing address:
Dr Giuseppe Varvara,
Department of Medical, Oral and Biotechnological Sciences,
University of Chieti–Pescara, Via Dei Vestini 31,
66100 Chieti, Italy
Tel.: +39 0871 3554125 - Fax: +39 0871 3554148
e-mail: gvarvara@unich.it

0393-974X (2016)

DISCLOSURE: ALL AUTHORS REPORT NO CONFLICTS OF INTEREST RELEVANT TO THIS ARTICLE.

be preceded by an adequate clinical and radiological diagnosis; intra or post-operative complications should be included in the informed consent. Clinicians attempting these procedures should ensure adequate access, appropriate bone removal if necessary, and luxation force control; finger guidance may be useful to avoid tooth displacement. In case of tooth or root fragment displacement, the dentist should suspend the procedure and refer the patient to an oral and maxillofacial surgeon as soon as possible. If the referral is not immediate, the socket should be cleaned, the wound sutured and antibiotics administrated. The timing of the retrieval attempt led to various approaches proposed in literature. It has been suggested that delay may induce fibrosis and thus an advantageous "stabilization" of the tooth or fragment (7). Moreover, an MTM displaced into the sublingual space was asymptomatic after 2 years of follow-up (8). However, a recent review found that when there was a delay in referral of more than 24 hours the result was more pain, more swelling and trismus (9). Furthermore, some reports described infection and migration subsequent to a delayed referral (10).

This paper describes the management of a failed mandibular third molar extraction, resulting in tooth displacement in the sublingual space; its diagnosis and medicolegal considerations.

C*ase report*

A 28-year-old male patient came to the clinician's attention complaining of local pain at the right side of the mandible, difficult mouth opening and paraesthesia of the right side of the tongue. He reported that 2 weeks previously, he had undergone an unsuccessful removal attempt of the right MTM by a general dentist, stating that the procedure had been traumatic and the dentist had lost visual contact of the tooth after luxation before its removal from the oral cavity. The post-op management performed by the previous dentist was limited to anti-inflammatory drugs and antibiotics (Clarithromycin 250mg twice a day for 10 days and Ibuprofen 600 mg twice a day for 3 days). Clinical examination revealed the postextraction site in the 4.8 area, local pain, combined with trismus caused by local and temporomandibular joint pain. Asymptomatic mouth opening was limited to 11 mm; a 16 mm opening was achievable with severe pain. Orthopantomography (OPG) was immediately performed to locate the tooth. The x-ray image showed the tooth over the lower edge of the mandibular angle, suggesting its displacement into the posterior part of the sublingual space (Fig. 1a), especially when compared to the pre-operative OPG provided by the patient (Fig. 1b). The patient was treated with miorelaxing drugs to reduce trismus (Thiocolchisoside 4 mg twice a day for 2 days) and was given instructions for exercises to do at home in order to improve mouth opening; the aim was to allow an intraoral removal of the displaced tooth. Three weeks after the failed extraction attempt, maximum mouth opening increased to 26 mm. The paraesthetic elliptic area on the tongue was measured, with a major axis of 10 mm and a minor axis of 7 mm and detected by sensory tests as brush directional touch, 2-point discrimination, temperature change, and pinprick. Cone beam computer tomography (CBCT) was then performed to plan intraoral removal of the displaced tooth: it showed the displaced tooth with anchored lingual cortical fragment displaced in the sublingual space (Fig. 2a, b, c). Antibiotic therapy was restarted with a different drug (amoxicillin + clavulanic acid 875 + 125 mg twice a day for six days) to manage swelling due to the presence of the contaminated tooth. The tooth removal was planned in an operating room, under general anaesthesia. A lingual mucoperiosteal flap extending from the ramus to the molar/premolar border was made. Post-operative OPG was taken, showing the complete tooth removal (Fig. 3). Although still present, the paresthetic area did not enlarge after retrieval surgery.

DISCUSSION

In the case described, extraction was attempted without flap elevation and bone removal, even if osteotomy was probably necessary if we consider the pre-operative OPG. This led to the fracture of the already fenestrated lingual plate, since it was the most fragile bony wall around the examined third molar. In the present case, referral was not

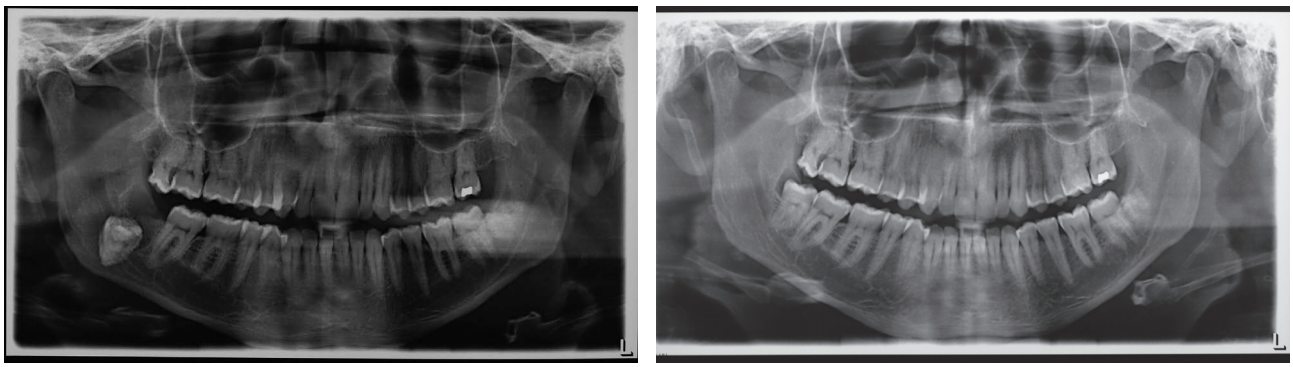

a **b**

Fig. 1. *OPG after displacement (**a**) and pre-displacement OPG (**b**).*

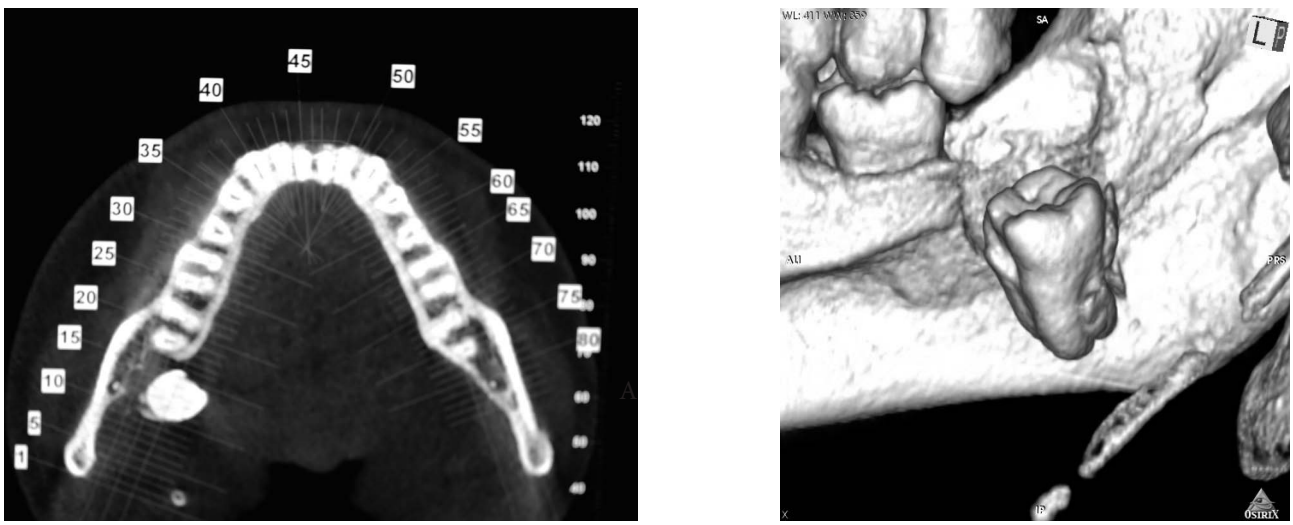

a ***c***

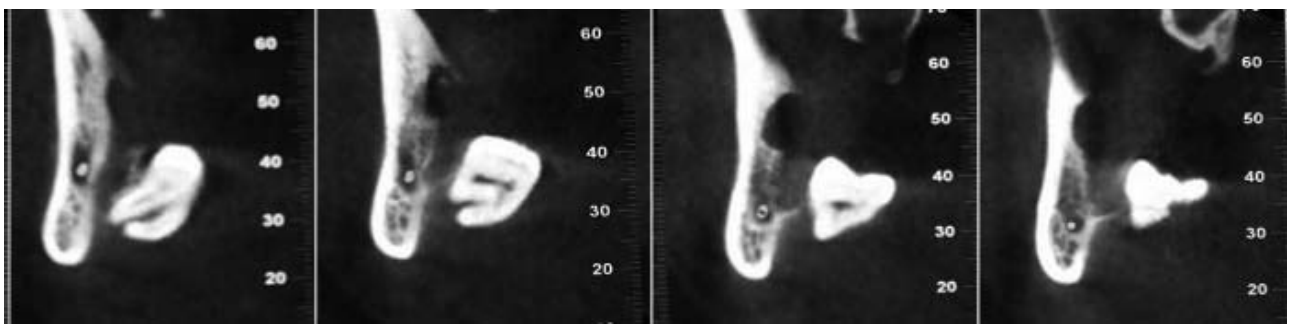

b

Fig. 2. *CBCT axial section (**a**), cross sections (**b**) and 3D reconstruction (**c**).*

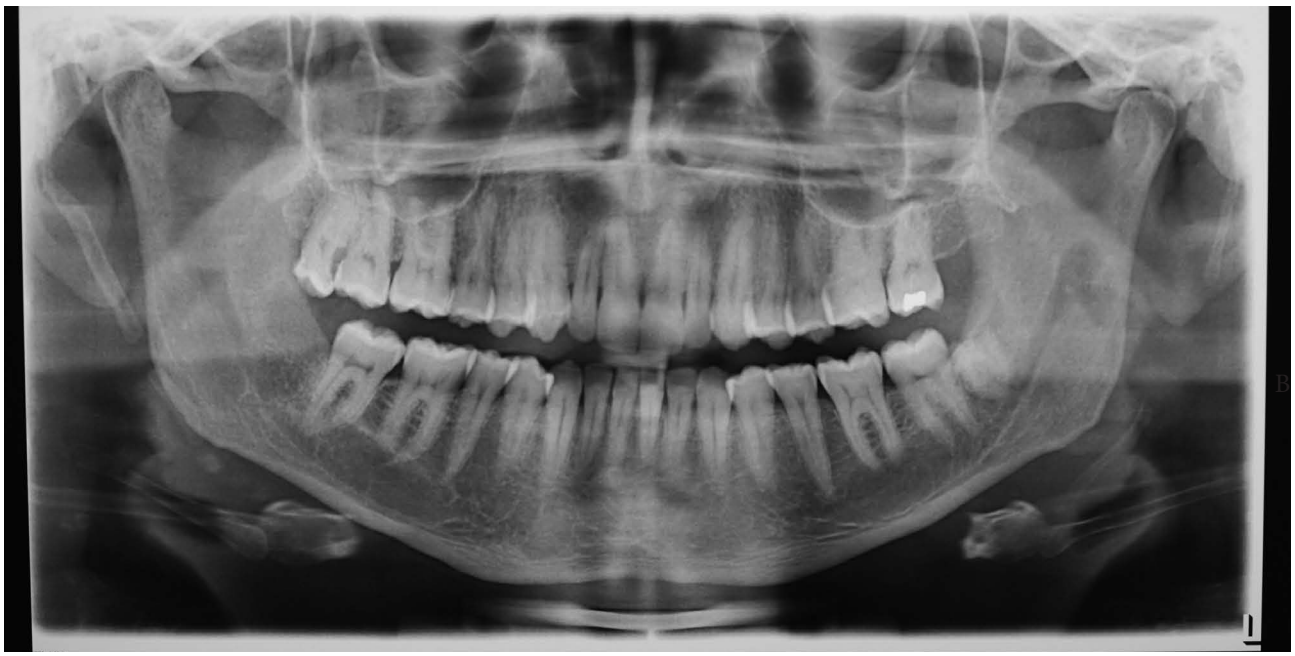

Fig. 3. *Final OPG after tooth retrieval.*

organized at all, allegedly because the tooth was no longer a problem due to the lack of communication with the oral cavity; this led to many of the symptoms mentioned in literature. To allow a correct localization of the displaced element, radiographs taken in at least 2 planes are needed. An OPG is a common first instance radiograph and was also requested in the case reported, but it did not provide information regarding the position in the frontal plane. A recovery attempt on the basis of an OPG only determined a failure; a later submentovertex view showed the displaced tooth to be in the sublingual space (8). A further attempt based on an OPG also failed (8). The addition of an occlusal film to be used in conjunction with the OPG has been recommended (9); posteroanterior and submentovertex films have been suggested, but are less common (8). The intraoral periapical radiography is not very useful in this clinical situation (10). However, in the case described in this paper the CBCT scan offered a complete three-dimensional detail of the displacement with a single exam, after the usual OPG. An up-to-date radiological protocol could be composed by an immediate OPG, for a preliminary evaluation followed by a CBCT scan for a correct three-dimensional assessment of the situation. To retrieve lingual displaced teeth or root fragments, intraoral, extraoral, and combined procedures have been used (7, 10). In the case described in the present paper, the patient experienced a lingual paraesthesia following the failed extraction attempt. In literature, the reported incidence of LN temporary deficit after MTM surgery widely ranges from 0% to 23%; the reported percentage of permanent LN sensorial disturbances varies between 0% and 8% (6). The timing of LN repair remains controversial. Several studies reported a spontaneous recovery of neurosensory deficit after MTM surgery in the first 6-24 postoperative months (11). An informed consent form is an excellent way of communicating potential risks and complications to a patient. Indeed, the potential risk and complications of injury or damage to the LN should be included on the informed consent to avoid liability in cases of lawsuits. Therefore, it could be questionable if the surgeon has to refer an unpredictable event that could occur, although the surgical execution falls within the standard of good medical/dental practice without negligence, imprudence or inexperience (6). Postoperative LN deficit could occur in spite of careful treatment and without malpractice, as it can be unpredictable and somehow unavoidable because

of several factors, such as anatomical ones (6). From a medico-legal point of view, a thorough and complete clinical documentation is vital in order to establish a correct judgment relating to professional conduct and the correct evaluation of any damage that might have been caused, to better assess any pre-existing clinical conditions of the patient. A negative outcome owing to a simple complication in conjunction with the lack of or incomplete documentation, can therefore lead to a judgement of liability for negligence even in cases that were possibly not affected by any technical errors. Indeed, according to Italian civil law, the dentist has the burden of disproving liability by proving that he followed the adequate standards of care (12). In conclusion, the displaced mandibular third molar is an uncommon but potentially serious complication of extraction, and should be taught more extensively to general dentists. This complication should be avoided with a correct diagnosis and surgical technique. When the incident occurs, A CBCT exam is a suitable option to provide correct three-dimensional assessment of the relative position of the displaced tooth, allowing a correct surgical planning for the retrieval attempt. The general dentist should immediately manage the complication within the limits of his surgical skills, or refer the patient to an oral and maxillofacial surgeon as soon as possible to avoid liability.

REFERENCES

1. Brauer HU. Unusual complications associated with third molar surgery: a systematic review. Quintessence Int 2009; 40:565-72.
2. Aznar-Arasa L, Figueiredo R, Gay-Escoda C. Iatrogenic Displacement of Lower Third Molar Roots Into the Sublingual Space: Report of 6 Cases. J Oral Maxillofac Surg 2012; 70:107-15.
3. Xavier CB, Gonçalves FR, Batista SH, Veras Filho Rde O, Vogt BF. Spontaneous migration of third molar following displacement to pterygomandibular fossa. J Oral Maxillofac Surg 2011; 69:1004-7.
4. Shahakbari R, Mortazavi H, Eshghpour M. First report of accidental displacement of mandibular third molar into infratemporal space. J Oral Maxillofac Surg 2011; 69:1301-3
5. Bouloux GF, Steed MB, Perciaccante VJ. Complications of third molar surgery. Oral Maxillofac Surg Clin North Am 2007; 19:117-28.
6. Boffano P, Roccia F, Gallesio C. lingual nerve deficit following mandibular third molar removal: review of the literature and medicolegal considerations. Oral Surg Oral Med Oral Path Oral Radiol 2012; 113: 10-18.
7. Esen E, Aydogan LB, Akcali MC. Accidental displacement of an impacted mandibular third molar into the lateral pharyngeal space. J Oral Maxillofac Surg 2000; 58:96-7.
8. Mellor TK, Finch LD. Displaced third molar. Oral Surg Oral Med Oral Pathol 1987; 64:131.
9. Huang IY, Wu CW, Worthington P. The displaced lower third molar: a literature review and suggestions for management. J Oral Maxillofac Surg 2007; 65:1186-90.
10. Gay-Escoda C, Berini-Aytes L, Pinera-Penalva M. Accidental displacement of a lower third molar. Report of a case in the lateral cervical position. Oral Surg Oral Med Oral Pathol 1993; 76:159-60.
11. Cheung LK, Leung YY, Chow LK, Wong MC, Chan EK, Fok YH. Incidence of neurosensory deficits and recovery after lower third molar surgery: a prospective clinical study of 4338 cases. Int J Oral Maxillofac Surg 2010; 39:320-26.
12. Pinchi V, Varvara G, Pradella F, Focardi M, Donati MD, Norelli G. Analysis of professional malpractice claims in implant dentistry in Italy from insurance company technical reports, 2006 to 2010. Int J Oral Maxillofac Implants 2014; 29:1177-84.

LETTER TO THE EDITOR

EFFICACY OF PULSED LOW-INTENSITY ELECTRIC NEUROMUSCULAR STIMULATION IN REDUCING PAIN AND DISABILITY IN PATIENTS WITH MYOFASCIAL SYNDROME

P. IODICE[1], G. LESSIANI[2], G. FRANZONE[2] and G. PEZZULO[1]

[1]Institute of Cognitive Sciences and Technologies, National Research Council, Rome, Italy;
[2]Center of Intensive Rehabilitation, 'S'Agnese", Pineto (TE), Italy

Received February 1, 2016 – Accepted May 3, 2016

Myofascial pain syndrome (MPS) is characterized by chronic pain in multiple myofascial trigger points and fascial constrictions. In recent years, the scientific literature has recognized the need to include the patient with MPS in a multidimensional rehabilitation project. At the moment, the most widely recognized therapeutic methods for the treatment of myofascial syndrome include the stretch and spray pressure massage. Microcurrent electric neuromuscular stimulation was proposed in pain management for its effects on normalizing bioelectricity of cells and for its sub-sensory application. In this study, we tested the efficacy of low-intensity pulsed electric neuromuscular stimulus (PENS) on pain in patients with MPS of cervical spine muscles. We carried out a prospective-analytic longitudinal study at an outpatient clinic during two weeks. Forty subjects (mean age 42±13 years) were divided into two groups: treatment (TrGr, n=20) and control group (CtrlGr, n=20). Visual-analog scale (VAS) values, concerning the spontaneous and movement-related pain in the cervical-dorsal region at baseline (T0) and at the end of the study (T1), showed a reduction from 7 to 3.81 ($p< 0.001$) in TrGr. In the CtrlGr, VAS was reduced from 8.2 to 7.2 (n.s.). Moreover, the pressure pain threshold at T0 was 2.1 vs 4.2 at T1 ($p <0.001$) in TrG. In the CtrlGR we observed no significant changes. Modulated low-intensity PENS is an innovative therapy permitting to act on the transmission of pain and on the restoration of tissue homeostasis. It seems to affect the transmission of pain through the stimulation of A-beta fibers. The above results show that low-intensity PENS can be considered as an effective treatment to reduce pain and disability in patients with MPS.

Pain is an unpleasant sensory and emotional experience associated with actual or potential tissue damage, or described in terms of such damage (1). Myofascial syndromes are described as painful muscular syndromes characterized by somatic-related pain, dysfunction, and autonomic phenomena and are caused by trigger points (2). These are sites of hyperirritability located in a muscle or its fascia in specific areas in a state of contracture (taut band), locally hardened, painful to pressure; if adequately hypersensitive, they can cause pain and tenderness (2). Myofascial pain syndrome (MPS) is one of the most important causes of disability among the musculoskeletal system diseases; its frequency is 37% in men and 65% in women between 30 and 60 years of age (2).

The most widely accepted pathogenetic hypothesis on the onset of MPS is the so-called theory of the

Key words: A-beta fibers, micro currents, myofascial syndrome, pain

Mailing address:
Dr Pierpaolo Iodice,
Institute of Cognitive Sciences and Technologies,
National Research Council,
Via S. Martino della Battaglia, 44, 00185 Roma, Italy
Tel.: +39 06 44595206 - Fax: +39 06 4459 5243
e-mail: pierpaolo.iodice@istc.cnr.it

0393-974X (2016)

'energy crisis' (2, 3). Excessive muscular overuse, caused by direct or indirect factors, results in damage to the sarcoplasmic reticulum, with the release of calcium ions independent from the spreading of the action potential to the T-tubules. The damage would impede the ion reuptake after each cycle of contraction; given the accumulation of calcium, it would create a state of permanent contracture with the development of local ischemia (3). In turn, ischemia would lead to a reduction in the energy intake, and the consequent deficit of adenosine triphosphate (ATP) would result in a state of contraction due to the failure of the acto-myosin complex dissociation. Ischemia, by inducing muscular damage, also stimulates the release of vasoactive substances such as serotonin, histamine, and bradykinin, with algogenic and sensitizing activity on the muscle nociceptors (3).

Simons et al. (2008) correlated the presence of trigger points in the muscles of the cervical-dorsal region to the genesis of mechanical cervical pain. Recent studies show that in patients with migraine and headache there is a greater number of trigger points in the muscles of the cervical-dorsal spine and that the deactivation of trigger points is related to the reduction in the number of migraine attacks (4). This symptom hampers daily activities, mainly sleep disorders, besides psychological and emotional alterations that affect patients' well-being and their maintenance of social and leisure activities, producing mood swings and decreasing quality of life (5).

In recent years, the scientific literature recognizes the need to include the patient with MPS in a multidimensional rehabilitation project to reduce both symptoms and perpetuating factors, the latter due to the onset of new attacks (3). At the moment, the most widely recognized therapeutic methods for the treatment of myofascial syndrome include the stretch and spray pressure massage, ischemic compression, and infiltration of trigger points (dry, local anesthetics, corticosteroids, saline solution) (6). The most widely used physical therapies are laser therapy, ultrasound and pharmaphoresis (3, 6).

Electric neuromuscular stimulation is a sub-sensory type of stimulus (not associated with unpleasant feelings as with other currents, i.e. painless). Low-intensity electric stimulation started to be used in wound healing after the discovery of the endogenous production of electric fields in tissue injuries, resulting from the sodium channels in the membrane that permit internal sodium diffusion (7). Microcurrent creates potential differences across sensitive channels of the cells within the body. Based on these concepts, the physiological effects include the re-establishment of tissue bio-electricity with increased transportation through the plasma membrane, increased ATP synthesis, protein generation (by stimulating the chemical processes of $Ca2^{+}$ ion), stimulation of cell recovery and relief from pain (8).

In this prospective analytic longitudinal study, we assessed the effectiveness of modulated low-intensity pulsed electric neuromuscular stimulus (PENS) - an innovative therapeutic stimulus which can hypothetically be able to affect the transmission of pain by stimulation of A-beta fibers and improve the energy status of tissue (9, 10) in patients with diagnosis of myofascial syndrome of the cervical spine muscles. In keeping with the previous discussion, we hypothesized that the shift would occur rapidly and be permanent.

MATERIALS AND METHODS

The study protocol conforms to the ethical guidelines of the 1975 Declaration of Helsinki and was approved by the institution's human research committee. After giving written, informed consent, 40 subjects were enrolled in the study (Fig. 1).

Treatment and control

The subjects were randomly allocated into 2 groups by chit method. Participants in the Treatment Group (n=20, GrTr), aged between 20 and 58 years (mean age 41 years) received low-intensity PENS treatment (Algotech®, Talamonti Group, San Benedetto, Italy), for 6 sessions in 14 days, on muscular trigger points in the cervical and dorsal region. Each treatment session lasted for 20/25 minutes. Participants in the Control Group (n=20, CtrlGr), aged between 27 and 60 years (mean age 44 years), received the same procedure as GrTr with an identical "sham" instrument (identical

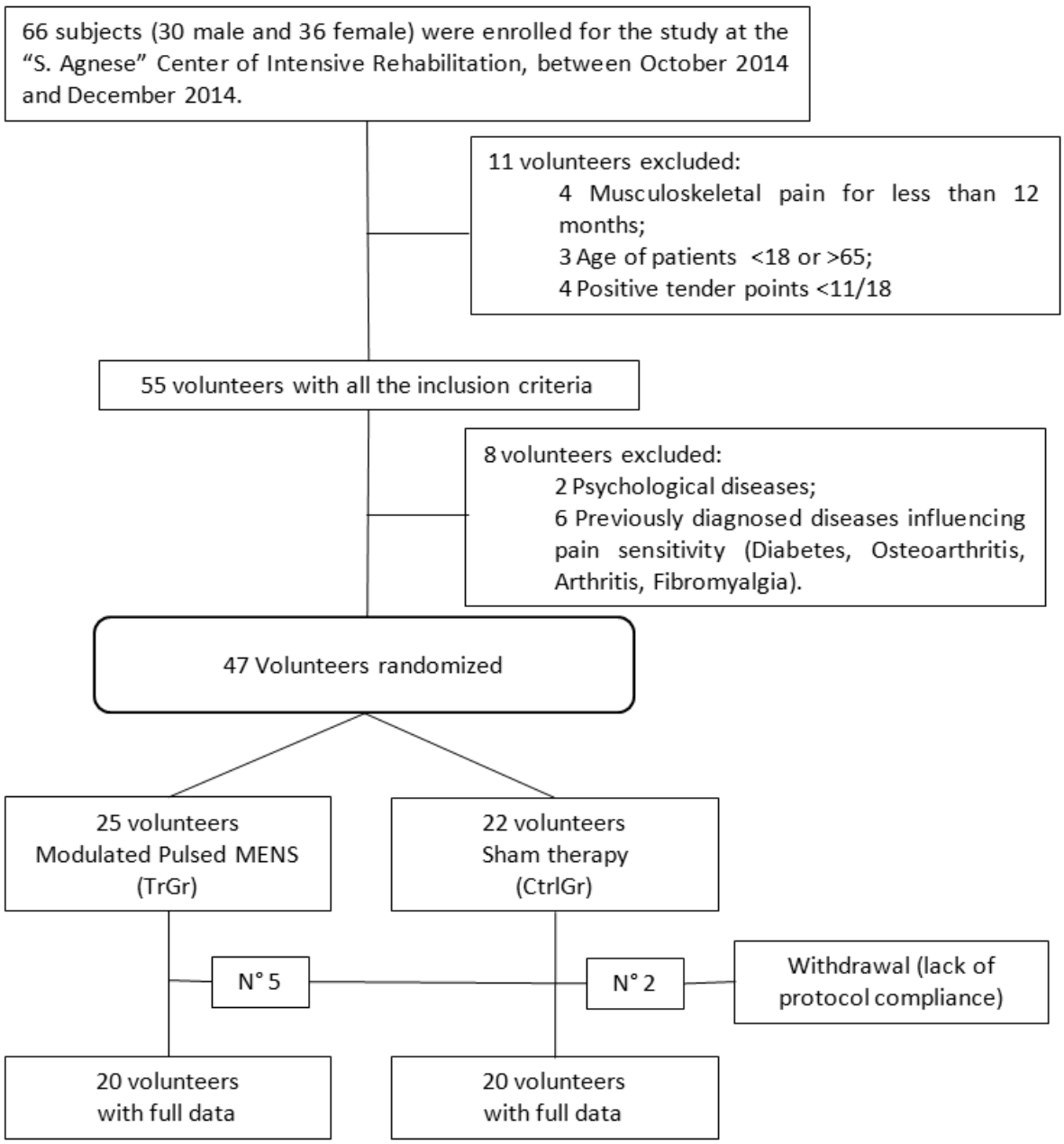

Fig. 1. *Eligibility and exclusion flowchart.*

design) - but the current delivery output was impeded on this instrument.

Equipment

The Algotech® (Talamonti Group, San Benedetto, Italy) was used in this study. The current is pulsed, starting negatively with a range from -58V to 8V and a frequency of approximately 150Hz. This device contains dedicated software able to calculate the skin resistance of the treated area. Based on this software, each pulse, voltage and duration, was in-time modulated (approximately every 20 μs). Furthermore, voltage, from -58V to 8V, and duration, from 10 to 50 μs, of each electric pulse was adapted to the tissue conductance state using a feedback loop. Patch electrodes of 4 × 6 cm2 were placed at

opposite sides of the trigger point area.

An identical "sham" instrument was used for CtrlGr treatment, but the current delivery output was impeded on this instrument. Prior to the study, the devices were labeled either A or B by an independent investigator.

Collection of data

All subjects were evaluated before starting the experimental protocol (T0) and at the end of the study (T1). The outcome measures were the maximum subjective pain intensity assessed by the Scott-Huskinsson visual-analog scale (VAS), the pressure pain threshold of each trigger point was calculated with Fischer algometer, and the level of disability calculated by the Neck Disability Index (11).

Statistical analysis

All data in Figs. 2 and 3 are reported as means ± SD. Differences between mean values before and after treatment programs were tested for significance using Student's *t*-test for paired observations. One-way analysis of variance (ANOVA) was performed with one within-subject factor (periods: T0, T1) to compare the responses to protocols in the two groups. The dependent variables were VAS, Fischer algometer variables and level of disability.

A post-hoc analysis with Bonferroni's Multiple Comparison correction was used to compare between periods and their interactions. The minimum level of statistical significance was set at $p<0.05$. GraphPad Prism (version 5) software (Abacus Concepts GraphPad Software, San Diego, CA, USA) was used for statistical analysis.

RESULTS

The analysis of the VAS scale values (concerning the spontaneous and movement-related pain in the cervical-dorsal region and determined by myofascial syndrome at baseline and at the end of the study) showed a significant reduction from the initial score of 7 to the final score 3.81 ($p< 0.001$) in TrGr. In the control group the mean value of the VAS scale was reduced from 8.2 to 7.2 (n.s.) (Fig. 2)

The pressure pain threshold (Fig. 2), expressed in kg/cm^2 and calculated by Fischer algometer, showed a significant increase from an initial average value of 2.1 to a final of 4.2 ($p <0.001$) in TrGr; in the control group pressure pain threshold had risen from an initial average value of 1.9 to a final of 2.3. (ns) (Fig. 3).

DISCUSSION

The main finding of the present study is that a treatment (6 sessions in 14 days) with a low-intensity PENS therapy is associated with changes in

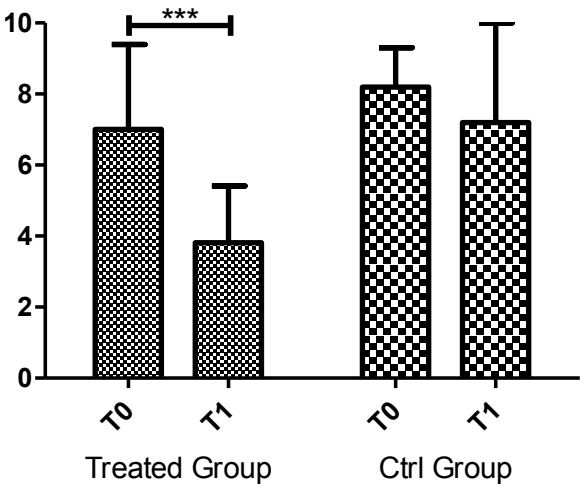

Fig. 2. *Trend of subjective pain (VAS) at T0 and T1, compared in the treatment and control group. The graph shows a significant reduction of the VAS values for TrGr ($p <0.001$) compared to the Ctrl group (ns).*

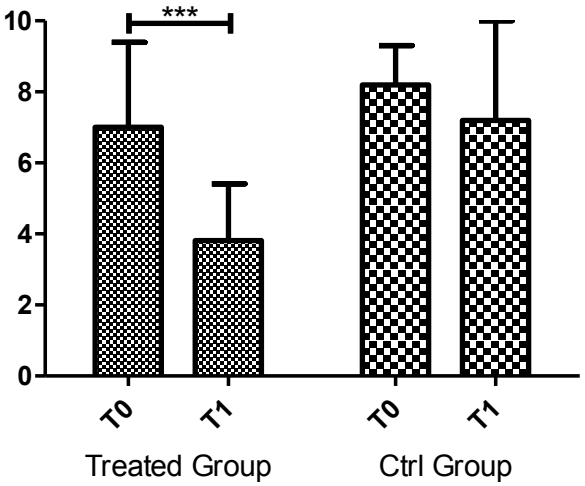

Fig. 3. *Pressure pain threshold assessed with Fischer algometer at T0 and T1, compared in the treatment group and control. The graph shows an increase in pressure pain threshold in both groups, the result is statistically significant (p <0.001) in TrGr.*

pain perception, possibly mediated by a restoration of tissue homeostasis in patients with myofascial syndrome.

Thus, using pain as a proxy for changes in tissue, this study provides a mechanistic support for the recent evidence that microcurrent pulses can induce the shifting of the membrane potential from the resting values towards the most positive ones (depolarization) - and this process may allow the blocking of pain transmission (9, 10).

The modulation of micro-pulses voltage, frequency and duration of each stimulus in relation to skin resistance (using the Algotech® software) causes, by a mechanical process, the passage of the connective tissue from the state of *gel* (integrated network) to that of *sol* (colloidal solution) (8). This allows decongesting the tissue itself and making the most of the piezoelectric ability, permitting the stimulus to spread deeper.

The membrane depolarization increases its own permeability, allowing the entry of ions into the cell and increasing the energy charge (7, 9). This leads to a cellular reactivation with increase in ATP production due to the mitochondrial stimulation, an increase in the activity of sodium-potassium pump, and an increase in ion exchange (9).

Furthermore, the ionic flow, interacting with cells, produces a cascade effect, with recovery of venous-lymphatic functions (12) and activation of the potential action of the motor neuron, with subsequent muscle contraction. Therefore, the activation of the muscular and cellular pump, through the lymphatic recovery, allows the mobilization of harmful substances accumulated in the interstitial spaces.

Our hypothesis is confirmed by the data of pressure pain threshold, which reveal the complete disappearance of trigger points or any tissue alteration in patients at the end of protocol therapy. These events lead to the restoration the homeostatic function, which had been altered in the tissue as a result of the myofascial syndrome.

The study limitations include the lack of a control group of other type of therapy treatment protocol, e.g., a conventional stretch and spray massage for MPS.

In conclusion, our study demonstrates that short-term, low-intensity, modulated PENS therapy has broad beneficial effects on pain perception of patients affected by MPS, with an evident normalization of cell bioelectricity.

REFERENCES

1. Portenoy R K. Report from the International Association for the Study of Pain Task Force on cancer pain. J. Pain Symptom Manage 1996; 12, 2:93-96.

2. Simons DG. New view of myofascial trigger points: etiology and diagnosis. Arch Phys Med Rehabil 2008; 89:157-9.
3. Srbely JZ. New trends in the treatment and management of myofascial pain syndrome. Curr Pain Headache Rep 2010; 14(5):346-52.
4. Giamberardino MA, Tafuri E, Savini A, et al. Contribution of myofascial trigger points to migraine symptoms. J Pain 2007; 8(11):869-78.
5. Schlenk EA, Erlen JA, Dunbar-Jacob J, et al. Health-related quality of life in chronic disorders: a comparison across studies using the MOS SF-36. Qual Life Res 1998; 7(1):57-65.
6. Saggini R, Bellomo RG, Saggini A, Iodice P, Toniato E. Rehabilitative treatment for low back pain with external pulsed electromagnetic fields. Int J Immunopathol Pharmacol 2009; 22(S3):25-28.
7. Balakatounis KC, Angoules AG. Low-intensity electrical stimulation in wound healing: review of the efficacy of externally applied currents resembling the current of injury. J Plastic Surg 2008; 8:283-91.
8. Jeong JW. A study on the effects of pain reduction using microcurrent. J Korean Soc Phys Ther 1991; 12:195-205
9. Cheng N The effect of electric currents on ATP generation, protein synthesis and membrane transport in rat skin. Clinical Orthopedics 1982; 171:264-72.
10. Lessiani G, Galati V, Franzone G, Iodice P. Efficacy of modulated microcurrent stimulation in pressure ulcers treatment: A monocentric, prospective, double-blind, randomized study. J Nov Physiother 2014; 4:4.
11. Vernon H, Mior S. The Neck Disability Index: a study of reliability and validity J Manipulative Physiol Ther 1991;14(7):409-15.
12. Saggini R, Iodice P, Bellomo RG, Lessiani G. Venous insufficiency and foot dysmorphism: effectiveness of visco-elastic rehabilitation system on veno-muscle system of the foot and of the calf. Int J Immunopathol Pharmacol 2009; 22(S3): 1-8.

LETTER TO THE EDITOR

COMPARISON BETWEEN INTRARTICULAR INJECTION OF HYALURONIC ACID, OXYGEN OZONE, AND THE COMBINATION OF BOTH IN THE TREATMENT OF KNEE OSTEOARTHROSIS

A. GIOMBINI[1], F. MENOTTI[1], A. DI CESARE[2], F. GIOVANNANGELI[3], M. RIZZO[3], S. MOFFA[4] and M. MARTINELLI[3]

[1]Department of Human, Motor and Health Sciences, University of Rome "Foro Italico", Rome, Italy; [2]UOC Unit of Physical Medicine and Rehabilitation, Azienda Ospedaliera Policlinico Umberto I, Rome, Italy; [3]Unit of Ozonetherapy, S.Pietro Fatebenefratelli Hospital, Rome; [4]University of Molise, Campobasso, Italy

Received February 21, 2016 – Accepted May 1, 2016

This study aimed to compare short-term clinical outcomes between intra-articular injection of hyaluronic acid (HA), oxygen ozone (O2O3), and the combination of both, in patients affected by osteoarthrosis (OA) of the knee. Seventy patients (age 45-75 years) with knee OA were randomized to intra-articular injections of HA (n=23), or O2O3 (n=23) or combined (n=24) one per week for 5 consecutive weeks. KOOS questionnaire and visual analog scale (VAS), before treatment (pre) at the end (post), and at 2 months after treatment ended (follow-up) were used as outcome measures. Analysis showed a significant effect (P<0.05) of the conditions (pre, post and follow-up) in all parameters of the KOOS score and a significant effect (P<0.05) of groups (HA, O2O3 and combined) for pain, symptoms, activities of daily living and quality of life. The combined group scores were higher compared to the HA and O2O3 groups, especially at follow-up. The combination of O2O3 and HA treatment led to a significantly better outcome especially at 2-month follow-up compared to HA and O2O3 given separately to patients affected by OA of the knee.

Knee OA is a common disease associated with significant morbidity, which is frequently associated with pain, limitation in range of motion, and muscle weakness (1). In a recent review, Miller et al. summarized that visco supplementation was an effective treatment for knee OA with beneficial effects on pain, function, and patient global assessment (2). Recently, intramuscular and intra-articular injection of O2O3 in therapeutic concentration between 10µg/mL and 30µg/mL ozone in oxygen gained popularity as an alternative therapy for either relief of pain, or physical disability, without significant side effects, in several chronic diseases in many European, South American and Asian countries (3). To the best of the authors' knowledge, there is one uncontrolled study by Moretti (4) on the combined effect of HA and O2O3 in the treatment of middle-aged patients affected by grade II knee OA, in which the Author demonstrated a reduction of pain, by means of a NRS scale, after three sessions of a combined intra-articular infiltration of HA and O2O3 with only a slight resumption in pain score, at three-month

Key words: oxygen-ozone, ozone therapy, knee osteoarthrosis, hyaluronic acid

Mailing address:
Annalisa Di Cesare, MD,
UOC Unit of Physical Medicine and Rehabilitation,
Azienda Ospedaliera Policlinico Umberto I,
Piazzale Aldo Moro 5, 00185Rome, Italy
Tel.: +393384280738
e-mail: annalisa.dicesare@gmail.com

0393-974X (2016)

follow-up. The study of Li et al. (5), although only the abstract is available in English, was conversely the only controlled study on knee OA patients treated with ozone; that study showed that the combination of intra-articular O2O3 and Chinese medicine was more effective on pain, joint stiffness and score of daily living activities with an effective rate of 76%. The present study was therefore designed to compare the short-term clinical outcomes of 3 intra-articular treatments for knee OA, one performed with HA, another performed with O2O3 and a third based on a combination of both. Our hypothesis was that the combination of both treatments would have yielded higher improvements in pain and disability than the other two treatments used alone.

MATERIALS AND METHODS

Study population

The study was approved by the Local Ethics Committee and conducted in accordance with the principles of the Declaration of Helsinki. All patients gave informed consent prior to enrollment. This was a prospective randomized comparative study involving a study population of 83 patients, aged from 57 to 74 years, of both sexes with OA of the knee (Table I) treated in two medical centers: the outpatient Ozone Therapy Unit of S. Pietro Fatebenefratelli Hospital and the Physical Medicine and Rehabilitation Complex Unit Azienda Ospedaliera Policlinico Umberto I, in Rome, between June 2014 and July 2015. The following inclusion criteria for patient selection were used: patients with knee OA (based on American College of Rheumatology criteria), with symptom duration of more than 6 months, and confirmatory knee X-ray diagnosis (Kellgren–Lawrence grade II, III) within the previous 3 months. All patients had previously been treated conservatively using analgesics and NSAIDs without success for at least 3 months. Exclusion criteria included secondary OA, history of diabetes mellitus, immunodeficiency and collagen vascular disorders, history or presence of malignant disorders, infection or severe trauma to the knee, autoimmune and platelet disorders, use of NSAIDs 3 days prior to injection, history of knee intra-articular injections of HA or corticosteroids during the previous 3 months or use of systemic corticosteroids 2 weeks before the start of the trial, hypersensitivity to HA. On admission, every eligible patient underwent a complete physical examination and weight-bearing X-rays of the affected knee. After having met the inclusion and exclusion criteria, a sample of 70 subjects were assigned to one of the three treatment groups on the basis of block randomization, by using a computer-generated random-sequence table generated at the trial coordinating center. The intra-articular HA injection group (HA) (n=23) were treated with 20 mg/2.0mL of intra-articular HA injection (Hyalgan®) (Fidia Farmaceutici S.p.A., Abano Terme, Italy) into the affected knee via a lateral parapatellar approach, using a 2.5 mL syringe with a 25-gauge (19 mm) needle, once a week for 5 consecutive weeks. Hyalgan, is a viscous solution consisting of a fraction of purified natural sodium hyaluronate (molecular weight 500,000–730,000 Da), in buffered physiological sodium chloride, having a PH of 6.8–7.5. The intra-articular 0203 (O2O3) group (n=23) received 5 intra-articular infiltrations (once a week for 5 consecutive weeks) of an O2O3 mixture (15 mL) with an O3 concentration of 15 μg /mL, obtained by means of an ozone generator (AlnitecOzo2 Futura, Alnitec s.r.l, Cremosano, CR, Italy). The intra-articular injection was administered with the patient in a supine position using a lateral parapatellar approach, using a 20 mL syringe with a 25-gauge (19 mm) needle. The intra-articular 0203 and HA (combined) group (n=24) received 5 intra-articular infiltrations (once a week for 5 consecutive weeks) of an O2O3 mixture (15 mL) with an O3 concentration of 15 μg/mL. The intra-articular injection was administered in the same position as the other two groups, but first the O2O3 gas mixture was injected using a 25-gauge 19-mm butterfly needle, followed after 60 s by the 20 mg/2.0mL HA solution. All procedures were performed under sterile conditions, by the same two experienced physicians. Subjects were evaluated with the KOOS questionnaire and VAS before treatment (Pre), at the end (Post), and at two months after the end of treatment (follow-up). The KOOS is a patient-based, site-specific questionnaire developed to be used for short- and long-term follow-up of knee injury and knee osteoarthritis. Demographic characteristics of the patients as well as complications and adverse events during treatment were recorded. At each follow-up visit, physical examination also assessed possible swelling of the affected joint, tenderness, subjective pressure, and local pain during motion and at rest.

Statistical analysis

All data were normally distributed in terms of skewness and kurtosis (all values<2). Statistical comparisons of the parameters (pain, symptoms, ADL, sport/recreation, QoL, VAS), between groups (O2O3, HA and combined) at the 3 time points (pre, post and follow up) were carried out by Two-Way ANOVA for repeated measures, followed by One-Way ANOVA and Student's *t*-tests with Bonferroni correction where appropriate. Statistical significance levels were set at P<0.05. Unless otherwise specified, data were reported as mean ± standard deviation (SD).

RESULTS

KOOS questionnaire

The two-way ANOVA for Pain showed a significant effect of group (P<0.05) and a significant effect of condition (P<0.05). The post-hoc analysis showed that the Pain scores were significantly higher in the O2O3 group and the combined group in respect to the HA group at the post condition (P<0.05) and follow-up (P<0.05). Similarly, the two-way ANOVA for symptoms showed significant effect of group (P<0.05) and a significant effect of condition (P<0.05). The post-hoc analysis showed that the symptom scores were higher in the O2O3 group and the combined group in respect to the HA group at post condition (p<0.05) and follow-up (P<0.05) and, in addition, the symptom scores in the combined group were significantly higher in respect to the O2O3 group at follow-up only (P<0.05). The two-way ANOVA for ADL showed significant effects of group (P<0.05) and a significant effect of condition (P<0.05). The post-hoc analysis showed that the ADL scores (Fig. 1) were higher in the O2O3 group and the combined group in respect to the HA group at post condition (P<0.05), and in the combined group only the ADL scores were higher in respect to the HA group at follow-up (P<0.05). Furthermore, the two-way ANOVA for QoL showed significant effect of group (P<0.05) and a significant effect of condition (P<0.05). The post-hoc analysis showed that the QoL scores were higher in the combined group in respect to the HA group at follow-up only (P<0.05). The two-way ANOVA for Sport/recreation scores showed significant effect of condition (P<0.05) while it did not show significant effect of groups (pre group: 22.92%±15.22, 25.43%±16.34, 17.73%±10.11; post group: 39.13%±14.36, 41.52%±19.80, 42.71±13.35; follow-up group: 56.30%±13.10, 53.70%±23.22, 61.46%±16.45 in HA, O2O3 and combined groups, respectively).

VAS scale

The two-way ANOVA for the VAS scale showed significant effect of condition (P<0.05) while it did not show significant effect of groups (Pre: 6.90±0.68 cm, 6.62±0.84 cm, 7.05±0.55 cm; Post: 4.58±0.44cm, 3.98±1.10 cm, 3.99±0.55 cm, follow-up: 2.40±0.48 cm, 2.40±1.41 cm, 1.75±0.65 cm in

Table I. *Baseline characteristics of HA, O2O3 and HA+O2O3 groups, mean values (SD) at baseline.*

	Group HA	***Group 0203***	***Group HA+0203***
Sex	*12 F/11M*	*11F/12M*	*14F/10M*
Age (years)	64±4.52	68±5.36	61±3.41
BMI	24.4±4.5	27.7±4.9	26.3±3.5
Pain Duration (months)	*28*±4	*27*±1	*26*±6
Kellgren and Lawrence OA	*10 (III)/13(II)*	*12 (III)/11(II)*	*11 (III)/13(II)*
Vas	6.93±0.68	6.71±0.87	7±0.55

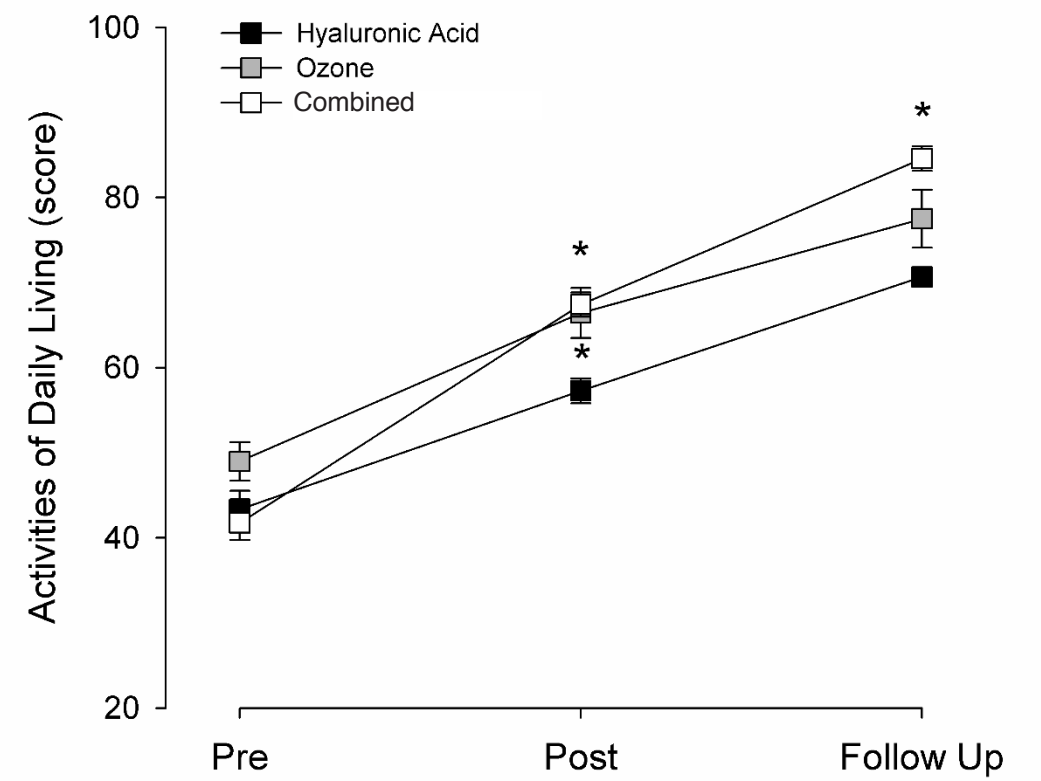

Fig. 1. *Activities of Daily Living scores (Mean±SD) reported by patients* during *the pre, post and follow-up conditions in HA group (black squares), O2O3 group (grey squares) and combined group (white squares). * Significantly different from HA group.*

HA, O2O3 and combined groups respectively).

DISCUSSION

The main finding of this study was that five sessions once a week of intra-articular injection with O2O3 in combination with HA therapy yielded higher improvements in pain, symptoms and ADL than the treatment with HA alone. At follow-up, two months after the end of the treatment, the combination of O2O3 therapy with HA obtained higher improvements in symptoms, ADL and QoL than the other two treatments used alone. HA is reported to serve as a lubricant to maintain the cartilage matrix integrity and to have an anti-inflammatory effect (2), while the action of O2O3 mixture could be explained with the biochemical properties of O3 (6, 7). The O2O3 mixture acts as a bioregulator when it comes into contact with a biological liquid, releasing factors from human endothelial cells, normalizing the cellular redox balance and stimulating important biochemical pathways (8-10). Borrelli et al. (11) stated that O2O3, when injected into the knee, after its solubilization in the synovial fluid, generates reactive oxygen species (ROS) and lipid oxidation products (LOP) which, in turn, are responsible for several effects: a possible inactivation and inhibition of the release of proteolytic enzymes and proinflammatory cytokines; induction of the proliferation of chondrocytes and fibroblasts; release of the synthesis of antioxidant enzymes such as superoxide dismutase (SOD), glutathione peroxidase (GSH-Px) and catalase. Our results seem to be comparable in terms of pain reduction in the short term to those obtained by Moretti (4) and those of Mishra et al. (12) who demonstrated the effectiveness, with a 90% success rate, of intra-articular injection of O2O3 compared

to methylprednisolone in patients with grade I and II knee OA. Intra-articular injection of a combination of O2O3 and HA obtained a better improvement in clinical symptoms, ADL and QoL in patients affected by grade II and III knee OA, maintaining the effect in a short term. Limitations included the limited number of patients, lack of a placebo control group, not being blinded and a short follow-up. Further prospective randomized controlled studies are needed to confirm our findings

REFERENCES

1. Fibel KH, Hillstrom HJ, Halpern BC. State-of-the-Art management of knee osteoarthritis. World J Clin Cases 2015; 3:89-101.
2. Miller LE, Block JE. US-approved intra-articular hyaluronic acid injections are safe and effective in patients with knee osteoarthritis: systematic review and meta-analysis of randomized, saline-controlled trials. Clin Med Arthritis Musculoskelet Disord 2013; 6:57-63.
3. Bocci V, Borrelli E, Zanardi I, Travagli V. The usefulness of ozone treatment in spinal pain. Drug Des Devel Ther 2015; 9:2677-85.
4. Moretti M. Effectiveness of treatment with oxygen-ozone and hyaluronic acid in osteoarthritis of the knee. Int J Ozone Ther 2010; 9:25-29.
5. Li JH, Zhou LX, Li GY, Cheng B. Treatment of middle-aged and aged patients with knee osteoarthritis of yang-deficiency induced cold-damp syndrome by ozone combined Chinese materia medica: a clinical research. Hongguo Zhong Xi Yi Jie He Za Zhi 2013; 33:471-75.
6. Bocci V. How a calculated oxidative stress can yield multiple therapeutic effects. Free Radic Res 2012; 46:1068-75.
7. Bocci V. Scientific and medical aspects of ozone therapy. State of the art. Arch Med Res 2006; 37:425-35.
8. Bocci V. Ozone as a bioregulator. Pharmacology and toxicology of ozonetherapy today. J Biol Regul Homeost Agents 1996; 10:29-33.
9. Melchionda D, Milillo P, Manente G, Stoppino L, Macarini L. Treatment of radiculopathies: a study of efficacy and tollerability of paravertebral oxygen-ozone injections compared with pharmacological anti-inflammatory treatment. J Biol Regul Homeost Agents 2012; 26:467-74
10. Bocci V, Valacchi G, Corradeschi F, Aldinucci C, Silvestri S, Paccagnini E, Gerli R. Studies on the biological effects of ozone: 7. Generation of reactive oxygen species (ROS) after exposure of human blood to ozone. J Biol Regul Homeost Agents 1998; 12:67-75.
11. Borrelli E, Alexandre A, Iliakis E, Alexandre A, Bocci V. Disc herniation and knee arthritis as chronic oxidative stress diseases: the therapeutic role of oxygen ozone therapy. J Arthritis 2015; 4:161-66.
12. Mishra S, Pramanik R, Das P, Das PP, Palit AK, Ray J, Halder RN. Role of intraarticular ozone in ostheoarthritis of the knee for functional and symptomatic improvement. Int J Phys Med Rehab 2011; 22:65-69.